

AD _____

Award Number: W81XWH-FFEEEG G

TITLE: ~~DEPARTMENT OF DEFENSE~~ INFORMATION REPORT

PRINCIPAL INVESTIGATOR: ~~DR. JOHN M. HARRIS~~

CONTRACTING ORGANIZATION: ~~U.S. ARMY MEDICAL RESEARCH AND MATERIALS COMMAND~~

REPORT DATE: ~~1 AUG 2001~~

TYPE OF REPORT: Annual

PREPARED FOR: U.S. Army Medical Research and Materiel Command
Fort Detrick, Maryland 21702-5012

DISTRIBUTION STATEMENT: Approved for public release; distribution unlimited

The views, opinions and/or findings contained in this report are those of the author(s) and should not be construed as an official Department of the Army position, policy or decision unless so designated by other documentation.

REPORT DOCUMENTATION PAGE

*Form Approved
OMB No. 0704-0188*

Public reporting burden for this collection of information is estimated to average 1 hour per response, including the time for reviewing instructions, searching existing data sources, gathering and maintaining the data needed, and completing and reviewing this collection of information. Send comments regarding this burden estimate or any other aspect of this collection of information, including suggestions for reducing this burden to Department of Defense, Washington Headquarters Services, Directorate for Information Operations and Reports (0704-0188), 1215 Jefferson Davis Highway, Suite 1204, Arlington, VA 22202-4302. Respondents should be aware that notwithstanding any other provision of law, no person shall be subject to any penalty for failing to comply with a collection of information if it does not display a currently valid OMB control number. **PLEASE DO NOT RETURN YOUR FORM TO THE ABOVE ADDRESS.**

1. REPORT DATE (DD-MM-YYYY) July 2013	2. REPORT TYPE Annual	3. DATES COVERED (From - To) 1 July 2012 - 30 June 2013		
4. TITLE AND SUBTITLE Assessment of Nanobiotechnology-Targeted siRNA Designed to Inhibit NF-kappaB Classical and Alternative Signaling in Breast Tumor Macrophages "			5a. CONTRACT NUMBER	
			5b. GRANT NUMBER W81XWH-11-1-0242	
			5c. PROGRAM ELEMENT NUMBER	
6. AUTHOR(S) Fiona Yull Ryan Ortega E-Mail: fiona.yull@vanderbilt.edu			5d. PROJECT NUMBER	
			5e. TASK NUMBER	
			5f. WORK UNIT NUMBER	
7. PERFORMING ORGANIZATION NAME(S) AND ADDRESS(ES) The Vanderbilt University Nashville, TN 37240			8. PERFORMING ORGANIZATION REPORT NUMBER	
9. SPONSORING / MONITORING AGENCY NAME(S) AND ADDRESS(ES) U.S. Army Medical Research and Materiel Command Fort Detrick, Maryland 21702-5012			10. SPONSOR/MONITOR'S ACRONYM(S) " " "	
			11. SPONSOR/MONITOR'S REPORT NUMBER(S) " " "	
12. DISTRIBUTION / AVAILABILITY STATEMENT Approved for Public Release; Distribution Unlimited				
13. SUPPLEMENTARY NOTES				
14. ABSTRACT Macrophages have been proposed as a potential target for manipulation of the microenvironment in breast cancer because they are potent effectors of the immune system. NF-kappaB (NF- κ B) signaling in macrophages contributes to their impact during breast tumorigenesis. Thus, macrophage-targeted modulation of NF- κ B has potential as a novel therapeutic approach for breast cancer. NF- κ B signaling is mediated via two major pathways; the canonical/classical pathway and the alternative pathway. Our strategy is designed to develop a nanobiotechnology-based method to target siRNA designed to inhibit NF- κ B classical and alternative signaling specifically to tumor associated macrophages to modulate the tumor microenvironment and to test the therapeutic potential of this approach. In this highly collaborative study, we have synthesized and characterized in vitro both mannoseylated and untargeted nanoparticles. We have compared the efficiency of transfection of bone marrow derived macrophages between nanoparticles and commercial transfection reagents. We have started to investigate the effects of modulation of the NF- κ B pathways on macrophage phenotype. Finally, we have performed initial in vivo studies that suggest that tumor associated macrophage specific targeting will be feasible in the context of primary tumors and metastases in the lung.				
15. SUBJECT TERMS Nanoparticles, NF-kappaB, macrophages, alternative NF-kappaB				
16. SECURITY CLASSIFICATION OF:			17. LIMITATION OF ABSTRACT UU	18. NUMBER OF PAGES 301
a. REPORT U	b. ABSTRACT U	c. THIS PAGE U	19a. NAME OF RESPONSIBLE PERSON USAMRMC 19b. TELEPHONE NUMBER (include area code)	

Table of Contents

Introduction.....	1
Body.....	2
Key Research Accomplishments.....	9
Reportable Outcomes.....	10
Conclusions.....	13
References.....	14
Appendices.....	15

Introduction

Macrophages have been proposed as a potential target for manipulation of the microenvironment in breast cancer because they are potent effectors of the immune system, demonstrating the ability to secrete a wide range of intercellular signals from pro-inflammatory cytokines and chemokines, to growth and pro-angiogenic factors [1, 2]. NF-kappaB (NF- κ B) signaling in macrophages contributes to their impact during breast tumorigenesis [3-9]. Thus, macrophage-targeted modulation of NF- κ B has potential as a novel therapeutic approach for breast cancer. NF- κ B signaling is mediated via two major pathways; the canonical/classical pathway and the alternative pathway both of which have been implicated in oncogenesis [10-13] (Figure 1). Our strategy is designed to use siRNA-mediated knockdown of expression of key proteins within each pathway to examine their individual and combined roles with respect to potential breast cancer immunotherapy. We selected as our initial targets the IKK β activator (canonical) or p52 (alternative) proteins. In order to harness inhibition of these pathways to modulate the tumor microenvironment we intend to deliver siRNA specifically to tumor-associated-macrophages (TAMs). Therefore, the proposed work seeks to synthesize, characterize and assess multifunctional nanoparticles for siRNA delivery specifically to tumor-associated-macrophages (TAMs). The nanoparticles will have the capacity for siRNA association, protection and endosome release combined with tissue/cell specific delivery. They are intended to knockdown protein expression of NF- κ B modulators with exceptional specificity for TAMs. TAM-specific nanoparticle targeting offers an innovative approach to enable NF- κ B modulation *in vivo* through highly localized siRNA knockdown of critical, pathway-specific proteins that control NF- κ B. The proposed approach is a novel combination intended to treat primary and metastatic breast cancer, the phase of this disease with the poorest clinical outcomes.

The ***hypothesis*** to be tested is that siRNA-mediated inhibition of NF- κ B signaling in TAMs will decrease primary tumor growth and metastatic potential. Our ***objectives*** are (1) exploration of macrophage response to inhibition of NF- κ B activation by the canonical and alternative pathways, separately and in combination using siRNA knockdown *in vitro* and (2) development of a nanobiotechnology delivery vehicle with the capacity for siRNA delivery TAMs for the purpose of pathway-specific NF- κ B knockdown *in vivo*.

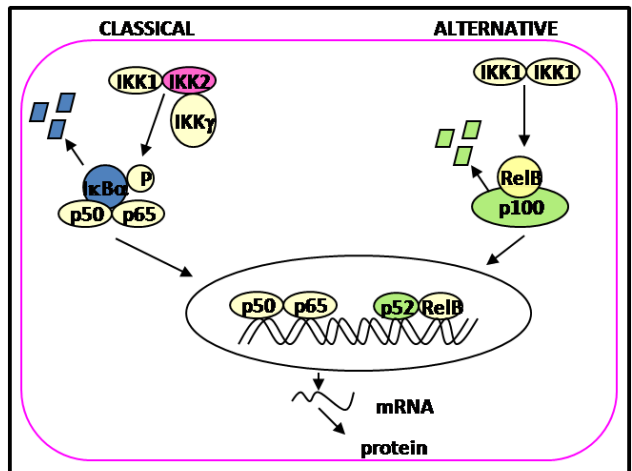


Figure 1. Classical and alternative NF- κ B signaling pathways.

Body

Specific Aim 1. Generate siRNA-delivering nanoparticles and optimize dosage *in vitro* in cell cultures of murine bone marrow derived macrophages (BMDM):

1a. Synthesize and fluorescently tag copolymer poly-HPMA-bl-DMAEMA-bl-[DMAEMA-co-PAA-co-BMA], and attach macrophage targeting peptide onto the HPMA end.

Completed previously by the Giorgio lab (see BC102696 annual report 2012 for details).

1b. Verify pH-responsive endosomolytic activity of new copolymer in hemolysis assays, and characterize polymer physical properties (light scattering, TEM, siRNA complexation assays).

Completed previously by the Giorgio lab (see BC102696 annual report 2012 for details).

1c. Expose BMDM from NGL reporter transgenics in culture to the nanoparticles. Quantify peptide-specific & dose-dependent delivery of nanoparticles to the BMDMs by fluorescence microscopy and flow cytometry.

Our previous work demonstrated the basic effectiveness of the mannosylated nanoparticle carrier for siRNA delivery to macrophages (BC102696 annual report 2012, published in *Molecular Pharmaceutics*, Yu et al, 2013). The goal then became to further characterize the particles *in vitro* as we moved towards *in vivo* application. With this in mind, one of the major concerns addressed by the Yull lab was the biocompatibility of the mannosylated nanoparticle carrier. In order to test the *in vitro* biocompatibility of the Mn-NP siRNA delivery agent, Mn-NP siRNA complexes were incubated with BMDMs for 24 hours with untransfected cells as a negative control and 0.5% Triton as a positive control for loss of viability. In order to compare the nanoparticles to a commercial transfection agent, Lipofectamine was also tested in the same fashion. The experiment was run with and without the presence of TNF- α stimulation and with either 10 nM or 50 nM siRNA. As the amount of siRNA used increases, the amount of Mn-NP used increases to maintain an N:P ratio of 4 as previously described [14]. This N:P ratio indicates a mass of 160 ng of Mn-NP per pmol of siRNA. Our results show that there was a small, but significant decrease in cell viability associated with the use of Lipofectamine in conjunction with the presence of TNF- α . There was no significant decrease in cell viability associated with the use of Mn-NP under any condition (**Figure 2**).

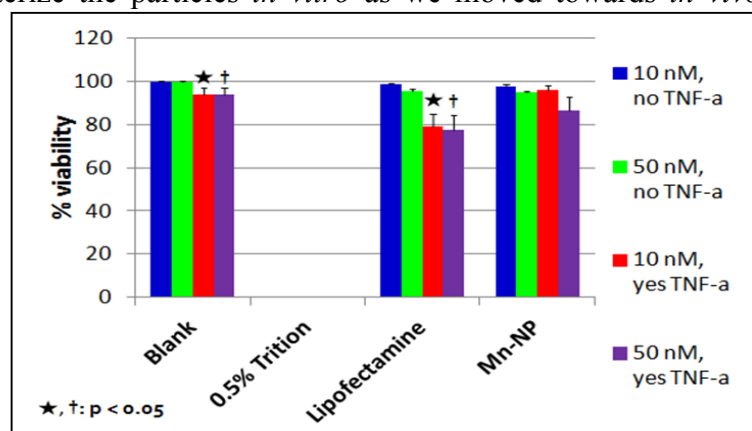


Figure 2: Mn-NP transfected BMDMs have no significant decrease in cell viability at low and high concentrations, +/- the presence of TNF- α compared to untransfected cells.

1d. Deliver IKK2 and p52 siRNA alone and in combination to BMDMs from NGL reporter transgenics *in vitro* and assess modulation of NF- κ B activity by luciferase assay and western analysis of nuclear protein extracts to quantify p65 or p52 translocation to the nucleus as a measure of activation of the canonical and alternative NF- κ B pathways. Further, assess resulting phenotype with respect to M2 → M1 markers by RT-

PCR to quantify expression of target genes correlated with M1 (*iNOS*, *MIPI- α* , *IL-12*) or M2 (*IL-10*, *CCL17*, mannose receptor) phenotypes.

As described in the previous annual report HiPerFect, was initially selected as the commercial transfection agent control based on manufacturers' claims and previous studies indicating that its formulation was optimal for transfecting macrophages due to the lower cationic charge of the lipids used to form the transfection complexes (see HiPerFect data from previous report). To form transfection complexes, a control siRNA against luciferase was incubated with HiPerFect for 1 hour before the transfection solution was added to the cells' media. siRNA concentration and HiPerFect volume were varied. BMDMs were then transfected for 6 hours with the HiPerFect_siRNA complexes. After transfection, the cells were washed and stimulated with TNF- α for 6 hours to activate the NF- κ B pathways as evidenced by an increase in luciferase production. Practical application of the HiPerFect transfection agent would prove difficult. Experiments with HiPerFect demonstrated poor repeatability when NF- κ B relevant siRNA were used and the amount of HiPerFect needed to perform the optimized protocol was cost prohibitive due to the large number of experiments being performed. For these reasons, Lipofectamine RNAiMAX (referred to hereafter as 'Lipofectamine') was investigated as a replacement for HiPerFect. Lipofectamine protocols were developed with varying transfection times and siRNA concentrations. Initial experiments with Lipofectamine expanded the siRNA screen reported in the previous report (Figure 3). Several NF- κ B specific sequences of siRNAs were investigated for efficacy in knocking down total NF- κ B activity in the stimulated NGL BMDM model. 3 different sequences of siRNAs were selected (indicated by A, B, and C) for the following initial targets: IKK β , p65 (RelA), and p52/p100. Preliminary studies were done with single sequences of the following targets: p50 and IKK α . Transfections were done in 12 well plates with NGL BMDMs cultured with 300,000 cells per well. 10 nM siRNA was delivered with 2 μ l of Lipofectamine per well with a total volume of 1 ml of media per well. Total NF- κ B knockdown was measured via luciferase assay.

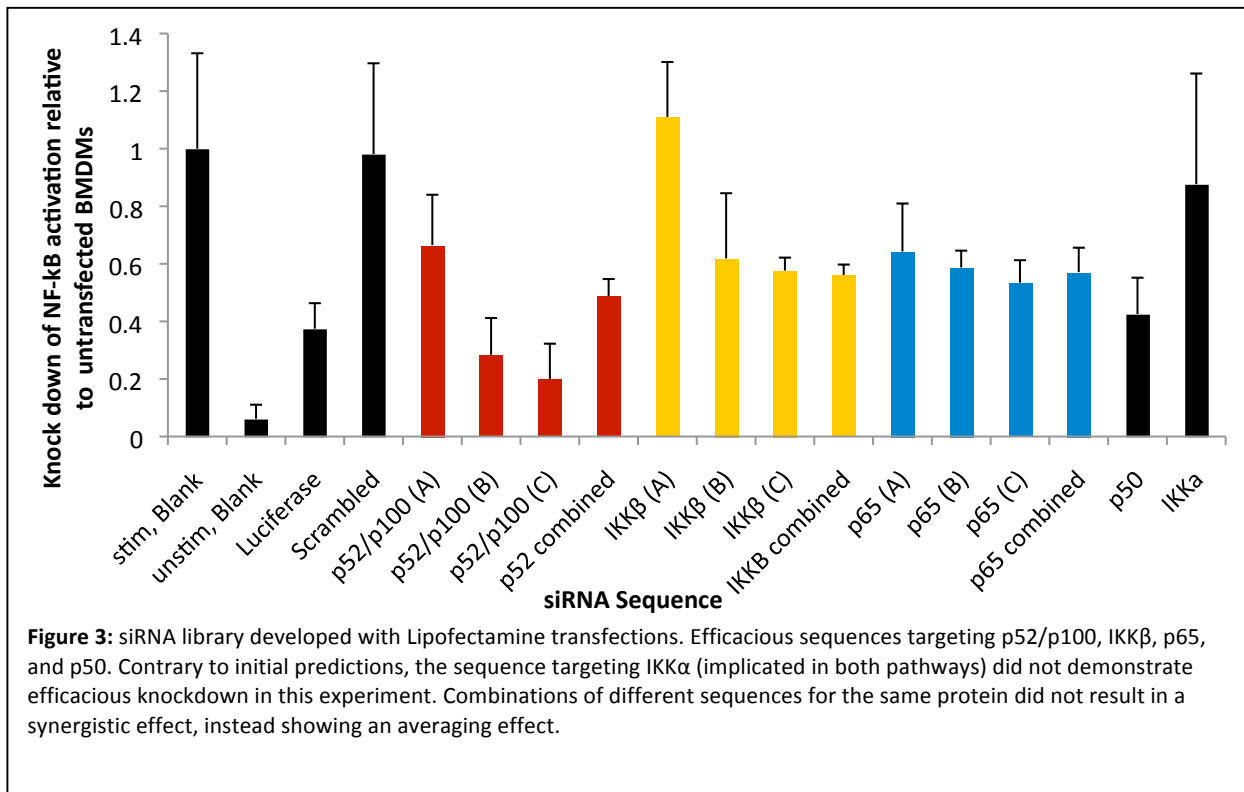
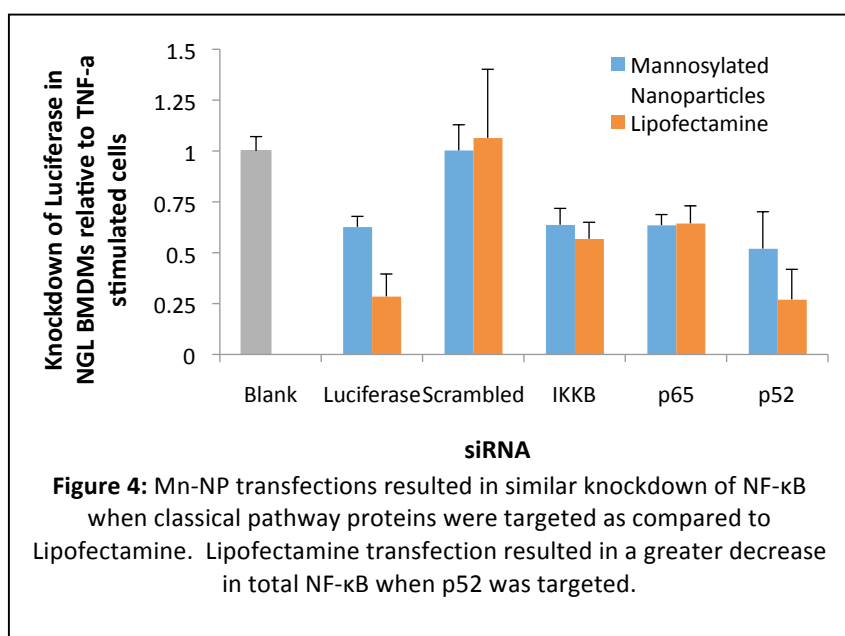


Figure 3: siRNA library developed with Lipofectamine transfections. Efficacious sequences targeting p52/p100, IKK β , p65, and p50. Contrary to initial predictions, the sequence targeting IKK α (implicated in both pathways) did not demonstrate efficacious knockdown in this experiment. Combinations of different sequences for the same protein did not result in a synergistic effect, instead showing an averaging effect.

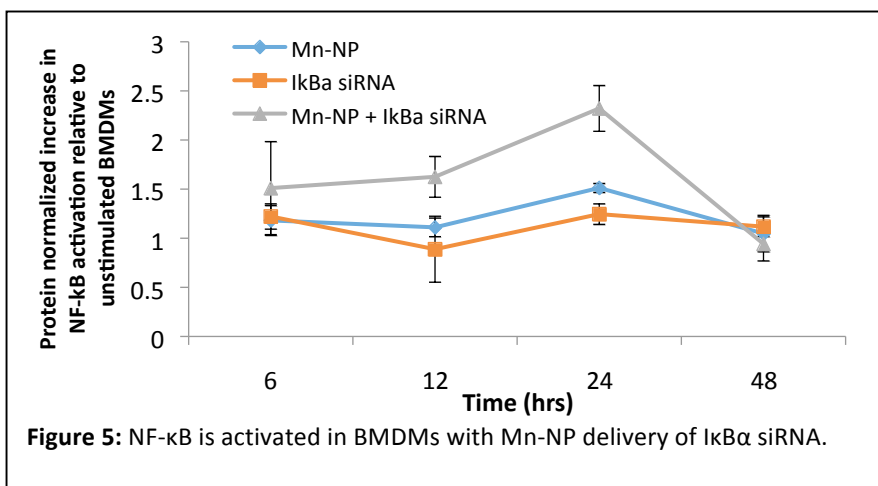
We are currently in the process of repeating the above transfection experiments and isolating cell mRNA in order to perform an analysis of phenotypic changes associated with NF- κ B modulation in these macrophages.

Phenotypic changes will be correlated with established macrophage phenotypic paradigms (M1/M2). We have attempted to utilize combinations of siRNA sequences to knock down both pathways simultaneously, but have seen significant toxicity associated with this approach consistent with the role of NF- κ B in cell survival.



Having determined that the commercial agent Lipofectamine could be used as a positive control for transfection experiments, we proceeded to test the most efficacious NF- κ B siRNAs (**Figure 3**) in conjunction with nanoparticle delivery. In these experiments BMDMs were transfected for 18 hrs, followed by stimulation with TNF- α for 6 hrs. Transfections were performed on a cell rocker to introduce convective fluid motion with a rate of 10 rocks per minute. Under these conditions, the use of Mn-NPs resulted in significant total NF- κ B knockdown; in many cases comparable to that measured with the use of Lipofectamine (**Figure 4**).

In the previous annual reports from the Yull and Giorgio labs, it was shown that the initial NF- κ B target IKK2 may not have been an optimal target for manipulating the classical NF- κ B pathway as the mRNA for this protein was not upregulated to a large degree during pathway activation. We tested other targets for efficacy using more siRNA sequences (see Figures 3 and 4). One interesting result of experiments using Mn-NP to deliver siRNA against NF- κ B proteins to BMDMs is the observation that NF- κ B can be activated by using siRNA to knockdown the I κ B α classical inhibitor protein in these cells (**Figure 5**). When free siRNAs or empty Mn-NPs are incubated with BMDMs, there is no effect. However, when the two are combined, there is an increase in total NF- κ B activation as measured in NGL BMDMs dosed with the complexes for 24 hours. The Yull lab has recently shown that strategic activation of the classical pathway can result in a significantly decreased metastatic burden in a murine tail vein lung metastasis model [15]. This unexpected finding has suggested the concept of using Mn-NP delivered siRNA for I κ B α to specifically activate the classical pathway as a novel approach for manipulation of macrophage phenotype with the potential to produce macrophages capable of demonstrating direct and/or indirect tumor cytotoxicity. This new idea, while not proposed as part of the current funded work, has become the basis for several new grant proposals.



Milestone #1: The result of subtasks 1a-1c is the production of a material capable of quantitatively predictable uptake into BMDMs. The result of subtask 1d is the *in vitro* validation and dose-response behavior of siRNA

mediated knockdown of the canonical and alternative NF- κ B pathways alone and in combination. The interplay of the canonical and alternative NF- κ B pathways in modulating BMDM phenotype will be assessed. These methods serve as a baseline to quantitatively evaluate the novel approaches described in the subsequent specific aims.

Specific Aim 2. Optimize delivery and efficacy of siRNA-delivering nanoparticles to inhibit canonical and alternative NF- κ B, alone and in combination, in macrophages *in vivo*:

2a. Evaluate population distribution of nanoparticles associated with macrophages *in vivo* by flow cytometry. Use the mouse model of metastatic human breast cancer provided by the FVB mice, tail-vein-injected with PyVT mammary tumor cell lines. Macrophage phenotype (M1/M2) will be correlated with high and low particle delivery following flow cytometric cell sorting.

Sub-aim 2a was partially completed previously in the Giorgio and Yull labs (see BC102696 annual report 2012 for details). We are currently planning studies to improve upon previous experiments by altering dosing amount and timing and developing an efficacious flow cytometry panel for analysis of macrophage phenotype.

We have performed preliminary *in vivo* biocompatibility tests on the Mn-NP by looking for signs of liver and kidney damage in wild type FVB mice after repeated injections of Mn-NP. Mannosylated nanoparticles complexed with DNA at an N:P ratio of 4 were delivered to wild type FVB mice at a dose of 5 mg/kg once per day for 3 days via retro-orbital injection. Serum was collected from the mice 24 hours after the last injection and tested for aspartate transaminase (AST) and alanine transaminase (ALT) levels as a measure of liver toxicity and blood urea nitrogen (BUN) and creatinine levels as a measure of kidney toxicity. All blood tests were performed at the Vanderbilt Comparative Pathology core lab. The result of this study showed no significant liver or kidney toxicity associated with the dosing regimen used as seen in **table 1**.

	1	2	3	4	Average	stdev	normal range
ALT (U/L)	37	49	73	105	66	30	26-120
AST (U/L)	96	86	213	140	133.75	57.80643	69-191
BUN (mg/dL)	21	23	27	23	23.5	2.516611	19-34
CREAT (mg/dL)	0.4	0.3	0.3	0.4	0.35	0.057735	0.5-0.8

Table 1: Average blood serum measurements for liver and kidney damage in mice showed no significant toxicity in these organs in mice receiving a daily 5 mg/kg dose of Mn-NP_DNA complexes over the course of 3 days

2b. Using optimized nanoparticle dosage from tasks 1c and 1d, in combination with *in vivo* delivery results from task 2a, evaluate pharmacokinetics of nanoparticles in NGL-reporter mice with overt lung metastases generated by tail vein injection of Polyoma-derived breast cancer cells using *in vivo* fluorescence imaging. This system enables detection of host response during tumor progression with respect to NF- κ B activity. Use model to further optimize delivery strategy of nanoparticles in terms of dispersibility, accumulation in lung tissue, dose, and duration of treatment.

These studies are scheduled for the 3rd (extension) year of this multi-year project.

2c. Functional amendments to the nanoparticle design will be carried out based on *in vivo* pharmacokinetic results of task 2b. The specific changes will be dictated by *in vivo* performance, but may include adjustment of the surface functionalizations for improved biodistribution and/or altered siRNA content per particle to optimize dosing based on achievable administration volumes and frequencies.

Based on current *in vivo* and *in vitro* experiments, no significant changes to nanoparticle design are currently planned. However, work in the Giorgio lab, with help from Dr. Craig Duvall, has produced PEG shielded, proximity activated, folate-targeted endosomal escape particles. Briefly, these particles utilize a shape-engineered PEG layer for biological stealthing as well as a matrix metalloproteinase sensitive proximity activated folate molecule; a particle design that could be implemented with our mannosylated particles. For further information, see Appendix items 11 and 13 (pgs. 114-135, 138-151).

2d. *Using siRNA sequence from task 1d and optimized nanoparticle administration conditions (tasks 2a-2b), assess modulation of NF- κ B activity by luciferase assay and western blots of nuclear extracts from lung tissue containing overt lung metastases to determine translocation of p65 or p52 to the nucleus. In addition, in vivo imaging of reporter mice will determine if impact is sufficient to be significant in intact live animals. Determine effects on local macrophage populations by RT-PCR of RNA to quantify expression of target genes correlated with M1 (iNOS, MIP1- α , IL-12) or M2 (IL-10, CCL17, mannose receptor) phenotype.*

These studies are scheduled for the 3rd (extension) year of this multi-year project.

2e. *Isolate TAMs from lung tissue containing overt metastases using anti-CD11 antibody-mediated magnetic separation and assess NF- κ B activity by luciferase assay and westerns, and macrophage phenotype (M1/M2) by RT-PCR.*

The NF- κ B pathways are complex and regulate hundreds of genes in macrophages and respond to many different stimuli. In order to show efficacious macrophage phenotype manipulation in macrophages by nanoparticle delivered siRNA it is important to identify NF- κ B regulated gene targets that may contribute to a pro- or anti-tumor phenotype. To that end, we have isolated mRNA from murine macrophages that have up-regulated classical NF- κ B pathway activation, up-regulated alternative NF- κ B pathway activation, and also from primary mammary tumor associated macrophages. mRNA from these cells was delivered to the Vanderbilt Technologies for Advanced Genomics (VANTAGE) core facility for analysis. We intend to identify differences in gene activation between these three groups and identify which genes in the classical or alternative pathway could potentially contribute to a pro- or anti-tumor phenotype. This analysis will provide targets for quantitative RT-PCR analysis of macrophages transfected with siRNAs for different NF- κ B pathway proteins. Currently, alternative pathway samples and TAM samples are awaiting microarray hybridization and analysis. Preliminary analysis of classically activated samples indicates an increase in inflammatory cytokines such as CXCL9 and immune cell chemoattractants such as CCL8, and a decrease in redox regulating proteins such as CYP family proteins.

Milestone #2: The result of subtasks 2a-2d is *in vivo* testing of novel multifunctional nanomaterials capable of modulating NF- κ B locally at tumor sites and location reporting by fluorescence imaging. These aims include sufficient controls to enable preparation of a manuscript for peer-reviewed publication in a nanomedicine or immunology journal.

Specific Aim 3. Utilize siRNA-delivering nanoparticles to inhibit classical or alternative NF- κ B activity alone and in combination in macrophages and determine effects on tumor progression:

3a. *Optimize generation of PyVT:NGL double transgenics. We currently have breeding colonies of PyVT and NGL transgenics. We have previously generated homozygous NGL transgenics demonstrating the feasibility of this approach. Due to the pathology of the PyVT model, only heterozygous males are competent for breeding. We will generate a breeding colony of PyVT heterozygous:NGL homozygous mice to improve the efficiency of generating experimental animals.*

We have generated the necessary breeding colonies for the most efficient generation of experimental mice for the ongoing studies.

3b. Evaluate primary tumor response to treatment by measurement of tumor latency, weight, and size in two dimensions. Evaluate tumor response to treatment by immunohistochemical analysis of sections, including assessment of TAM populations (anti-F4/80 antibody), cell proliferation (Ki67 staining), and survival (TUNEL staining). Evaluate nanoparticle delivery by fluorescence microscopy of tumor sections.

We have performed a preliminary study to provide evidence that the nanoparticle formulations can deliver siRNA to macrophages in the context of primary mammary tumors. PyVT mice rapidly produce multifocal mammary adenocarcinomas together with secondary metastatic tumors in the lung by 12 weeks. PyVT mice in which a significant load of primary mammary tumors had developed were injected i.v. (retro-orbital) with mannosylated and non-mannosylated nanoparticle versions containing fluorescently labeled (FAM) siRNA. 24 hours after injection, mammary and liver tissue was harvested. Immunostaining of frozen sections demonstrated co-localization of delivered siRNA with CD206 (mannose receptor)-expressing cells in tumor sections (images in appendix). No overt liver damage was seen, in agreement with the blood chemistry presented above. This is in agreement with previously reported, flow cytometry analysis that demonstrated co-localization of delivered siRNA with tumor-associated F4/80⁺ cells. This data supports the feasibility of targeted delivery of specific siRNAs into tumor-associated macrophages.

Additionally, we have begun *ex vivo* experiments using murine mammary tumor associated macrophages (TAMs) in order to show efficacy of siRNA delivery in a cell type relevant to the *in vivo* target cell. TAMs were isolated from the mammary tumors of mice bearing the polyoma middle T oncogene (PyVT) targeted to the mammary epithelium by a 60 minute rapid adhesion protocol and plated in 12 well plates. The rapid adhesion protocol allows us to isolate primary macrophages from a mixed single-cell suspension using inherent characteristics of macrophages rather than modifying the cells and isolating them based on that modification. FAM labeled scrambled siRNA was delivered to the cells either (1) in free form, (2) with Lipofectamine, a(3) with Mn-NP or (4) with alcohol terminated nanoparticles (OH-NP).

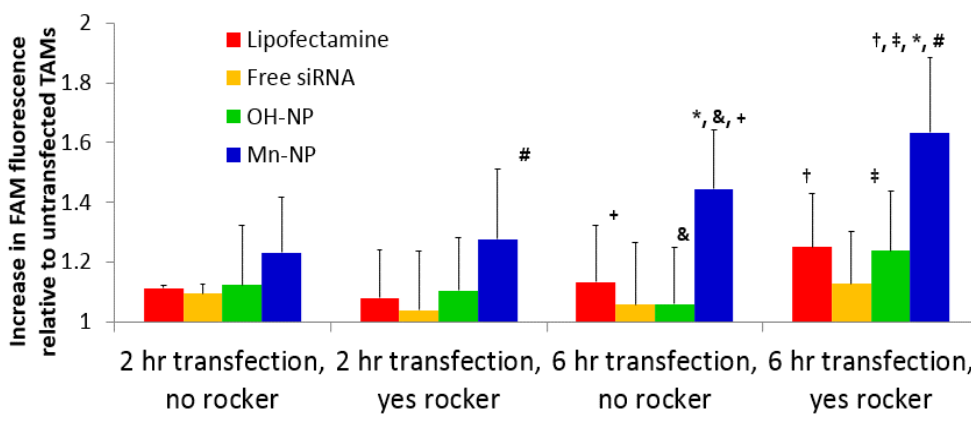


Figure 6: Delivery of FAM labeled siRNA to TAMs with different transfection agents under differing transfection conditions.

transfection times were used and TAMs were transfected both with and without fluid motion in the wells. Fluid motion was created with a cell rocker installed in the incubator, rocking at a rate of approximately ten rocks per minute. Following transfection, cells were washed with PBS to remove any non-uptaken siRNA and particles. FAM fluorescence was then measured, as an indication of uptake, using a Tecan Infinite M1000 Pro plate reader. The Mn-NP treatment resulted in the most FAM fluorescence under all conditions (**Figure 6**). This effect was more pronounced with the longer transfection time and with fluid motion in the well. Previous work by the Giorgio lab has shown that convective fluid flow increases delivery of nucleotide containing transfection

agents to cells. The Mn-NP treatment resulted in the most FAM fluorescence under all conditions (**Figure 6**). This effect was more pronounced with the longer transfection time and with fluid motion in the well. Previous work by the Giorgio lab has shown that convective fluid flow increases delivery of nucleotide containing transfection

particles, and it is expected that this effect is more pronounced in particles targeting an endosomal receptor such as the mannose receptor.

Together, these data indicate that Mn-NP's are effective in delivering siRNA to tumor associated macrophges both in a culture setting (when cells are isolated from primary Polyoma mammary tumors and treated ex vivo) and *in vivo* when particles are delivered systemically. We are currently performing a series of *in vivo* experiments designed to test mannosylated nanoparticle targeting in a PyVT mouse mammary tumor model. Fluorescently labeled nucleotides are complexed with the nanoparticles and then delivered to the spontaneously generated mammary tumors. After 3 days of daily, 5 mg/kg doses, the tumors are digested to a single cell suspension and the macrophages are isolated by a 30 minute rapid adhesion protocol. The cells are then analyzed for total internalized fluorescence. Preliminary data indicates that injection of the mannosylated particle-fluorescent nucleotide complex results in more internalized fluorescense in TAMs than injection of free nucleotides.

3c. Evaluate tumor response to treatment by macrometastasis count on lung tissue. Evaluate micrometastases and tumor response to treatment by immunohistochemical analysis of lung tissue sections, including assessment of TAM populations (anti-F4/80 antibody), cell proliferation (Ki67), survival (TUNEL), matrix remodeling (MMP-9 and MMP-12 zymography) and angiogenesis (vWF, VEGF staining). Evaluate nanoparticle delivery by fluorescence microscopy of lung tissue sections.

These studies are scheduled for the 3rd (extension) year of this multi-year project.

3d. Establish correlations among nanoparticle delivery, NF- κ B activity, TAM phenotype, and tumor response to treatment.

These studies are scheduled for the 3rd (extension) year of this multi-year project.

Milestone #3: The results from Specific Aim 3 include localized modulation of NF- κ B activity and TAM phenotype *in vivo* and correlation of the modulated phenotype with primary and metastatic tumor characteristics. These results will be reported as a peer-reviewed paper in a high-impact breast cancer journal.

Key Research Accomplishments

During this Reporting Period:

1. We have maintained a highly collaborative and scientifically integrated partnership. We continue to have regular combined group meetings and Ryan Ortega (predoctoral student) represents a direct link between the two groups. This collaborative study is proving educational for members of both research teams and we have developed a shared interest in the progress and outcome of these studies. Several grants that would continue this collaboration have been submitted in order to carry on this work.
2. We have confirmed the biocompatibility of the nanomaterials both *in vitro* and *in vivo*. The mannosylated nanoparticles are biocompatible with cells at high doses for extended periods of time and are biocompatible in a murine model at doses as high as 5 mg/kg with repeated dosing.
3. We have identified a small library of siRNA sequences that are effective at knocking down NF- κ B activation in bone marrow derived macrophages. The most promising of these sequences will be used in the *in vivo* aims of this work.
4. We have shown the highly novel result that it is possible to manipulate the NF- κ B pathways in an unpredicted fashion: namely activation of the classical pathway by knocking down an inhibitor protein using nanoparticle delivered siRNA. This mechanism of NF- κ B manipulation shows high therapeutic potential and merits further investigation
5. We have compared the mannosylated nanoparticles to a commercial agent in an *in vitro* test for siRNA delivery and total NF- κ B knockdown. The nanoparticle exhibited total NF- κ B knockdown similar to the commercial agent with the added benefit of high biocompatibility.
6. We have isolated mRNA samples from TAMs, classical NF- κ B up-regulated macrophages, and alternative NF- κ B unregulated macrophages. The mRNA will be used to analyze phenotypic differences and similarities between these cell populations
7. We have become proficient in a macrophage isolation protocol that utilizes the rapidly adhesive properties of macrophages to isolate primary macrophages from whole tissue samples. This methodology allows us to isolate these cells without external modification.
8. We have shown that the mannosylated particles are capable of transfecting TAMs more effectively than untargeted, OH- terminated nanoparticles in an *ex vivo* cell culture of mammary TAMs.
9. We continue to maintain colonies of NGL and PyVT transgenic mice.

Reportable Outcomes

Manuscripts, Abstracts, Presentations

1. Ortega RA, Barham W, Tikhomirov O, Kumar B, Yull FE, Giorgio TD: A Targeted Endosomal Nanoparticle for Engineering Tumor Immunity in Macrophages. Biomedical Engineering Society Annual Meeting. Seattle, WA, September 2013. {accepted abstract; poster to be presented September 2013} **[abstract on appendix page 21]**
2. Ortega RA, Barham W, Kumar B, Yull FE, Giorgio TD: Investigating the Effects of NF-κB Pathway Modulation in Macrophages using Modular Endosomal Escape Nanoparticles. Cancer Immunotherapy annual meeting. Mainz, Germany, May 2013. {accepted abstract and poster presentation} **[abstract on appendix page 22; poster on appendix page 23]**
3. Yu SS, Lau CM, Barham W, Nelson CE, Li H, Smith CA, Yull FE, Duvall CL, Giorgio TD: Targeting Tumor-Associated Macrophages for Immunotherapy via RNA Interference using Smart, Environmentally-Responsive Nanoparticles. Cancer Immunotherapy annual meeting. Mainz, Germany, May 2013. {accepted abstract and podium talk} **[abstract on appendix page 24; presentation on appendix pages 25-41]**
4. Ortega RA, Barham W, Kumar B, Yu SS, Yull FE, Giorgio TD: Reprogramming Tumor Associated Macrophages toward an Anti-Tumor Phenotype by Targeting the NF-κB Pathway Using Novel Targeted Nanotherapeutics. American Association for Cancer Research annual meeting. Washington, D.C., April 2013. {accepted abstract and poster presentation} **[abstract on appendix page 42; poster on appendix page 43]**
5. Barham W, Tikhomirov O, Chen L, Ortega RA, Gleaves L, Onishko H, Sherrill T, Yu S, Connelly L, Giorgio TD, Blackwell TS, Yull FE: Education of macrophages through modulation of NF-kappaB: an opportunity for targeted therapy. American Association for Cancer Research annual meeting. Washington, D.C., April 2013. {accepted abstract and poster presentation} **[abstract on appendix page 44; poster on appendix page 45]**
6. Giorgio TD: Biofunctional nanomaterials for the modulation of macrophage phenotype and polarization. University of Minnesota Department of Biomedical Engineering Invited talk. Minneapolis, MN, April 2013. {invited podium talk} **[presentation on appendix pages 46-70]**
7. Ortega RA, Barham W, Kumar B, Yull FE, Giorgio TD: Modular, Endosomal-Escape Nanoparticles for the Delivery of Therapeutic Agents to Tumor Associated Macrophages. Tennessee Biomaterials Day annual meeting. Nashville, TN, March 2013. {accepted abstract and podium talk} **[abstract on appendix page 71; presentation on appendix pages 72-77]**
8. Yull FE: Macrophage targeting in Benign and Malignant Disease. Vanderbilt University Department of Medicine's Dinner and Data meeting. Nashville, TN, March 2013. {invited podium talk} **[presentation on appendix pages 78-86]**
9. Giorgio TD: Nanostructure Design for Modulation of Inflammation. Vanderbilt University Department of Medicine's Dinner and Data meeting. Nashville, TN, March 2013. {invited podium talk} **[presentation on appendix pages 87-100]**

10. Yu SS, Lau CM, Barham WJ, Onishko HM, Nelson CE, Li H, Smith CA, Yull FE, Duvall CL and Giorgio TD: Macrophage-Specific RNA Interference Targeting via 'Click', Mannosylated Polymeric Micelles. Molecular Pharmaceutics. January 2013. {published scientific manuscript} **[manuscript on appendix pages 101-113]**
11. Li H, Duvall CL, Giorgio TD: Tissue specific, proximity-activated, folic acid dual targeting polymeric nanoparticles for siRNA drug carrier. Invention disclosure form to begin patent process. **[invention disclosure form on appendix pages 114-135]**
12. Ortega RA, Barham W, Kumar B, Yull, FE, Giorgio TD: Manipulation of the NF- κ B Pathway in Macrophages Using Targeted Nanotherapeutics to Achieve an Anti-Tumor Phenotype. Host-Tumor Interactions Program & Department of Cancer Biology 12th Annual Joint Retreat. Nashville, TN, November 2012. {accepted abstract and poster presentation} **[abstract on appendix page 136; poster on appendix page 137]**
13. Li H, Miteva M, Cheng MJ, Giorgio TD, Duvall CL: Dual MMP-7-Proximity-Activated and Folate Targeted Nanoparticles for siRNA Delivery. Biomedical Engineering Society Annual Meeting. Atlanta, GA, October 2012. {accepted abstract and podium talk} **[abstract on appendix page 138; presentation on appendix pages 139-151]**
14. Yu SS, Lau CM, Barham WJ, Nelson CE, Yull FE, Duvall CL, and Giorgio TD: Achieving Cancer Immunotherapy Through RNAi Interference in Tumor-Associated Macrophages via 'Click', Mannosylated Polymeric Nanoparticles. Biomedical Engineering Society Annual Meeting. Atlanta, GA, October 2012. {accepted abstract and podium talk; *winner of the 2012 Design and Research Awards from the Biomedical Engineering Society*} **[abstract on appendix page 152; presentation on appendix pages 153-189]**
15. Ortega RA, Kumar B, Yu SS, Yull FE, Giorgio TD: Targeted Knockdown of NF- κ B in Tumor Associated Macrophages. Biomedical Engineering Society Annual Meeting. Atlanta, GA, October 2012. {accepted abstract and poster presentation} **[abstract on appendix page 190; poster on appendix page 191]**
16. Barham W, Chen L, Onishko H, Tikhomirov O, Sherrill T, Ortega RA, Connelly L, Blackwell TS, and Yull FE: Education of macrophages through modulation of NF- κ B: an opportunity for targeted therapy. MD Anderson Symposium on Cancer Research. Houston, TX, September 2012. {accepted abstract and podium talk} **[abstract on appendix page 192; presentation on appendix pages 193-202]**
17. Swartz MA, Lida N, Roberts EW, Sangaletti S, Wong MH, Yull FE, Coussens LM, DeClerk YA: Tumor microenvironment complexity: emerging roles in cancer therapy. Cancer Research. March 2012. {published scientific manuscript} **[manuscript on appendix pages 203-211]**
18. Yu SS, Lau CM, Thomas SN, Jerome WG, Maron DJ, Dickerson JH, Hubbell JA, Giorgio TD: Size- and charge-dependent non-specific uptake of PEGylated nanoparticles by macrophages. International Journal of Nanomedicine. February 2012. {published scientific manuscript} **[manuscript on appendix pages 212-226]**

Funding applied for based on work supported by this award

1. Fiona Yull. **Targeted activation of macrophages as breast cancer therapy.** NIH, NCI R01 application, submitted October 2012; re-submitted July 2013.
2. Fiona Yull. **Induction of tumoricidal tumor-associated macrophages as lung cancer therapy.** NIH, NCI R21 application, submitted June 2013.
3. Fiona Yull. **Generation of cytotoxic tumor-associated macrophages by nanoparticle-mediated siRNA delivery as lung cancer therapy.** Department of Defense Lung Cancer Research Program (LCRP) Idea Development Award application, submitted June 2013.
4. Fiona Yull and Todd D. Giorgio. **Nanoparticle-mediated siRNA delivery to tumor-associated macrophages as metastatic breast cancer therapy.** Department of Defense Breast Cancer Research Program (BCRP) Breakthrough Award pre-application, submitted June 2013.

Employment or research opportunities applied for and/or received based on experience/training supported by this award

1. Lianyi Chen, a research assistant in Fiona Yull's laboratory was partially supported by this award. She gained experience in managing transgenic mouse colonies and in molecular techniques for the analysis of both cell lines and mouse tissue through working on the funded studies. As a result of this experience, she was recently able to secure a position in the Department of Anesthesiology at Vanderbilt, and was promoted to Research Assistant II.
2. Undergraduate student Cheryl Lau applied to the Graduate School of Georgia Tech based citing research experience gained while working on this project. She was accepted into the Graduate School of Georgia Tech in 2012.
3. Graduate Student and Doctoral Candidate Ryan Ortega (supported by this award) developed a PhD thesis proposal based on work completed on and experience received from this project. His proposal was accepted by his committee of advisors and by the Graduate School of Vanderbilt University in May, 2013. **[thesis proposal on abstract pages 227-260; thesis presentation on abstract pages 261-281]**
4. Former Graduate Student and current PhD, Shann Yu, obtained his PhD based on work accomplished for this project. He applied for and received a post-doctoral position at the Laboratory of Lymphatic and Cancer Bioengineering at the Ecole Polytechnique Federale de Lausanne in Lausanne, Switzerland based on experience gained while funded by this grant.

Conclusions

The ***hypothesis*** to be tested in these studies is that siRNA-mediated inhibition of NF- κ B signaling in TAMs will decrease primary tumor growth and metastatic potential. Our ***objectives*** are (1) exploration of macrophage response to inhibition of NF- κ B activation by the classical and alternative pathways, separately and in combination using siRNA knockdown *in vitro* and (2) development of a nanobiotechnology delivery vehicle with the capacity for siRNA delivery TAMs for the purpose of pathway-specific NF- κ B manipulation *in vivo*.

In order to reach our ultimate goal of testing the efficacy of this approach in *in vivo* tumor models three major milestones will need to be reached; 1) synthesis and development of the nanoparticles (published), 2) selection of appropriate siRNA (completed), 3) optimization of delivery of nanoparticles (initial *in vivo* treatment has proved not to be toxic via i.v. route and to deliver with some specificity to a population of macrophages in both primary tumor and lung metastases).

In vitro testing of the mannosylated carrier has shown these materials capable of efficaciously delivering siRNA into macrophages and altering the NF- κ B pathway. We have reported the unexpected result that targeted, acute activation of the classical pathway can be accomplished using siRNA to knock down an inhibitor protein and that this may provide a novel avenue for therapeutic NF- κ B manipulation in macrophages. *In vivo* testing is underway and no toxicity has been observed from the nanoparticles at large doses in murine models. With the addition of the no-cost extension year, we believe that we are “on track” to achieving our stated goal of performing an initial set of tumor response studies.

References

1. Mantovani, A., et al., *Macrophage polarization: tumor-associated macrophages as a paradigm for polarized M2 mononuclear phagocytes*. Trends Immunol, 2002. **23**:549-55.
2. Miselis, N.R., et al., *Targeting tumor-associated macrophages in an orthotopic murine model of diffuse malignant mesothelioma*. Mol Cancer Ther, 2008. **7**:788-99.
3. de Visser, K.E., A. Eichten, and L.M. Coussens, *Paradoxical roles of the immune system during cancer development*. Nat Rev Cancer, 2006. **6**:24-37.
4. Dirkx, A.E., et al., *Monocyte/macrophage infiltration in tumors: modulators of angiogenesis*. J Leukoc Biol, 2006. **80**:1183-96.
5. Murdoch, C., et al., *The role of myeloid cells in the promotion of tumour angiogenesis*. Nat Rev Cancer, 2008. **8**:618-31.
6. Pollard, J.W., *Macrophages define the invasive microenvironment in breast cancer*. J Leukoc Biol, 2008. **84**:623-30.
7. Stout, R.D., et al., *Macrophages sequentially change their functional phenotype in response to changes in microenvironmental influences*. J Immunol, 2005. **175**:342-9.
8. Watkins, S.K., et al., *IL-12 rapidly alters the functional profile of tumor-associated and tumor-infiltrating macrophages in vitro and in vivo*. J Immunol, 2007. **178**:1357-62.
9. Connelly L, Barham W, Onishko HM, Chen L, Sherrill T, Zabuwala T, Ostrowski MC, Blackwell TS, Yull FE. *NF-kappaB activation within macrophages leads to an anti-tumor phenotype in a mammary tumor lung metastasis model*. Breast Cancer Res. 2011; **13**:R83.
10. Cao, Y. and M. Karin, *NF-kappaB in mammary gland development and breast cancer*. J Mammary Gland Biol Neoplasia, 2003. **8**:215-23.
11. Eliopoulos, A.G., et al., *Epstein-Barr virus-encoded latent infection membrane protein 1 regulates the processing of p100 NF-kappaB2 to p52 via an IKKgamma/NEMO-independent signalling pathway*. Oncogene, 2003. **22**(48):7557-69.
12. Perkins, N.D., *Oncogenes, tumor suppressors and p52 NF-kappaB*. Oncogene, 2003. **22**:7553-6.
13. Romieu-Mourez, R., et al., *Roles of IKK kinases and protein kinase CK2 in activation of nuclear factor-kappaB in breast cancer*. Cancer Research, 2001. **61**:3810-8.
14. Yu. S. S., et al. *Macrophage-Specific RNA Interference Targeting via “Click: Mannosylated Polymeric Micelles*. Molecular Pharmaceutics. 2013. **10**(3): 975-987.
15. Connelly, L. et al. *NF-kappaB activation within macrophages leads to an anti-tumor phenotype in a mammary tumor lung metastasis model*. Breast Cancer Res **13**, R83

Appendices

Appendix materials start with Biographical Sketches for the PIs (Giorgio, Todd D. and Yull, Fiona E.) and the other major personnel contributing to this research effort during the award period (July 2012-July 2013)

1. Giorgio, Todd D., Biographical Sketch **[appendix pages 1-4]**
2. Yull, Fiona E., Biographical Sketch **[appendix pages 5-8]**
3. Barham, Whitney J., Biographical Sketch **[appendix page 9]**
4. Chen, Lianyi, Biographical Sketch **[appendix page 10]**
5. Ortega, Ryan A., Biographical Sketch **[appendix pages 11-13]**
6. Tikhomirov, Oleg Y., Biographical Sketch **[appendix pages 14-16]**
7. Yu, Shann S., Biographical Sketch **[appendix pages 17-20]**

Following Biographical Sketches, each item identified as a ‘reportable outcome’ for this project is included in appendices. The appendix materials appear in inverse chronological order (newest first) in agreement with the order shown as ‘reportable outcomes’ and identified below:

Manuscripts, Abstracts, Presentations

8. Ortega RA, Barham W, Tikhomirov O, Kumar B, Yull FE, Giorgio TD: A Targeted Endosomalytic Nanoparticle for Engineering Tumor Immunity in Macrophages. Biomedical Engineering Society Annual Meeting. Seattle, WA, September 2013. {accepted abstract; poster to be presented September 2013} **[abstract on appendix page 21]**
9. Ortega RA, Barham W, Kumar B, Yull FE, Giorgio TD: Investigating the Effects of NF-κB Pathway Modulation in Macrophages using Modular Endosomal Escape Nanoparticles. Cancer Immunotherapy annual meeting. Mainz, Germany, May 2013. {accepted abstract and poster presentation} **[abstract on appendix page 22; poster on appendix page 23]**
10. Yu SS, Lau CM, Barham W, Nelson CE, Li H, Smith CA, Yull FE, Duvall CL, Giorgio TD: Targeting Tumor-Associated Macrophages for Immunotherapy via RNA Interference using Smart, Environmentally-Responsive Nanoparticles. Cancer Immunotherapy annual meeting. Mainz, Germany, May 2013. {accepted abstract and podium talk} **[abstract on appendix page 24; presentation on appendix pages 25-41]**
11. Ortega RA, Barham W, Kumar B, Yu SS, Yull FE, Giorgio TD: Reprogramming Tumor Associated Macrophages toward an Anti-Tumor Phenotype by Targeting the NF-κB Pathway Using Novel Targeted Nanotherapeutics. American Association for Cancer Research annual meeting. Washington, D.C., April 2013. {accepted abstract and poster presentation} **[abstract on appendix page 42; poster on appendix page 43]**
12. Barham W, Tikhomirov O, Chen L, Ortega RA, Gleaves L, Onishko H, Sherrill T, Yu S, Connelly L, Giorgio TD, Blackwell TS, Yull FE: Education of macrophages through modulation of NF-kappaB: an opportunity for targeted therapy. American Association for Cancer Research annual meeting. Washington, D.C., April 2013. {accepted abstract and poster presentation} **[abstract on appendix page 44; poster on appendix page 45]**

13. Giorgio TD: Biofunctional nanomaterials for the modulation of macrophage phenotype and polarization. University of Minnesota Department of Biomedical Engineering Invited talk. Minneapolis, MN, April 2013. {invited podium talk} **[presentation on appendix pages 46-70]**
14. Ortega RA, Barham W, Kumar B, Yull FE, Giorgio TD: Modular, Endosomal-Escape Nanoparticles for the Delivery of Therapeutic Agents to Tumor Associated Macrophages. Tennessee Biomaterials Day annual meeting. Nashville, TN, March 2013. {accepted abstract and podium talk} **[abstract on appendix page 71; presentation on appendix pages 72-77]**
15. Yull FE: Macrophage targeting in Benign and Malignant Disease. Vanderbilt University Department of Medicine's Dinner and Data meeting. Nashville, TN, March 2013. {invited podium talk} **[presentation on appendix pages 78-86]**
16. Giorgio TD: Nanostructure Design for Modulation of Inflammation. Vanderbilt University Department of Medicine's Dinner and Data meeting. Nashville, TN, March 2013. {invited podium talk} **[presentation on appendix pages 87-100]**
17. Yu SS, Lau CM, Barham WJ, Onishko HM, Nelson CE, Li H, Smith CA, Yull FE, Duvall CL and Giorgio TD: Macrophage-Specific RNA Interference Targeting via 'Click', Mannosylated Polymeric Micelles. Molecular Pharmaceutics. January 2013. {published scientific manuscript} **[manuscript on appendix pages 101-113]**
18. Li H, Duvall CL, Giorgio TD: Tissue specific, proximity-activated, folic acid dual targeting polymeric nanoparticles for siRNA drug carrier. Invention disclosure form to begin patent process. **[invention disclosure form on appendix pages 114-135]**
19. Ortega RA, Barham W, Kumar B, Yull, FE, Giorgio TD: Manipulation of the NF-κB Pathway in Macrophages Using Targeted Nanotherapeutics to Achieve an Anti-Tumor Phenotype. Host-Tumor Interactions Program & Department of Cancer Biology 12th Annual Joint Retreat. Nashville, TN, November 2012. {accepted abstract and poster presentation} **[abstract on appendix page 136; poster on appendix page 137]**
20. Li H, Miteva M, Cheng MJ, Giorgio TD, Duvall CL: Dual MMP-7-Proximity-Activated and Folate Targeted Nanoparticles for siRNA Delivery. Biomedical Engineering Society Annual Meeting. Atlanta, GA, October 2012. {accepted abstract and podium talk} **[abstract on appendix page 138; presentation on appendix pages 139-151]**
21. Yu SS, Lau CM, Barham WJ, Nelson CE, Yull FE, Duvall CL, and Giorgio TD: Achieving Cancer Immunotherapy Through RNAi Interference in Tumor-Associated Macrophages via 'Click', Mannosylated Polymeric Nanoparticles. Biomedical Engineering Society Annual Meeting. Atlanta, GA, October 2012. {accepted abstract and podium talk; *winner of the 2012 Design and Research Awards from the Biomedical Engineering Society*} **[abstract on appendix page 152; presentation on appendix pages 153-189]**
22. Ortega RA, Kumar B, Yu SS, Yull FE, Giorgio TD: Targeted Knockdown of NF-kB in Tumor Associated Macrophages. Biomedical Engineering Society Annual Meeting. Atlanta, GA, October 2012. {accepted abstract and poster presentation} **[abstract on appendix page 190; poster on appendix page 191]**

23. Barham W, Chen L, Onishko H, Tikhomirov O, Sherrill T, Ortega RA, Connelly L, Blackwell TS, and Yull FE: Education of macrophages through modulation of NF-κB: an opportunity for targeted therapy. MD Anderson Symposium on Cancer Research. Houston, TX, September 2012. {accepted abstract and podium talk} **[abstract on appendix page 192; presentation on appendix pages 193-202]**
24. Swartz MA, Lida N, Roberts EW, Sangaletti S, Wong MH, Yull FE, Coussens LM, DeClerk YA: Tumor microenvironment complexity: emerging roles in cancer therapy. Cancer Research. March 2012. {published scientific manuscript} **[manuscript on appendix pages 203-211]**
25. Yu SS, Lau CM, Thomas SN, Jerome WG, Maron DJ, Dickerson JH, Hubbell JA, Giorgio TD: Size- and charge-dependent non-specific uptake of PEGylated nanoparticles by macrophages. International Journal of Nanomedicine. February 2012. {published scientific manuscript} **[manuscript on appendix pages 212-226]**

Employment or research opportunities applied for and/or received based on experience/training supported by this award

26. Graduate Student and Doctoral Candidate Ryan Ortega (supported by this award) developed a PhD thesis proposal based on work completed on and experience received from this project. His proposal was accepted by his committee of advisors and by the Graduate School of Vanderbilt University in May, 2013. **[thesis proposal on abstract pages 227-260; thesis presentation on abstract pages 261-281]**

BIOGRAPHICAL SKETCH

ÓÖWÔŒV/ØPØVÜŒDΦÖÄ(Begin with baccalaureate or other initial professional education, such as nursing, include postdoctoral training and residency training if applicable.)Ä

ΦÙVØWØVØPØ Á ØÆSU ØCØVØPØ	ØØÙØØA (if applicable)	T T ÙÙYÁ	ØØSØÁØÙVØYÁ
Á S̄ @ { ÁW } Á@{ · Á EÓ@{ @ { EÚOA	Á ÓÙÙA	Á E ÙGÁ	Á Ø@{ Á@{ Á } * Á Á@{ Á@{ Á } * Á
Á Ü ÁN } Á@{ · Á EAP [^ • d } EAVYÁ	Á ÚØØA	Á FFÙ Ù Á	Á Ø@{ Á@{ Á } * Á Á@{ Á@{ Á } * Á
Á	Á	Á	Á

A. Personal Statement

B. Positions and Honors

Positions and Employment

Honors

C. Selected Peer-reviewed Publications (in reverse chrono order; from a total of 57)

ÚÍ[*] ÁS AÖä^&d; HÚíä &d; ÁKQç^• ZÉS ÁSæ dÁo• dÁT ÁSå^&d; Á

|ʌ| |çæ| ð| cæs̥ɪ^*| æ̥æ̥| } Á| Á| ð| C| [| j̥ | ^| ð| [| •| | å| ^| å| [| ^| { | | | å| &æ| | å| | ð|

Ó&{ æ&{ { { |& |• AGEFFÆGÆHÍ ÆHÍ ÆA{ æFEEFGFA{ GEFHG \ EAUT ØKGEGTÍ H JÁ

D. Research Support

Ongoing Research Support

DE^} & KÄÖ^] æd^ ^} d^ ÄÖ^A} •^A
i GEÄ@^ a^! Äüd^A
d^ | ÄÖ^d^ ÄT ÖÄGFI EGFI Ä
Ö^ } d^d^ * ÄU~ä^! KÄY ^} ä^ ÄÖZÖa^! Ä
E^•^•^ { ^} d^ ÄP@^ [ä^! & @ [|| *^ E^@^ *^ c^äÄ üpÖÄ^•^ ä} ^äÄ[ÄQ @^äÄ ÖS@^] ÄÖÄ|æ•^d^ Ä
D^F^ } ä^ä^ ÄU^ } ä^ * ÄÖ^A^ æ d^V^ { [!ÄT ä^! [] @^ ^•^ä^
Ü! ä^ ä^ ÄQç^•^ d^ ä^! KÄV[ääÄÖZÖä! *^ Ä
Ü[|^ KÄU; ä^ ä^ ÄQç^•^ d^ ä^! Ä
F^ E^ Ä A^ } ^ ä^A- { !Ä
Ü! ä^ ä^ KR | ÄEGERFER } ^ ÄEGERFI Ä
Ä

The research focuses on developing smart nanomaterials to modulate breast cancer development and progression through inhibition of NF- κ B mediated macrophage activation. Both the classical and alternative NF- κ B pathways will be modulated, individually and together. The novel delivery system enables *in vivo* use of this powerful approach. No overlap with the current application.

The research focuses on the translation of new molecular targeting approaches for the delivery of chemotherapies and gene therapies as treatments for multidrug resistant metastatic breast cancer. No overlap with the current application.

DE^} & KÁK& å^|à&ÓW ã^|• ÁO& [ç^| ^ ÁO|& Ó|[*|& Á
FÉ| ÁS| |& áP&| Á
Pæ @é|^ÉV|P ÁH| G €Á
Ó[} d&c| * ÁU ~Å| KÓ|á å^|c@Ó|& å|& å|& å|
+|^&c|^ Á@{| { æ| Á|a|æ| } Á| Á| || |^&c| Á| { [| Á| ^|| Á| ^ Á| ^ |c| } &c| } & Á| |^| { |^|& Á| @| Á| | • Á
Ú| å| &| æ|Q|ç| • c| æ| KÁ| å|å| Á| Ó| Ó| |*| å| Á
Ü| | KÓ|ç| • c| æ| I| €| Á| DA
Ú| å| KÁ| æ| Á| F| E| G| G| Á| } ^| Á| E| G| F| H| Á

This pilot project will test the feasibility of local thermal ablation of tissues in direct contact with a mucoadhesive thin film containing nanophotonic materials and deployed during endoscopy. No overlap with the current application.

OE^} & KAX& å^|à^|å^|Qææ^|A ÁU^|*|^|A å^|Å^} * å ^|ä^|ä^|A
E^|E@ @^|E^|Å^|æ^|@^|A^|A^|c^|A^|å^|Å^|à^|c^|d^|B^|A^|*|^|ä^|A
Ú|ä^|ä^|æ^|Q^|ç^|c^|æ^|KX&*|A å^|Å^|} • æ^|} ^|A
Ü| |KÖ| EÜ|ä^|æ^|Q^|ç^|c^|æ^|LÄ
Ú|ä^|å^|k^|F^|T^|æ^|A^|G^|F^|G^|A^|H^|A^|d^| à^|A^|G^|F^|H^|A

BIOGRAPHICAL SKETCH

Provide the following information for the Senior/key personnel and other significant contributors in the order listed on Form Page 2.
Follow this format for each person. **DO NOT EXCEED FOUR PAGES.**

NAME Yull, Fiona Elizabeth, D.Phil.	POSITION TITLE Associate Professor of Cancer Biology		
ERA COMMONS USER NAME (credential, e.g., agency login) FIONA_YULL			
EDUCATION/TRAINING (<i>Begin with baccalaureate or other initial professional education, such as nursing, include postdoctoral training and residency training if applicable.</i>)			
INSTITUTION AND LOCATION	DEGREE (if applicable)	MM/YY	FIELD OF STUDY
University of St. Andrews, St. Andrews, UK	B.Sc. (Hons)	1985	Biochemistry w/Microbiology
University of Oxford, Oxford, U.K.	D.Phil.	1989	Biochemistry

A. Personal Statement

I have a longstanding 21-year experience with the design, generation and characterization of multi-mutation transgenic and knockout mice. My group develops murine models to investigate the role of the NF-κB family of transcription factors in disease, particularly cancer. We have successfully used these in a large number of collaborative studies relating to the contribution of NF-κB signaling in several types of cancer including lung, breast, prostate and skin. My main interests have been on mammary cancer progression from primary tumor, through metastasis in the circulation to the establishment of final metastatic tumors in a secondary site and on how inflammation contributes to lung cancer. To address the roles of NF-κB in these processes we have developed a modular inducible “tool kit” of transgenics. These enable up and down-regulation of NF-κB signaling directed to specific cell types (mammary epithelium, macrophages and lung epithelium) providing the opportunity to address the roles of NF-κB in specific cells in the tumor microenvironment and defined stages of progression. Given the potential for macrophages to play a critical role in cancer progression and our exciting preliminary data, I now plan to investigate methodologies to modulate NF-kappaB signaling specifically within macrophages to define new therapeutic approaches.

B. Positions and Honors

Positions and Employment

- 1985-1989 Predoctoral Fellow under the direction of Drs. A. and S. Kingsman, Oxford University, UK
- 1989-1995 Postdoctoral Fellow under the direction of Dr. J. Clark, The Roslin Institute, Roslin, Edinburgh, UK
- 1995-1998 Postdoctoral Fellow, Dept. of Microbiology and Immunology, under the direction of Dr. L. Kerr, Vanderbilt University Medical Center, Nashville, Tennessee
- 1998-1998 Research Instructor, Dept. of Cell Biology, working with Dr. L. Kerr, Vanderbilt University. Awarded US Army Breast Cancer Research Program Fellowship
- 1998-1999 Research Asst. Professor, Dept. of Cell Biology. Acting Principal Investigator during absence of Dr. L. Kerr on Robert Woods Johnson Fellowship in Washington. Awarded American Cancer Society Institutional Research Grant
- 2000-2004 Research Assistant Professor, Department of Cancer Biology, Vanderbilt University Medical Center, Nashville, Tennessee
- 2004-2010 Assistant Professor of Cancer Biology, Department of Cancer Biology, Vanderbilt University Medical Center, Nashville, Tennessee
- 2010-Pres. Associate Professor, Dept. of Cancer Biology, VUMC, Nashville, TN

Other Experience and Professional Memberships

- 2000-2007 Deputy Director, Department of Medicine PPG Core B
- 2003 Deputy Director of Cancer Biology Graduate Course
- 2004-2006 Reviewer for Susan G Komen Foundation Postdoctoral Fellowships
- 2004-Pres. Director of Cancer Biology Graduate Course

- 2007-Pres. Member of Research Safety Subcommittee
 2009-Pres. Member of Vanderbilt University IACUC Committee
 2010,11,13 Ad hoc member, DOD BCRP FY10 Programmatic Review Panel
 2011 Ad hoc reviewer NIH MESH study section
 2013 Ad hoc reviewer NIH SEP Cancer Health Disparities and Diversity in Basic Cancer Research
- 1986-Pres. Member of Society of General Microbiology
 1997-Pres. Member of Society of Developmental Biology
 1998-Pres. Member of American Association of Cancer Research

Honors

- 2000-2004 Aventis Leadership Development Program Fellow

C. Selected Peer-reviewed Publications (from 64 peer-reviewed publications)

1. Connelly L, Robinson-Benion C, Chont M, Saint-Jean L, Li H, Polosukhin VV, Blackwell TS, Yull FE, A transgenic model reveals important roles for the NF- κ B alternative pathway (p100/p52) in mammary development and links to tumorigenesis. *J Biol Chem.* 282: 10028-35, 2007. PMID: 17261585.
2. Stathopoulos GT, Sherrill TP, Cheng DS, Scoggins RM, Han W, Polosukhin VV, Connelly L, Vassiliou S, Karatza M, Yull FE, Fingleton B, Blackwell TS. Epithelial nuclear factor- κ B activation promotes urethane-induced lung carcinogenesis. *Proc Natl Acad Sci.* 104(47):18514-18519, 2007. PMCID: PMC2141808
3. Han W, Joo W, Everhart MB, Christman JW, Yull FE, Blackwell TS. Myeloid cells control termination of lung inflammation through the NF- κ B pathway. *Am J Physiol.: Lung Cell Mol Physiol.* 296(3): L320-7, 2009. PMCID: PMC2660215.
4. Yang J, Splittgerber R, Yull FE, Kantrow S, Ayers GD, Karin M, Richmond A. Conditional ablation of IKKB inhibits melanoma tumor development in mice. *J Clin Invest* 120:2563-74, 2010. PMCID: PMC2898608
5. Connelly, L., Barham, W., Pigg, R., Saint-Jean, L., Sherrill, T., Cheng, D-S., Chodosh, L.A., Blackwell, T.S. Yull FE. 2010. Activation of NF-kappaB in mammary epithelium promotes milk loss during mammary development and infection. *Journal of Cellular Physiology* 222:73-81. PMCID: PMC2783968.
6. Connelly L, Barham W, Onishko HM, Sherrill T, Chodosh LA, Blackwell TS, Yull FE. Inhibition of NF-kappaB activity in mammary epithelium increases tumor latency and decreases tumor burden. *Oncogene* 30:1402-12, 2010. PMCID: PMC3063854
7. Zaynagetdinov R, Stathopoulos GT, Sherrill TP, Cheng DS, McLoed AG, Ausborn JA, Polosukhin VV, Connelly L, Zhou W, Fingleton B, Peebles RS, Prince LS, Yull FE, Blackwell TS. Epithelial nuclear factor- κ B signaling promotes lung carcinogenesis via recruitment of regulatory T lymphocytes. *Oncogene*. 2011. PMID: 22002309.
8. Zaynagetdinov R, Sherrill TP, Polosukhin VV, Han W, Ausborn JA, McLoed AG, McMahon FB, Gleaves LA, Degryse AL, Stathopoulos GT, Yull FE, Blackwell TS. 2011. A critical role for macrophages in promotion of urethane-induced lung carcinogenesis. *J Immunol.* 187:5703-11. PMID: 22048774.
9. Karabela SP, Psallidas I, Sherrill TP, Kairi CA, Zaynagetdinov R, Cheng DS, Vassiliou S, McMahon F, Gleaves LA, Han W, Stathopoulos I, Zakynthinos SG, Yull FE, Roussos C, Kalomenidis I, Blackwell TS, Stathopoulos GT. Opposing effects of bortezomib-induced nuclear factor- κ B inhibition on chemical lung carcinogenesis. *Carcinogenesis*. 2012. PMID:22287559.
10. Blackwell, TS, Hipps, AN, Yamamoto, Y, Han, W, Barham, WJ, Ostrowski, MC, Yull, FE, Prince, LS. 2011. NF-kappaB Signaling in Fetal Lung Macrophages Disrupts Airway Morphogenesis. *J Immunol.* 187:2740-7. PMID: 21775686.
11. Connelly L, Barham W, Onishko HM, Chen L, Sherrill T, Zabuwala T, Ostrowski MC, Blackwell TS, Yull FE. NF-kappaB activation within macrophages leads to an anti-tumor phenotype in a mammary tumor lung metastasis model. *Breast Cancer Res.* 13:R83. 2011. PMID: 21884585.
12. Swartz MA, Iida N, Roberts EW, Sangaletti S, Wong MH, Yull FE, Coussens LM, Declerck YA. Tumor Microenvironment Complexity: Emerging Roles in Cancer Therapy. *Cancer Res.* 2012 PMID: 22414581.

13. Barham W, Sherrill T, Connelly L, Blackwell TS, Yull FE. Intraductal Injection of LPS as a Mouse Model of Mastitis: Signaling Visualized via an NF-κB Reporter Transgenic. *J Vis Exp.* (67). pii: 4030. 2012. PMID:22971993
14. Han W, Li H, Cai J, Gleaves LA, Polosukhin VV, Segal BH, Yull FE, Blackwell TS. 2013. NADPH Oxidase Limits Lipopolysaccharide-Induced Lung Inflammation and Injury in Mice through Reduction-Oxidation Regulation of NF-κB Activity. *J Immunol* 190:4786-94. PMID:23530143 PMCID: PMC3633681
15. Yu SS, Lau CM, Barham WJ, Onishko HM, Nelson CE, Li H, Smith CA, Yull FE, Duvall CL, Giorgio TD. Macrophage-Specific RNAi Targeting via 'Click', Mannosylated Polymeric Micelles. *Mol Pharm.* 2013 PMID:23331322 PMCID:PMC3595119

D. Research Support

Ongoing Research Support

W81XWH-11-1-0242 (Yull) 07/01/11-06/30/13 (No cost extension – 06/30/14)
 Department of Defense
 "Assessment of nanobiotechnology-Targeted siRNA Designed to Inhibit NF-kappaB Classical and Alternative signaling in Breast Tumor Macrophages"
 Goals are; 1) exploration of macrophage response to inhibition of NF-κB activation by the canonical and alternative pathways using siRNA *in vitro*, 2) develop nanobiotechnology delivery vehicle for specific delivery of siRNA to tumor associated macrophages *in vivo* to modulate NF-κB activity.

5 R01 HL 097195-02 (Prince) 09/14/09 - 07/31/14
 NIH/NHLBI

"Role of Fetal Lung Macrophages in Bronchopulmonary Dysplasia"
 Goal: This proposal tests the role of fetal lung macrophages in bronchopulmonary dysplasia pathogenesis. Specifically, we will test if macrophages are required for inhibition of normal lung development by innate immune stimuli, if NF-κB activation in macrophages mediates global fetal lung inflammation, and how early exposure of fetal lung macrophages to inflammatory stimuli alters macrophage phenotype as lungs mature.
 Aims: To identify the role of the NF-κB pathway in inhibition of lung development following innate immune activation. To determine if early activation of fetal lung macrophages alters the macrophage phenotype as lungs mature.

1 R01 HL 116358-01 (Blackwell/Prince, Co-PI's) 09/25/12 - 06/30/15
 NIH/NHLBI

Imaging Activated Macrophages in the Lungs
 Lung macrophages are critical for initiating the innate immune response to microbial and environmental stimuli, resolving acute inflammation, and promoting repair following injury. In this proposal, we hypothesize that developing molecular imaging techniques to identify functional subsets of activated macrophages will advance understanding of inflammatory lung diseases and could lead to novel, macrophage-targeted therapies. These studies will optimize imaging probes based on FRβ expression and explore new imaging targets present on the surface of activated macrophages. These new strategies can then be applied to the study of inflammatory lung diseases in humans.

W81XWH-11-1-0509 (Wilson) 07/25/11-08/24/13 (No cost extension – 08/24/14)
 Department of Defense

Nuclear factor-kappaB Activity in the Host-tumor Microenvironment of Ovarian Cancer
 Study the patterns of nuclear factor-kappa B activity in the host versus the tumor epithelium during progression of ovarian cancer in a murine model. Bioluminescent reporters in ovarian cancer cell lines or transgenic mice will determine patterns of NF-κB activity and responses to pharmacologic interventions during tumor progression.

5 R01 HL 085317 (Blackwell) 04/01/12 - 02/28/16

NIH/NHLBI

"Epithelial-Fibroblast Interactions in Lung Fibrosis"

Goal: This proposal uses novel mouse models to test the hypothesis that specific phenotypic alterations in alveolar epithelial cells affect the response to injurious stimuli, impact fibroblast activation, and determine the severity and progression of lung fibrosis.

Aims: To define the extent of epithelial-mesenchymal transition as a source of fibroblasts in experimental pulmonary fibrosis. In these studies, we will determine the proportion of lung fibroblasts derived from epithelium via EMT and examine the phenotypic characteristics of epithelial-derived fibroblasts.

5 R01 78188-02 (McGuinness)

06/01/09 - 05/31/14

NIH/NCI

Impact of Inflammation on the control of muscle

Goal: Identify the steps controlling MGU that are impacted by inflammation so that future therapies can have a more targeted approach in correcting MGU during an inflammatory stress such as sepsis

Aims: The impact of LPS on the relative control glucose transport and glucose phosphorylation have in determining MGU. If inflammatory stress amplifies the impact LCFA and glucose availability have in modulating MGU. If modulating oxidative stress (Nitric oxide availability and NF- κ B activation) will improve MGU by augmenting glucose phosphorylation and mitochondrial ATP flux.

Overlap: There is no overlap between the currently funded grants listed above and this application.

BIOGRAPHICAL SKETCH

Á	
ÞÓET ÓÁ Óæ@æ ßÝ @æ ^^ Á Á	ÚÚÙQWIPÁ/QSHÓÁ Ü^•^æ&@œ•ã ææ oÁÁ
Í	
ΦÙNQWWIPÁ ØÖSUÔOE/WIPÁ	ØÖÖÜØÓÁ (if applicable)
Ü@å^•ÁÔ ^*^Á Á Á Á	ÓÈÜÉP } • ßÁ Á Á Á
	QE ECE Á Á Á Á
	Ô@{ ãd^Ó{ &@{ ãd^DÁ Á Á Á Á

A. Positions and Honors

B. Peer-reviewed publications in chronological order.

Á Á Á Á

I I L SK

NAME Chen, Lianyi	POSITION TITLE Research Assistant I
----------------------	--

INSTITUTION AND LOCATION	DEGREE (if applicable)	YEAR(s)	FIELD OF STUDY
Capital Normal University, Beijing, China	S	1992- 1996	Biology
West Virginia University, Morgantown, WV	M.S.	2005-2008	Animal and Nutrition Science

positions

1996 - 2000 **Senior Researcher** College of Food Science & Nutritional Engineering, China Agricultural University, Beijing, China.

2009-Pres Research Assistant, Dept. Cancer Biology. Principal Investigator Fiona Yull, Vanderbilt University Medical Center (VUMC), Nashville, TN

Peer reviewed publications in chronological order

1. Connelly, L.*, Barham, W. , Onishko, H.M., Chen L , Sherrill, T.P., Zabuawala, T., Ostrowski, M.C., Blackwell, T.S., and Yull, F.E. NF-kappaB activation within macrophages leads to an anti-tumor phenotype in a mammary tumor lung metastasis model. Breast Cancer Research 2011. 13(4):R83. PMID: 21884585. (*these authors contributed equally).

BIOGRAPHICAL SKETCH

<p>ÞÓE ÒÁ Ü^ æ ÁU;c^* æ ^Ü<u>Æ</u>TT U<u>Þ</u>ÁN<u>Ü</u>Æ<u>Þ</u> ÓÁ Á</p>	<p>Á Ú<u>Þ</u>Á<u>Q</u> Ó!æ^ æ^ ÁU;c å^} dÜ^•^æ&@!Á</p>
--	---

ÖÖWÖÖE/ÖÖPÖVÜÖÖPÖÖ (Begin with baccalaureate or other initial professional education, such as nursing, and include postdoctoral training.)

ΦÙVQWVQFÁPÖÖSUÖCEVQFPA	ÖÖÖÜÖÖA (if applicable)	ÝÖÄÜÇDÁ	ØÖSÖÁØÙVWÖYÁ
Xǣ å̄!à̄fÁW} ã̄!•ã̄ Á Á	ÓÐEÁ	GEEI ßGEEI Á	Óä { ^å̄!à̄fÁW} * ã̄!•ã̄ * Á
Xǣ å̄!à̄fÁW} ã̄!•ã̄ Á Á	T ÐUÉÁ	GEEI ßGEEFÁ	Óä { ^å̄!à̄fÁW} * ã̄!•ã̄ * Á
Xǣ å̄!à̄fÁW} ã̄!•ã̄ Á Á	ÚGÖDÁ	GEFHÁ GÇ] ^&CáDÁ	Óä { ^å̄!à̄fÁW} * ã̄!•ã̄ * Á
	Á	Á	Á

A

Positions and Employment

CECÉTÉ! ^•^} dÁ Ó! ^•^ æ ÁUc á^} dÜ^•^ æ &@! ÁeÁKæ á^! àééÁW} ã^! • ã Ö^} æd ^} ã! ÁÓä { ^åéééÁ
Ó} * ã ^•^ ã * ÉA [\! ã * Á æ &@! ÉA! áá ÁÖÉZÖ! * ã Á ÁÓä } æ [^•^ &@! [| * ^ Á
CEFFÉ! ^•^} dÁ Ó! ^•^ æ ÁUc á^} dÜ^•^ æ &@! ÁeÁKæ á^! àééÁW ^åéééÖ! } d! Ö^} æd ^} ã! ÁÓä &! ÁÓä | | * ^ ÉA
, [\! ã * Á æ &@! ÉA! } æ ^•^ | | Á ÁÓä &! ÁÓä { ^ } | | * ^ Á
CECÉTÉ! Á W! á^! * | ^•^ æ ÁUc á^} dÜ^•^ æ &@! ÁeÁKæ á^! àééÁW} ã^! • ã Ö^} æd ^} ã! ÁÓä { ^åéééÁ
Ó} * ã ^•^ ã * ÉA [\! ã * Á æ &@! ÉA! ÉA! æ ^•^ Á @ d! ^•^ Á * ^ Á! * ã ^•^ ã * ^ Á! ^•^ Á! ^•^ Á
CECÉTÉ! Á W! á^! * | ^•^ æ ÁUc á^} dÜ^•^ æ &@! ÁeÁKæ á^! àééÁW} ã^! • ã Ö^} æd ^} ã! Á! | | ^& | ^ A
Ó! | | ^ Á! | | ^ Á æ &@! ÉA! ÉA! | | Á! ^•^ &@! } Á! ^•^ Á! | | ^ A! | | ^ A! | | ^ A! | | ^ A!

A

B. Selected peer-reviewed publications (in reverse chronological order).

Journal of Nanoparticle Research. A K F G E F G E
Journal of Nanomedicine and Nanobiotechnology. A K F G E F F A

VĚU[á ^ EÖES EÅd ^ ~ EÖEÖ~ ^ æ EÅEÅ! c* aÅT EÅVæ cæ ^ EÖEÅÅ [EÅEÅEÅ @e d ÅO } * å ^ v | * ÅÅT aæ! åÅÅU` | -æ & ^ Á | Á
Ö!` * ÅÖ` | äv | ^ Aæ åÅQ æ å * Å • å * ÅSæ ^ | Eå ^ EÅSæ ^ | ÅOE• ^ { à | Å | ÅD } &c } aÅ ^ åÅPæ [] æc | ^ EÅAdv. Mater. ÅGGÅ
FHUGEFHJÍ EÅGEFEEÅ

Á Á Á Á

C. Talks

A

ÜEDEAU|C* æEY EØæ @ø EØÉS~ { æEØEØEY||EVEØEØ{ * å ÆT [å |æEØ} å[• [{ æEØ• &ø ^Áø [] åEø^• Á | Á@ Á
Ö|æ^• ^ Á@|æ ^ c&Ø^ } o Á| Á~ { [|ÁØ• [&ø^• å Á å [] @^• E Tennessee Biomaterials Day annual
meeting. Áæ @å^ EØP EAT æ@&GEFHÈ

ÜEDEAU |c* ǣV̄EDEZÖA| * ፩ ይጋግጣ, አት [å̄ | Á ÁQ } ÁU cā̄^ÁP ǣ] ǣcā̄^ÁT ǣ } ^cā̄ÁU [] ስ|ቁ• Át ÁŌ የለAŌ• Á } Á ÁP [c̄^ÁP ǣ] { ǣ |ǣ ይBiomedical Engineering Society annual meeting. ጥቁቄ.

Á

D. Posters

ÜEDEAU | c* æF̄ ðOæ @æ ÆU Ævå @ { [ã[çÆÓES̄` { æÆAOðEY` ||ÆVÆðÆOñ! * f̄ ÆOAæ* ^cååð} å[• [{ æf̄ cÅ
þø [] æcå^A{ [ãð} * æ ^v; æ * Á` { [!ÁQ { ` } æf̄ Át æ! [] @æ ^• ÆBiomedical Engineering Society Annual
MeetingÆU ^æcå^ÆY ØEUAU} c{ à^! AGEFHEÅ

ÜEDEAU | c * æ^Y ððæ^c æ^c ðððð^c { æ^c ðððð^c ðð^c || ðð^c ðððð^c { * ð^c ðð^c ç^c • c^c æ^c * Á@À^c & Á^c Á^c Ø^c Ó^c Á^c æ^c Á^c T[å^c | æ^c } Á^c Á^c æ^c [] @^c ^• Á^c • ð^c * Á^c [å^c | æ^c ð^c } å^c [• [{ æ^c ð^c & ð^c ^• Á^c ð^c [] æ^c ^• ð^c Cancer Immunotherapy annual meeting@A^c æ^c : ðð^c { æ^c ^• ð^c æ^c Á^c G^c F^c H^c A

ÜEDEÁU|c* æÉY ÞÓæ@ cE ÞÓES` { æEÚEUÉY~ ÞÓðÓÉY~ ||EAVÞÓÞÓs` |* f EÜ^] | [*|æ { f * Á~ { | |ÁÓ• | &ææåÁ
T æ[] @e^ ^ Á[, æå ÁÓ ÞÓ ÞÓ` { | ÁU@)[c] ^ Á^ Áæ* ^ç* Á@ ÁÓ ÓÁÚæ@ æ Áñ ã* Á[ç^ Á/æ* ^ç^ åÁ
þæ[c@|æ ^` ÞÓ American Association for Cancer Research annual meeting. Y æ @* q] ÞÓÞÓÞÓH@ ÁGÆFHÁ

ÜEDEUIC* AZOS } æEUEEY~ EVEOUI* åEVa*^cåÅS } & å[,] ÁÁPØEÓÁÁ~{ [IAE•] &æcåÁTa&[] æe•ÁBiomedical Engineering Society annual meetingEOEazÅOEUIC* azÅEGFÁ

Á

A

UEDEAU [c* aEUEUEAY~ EEVEDO@] * Á ÉT [a^@] @ Á@Á æ } ^c@Á| [] ^{c@• Á Á~] ^{]} æ@æ æ } ^c@Á| } Á c@^Á
} æ [] æc@^• Á@æ * ^@ Á | a^@! ^@ Á~ • c! • Tennessee Biomaterials Day annual meeting. Á ^{] @ E@P E@GEFF@

A

A
6

A

E. Research Support

A

Ongoing Research Support

ÓÔFEG JÎ Á Á Óä! * á ÁÜÖÄY ||Á&[EÜÖÁ Á Á ï DÉÖFFÁ ÁU!^•^} oÁ

Completed Research Support

ÓÔEÍ Í JJÁ Á ÕÉ! * Á ÁÚÓÁ Á Á Á Á Í ÓEEÍ Á ÁEÍ EEEÁ
Q] [cä * ÁØæ! ^ ÁØ^æ & } Á Á! ^ æ æ Øæ! ^ Á Á! ^ æ æ & ÁÅ } æ & ^ ÁÅ æ } ^ ÄÄÜ^æ [} æ & ^ ÁQ æ ä * ÁW ä * Á
P[c^] ÄÖ! [..! Eä! ^ å ÁQ } ÁU cä! ^ ÁP æ [] æ cä! ^ ÁÖ! • c! • ÁA
V@ Á [! Áæ! ^] cä! ^ Á! } c@ • ä! ^ Áæ! ^ Áæ! ^ c! ^ Áæ! [c^] Áé! ^ E! ^ [} • Ä! ^ Á æ [E! { } [• Ä! ^ Á! | Áæ! ^ Á! ^ æ c! ^
æ & ! ^ Áæ! ^ Áæ! ^ cæ cæ a! ^ Á! ^ æ & } Á! ^ Á æ } ^ c! ^ Á! ^ [} æ & ^ ÁQ ÜD! æ ä * E!

BIOGRAPHICAL SKETCH

<p>þœt öðr A—————vã @ { á[çÁ ^* ÄÈ Á</p>	<p>Á úúúq@þÁ/qšöA Ü^•^æ&@Ó•d^ &q !Á</p>
--	---

ÖÖVÖÄE/VÖPÄVÜÄE/PÖÄKBegin with baccalaureate or other initial professional education, such as nursing, and include postdoctoral training.)

ΦÙVQWVWVÁÅÖÖŠUÔC/WPÁ	ÖÖÖÜÖÖÄ (if applicable)	ÝÒCÆGÁ	ØØSÖÁØÙVWÖÝÁ
GáÁT [• & , ÅÙæv ÁT ^å^æ^éÅBæ^ { ^ÉU^ • • åÁ	ÅÅT ÆDEÁ	FJÍ Í ÙJÌ GÁ	T ^å^æ^éÅB [@ • åÁ
Q•æ^ c Á ÄÖ] å^ { ^ÉU^ • • åÁ	ÅÅP EDÉA	FJÍ Í ÙJÌ Í Á	Ø] å^ { ^ÉU^ • • åÁ
Q•æ^ c Á ÄÖ] å^ { ^ÉU^ • • åÁ	ÅÅP EDÉA	FJÍ Í ÙJÌ Í Á	Óä c &@ [* ^ Á
Q•æ^ c Á ÄÖ] å^ { ^ÉU^ • • åÁ	ÅÅP EDÉA	FJÍ JÙJJÍ Á	Q { ^ } [* ^ Á
Xæ å^ àäCÅW å^ { ^ÉU&@ [Á Ä ^å^æ^á ^ Á	ÅÅP EDÉA	FJJÍ ÆGEFGÁ	Q { ^ } [* ^ ÉÖä &@ { äd^ Á

A. Positions and Honors

Positions and Employment:

- | | |
|--------------|--|
| 1982-1985 | Microbiologist, Mechnikov Institute of Vaccine and Sera, Moscow, Russia |
| 1985-1986 | Junior Researcher, Institute of Epidemiology, Moscow, Russia |
| 1986-1988 | Researcher, Institute of Agricultural Biotechnology, Moscow, Russia |
| 1989-1994 | Researcher, Institute of Experimental Cardiology,
Cardiology Research Center, Moscow, Russia |
| 1995-1997 | Research Fellow, Vanderbilt University Medical Center,
Department of Medicine, Division of Rheumatology and Immunology |
| 1997-2002 | Research Fellow, Vanderbilt University School of Medicine,
Department of Biochemistry |
| 2002-2003 | Research Instructor, Vanderbilt University School of Medicine,
Department of Biochemistry |
| 2003-2005 | Research Assistant Professor, Vanderbilt University School of Medicine,
Department of Biochemistry |
| 2005-2008 | Research Assistant Professor, Vanderbilt University School of Medicine,
Department of Medicine, Division of Hematology/Oncology |
| 2008-2011 | Research Assistant Professor, Vanderbilt University School of Medicine,
Department of Biochemistry |
| 2011-present | Research Instructor, Vanderbilt University School of Medicine,
Department of Cancer Biology |

B. Publications: 1. Ermolin G.A., Dikov M.M., Tikhomirov O.Y. Enzyme immunoassay in evaluation of homeostasis and diagnostics of its disorders. In: New in Cardiology. (ed. Chazov E.I.) Moscow, Vneshtorgizdat, 1985, 141-144.

2. Tikhomirov O.Yu., Ermolin G.A., Dikov M.M. Detection of myoglobin by enzyme immunoassay. USSR Pharm. Art. 42-39BC-1986.

3. Efremov E.E., Ermolin G.A., Dikov M.M., Tikhomirov O.Y. Detection of fibronectin by enzyme immunoassay. USSR Pharm. Art. 42-28BC-1986.

4. Ermolin G.A., Tikhomirov O.Y., Dikov M.M. Detection of fibrinogen and fibrin-fibrinogen degradation products by enzyme immunoassay. USSR Pharm Art. 42-37BC-1986.
5. Ermolin G.A., Shelepova T.M., Dikov M.M., Tikhomirov O.Y. Application of enzyme immunoassay for detection of myoglobin, fibronectin, fibrinogen and fibrin-fibrinogen degradation products in diagnostics of somatic diseases. Bull.Cardiol.Cent USSR(1):33-37, (1987).
6. Plaksin D.Yu., Ermolin G.A., Dikov M.M., Tikhomirov O.Y. Ultramicromethod of erythrocytes immunoadsorption in screening for somatic antigens in acute myocardial infarction. Bull.Cardiol.Cent.USSR(2):21-25, (1987).
7. Dikov M.M., Tikhomirov O.Y., Ratner G.M., Ermolin G.A. Detection of antibodies to myoglobin by enzyme immunoassay. USSR Pharm.Art. 42-17BC-1991.
8. Dikov M.M., Tikhomirov O.Y., Ratner G.M. Detection of insulin and antibodies to insulin by enzyme immunoassay. USSR Pharm Art. 42-86BC-1992.
9. Lakeev Iu.V., Kosykh V.A., Kozenkov E.I., Tsibul'skii V.P., Tikhomirov O.Y., Antonov I.A., Repin V.S. Producol and alpha-tocopherol stimulate the synthesis of bile acids in cultured rabbit hepatocytes. Biochemistry (Moscow) (1993), 58(3): 406-415.
10. Kazantseva I.A., Kalinin A.P., Polyakova G.A., Davydova I.Y., Tikhomirov O.Y.. A retrospective clinico-morphologic study of insulinoma. Arkhiv Patologii USSR (1995), 57(3): 31-35.
11. Khaspekova S.G., Byzova T.V., Lukin V.V., Tikhomirov O.Y., Berndt M., Kouns W., Mazurov A.V. Conformational changes of the platelet membrane glycoprotein IIb-IIIa complex stimulated by a monoclonal antibody to the N-terminal segment of glycoprotein IIIa. Biochemistry (Moscow) (1996), 61(3): 412-428.
12. Mazurov A.V., Khaspekova S.G., Byzova T.V., Tikhomirov O.Y., Berndt M.C., Steiner B., Kouns W.C. Stimulation of platelet glycoprotein IIb-IIIa (alpha IIb beta 3-integrin) functional activity by a monoclonal antibody to the N-terminal region of glycoprotein IIIa. FEBS Letters (1996), 391(1-2): 84-88.
13. Tsibulsky V.P., Yakushkin V.V., Tikhomirov O.Y., Preobrazhensky S.N. Immunoenzyme assessment of human apoB-lipoprotein binding to immobilized receptor of low density lipoproteins. 1. Preparation of anti-receptor monoclonal antibodies. Biochemistry (1997), 62(6): 596-602.
14. Tikhomirov O.Y., Thomas J.W. Restricted V gene repertoire in the secondary response to insulin in young BALB/c mice. Journal of Immunology (1997), 158(9): 4292-4300.
15. Semenov A.V., Romanov Y.A., Loktionava S.A., Tikhomirov O.Y., Khachikian M.V., Vasil'ev S.A., Mazurov A.V. Production of soluble P-selectin by platelets and endothelial cells. Biochemistry (Moscow) (1999), 64(11): 1326-35.
16. Tikhomirov O.Y., Thomas J.W. Alanine scanning mutants of rat proinsulin I show functional diversity of antiinsulin monoclonal antibodies. Journal of Immunology (2000), 165(7): 3876-82.
17. Tikhomirov O.Y., Thomas J.W. Preference for IgG mAb binding insulin in solution or on surfaces is related to immunoglobulin variable region structures. Journal of Autoimmunity (2000), 10(6): 541-549.
18. Tikhomirov O., Carpenter G. Geldanamycin induces ErbB-2 degradation by proteolytic fragmentation. The Journal of Biological Chemistry (2000), 275(34): 26625-31.
19. Tikhomirov O., Carpenter G. Caspase-dependent cleavage of ErbB-2 by geldanamycin and staurosporin. The Journal of Biological Chemistry (2001), 276(36): 33675-33680.
20. Tikhomirov O., Carpenter G. Identification of ErbB-2 kinase domain motifs required for geldanamycin-induced degradation. Cancer Research (2003), 63, 39-43.

21. Tikhomirov O., Carpenter G. Epidermal growth factor (EGF) signaling. In: “Encyclopedia of hormones and related cell regulators” (H.L.Henry and A.W. Norman, eds), Academic Press (2003), Vol.I, 549-556.
22. Qiu-Chen Cheng, Tikhomirov O., Zhou W., Carpenter G. Ectodomain cleavage of ErbB-4: Characterization of the cleavage site and m80 fragment. *The Journal of Biological Chemistry* (2003), 278, 38421-38427.
23. Tikhomirov O., Carpenter G. Ligand-induced p38-dependent apoptosis in cells expressing high levels of EGFR and ErbB-2. *The Journal of Biological Chemistry* (2004), 279, 12988-12996.
24. Tikhomirov O., Carpenter G. Identification of the proteolytic fragments from ErbB-2 that induce apoptosis. *Oncogene* (2005), 24:3906-3913.
25. Tikhomirov O., Carpenter G. Bax activation and translocation to mitochondria mediate EGF-induced programmed cell death. *Journal of Cell Science* (2005), 118:5681-90.
26. Sergey V. Novitskiy, Sergey Ryzhov, Rinat Zaynagetdinov, Anna E. Goldstein, Yuhui Huang, Oleg Y. Tikhomirov, Michael R. Blackburn, Italo Biaggioni, David P. Carbone, Igor Feoktistov, Mikhail M. Dikov. Adenosine receptors in regulation of dendritic cell differentiation and function. *Blood* (2008), 112: 1822-1831.

BIOGRAPHICAL SKETCH

ÞÓR ÓÁ Ú{ ÁÉY~ Á ^ÜCEÓUTT UÞÚÁNUÓUÁ CÉ ÓÁ{^á} {^á} & Á * á D • @{ } ^~ Á	Á ÚÚÓQÓPÁQŠÓÁ Ú[• c{] &q a{ Á^• ^a{ &@{ } [&a{ ^E{ Q• c{ c{ Á ~ Á Ó{ ^} * á ^{ á * Á
---	--

ÖÖWÖCE/ØPØVÜCE/ØÖÄ Begin with baccalaureate or other initial professional education, such as nursing, include postdoctoral training and residency training if applicable.)

ΦÙVQWVØPÅ ØÖSNUÓCE/WØPÁ	ØÖSÙØÖA (if applicable)	T T ÆYÁ	ØØSØÁØÅVMØYÁ
Ü&^ÁN} Æ^!••Æ ÈP[^ •ç } ÈVYÁ	ØEJÄ	E EEE Á	Óa ^ } * æ ^!ä * Á
Xæ å^!àæÁN} Æ^!••Æ ÈPæ @ç! ÈVpÁ	T ÈUÄ	FØDEEJÁ	Óa { ^å^!æ@ç! } * æ ^!ä * Á
Xæ å^!àæÁN} Æ^!••Æ ÈPæ @ç! ÈVpÁ	Ú@ç!Ä	FØDEFGÁ	Óa { ^å^!æ@ç! } * æ ^!ä * Á

A. Positions and Honors

Research Experience

GEE EEE Á W à^* i^* i^* ÁÜ^* ^z&@Á• ã z̄e d̄s̄ Á ÁU[-ÉR^ } } à^ Á ^* d̄z̄ Ö^] z̄d̄ ^* ã^ ÁÖ^ * è^ v^* È Á
 Üz̄ ÁV^ f̄^* i^* ÈP[^* d̄ } ÈV Y Á
 GEE EEEFGÁ Ó i^* ÁÜ^* ^z&@Á• ã z̄e d̄s̄ Á ÁU[-ÉV[åå ÁÖ^ * è^ ÈÖ^] z̄d̄ ^* ã^ ÁÖ{ ^å^z̄ ÁÖ } * è^ v^* È Á
 Xz̄ a^* à^z̄ ÁW^ f̄^* i^* ÈP[@z̄ ÈV PA
 GFGÁ Xz̄ a^* ÁÜ^* ^z&@Á{ ||, d̄s̄ Á ÁU[-ÉP[i^* ÁÖ^ a^ ÈV{ [| Á a^ &^ ÁÖ{ ^* } ÁÖz̄ &^ Á { ^ } [@|z̄ ^ Á
 V|z̄ ÁP^ c[| | ÈV^ f̄^* i^* È Á z̄ @^* d̄ } Á^* ÁÖ^ z̄ ÈV PA
 GEFHEU^* ^* } ÁU[• @^* &^ | z̄ ÁÜ^* ^z&@Á• | &^ z̄ Á ÁU[-ÉT^* | à^ ÁU, z̄c ÈQ• @^ c Á ÁÖ^ * è^ v^* È Á & | Á
 U[| | @^* ÁÖ. å.. | å^* ÁSæ• z̄ } ^ ÈSæ• z̄ } ^ ÈU, è^ s|z̄ å Á

A

Awards and Honors

Professional Memberships

GEET EÜ|A•A} AÜC å^} ØT ^{ à^|EØA { ^åÅæAO}* å^|æ* ÅU[&æc Á
GEEU EÜ|A•A} AÜC å^} ØT ^{ à^|EÅU &æc ÁF|AØA { æ^|æ* Á

C. Peer-reviewed Publications

Talks

T æ AGEFHÁ ÚEJÉAY EÔÈT EÑæé EÝ EREÓæ @ EÔÈDÉP^@[] EEP EÑAZÓEDEU{ æCÓDÉAY^|||EÔÈSÉÖ çæ|EBA|EØÉ
Óä|* ä|Eñæé^çä|* Á^{|[|EDE•[&æ^æ ÁT æ{|[| @æ^•Á|IÁ{|[| @|!æ| ^Aæ|UPQç|!-|^{|} &Á
^•ä|* Á{| æEÓ} çä|[{| ^EÜ^@|[| •ä|* ÁPæ|[| æç^•EAGEFHÁCancer Immunotherapy Annual
Meeting@æ|:EÓ^{|æ| ^EA

Conference Abstracts

U&EAEFGÁ ÚUEJAY~ EÖRÉT EÅSÅE EÅY EÅRÖÅt @Å EÅO EÅP^|[] EÅO EÅY~ || EÅO EÅO~ çÅ EÅBÅ/EÅEÅ! * å EÅQ@çå * Å
ÖÅ &@ÅQ { ^ } [c@! å^ Á@[^ * @ÅP@Qç@^@^ } &@Å Á~ { [| EÅE•[&@Å åÅT å! [] @Å ^@Å ÅÅÅ
ÅÅÅ åÅT å } [•^ åÅ åÅU | { | åÅÅ åÅ } åÅ åÅ^• EÅEFGÅ } ^ åÅT c@ Å Å@Åå { ^ åÅ åÅÅ } * å @@| å * Å
ÅU &@c EÅQ@ç@ÅÅÅ
U&EAEFGÁ ÖÅEÅO~ çÅ EÅO EÅP^|[] EÅP EÅSÅU EÅJAY~ EÅRÉT EÅQ@å•[] EÅU EÅO~ ^@Å EÅBÅ/EÅEÅ! * å EÅN &@Å åÅ
Vå* ^ c@Å åÅP@Qç@^@^ Á^&@ [| [* å• EÅEFGÅ } ^ åÅT c@ Å Å@Åå { ^ åÅ åÅÅ } * å @@| å * ÅU [&@c EÅ
ÅQ@ç@ÅÅÅ

A Targeted Endosomalytic Nanoparticle for Engineering Tumor Immunity in Macrophages

Ryan Ortega, Whitney Barham, Oleg Tikhomirov, Bharat Kumar, Fiona Yull, Todd Giorgio

Introduction: Tumor associated macrophages (TAMs) can modify the tumor microenvironment to create a pro-tumor niche. Dysregulation of the NF- κ B pathways has been implicated in creating a pro-tumor phenotype in TAMs. NF- κ B regulation of gene activation consists of a well-described classical activation pathway and a less understood alternative pathway. Manipulation of TAM phenotype is a promising therapeutic approach to engage anti-cancer immunity, but macrophages are difficult to specifically target and transfect. We have successfully utilized mannosylated polymer nanoparticles (Mn-NP) capable of escaping the endosomal compartment to deliver siRNA for RNAi of NF- κ B proteins in bone marrow derived macrophages (BMDMs). Mannose serves as a macrophage targeting ligand via the mannose receptor (CD206). The goals of this work are (a) to show that these nanomaterials are efficacious for targeted delivery of functional nucleic acid sequences into macrophages and (b) to use the Mn-NP to investigate the effects that manipulation of the NF- κ B pathways, particularly the alternative pathway, has on macrophage phenotype.

Materials and Methods: Mannosylated polymeric micelles were prepared as previously described¹. Briefly, a triblock polymer is formed with a poly(BMA-*co*-PAA-*co*-DMAEMA) core, a DMAEMA siRNA condensing block, and an azide-containing outer block for further functionalization. Alkyne functionalized mannose is then “clicked” onto the surface of the polymer. *In vitro* cell studies were done primarily with (BMDMs) from FVB mice which express luciferase as a reporter of NF- κ B activity (NGL mice). Bone marrow was cultured in M-CSF containing media for 6 days. The BMDMs were transfected with siRNA (10 nM) using Lipofectamine or Mn-NP for 24 hours on a rocking platform. After transfection, cells were stimulated with TNF- α for 6 hours to elicit strong NF- κ B activity. After stimulation, cells were frozen in a lysis buffer and analyzed for luciferase activity normalized to total protein per sample. In viability studies of Mn-NP and Lipofectamine transfected cells, cell viability was assessed with trypan blue staining after transfection, prior to freezing.

Results and Discussion: At 10 nM siRNA, the Mn-NP formulations are capable of delivering functional siRNA for NF- κ B pathway protein knockdown in NGL BMDMs. Knockdown of only the classical pathway results in an approximately 50% decrease in NF- κ B activity, consistent with the interpretation that this pathway is responsible for only a portion of the total NF- κ B activity. Knockdown of only the alternative pathway results in a 75% decrease in NF- κ B activity. NF- κ B activation is modulated by interactions among proteins in the classical and alternative pathways. Mn-NPs mediate a 30% greater intracellular delivery of FAM labeled siRNA compared to Lipofectamine. This difference increased to almost 40% when transfection was carried out in the presence of convective transport provided by gentle rocking. Rocking increased intracellular siRNA delivery by 40% as compared to Mn-NP transfections carried out in the absence of fluid motion. The combination of 10 nM siRNA delivered by 2 μ L/mL Lipofectamine RNAi max with TNF- α treatment results in 20% BMDM cell death within 6 hours. The same dose of siRNA delivered by 1.6 μ g/mL Mn-NPs followed by TNF- α treatment results in < 5% loss of BMDM viability.

Conclusions: Mannosylated endosomalytic nanoparticles are capable of delivering functional siRNA into macrophages. The resulting RNAi of specific classic or alternative pathway proteins decreases activation of the NF- κ B following TNF- α stimulation. Intracellular siRNA delivery mediated by Mn-NPs is greater than that for Lipofectamine and is additionally increased by convective fluid motion. Mn-NPs induce no significant loss of cell viability at low siRNA concentrations (10 nM), even in the presence of strong stimulation by TNF- α , and reduce NF- κ B activation similar to commercial agents. These particles represent a novel delivery mechanism targeted to macrophages, which are an emerging objective for engineering tumor immunity *in vivo*. Current work consists of delivering functional siRNA to TAMs in *in vivo* murine models and elucidating novel interactions between the classical and alternative NF- κ B pathways in macrophages using our nanoparticles as a tool for targeted RNAi therapy.

References:

¹S.S. Yu, et al. *Mol. Pharmaceutics*. 2013. 10, 975-987

Investigating the Effects of NF- κ B Pathway Modulation in Macrophages using Modular Endosomal Escape Nanoparticles

Ü^ æ ÁEÚ!ç* æÉY @, ^ ÁREÓæ @, GÉÓ@æs^ { æFÉÓ } æÓÉY || ÉV[ååÅEÓ!ç! * f FÉÁ

FÖ^] æd{ ^} ðf{ Áð{ { ^å^æ^ð{ Á} * ð{ ^w{ ð{ * Þ{ ð{ á^| å^| å^ð{ ÁW{ ð{ w{ • ð{ Á}

¶ ÖÖ] æd ^} of Áðæ & | Áðæ [| * ^ EKæ å^| àæd | * | æ Áðæ & | Áðæ } c | Á

“HÖ] æd ^} of -A@{ ææAå åAO@{ [|^& |æAO}* å ^|^å * EÅæ å^|åæAW] å^|• Å A

A

Investigating the Effects of NF- κ B Pathway Modulation in Macrophages using Modular Endosomal Escape Nanoparticles

VANDERBILT
School of Engineering

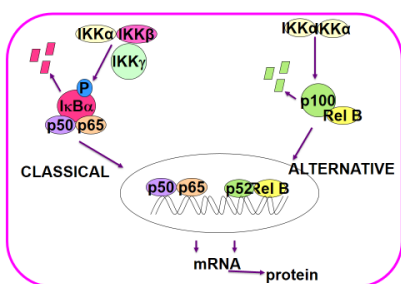
laboratory for
bionanotechnology
AND
nanomedicine

Ryan A. Ortega^{1,2}, Whitney Barham², Bharat Kumar¹, Fiona Yull², Todd D. Giorgio^{1,2}

¹Department of Biomedical Engineering, Vanderbilt University, Nashville, TN, ²Department of Cancer Biology, Vanderbilt University Medical Center, Nashville TN

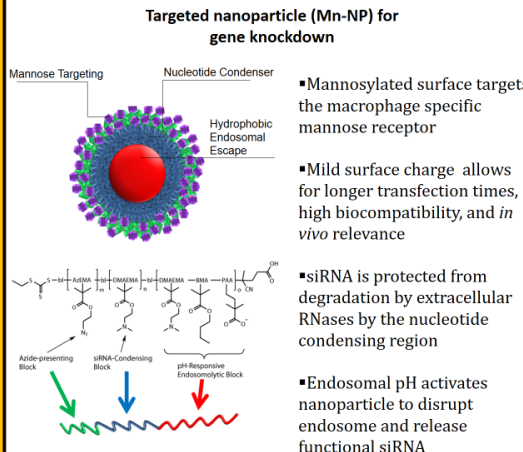
NF- κ B is a promising target for therapeutic manipulation of tumor associated macrophages (TAMs)

- NF- κ B is implicated in creating a TAM phenotype
- Characterized by constant low levels of inflammation, the recruitment of pro-tumorigenic cells, and the restructuring of local tissue.
- Classical and alternative NF- κ B activation offer highly varied therapeutic targets and effects, specific to each pathway



- Knocking down key NF- κ B proteins with targeted nanotherapeutics could wipe out the TAM phenotype
- Selectively activating a cytotoxic (M1) phenotype could produce a strong anti-tumor inflammatory response that is local and transient

Nanotherapeutic Scheme

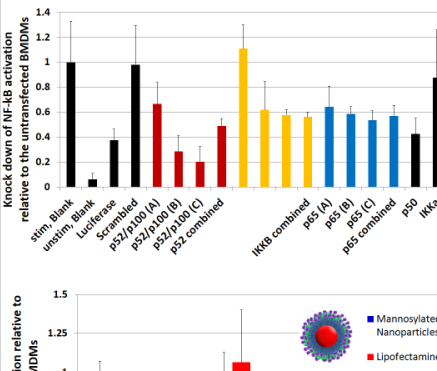


- Mannosylated surface targets the macrophage specific mannose receptor
- Mild surface charge allows for longer transfection times, high biocompatibility, and *in vivo* relevance
- siRNA is protected from degradation by extracellular RNases by the nucleotide condensing region
- Endosomal pH activates nanoparticle to disrupt endosome and release functional siRNA

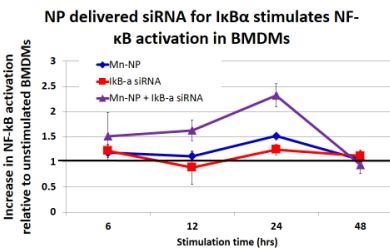
In vitro bone marrow derived macrophage (BMDMs) culturing and transfection procedure

- Bone marrow was harvested from the femurs of NGL reporter mice on an FVB background.
- NGL mice express luciferase and GFP as a reporter of total NF- κ B activity.
- Bone marrow is cultured in media containing a supplemental source of M-CSF for 6 days.
- BMDMs are transfected with siRNA (10 nM) using commercial agent, Lipofectamine (2 μ l/ml), or using nanoparticles (4 μ g/ml); or cells are stimulated with an NF- κ B activating agent.
- Cells are transfected for 24 hours on a rocking platform (10 rocks per minute)
- For siRNA transfected cells: After 6 hrs of transfection, cells are stimulated with TNF- α for 6 hrs to elicit strong NF- κ B activation.
- For drug stimulated cells: Cells are exposed to L-MTP-PE or other agent for varying time points. Cells are dosed every 24 hours and media is refreshed.

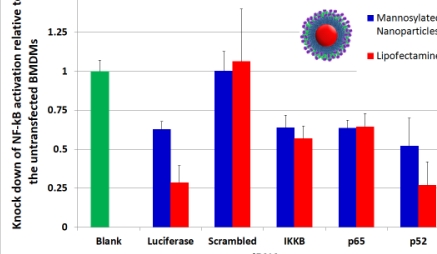
siRNA successfully decreases luciferase as a readout of NF- κ B



Controlled *in vitro* activation of NF- κ B requires longer dosing times

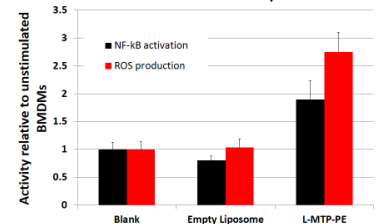


- The transfection times necessary to effectively stimulate NF- κ B by knocking down IκBα with siRNA are difficult to achieve using commercial agents



- Nanoparticle siRNA delivery efficiency is comparable to commercial agents with the added bonus of increased feasibility for *in vivo* use and targetability

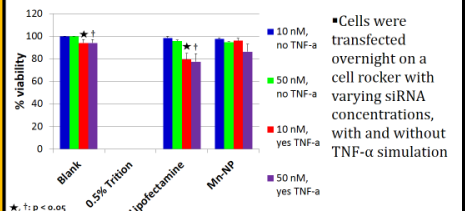
Stimulation of BMDMs with L-MTP-PE (clinical Mφ activator) shows an increase in NF- κ B activation and ROS production



Acknowledgments

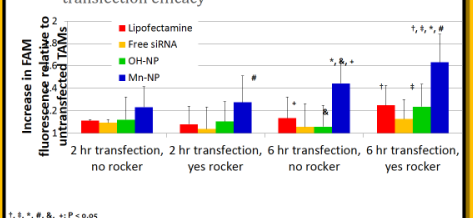
This work was made possible in part by a grant from the United States Department of Defense's (USDoD) Congressionally Directed Medical Research Programs (CDMRP) Breast Cancer Research Program (BCRP): Grant BC102696.

Mn-NP have low toxicity as measured by trypan blue viability assay



Longer transfection times and convective fluid motion improve transfection of TAMs with Mn-NP

- TAMs were harvested from murine mammary tumors from MMTV-PyVT mice
- TAMs were transfected with FAM-labeled, scrambled siRNA with different transfection agents
 - Transfection time and the presence of convective fluid motion was varied
 - FAM fluorescence was measured as a reporter of transfection efficacy



Conclusions

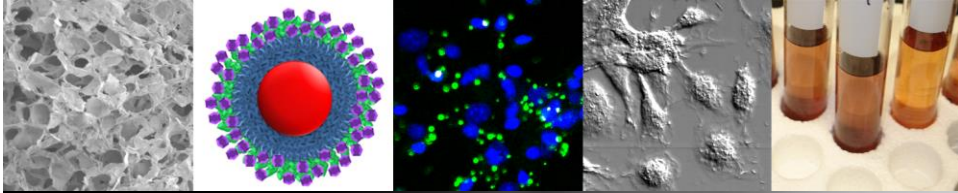
- NF- κ B specific siRNA are capable of knocking down specific pathway proteins.
- Mannosylated nanoparticles exhibit transfection efficiencies comparable to commercial agents and show preferential TAM uptake.
- Targeted activation was achieved via Mn-NP mediated delivery of siRNA for the IκBα inhibitor protein.

Impact

The novel mannosylated nanoparticles presented here are a promising therapeutic tool for targeted *in vivo* manipulation of macrophage phenotype.

Targeting Tumor-Associated Macrophages for Immunotherapy via RNA Interference using Smart, Environmentally-Responsive Nanoparticles

Targeting Tumor-Associated Macrophages for Immunotherapy via RNA Interference



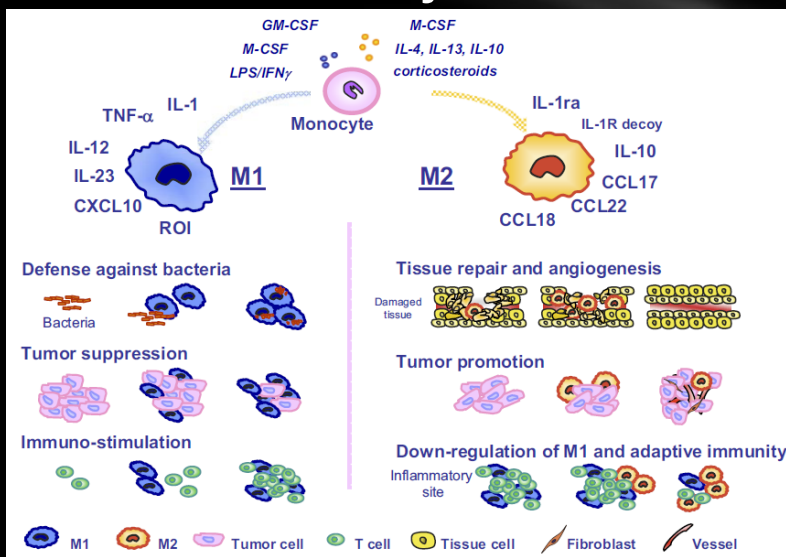
Shann S. Yu¹, C.M. Lau, W.J. Barham, C.E. Nelson, H. Li, C.A. Smith, F.E. Yull, C.L. Duvall, & Todd D. Giorgio

May 16, 2013

CIMT Annual Meeting – Mainz, Germany

¹Current Address: École Polytechnique Fédérale de Lausanne, Lausanne, Switzerland

Macrophages are versatile, multifunctional cells that have been ‘hijacked’ in cancer.

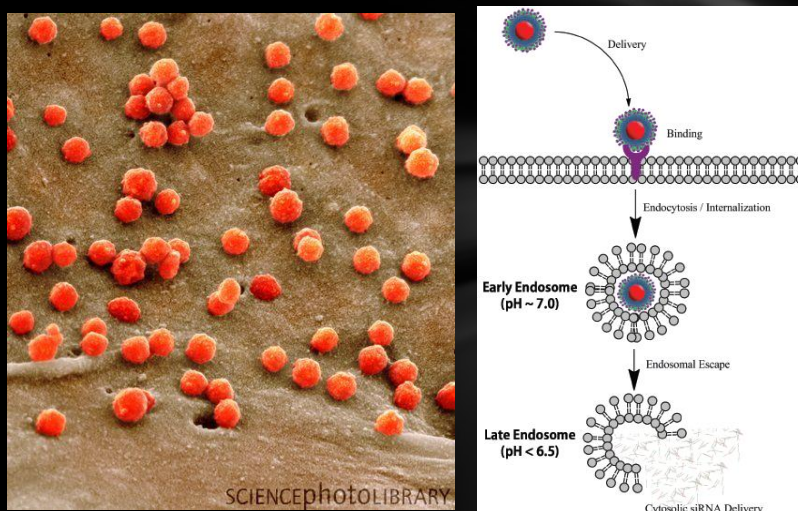


G. Solinas et al. (2009) *J. Leukocyte Biol* 86: 1066.

Re-polarization of Tumor-Associated Macrophages Reactivates an Anti-Tumor Immune Response

- C. Guiducci et al. (2005) *Cancer Research*
- A. Saccani et al. (2006) *Cancer Research*
- T. Hagemann et al. (2008) *J Exp Med*
- GL Beatty et al. (2011) *Science*

Using Polymers to Mimic Viruses for TAM-Targeted, Intracellular Drug Delivery



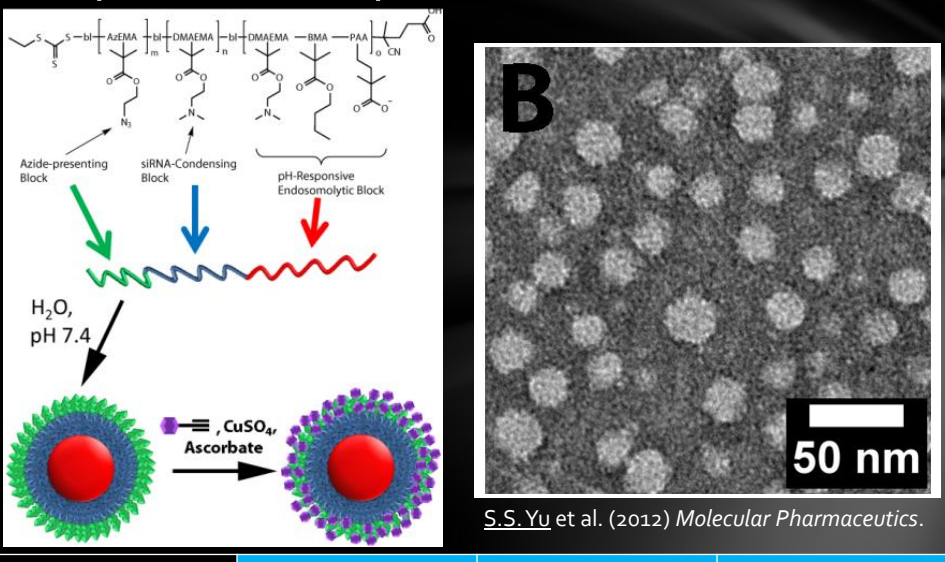
Design & Synthesis

Controlled Release

In Vitro Assays

In Vivo Behavior

Schematic of Completed Triblock Polymeric Nanoparticles



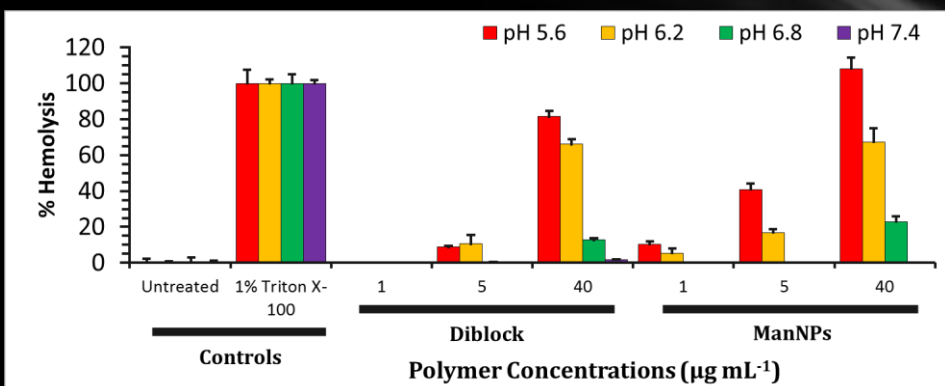
Design & Synthesis

Controlled Release

In Vitro Assays

In Vivo Behavior

Diblocks and ManNPs Exhibit pH-Responsive Hemolysis

S.S. Yu et al. (2012) *Molecular Pharmaceutics*.

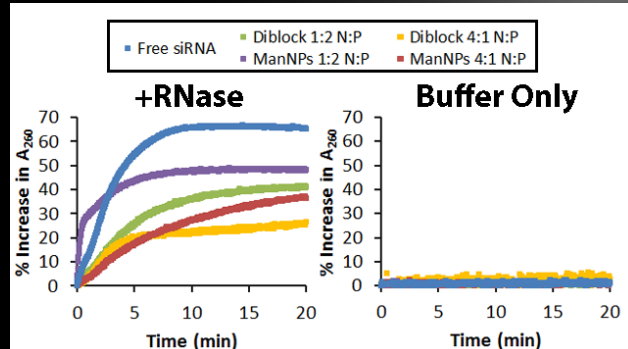
Design & Synthesis

Controlled Release

In Vitro Assays

In Vivo Behavior

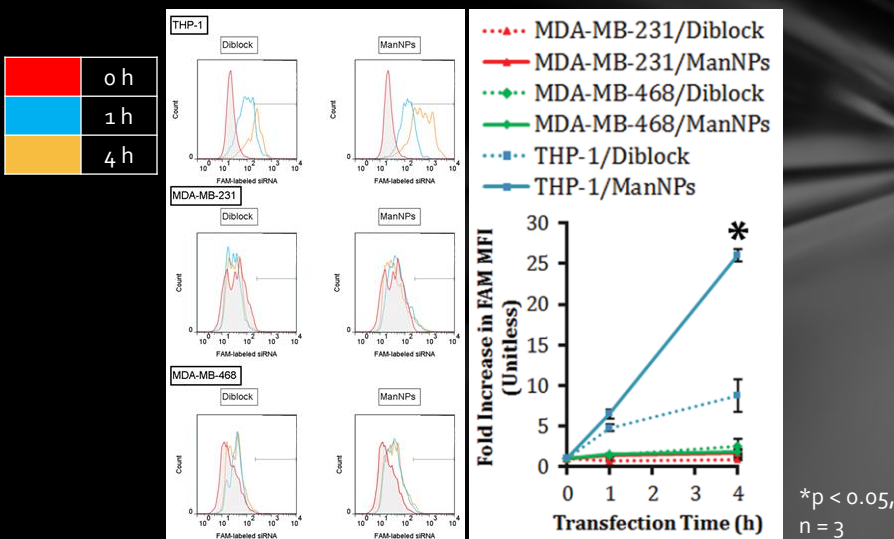
ManNPs Electrostatically Complex siRNA and Protect it from RNases



S.S. Yu et al. (2012) *Molecular Pharmaceutics*.

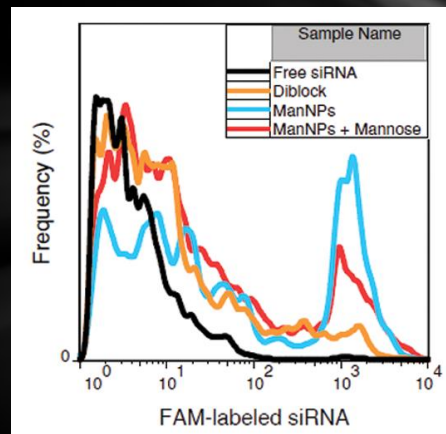
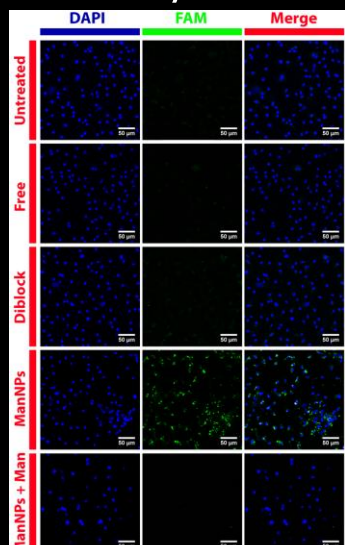
Design & Synthesis **Controlled Release** **In Vitro Assays** **In Vivo Behavior**

ManNPs Enhance siRNA Delivery into Immortalized Macrophages



Design & Synthesis **Controlled Release** **In Vitro Assays** **In Vivo Behavior**

ManNPs Enhance siRNA Delivery into Primary Macrophages



S.S. Yu et al. (2012) *Molecular Pharmaceutics*.

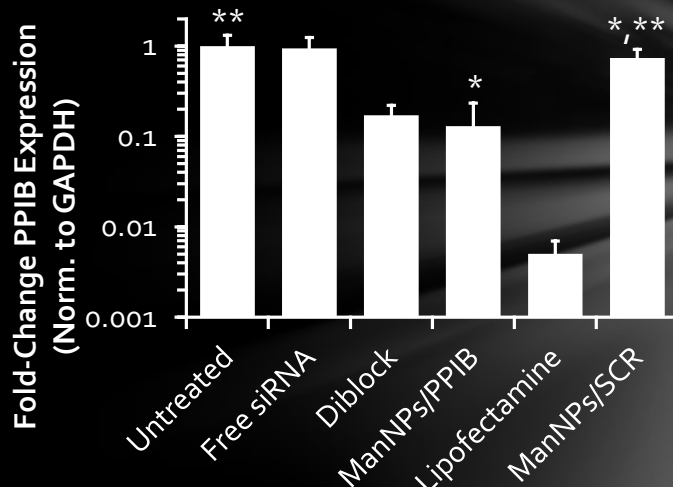
Design & Synthesis

Controlled Release

In Vitro Assays

In Vivo Behavior

siRNA Delivered through ManNPs Retains Ability to Knock Down Target Gene Expression



*p < 0.05; n = 3

** p > 0.05; n = 3

S.S. Yu et al. (2012) *Molecular Pharmaceutics*.

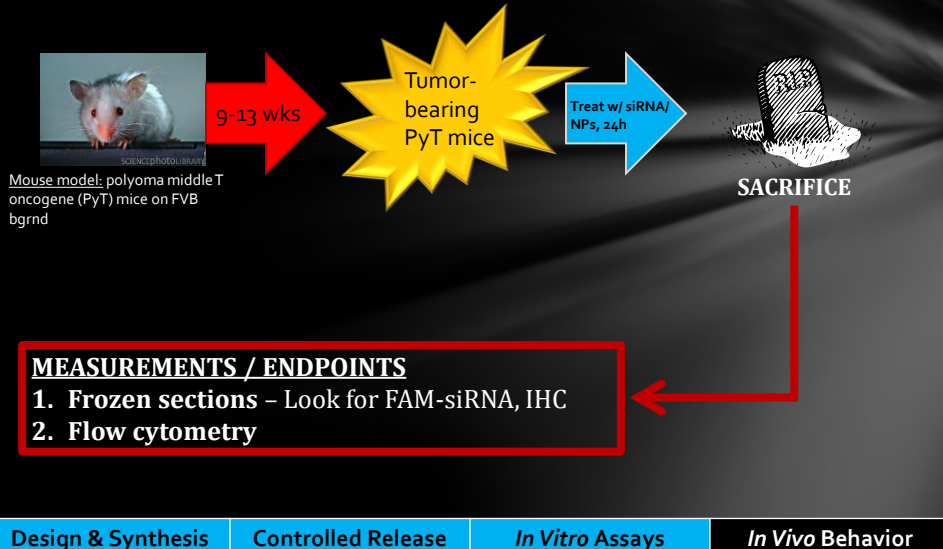
Design & Synthesis

Controlled Release

In Vitro Assays

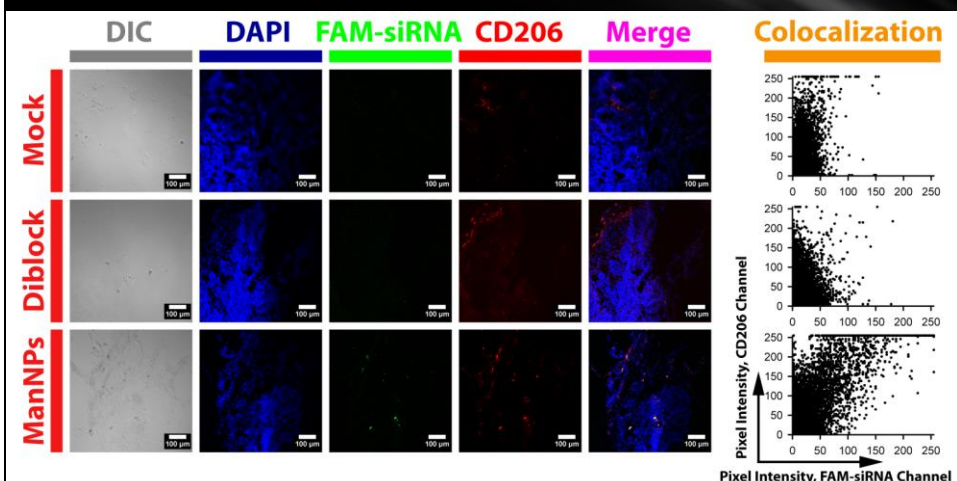
In Vivo Behavior

In Vivo Biodistribution of ManNPs in Primary Tumor Model



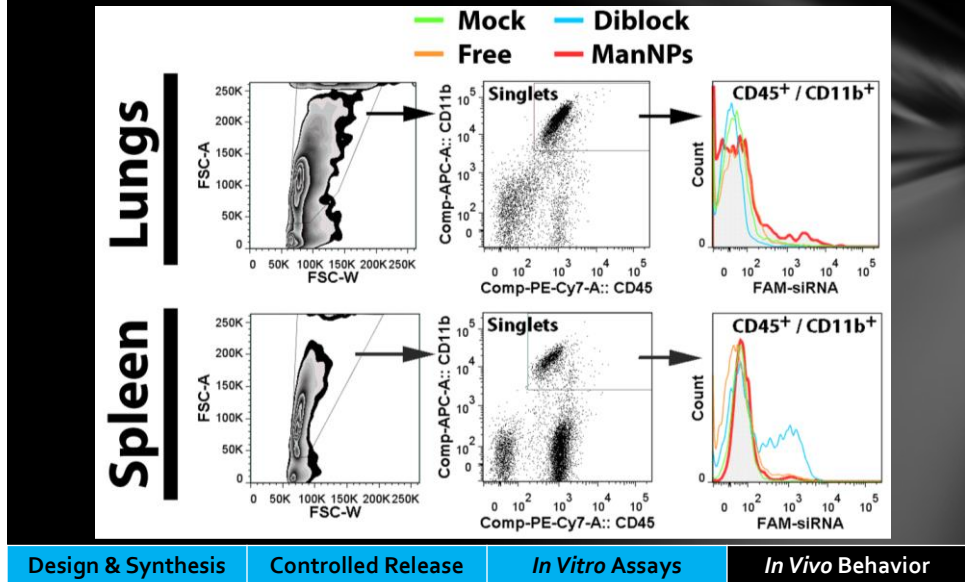
Design & Synthesis Controlled Release *In Vitro* Assays *In Vivo* Behavior

ManNPs Target CD206⁺ Cells in Primary Tumor Model



Design & Synthesis Controlled Release *In Vitro* Assays *In Vivo* Behavior

Nanoparticles May Also Bind Resident Leukocytes in the Lungs or Spleen



Design & Synthesis

Controlled Release

In Vitro Assays

In Vivo Behavior

In Vivo Biodistribution of ManNPs in Metastatic Tumor Model



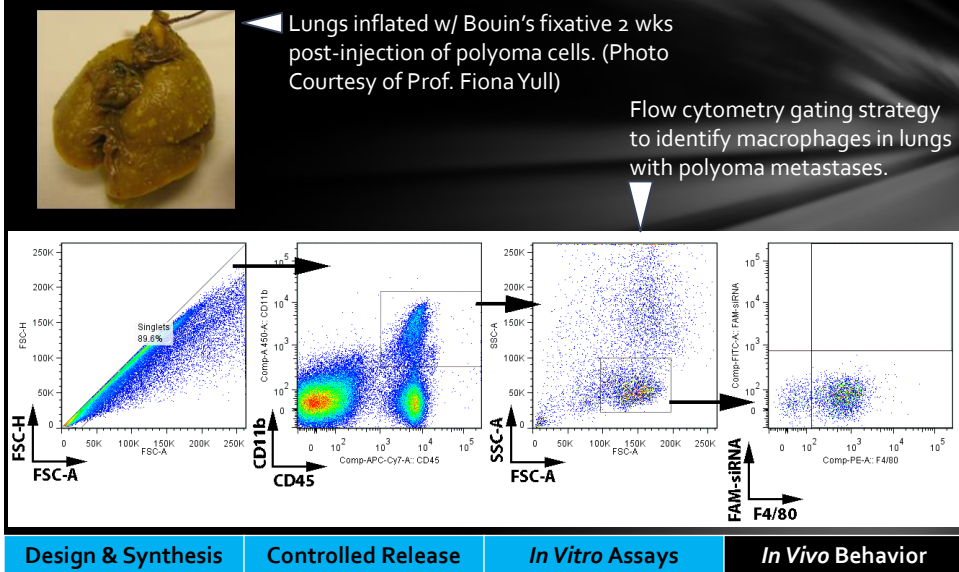
Design & Synthesis

Controlled Release

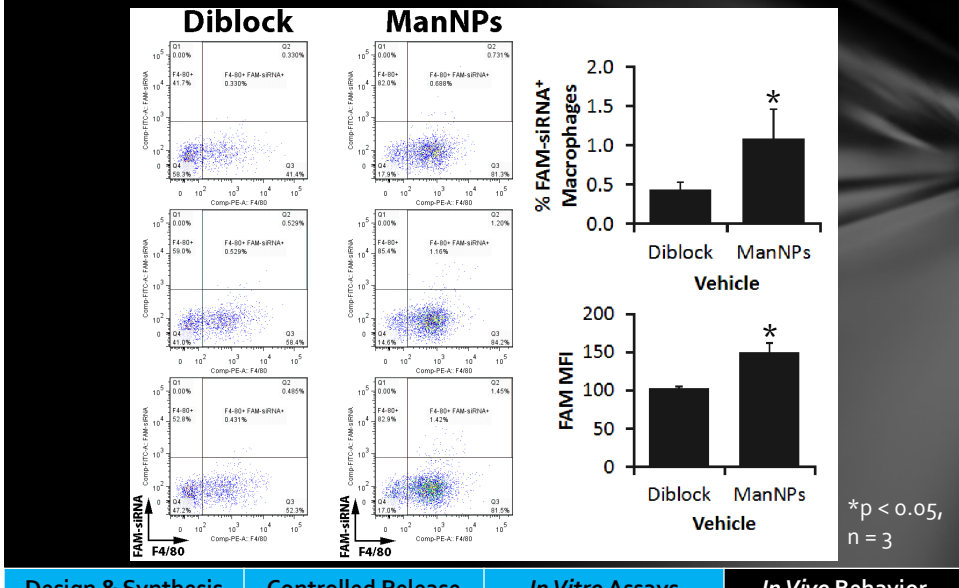
In Vitro Assays

In Vivo Behavior

Formation of Lung Metastases in Tail Vein Injection Model, and Quantification of Macrophages via Flow Cytometry



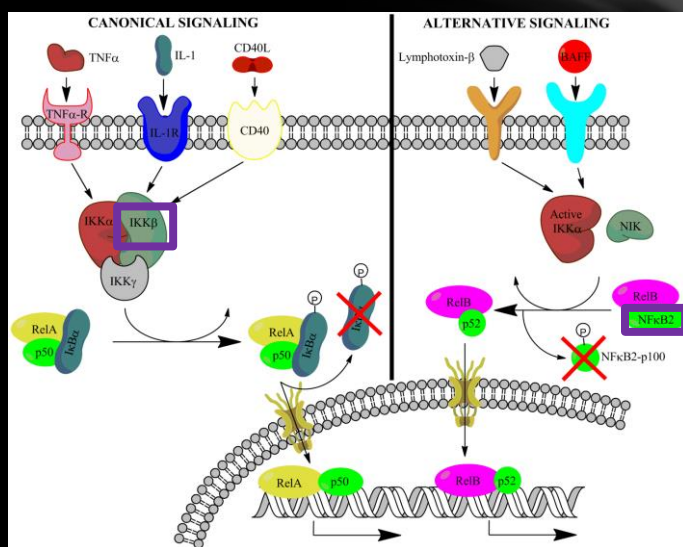
ManNPs Enhance siRNA Delivery Into Macrophages in Lungs of Mice w/ Overt Lung Metastases

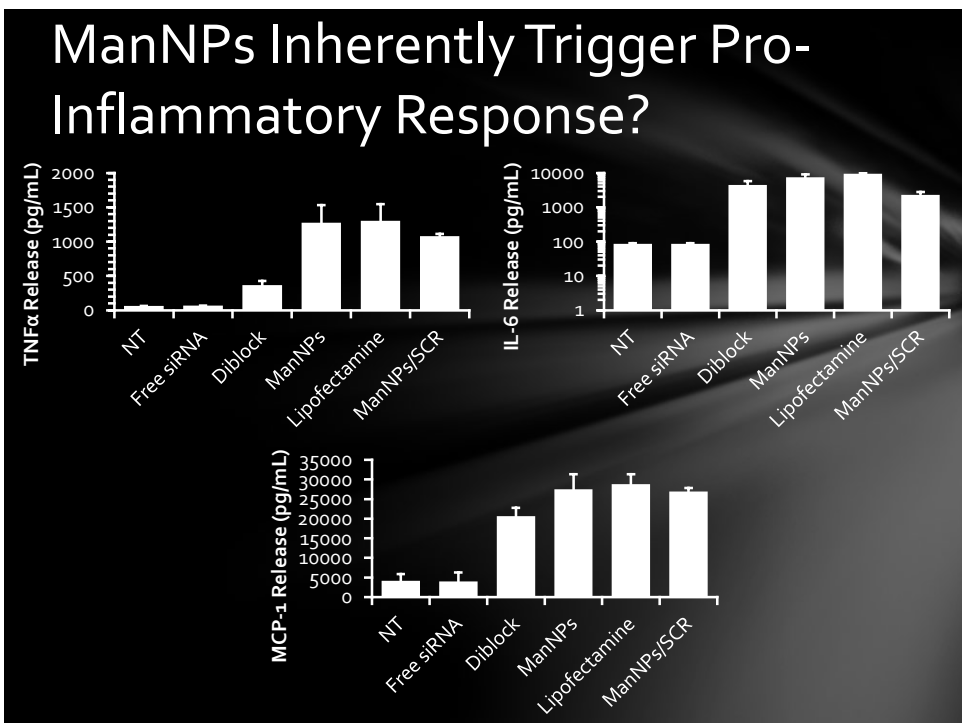
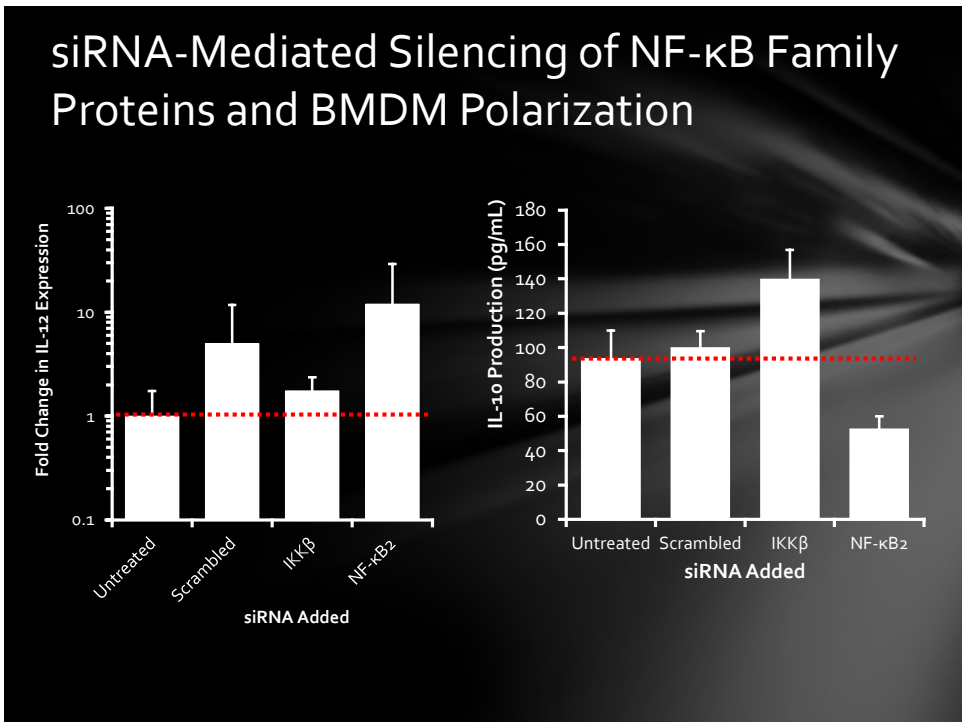


Summary

- Multifunctional triblock copolymers enable systemic targeting of TAMs
 - “ pH-Responsive behavior enables cytosolic drug delivery
 - “ Cationic block enables complexation of nucleic acids
 - “ Azido corona enables attachment of targeting ligands via ‘click’ chemistry
- ManNPs enhance siRNA delivery into primary macrophages *in vitro*
- ManNPs co-localize with CD206⁺ cells in PyMT mice

Next Steps: What's the Therapeutic Target?





Acknowledgments



FUNDING SOURCES

- Department of Defense
- Vanderbilt University
- NIH Cancer Center Grant

Vanderbilt University

- Todd Giorgio
- Craig Duvall
- Fiona Yull
- Cheryl Lau
- Rachel Koblin
- Chelsey Smith
- Whitney Barham
- Ryan Ortega
- Christopher Nelson
- Hongmei Li
- Rinat Zaynagetdinov
- Kwangho Kim



THANK YOU!!!

Be sure to check out our posters! Abstracts # 243-244.

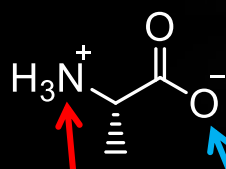


A shot I took of Mt. Rainier (Seattle, WA, USA) as I was flying out of Seattle at sunrise in Sept. 2012.

Supplementary Slides

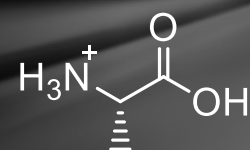
pH-Responsive Polymers are Inspired by Lessons from Nature

pH = 7.4



NET CHARGE =
NEUTRAL!!!

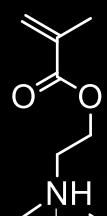
pH < 2.3



NET CHARGE =
POSITIVE

-35

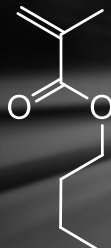
Building pH-Responsive, Endosomolytic Polymers: Rational Monomer Selection



DMAEMA
pKa ~ 7.5



PAA
pKa ~ 6.7



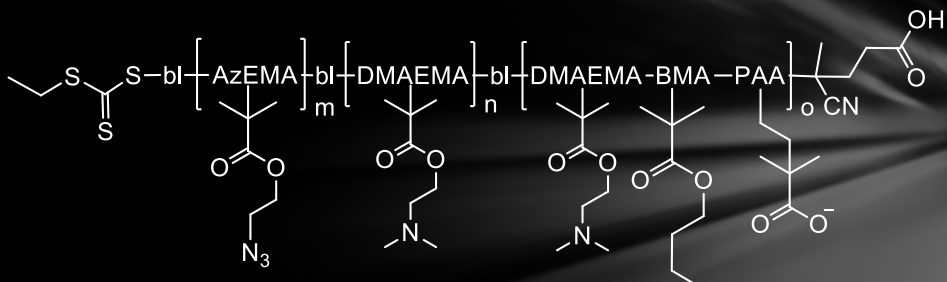
Hydrophobic
comonomer

S Grainger & MEH El-Sayed. (2010) in **Biologically Responsive Hybrid Biomaterials**, E Jabbari & A Khademhosseini (Eds.): 171-190.

AJ Convertine et al. (2009) **J Controlled Release**.

Design & Synthesis	Controlled Release	In Vitro Assays	In Vivo Behavior
--------------------	--------------------	-----------------	------------------

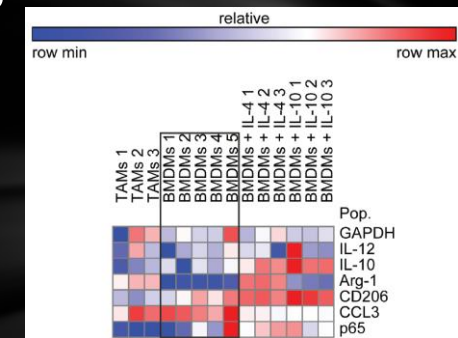
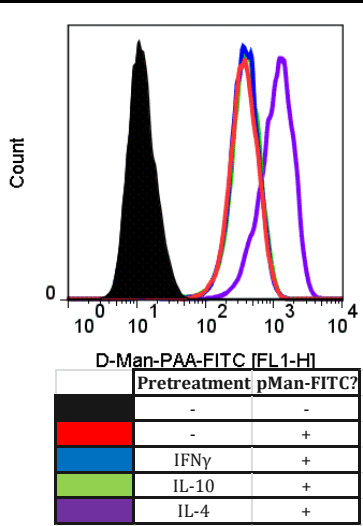
Azide-Containing Block is Added to Enable 'Click' Functionalization



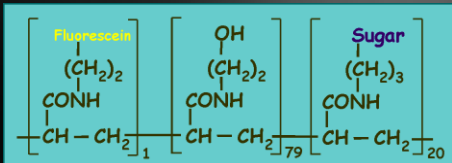
Polymer	dn/dc (mL/g)	Target M _n (Da)	M _n (Da)	M _w (Da)	PDI	D _h (nm)	ζ-Potential (mV)
Terpolymer	0.081	14000	11400	13900	1.22		
Diblock	0.049	21000	16800	20700	1.23	34.2 ± 2.2	$+10.8 \pm 11.2$
Triblock (Before 'click')	---	22000	22300	28900	1.29	28.0 ± 1.5	$+19.6 \pm 11.7$

Design & Synthesis	Controlled Release	In Vitro Assays	In Vivo Behavior
--------------------	--------------------	-----------------	------------------

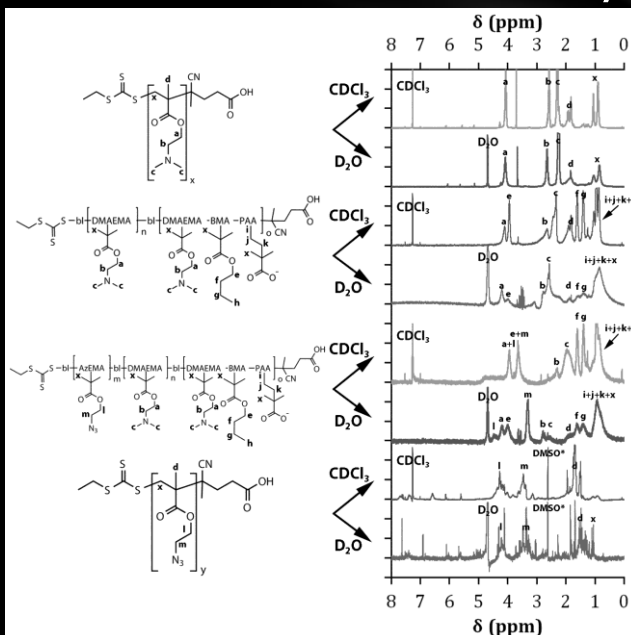
Mannose Receptor Activity vs. Phenotype?



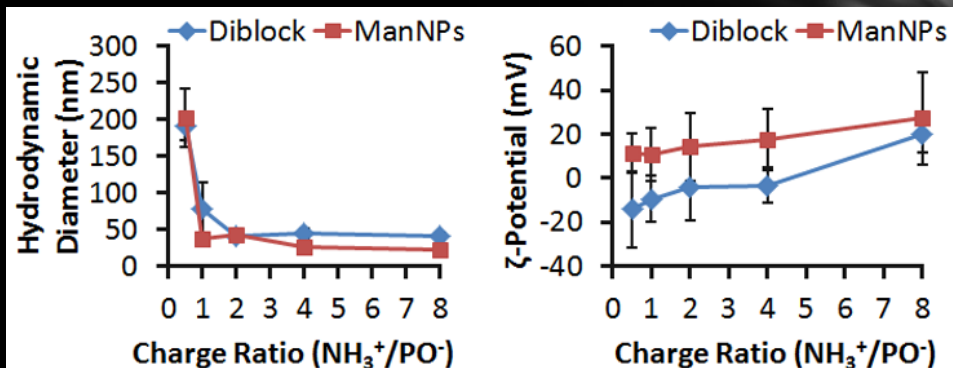
Manufacturer-provided chemical structure of pMan-FITC (Glycotech).



NMR Characterization of Polymers

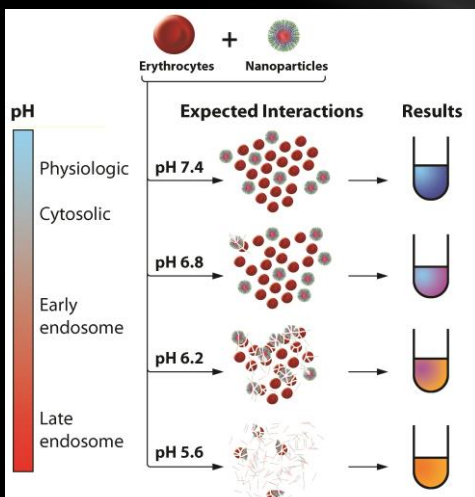


NP Size and ζ -Potential After Loading w/ siRNA



Design & Synthesis Controlled Release In Vitro Assays In Vivo Behavior

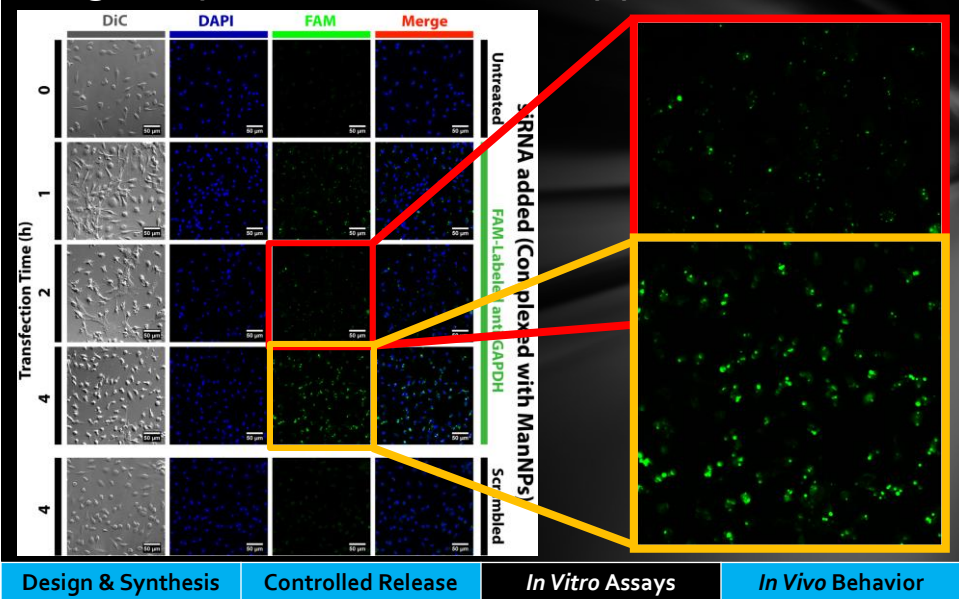
Using the Hemolysis Assay to Model Endosome-Nanoparticle Interactions



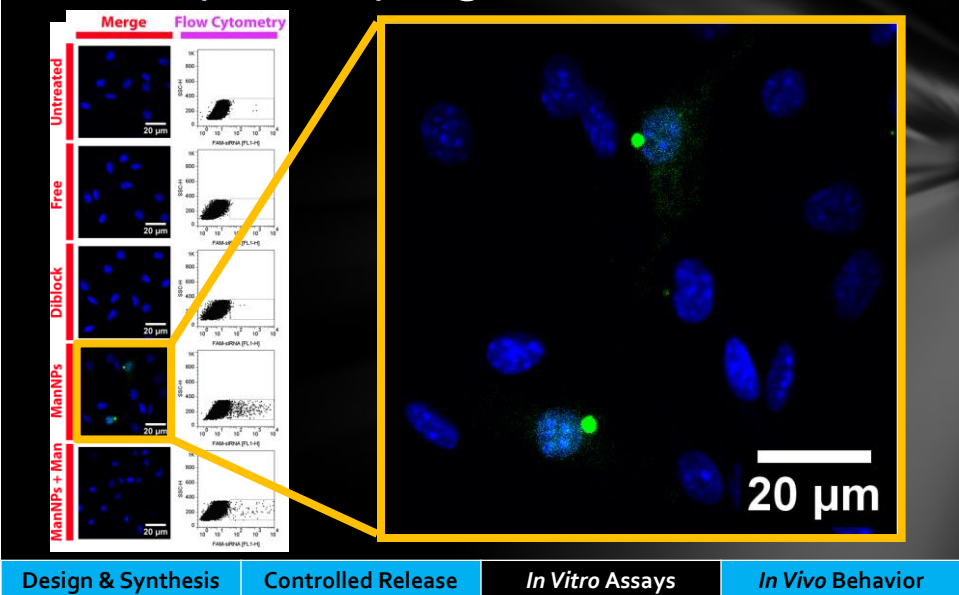
BC Evans, CE Nelson, SS Yu, et al. (2012) *J Visualized Exp.* (in press).

Design & Synthesis Controlled Release In Vitro Assays In Vivo Behavior

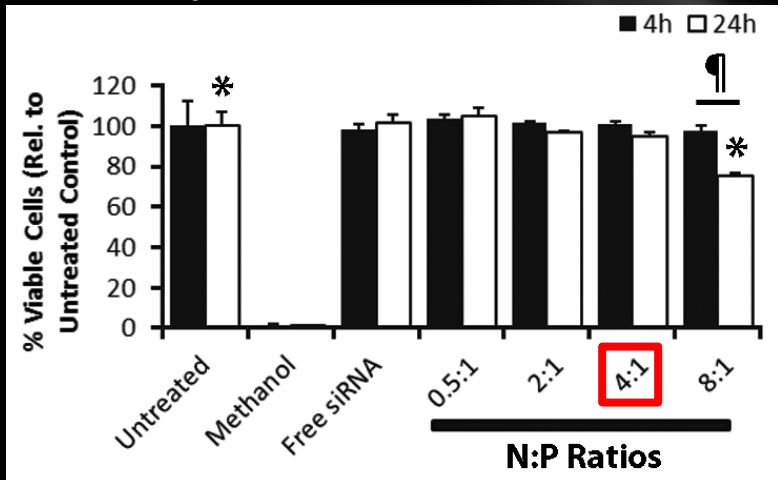
Kinetics of Primary Macrophage Transfection Imaged by Confocal Microscopy



ManNPs Enhance siRNA Delivery Into Primary Macrophages



siRNA-Loaded ManNPs Exhibit Low Cytotoxicity at N:P < 8:1



Cell model = THP-1 (immortalized human macrophages); *, ¶ p < 0.01 / n = 3

siRNA dose = 50 nM S.S. Yu et al. (2012) *Molecular Pharmaceutics* (Revisions requested).

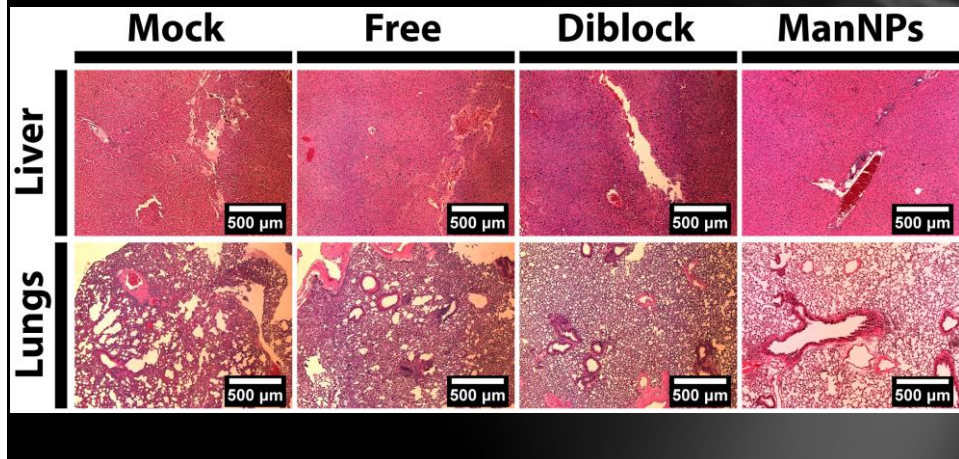
Design & Synthesis

Controlled Release

In Vitro Assays

In Vivo Behavior

No Significant Changes in Lungs / Liver Morphology within 24 h



Design & Synthesis

Controlled Release

In Vitro Assays

In Vivo Behavior

Reprogramming Tumor Associated Macrophages toward an Anti-Tumor Phenotype by Targeting the NF-κB Pathway Using Novel Targeted Nanotherapeutics

Ryan Ortega, Whitney Barham, Bharat Kumar, Shann Yu, Fiona Yull, and Todd Giorgio

Tumor associated macrophages (TAMs) can modify the tumor microenvironment to create an inflammatory, pro-tumor niche. Activation of the NF-κB pathway has been implicated in creating a pro-tumor phenotype in TAMs. Manipulation of TAM phenotype is a new approach to engage anticancer immunity, but has been limited by a lack of methods capable of therapeutic delivery to TAMs *in vivo*. We have successfully utilized mannosylated polymer nanoparticles capable of disrupting the endosomal compartment to deliver siRNA for RNAi of NF-κB proteins into bone marrow derived macrophages (BMDMs) derived from transgenic mice with a GFP/Luciferase reporter of NF-κB activity (NGL). In *in vitro* studies, the nanoparticles are comparable to commercial transfection agents using both gene and protein level readouts for knockdown. The transfection protocol utilizing these novel vehicles has been optimized with respect to transfection time, siRNA dose, and siRNA:polymer ratio with the intent to inform *in vivo* experiments. The presence of serum does not significantly affect transfection efficiency *in vitro*, presumably due to an almost neutral particle surface charge. Preliminary *in vivo* studies have revealed no significant particle toxicity. Delivering siRNA specific to the p52/p100 protein in the alternative pathway achieves knockdown of total NF-κB activity by approximately 80% in NGL BMDMs stimulated by TNF- α . By targeting proteins in the classical pathway, we have decreased total NF-κB activity by approximately 50% in the same model. While inhibition of NF-κB activity may be desirable in some contexts, we recently reported that induced activation of NF-κB in macrophages can result in anti-tumor activity. We have delivered a liposomal formulation of muramyl tripeptide (Mifamurtide), a synthetic derivative of a bacterial cell wall peptide and an activator of macrophages, to NGL BMDMs. Mifamurtide delivery increases both NF-κB activity, and the production of reactive oxygen species, indicating a preliminary mechanistic explanation for the therapeutic potential of NF-κB activation. Mifamurtide is used clinically in the European Union to treat osteosarcoma, potentially providing an avenue for rapid clinical translation of NF-κB modulating therapy for other tumor types. However, Mifamurtide has the potential to activate multiple pathways simultaneously. A more elegant approach would be to target knockdown of an NF-κB inhibitor to macrophages to mediate pathway specific activation. In preliminary studies we have demonstrated the ability to increase total NF-κB activity by treating NGL macrophages with nanoparticles carrying siRNA against the IκB α inhibitor of NF-κB. Our data provides evidence that delivering siRNA specifically to macrophages to modulate their functions using nanoparticles has potential as a therapeutic approach to cancer treatment.

Reprogramming Tumor Associated Macrophages toward an Anti-Tumor Phenotype by Targeting the NF- κ B Pathway Using Novel Targeted Nanotherapeutics



VANDERBILT
School of Engineering

Ryan A. Ortega^{1,2}, Whitney Barham², Bharat Kumar¹, Shann S. Yu³, Fiona Yull², Todd D. Giorgio^{1,2}

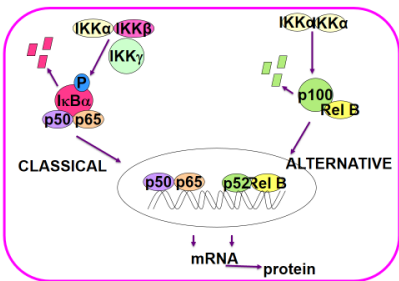
¹Department of Biomedical Engineering, Vanderbilt University, Nashville, TN, ²Department of Cancer Biology, Vanderbilt University Medical Center, Nashville TN

³École Polytechnique Fédérale de Lausanne

laboratory for
bionanotechnology
AND
nanomedicine

NF- κ B is a promising target for therapeutic manipulation of tumor associated macrophages (TAMs)

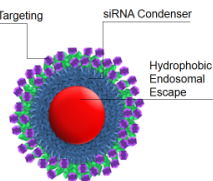
- NF- κ B is implicated in creating a TAM phenotype
- Characterized by constant low levels of inflammation, the recruitment of pro-tumorigenic cells, and the restructuring of local tissue.
- Classical and alternative NF- κ B activation offer highly varied therapeutic targets and effects, specific to each pathway



- Knocking down key NF- κ B proteins with targeted nanotherapeutics could wipe out the TAM phenotype
- Selectively activating a cytotoxic (M1) phenotype could produce a strong anti-tumor inflammatory response that is local and transient

Nanotherapeutic schemes

Targeted nanoparticle (Mn-NP) for gene knockdown

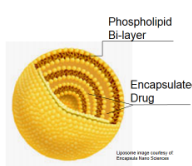


- Mannosylated surface targets the macrophage specific mannose receptor

- Mild surface charge allows for longer transfection times, high biocompatibility, and *in vivo* relevance

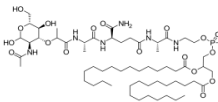
- Endosomal pH activates nanoparticle to disrupt endosome and release functional siRNA

Multilamellar liposome for drug delivery



- Liposome ensures preferential uptake by macrophages

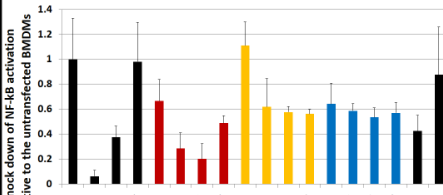
- Encapsulated drug, muramyl tripeptide phosphatidylethanolamine (L-MTP-PE), is a synthetic analog of a bacterial protein. Used clinically in the EU to treat osteosarcoma.



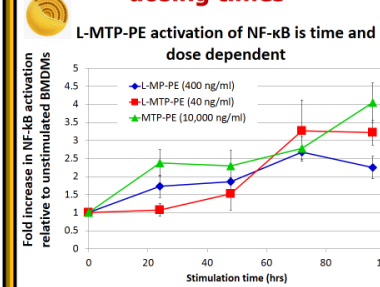
In vitro bone marrow derived macrophage (BMDMs) culturing and transfection procedure

- Bone marrow was harvested from the femurs of NGL reporter mice on an FVB background.
- NGL mice express luciferase and GFP as a reporter of total NF- κ B activity.
- Bone marrow is cultured in media containing a supplemental source of M-CSF for 6 days.
- BMDMs are transfected with siRNA (10 nM) using commercial agent, Lipofectamine (2 μ l/ml), or using nanoparticles (4 μ g/ml); or cells are stimulated with an NF- κ B activating agent.
- Cells are transfected for 24 hours on a rocking platform (10 rocks per minute)
- For siRNA transfected cells: After 6 hrs of transfection, cells are stimulated with TNF- α for 6 hrs to elicit strong NF- κ B activation.
- For drug stimulated cells: Cells are exposed to L-MTP-PE or other agent for varying time points. Cells are dosed every 24 hours and media is refreshed.

siRNA successfully decreases luciferase as a readout of NF- κ B

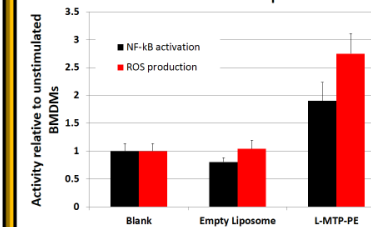


Controlled *in vitro* activation of NF- κ B requires longer dosing times



- Liposomal encapsulation of muramyl tripeptide increases its stimulatory effect more than 100 fold

Stimulation of BMDMs with L-MTP-PE (400 ng/ml, 24 hrs) shows an increase in NF- κ B activation and ROS production



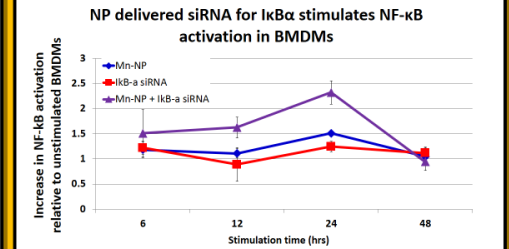
Acknowledgments

This work was made possible in part by a grant from the United States Department of Defense's (USDoD) Congressionally Directed Medical Research Programs (CDMRP) Breast Cancer Research Program (BCRP): Grant BC102696.

Lung macrophages with constitutively activated IKK2 isolated from murine lung upregulate inflammatory cytokines

Gene	Fold-Change	Function
Cxcl9	11.89	Inflammation
Mpa2l	11.84	Macrophage activation
Ccl8	6.55	Inflammation
Gzma	5.78	Apoptosis
IL-27	5.31	Inflammation
Stat1	5.05	Apoptosis
CXCL10	3.91	Inflammation

Knock down of the IκB inhibitor protein using Mn-NP activates the classical NF- κ B pathway



- The transfection times necessary to effectively stimulate NF- κ B by knocking down IκBα with siRNA are impossible to achieve using commercial agents

Conclusions

- NF- κ B specific siRNA are capable of knocking down specific pathway proteins
- Mannosylated nanoparticles exhibit transfection efficiencies comparable to commercial agents
- Using a clinical agent, strategic NF- κ B activation correlates to an increase in ROS.
- Targeted activation was achieved via Mn-NP mediated delivery of siRNA for the IκBα inhibitor protein.

Impact

The novel mannosylated nanoparticles presented here are a promising therapeutic tool for targeted *in vivo* manipulation of macrophage phenotype.

AACR Abstract

Title: Education of macrophages through modulation of NF-kappaB: an opportunity for targeted therapy

Authors: Whitney Barham¹, Oleg Tikhomirov¹, Lianyi Chen¹, Ryan Ortega¹, Linda Gleaves¹, Halina Onishko¹, Taylor Sherrill¹, Yu S¹, Linda Connelly², Giorgio TD¹, Timothy S. Blackwell¹, Fiona E. Yull¹. ¹Vanderbilt-Ingram Cancer Ctr., Nashville, TN; ²University of Hawaii at Hilo, Hilo, HI

Abstract:

Macrophages are a plastic cell type, capable of adapting to numerous signals within their environment. As part of the innate immune system, macrophages were traditionally considered anti-tumor (M1), but it has been well established that macrophages can also help to create a pro-tumor, pro-metastatic tumor niche (M2). NF-κB transcription factors can regulate both pro-(MMP's, VEGF) and anti-tumor (iNOS) downstream targets within macrophages, suggesting that modulation of NF-κB may play a role in the two different macrophage phenotypes. However, our understanding of NF-κB signaling specifically within macrophages during tumor progression is limited. To this end, we have developed murine transgenic models that enable us to induce expression of an activator or dominant inhibitor of NF-κB in macrophages by adding doxycycline to the drinking water of mice. We have combined these novel transgenics with the polyoma model of mammary cancer for our studies.

We have recently shown that activation of NF-κB in macrophages significantly limits metastasis in a tail vein model of tumor progression. In this model, constitutive IKK2 activity within macrophages leads to an anti-tumor immune response including altered immune cell populations within the lung microenvironment, changes in chemokine and cytokine expression and rapid killing of tumor cells during the seeding phase mediated by reactive oxygen species. Our current work has extended these findings to an orthotopic mammary tumor model. Again, we find that activation of NF-κB in macrophages results in decreased primary tumor growth and decreased tumor seeding into the blood. To model this activation *in vitro*, we have utilized immortalized bone marrow derived macrophages from IκBα knock-out mice compared to a wild type line. IκBα KO macrophages display changes in morphology and adhesion relative to wild type macrophages. This correlates with increased cytotoxic behavior in co-culture with polyoma tumor cells, mirroring the *in vivo* phenotype of the cIKK2 expressing macrophages. Given these findings, we believe that targeted activation of NF-κB signaling in macrophages could be harnessed to overcome the education of macrophages by tumor cells, and could be exploited as a novel targeted therapy.

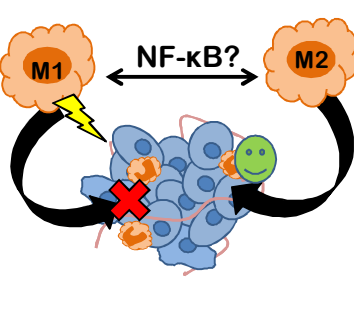
Abstract #1545

Education of macrophages through modulation of NF- κ B: an opportunity for targeted therapy

Whitney Barham¹, Oleg Tikhomirov¹, Lianyi Chen¹, Ryan Ortega¹, Linda Gleaves¹, Halina Onishko¹, Taylor Sherrill¹, Shann Yu¹, Linda Connelly², Todd D. Giorgio¹, Timothy S. Blackwell¹, Fiona E. Yull¹. ¹Vanderbilt-Ingram Cancer Ctr., Nashville, TN; ²University of Hawaii at Hilo, Hilo, HI

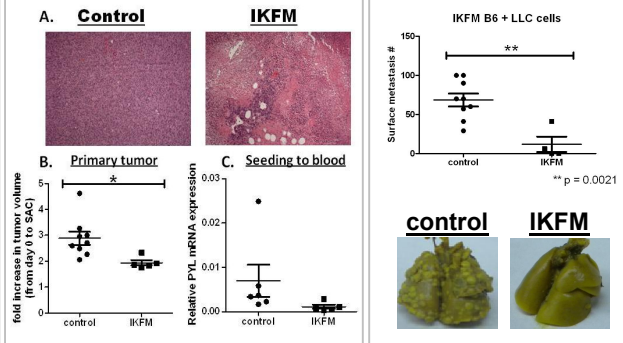
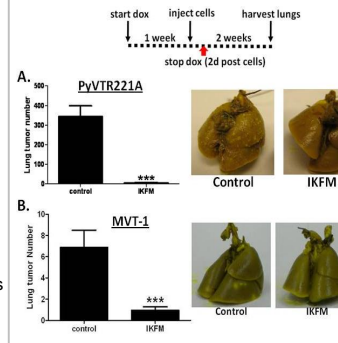
Motivation

Macrophages are a plastic cell type, capable of adapting to numerous signals within their environment. As part of the innate immune system, macrophages were traditionally considered anti-tumor (M1), but it has been well established that macrophages can also help to create a pro-tumor, pro-metastatic tumor niche (M2). NF- κ B transcription factors can regulate both pro-(MMP β , VEGF) and anti-tumor (iNOS) downstream targets within macrophages, suggesting that modulation of NF- κ B may play a role in the two different macrophage phenotypes. However, our understanding of NF- κ B signaling specifically within macrophages during tumor progression is limited.

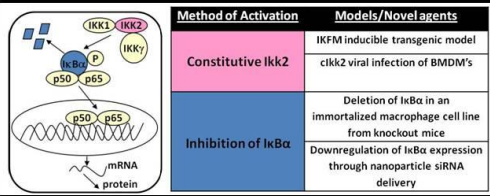


Results

Macrophages expressing cIKK2 prevented tumor seeding in a tail vein metastasis model and inhibited tumor growth in primary mammary orthotopic tumors. This anti-tumor phenotype was also apparent in a tail vein assay which utilized Lewis Lung Carcinoma cells (LLCs).

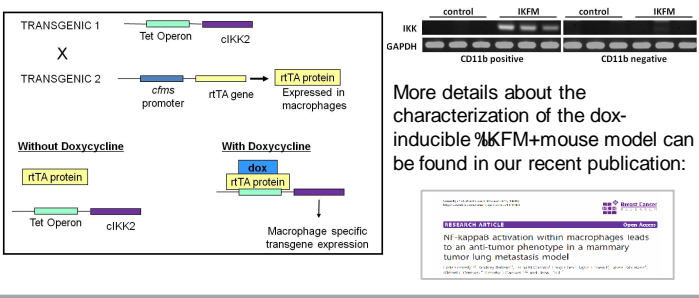


Methods

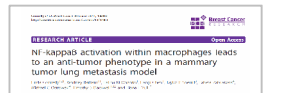


Using a variety of approaches, we can activate NF- κ B specifically within macrophages both *in vitro* and *in vivo*. With these models, we can determine how increased levels of NF- κ B signaling affects macrophage phenotype and ultimately, tumor progression.

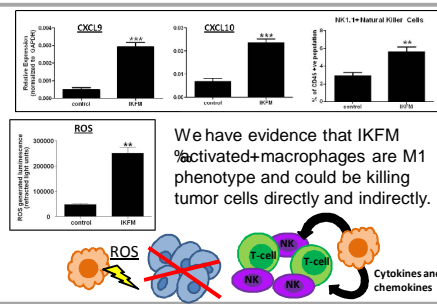
We have generated a novel, transgenic mouse model to activate NF- κ B signaling within macrophages *in vivo*. Transgene expression is tissue specific and doxycycline inducible.



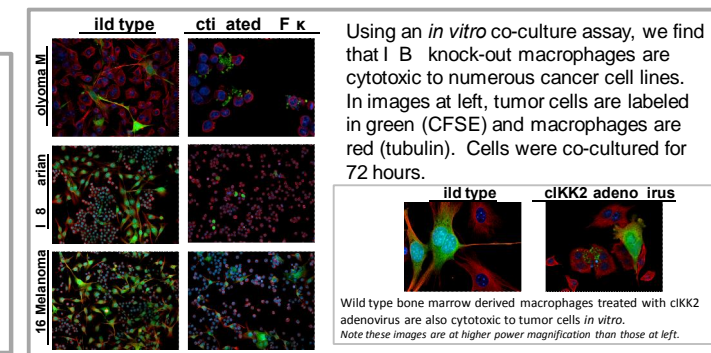
More details about the characterization of the dox-inducible IKFM+mouse model can be found in our recent publication:



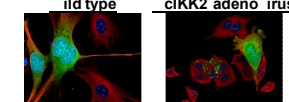
Mechanism



We have evidence that IKFM activated+macrophages are M1 phenotype and could be killing tumor cells directly and indirectly.



Using an *in vitro* co-culture assay, we find that I κ B knock-out macrophages are cytotoxic to numerous cancer cell lines. In images at left, tumor cells are labeled in green (CFSE) and macrophages are red (tubulin). Cells were co-cultured for 72 hours.

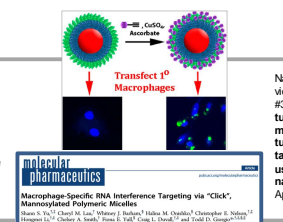


Wild type bone marrow derived macrophages treated with cIKK2 adenovirus are also cytotoxic to tumor cells *in vitro*. Note these images are at higher power magnification than those at left.

Conclusions

Contrary to the largely pro-tumor role that NF- κ B signaling plays within epithelial cells, our data indicates that activation of this pathway specifically within macrophages endows them with *anti-tumor* characteristics. This finding has extremely significant implications for a broad range of cancers and other disease states.

So far, we have obtained these data using genetically modified murine and cell culture models. Therapeutics that could modulate NF- κ B specifically in macrophages are the next logical step.



Nanoparticle data can be viewed by viewing poster #3881 - *Anti-promoting tumor associated macrophages to aid an anti tumor p. eotype by targeting the Fc p. ay using no el targeted nanop. erapeutics*. Tuesday, Apr 09, 1:00 - 5:00 PM

VANDERBILT UNIVERSITY MEDICAL CENTER

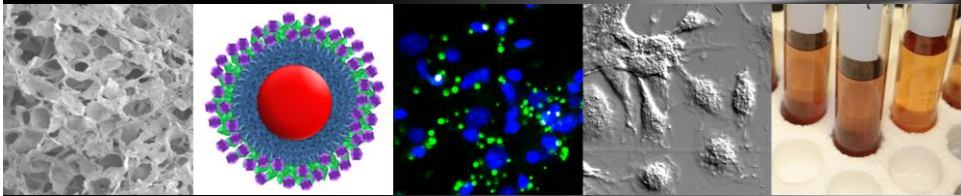
Comprehensive Clinical Medical Research Program

CDMRP Department of Defense

NATIONAL CANCER INSTITUTE

molecular pharmacology
Macrophage-Specific RNA Interference Targeting via "Click".
Hong J, Yu X, Yull FE, Yell J, Sogami M, Capillo C, Christopher E, Nelson JZ, Haugen LS, Cheley A, Smith P, Penn E, Yull F, Cong L, Dardik A, and Todd D. Giorgio^{1,2,3}

Biofunctional nanomaterials for the modulation of macrophage phenotype and polarization



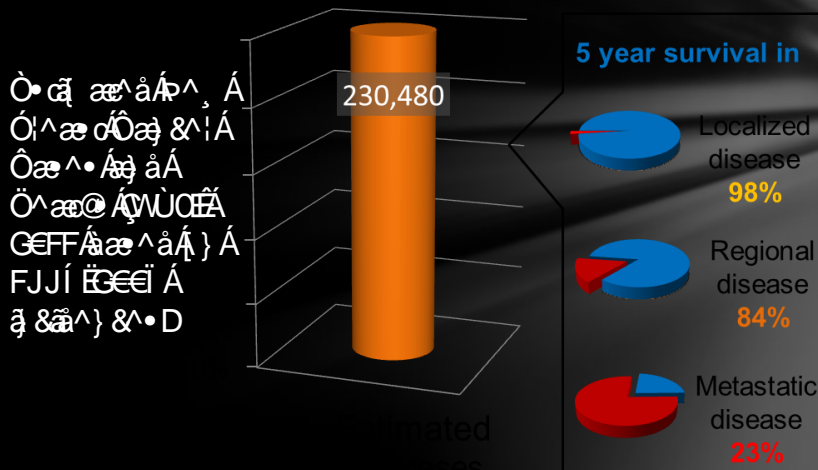
Todd Giorgio

Departments of Biomedical Engineering and Cancer Biology

29 April 2013

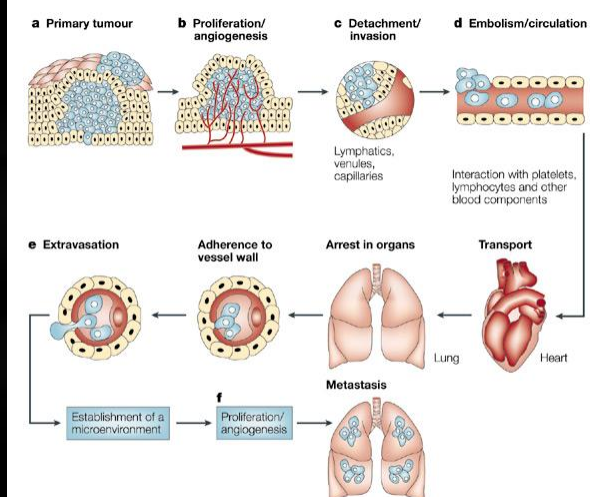
University of Minnesota, Department of Biomedical Engineering

Tumor Metastasis: Treatment Failure Reduces Five-Year Survival Rate



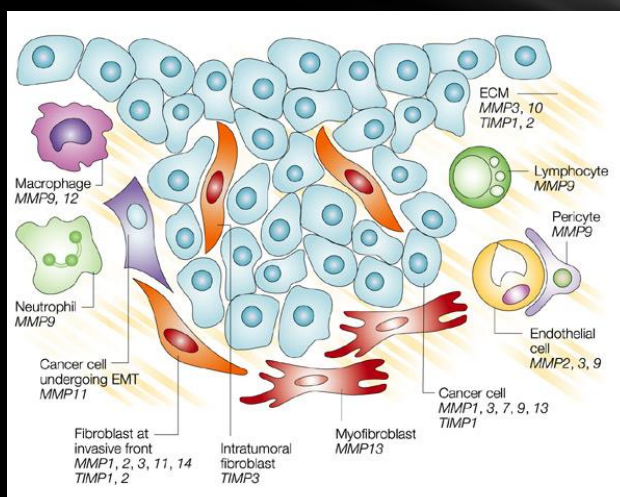
Direct Treatment of Distributed Disease (Metastases) is Systemic, not Local

- “ Complete surgical resection is associated with good clinical outcomes (a)
- “ Distributed disease occurs broadly and may also be below the threshold of detection (f)
- “ Treat metastases using systemically administered therapies
- “ Selection pressure results in tumor cells resistant to cytotoxic therapy
- “ ***But the tumor is also composed of non-tumor cells***



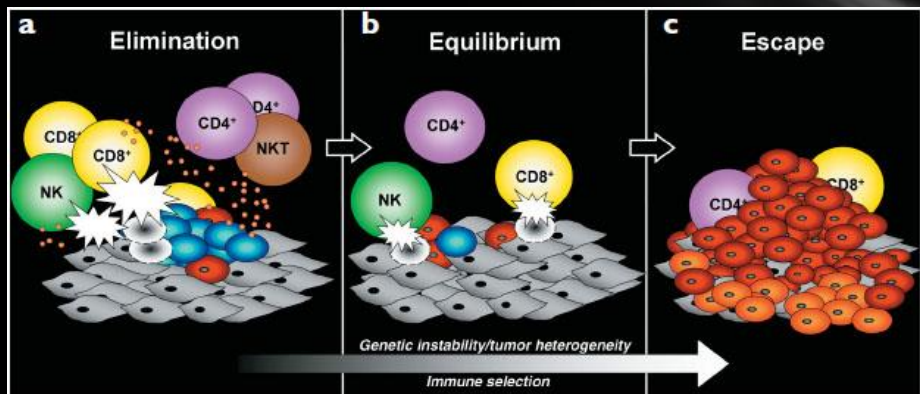
Nature Reviews | Cancer

Tumor Stroma is Composed of Immune Cells, Secreted Modulators and Substrate



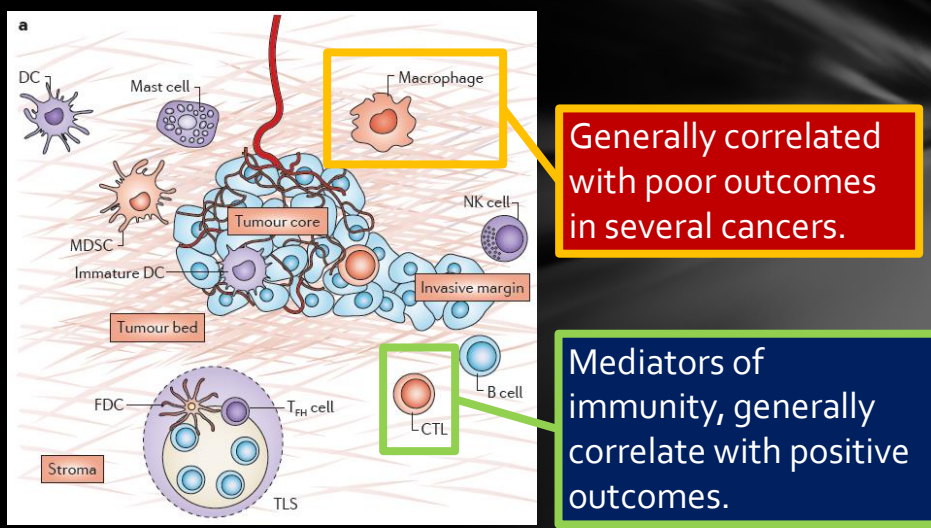
Egeblad, M. & Werb, Z., 2002. New functions for the matrix metalloproteinases in cancer progression. *Nat Rev Cancer*, 2(3), pp.161–174.

Disease Progression = Failure of Anti-Cancer Immunity



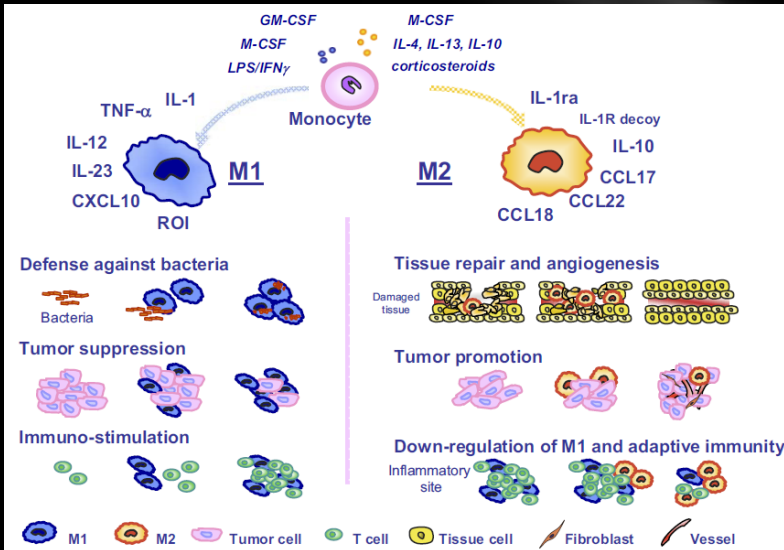
GP Dunn et al. (2007) *Nature Immunol.*

Various Tumor-Infiltrating Immune Cell Subtypes Play Different Roles In Tumors



Fridman et al. (2012) *Nat Rev Cancer.*

Macrophages Are Multifunctional Cells That Have Been 'Hijacked' In Cancer



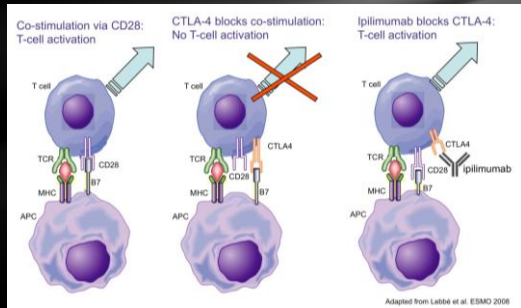
G. Solinas et al. (2009) *J. Leukocyte Biol.* 86: 1066.

Re-polarization of Tumor-Associated Macrophages Reactivates an Anti-Tumor Immune Response

- C. Guiducci et al. (2005) *Cancer Research*
- A. Saccani et al. (2006) *Cancer Research*
- T. Hagemann et al. (2008) *J Exp Med*
- G.L. Beatty et al. (2011) *Science*

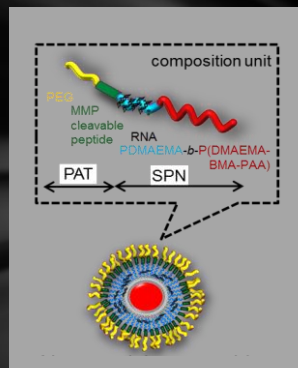
Modulate Macrophages Locally: WHY?

- Example: Cancer Immunology
 - “ Acute inflammation = anti-tumor microenvironment
 - “ Chronic inflammation = pro-tumor microenvironment
- “ New therapeutics intended to stimulate anti-cancer immunity possess significant self-recognition consequences
- “ What about siRNA?
- “ Limitations might be relieved with localized delivery to specific cells, tissues



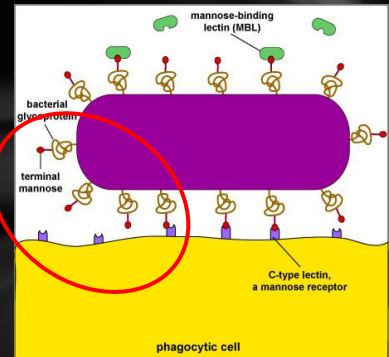
Design of Nanomaterials?

- Engineering approaches enable the principled design of nanomaterials to provide specific and unique functions *in vivo*
- Multiple, co-localized functions, including site-specific activation
- Generation of ‘smart’ materials
- TODAY: Modulate the phenotype of tumor associated macrophages (TAMs) – but **not** macrophages localized in other tissues



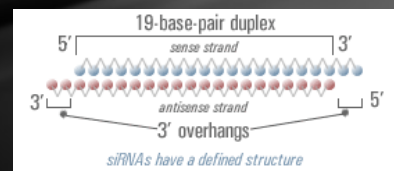
Design of Materials: TAM Modulation

- RAFT polymerization enables controlled size appropriate for EPR
- Surface functionalization enables macrophage-specific binding: mannose
- Cationic layer for siRNA condensation / protection
- pH responsive endosomolysis
- Hydrophobic core as a drug reservoir

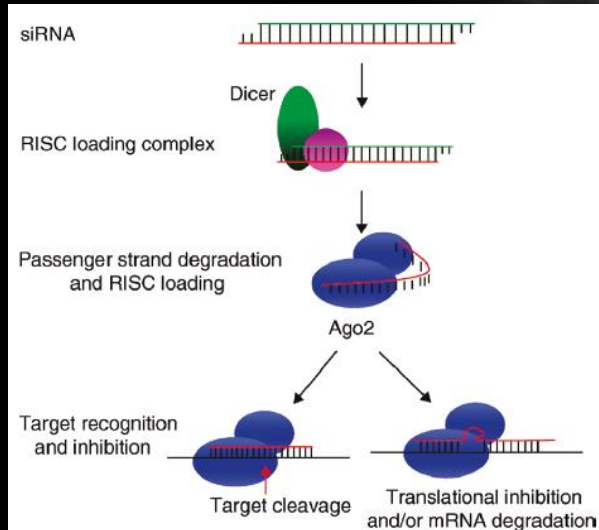


Design of Materials: TAM Modulation

- RAFT polymerization enables controlled size appropriate for EPR
- Surface functionalization enables macrophage-specific binding: mannose
- Cationic layer for siRNA condensation / protection
- pH responsive endosomolysis
- Hydrophobic core as a drug reservoir



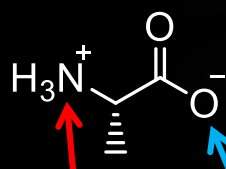
Reprogramming TAMs with siRNA: Silencing Pathologic Gene Pathways



MG Stanton & SL Colletti. (2010) *J Medicinal Chem*, 53: 7887-7901.

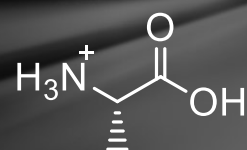
pH-Responsive Polymers are Inspired by Lessons from Nature

pH = 7.4



NET CHARGE = NEUTRAL!!!

pH < 2.3



NET CHARGE = POSITIVE

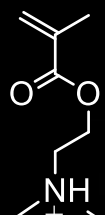
Design & Synthesis

Controlled Release

In Vitro Assays

In Vivo Behavior

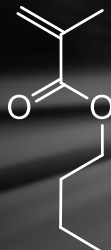
pH-Responsive, Endosomolytic Polymers: Rational Monomer Selection



DMAEMA
pKa ~ 7.5



PAA
pKa ~ 6.7

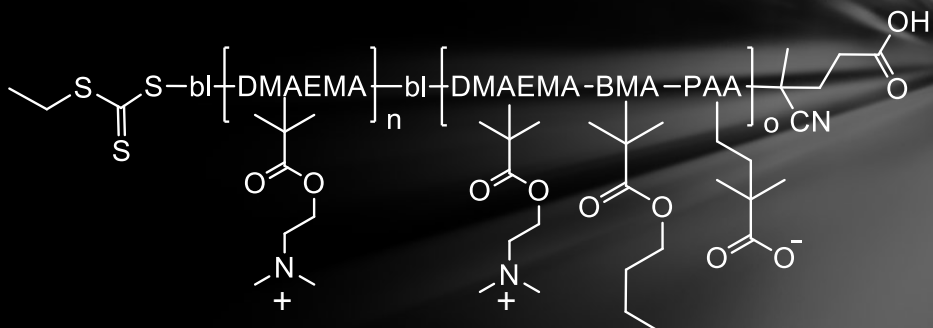


Hydrophobic comonomer

S Grainger & MEH El-Sayed. (2010) in **Biologically Responsive Hybrid Biomaterials**, E Jabbari & A Khademhosseini (Eds.): 171-190.
 AJ Convertine et al. (2009) **J Controlled Release**.

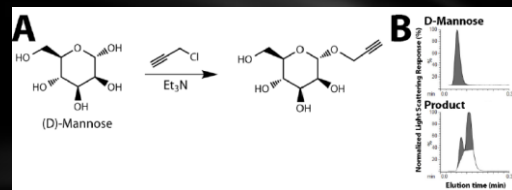
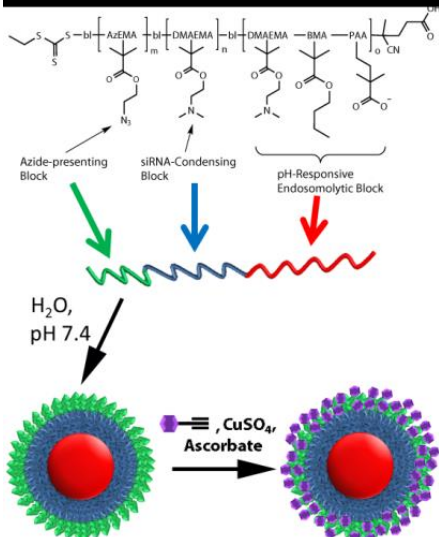
Design & Synthesis	Controlled Release	In Vitro Assays	In Vivo Behavior
--------------------	--------------------	-----------------	------------------

Hydrophobic Polymer + pH-Responsive Polymer = Amphiphilic Block Copolymer



Design & Synthesis	Controlled Release	In Vitro Assays	In Vivo Behavior
--------------------	--------------------	-----------------	------------------

Triblock Polymer With 'Clickable' Corona for Mannose Decoration



- Mannose binds to CD206 (mannose receptor)

- ✓ Expressed near-exclusively on macrophages and DCs
- ✓ Upregulated in tumor-associated macrophages
- ✓ Facilitates endocytosis

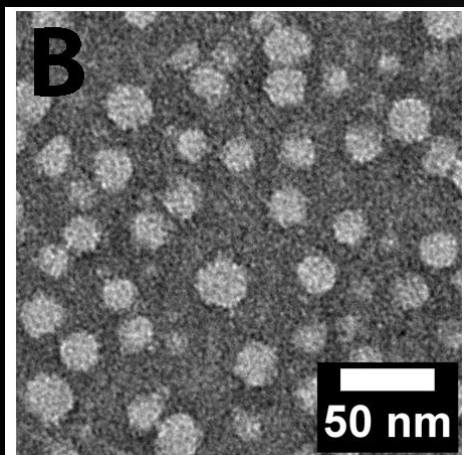
Design & Synthesis

Controlled Release

In Vitro Assays

In Vivo Behavior

Copolymers Self-Assemble into Micelles With Appropriate Size for EPR



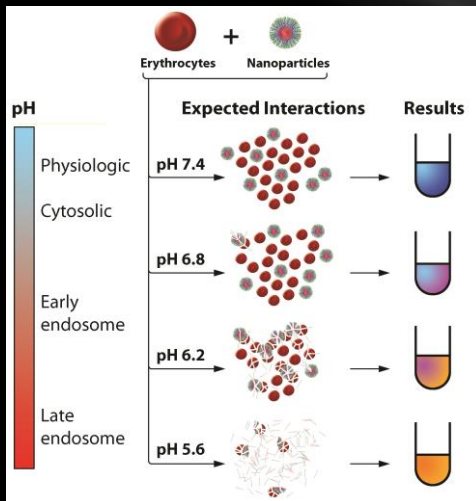
Design & Synthesis

Controlled Release

In Vitro Assays

In Vivo Behavior

Hemolysis Assay to Model Endosome-Nanoparticle Interactions



BC Evans, CE Nelson, SS Yu, et al. (2012) *J Visualized Exp.* (in press).

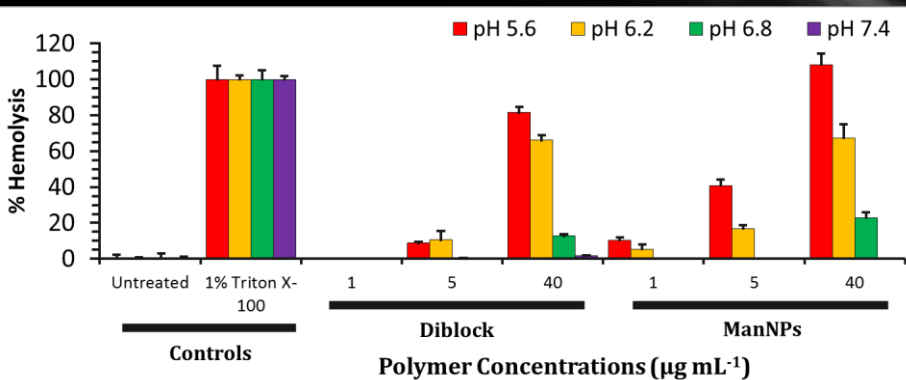
Design & Synthesis

Controlled Release

In Vitro Assays

In Vivo Behavior

Diblocks and ManNPs Exhibit pH-Responsive Hemolysis



S.S. Yu et al. (2012) *Molecular Pharmaceutics* (Accepted).

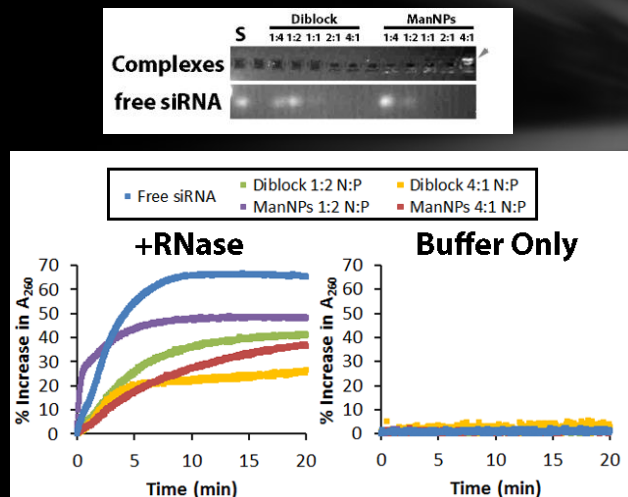
Design & Synthesis

Controlled Release

In Vitro Assays

In Vivo Behavior

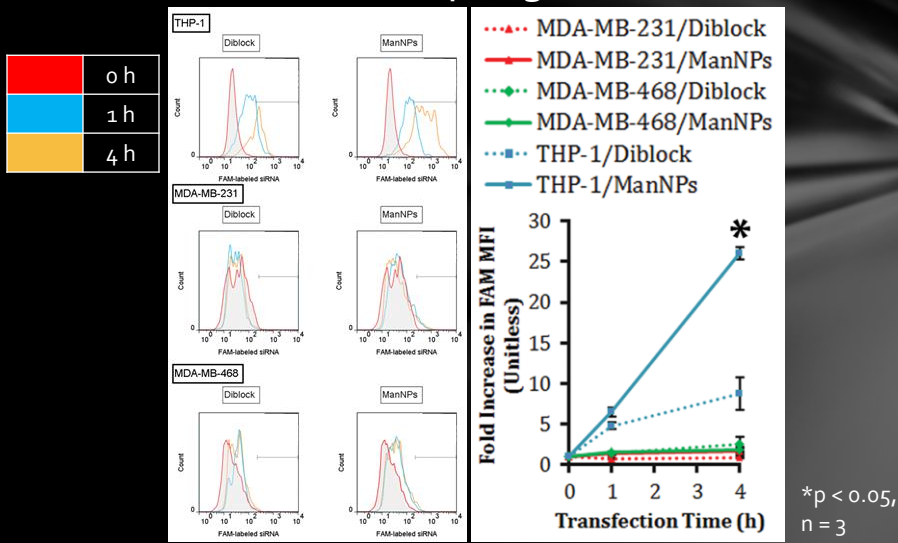
ManNPs Electrostatically Complex siRNA and Protect it from RNases



S.S. Yu et al. (2012) Molecular Pharmaceutics (Accepted).

Design & Synthesis **Controlled Release** **In Vitro Assays** **In Vivo Behavior**

ManNPs Enhance siRNA Delivery into Immortalized Macrophages



Design & Synthesis **Controlled Release** **In Vitro Assays** **In Vivo Behavior**

Uptake Assays: Methods

■ Cell source¹

- “ FVB mice (albino; wild-type)
- “ Bone marrows excised from adults and flushed
- “ Bone marrow cells differentiated *in vitro* for 6 days in M-CSF-rich media

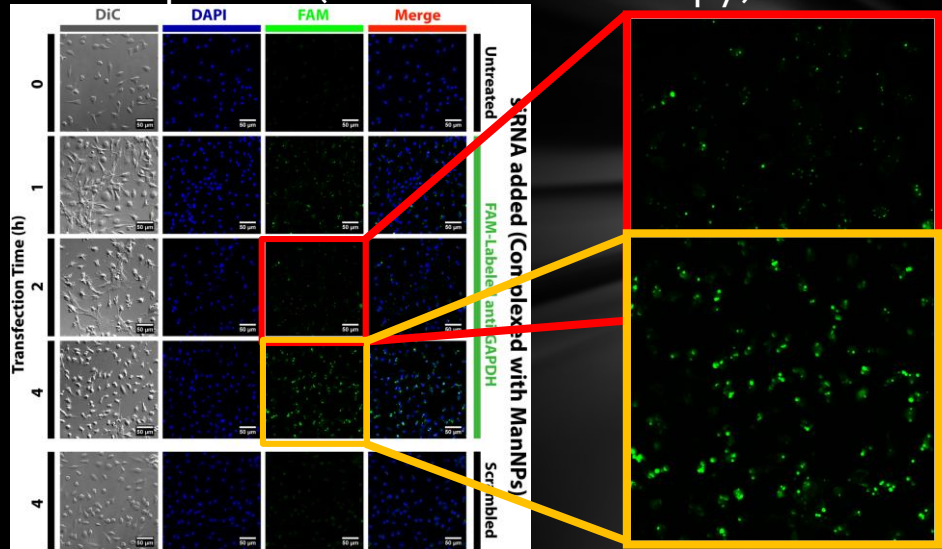
■ Nanoparticles/siRNA

- “ FAM-labeled siRNA (FAM = similar to fluorescein)
- “ Electrostatically complexed with polymers at N:P = 4:1
- “ Added to cells at final [siRNA] = 50 nM

¹ J. Weischenfeldt & B. Porse. (2008) *Cold Spring Harb Protoc* pdb.prot5080.

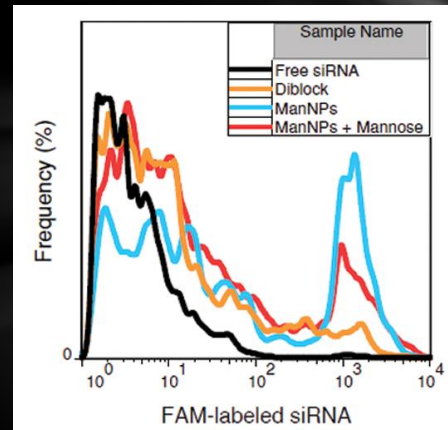
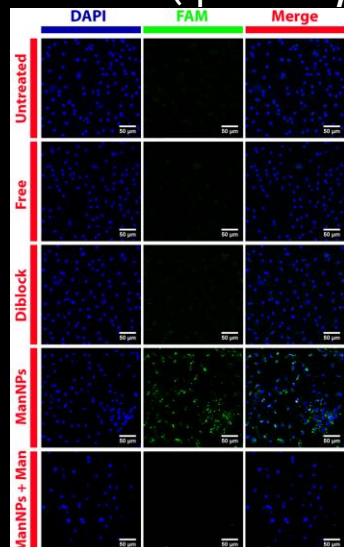
Design & Synthesis Controlled Release In Vitro Assays In Vivo Behavior

Extensive siRNA Delivery into BMDMs After 4 Hours (Confocal Microscopy)



Design & Synthesis Controlled Release In Vitro Assays In Vivo Behavior

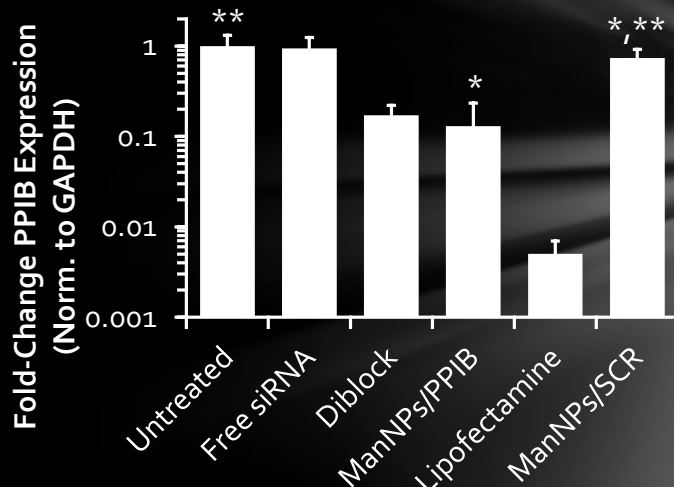
ManNPs Enhance siRNA Delivery into BMDMs (4 Hours, Flow Cytometry)



S.S. Yu et al. (2013) *Molecular Pharmaceutics* (Accepted).

Design & Synthesis Controlled Release In Vitro Assays In Vivo Behavior

siRNA/ManNPs Knock Down Target Gene Expression



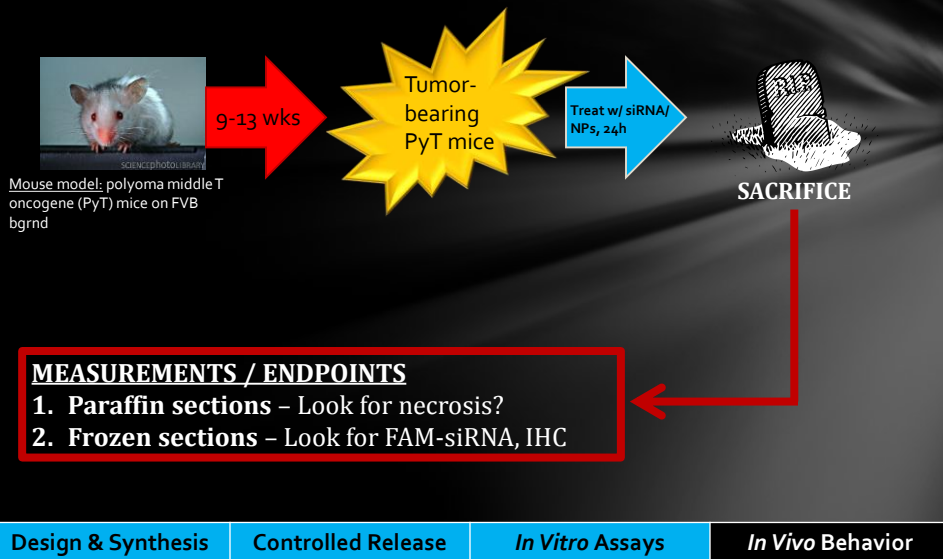
*p < 0.05; n = 3

** p > 0.05; n = 3

S.S. Yu et al. (2013) *Molecular Pharmaceutics* (Accepted).

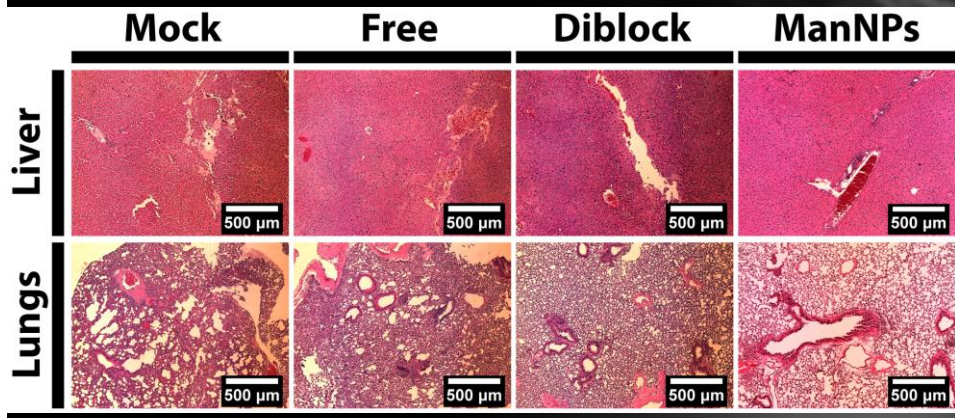
Design & Synthesis Controlled Release In Vitro Assays In Vivo Behavior

In Vivo Biodistribution of ManNPs in Primary Tumor Model



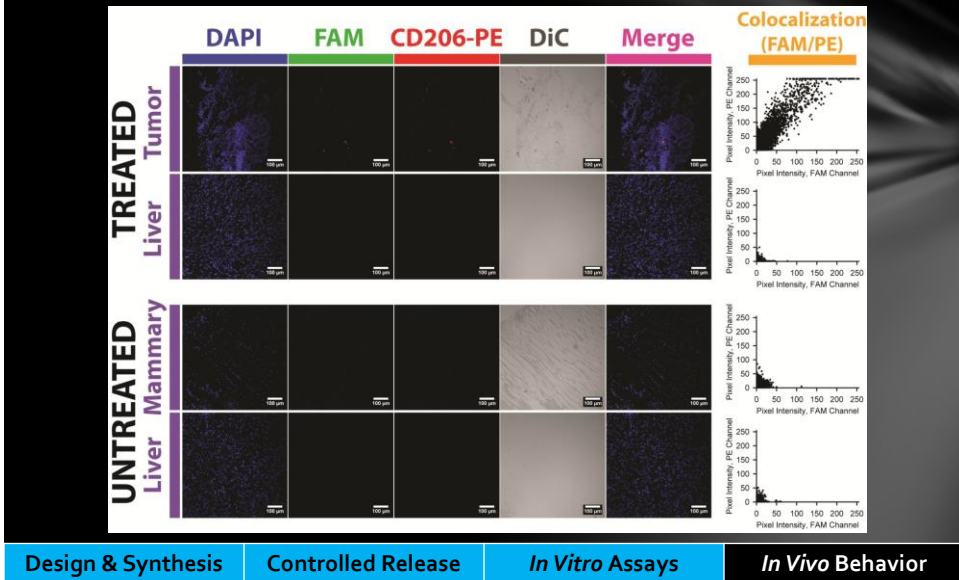
Design & Synthesis Controlled Release *In Vitro* Assays *In Vivo* Behavior

No Significant Changes in Lung / Liver Morphology within 24 h

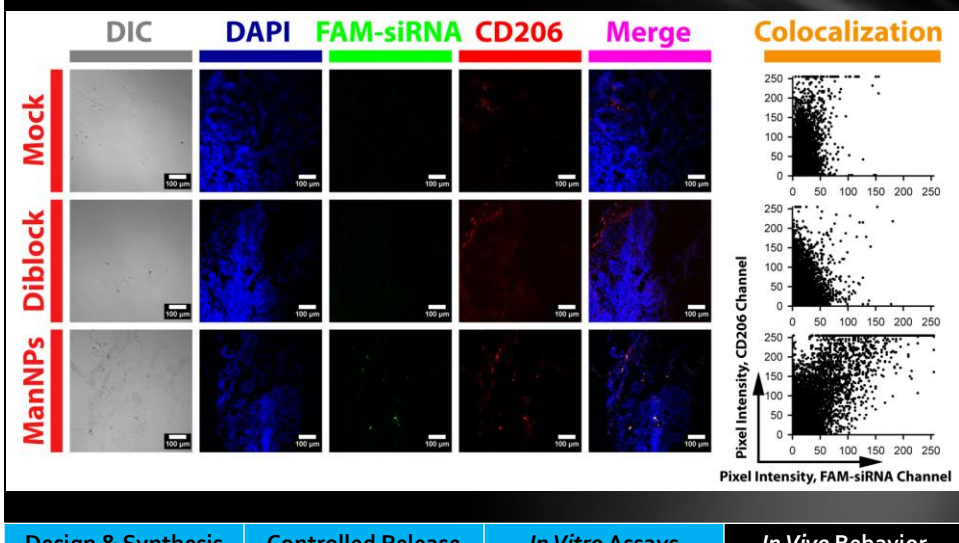


Design & Synthesis Controlled Release *In Vitro* Assays *In Vivo* Behavior

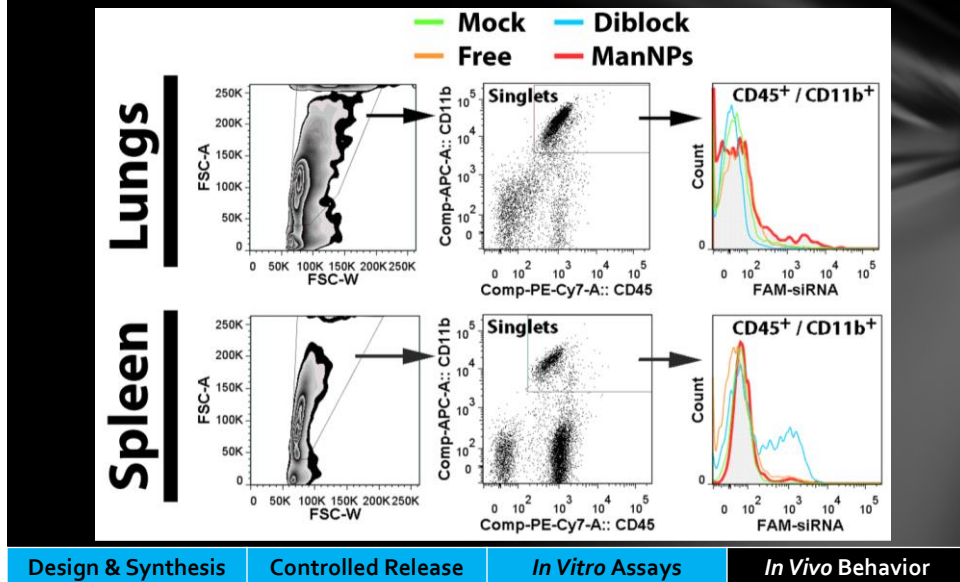
ManNPs Target CD206⁺ Cells in Primary Tumor Model



ManNPs Target CD206⁺ Cells in Primary Tumor Model



Nanoparticles are Also Found in Leukocytes from the Lung and Spleen



Design & Synthesis

Controlled Release

In Vitro Assays

In Vivo Behavior

In Vivo Biodistribution of ManNPs in Metastatic Tumor Model



MEASUREMENTS / ENDPOINTS

1. Flow cytometry – FAM-siRNA localization?

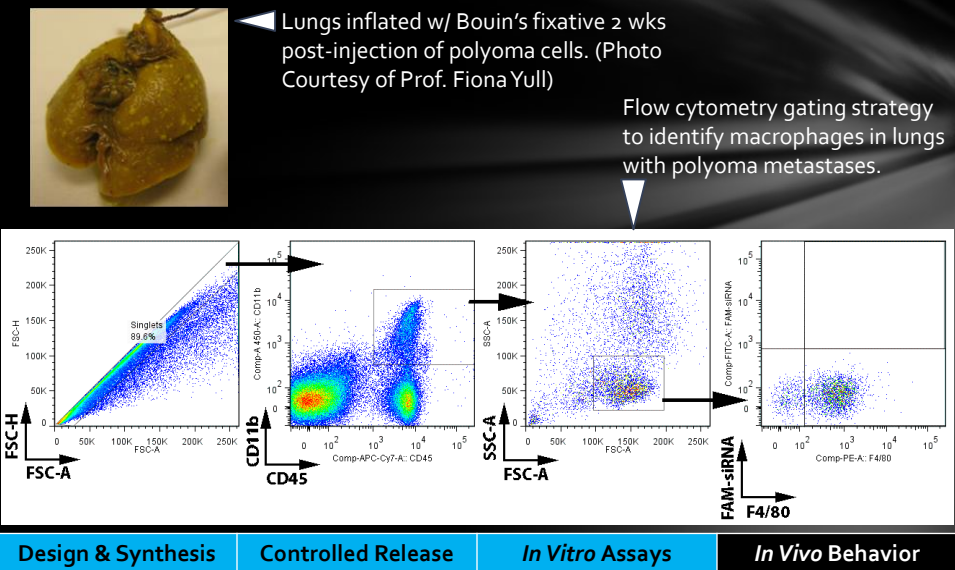
Design & Synthesis

Controlled Release

In Vitro Assays

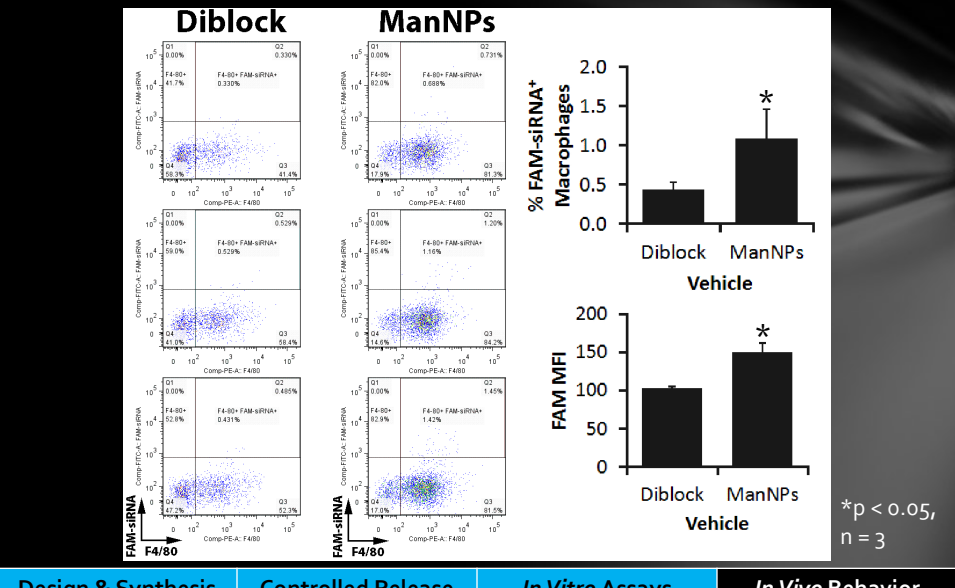
In Vivo Behavior

Macrophages from Lung Metastases can be Quantified by Flow Cytometry



Design & Synthesis **Controlled Release** **In Vitro Assays** **In Vivo Behavior**

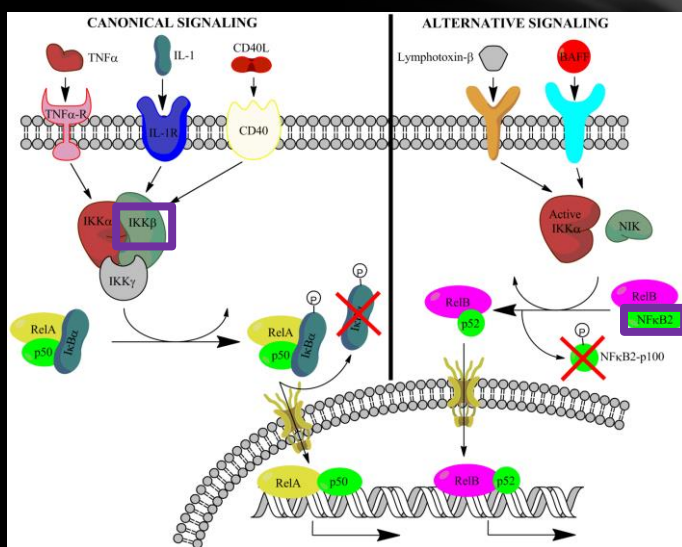
ManNPs Enhance siRNA Delivery Into Macrophages in Lungs of Mice w/ Overt Lung Metastases



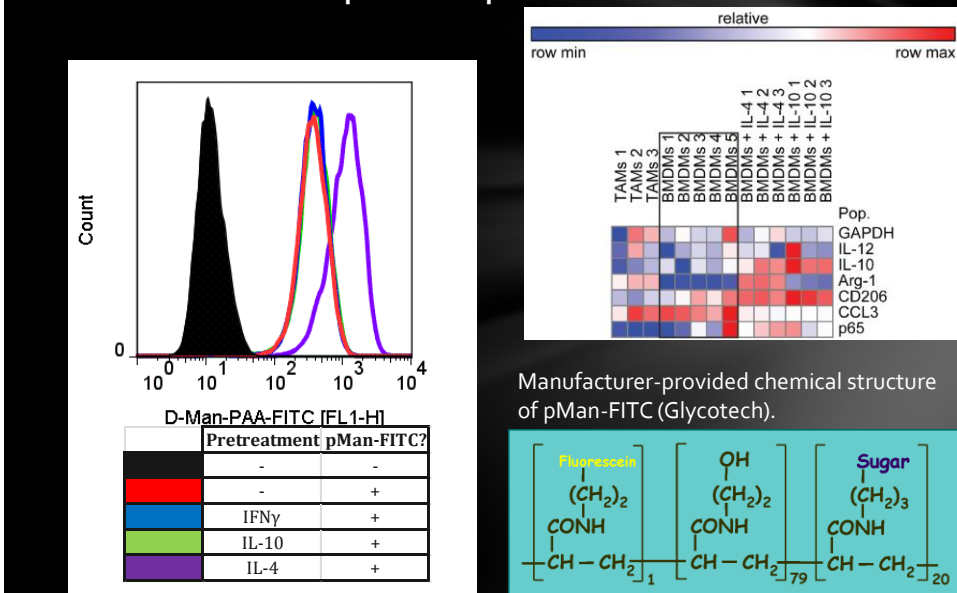
Summary: ManNPs for Systemic Targeting of TAMs

- Multifunctional triblock copolymers enable systemic targeting of TAMs
 - “ pH-Responsive behavior enables cytosolic drug delivery
 - “ Cationic block enables complexation of nucleic acids
 - “ Azido corona enables attachment of targeting ligands via ‘click’ chemistry
- ManNPs enhance siRNA delivery into primary macrophages *in vitro*
- ManNPs co-localize with CD206⁺ cells in PyMT mice

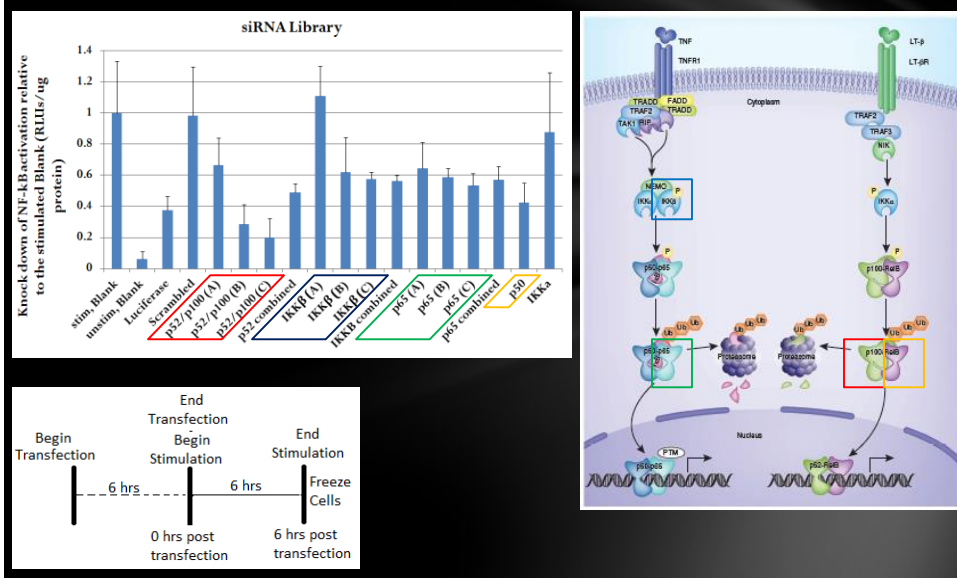
Next Steps: What's the Therapeutic Target?

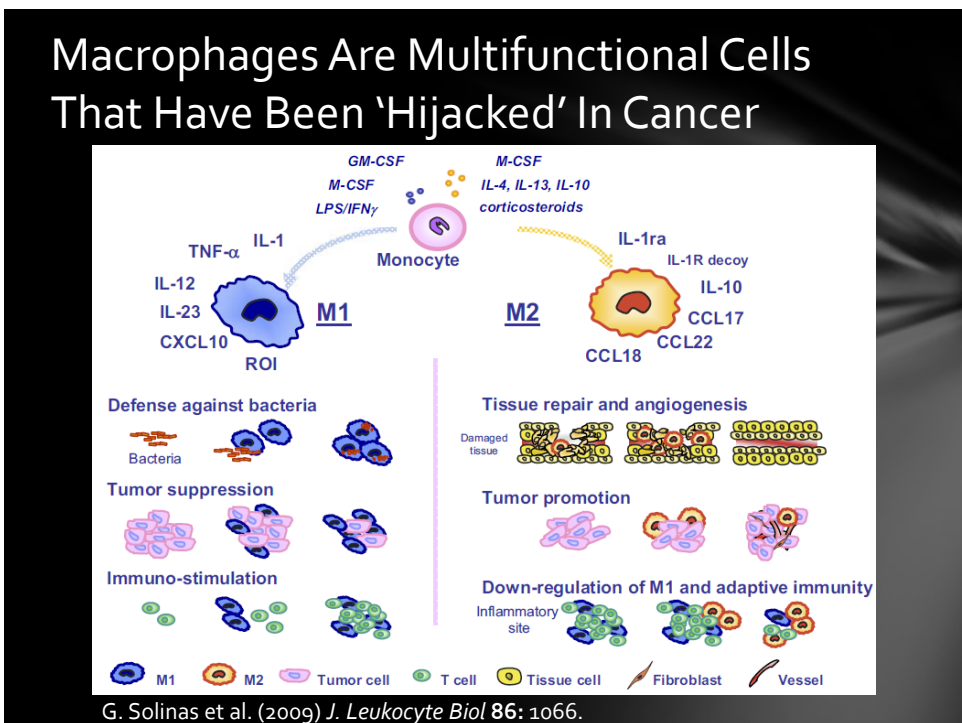
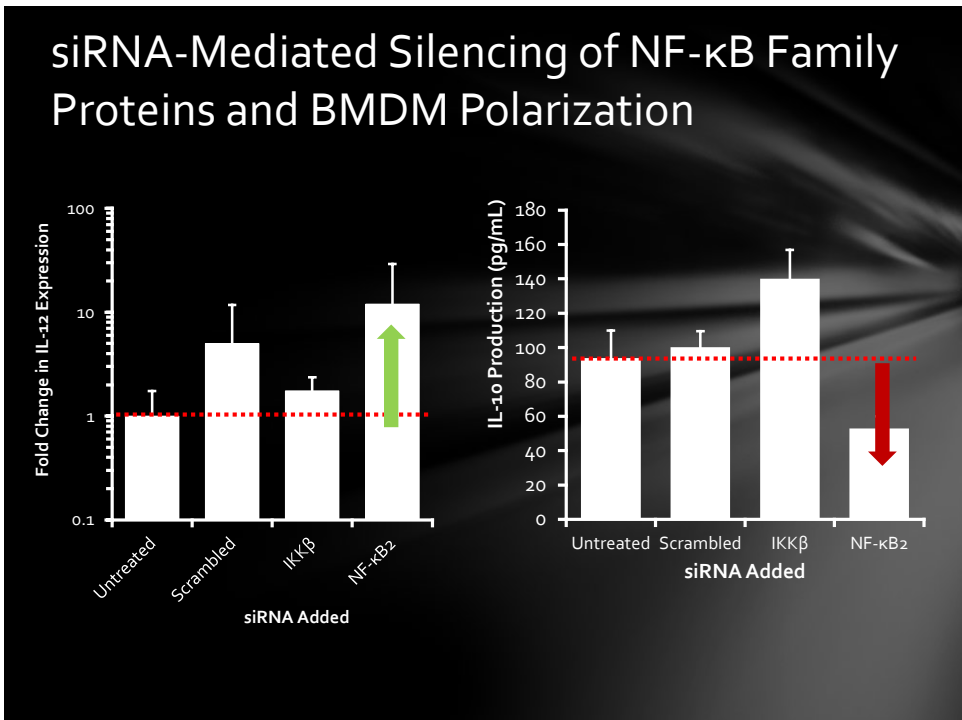


Macrophage Phenotype and Activation and Mannose Receptor Expression



Knockdown of NF- κ B Activity by siRNAs for p52, p65 or IKK β





In Vivo Function of ManNPs in Primary and Metastatic Tumor Models

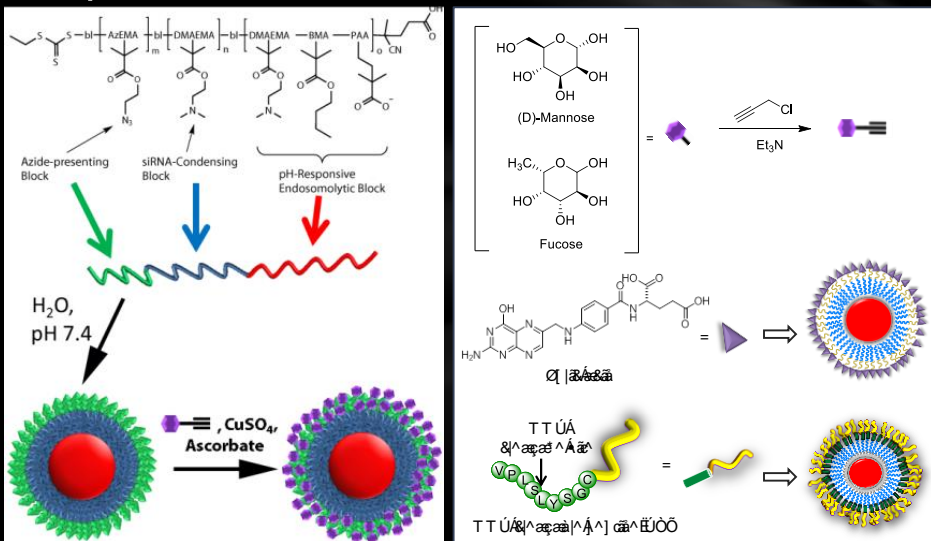


- ” ManNP delivery by flow cytometry
 - ” TAM phenotype by microarray / PCR
 - ” Cytokine expression in tumor tissues
 - ” Tumor growth / survival

” STUDIES IN PROGRESS

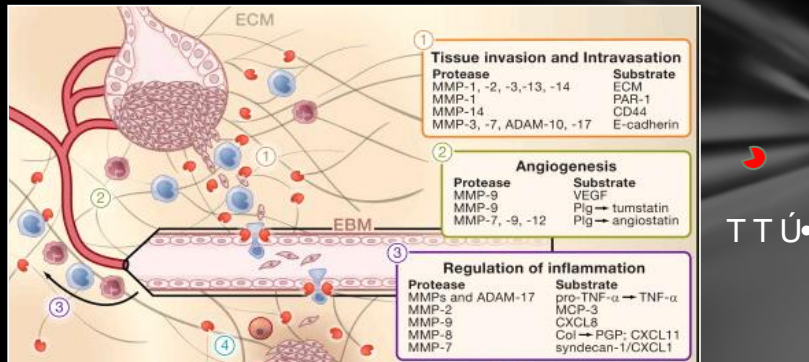
Design & Synthesis Controlled Release *In Vitro* Assays *In Vivo* Behavior

Design of Other Micelle-Forming Polymers: Alternative *In Vivo* Functions



Design & Synthesis Controlled Release *In Vitro* Assays *In Vivo* Behavior

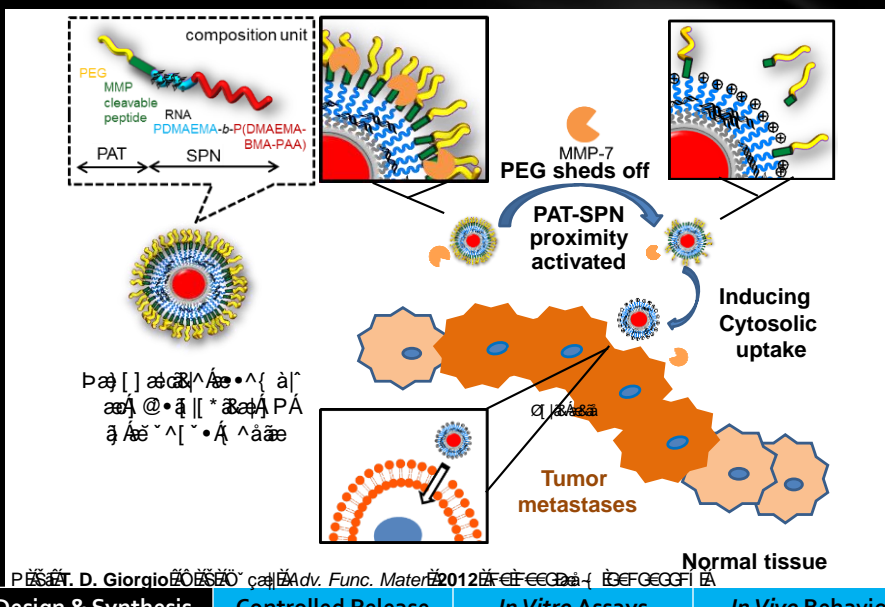
Matrix Metalloproteinases (MMPs) are Hallmarks of Metastatic Cancers



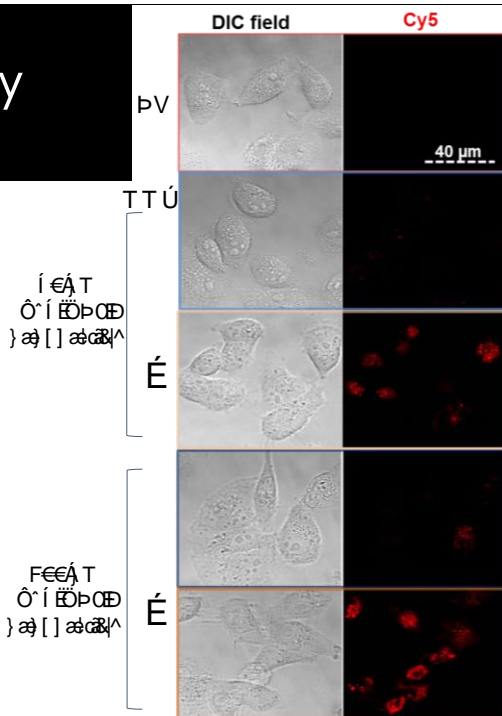
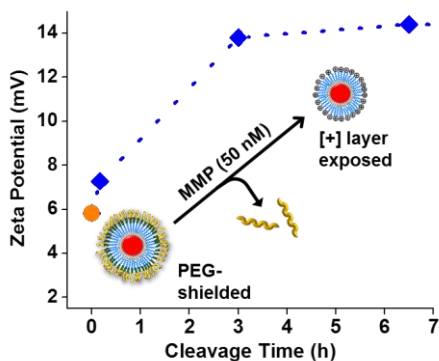
TTÚ• æ^ [ç^{:}Éç] {^••^å å o@] :[çæ æ [~ c { [:
 { ^œœ œœ ^•È

SÉS^••^} à! [& ^Éç Cell 2010 41 Éç

Design for MMP-Activation

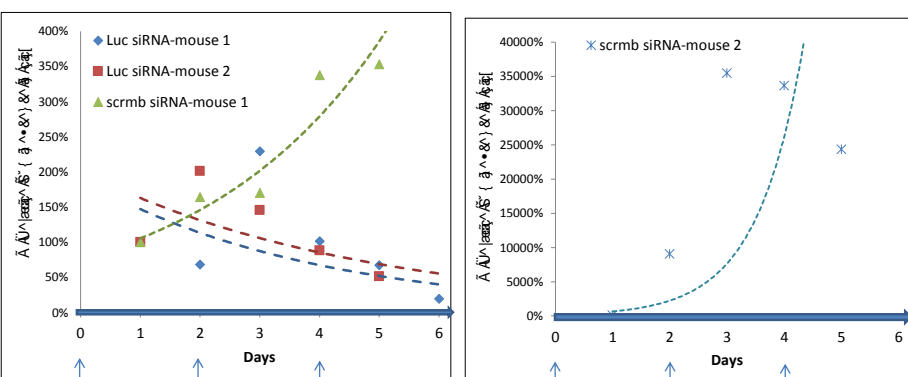


Delivery Triggered by MMP-Activation



PESCARA D. Giorgio - 2012 - Adm. Func.
Mater. 2012 - Adm. Func.

QÁÃ[Á^} ^Á}{ & å[, } Á Á^}{ * | æc{ [^•^Á
à^æé * Á & å^æ^Ëç}{ | ^•^æåç{ [| •



Q&{ } Á ã@í ÜPQE
[æ^åÅ æ [] ææ^

Q18 & Q19 } A. ଅଭ୍ୟାସିତରେ
[ଅନୁଷ୍ଠାନିକ [] ଅନୁଷ୍ଠାନିକ



Acknowledgments



Ó[||æ[|æœ[^
Ó[æ•[} Ó[æ•[K
Y I FYY PEEFEEU I I I I
€ I I



Ú[
V[äååññ I * ñ
Ó[æœ[AÖçœ[

Ú[•ä[&Ä
P[} * { ^äññä

Ó[æœ[c å^} dÄ
Ù@{ } Ä~ ÄÜ@D
T æœ[æœ[ßœçœ
Ó@ä Äp^•[}

W[ä^I * |æœ[ñœ[^^Ä
V@{ æÄ^ v|Ä





Acknowledgments

FUNDING SOURCES

- Department of Defense
- Vanderbilt University
- NIH Cancer Center Grant

POSTDOCTORAL

- Hongmei Li

PREDCTORAL

- Ryan Ortega
- Christopher Nelson
- Angela Zachman

FACULTY COLLABORATORS

- Fiona Yull
- Craig Duvall
- Hak-Joon Sung

THANKS TO

- Whitney Barham (VUSM)
- Rinat Zaynagetdinov (VUMC)
- Susan Thomas (GaTech)
- Nora Disis (UW/FHCRC)

UNDERGRADS

- Cheryl Lau, Elaine Simpson
- Rachel Koblin, Bharat Kumar
- Chelsey Smith

Modular, Endosomal-Escape Nanoparticles for the Delivery of Therapeutic Agents to Tumor Associated Macrophages

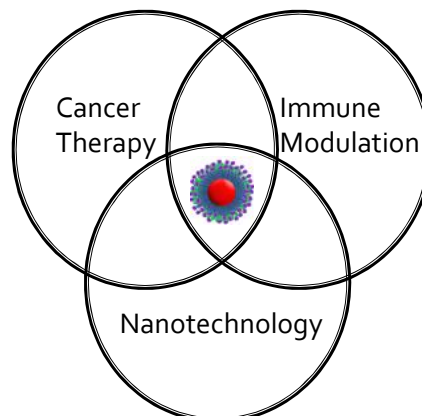
Tumor associated macrophages (TAMs) can modify the tumor microenvironment to create an inflammatory pro-tumor niche. Manipulation of TAM phenotype is a new approach to engage anticancer immunity, but has been limited by a lack of methods capable of therapeutic delivery to TAMs *in vivo*. Using a modular, endosomal escape nanoparticle, we have successfully delivered siRNA for RNAi of the translation of key proteins in the NF- κ B pathway, a major controlling pathway of macrophage phenotype. In *in vitro* studies, the nanoparticles are comparable to commercial transfection agents using both gene and protein level readouts for knockdown. The transfection protocol utilizing these novel vehicles has been optimized with respect to transfection time, siRNA dose, and siRNA:polymer ratio with the intent to inform *in vivo* experiments. The presence of serum does not significantly affect transfection efficiency *in vitro*, presumably due to an almost neutral particle surface charge. This characteristic also allows for increased transfection times and repeated dosing regimens. Preliminary *in vivo* studies have revealed no significant particle toxicity. Delivering siRNA to single proteins in the NF- κ B family of pathways has resulted in a 50-80% decrease in total NF- κ B activity. While inhibition of NF- κ B activity may be desirable in some contexts, we recently reported that strategically induced activation of NF- κ B in macrophages can also result in anti-tumor activity. In preliminary studies we have demonstrated the ability to increase total NF- κ B activity by treating murine macrophages with nanoparticles carrying siRNA against the I κ B α inhibitor of NF- κ B, increasing total NF- κ B activity.

Modular, Endosomal-Escape Nanoparticles for the Delivery of Therapeutic Agents to Tumor Associated Macrophages

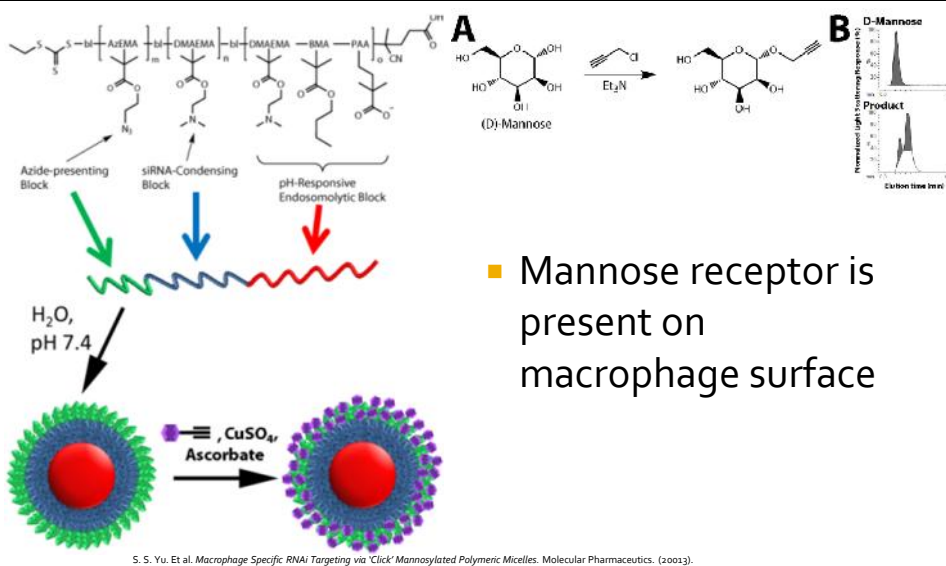
Ryan Ortega
Biomaterials Day
3/15/2013

A multidisciplinary team for a complex design problem

- Todd Giorgio
 - Nanotechnology and gene therapy
- Fiona Yull
 - Mouse models and molecular biology
- Craig Duvall
 - Polymer chemistry



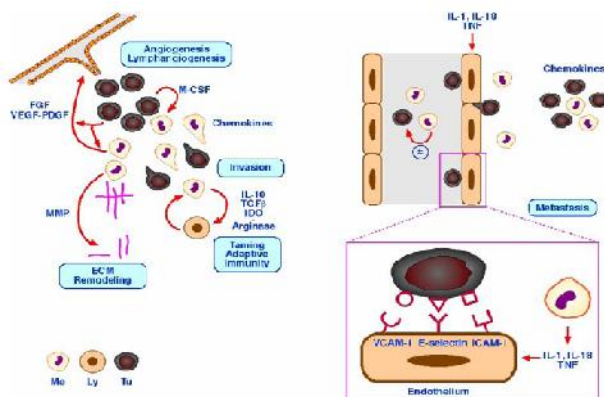
Our tri-block polymer nanoparticle targets macrophages



- Mannose receptor is present on macrophage surface

Tumor Associated Macrophages (TAMs) have a pro-tumor phenotype

- TAMs display traits of multiple established macrophage phenotypes.



A. Mantovani. Et al. Role of tumor-associated macrophages in tumor progression and invasion. Cancer Metastasis Rev. (2006); 25:315-322.

TAMs display a mixed phenotype

M1-like

- Low level local inflammation
 - TNF- α
 - IL -1
 - Low level ROS

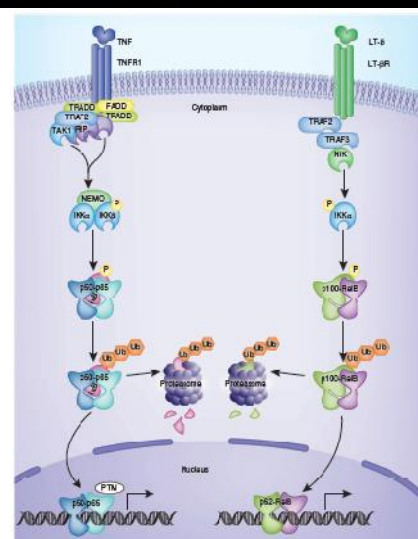
M2-like

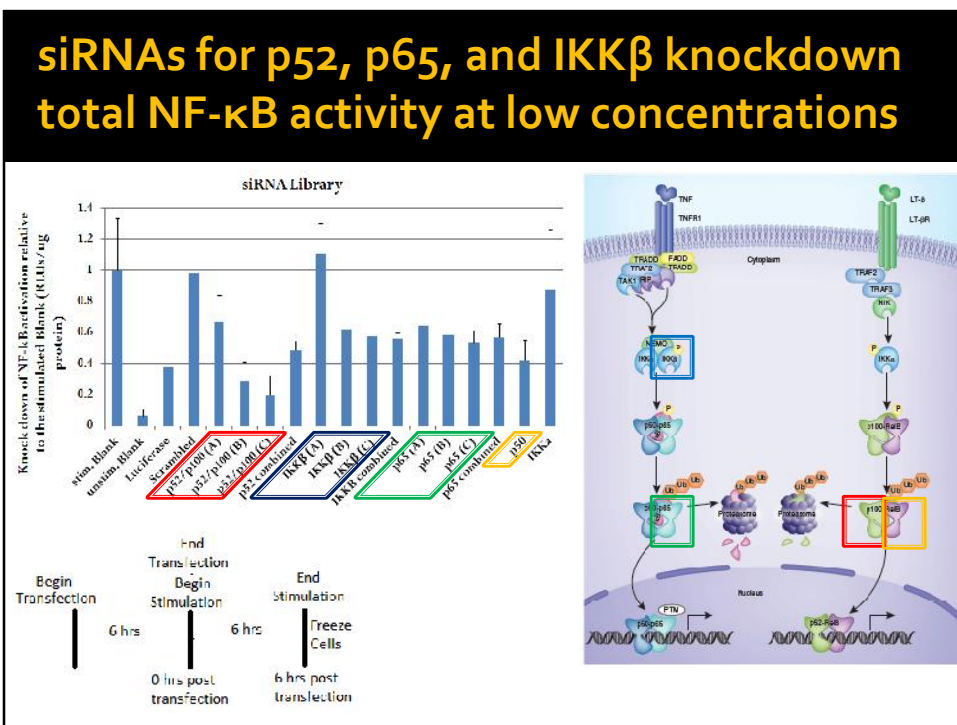
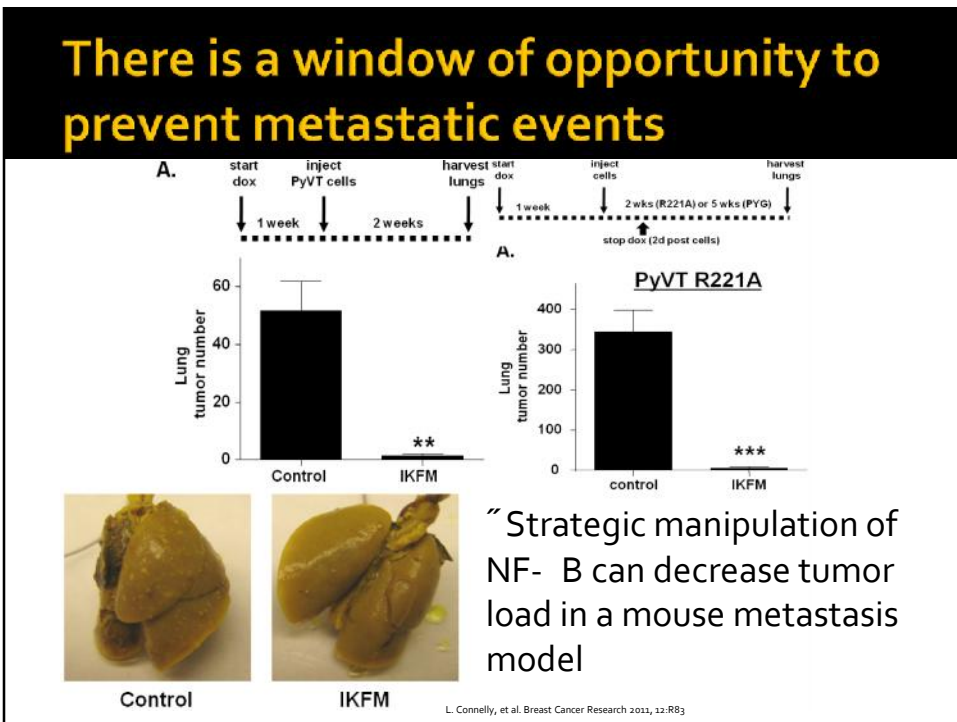
- CSF-1
- Angiogenesis
- Eosinophilia
- IL -10
- TGF- β

- “ Tumor cells induce TAMs to display a very ‘plastic’ phenotype
- “ TAMs recruit or depress other cells as needed
- “ TAMs and tumor cells interact differently depending on location and tumor life cycle

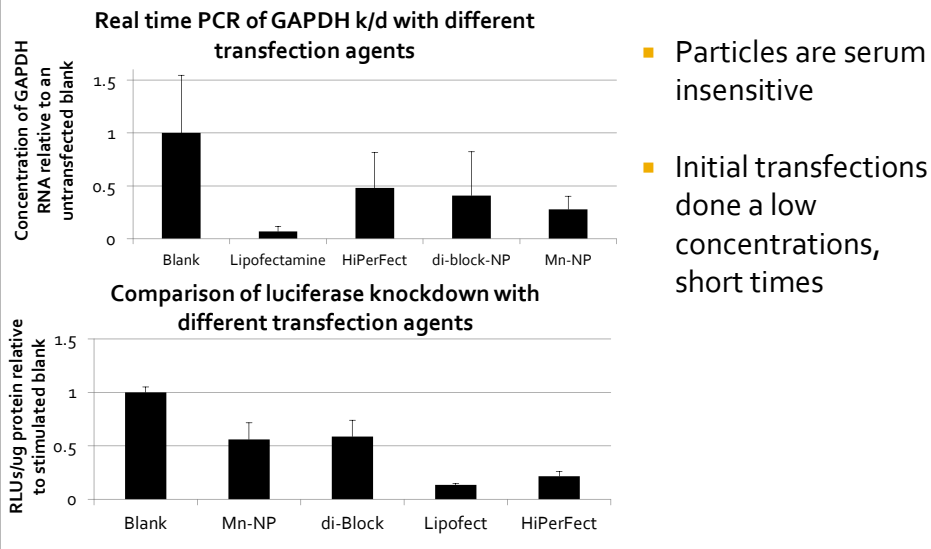
NF- κ B is an attractive therapeutic target for genetic modification

- Genetic ‘master switch’
- Controls inflammation and tissue development
- Modulates macrophage plasticity
 - Receptors
 - Cytokines
 - Chemokines

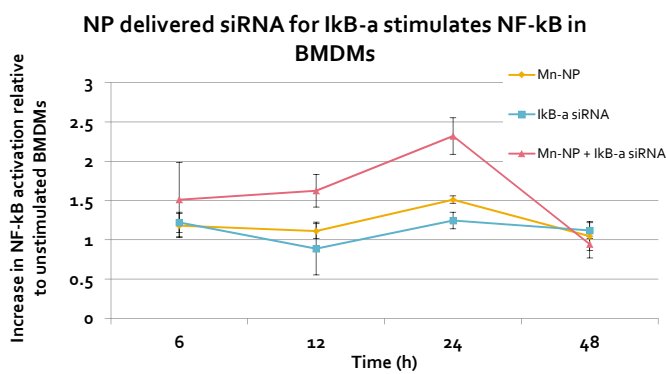




Initial experiments with particles show knockdown similar to commercial agents



Stimulation of NF- κ B with siRNA can only be done with nanoparticle transfection



- Stimulation via k/d of inhibitor requires longer, repeated dosing

Acknowledgements

- Coauthors

- Dr. Todd Giorgio
- Dr. Fiona Yull
- Whitney Barham
- Bharat Kumar

- Collaborators and labmates

- Dr. Craig Duvall
- Dr. Shann Yu
- Dr. Oleg Tikhomirov
- Dr. Hongmei Li
- Dr. Virginia Pensabene
- Ian McFadden
- Charleson Bell
- Lianyi Chen
- Chelsey Smith

- Funding

- DoD CDMRP BCRP BC102696

- Vanderbilt Resources

- Molecular Cell Biology Resource core
- Vanderbilt Technologies for Advanced Genomics (VANTAGE)
- Vanderbilt Institute of Nanoscale Science and Engineering (VINSE)



Macrophage targeting in Benign and Malignant Disease

Fiona E. Yull

Dinner and Data March 11 2013

NF- κ B in Epithelium is important for mammary ductal development

Inhibitor of NF- κ B targeted specifically to mammary epithelium with doxycycline inducible transgenic results in decreased ductal extension



DNMV mice and littermate controls were treated with dox from 3-6 weeks of age. DN- κ B α transgene expression resulted in stunted ductal length (quantified as distance past lymph node).

Macrophages are important for ductal development

[Postnatal mammary gland development requires macrophages and eosinophils.](#)

Gouon-Evans V, Rothenberg ME, Pollard JW.

Development. 2000 Jun;127(11):2269-82.

[Colony stimulating factor-1 is required to recruit macrophages into the mammary gland to facilitate mammary ductal outgrowth.](#)

Van Nguyen A, Pollard JW.

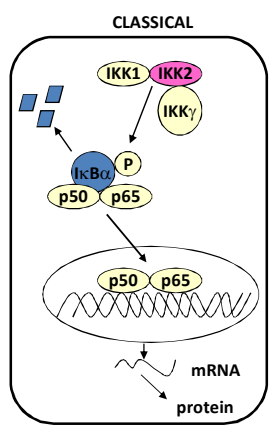
Dev Biol. 2002 Jul 1;247(1):11-25.

[Requirement of macrophages and eosinophils and their cytokines/chemokines for mammary gland development.](#)

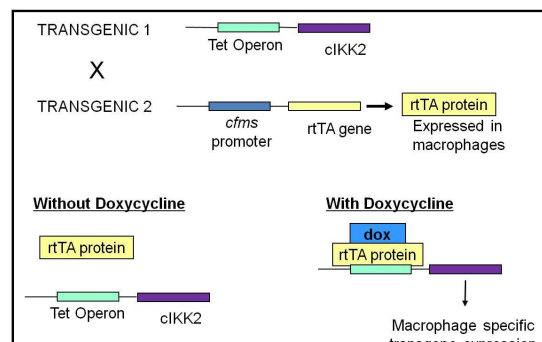
Gouon-Evans V, Lin EY, Pollard JW.

Breast Cancer Res. 2002;4(4):155-64.

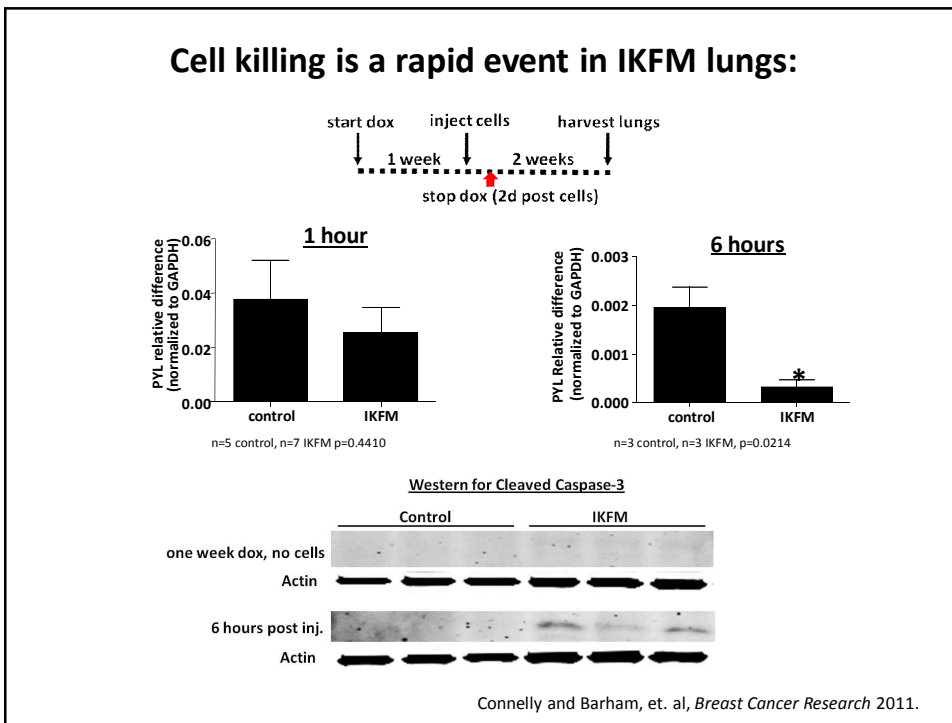
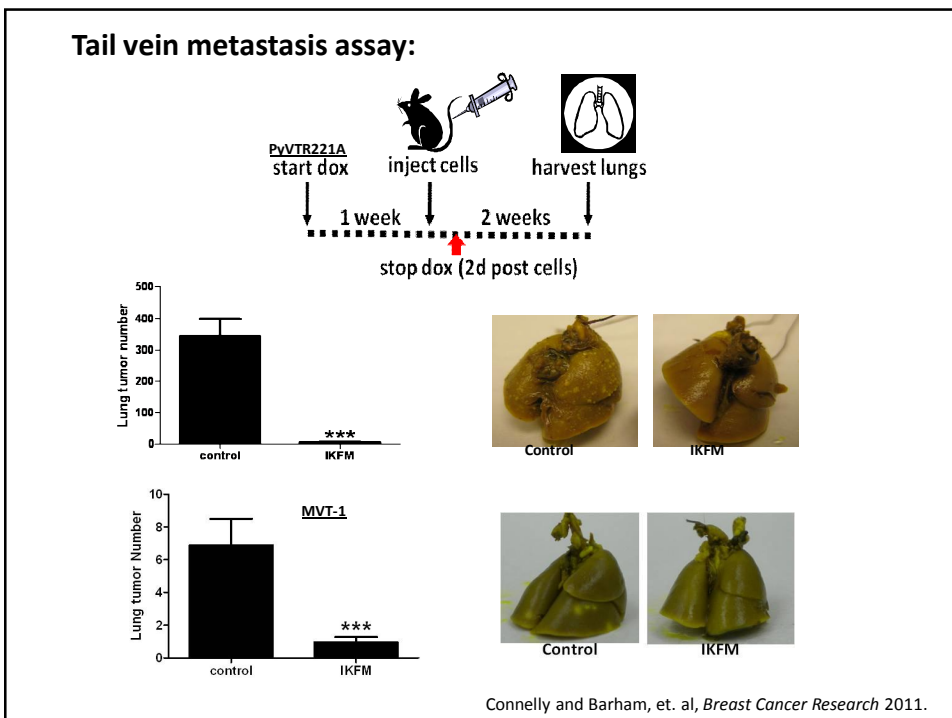
Transgenic mouse model for activation of NF- κ B in Macrophages:



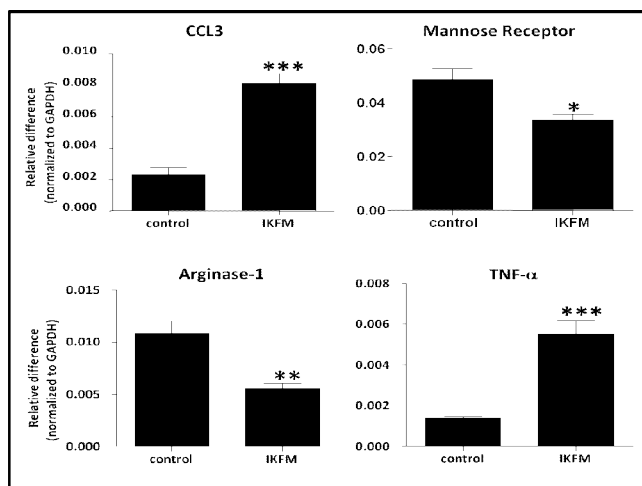
Constitutively active IKK2 = increased activity



IKFM = increased NF- κ B signaling in macrophages

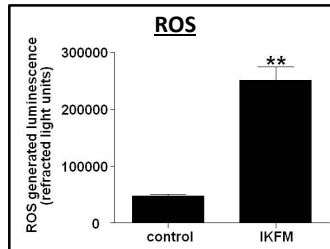


IKFM lungs exhibit an “M1” phenotype:

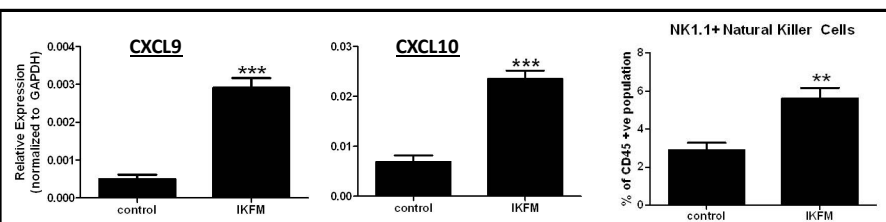


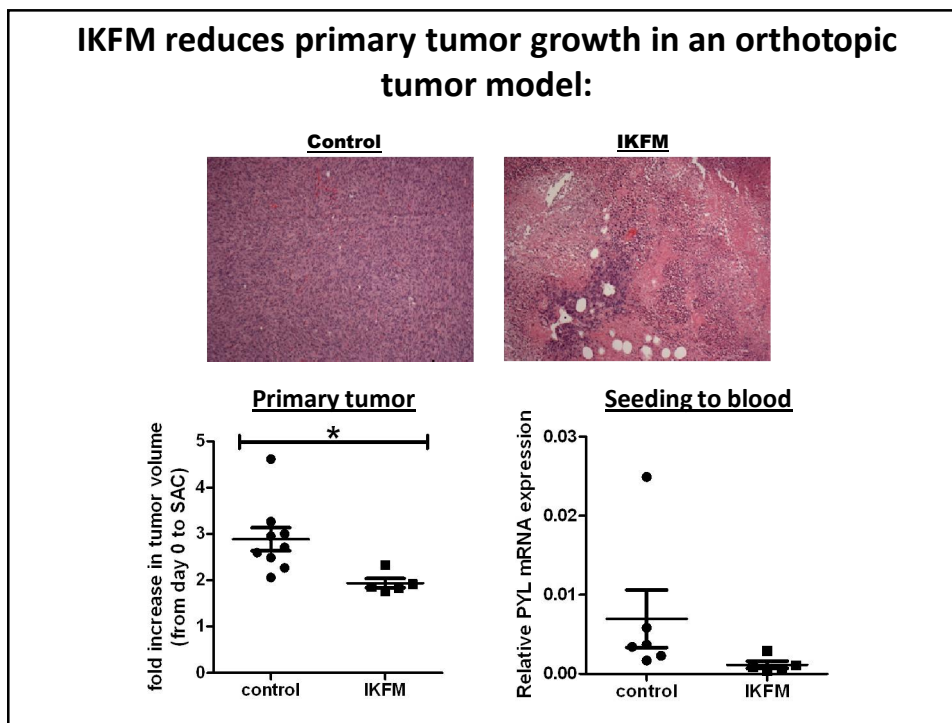
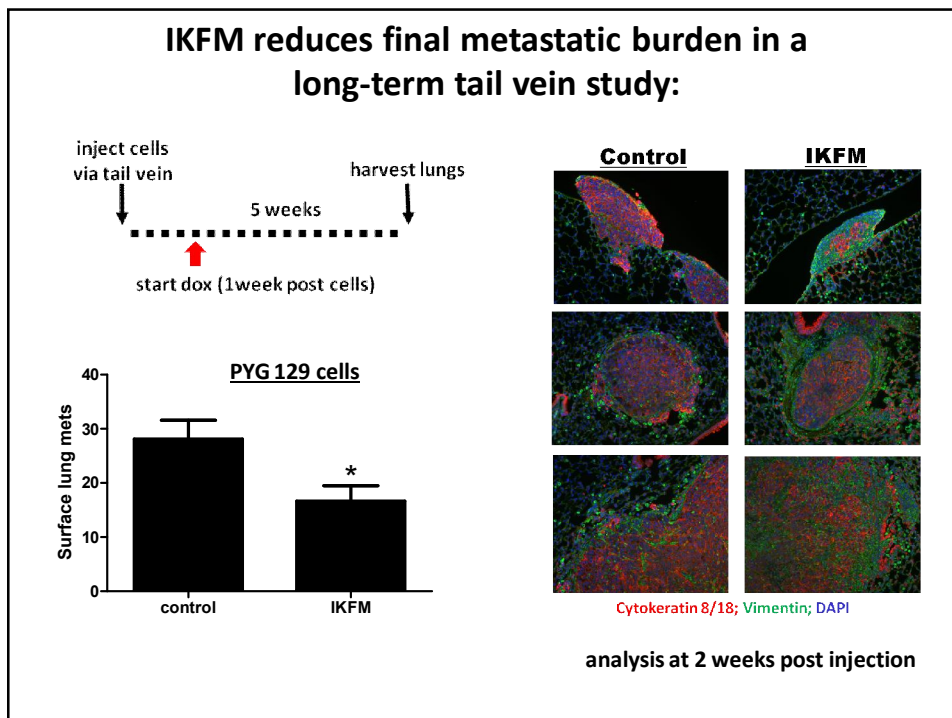
Tumor cell cytotoxicity may be direct or indirect:

Direct:

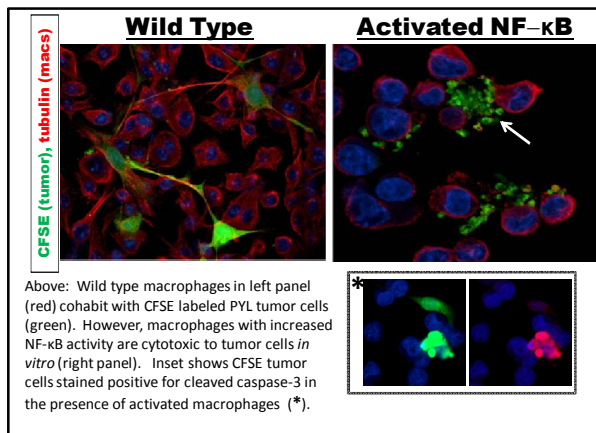


Indirect:



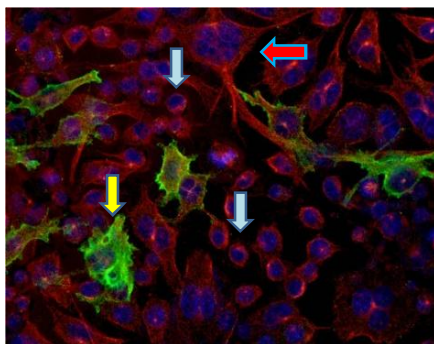


In vitro studies: Polyoma mammary tumor cells and NF-κB activated macrophages

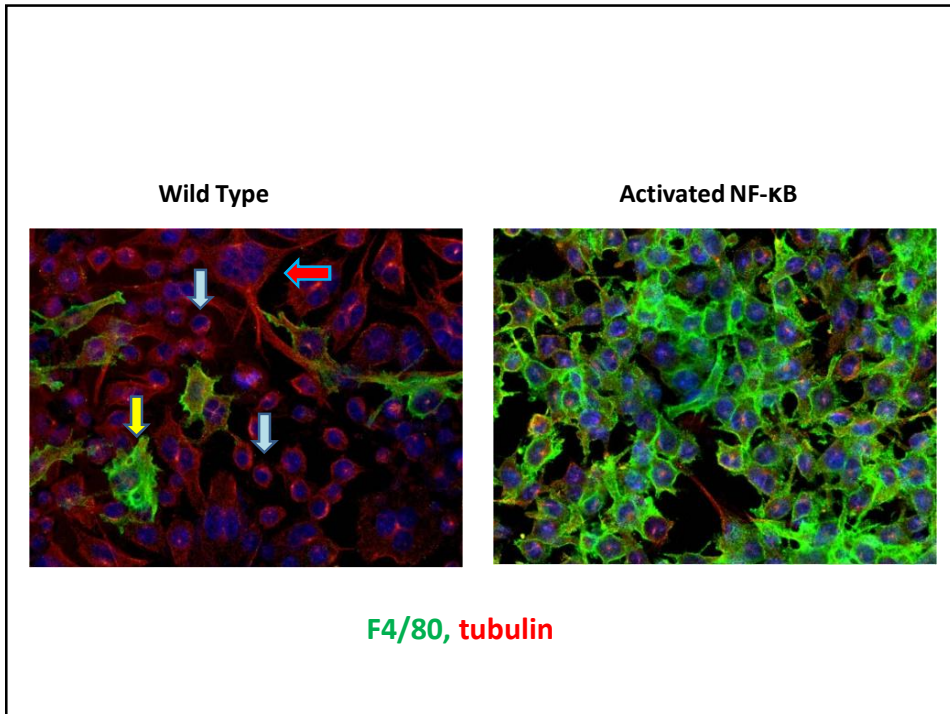


Macrophages responding to mammary tumor cells are highlighted by F4/80 IHC

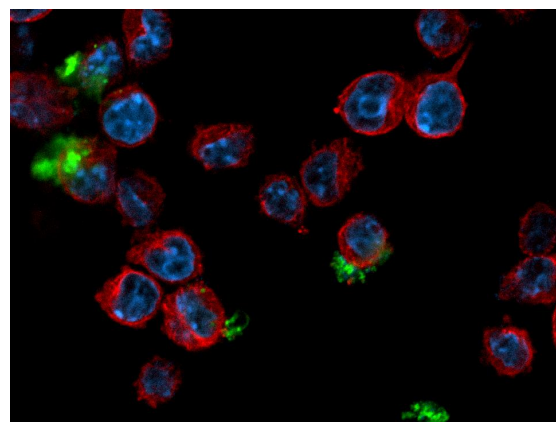
Wild Type



F4/80, tubulin



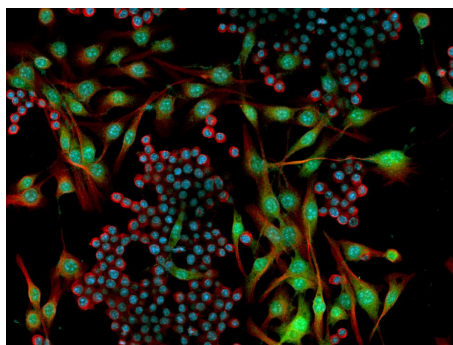
Met1 mammary tumor cells and NF- κ B activated macrophages



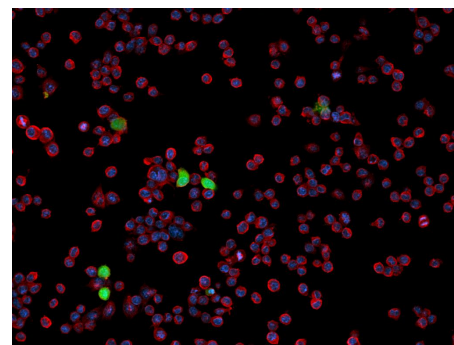
Green: CFSE tumor
Red: tubulin

**ID8 Ovarian tumor cells + macrophages
(3 days of coculture)**

Wild Type



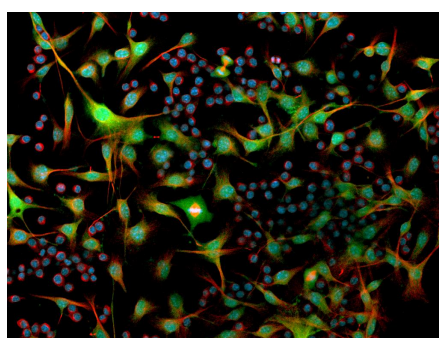
Activated NF-κB



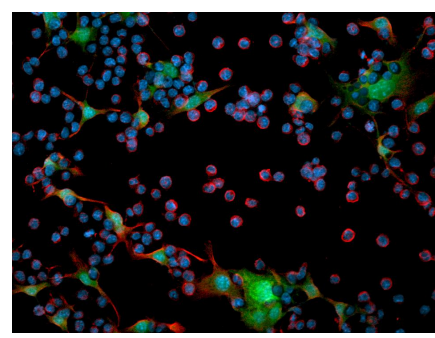
Green: CFSE tumor
Red: tubulin

**B16 Melanoma tumor cells +
macrophages (3 days of coculture)**

Wild Type



Activated NF-κB



Green: CFSE tumor
Red: tubulin

Summary

- “ Our novel transgenic mouse models enabling macrophage specific activation of NF-κB during defined time periods highlight potential anti-tumor effects in multiple *in vivo* models of breast cancer tumorigenesis including primary tumor and metastatic growth .
- “ *In vitro* studies suggest that activation of NF-κB in macrophages can be directly cytotoxic with effects on breast, ovarian and melanoma tumor cells.
- “ How can we achieve modulation of NF-κB signaling to manipulate macrophage behavior as potential clinical cancer therapy? *Nanoparticle therapeutics...*

Yull lab:

Whitney Barham
 Lianyi Chen
 Oleg Tikhomirov
 Ryan Ortega
 Halina Onishko
 Linda Connelly (University of Hawaii at Hilo)

Vanderbilt University:

Timothy S. Blackwell
 Taylor Sherrill
 Rinat Zaynagetdinov
 Linda Gleaves

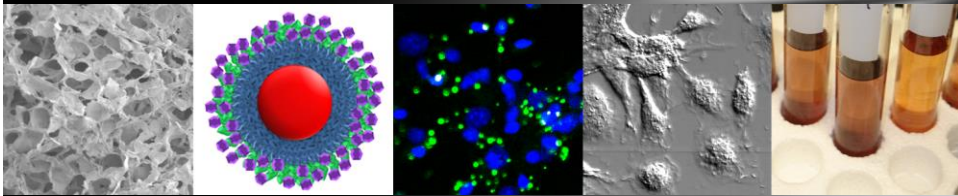
Ohio State University:

Mike Ostrowski

Funding: DOD Breast Cancer Program – IDEA and Concept grants


Urban-photos.com

Nanostructure Design for Modulation of Inflammation



Todd Giorgio

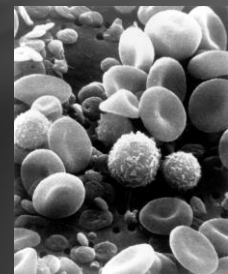
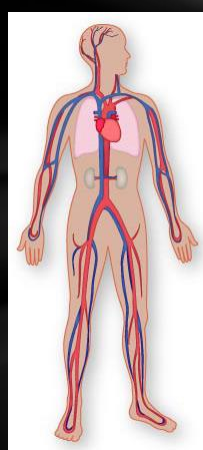
Departments of Biomedical Engineering and Cancer Biology

11 March 2013

VU Department of Medicine: Dinner and Data

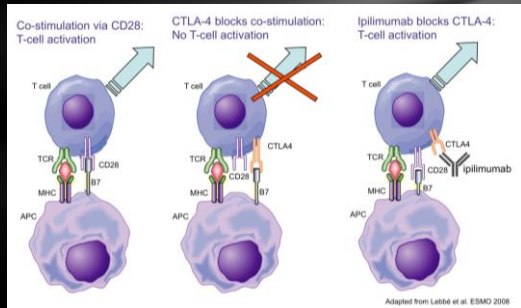
Modulate Inflammation Locally: WHY?

- Advanced approaches require site-specific activity
 - Current therapeutics are small molecule, systemic
 - Dysregulation of inflammation is often cell or tissue specific
 - New therapeutic approaches can be limited by powerful effects in non-target tissues



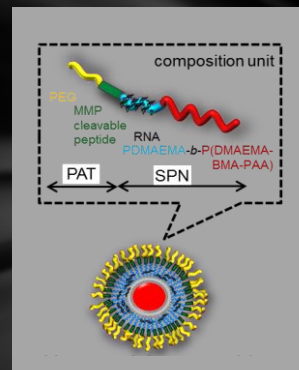
Modulate Inflammation Locally: WHY?

- Example: Cancer Immunology
 - Acute inflammation = anti-tumor microenvironment
 - Chronic inflammation = pro-tumor microenvironment
- New therapeutics intended to stimulate anti-cancer immunity possess significant self-recognition consequences
- What about siRNA?
- Limitations might be relieved with localized delivery to specific cells, tissues



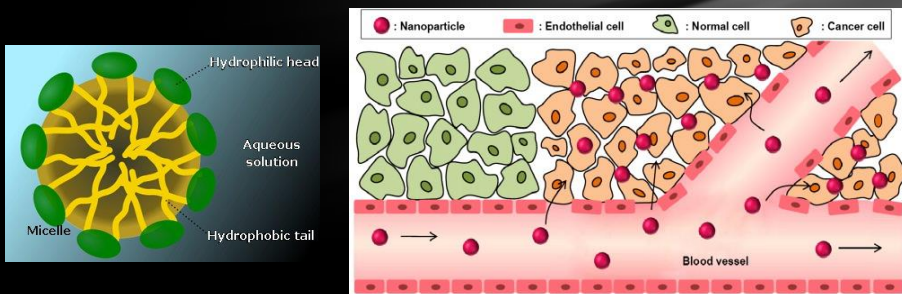
Design of Nanomaterials?

- Engineering approaches enable the principled design of nanomaterials to provide specific and unique functions *in vivo*
- Multiple, co-localized functions, including site-specific activation
- Generation of 'smart' materials
- TODAY: Modulate the phenotype of tumor associated macrophages (TAMs) – but **not** macrophages localized in other tissues



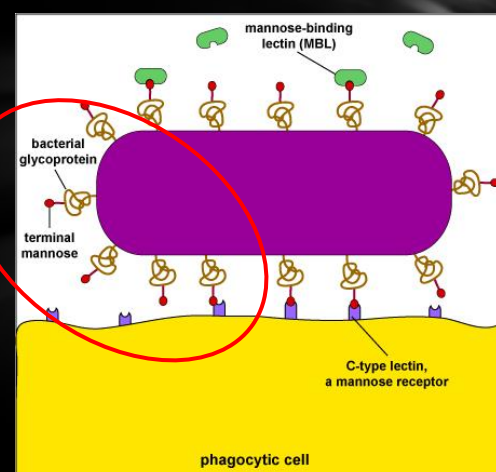
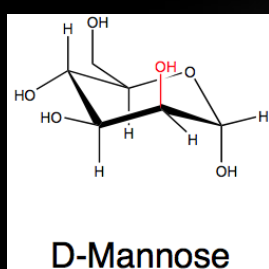
Design of Materials: TAM Modulation

- Molecular design for self assembly into micelles: nontoxic
- Nanoscale size controls tumor extravasation: EPR



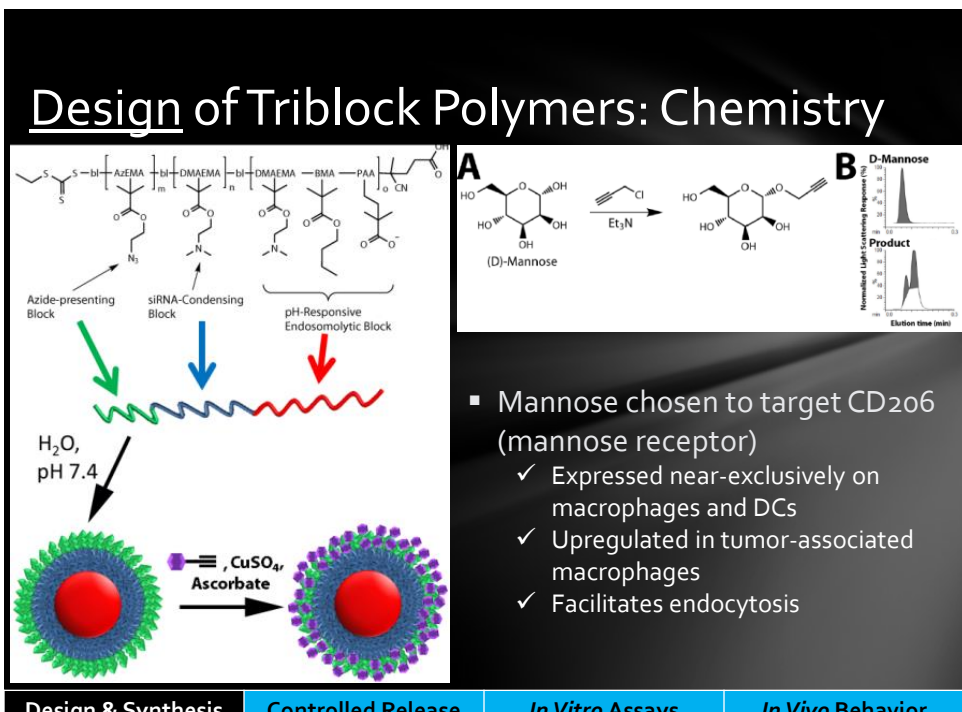
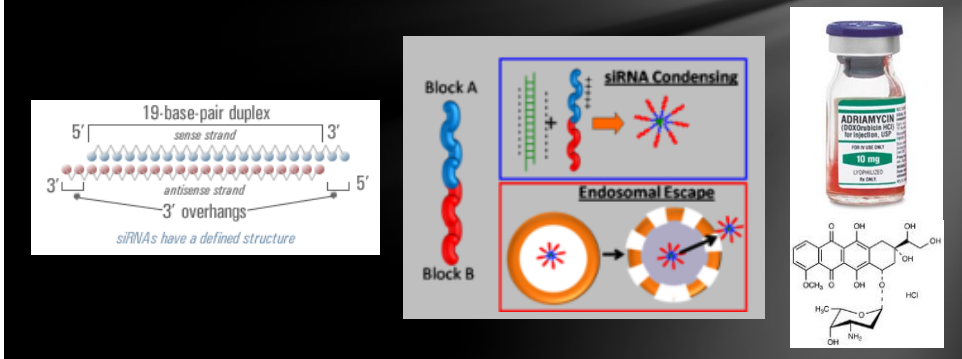
Design of Materials: TAM Modulation

- Surface functionalization enables cell-specific binding: mannose



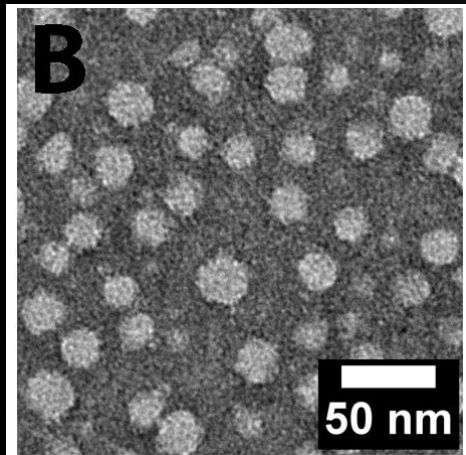
Design of Materials: TAM Modulation

- Interior functionalization enables knockdown of protein expression: siRNA+ endosomolytic
- Core provides a reservoir for other therapeutic payloads: hydrophobic small molecule drugs



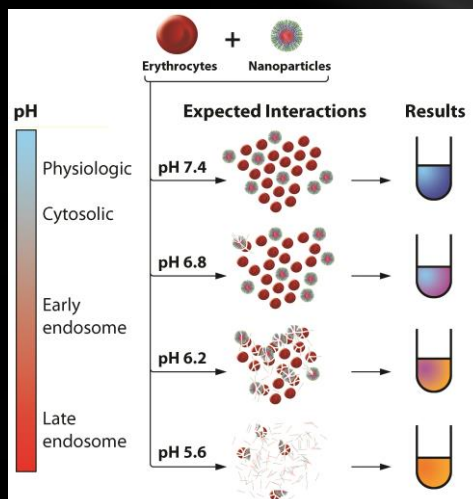
- Mannose chosen to target CD206 (mannose receptor)
 - ✓ Expressed near-exclusively on macrophages and DCs
 - ✓ Upregulated in tumor-associated macrophages
 - ✓ Facilitates endocytosis

Self-Assembly Into Micelles with Appropriate Nanoscale Size for EPR



[Design & Synthesis](#) [Controlled Release](#) [In Vitro Assays](#) [In Vivo Behavior](#)

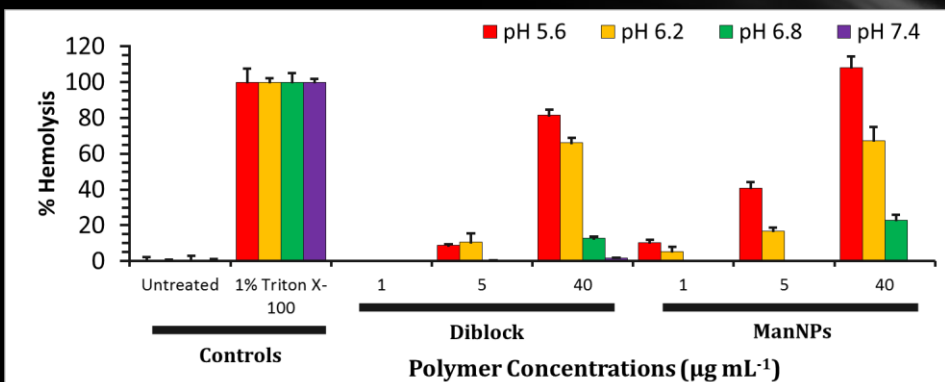
Using the Hemolysis Assay to Model Endosome-Nanoparticle Interactions



BC Evans, CE Nelson, SS Yu, et al. (2013) *J Visualized Exp.* (in press).

[Design & Synthesis](#) [Controlled Release](#) [In Vitro Assays](#) [In Vivo Behavior](#)

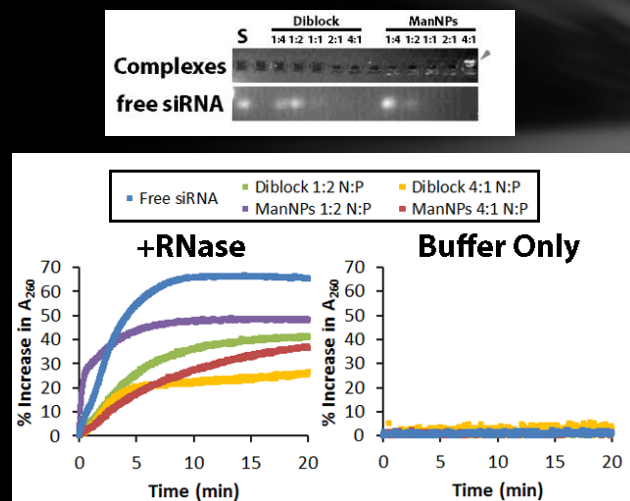
Diblocks and ManNPs Exhibit pH-Responsive Hemolysis



S.S. Yu et al. (2013) *Molecular Pharmaceutics* (in press).

[Design & Synthesis](#) [Controlled Release](#) [In Vitro Assays](#) [In Vivo Behavior](#)

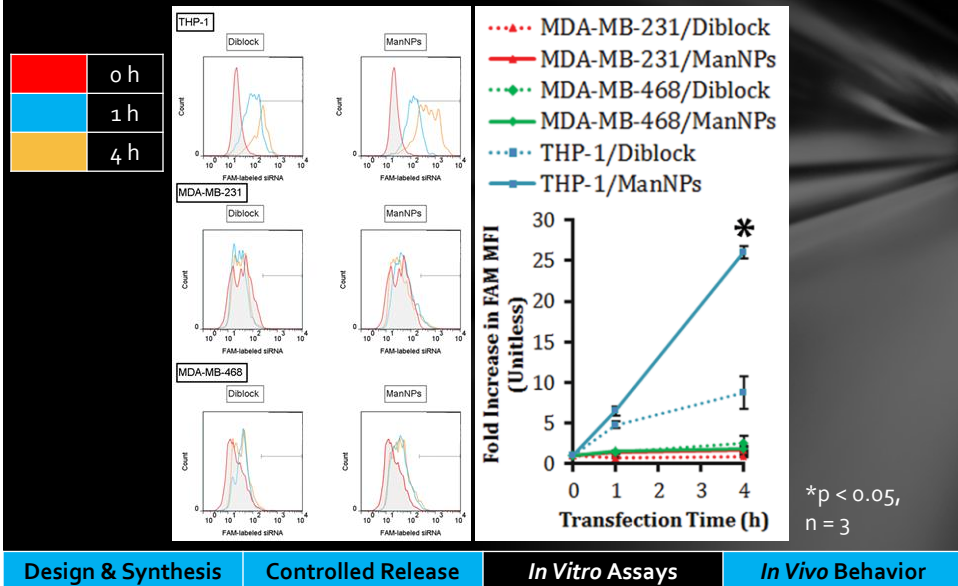
ManNPs Electrostatically Complex siRNA and Protect it from RNases



S.S. Yu et al. (2012) *Molecular Pharmaceutics* (in press).

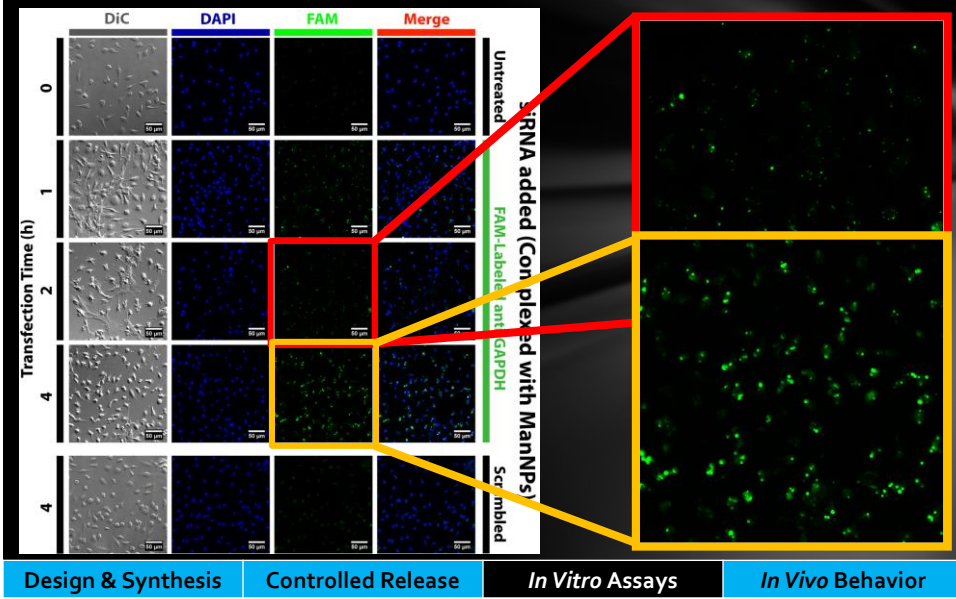
[Design & Synthesis](#) [Controlled Release](#) [In Vitro Assays](#) [In Vivo Behavior](#)

ManNPs Enhance siRNA Delivery into Immortalized Macrophages



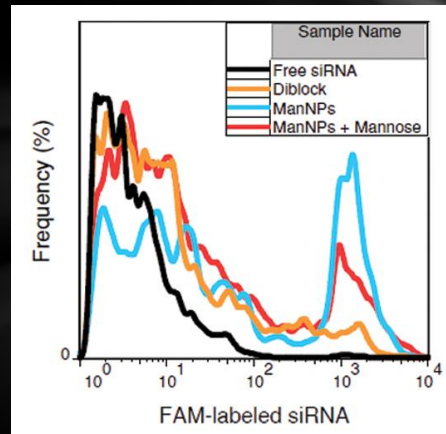
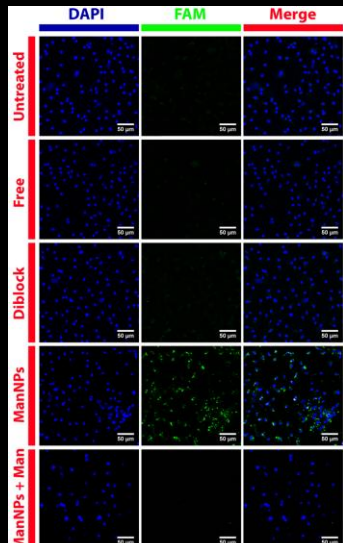
Design & Synthesis Controlled Release In Vitro Assays In Vivo Behavior

Kinetics of Primary Macrophage Transfection Imaged by Confocal Microscopy



Design & Synthesis Controlled Release In Vitro Assays In Vivo Behavior

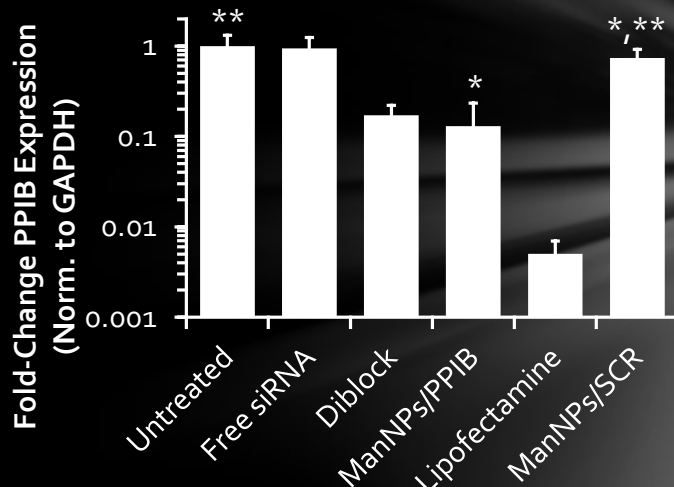
ManNPs Enhance siRNA Delivery into Primary Macrophages



S.S. Yu et al. (2013) *Molecular Pharmaceutics* (in press).

Design & Synthesis Controlled Release In Vitro Assays In Vivo Behavior

siRNA Delivered through ManNPs Retains Ability to Knock Down Target Gene Expression



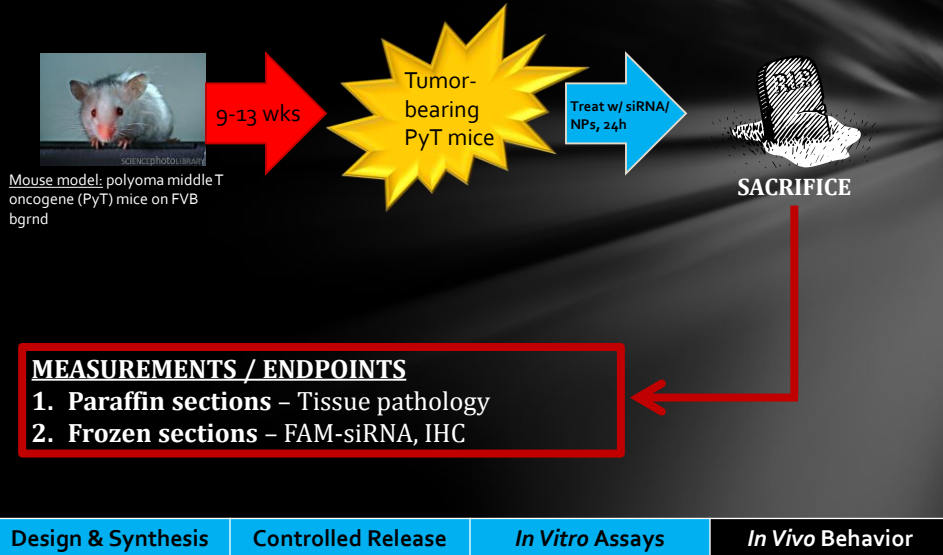
*p < 0.05; n = 3

** p > 0.05; n = 3

S.S. Yu et al. (2013) *Molecular Pharmaceutics* (in press).

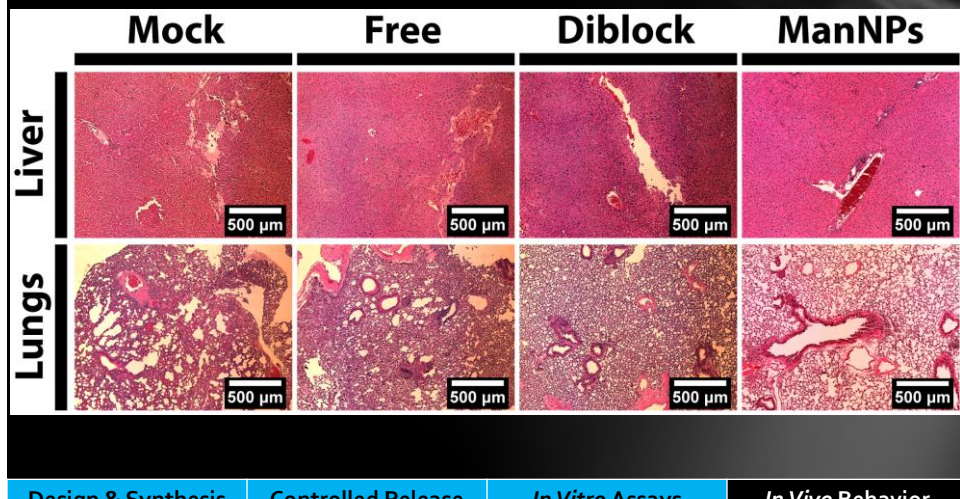
Design & Synthesis Controlled Release In Vitro Assays In Vivo Behavior

In Vivo Biodistribution of ManNPs in Primary Tumor Model

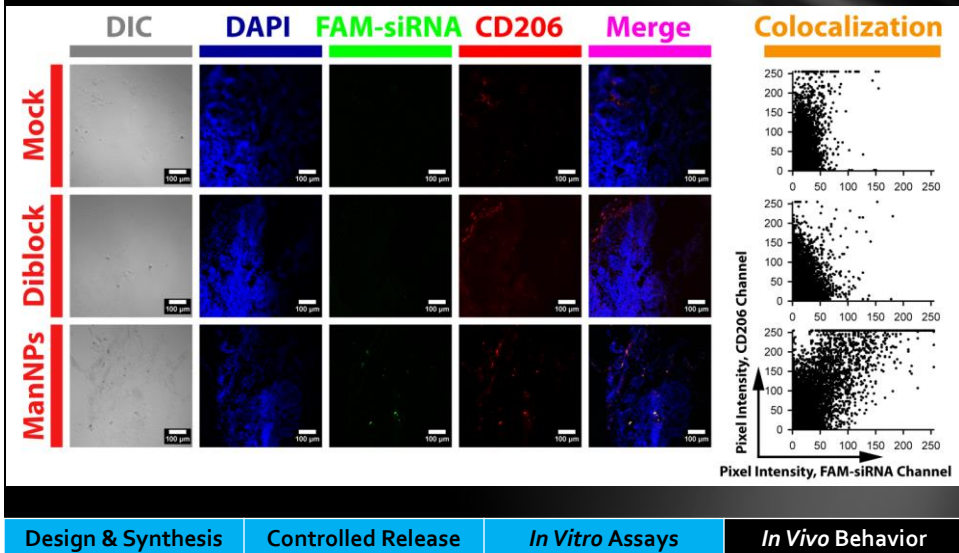


Design & Synthesis Controlled Release *In Vitro* Assays *In Vivo* Behavior

No Significant Changes in Lungs / Liver Morphology within 24 h



ManNPs Target CD206⁺ Cells in Primary Tumor Model



Design & Synthesis

Controlled Release

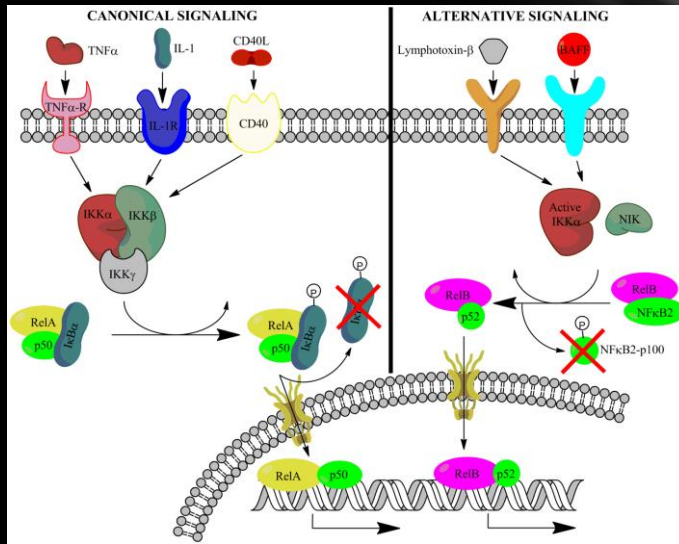
In Vitro Assays

In Vivo Behavior

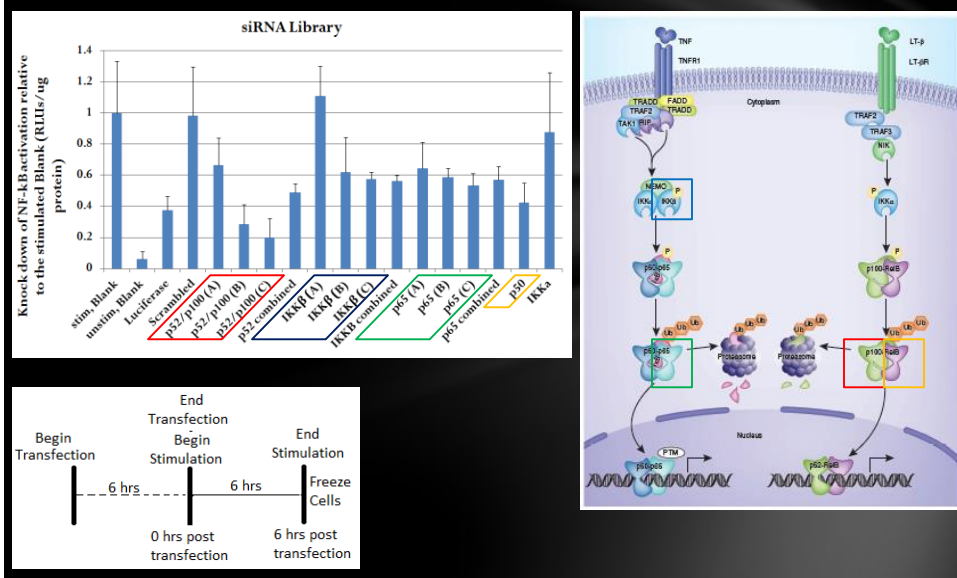
Summary: ManNPs for Systemic Targeting of TAMs

- Multifunctional triblock copolymers enable systemic targeting of TAMs
 - pH-Responsive behavior enables cytosolic drug delivery
 - Cationic block enables complexation of nucleic acids
 - Azido corona enables attachment of targeting ligands via 'click' chemistry
- ManNPs enhance siRNA delivery into primary macrophages *in vitro*
- ManNPs co-localize with CD206⁺ cells in PyMT mice

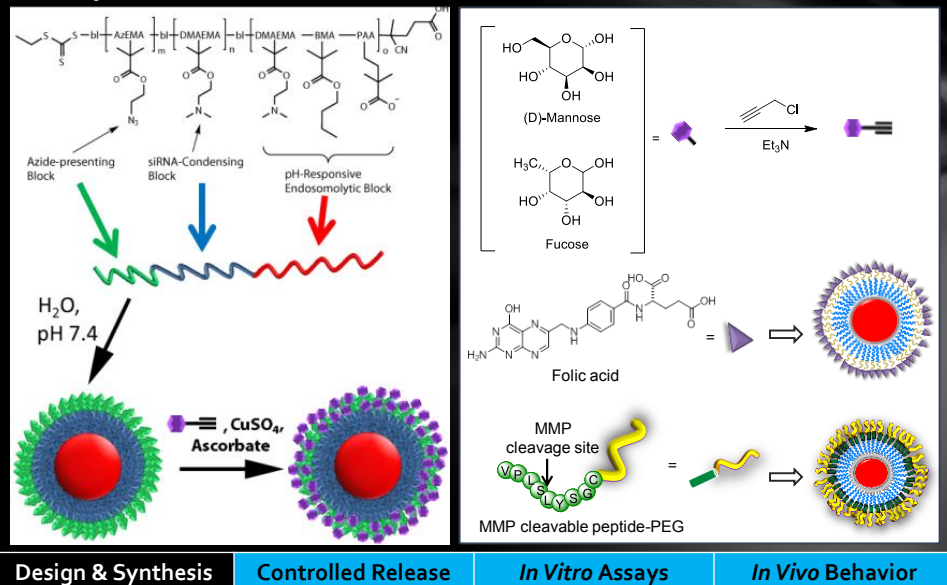
Inflammation and TAMs: What's the Therapeutic Target?



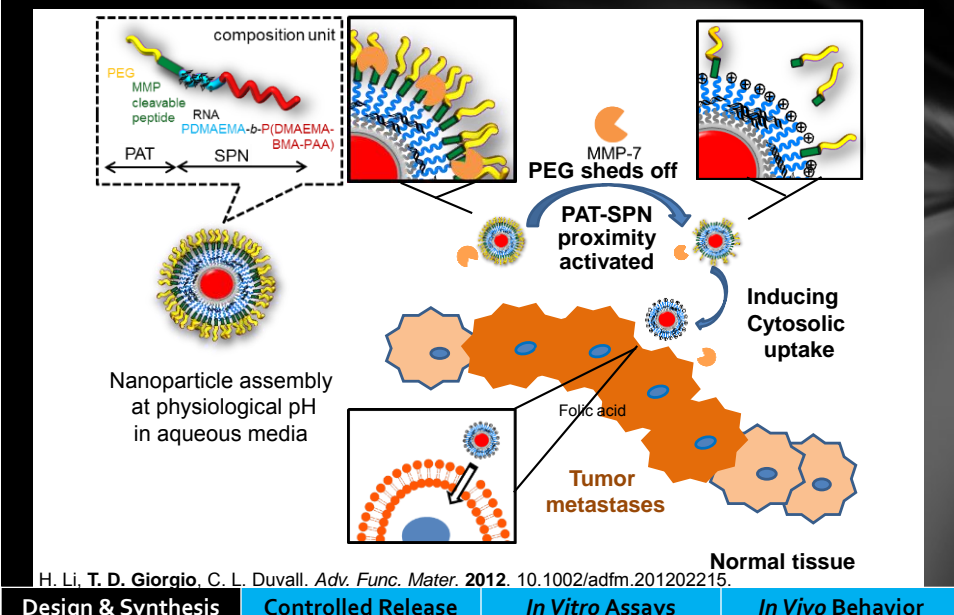
Knockdown of NF- κ B Activity by siRNAs for p52, p65 or IKK β



Design of Other Micelle-Forming Polymers: Alternative *In Vivo* Functions

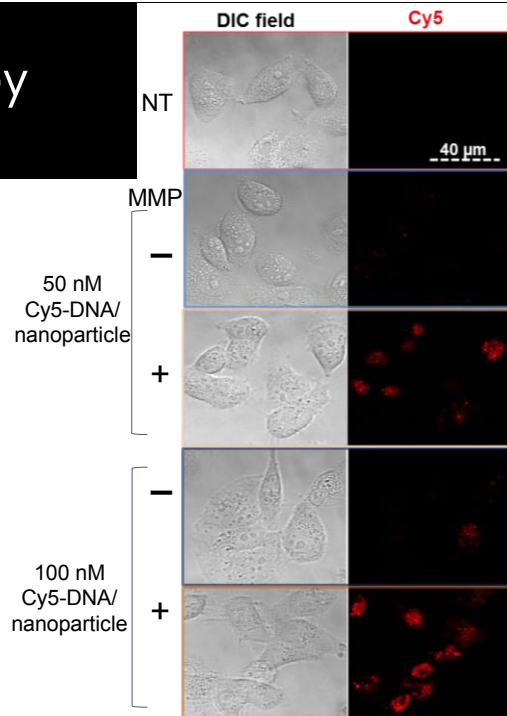
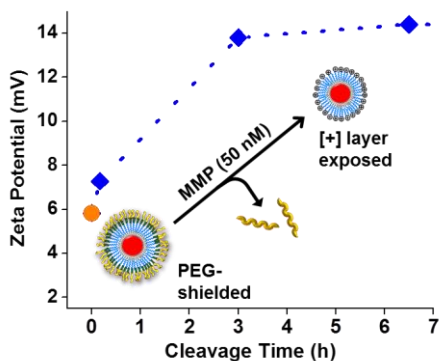


Design for MMP-Activation



Design & Synthesis Controlled Release In Vitro Assays In Vivo Behavior

Delivery Triggered by MMP-Activation



H. Li, T. D. Giorgio, C. L. Duvall. *Adv. Func. Mater.* 2012. 10.1002/adfm.201202215.

Giorgio Lab

Shann Yu

Hongmei Li

Ryan Ortega



VANDERBILT
School of Engineering





Acknowledgments

FUNDING SOURCES

- Department of Defense
- Vanderbilt University
- NIH Cancer Center Grant

POSTDOCTORAL

- Hongmei Li

PREDCTORAL

- Ryan Ortega
- Christopher Nelson
- Angela Zachman

FACULTY COLLABORATORS

- Fiona Yull
- Craig Duvall
- Hak-Joon Sung

THANKS TO

- Whitney Barham (VUSM)
- Rinat Zaynagetdinov (VUMC)
- Susan Thomas (GaTech)
- Nora Disis (UW/FHCRC)

UNDERGRADS

- Cheryl Lau, Elaine Simpson
- Rachel Koblin, Bharat Kumar
- Chelsey Smith

Macrophage-Specific RNA Interference Targeting via “Click”, Mannosylated Polymeric Micelles

Shann S. Yu,^{†,‡} Cheryl M. Lau,[†] Whitney J. Barham,[§] Halina M. Onishko,[§] Christopher E. Nelson,^{†,‡} Hongmei Li,^{†,‡} Chelsey A. Smith,[†] Fiona E. Yull,[§] Craig L. Duvall,^{†,‡} and Todd D. Giorgio*,^{†,‡,§,||}

[†]Department of Biomedical Engineering, Vanderbilt University, Nashville, Tennessee 37235, United States

[‡]Vanderbilt Institute for Nanoscale Science and Engineering, Vanderbilt University, Nashville, Tennessee 37235, United States

[§]Department of Cancer Biology, Vanderbilt-Ingram Cancer Center, Nashville, Tennessee 37232, United States

^{||}Department of Chemical and Biomolecular Engineering, Vanderbilt University, Nashville, Tennessee 37235, United States

Supporting Information

ABSTRACT: Macrophages represent an important therapeutic target, because their activity has been implicated in the progression of debilitating diseases such as cancer and atherosclerosis. In this work, we designed and characterized pH-responsive polymeric micelles that were mannosylated using “click” chemistry to achieve CD206 (mannose receptor)-targeted siRNA delivery. CD206 is primarily expressed on macrophages and dendritic cells and upregulated in tumor-associated macrophages, a potentially useful target for cancer therapy. The mannosylated nanoparticles improved the delivery of siRNA into primary macrophages by 4-fold relative to the delivery of a nontargeted version of the same carrier ($p < 0.01$). Further, treatment for 24 h with the mannose-targeted siRNA carriers achieved $87 \pm 10\%$ knockdown of a model gene in primary macrophages, a cell type that is typically difficult to transfect. Finally, these nanoparticles were also avidly recognized and internalized by human macrophages and facilitated the delivery of 13-fold more siRNA into these cells than into model breast cancer cell lines. We anticipate that these mannose receptor-targeted, endosomolytic siRNA delivery nanoparticles will become an enabling technology for targeting macrophage activity in various diseases, especially those in which CD206 is upregulated in macrophages present within the pathologic site. This work also establishes a generalizable platform that could be applied for “click” functionalization with other targeting ligands to direct siRNA delivery.

KEYWORDS: mannose, nanoparticles, macrophages, siRNA, drug delivery, immunotherapy



INTRODUCTION

Macrophages perform diverse functions, some of which have cytotoxic effects (i.e., when fighting infection) and others that promote cell growth, matrix remodeling, and wound healing.¹ However, the dysregulation of these multifaceted activities can initiate pathogenesis and promote disease progression. For example, in many cancers, significant levels of resident macrophages have been observed, and this has been correlated with poor prognoses.² This is hypothesized to occur because tumor-associated macrophages (TAMs) overexpress angiogenic growth factors such as VEGF, and matrix-remodeling enzymes, including cathepsins and metalloproteinases, promoting tumor growth and invasiveness.³ Macrophages also secrete immuno-suppressive cytokines, including IL-10 and TGF- β , which discourage the infiltration of antitumor lymphocytes and further promote an environment conducive to unchecked tumor progression.⁴ Therefore, macrophages potentially represent a viable therapeutic target that can address a major underlying cause of cancer progression. On the basis of this hypothesis, technologies that allow cell-specific phenotypic modulation of aberrant macrophage activity would have an especially strong impact in cancer research.

A promising strategy for reprogramming macrophage behavior is through the use of RNA interference (RNAi) therapy. One approach to therapeutically harnessing RNAi involves the delivery of small interfering RNA (siRNA). siRNA is processed by the target cell's inherent transcriptional regulation machinery, with the ultimate effect of gene silencing through cleavage and degradation of mRNA complementary to the antisense strand of the delivered siRNA duplex.⁵ By silencing master genes that regulate undesirable macrophage activity, RNAi therapy has the potential to directly block macrophage functions that lead to disease progression. A number of studies in genetically engineered knockout models suggest that genes within the Jak/Stat pathways drive pathologic macrophage polarization and activity in a variety of diseases.^{6–9} Recently, Kortylewski et al. showed that siRNA-mediated silencing of Stat3 in tumor-infiltrating leukocytes drove immune-mediated tumor rejection.¹⁰ In a related

Received: August 7, 2012

Revised: December 20, 2012

Accepted: January 19, 2013

approach, it has also been shown that siRNA-mediated knockdown of CCR2 in monocytes weakens their ability to enter tumor sites, resulting in fewer TAMs and reduced tumor volumes.¹¹ Finally, in a study aimed at reducing the level of classically activated, pro-inflammatory macrophages, Aouadi et al. showed that siRNA-mediated silencing of Map4k4 suppressed systemic inflammation by reducing the level of production of TNF α by macrophages.¹² The authors note that this approach can be applied to autoimmune diseases and atherosclerosis, where classically activated macrophages promote disease progression. These studies provide a strong precedent for the use of RNAi to modulate macrophage function and further motivate the broad applicability of macrophage-targeted siRNA nanocarriers for the treatment of a variety of diseases.

Because of their highly degradative phagocytic, endosomal, and lysosomal compartments, delivery and cytoplasmic release of siRNA in macrophages are particularly challenging, especially in primary cells.¹³ Conventional transfection methods have led to limited success, because many of these methods are based on strongly cationic materials that can be cytotoxic and have been largely restricted to the laboratory bench.¹⁴ While strategies exist for targeting macrophages at pathologic sites, some of these strategies require prior knowledge of their locations so that local delivery can be achieved by injection directly into the site of the macrophages.^{10,15} For example, intratumoral or peritumoral injections may be useful when treating a primary tumor site but are poorly translated to the treatment of dispersed, metastatic cancers. Alternative strategies require expensive technologies with uncertain practical clinical applicability, such as macrophage extraction, ex vivo modification, and adoptive transfer;⁸ antibody–nanoparticle conjugates;^{16,17} or custom phospholipids,¹⁸ as reviewed elsewhere.¹⁹ Very few of these proposed approaches can be practically scaled for pharmaceutical purposes. Some of these methods deliver drugs to multiple cell types nonspecifically, and systemic interference with macrophage behavior may lead to unintended side effects, including autoimmune manifestations. Therefore, the clinical translation of macrophage-targeted drug delivery is complicated by barriers, including targeting method, synthesis, and cost.

We designed and evaluated a polymeric glycoconjugate that can be assembled into pH-responsive, endosomolytic nanocarriers for macrophage-specific siRNA delivery (Figure 1). These agents expand on a nontargeted polymeric formulation previously reported by Convertine et al.,²⁰ which is capable of mediating the escape of its cargo from the endosomal pathway, because of their ability to disrupt phospholipid membranes in the acidic environment characteristic within late endosomes ($pH < 6.5$).

The macromolecular structure includes a hydrophobic, pH-responsive block, a cationic, siRNA-condensing block, and a terminal block with reactive sites for “click” bioconjugation (Figure 1). These multifunctional polymers were synthesized via reverse addition–fragmentation chain transfer (RAFT) polymerization, which has the advantage of allowing the polymerization of a variety of monomers displaying a wide range of chemical functionalities.²¹ Additionally, RAFT yields highly monodisperse polymers and is an industrially scalable method, making it appropriate for pharmaceutical applications. In aqueous media at $pH 7.4$, the polymers self-assemble into stable micelles that can be surface-functionalized with a wide range of possible molecular structures through the azide–

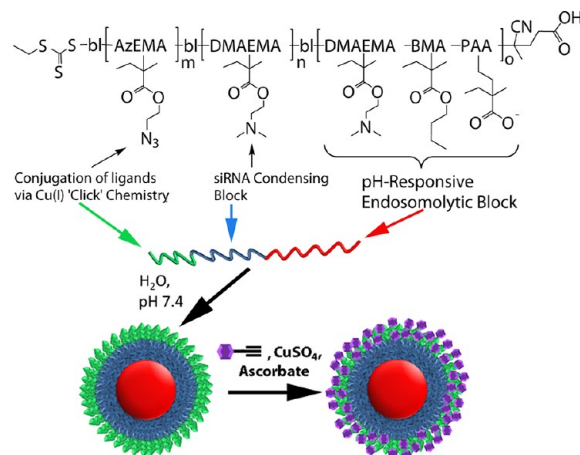


Figure 1. Smart polymeric nanoparticles for mannose receptor-targeted cytosolic delivery of siRNA. Schematic representation of the triblock copolymers and formulation into multifunctional nanoscale siRNA delivery vehicles. The blocks include a pH-responsive block that is capable of disrupting endosomes at low pH (red), a cationic block for condensation of nucleic acids (blue), and an azide-displaying block (green) for conjugation of targeting motifs (purple) via click chemistry.

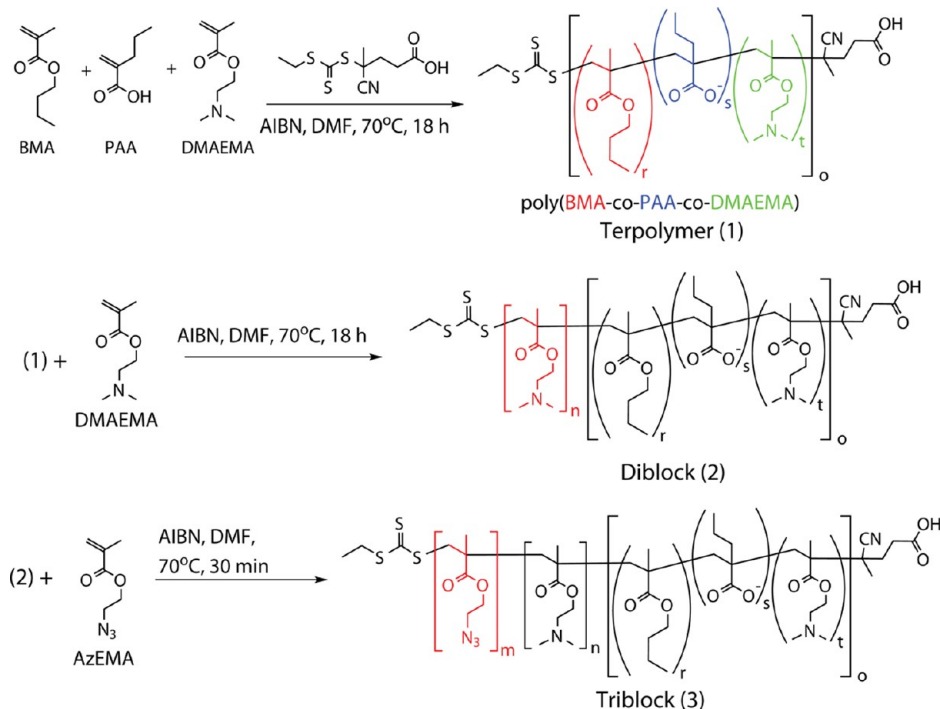
alkyne click reaction chemistry. Because of their orthogonality, specificity, speed, and efficiency,²² “click” reactions have been widely employed to perform covalent conjugations for biological applications.

Mannose was chosen as the targeting motif, because mannose receptor (CD206) is primarily expressed by alternatively activated, M2-like macrophages and some dendritic cells.^{23,24} In these cells, CD206 mediates the recognition and endocytosis of mannosylated, fucosylated, or N-acetylglucosaminated substrates, which occurs via clathrin-coated vesicles.²⁵ While most macrophages express low baseline levels of CD206, mannose receptor is upregulated in TAMs, and the potential to directly target this specific macrophage subset via mannose has not been explored.^{4,26} Mannose is also readily available at significantly lower costs than most alternative targeting motifs (i.e., antibodies and peptides), improving the practicality of the approach. We believe that coupling mannose-mediated targeting with pH-responsive endosomolytic polymers will lead to a reliable and translatable platform for macrophage-targeted RNAi therapies and investigational reagents.

In this study, the capabilities of the mannose receptor-targeted nanoparticles (ManNPs) were evaluated for cytosolic delivery and gene knockdown in primary, murine bone marrow-derived macrophages (BMDMs). The specificity of the carriers was examined on the basis of the ability of the glycoconjugated nanoparticles to preferentially deliver siRNA into immortalized human macrophages relative to cancer cell lines. Results support the idea that the described carrier offers significant opportunities for targeting of drugs and siRNA to TAMs.

EXPERIMENTAL SECTION

Materials. All reagents and materials were purchased from Sigma-Aldrich (St. Louis, MO) and used as received unless described otherwise. Monomers for radical polymerization, including BMA, DMAEMA, PAA, and AzEMA, were all purified by vacuum distillation and stored at 4 °C in

Scheme 1. RAFT Polymerizations^a

^aSynthetic scheme for RAFT polymerization of triblock copolymers composed of blocks of 2-azidoethyl methacrylate (AzEMA), 2-dimethylaminoethyl methacrylate (DMAEMA), and the BMA-co-PAA-co-DMAEMA terpolymer (BMA, butyl methacrylate; PAA, 2-propylacrylic acid).

inhibitor-free containers. Riboshredder RNase blend was purchased from Epicenter (Madison, WI). Immortalized cell lines were acquired from American Type Culture Collection (Manassas, VA). Cell culture supplies, including media, fetal bovine serum, antibiotics, and nonessential amino acids, were obtained from Life Technologies (Carlsbad, CA). The following siRNA sequences were purchased for transfections: FAM-labeled anti-GAPDH siRNA (FAM-siRNA, Life Technologies) and anti-PPIB siRNA (Integrated DNA Technologies, Coralville, IA). Horse serum was purchased from Atlanta Biologicals (Norcross, GA).

Synthesis of 2-Azidoethyl Methacrylate (AzEMA). In a 500 mL round-bottom flask, 15.6 g of sodium azide (0.24 mol) was dissolved in 100 mL of nanopure water, followed by the addition of 5.67 mL of 2-bromoethanol [10 g, 0.08 mol (Figure S1 of the Supporting Information)]. After the flask had been capped with a septum, the reaction mixture was heated to 80 °C and allowed to stir overnight, during which the color of the reaction mixture changed from yellow to orange. Next, the reaction mixture was allowed to cool to room temperature, and the product was extracted four times with 75 mL of diethyl ether. Following two extractions, the color of the aqueous phase changed from orange to clear. The pooled organic fractions were concentrated by rotary evaporation to yield pure 2-azidoethanol (>90% by HPLC, UV trace at 215 nm), which is a clear, colorless oil: 95% yield (6.66 g, 27.6137 g – 20.9532 g); ¹H NMR [400 MHz, (CD₃)₂SO] δ 3.20–3.27 (t, 2H, CH₂N₃), 3.44 (s, 1H, OH), 3.54–3.60 (q, 2H, CH₂O); FT-IR (KBr pellet) 3380 (broad, O-H), 2100 (N₃), 1295 (C-N), 1050 cm⁻¹ (C-O).

In a round-bottom flask, 10 g of 2-azidoethanol (0.11 mol) was mixed with 30.6 mL of Et₃N (22.3 g, 0.22 mol) in 50 mL of CH₂Cl₂ in a dry ice/acetone bath [−78 °C (Figure S1 of the

Supporting Information)]. The reaction vessel was capped with a septum and degassed by alternating evacuation of the vessel and equilibration with nitrogen gas (six times). Next, 8.6 mL of methacryloyl chloride (9.2 g, 0.088 mol) was injected into the system dropwise, and the reaction was allowed to proceed overnight. **Caution:** Azide compounds may become shock-sensitive above 75–80 °C, and this step is highly exothermic. The dry ice/acetone bath was allowed to warm to room temperature during this reaction. The crude product was extracted three times with 1 N hydrochloric acid to remove excess Et₃N, extracted twice with 1 N aqueous NaOH, and precipitated in nanopure water. After the organic fraction had been dried over MgSO₄, the product was concentrated under rotary evaporation to yield a dark red-orange liquid, which was further distilled under high vacuum to produce pure 2-azidoethyl methacrylate. RAFT polymerization kinetics of AzEMA are shown in Figure S2 of the Supporting Information: ¹H NMR (400 MHz, CDCl₃) δ 1.97 (s, 3H, CH₃), 3.5 (t, 2H, CH₂N₃), 4.33 (t, 2H, CH₂O), 5.62 (s, 1H), 6.18 (s, 1H).

Synthesis of Alkyne-Functionalized Mannose. The reaction diagram is shown in Figure S3A of the Supporting Information. In a round-bottom flask, 11 g of D-mannose (60 mmol) was dissolved in 30 mL of dimethyl sulfoxide (DMSO). To activate the sugar into a nucleophile, 10 mL of Et₃N (triethylamine, 72 mmol) was added to the reaction mixture, followed by the addition of 5 g of propargyl chloride (67 mmol). After the mixture had been purged with argon, the reaction proceeded for 24 h at 40 °C. Excess reagents were removed by extraction into diethyl ether (five times). The remaining ether-insoluble phase was dissolved into nanopure water and further extracted five times with dichloromethane to remove other byproducts and DMSO. The product was flash-frozen in liquid N₂ and lyophilized. HPLC characterization and

Table 1. Characterization of Polymers Synthesized via RAFT Polymerization

polymer	abbreviation	$\frac{dn}{dc}$ (mL/g) ^a	target M_n (Da)	M_n (Da) ^b	M_w (Da) ^b	PDI	D_h (nm)	ζ -potential (mV)
poly(BMA-co-PAA-co-DMAEMA) ^c	terpolymer	0.081	14000	11400	13900	1.22		
poly(BMA-co-PAA-co-DMAEMA)-bl-poly(DMAEMA)	diblock	0.049	21000	16800	20700	1.23	32.2 ± 6.8	15.0 ± 5.3
poly(BMA-co-PAA-co-DMAEMA)-bl-poly(DMAEMA)-bl-poly(AzEMA)	triblock	—	22000	22300	28900	1.29	28.0 ± 1.5	19.6 ± 11.7

^aMeasured in off-line batch mode in a Shimadzu RID-10A differential refractive index (dRI) detector, with DMF and 0.1 M LiBr as the solvent.

^bMeasured via gel-permeation chromatography with MALS and dRI in-line with columns. ^cThe terpolymer was insoluble in aqueous buffer at pH 7.4, so no D_h or ζ -potential could be measured via DLS.

¹H and ¹³C NMR are presented in Figure S3B–D of the Supporting Information.

RAFT Polymerizations. Syntheses of the RAFT chain transfer agent (CTA) 4-cyano-4-(ethylsulfanylthiocarbonyl)-sulfanylpentanoic acid (ECT) and 2-propylacrylic acid monomer have been described in detail previously.^{20,27} Block copolymers were synthesized on the basis of the reaction shown in Scheme 1.

Polymerization of the 47%BMA–25%PAA–28%DMAEMA terpolymer (**1** in Scheme 1, compositions based on the ¹H NMR of the product; target composition was 50%BMA–25%PAA–25%DMAEMA) was conducted at 70 °C under N₂ for 18 h with DMF as the solvent (90 wt % in feed), an initial monomer:CTA molar ratio of 100, and a CTA:initiator molar ratio of 10. After the reaction mixture had been rapidly cooled in an ice bath, the organic mixture was mixed in a 1:1 ratio (by volume) with aqueous HCl at pH 2, which initially results in a turbid mixture that quickly turns clear-yellowish. Next, the polymer was precipitated seven times in hexanes and twice in diethyl ether to remove residual, unreacted monomers. Finally, the polymers were dialyzed across a 10 kDa molecular mass cutoff membrane (Pierce, Rockford, IL) against nanopure water (pH 5) overnight. Lyophilization yielded the pure terpolymer, which was a yellowish powder (Table 1).

The same monomer:macroCTA:I molar ratios and 90 wt % DMF conditions were used to polymerize the DMAEMA block onto the terpolymer macroCTA (**1**). To purify the poly(BMA-co-PAA-co-DMAEMA)-bl-poly(DMAEMA) diblock copolymers (**2** in Scheme 1, henceforth termed diblock), the reaction mixture was precipitated in diethyl ether at –20 °C for 1 h and then pelleted by centrifugation at 800g for 5 min. The polymer was dialyzed against deionized water for 48 h using a 10 kDa molecular mass cutoff membrane, and lyophilization yielded a light yellow powder.

Finally, the AzEMA block was polymerized from the diblock (**2**) to form poly(BMA-co-PAA-co-DMAEMA)-bl-poly(DMAEMA)-bl-poly(AzEMA) triblock copolymers (**3** in Scheme 1, henceforth termed triblock) using similar reaction conditions. This mixture was then dialyzed against nanopure water across a 10 kDa molecular mass cutoff membrane overnight to yield pure triblock. The triblock copolymer was dissolved in deionized water at a concentration of 1 mg/mL and stored at –20 °C until it was ready for use in click reactions.

¹H NMR spectra for all polymers are shown in Figure S4 of the Supporting Information.

Mannose Click Functionalization. In a scintillation vial, 1 mL of poly(BMA-co-PAA-co-DMAEMA)-bl-poly(DMAEMA)-bl-poly(AzEMA) copolymer (**3**, 1 mg/mL in nanopure H₂O) was mixed with 6 mg of alkyne-functionalized mannose (27.5 mmol). After the addition of CuSO₄ and sodium ascorbate to final concentrations of 1 and 5 mM, respectively, the reaction

was allowed to proceed at 37 °C on an orbital shaker in the dark for 48 h. Excess copper was removed by treating the crude product with Chelex 100 Resin (Bio-Rad Laboratories, Hercules, CA) according to the manufacturer's instructions. The product was filtered through a 0.45 μm Teflon filter to remove the resin and then dialyzed through a 2 kDa molecular mass cutoff membrane against deionized water to remove excess reactants. Lyophilization yielded the ManNPs, which were reconstituted in nuclease-free water at a concentration of 1–4 mg/mL before being used in experiments. ¹H NMR characterization of the micelles before and after click chemistry is shown in Figure S5 of the Supporting Information.

Characterization of Polymer-Mediated siRNA Complexation and Nuclease Protection. FAM-labeled siRNA (50 pmol) was complexed with mannosylated nanoparticles at N:P (NH⁺:PO₄[−]) ratios of: 1:2, 1:1, 2:1, and 4:1. Ratios were calculated by using the concentration of NH⁺ (based on the degree of polymerization of the DMAEMA homopolymer block) and PO₄[−] (based on the number of siRNA base pairs). Because the pK_a of DMAEMA is ~pH 7.5, we assumed that the DMAEMA polymer block was 50% charged for the calculation of N:P ratios. The complexes were loaded onto a 2% agarose gel containing 1.5 μM ethidium bromide.

By measuring the hyperchromic effect, protection of siRNA from RNase degradation was assessed in untargeted nanoparticles comprised of the diblock copolymers or mannosylated nanoparticles (1:2 or 4:1 N:P ratios), as described previously.²⁸

Hemolysis Assays. Assays were performed as described previously.²⁹ Briefly, human blood samples were obtained from consenting, anonymous, healthy adults under a protocol approved by the Vanderbilt University Institutional Review Board (IRB). Plasma was removed, and RBCs were washed with 150 mM NaCl. RBCs were ultimately diluted into phosphate buffers adjusted to pH 5.6, 6.2, 6.8, or 7.4, and the percent hemolysis in these buffers was assessed for polymers at concentrations of 1, 5, and 40 μg/mL. PBS (negative control) or 20% Triton X-100 (positive control) was used as a control. Polymer/RBC solutions were incubated at 37 °C in a 5% CO₂ incubator for 1 h and centrifuged at 1500 rpm for 5 min, and supernatants were transferred to a new plate. The percent RBC lysis was quantified on the basis of the absorbance at 450 nm relative to samples treated with Triton X-100 (assume 100% lysis) and PBS (to subtract background absorbance).

Animals and Cell Lines. Animal work was approved by the Vanderbilt University Institutional Animal Care and Use Committee. All mice were on an FVB background strain. Bone marrow-derived macrophages were isolated from tibiae and femurs immediately after the mice had been sacrificed and cultured as described previously.³⁰ Cells were seeded at a density of 300000 cells/cm² for all experiments. Detailed information about culturing of immortalized cell lines can be found in the Supporting Information.

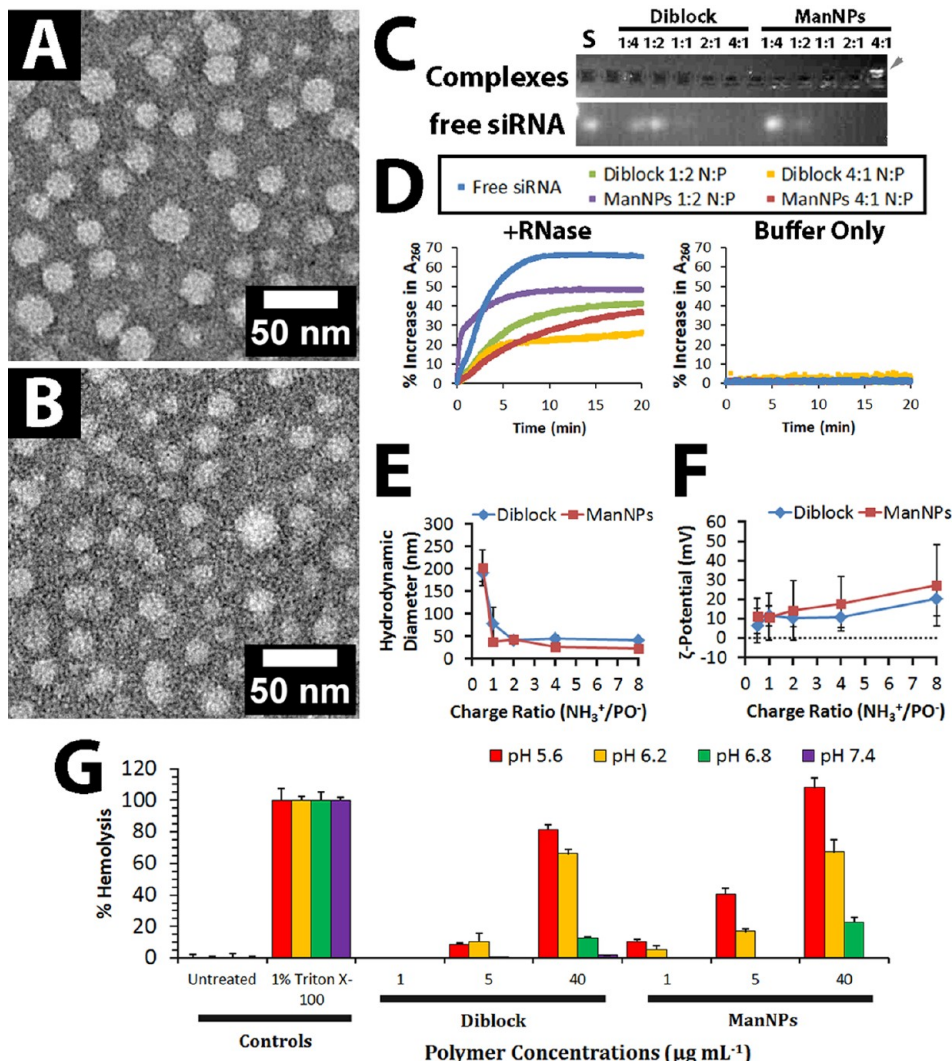


Figure 2. Morphologic and functional characterization of micelles composed of diblock copolymers and mannosylated triblock copolymers. (A and B) Uranyl acetate-counterstained transmission electron micrographs. (A) Dehydrated micelles of diblock copolymers (see 2 in Scheme 1) had an average diameter of 13.0 ± 6.1 nm ($n = 367$). (B) Dehydrated ManNPs had an average diameter of 9.7 ± 6.2 nm ($n = 415$). Scale bars are 50 nm. (C) Gel retardation assay of siRNA-loaded ManNPs confirmed an increased level of complexation of siRNA with increasing N:P ratios. Free FAM-labeled siRNA (S) appears as a control. (D) Protection of siRNA from degradation by RNases. Micelle–siRNA complexes were incubated with RNase cocktails. RNase-mediated degradation of siRNA was characterized by a hyperchromic effect at 260 nm, and within 10–15 min, all siRNA in each sample had completely degraded as signified by asymptotic behavior of the results. siRNA and micelle–siRNA complexes that were left in buffer without RNases did not exhibit this hyperchromic effect. (E and F) Dynamic light scattering was used to analyze the (E) hydrodynamic diameters and (F) ζ -potentials of the polymeric micelles following complexation with siRNA. (G) Both polymers exhibit pH- and concentration-dependent hemolysis, with minimal disruption of erythrocyte phospholipid membranes at physiologic pH, but an increased level of disruption in pH ranges mimicking the endosomal pH (pH < 6.5). Error bars represent the standard deviation of four replicates.

Transfections. ManNP formulations were prepared as described above, and Lipofectamine RNAiMAX (Life Technologies) was used according to the manufacturer's instructions as a commercially available benchmark. Cells were rinsed twice with PBS and given serum-free medium, which is composed of DMEM with 4.5 g/L glucose, 1 unit/mL penicillin, 1 $\mu\text{g}/\text{mL}$ streptomycin, and 2 mM L-glutamine. Complexes were then added to the wells such that the final concentration of siRNA in the wells was 50 nM (10-fold dilution from stock). For some experiments, cells were co-incubated with complexes and 100 mg/mL free D-mannose (Sigma-Aldrich) to examine the CD206 dependence of nanoparticle-mediated siRNA delivery. At set time points, wells were rinsed with PBS and processed according to the desired experiment as described below.

Transfected cells were analyzed for cell viability using a Live-Dead kit (Life Technologies) according to the manufacturer's instructions. Quantification of live and dead cells was conducted by flow cytometry.

Quantitative Real-Time PCR. Total RNA was isolated from cell samples using the RNeasy Kit and QiaShredder columns (Qiagen). After the removal of genomic contamination through DNase treatment (DNA-free kit, Life Technologies), cDNA libraries were constructed using a reverse transcriptase kit (Life Technologies).

For qRT-PCR, primers were purchased from Integrated DNA Technologies: PPIB, 5'-TTCCATCGTGTCAAG-3' (sense) and 5'-GAAGAACTGTGAGCCATT-3' (antisense); GAPDH, 5'-TGAGGACCAGGTTGTCTCCT-3' (sense) and 5'-CCCTGTTGCTGTAGCCGTAT-3' (antisense). qRT-PCR

was conducted using SYBR Green PCR Master Mix. Details of data analysis for relative GAPDH expression can be found in the Supporting Information.

Flow Cytometry. Flow cytometry was performed on a BD (Franklin Lakes, NJ) FACSCalibur system, operated via BD Cellquest Pro, version 5.2. The FL1 channel (emission filter at 530 ± 15 nm) was used for the quantification of the FAM emission of each cell.

Confocal Microscopy. Transfections were performed as described above for 1, 2, or 4 h. To prepare cells for confocal microscopy, they were washed with PBS, fixed for 15 min with 10% buffered formalin, rinsed three times with PBS, and then stained with DAPI (Invitrogen, Carlsbad, CA) for 10 min. After the cells had been rinsed three times with PBS, slides were mounted with the Invitrogen ProLong Antifade kit. Imaging was performed on a Zeiss (Oberkochen, Germany) LSM 710 system. Image processing is described in the Supporting Information.

Statistical Analysis. For all experiments, statistical significance was assessed using the unpaired Student's *t* test or one-way ANOVA as appropriate and indicated in the text, with $p < 0.05$ considered significantly different.

RESULTS

Modular Design, Synthesis, and Characterization of Mannosylated siRNA Delivery Vehicles. The synthesis of the mannosylated delivery vehicles was successfully completed through three stages. (I) The polymeric components were synthesized in three sequential iterations of RAFT polymerization and purification (Figure 1 and Scheme 1). (II) Alkyne-functionalized mannose was separately synthesized (Figure S3 of the Supporting Information). (III) The polymers from stage I are formed into micelles and reacted with the alkyne-functionalized mannose from stage II. These steps result in immobilization of mannose onto the micelle corona through reaction with the distal azide groups via click chemistry (Figure 1).

The polymers that make up the ManNPs were synthesized via RAFT polymerization. These modules include a pH-responsive block (Figure 1, red), a cationic block for condensing nucleic acids (blue), and an azide-presenting block (green) for the attachment of alkyne-functionalized ligands. First, a ~14 kDa random terpolymer block composed of 47% butyl methacrylate (BMA), 25% 2-propylacrylic acid (PAA), and 28% 2-dimethylaminoethyl methacrylate (DMAEMA) was synthesized (Scheme 1 and Table 1). The percentages represent the molar composition of each monomer in the copolymer structure, as determined by ^1H NMR (Figure S4 of the Supporting Information). The terpolymer forms a turbid suspension upon being exposed to aqueous media at pH 7.4 but dissolves effectively when the pH is lowered to <6.0 , consistent with the pH-sensitive characteristics of this block.

To form a hydrophilic, corona-forming segment, a cationic DMAEMA block (8.9 kDa by ^1H NMR) was polymerized from the terpolymer macroCTA, yielding a diblock copolymer [22.8 kDa (Figure 1, red and blue, and Table 1)]. This diblock copolymer self-assembles into micellar nanoparticles upon being exposed to aqueous media (Figure 2A), consistent with previous work by others.^{20,31–33} Diameters of the diblock copolymer micelles were measured to be 13.0 ± 6.1 nm in a dehydrated state by TEM and 32.2 ± 6.8 nm in a hydrated state by DLS.

Finally, an azide-presenting block composed of 2-azidoethyl methacrylate (AzEMA) was extended from the DMAEMA terminus of these polymers (Figure S4 of the Supporting Information). The synthetic route for AzEMA (Figure S1 of the Supporting Information) was modified from published schemes for the synthesis of 3-azidopropyl methacrylate, a similar monomer.^{34,35} The controlled polymerization kinetics of AzEMA are also presented (Figure S2 of the Supporting Information).

The resulting triblock copolymers retained the ability to self-assemble into micelles in aqueous media. Morphologically, the triblock copolymers are expected to form assemblies as depicted in Figure 1, where the azide-presenting block effectively shields the DMAEMA block in the final micellar structures. Because addition of the final, AzEMA block to the base diblock leads to a 4 nm decrease in the hydrodynamic diameter of the resulting micelles and a slight increase in the ζ -potential (Table 1), NMR spectra of the micelles were obtained in D_2O to improve our understanding of the particle morphology in aqueous environments (Figure S4 of the Supporting Information). The base diblock micelles [poly-(BMA-co-PAA-co-DMAEMA)-bl-poly(DMAEMA), 2] featured peaks in chemical shift regions characteristic of pure poly(DMAEMA), while the micelles composed of the triblock [poly(BMA-co-PAA-co-DMAEMA)-bl-poly(DMAEMA)-bl-poly(AzEMA), 3] produced peaks corresponding to the azido protons in addition to poly(DMAEMA) peaks (Figures S4 and S5 of the Supporting Information). Therefore, micelles consisting of the diblocks display a corona of DMAEMA, while the triblock copolymers form micelles that present azide groups at their corona, allowing the facile immobilization of alkyne-functionalized ligands onto the micelles.

The synthesis of alkyne-functionalized mannose (Figure S3A of the Supporting Information) was adapted from a synthetic scheme for derivatized sugars presented by Plotz and Rifai.³⁶ The resulting NMR spectra of the product indicated the successful alkyne functionalization of the monosaccharide (Figure S3C,D of the Supporting Information). HPLC confirmed that the product is 70–80% pure following synthesis. No further purification was conducted, and nonfunctionalized mannose was subsequently removed via dialysis of the final ManNPs.

Following the click reaction to functionalize the polymers with mannose, the polymers retained the ability to form micellar nanoparticles, similar to those formed by the diblock copolymers lacking the azide block and mannose (Figure 2A,B). The ManNPs exhibited diameters of 9.7 ± 6.2 nm in a dehydrated state by TEM and 21.8 ± 2.6 nm in a hydrated state by DLS. The ManNPs also exhibited a distinct NMR signature compared to that of the micelles made of triblock copolymer before the click mannosylation reaction (Figure S5 of the Supporting Information). This is particularly evident in the 3.2–3.7 ppm region, where the appearance of peaks corresponding to mannose is consistent with the success of the click reaction.

ManNPs Form Complexes with siRNA and Protect Cargo from Degradation. Like the diblock copolymers, the completed ManNPs are able to complex siRNA in an N:P ratio-dependent fashion as evidenced by a gel retardation assay (Figure 2C). The brightness of the free, uncomplexed siRNA band apparent in the gel decreased with an increased N:P ratio. We also performed experiments to characterize the ability of ManNPs to protect siRNA cargo from nuclease degradation

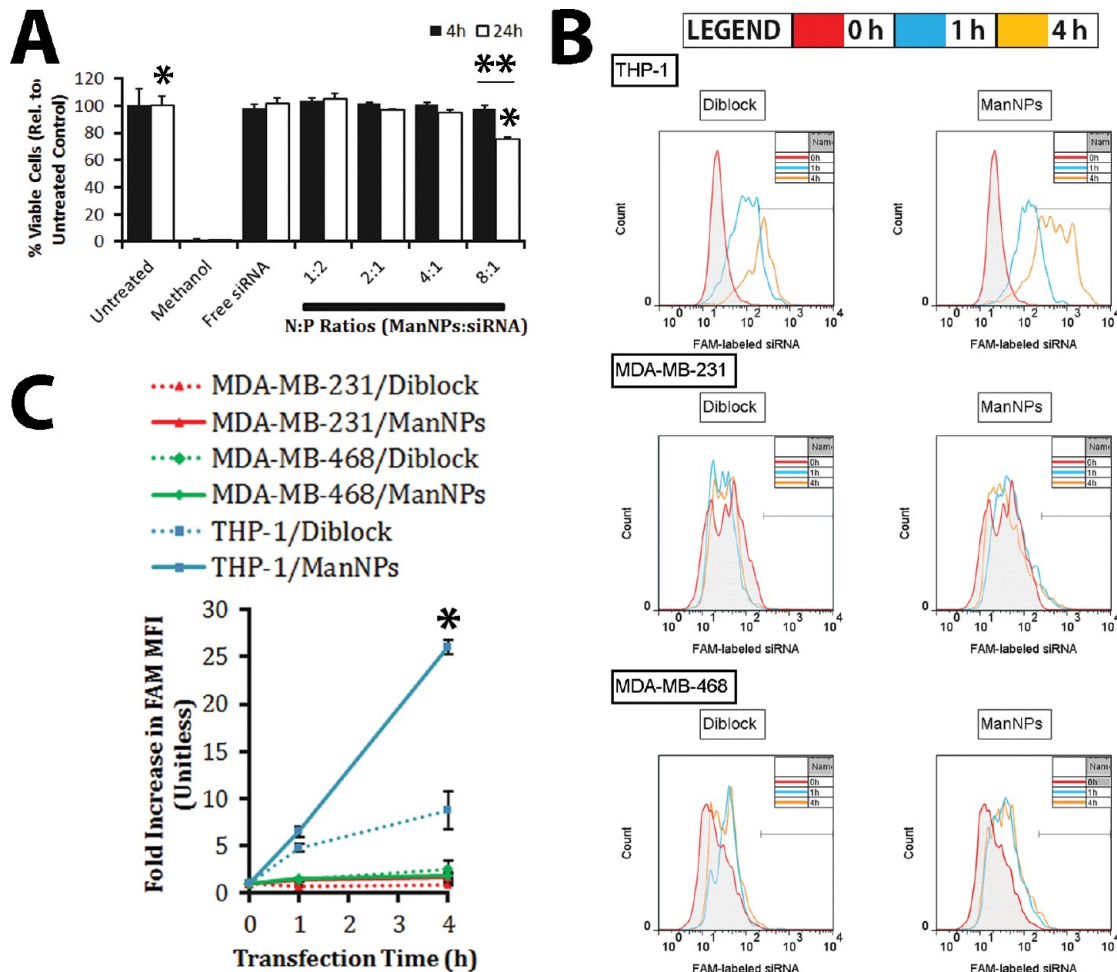


Figure 3. ManNPs are cytocompatible and selectively enhance the delivery of siRNA into immortalized human macrophages. (A) Cytotoxicity assay of immortalized THP-1 macrophages, treated with ManNPs complexed with siRNA at various N:P ratios. Error bars represent the standard deviation from three experiments (*, ** $p < 0.01$; $n = 3$). (B) Representative flow cytometry histograms of THP-1, MDA-MB-231, and MDA-MB-468 cells 0 (red), 1 (blue), or 4 h (orange) after transfection with FAM-siRNA loaded into diblock micelles (left) or ManNPs (right). (C) Mean fluorescence intensities of all of the groups in panel B have been quantified and are shown. Error bars represent the standard deviation of three experiments. ManNPs enhanced the delivery of siRNA into macrophages up to 26-fold over two model breast cancer cell lines and 3-fold in macrophages relative to untargeted diblock carriers, as measured via flow cytometry (* $p < 0.01$ vs all other treatment groups at the 4 h time point).

(Figure 2D). In this study, the degradation of siRNA results in a hyperchromic effect, which is characterized by increased sample absorbance at 260 nm.²⁸ The 65% increase in Abs_{260} of free siRNA within 10 min of RNase treatment is a demonstration of this effect and is used as a positive control. The same siRNA incubated in buffer alone did not exhibit this trend, confirming that RNase activity is necessary for the hyperchromic effect. Both polymers were able to protect their cargo from rapid degradation by RNases, and this ability is enhanced at higher N:P ratios.

Finally, dynamic light scattering confirmed that the hydrodynamic diameter of the siRNA–polymer complexes increased with a decreasing N:P ratio [less polymer per siRNA, from 8:1 to 1:2 (Figure 2E)]. However, at N:P ratios of <2 , these complexes became less stable, and >100 nm diameter aggregates were measured. Decreasing N:P ratios also corresponded to decreasing nanoparticle ζ -potential (Figure 2F). Both polymers formed complexes with siRNA that exhibited ζ -potentials of <25 mV, and these complexes remain colloidally stable if left at room temperature for at least 24 h without any observable flocculation.

ManNPs Exhibit pH-Dependent Hemolysis and Are Cytocompatible.

We next sought to investigate the ability of the ManNPs to create pH-dependent membrane disruption of red blood cells as a surrogate measure for escape from acidified endosomes following endocytotic uptake. Erythrocyte hemolysis assays are commonly employed to model polymer–endosome interactions because relative membrane disruption can be quantified through the release of hemoglobin from the cells (Figure 2G).²⁹ Neither the diblock nor the ManNPs caused significant levels of hemolysis at pH 7.4 (1.8 ± 2 and $0.0 \pm 0.1\%$, respectively, at a $40 \mu\text{g/mL}$ dose, relative to detergent-treated erythrocytes; $n = 4$). However, as the environmental pH was decreased to 6.2, significantly higher levels of hemolysis were measured (66.1 ± 2.7 and $67.3 \pm 7.6\%$ for diblocks and ManNPs, respectively). This effect was even greater at pH 5.6 ($81.5 \pm 3.1\%$ for diblock and $108.2 \pm 6.1\%$ for ManNPs), which is similar to pH ranges encountered in late endosomes and lysosomes.²⁹ These data suggest that, during circulation, the nanoparticles are unlikely to cause adverse effects because of cell membrane lysis. Importantly, these results also suggest that, following endocytosis, the polymeric components will be

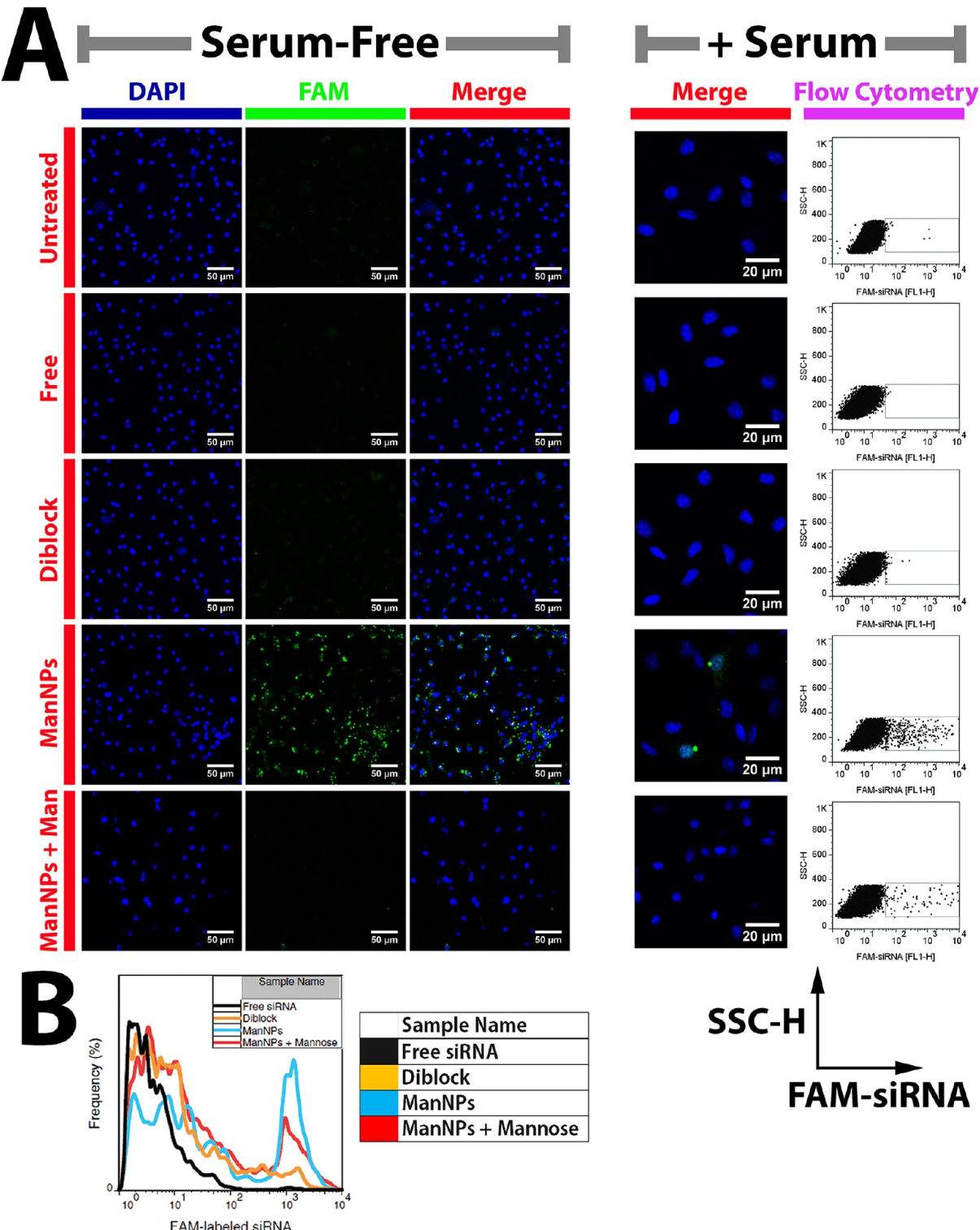


Figure 4. CD206-dependent delivery of siRNA to primary macrophages using ManNPs. (A) Following transfection with FAM-siRNA for 4 h (green; free or complexed into nanoparticles), BMDMs were fixed, and nuclei were stained with DAPI (blue) and imaged via confocal microscopy. Scale bars are 50 μ m for serum-free and 20 μ m for serum. Mannosylation of the polymeric vehicles enhanced their internalization by BMDMs. This could be competitively inhibited through co-administration of the ManNPs with D-mannose. A similar trend was observed when transfactions were performed under serum conditions. The FAM brightness and contrast were enhanced equally for all samples with serum but unaltered for the serum-free condition. For the serum-free condition, the brightness and contrast were also enhanced in the DAPI channel to account for small differences in staining between samples. (B) Flow cytometry quantification of delivery of FAM-siRNA into BMDMs via ManNPs (blue) relative to untargeted nanoparticles (orange) or free siRNA without vehicle (black) within 4 h of administration under serum-free conditions. Quantification of mean fluorescence intensity in each treatment group is shown in Figure S6 of the Supporting Information.

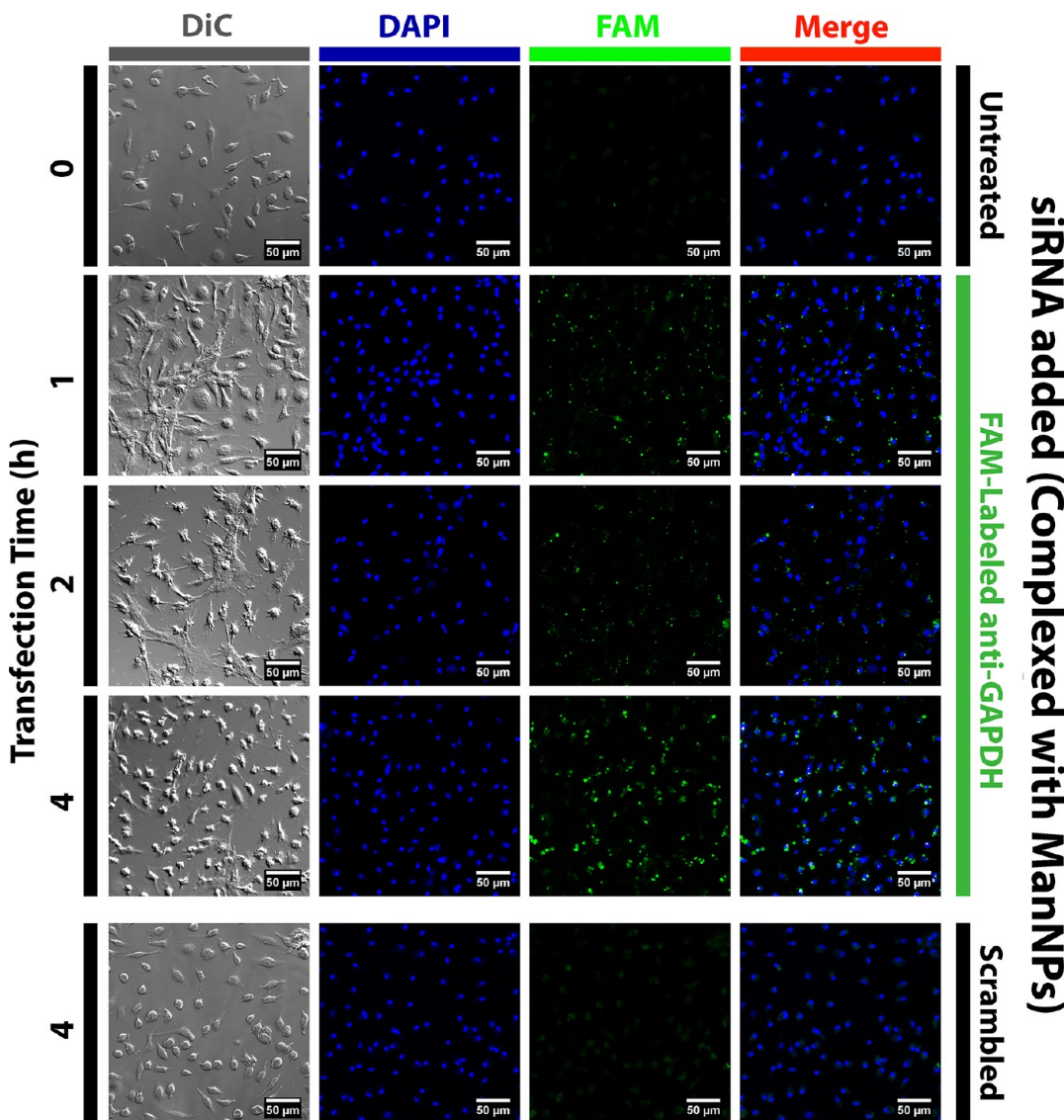


Figure 5. Kinetics of ManNP-mediated delivery of siRNA into primary macrophages. BMDMs were transfected with FAM-siRNA (green; complexed into ManNPs) for 1–4 h prior to being fixed, stained with DAPI (blue), and imaged via confocal microscopy. Scale bars are 50 μ m. As a comparison, BMDMs treated with nonfluorescent, scrambled siRNA (also complexed into ManNPs) are also shown. The brightness and contrast were enhanced in the DAPI channel to account for small differences in staining between samples. All settings were identical for FAM imaging. The punctate green signal is observed within 1–2 h of administration, suggesting internalization of siRNA into vesicles. At the 4 h time point, more green fluorescence has accumulated and the staining pattern is more diffuse, consistent with endosomal escape of the siRNA into the cytosol.

able to facilitate pH-dependent disruption of endosomal membranes and cytosolic delivery of the cargo.

To further demonstrate that the polymers do not cause significant cytotoxicity under physiologic pH conditions, immortalized human THP-1 macrophages were incubated with siRNA-loaded ManNPs at various N:P ratios, and cell viability was assessed via calcein AM/ethidium homodimer incorporation 4 or 24 h after ManNP delivery. Experimental groups were quantified via flow cytometry relative to untreated cells (100%) or methanol-killed cells [set to 0% (Figure 3A)]. For all N:P ratios investigated, negligible cytotoxicity was observed after treatment for 4 h. However, at 24 h, $76 \pm 1\%$ of the cells treated at the 8:1 N:P ratio remained viable, indicating that prolonged treatment of BMDMs with ManNPs and siRNA at this charge ratio resulted in mild but significant levels of cytotoxicity (*,** $p < 0.01$; $n = 3$). The 4:1 N:P ratio was

selected for further experiments on the basis of precedent^{20,27,37} and because it did not result in significant cytotoxicity at 24 h.

ManNPs Selectively Enhance Delivery to Human Macrophages. To examine the potential of using the ManNPs to selectively target TAMs, we incubated ManNPs loaded with FAM-siRNA with immortalized human macrophages (THP-1) or human breast cancer cell lines (MDA-MB-231 and MDA-MB-468) for up to 4 h. Cellular internalization of the siRNA was assessed via flow cytometry (Figure 3B,C). All measurements were normalized against the inherent FAM intensity measured in untreated cells. As controls, cells treated with siRNA-loaded micelles made with the diblock copolymers were also measured. For both breast cancer cell lines, modest intracellular delivery of FAM-siRNA/ManNPs was observed with either carrier investigated (diblocks or ManNPs). Both cell types experienced an approximately 2-fold increase in FAM mean fluorescence intensity (MFI) over the 4 h study period.

With the macrophages, the same treatment period led to a 26-fold increase in the FAM MFI of the cells, confirming that these cells preferentially internalize the constructs relative to the model cancer cell lines (Figure 3C; $*p < 0.01$ vs all other treatment groups at the 4 h time point). Further, ManNPs facilitated a 3-fold increase in the level of delivery of siRNA to the macrophages, relative to the diblock micelles.

ManNPs Mediate CD206-Dependent Intracellular siRNA Delivery and Target Gene Knockdown in Primary Murine Macrophages. siRNA delivery and gene knockdown were examined in primary murine bone marrow-derived macrophages (BMDMs). Within 4 h of siRNA administration, ManNPs improved delivery of FAM-siRNA into macrophages by more than 40-fold relative to the delivery of free siRNA or 4-fold relative to the delivery of untargeted, diblock copolymers (Figure 4 and Figure S6 of the Supporting Information; $p < 0.01$). Notably, the uptake of ManNPs can be partially blocked via co-administration with D-mannose, indicating that internalization of the ManNPs is mediated by mannose receptor CD206. These phenomena are also observed when transfections are performed in serum-containing media (Figure 4A, right).

In support of these observations, imaging of the uptake of fluorescently labeled siRNA into BMDMs was accomplished by confocal microscopy (Figures 4A and 5 and Figure S7 of the Supporting Information). Consistent with the flow cytometry results, mannose targeting significantly increased the rate of delivery of siRNA into macrophages, and co-administration of D-mannose with the ManNPs reduced the magnitude of the FAM-siRNA signal in the BMDMs. Significant levels of FAM-siRNA can be visualized in the BMDMs within 1–2 h of administration.

The enhanced delivery of siRNA via the ManNPs also corresponded to knockdown of expression of a model gene, cyclophilin B (PPIB) in BMDMs relative to nontransfected cells and cells treated with complexes of ManNPs with scrambled siRNA [ManNPs/SCR (Figure 6; $*p < 0.05$)]. The commercially available Lipofectamine RNAiMAX transfection reagent was a reliable positive control and was the most effective vehicle for facilitating the knockdown of PPIB expression ($0.5 \pm 0.2\%$ residual PPIB expression). Despite lower levels of delivery of siRNA into the BMDMs than into ManNPs (Figure 4), the diblock nanoparticles also facilitated a significant level of PPIB knockdown ($p = 0.55$ relative to ManNPs, via one-way ANOVA).

DISCUSSION

Because of their central role in promoting the progression of a number of debilitating diseases, such as cancer and atherosclerosis, macrophages represent an important target for immunotherapy.^{19,38} Nanoparticle-mediated drug delivery is an attractive way to achieve this goal, because macrophages are phagocytes capable of efficiently internalizing particulate substances.^{39,40} However, macrophages play functional roles in maintaining the healthy physiology of many tissues, including bone, liver, and spleen.^{41–43} Therefore, to reduce the likelihood of an off-target impact on healthy immune function, it is very important to specifically target macrophages at desired pathological sites. In this work, we demonstrated the design, synthesis, and characterization of mannosylated micellar nanoparticles to target CD206 expression, which is upregulated in tumor-associated macrophages.^{23,24,44,45} The creation of these nanoparticles centers around a generalizable platform that

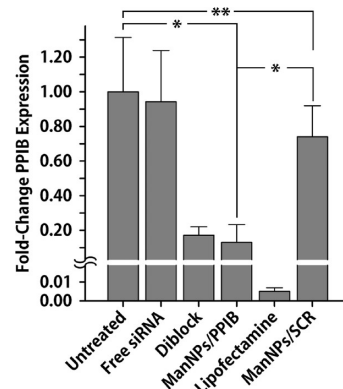


Figure 6. ManNPs mediate knockdown of PPIB expression in BMDMs. siRNA-mediated knockdown of PPIB expression using different transfection vehicles relative to controls. qRT-PCR confirmed ManNPs carrying anti-PPIB siRNA (ManNPs/PPIB) mediated an $87 \pm 10\%$ decrease in the level of target gene expression following treatment for 24 h, relative to nontransfected cells. Data were normalized to the expression of the housekeeping gene GAPDH as an internal control. Error bars represent the standard deviation of three independent experiments ($*p < 0.05$ by one-way ANOVA; **not statistically significant). Some BMDMs were also transfected with ManNPs carrying scrambled siRNA (ManNPs/SCR) as an additional negative control.

can be utilized for “clicking” ligands onto the surfaces of siRNA-condensing polymeric nanoparticles. We opted for this strategy, involving the highly efficient Huisgen 1,3-dipolar cycloaddition reaction, otherwise known as azide–alkyne click chemistry (Figure 1), because it provides the necessary orthogonal chemistry to allow the synthesis of the block copolymers for siRNA delivery, followed by site-selective functionalization of the nanocarrier coronas with the ligand of interest in the final step. The resulting ManNPs exhibited diameters of <40 nm (Figure 2), a size range that confers the additional advantage of exhibiting improved passive accumulation into tumors.^{39,46}

This approach extends previous work by Convertine et al. describing polymers for siRNA delivery applications, which exhibited nonselective transfection activity driven by their cationic corona.²⁰ The diblock copolymers tested in this work were patterned after these polymers and provide a reliable benchmark against which the ManNPs can be reasonably compared.^{20,47} To improve the cellular specificity of these carriers, variants that target folate receptor and CD22 have recently been developed.^{32,33} These polymers include a micelle core-forming terpolymer block, which confers pH responsiveness to the final polymers. Because of the pK_a values of these monomers (7.5 for DMAEMA and 6.7 for PAA),^{48,49} at pH 7.4, approximately 50% of the amine groups on DMAEMA are protonated (NH^+), and 50% of the carboxylic groups on PAA are deprotonated (COO^-). Therefore, the terpolymer is approximately charge neutral at pH 7.4 when DMAEMA cations and PAA anions are present in relatively balanced quantities, leading to the insolubility of the terpolymer in water at this pH. When the terpolymer is paired with a hydrophilic block to form an amphiphilic diblock structure, the terpolymer block’s electrostatic and hydrophobic interactions allow it to self-assemble into a micelle core at pH 7.4.^{20,27,47} With a decrease in pH, PAA and DMAEMA become increasingly protonated, leading to a net cationic charge on this block that triggers micelle disassembly.²⁰ The exposed terpolymer is

hypothesized to disrupt endosomal and lysosomal membranes and ferry siRNA into the cytoplasm. The block copolymers described here behave in a fashion consistent with this hypothesis, as they exhibit pH-dependent hemolysis at pH ranges that mimic the acidic environments of late endosomes (Figure 2G).

These polymeric siRNA nanocarriers have cationic ζ -potential because of the presence of the poly(DMAEMA) block (blue in Figure 1), and previous observations by others suggest that such agents can exhibit charge-dependent cytotoxicity.¹⁴ Consistent with these reports, a moderate level of cytotoxicity at N:P ratios of >4:1 was not surprising. As a result, all polyplexes for subsequent experiments were prepared at N:P ratios for which negligible cytotoxicity was observed at the 24 h treatment time (Figure 3A). Because of negligible cytotoxicity at a 4:1 N:P ratio, many test agents have been optimized and evaluated at this charge ratio.^{20,27,37} When our delivery system is optimally formulated with siRNA, it is anticipated that the system for preferential macrophage targeting can be safely leveraged to treat diseases, such as cancer, where infiltrating macrophages at pathologic sites exhibit upregulated CD206 expression.⁵⁰

The ManNPs show cell selectivity, and the data suggest that in a tumor environment where cancer cells coexist with a significantly smaller population of macrophages, the ManNPs will enter macrophages markedly faster than the cancer cells (Figure 3B,C). While this increased internalization rate in macrophages over cancer cells was also observed for the diblock copolymer micelles, the effect was enhanced for the mannosylated constructs.

The ManNPs also facilitated improved delivery of siRNA into primary murine macrophages and generated robust knockdown of a model gene (Figures 4–6). The untargeted, diblock polymers also achieved potent gene knockdown despite delivering significantly smaller amounts of siRNA into the macrophages. However, like the ManNPs, the diblock polymers are capable of efficiently escaping from the endosomal compartment in a pH-dependent manner, as modeled via the hemolysis assay (Figure 2G).²⁹ Therefore, even if the diblock copolymers are not as efficiently internalized into BMDMs as the ManNPs, the diblock copolymers still deliver sufficient siRNA to cause significant levels of gene knockdown. This effect can depend on the potency of the siRNA sequence itself, as different siRNA sequences against the same target gene can exhibit widely different abilities to recognize the targeted mRNA sequence for knockdown.⁵¹

These results are significant because primary macrophages possess highly degradative phagocytic, endosomal, and lysosomal compartments, providing a formidable barrier to the cytosolic delivery of siRNA.¹³ Moreover, because the ManNPs are internalized via an endocytotic receptor, these data indicate that ManNPs successfully mediate escape from the endosomal pathway, through a mechanism that is likely mediated by the pH-responsive, endosomolytic behavior of the core-forming terpolymer block.²⁰

CONCLUSIONS

This report demonstrates a novel nanocarrier design for selectively targeting CD206-positive macrophages. The ManNPs' hydrodynamic radius was ~20 nm by DLS, which is appropriate for in vivo tumor biodistribution through the enhanced permeation and retention effect. This novel carrier has finely tuned pH-dependent membrane disruptive behavior,

to overcome the macrophage's highly degradative phagosomal and endosomal compartments. Nanocarrier characteristics allow biologics to be delivered into the macrophage cytosol and promote access of the payload to intracellular drug targets. Importantly, this generalized azide-containing siRNA delivery platform also has potential for click functionalization with alternative targeting ligands, and this is, to the best of our knowledge, the first demonstration of a "clickable", pH-responsive, endosomolytic micelle for siRNA delivery. These strategies will potentially open up new areas in cancer immunotherapy, allowing selective intervention with siRNA therapeutics.

ASSOCIATED CONTENT

Supporting Information

Supplementary materials and methods and supplementary figures. This material is available free of charge via the Internet at <http://pubs.acs.org>.

AUTHOR INFORMATION

Corresponding Author

*Department of Biomedical Engineering, Vanderbilt University, 5824 Stevenson Center, Nashville, TN 37235. E-mail: todd.d.giorgio@vanderbilt.edu. Phone: (615) 322-3521. Fax: (615) 343-7919.

Author Contributions

S.S.Y. oversaw all materials design and synthesis, experimental design, and data collection, analysis, and interpretation, with extensive input from F.E.Y., C.L.D., and T.D.G. C.M.L. and C.A.S. collected, analyzed, and interpreted data. W.J.B. and H.M.O. designed and selected the biological models used in this study and assisted in biological experiments with S.S.Y. and C.M.L., under the oversight of F.E.Y. C.E.N. and H.L. helped design protocols for the synthesis and purification of polymeric products and contributed new reagents and analytic tools crucial to the experiments. S.S.Y. wrote the manuscript. All authors discussed the results and commented on the manuscript.

Notes

The authors declare no competing financial interest.

ACKNOWLEDGMENTS

This work is supported through a Concept Award through the Department of Defense CDMRP Breast Cancer Research Program (W81XWH-10-1-0684). Bone marrow-derived macrophages were supported through a multi-investigator, collaborative IDEA Award through the Department of Defense CDMRP Breast Cancer Research Program (W81XWH-11-1-0344 and W81XWH-11-1-0242). Polymer development was also supported in part through National Institutes of Health (NIH) Grant R21 EB012750. S.S.Y. gratefully acknowledges partial support from a 2012 Lai Sulin Scholarship from the Vanderbilt University. C.M.L. acknowledges partial support through a fellowship from the Vanderbilt Undergraduate Summer Research Program (VUSR). Portions of this work were performed at the Vanderbilt Institute of Nanoscale Science and Engineering, using facilities renovated under National Science Foundation Grant ARI-R2 DMR-0963361. Confocal microscopy was supported in part by National Cancer Institute Cancer Center Support Grant P30 CA068485, utilizing the Vanderbilt University Medical Center Cell Imaging Shared Resource. The Vanderbilt University Medical Center

Cell Imaging Shared Resource is also supported by NIH Grants DK020593, DK058404, DK059637, and EY08126. qRT-PCR was performed in the laboratory of Prof. David G. Harrison (Division of Clinical Pharmacology, Vanderbilt University Medical Center, Nashville, TN). The authors also acknowledge Ryan A. Ortega (Department of Biomedical Engineering, Vanderbilt University) for reading and editing the manuscript.

■ ABBREVIATIONS

AzEMA, 2-azidoethyl methacrylate; BMA, butyl methacrylate; BMDM, bone marrow-derived macrophage; CD206, macrophage mannose receptor; DLS, dynamic light scattering; DMAEMA, 2-dimethylaminoethyl methacrylate; FAM-siRNA, FAM-labeled anti-GAPDH siRNA; ManNPs, mannosylated triblock copolymer nanoparticles; MFI, mean fluorescence intensity; N:P ratio, charge ratio ($\text{NH}^+:\text{PO}_4^-$); PAA, 2-propylacrylic acid; PCR, polymerase chain reaction; PPIB, peptidyl-prolyl *cis-trans*-isomerase B (cyclophilin B); qRT-PCR, quantitative real-time PCR; RAFT, reverse addition-fragmentation chain transfer; TAM, tumor-associated macrophage; THP-1, immortalized human leukemic monocytes/macrophages.

■ REFERENCES

- (1) Kindt, T. J.; Goldsby, R. A.; Osborne, B. A.; Kuby, J. *Kuby Immunology*, 6th ed.; W. H. Freeman: New York, 2007; p xxii, 574, A-31, G-12, AN-27, I-27.
- (2) Lewis, C. E.; Pollard, J. W. Distinct role of macrophages in different tumor microenvironments. *Cancer Res.* **2006**, *66* (2), 605–612.
- (3) Dirkx, A. E.; Oude Egbrink, M. G.; Wagstaff, J.; Griffioen, A. W. Monocyte/macrophage infiltration in tumors: Modulators of angiogenesis. *J. Leukocyte Biol.* **2006**, *80* (6), 1183–1196.
- (4) Vasievich, E. A.; Huang, L. The Suppressive Tumor Microenvironment: A Challenge in Cancer Immunotherapy. *Mol. Pharmaceutics* **2011**, *8* (3), 635–641.
- (5) Fire, A.; Xu, S.; Montgomery, M. K.; Kostas, S. A.; Driver, S. E.; Mello, C. C. Potent and specific genetic interference by double-stranded RNA in *Caenorhabditis elegans*. *Nature* **1998**, *391* (6669), 806–811.
- (6) Mantovani, A.; Garlanda, C.; Locati, M. Macrophage Diversity and Polarization in Atherosclerosis: A Question of Balance. *Arterioscler., Thromb., Vasc. Biol.* **2009**, *29* (10), 1419–1423.
- (7) Porta, C.; Rimoldi, M.; Raes, G.; Brys, L.; Ghezzi, P.; Di Liberto, D.; Dieli, F.; Ghisletti, S.; Natoli, G.; De Baetselier, P.; Mantovani, A.; Sica, A. Tolerance and M2 (alternative) macrophage polarization are related processes orchestrated by p50 nuclear factor κ B. *Proc. Natl. Acad. Sci. U.S.A.* **2009**, *106* (35), 14978–14983.
- (8) Hagemann, T.; Lawrence, T.; McNeish, I.; Charles, K. A.; Kulbe, H.; Thompson, R. G.; Robinson, S. C.; Balkwill, F. R. “Re-educated” tumor-associated macrophages by targeting NF- κ B. *J. Exp. Med.* **2008**, *205* (6), 1261–1268.
- (9) Sica, A.; Bronte, V. Altered macrophage differentiation and immune dysfunction in tumor development. *J. Clin. Invest.* **2007**, *117* (5), 1155–1166.
- (10) Kortylewski, M.; Swiderski, P.; Herrmann, A.; Wang, L.; Kowolik, C.; Kujawski, M.; Lee, H.; Scuto, A.; Liu, Y.; Yang, C.; Deng, J.; Soifer, H. S.; Raubitschek, A.; Forman, S.; Rossi, J. J.; Pardoll, D. M.; Jove, R.; Yu, H. In vivo delivery of siRNA to immune cells by conjugation to a TLR9 agonist enhances antitumor immune responses. *Nat. Biotechnol.* **2009**, *27* (10), 925–932.
- (11) Leuschner, F.; Dutta, P.; Gorbatov, R.; Novobrantseva, T. I.; Donahoe, J. S.; Courties, G.; Lee, K. M.; Kim, J. I.; Markmann, J. F.; Marinelli, B.; Panizzi, P.; Lee, W. W.; Iwamoto, Y.; Milstein, S.; Epstein-Barash, H.; Cantley, W.; Wong, J.; Cortez-Retamozo, V.; Newton, A.; Love, K.; Libby, P.; Pittet, M. J.; Swirski, F. K.; Koteliansky, V.; Langer, R.; Weissleder, R.; Anderson, D. G.; Nahrendorf, M. Therapeutic siRNA silencing in inflammatory monocytes in mice. *Nat. Biotechnol.* **2011**, *29* (11), 1005–1010.
- (12) Aouadi, M.; Tesz, G. J.; Nicoloro, S. M.; Wang, M.; Chouinard, M.; Soto, E.; Ostroff, G. R.; Czech, M. P. Orally delivered siRNA targeting macrophage Map4k4 suppresses systemic inflammation. *Nature* **2009**, *458* (7242), 1180–1184.
- (13) Stacey, K. J.; Ross, I. L.; Hume, D. A. Electroporation and DNA-dependent cell death in murine macrophages. *Immunol. Cell Biol.* **1993**, *71* (2), 75–85.
- (14) Lv, H.; Zhang, S.; Wang, B.; Cui, S.; Yan, J. Toxicity of cationic lipids and cationic polymers in gene delivery. *J. Controlled Release* **2006**, *114* (1), 100–109.
- (15) Watkins, S. K.; Egilmez, N. K.; Suttles, J.; Stout, R. D. IL-12 rapidly alters the functional profile of tumor-associated and tumor-infiltrating macrophages in vitro and in vivo. *J. Immunol.* **2007**, *178* (3), 1357–1362.
- (16) Briley-Saebo, K. C.; Cho, Y. S.; Shaw, P. X.; Ryu, S. K.; Mani, V.; Dickson, S.; Izadmehr, E.; Green, S.; Fayad, Z. A.; Tsimikas, S. Targeted Iron Oxide Particles for In Vivo Magnetic Resonance Detection of Atherosclerotic Lesions With Antibodies Directed to Oxidation-Specific Epitopes. *J. Am. Coll. Cardiol.* **2011**, *57* (3), 337–347.
- (17) Lipinski, M. J.; Amirbekian, V.; Frias, J. C.; Aguinaldo, J. G.; Mani, V.; Briley-Saebo, K. C.; Fuster, V.; Fallon, J. T.; Fisher, E. A.; Fayad, Z. A. MRI to detect atherosclerosis with gadolinium-containing immunomicelles targeting the macrophage scavenger receptor. *Magn. Reson. Med.* **2006**, *56* (3), 601–610.
- (18) Cormode, D. P.; Skajaa, T.; van Schooneveld, M. M.; Koole, R.; Jarzyna, P.; Lobatto, M. E.; Calcagno, C.; Barazzza, A.; Gordon, R. E.; Zanzonico, P.; Fisher, E. A.; Fayad, Z. A.; Mulder, W. J. Nanocrystal core high-density lipoproteins: A multimodality contrast agent platform. *Nano Lett.* **2008**, *8* (11), 3715–3723.
- (19) Yu, S. S.; Ortega, R. A.; Reagan, B. W.; McPherson, J. A.; Sung, H.-J.; Giorgio, T. D. Emerging applications of nanotechnology for the diagnosis and management of vulnerable atherosclerotic plaques. *Wiley Interdiscip. Rev.: Nanomed. Nanobiotechnol.* **2011**, *3* (6), 620–646.
- (20) Convertine, A. J.; Benoit, D. S.; Duvall, C. L.; Hoffman, A. S.; Stayton, P. S. Development of a novel endosomolytic diblock copolymer for siRNA delivery. *J. Controlled Release* **2009**, *133* (3), 221–229.
- (21) Boyer, C.; Bulmus, V.; Davis, T. P.; Ladmiral, V.; Liu, J.; Perrier, S. Bioapplications of RAFT polymerization. *Chem. Rev.* **2009**, *109* (11), 5402–5436.
- (22) Kolb, H. C.; Sharpless, K. B. The growing impact of click chemistry on drug discovery. *Drug Discovery Today* **2003**, *8* (24), 1128–1137.
- (23) Allavena, P.; Chieppa, M.; Bianchi, G.; Solinas, G.; Fabbri, M.; Laskarin, G.; Mantovani, A. Engagement of the Mannose Receptor by Tumoral Mucins Activates an Immune Suppressive Phenotype in Human Tumor-Associated Macrophages. *Clin. Dev. Immunol.* **2010**, *2010*.
- (24) Taylor, P. R.; Gordon, S.; Martinez-Pomares, L. The mannose receptor: Linking homeostasis and immunity through sugar recognition. *Trends Immunol.* **2005**, *26* (2), 104–110.
- (25) East, L.; Isacke, C. M. The mannose receptor family. *Biochim. Biophys. Acta* **2002**, *1572* (2–3), 364–386.
- (26) Solinas, G.; Germano, G.; Mantovani, A.; Allavena, P. Tumor-associated macrophages (TAM) as major players of the cancer-related inflammation. *J. Leukocyte Biol.* **2009**, *86* (5), 1065–1073.
- (27) Nelson, C. E.; Gupta, M. K.; Adolph, E. J.; Shannon, J. M.; Guelcher, S. A.; Duvall, C. L. Sustained local delivery of siRNA from an injectable scaffold. *Biomaterials* **2012**, *33* (4), 1154–1161.
- (28) Kirkland-York, S.; Zhang, Y.; Smith, A. E.; York, A. W.; Huang, F.; McCormick, C. L. Tailored design of Au nanoparticle-siRNA carriers utilizing reversible addition-fragmentation chain transfer polymers. *Biomacromolecules* **2010**, *11* (4), 1052–1059.
- (29) Evans, B. C.; Nelson, C. E.; Yu, S. S.; Kim, A. J.; Li, H.; Nelson, H. M.; Giorgio, T. D.; Duvall, C. L. Ex Vivo Red Blood Cell Hemolysis

- Assay for the Evaluation of pH-responsive Endosomolytic Agents for Cytosolic Delivery of Biomacromolecular Drugs. *J. Visualized Exp.* **2013**, DOI: 10.3791/50166.
- (30) Connelly, L.; Jacobs, A. T.; Palacios-Callender, M.; Moncada, S.; Hobbs, A. J. Macrophage endothelial nitric-oxide synthase autoregulates cellular activation and pro-inflammatory protein expression. *J. Biol. Chem.* **2003**, 278 (29), 26480–26487.
- (31) Duvall, C. L.; Convertine, A. J.; Benoit, D. S.; Hoffman, A. S.; Stayton, P. S. Intracellular Delivery of a Proapoptotic Peptide via Conjugation to a RAFT Synthesized Endosomolytic Polymer. *Mol. Pharmaceutics* **2010**, 7 (2), 468–476.
- (32) Benoit, D. S. W.; Srinivasan, S.; Shubin, A. D.; Stayton, P. S. Synthesis of Folate-Functionalized RAFT Polymers for Targeted siRNA Delivery. *Biomacromolecules* **2011**, 12 (7), 2708–2714.
- (33) Palanca-Wessels, M. C.; Convertine, A. J.; Cutler-Strom, R.; Booth, G. C.; Lee, F.; Berguig, G. Y.; Stayton, P. S.; Press, O. W. Anti-CD22 antibody targeting of pH-responsive micelles enhances small interfering RNA delivery and gene silencing in lymphoma cells. *Mol. Ther.* **2011**, 19 (8), 1529–1537.
- (34) Crownover, E.; Duvall, C. L.; Convertine, A.; Hoffman, A. S.; Stayton, P. S. RAFT-synthesized graft copolymers that enhance pH-dependent membrane destabilization and protein circulation times. *J. Controlled Release* **2011**, 155 (2), 167–174.
- (35) Sumerlin, B. S.; Tsarevsky, N. V.; Louche, G.; Lee, R. Y.; Matyjaszewski, K. Highly Efficient “Click” Functionalization of Poly(3-azidopropyl methacrylate) Prepared by ATRP. *Macromolecules* **2005**, 38 (18), 7540–7545.
- (36) Plotz, P. H.; Rifai, A. Stable, Soluble, Model Immune-Complexes Made with a Versatile Multivalent Affinity-Labeling Antigen. *Biochemistry* **1982**, 21 (2), 301–308.
- (37) Benoit, D. S. W.; Henry, S. M.; Shubin, A. D.; Hoffman, A. S.; Stayton, P. S. pH-Responsive Polymeric siRNA Carriers Sensitize Multidrug Resistant Ovarian Cancer Cells to Doxorubicin via Knockdown of Polo-like Kinase 1. *Mol. Pharmaceutics* **2010**, 7 (2), 442–455.
- (38) Pollard, J. W. Macrophages define the invasive microenvironment in breast cancer. *J. Leukocyte Biol.* **2008**, 84 (3), 623–630.
- (39) Yu, S. S.; Lau, C. M.; Thomas, S. N.; Jerome, W. G.; Maron, D. J.; Dickerson, J. H.; Hubbell, J. A.; Giorgio, T. D. Size- and charge-dependent non-specific uptake of PEGylated nanoparticles by macrophages. *Int. J. Nanomed.* **2012**, 7, 799–813.
- (40) Daldrup-Link, H. E.; Golovko, D.; Ruffel, B.; DeNardo, D.; Castaneda, R.; Ansari, C.; Rao, J.; Tikhomirov, G. A.; Wendland, M. F.; Corot, C.; Coussens, L. M. MR Imaging of Tumor Associated Macrophages with Clinically-Applicable Iron Oxide Nanoparticles. *Clin. Cancer Res.* **2011**, 17, 5695–5704.
- (41) Martin, P. Wound Healing: Aiming for Perfect Skin Regeneration. *Science* **1997**, 276 (5309), 75–81.
- (42) Bouwens, L.; Baekeland, M.; de Zanger, R.; Wisse, E. Quantitation, tissue distribution and proliferation kinetics of Kupffer cells in normal rat liver. *Hepatology* **1986**, 6 (4), 718–722.
- (43) Felix, R.; Cecchini, M. G.; Hofstetter, W.; Elford, P. R.; Stutzer, A.; Fleisch, H. Rapid publication: Impairment of macrophage colony-stimulating factor production and lack of resident bone marrow macrophages in the osteopetrotic op/op Mouse. *J. Bone Miner. Res.* **1990**, 5 (7), 781–789.
- (44) Linehan, S. A.; Martinez-Pomares, L.; Gordon, S. Mannose receptor and scavenger receptor: Two macrophage pattern recognition receptors with diverse functions in tissue homeostasis and host defense. *Adv. Exp. Med. Biol.* **2000**, 479, 1–14.
- (45) Stahl, P. D.; Ezekowitz, R. A. B. The mannose receptor is a pattern recognition receptor involved in host defense. *Curr. Opin. Immunol.* **1998**, 10 (1), 50–55.
- (46) Larsen, E. K.; Nielsen, T.; Wittenborn, T.; Birkedal, H.; Vorup-Jensen, T.; Jakobsen, M. H.; Ostergaard, L.; Horsman, M. R.; Besenbacher, F.; Howard, K. A.; Kjems, J. Size-Dependent Accumulation of PEGylated Silane-Coated Magnetic Iron Oxide Nanoparticles in Murine Tumors. *ACS Nano* **2009**, 3, 1947–1951.
- (47) Convertine, A. J.; Diab, C.; Prieve, M.; Paschal, A.; Hoffman, A. S.; Johnson, P. H.; Stayton, P. S. pH-Responsive Polymeric Micelle Carriers for siRNA Drugs. *Biomacromolecules* **2010**, 11 (11), 2904–2911.
- (48) van de Wetering, P.; Moret, E. E.; Schuurmans-Nieuwenbroek, N. M.; van Steenbergen, M. J.; Hennink, W. E. Structure-activity relationships of water-soluble cationic methacrylate/methacrylamide polymers for nonviral gene delivery. *Bioconjugate Chem.* **1999**, 10 (4), 589–597.
- (49) Grainger, S. J.; El-Sayed, M. E. H. Stimuli-Sensitive Particles for Drug Delivery. In *Biologically-Responsive Hybrid Biomaterials*; Jabbari, E., Khademhosseini, A., Eds.; World Scientific: Singapore, 2010; pp 171–190.
- (50) Luo, Y.; Zhou, H.; Krueger, J.; Kaplan, C.; Lee, S.-H.; Dolman, C.; Markowitz, D.; Wu, W.; Liu, C.; Reisfeld, R. A.; Xiang, R. Targeting tumor-associated macrophages as a novel strategy against breast cancer. *J. Clin. Invest.* **2006**, 116 (8), 2132–2141.
- (51) Rettig, G. R.; Behlke, M. A. Progress toward in vivo use of siRNAs-II. *Mol. Ther.* **2012**, 20 (3), 483–512.



CTTC

Center for Technology Transfer
& Commercialization

Invention Disclosure Form

Thank you for disclosing your invention to the Center for Technology Transfer and Commercialization. We look forward to working with you to facilitate the translation of your new discovery into a commercial product/process. We are here to help in any way – please contact us with any questions you may have.

- CTTC Staff

Instructions

Why submit an Invention Disclosure Form:	<ul style="list-style-type: none">Completion of the Invention Disclosure Form is the first step in the commercialization process and supplies CTTC with the necessary information to begin assessing the invention.All federal funding sources and most other funding sources require invention reporting, and this document will facilitate Vanderbilt's compliance with those obligations.The Vanderbilt University Technology Policy governs the disposition of all inventions created or authored by faculty, staff and students.
How to complete the Invention Disclosure Form:	<ul style="list-style-type: none">Complete the form by typing directly in the text boxes.Create a Title to identify the invention. Enter it in the space provided in Parts I, III, and IV.When complete, print the form.Prior to submitting to CTTC, each contributor must:<ul style="list-style-type: none">Complete and sign a Contributor pageReview and sign the Assignment of Rights in Part IV (VU contributors only)
Where to send the form once it is completed:	<ul style="list-style-type: none">Scan the completed form and email it to cttc@vanderbilt.edu. If you have been in contact with one of our licensing staff, please note that person's name in the email. <p>OR</p> <ul style="list-style-type: none">Mail your completed form with all signatures to PMB 320.
Next steps:	<ul style="list-style-type: none">The CTTC office will create an official record of your disclosure and you will receive a confirmation email notifying of you this.Next, a member of our licensing staff will contact you within a few business days to discuss the next steps in the commercialization process.Click here for a visual representation of the commercialization process.

**CTTC**Center for Technology Transfer
& Commercialization

For Office Use Only:

VU Number: _____

Date Completed: _____

Invention Disclosure Form**Part I: Invention Information**

Invention Title: MMP and folic acid dual targeted polymeric nanoparticles for siRNA delivery

Provide a detailed description of the invention being disclosed: (Please attach any supporting information, such as a summary, PowerPoint, grant applications, draft manuscripts or abstracts.)	Here, a novel dual folic acid (FA) and proximity-activated targeting (PAT), pH-responsive, polymer-based nanomicelle for siRNA delivery is reported. Folate receptor overexpression is established for numerous cancer types, but its use for drug targeting is hindered by the fact that some noncancerous cell types also express this receptor. Elevated levels of MMP activity are another tumor characteristic that can be exploited for environmentally-triggered, PAT to tumors. Here, a dual folate and PAT delivery system has been synthesized for improved tumor targeting specificity. This system requires colocalization of both MMP activity and folate receptor expression to be active. This delivery system is comprised of two polymers. The first polymer, PAT-SPN, has a PEG corona-forming block linked by a matrix metalloproteinase (MMP) cleavable peptide to an underlying polymer segment that forms the core of a pH-responsive smart polymer nanoparticle (SPN). The second polymer, FA-SPN, is a FA-modified version of the same core polymer segment that forms the pH-responsive SPN. When assembled into micelles, the SPN portion of the polymers form a core that consists of positively-charged dimethyl aminoethyl methacrylate (DMAEMA) that functions as a siRNA-condensing block and a pH-responsive random terpolymer block in the micelle core containing DMAEMA, 2-propylacrylic acid (PAA), and butyl methacrylate (BMA) that mediates endosomal escape. This core forming portion of the delivery system enables formation of nanocarriers that are capable of packaging and cytosolic delivery of the siRNA payload. Mixed micelles were formed from a combination of these two polymers (FA-SPN and PAT-SPN) at various ratios to optimize the dual targeting functionality. Endowing the SPN with a PEG cloak linked by an MMP cleavable peptide enables particle activation specifically in the proximity of tumor tissue, mediating exposure of the underlying folic acid that will further facilitates uptake of the SPN and the associated siRNA cargo.
--	---

Folic acid (FA) receptors are overexpressed on numerous cancer cell types and are thus commonly utilized for drug targeting. However, several normal cell types also express low levels of FA receptor, which can lead to off-site effects. In order to increase cancer specificity, we designed a siRNA carrier that specifically targets tissues where there is a co-localization of cell-surface receptors (FA receptors) and environmental factors (high MMP activity) that are both hallmarks

**CTTC**Center for Technology Transfer
& Commercialization

For Office Use Only:

VU Number: _____

Date Completed: _____

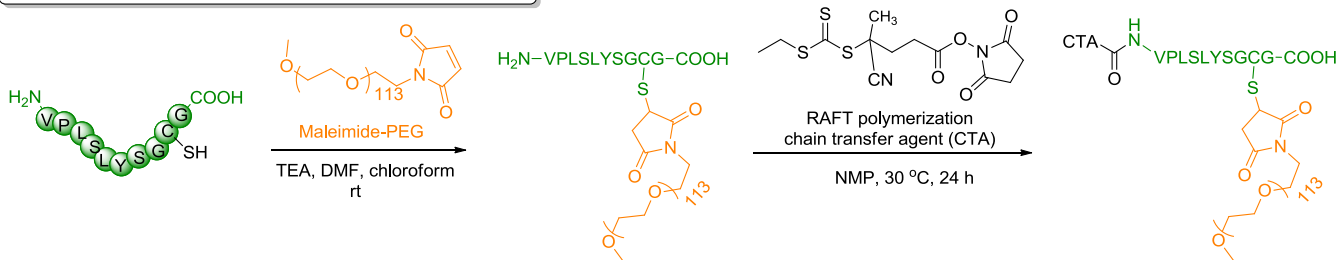
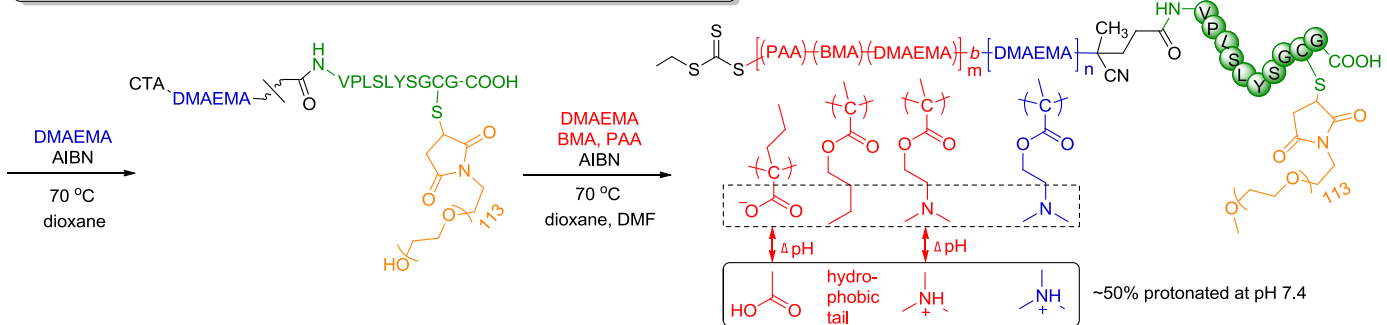
Invention Disclosure Form

of the cancer microenvironment. With this dual FA and MMP proximity-activated targeting (PAT) smart polymer nanoparticle (PAT-SPN/FA-SPN), FA is masked by an MMP-removable PEG “cloak” that, when removed by MMP activity, exposes FA and triggers uptake by FA receptor-expressing cells (see the mechanism in **Figure 1A in 2012 BMES abstract and slide 4 in BMES presentation**). The nanocarriers are co-assemblies of two polymer species with adjustable ratios in order to vary the density of the FA vs. the cleavable PEG shield on the nanoparticle surface in order to achieve optimal dual targeted function. The first polymer was made using **Scheme 1** and contained a 20 kDa Y-shaped PEG block (PAT_{20k}-Yshape-PEG-pD-pDPB). The second polymer constituent was a folic acid functionalized diblock copolymer (FA-PEG_{2kDa}-pD-pDPB) that was synthesized using **Scheme 2** below. In this scheme, folic acid was coupled to one terminus of a 2kDa PEG precursor, and a RAFT chain transfer agent was coupled to the other terminus, both using efficient, site-selective conjugation chemistries. UV-vis spectrophotometry was performed to confirm the composition of the FA-PEG_{2k}-macro-CTA (**Figure 3**). Subsequently, this FA-PEG_{2k}-macro-CTA was utilized in two sequential RAFT polymerizations to form FA-PEG_{2kDa}-pD-pDPB. These carriers were publicly disclosed for the first time as an oral presentation at the Annual BMES meeting in October 2012 in Atlanta, and the abstract for this talk can be seen on Appendices **2012 BMES abstract and 2012 BMES presentation slides**.

Synthesis of PEG_{20k}-peptide-pD-pDPB

Scheme 1 involved synthesis of the PAT component followed by polymerization of the polymer blocks that form the “base” SPN micelle. In this route, the PEG-peptide was pre-conjugated to the precursor that serves as the basic “building block” for the remainder of the SPN. This route enabled a nearly 100 percent substitution rate and thus a high density of PEG chains on the final PAT-SPN.

Invention Disclosure Form
Solid phase peptide synthesis

Synthesis of PEG-peptide based macro-CTA

Synthesis of smart polymeric composition with the macro-CTA


Scheme 1. Synthetic route for the fabrication of PAT-SPN building unit.

This new dual-targeted carrier represents an extension of the previously-disclosed SPNs endowed only with the MMP-dependent PAT targeting. The previous work has been accepted for publication at Advanced Functional Materials (Manuscript draft was sent with a previous disclosure, but we can re-send it if desired).

Using the synthetic route in **Scheme 1**, new versions of the PAT-SPNs have been synthesized with 20 kDa Y-shaped PEG. Cationic particle surface charge increases particle-cell surface interactions, and the neutralized surface charge on the particles with the 20kDa Y-shaped PEG is desirable to limit the nonspecific cellular uptake of the particles prior to removal of the MMP-cleavable PAT element. **Table 1** shows the diameter and size of the PAT-SPN containing the 20kDa PEG.

**CTTC**Center for Technology Transfer
& Commercialization

For Office Use Only:

VU Number: _____

Date Completed: _____

Invention Disclosure Form

Characterization of PAT_{20k} Yshape-PEG-pD-pDPB by GPC (**Figure 1**) and composition determination by both NMR and GPC (**Table 1**) are shown below, respectively.

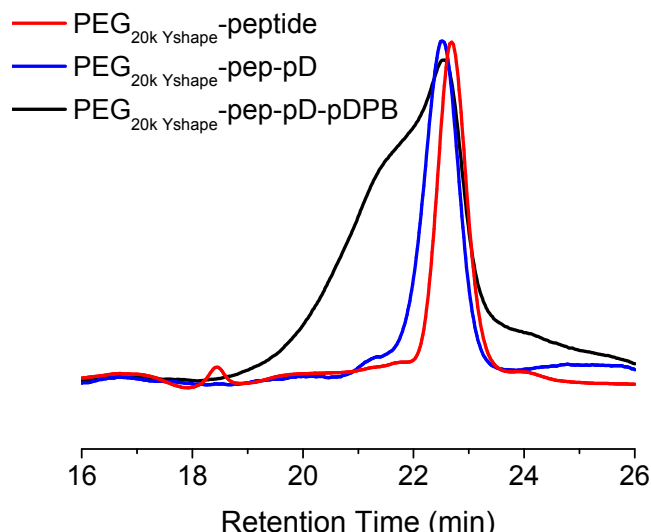
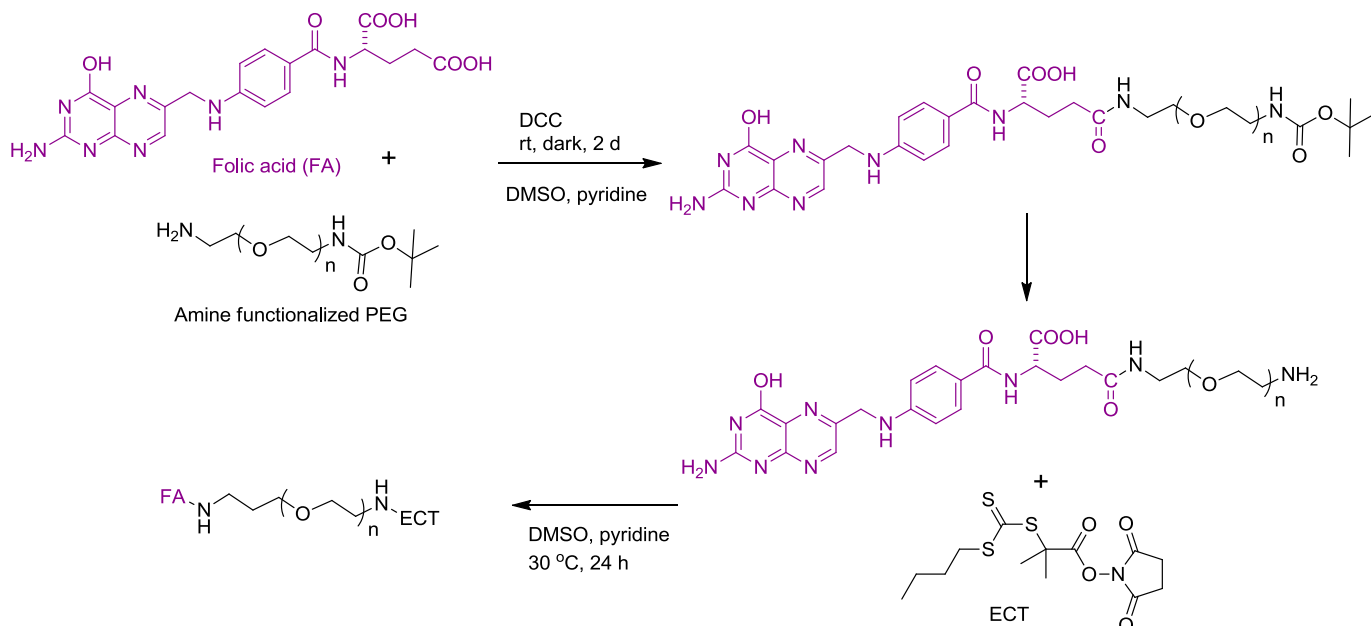
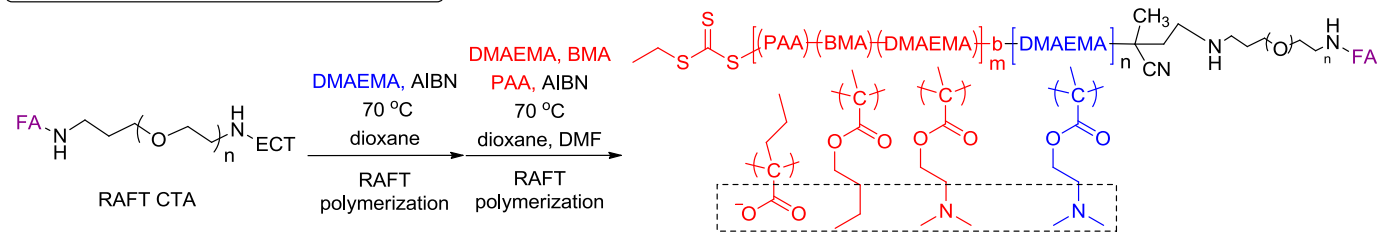


Figure 1. GPC confirmation of the syntheses of PEG_{20k}-peptide-pD-pDPB from PEG_{20k}-pep macroCTA. Synthesis of PAT_{20k-Yshape}-SPN was confirmed by the broadening of the GPC peak as compared to just PEG-peptide.

Table 1: Molecular weight (M_n) and composition of PEG_{20k}-peptide-pD-pDPB. pD represents poly(DMAEMA) and pDPB represents poly(DMAEMA-PPA-BMA).

	Total M_n (kDa)	PEG (kDa)	pD1 (kDa)	pDPB (kDa)	pD %	pP %	pB %
PAT _{20k Yshape-PEG} SPN	45	20 (Y-shaped)	6	25	24	22	54

Invention Disclosure Form
Synthesis of folic acid-PEG_{2k}-pD-pDPB
Synthesis of folate-PEG_{2k} macro-CTA

Synthesis of folate-PEG_{2k}-linked-SPN


Scheme 2. Synthetic scheme of folic acid modified, 2 kDa PEG linked diblock copolymer (FA-PEG_{2k}-pD-pDPB).

Following **Scheme 2** route, polymer FA-PEG_{2k}-pD-pDPB with approximate molecular weight with the PEG_{20k}-pep-pD-pDPB was synthesized and characterized by GPC (**Figure 2**). Functionalization of FA component was confirmed by the absorbance at 360 nm of purified polymer in aqueous solutions (**Figure 3**).



CTTC

Center for Technology Transfer
& Commercialization

For Office Use Only:

VU Number: _____

Date Completed: _____

Invention Disclosure Form

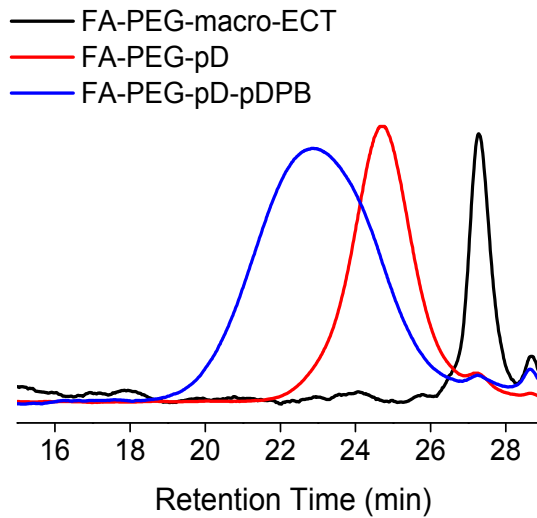


Figure 2. GPC confirmation of the synthesis of FA-PEG_{2k}-pD-pDPB from FA-PEG_{2k}-macro-CTA. The final product was the result of two successive RAFT polymerizations of DMAEMA, resulting in FA-PEG_{2k}-pD, and of the DPB terpolymer, resulting in FA-PEG_{2k}-pD-pDPB.

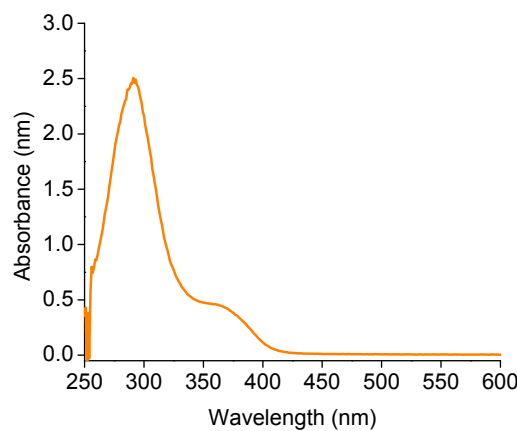


Figure 3. UV-vis spectrophotometry was performed to confirm the composition of the FA-PEG_{2k}-macro-CTA. The presence of absorbance peaks at 310 nm (RAFT CTA) and 360 nm (FA) confirms the synthesis of the FA-PEG_{2k}-macro-CTA. The mixed SPNs (PAT_{20k}-Y-shape-PEG-SPN/FA-SPN) were fabricated with ratios of 0, 25, 50, 75, and 100 mol% of the FA polymer constituent to PAT-SPNs and then characterized with DLS to confirm particle formation and size (**Table 2**). Sizing by DLS was similar for all combinations of the two polymeric components. Responsiveness of these particles to MMP-7

**CTTC**Center for Technology Transfer
& Commercialization

For Office Use Only:

VU Number: _____

Date Completed: _____

Invention Disclosure Form

was also assessed (**Figure 4**). In these studies, when PEG was shed through MMP-7 activity, particle diameter decreased and zeta potential increased, as expected. The nanoparticle containing only FA-SPN does not respond to the addition of MMP-7.

Size characterization of PAT/FA-SPN micelles by DLS and TEM

Micelles automatically assembled following dropping mix polymer methanolic solutions into PBS buffer. Mix micelles comprised of 0/100, 25/75, 50/50, 75/25, and 100/0 of PAT/FA components were prepared and confirmed the formation by DLS (**Table 2**).

Table 2. Nanoparticle sizes determination by DLS.

	Mol % of FA-SPN in $\text{PAT}_{20k\text{-Y-shape-PEG}}/\text{FA-SPNs}$				
	0	25	50	75	100
by DLS (nm)	53 ± 9.1	54 ± 8.9	56 ± 9.1	55 ± 10.8	61 ± 10.7

Confirmation of MMP responsiveness of PAT/FA-SPN micelles by the changes on particle diameter and surface charge

Upon the exposure to a pathologically relevant level of MMP-7 (50 nM), PAT/FA-SPNs exhibited a simultaneous increase in nanoparticle surface charge and a decrease on nanoparticle diameter over hours, indicating that the outer PEG layer sheds off after MMP-7 cleavage and unshields cationic charges from the inner pDMAEMA layer (**Figure 4**). The results also showed a faster MMP-7 cleavage profile for the formulations with a lower % of the PAT component in the mixed micelles. This would allow us to tune the environmental responsive rate for varied diseases.

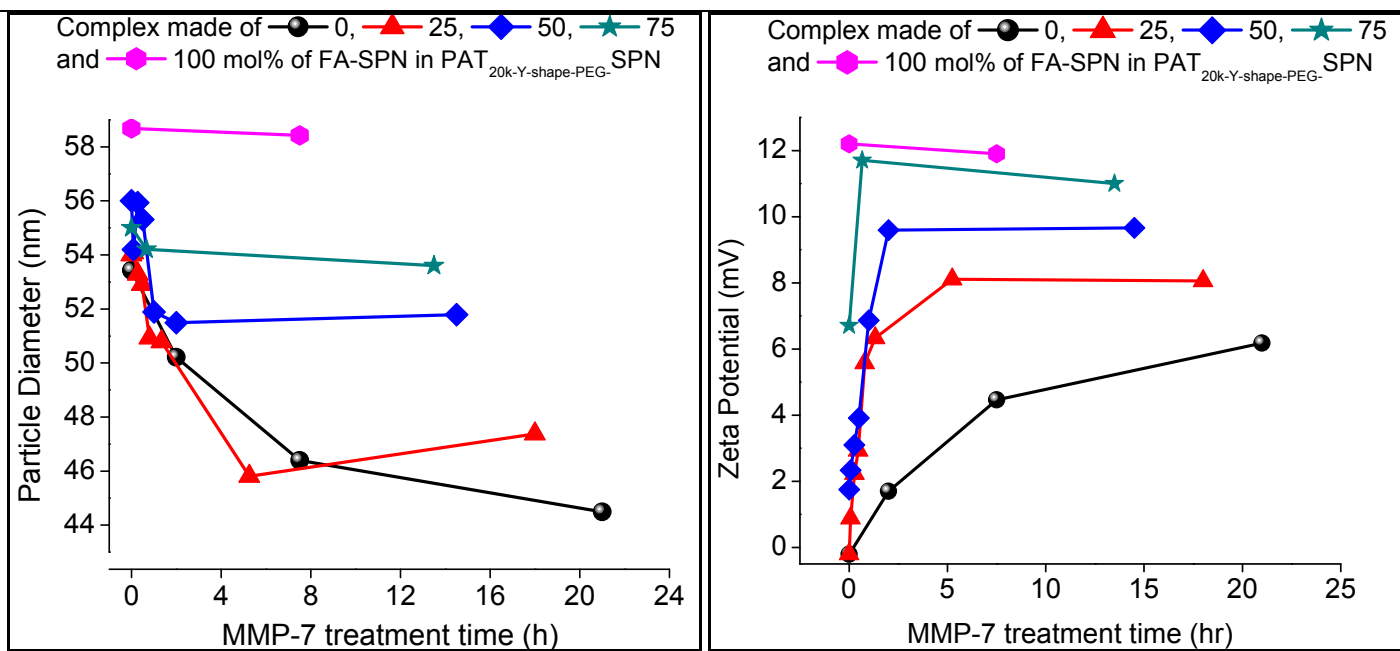
Invention Disclosure Form


Figure 4. Decreased particle diameter (left) and increased zeta potential (right) of PAT_{20k}Y-shape-PEG-SPN mixed micelles over time after treatment with MMP-7, triggering peptide cleavage and removal of the outer PEG layer.

PAT design minimizes undesirable interaction with whole blood

Many cationic-charge bearing transfection reagents are not compatible with intravenous delivery because of their high potential for interaction/aggregation/instability with blood components. This invention was designed to be delivered intravenously and subsequently reach cancerous tissues via leaky vasculature, or the enhanced permeation and retention (EPR) effect that occurs in tumors. **Figure 5** (as in **slide 6 in BMES presentation slides**) shows that PAT-SPNs do not interact with whole blood. As a contrast, commercial transfection reagent Lipofectamine™ had 60% - 76%, depending on exact formulation, partitioned with the red blood cells. In this assay, the nanocarriers were incubated with diluted whole blood, the solutions were centrifuged to pellet the cells, and the relative amount of siRNA partitioning with the cells vs. into the supernatant were quantified by fluorescence.



CTTC

Center for Technology Transfer
& Commercialization

For Office Use Only:

VU Number: _____

Date Completed: _____

Invention Disclosure Form

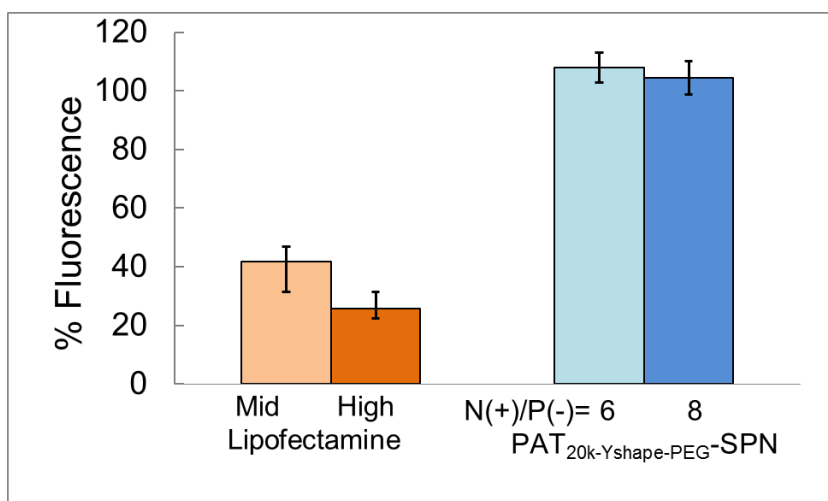


Figure 5. Assessment of interaction between whole blood and nanocarriers. DNA^{FAM} loaded PAT-SPN or Lipofectamine were mixed with whole blood. After incubation of the mixture for 1 h at 37°C, red blood cells were spun down. Fluorescent intensity from DNA^{FAM} in the supernatant was measured. Complexes suspended in PBS following the same procedure was set as 100% fluorescence (0% interaction) and complexes loaded with non-fluorescent, control DNA were set as 0% fluorescence.

pH-dependent membrane disruption facilitates endo/lysosomal escape

The pH-dependent membrane-disruptive behavior of the terpolymer that forms the SPN core was found to be retained in the PAT-modified SPN design, ensuring endosomolytic release of the siRNA into the cytosol where it functions (**Figure 6** as the representative figure in **slide 8 in BMES presentation slides**).

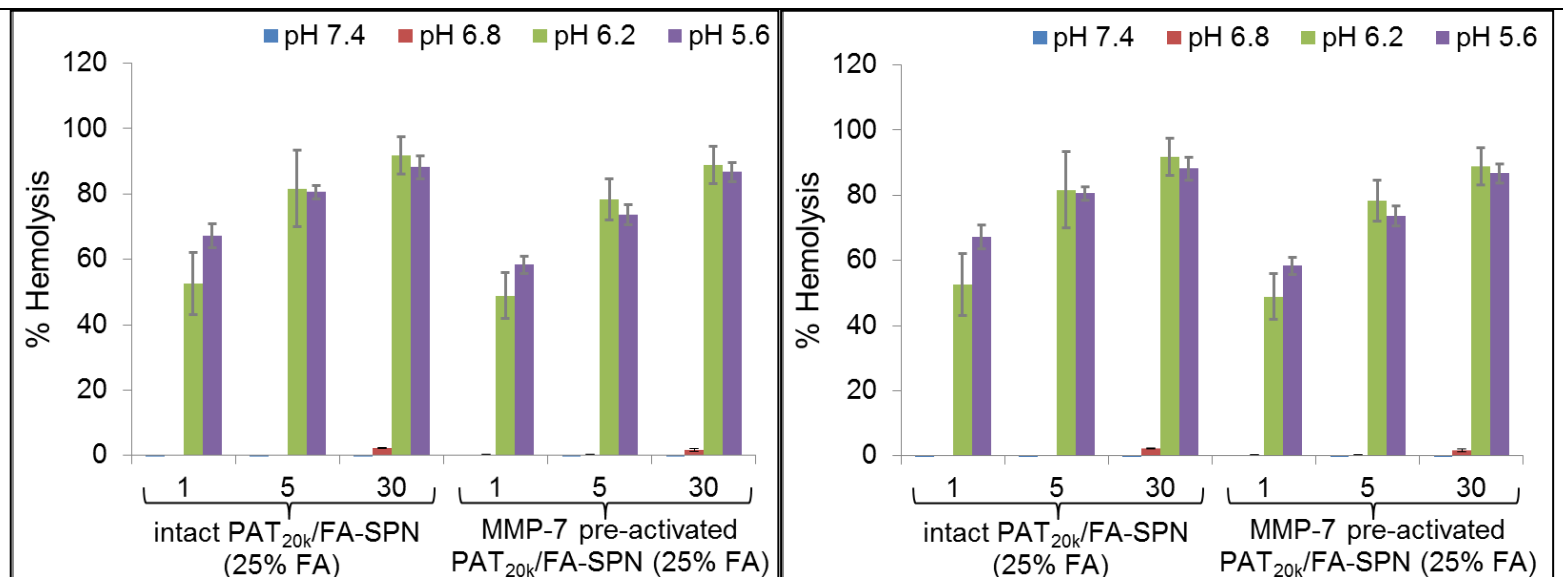
Invention Disclosure Form


Figure 6. pH-dependent membrane disruption. pH-dependent hemolysis of erythrocytes with 25 mol% (left) and 50 mol% (right) FA-SPN-containing mixed micelles was determined for intact PAT/FA-SPN and MMP-7 pretreated PAT/FA-SPN at 1, 5, and 30 μg/mL relative to 1% Triton X-100 as a positive control (100% lysis). Hemolysis was pH-dependent, with approximately 0% at extracellular pH 7.4 and more than 90% at pH 5.6. Hemolysis mediated by PAT-SPN is essentially unchanged following MMP-7 proteolytic activation. Error bars indicate standard deviation of n = 3.

PAT/FA-SPNs are cytocompatible

Cell viability of luciferase expressing MDA-MB-231 cancer cells after treatment with PAT_{20k-Y-shape-PEG}/FA-SPN/siRNA comprising 0, 25, 50, 75, 100 FA component was measured **Figure 7** (as seen in **slide 9 in BMES presentation slides**). Generally, very little cytotoxicity was observed for the charge ratios that we typically utilize for in vitro and in vivo experiments.

Invention Disclosure Form

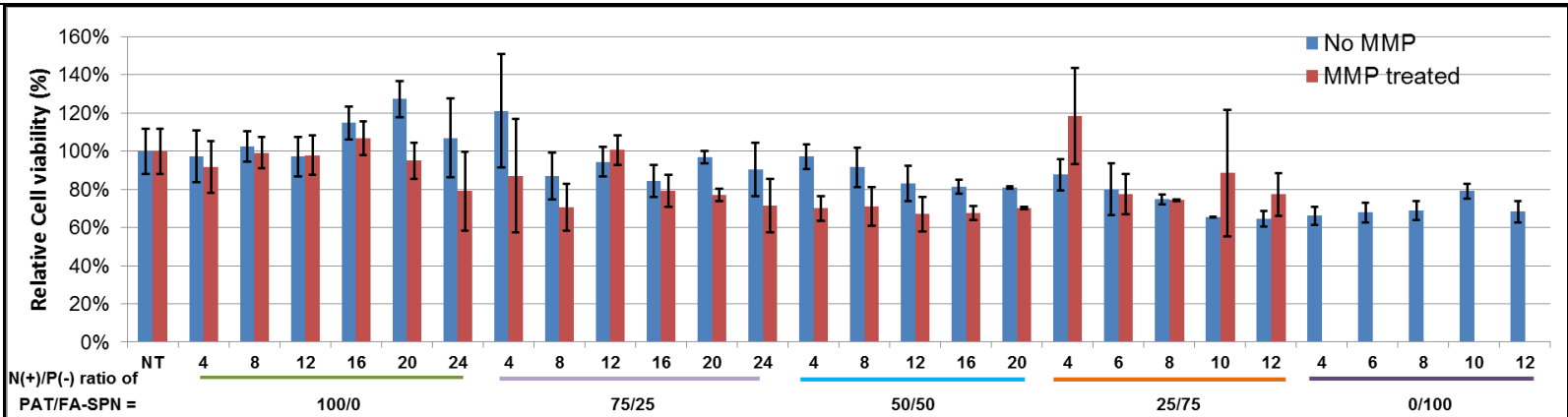


Figure 7. Cell viability of PAT/FA-SPNs across a range of N(+)/P(-) ratios assessed on luciferase expressing MDA-MB-231 cells. Cell viability was assessed by treating luciferase expressing MDA-MB-231 mammary tumor cells with PAT_{20k-Y-shape-PEG}/FA-SPNs loaded with 50 nM scrambled siRNA at a broad range of N(+)/P(-) ratio in the presence of MMP (50 nM) supplemented with Zn²⁺ (50 μM) (MMP+Zn²⁺). Cell viability was reported relative to non-treated cells (NT). No significant cytotoxicity was observed within the whole tested range of N(+)/P(-) for PAT_{20k-Y-shape-PEG}-SPN and very slight cytotoxicity was observed for 25/75 and 50/50 mol% of PAT/FA formulations at charge ratios above 12.

MMP-7 triggered dual PAT- and FA-targeting enhances cell internalization in cancer cells

MDA-MB-231 and MCF-7 are two known cancer cell lines with up-regulated expression of FA receptors. Cell uptake with or without pre-activation with MMP-7 was assessed by flow cytometry in MDA-MB-231 and MCF-7 (**Figure 8** as in **slide 10 in BMES presentation slides**) and confocal fluorescent imaging in MDA-MB-231 cells (**Figure 9** as in **slide 11 in BMES presentation slides**). The data shown in **Figures 8 and 9** demonstrate the dual targeting function of the PAT_{20k-Y-shape-PEG}/FA-SPN carrier; after pre-treatment with MMP-7 and in the absence of folate competition, all nanoparticle formulations had increased cellular uptake compared to the controls. This result is confirmed by the microscopic images in **Figure 9**.

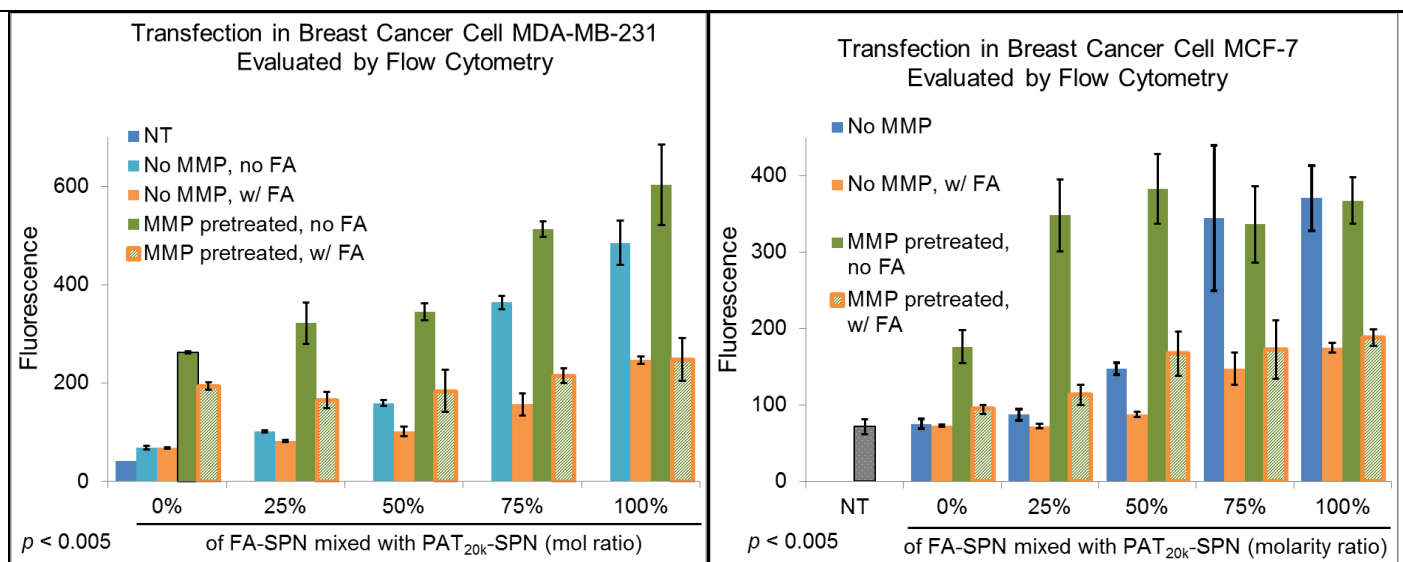
Invention Disclosure Form


Figure 8. Enhanced cell internalization mediated by on MDA-MB-231 (left) and MCF-7 (right) following exposure to MMP-7 and in the absence of free FA competition. Data presented as mean +/- standard error with n = 3. *p < 0.005 compared with NT.

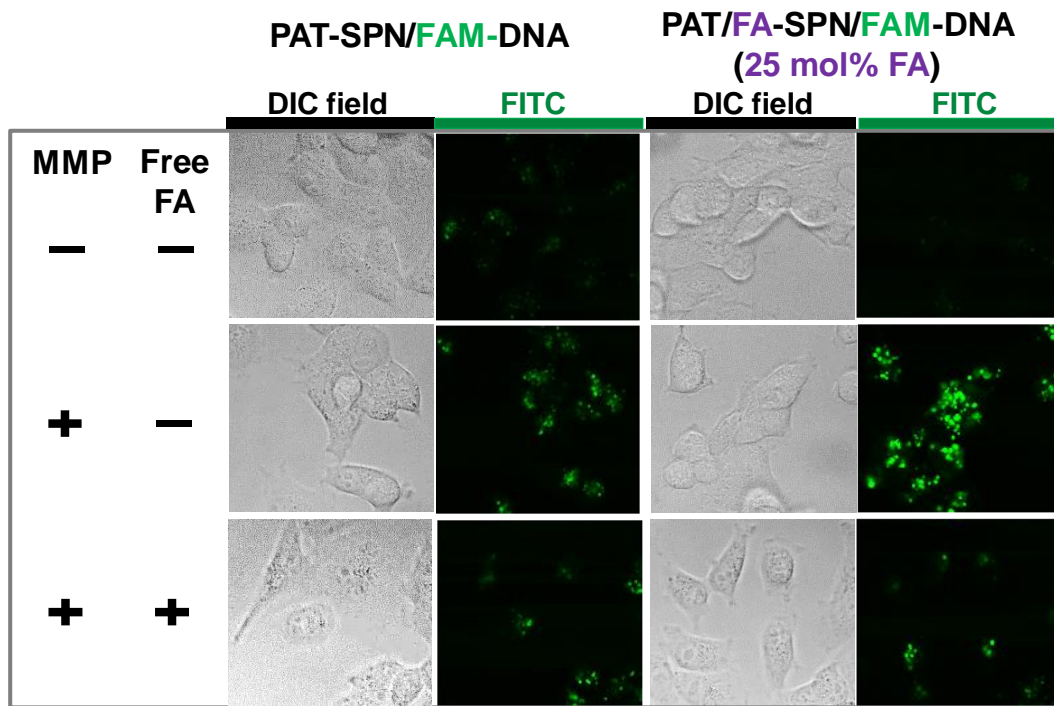


Figure 9. Enhanced cell internalization mediated by PAT-SPN/DNA^{FAM} (left panel) and PAT/FA-SPN/DNA^{FAM} (of 25 mol% FA, right panel) on MDA-MB-231 following exposure to MMP-7. The enhancement was blocked by addition of free FA to competitively inhibit nanocarrier uptake through binding to folate receptor. Data presented as mean +/- standard error with n = 3. *p < 0.005 compared with NT.

Invention Disclosure Form

MMP-triggered PAT- and FA-dual targeting induces prominent target protein suppression

Figure 10 (as in slide 11 in Cancer Bio Retreat presentation slides), which was first disclosed recently at the internal Vanderbilt Cancer Biology Retreat demonstrates the functional significance in terms of gene silencing bioactivity of the dual targeted carriers.

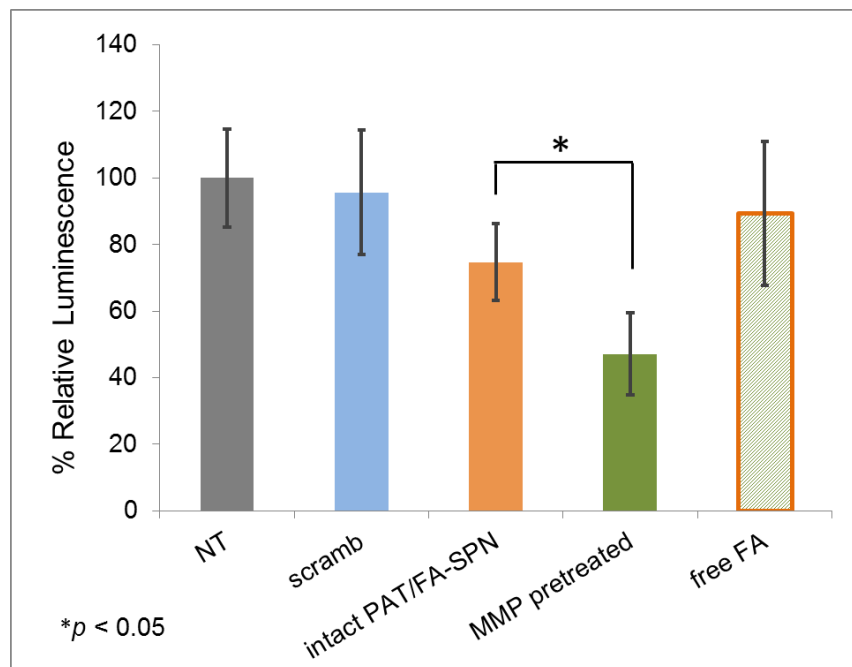


Figure 10. Enhanced target protein suppression in luciferase expressing MDA-MB-231 cells following MMP-7 pre-activation (53% suppression) relative to intact PAT/FA-SPN/luciferase-siRNA (consisting 50 mol% FA) (no MMP-7 pre-activation) or samples where the FA targeting was blocked by addition of free FA into the media. Data presented as mean +/- standard error with n = 3.

Briefly describe any problems this invention overcomes:	The SPN alone protects siRNA and mediates the intracellular delivery efficiently in vitro but is not amenable to IV delivery. FA targeting alone is susceptible to targeting healthy cells. Dual FA and PAT targeting makes the SPNs more hemocompatible due to the removable PEG corona. Dual MMP and folate receptor dependent targeting mechanisms have been incorporated to improve cancer specific delivery.
List any elements of the invention that you believe to be novel:	The PAT-component incorporates a reversible PEG corona that provides stealth in systemic circulation. The MMP-7 cleavability exposes FA for receptor targeting. The combination of environmental and cell receptor targeting is unique and is anticipated

**CTTC**Center for Technology Transfer
& Commercialization

For Office Use Only:

VU Number: _____

Date Completed: _____

Invention Disclosure Form

	to yield better targeting specificity <i>in vivo</i> .
List the likely potential product(s) or application(s) for this invention:	Tissue specific nanocarriers for siRNA drugs and chemo therapeutics
Describe the current developmental stage of the invention:	The dual targeted system has been thoroughly validated <i>in vitro</i> .
Please list any experiments that will be performed in the next 6 months:	<ol style="list-style-type: none">1. <i>In vivo</i> bio-distribution in a mouse model2. <i>In vivo</i> reduction of target gene in a mouse tumor model.
List any potential licensees or companies that may be interested in this invention:	Pharmaceutical companies, e.g., Novartis, PhaseRX, Alnylam, Tekmira, etc. http://rnaitherapeutics.blogspot.com/ etc.
List any current competitive or compatible technologies available, and describe the advantages of this invention over those technologies:	The base SPN is a competitive technology but does not enable IV injection or any type of targeting
Please list any recent literature or information that you are aware of that is similar to this invention:	<p><u>Hatakeyama et al., Gene Ther. (2007) 14, 68-77.</u> This manuscript is based on a liposome which has no pH responsiveness to further assist endosomal escape of the siRNA.</p> <p><u>Sarah L. Sewell a, Todd D. Giorgio. Materials Science and Engineering C 29 (2009) 1428–1432.</u> Giorgio is a co-applicant of the current invention, but his previous work was in diagnostic nanoparticles rather than for drug delivery.</p> <p><u>Zhang Y, So MK, Rao J. Protease-modulated cellular uptake of quantum dots. Nano Lett 2006;6(9):1988 - 92.</u> The design in this publication is used for diagnostic imaging instead of drug delivery.</p> <p>Hongmei Li, Shann S. Yu, Martina Miteva, Christopher E. Nelson, Thomas Werfel, Todd D. Giorgio*, Craig L. Duvall*. Matrix Metalloproteinase Responsive, Proximity-activated Polymeric Nanoparticles for siRNA Delivery. <i>Adv. Funct. Mater.</i>, 2012, 10.1002/adfm.201202215.</p> <p>Danielle S. W. Benoit, Selvi Srinivasan, Andrew D. Shubin, and Patrick S. Stayton. Synthesis of Folate-Functionalized RAFT Polymers for Targeted siRNA Delivery. <i>Biomacromolecules</i>, 2011, 12 (7), pp 2708–2714.</p> <p>(Folate targeting only)</p>

**CTTC**Center for Technology Transfer
& Commercialization

For Office Use Only:

VU Number: _____

Date Completed: _____

Invention Disclosure Form

Has this invention been described in either a publication or verbally outside of Vanderbilt?	Yes <input checked="" type="checkbox"/> No <input type="checkbox"/>
Please list where and when you disclosed or plan to disclose your invention.* (e.g. abstract, poster, publication, presentation, website, etc.)	<ol style="list-style-type: none">1. <i>Biomedical Engineering Society Annual Fall Meeting</i>, Atlanta, GA, Oct., 2012. (abstract and oral presentation)2. <i>12th Host-Tumor Interactions/Cancer Biology Retreat</i>, Nashville, TN, Nov 30th, 2012. (oral presentation)

* Please attach any files that contain the disclosure (e.g. PowerPoint, abstract, etc.).

**CTTC**Center for Technology Transfer
& Commercialization**Invention Disclosure Form****Part II: Reporting**

Funding Information: If you received full or partial support during any stage of your research resulting in this invention, or if you have acknowledged or plan to acknowledge a funding source in a publication or grant progress report in which you describe the invention, please indicate all source(s) of your funding by checking the appropriate box or boxes below. If you were not funded, please check none.

Federal Foundation Industry Internal Other State None

Please identify below each funding source's name and each corresponding grant, contract or award number/ID.

Funding Source Name (List primary funding source first)	Grant/Contract/Award Numbers/IDs (Not center numbers)
Congressionally Directed Medical Research Program	W81XWH-10-1-0445/-0446

Third Party Material: Was any material or equipment provided by a third party?	Yes <input type="checkbox"/> No <input checked="" type="checkbox"/> Unknown <input type="checkbox"/>
If yes, please provide details:	
If yes, was a material transfer agreement signed?	Yes <input type="checkbox"/> No <input type="checkbox"/>
Please indicate the material and from where you received the material:	

Export Control: Is this invention likely to have any export control sensitivity?*	Yes <input type="checkbox"/> No <input checked="" type="checkbox"/>
--	---

*Please check "yes" if you believe the invention may be subject to controlled disclosure under the United States Munitions List (defense and weaponry, explosives, space, national security, and/or biological materials to either protect or cause biological/chemical warfare) or the Commerce Control List (Categories: 0=Nuclear Materials, facilities and equipment; 1=Materials, Chemicals, Microorganisms and Toxins; 2=Material processing; 3=Electronics; 4=Computers; 5=Telecommunications and Information Security; 6=Sensors and Lasers; 7=Navigation and Avionics; 8=Marine; 9=Propulsion Systems, Space Vehicles and related equipment). Contact Vanderbilt Export Compliance at vec@vanderbilt.edu if you require assistance in making this determination.

**CTTC**Center for Technology Transfer
& Commercialization**Invention Disclosure Form****Part III: Revenue Sharing Agreement**

Invention Title: Tissue specific, proximity-activated, folic acid dual targeting polymeric nanoparticles for siRNA drug carrier

List **ALL** contributors and the percentage of their contribution below:

(*List percentage of contribution at the time of this disclosure. Inventorship has a legal meaning under patent law and will be finally determined by Vanderbilt-appointed patent counsel. CTTC understands that contributions may fluctuate as the technology is developed.)

Name: _____ Craig L. Duvall _____ 33 _____ %

Name: _____ Todd D. Giorgio _____ 33 _____ %

Name: _____ Hongmei Li _____ 33 _____ %

Have any non-Vanderbilt employees contributed to the invention?

Yes _____ No X _____

If yes, from what other institution(s)?

Contributor Information: Who will be the primary contact between the CTTC and other contributors?

Craig L. Duvall and Todd D. Giorgio

**CTTC**Center for Technology Transfer
& Commercialization**Invention Disclosure Form****Part IV: Assignment of Rights**

Invention Title: Tissue specific, proximity-activated, folic acid dual targeting polymeric nanoparticles for siRNA drug carrier

To be signed by Vanderbilt contributors only.

For good and valuable consideration, as described in the Policy on Technology and Literary and Artistic Works in the Vanderbilt University Faculty Manual, the sufficiency and adequacy of which are hereby acknowledged, I agree to assign and hereby do assign, sell, and transfer unto VANDERBILT UNIVERSITY, whose post-office address is 305 Kirkland Hall, Nashville, TN 37240, U.S.A., my entire right, title and interest in and to the inventions disclosed herein and related thereto, including but not limited to any associated intellectual property rights. I hereby agree to execute without further consideration any and all applications, petitions, oaths and assignments or other papers and instruments which may be necessary in order to carry into full force and effect, the sale, assignment, transfer and conveyance hereby made or intended to be made. I hereby agree that no assignment, sale, agreement or encumbrance has been or will be made or entered into which would conflict with this assignment. I further represent that to the best of my knowledge, the information provided herein and in the body of the Invention Disclosure, is true and accurate, and I agree to promptly disclose to the Center for Technology Transfer and Commercialization any updated or new information relating to the disclosed technology hereunder.

I have read and reviewed the information contained in the Disclosure Form and Assignment form and agree that all information, including contributor information, is accurate to the best of my knowledge.

Contributor Signature <u>and</u> Date	Printed Name
1. 10/12	Craig L. Duvall
2. 10/12	Todd D. Giorgio
3. 10/10/2012	Hongmei Li



Invention Disclosure Form

Accepted for Vanderbilt: _____

Contributor #1

Must be filled out by each Vanderbilt contributor.

Invention Title: Tissue specific, proximity-activated, folic acid dual targeting polymeric nanoparticles for siRNA drug carrier

Name: Craig L. Duvall	Position: Assistant Professor
Citizenship/Visa Status: United States	VUnet ID: duvallc
Primary Phone Number: 615-322-3598	Home Address: 2813 22 nd Ave S, Nashville, TN 37215
Please describe the nature of your contribution:	Co-proposed the idea of PAT/FA-SPN nanoparticles described in this form that was awarded research funding from CDMRP program, and provided extensive technical support through PAT/FA-SPN project in nanoparticle synthesis and biomedical assessments.
If you are a faculty member, please list the department and school to which you are appointed:	Biomedical Engineering Department
If you are not a faculty member, please list the department or center in which you are employed:	
If the research leading to the invention was supported by a university-recognized center, please list the supporting center(s):	1. ____ 4-22-430-3752 ____ 2. ____ 4-22-430-3762 ____ 3. ____
Please check the appropriate box below to describe your VA association:	No VA appointment <input checked="" type="checkbox"/> Dually Appointed <input type="checkbox"/> Without Comp <input type="checkbox"/>
If you checked Without Comp, are you performing any VA approved research activities?	Yes <input type="checkbox"/> No <input checked="" type="checkbox"/>
<i>I hereby agree to the Revenue Sharing Agreement as set forth in Part III of the Invention Disclosure Form.</i>	Signature: Date: 12/7/2012

**CTTC**Center for Technology Transfer
& Commercialization**Invention Disclosure Form****Contributor #2***Must be filled out by each Vanderbilt contributor.*

Invention Title: Tissue specific, proximity-activated, folic acid dual targeting polymeric nanoparticles for siRNA drug carrier

Name: Todd D. Giorgio	Position: Professor Chair of Biomedical Engineering
Citizenship/Visa Status: United States	VUnet ID: Giorgitd
Primary Phone Number: 615-322-3521	Home Address: 311 Whitworth Way, Nashville, TN 37205
Please describe the nature of your contribution:	Co-proposed the idea of PAT/FA-SPN nanoparticles described in this form that was awarded research funding from CDMRP program, and provided extensive technical support through PAT/FA-SPN project in nanoparticle synthesis and biomedical assessments.
If you are a faculty member, please list the department and school to which you are appointed:	Department of Biomedical Engineering
If you are not a faculty member , please list the department or center in which you are employed:	
If the research leading to the invention was supported by a university-recognized center, please list the supporting center(s):	1. ___ 4-22-430-3752 ___ 2. ___ 4-22-430-3762 ___ 3. _____
Please check the appropriate box below to describe your VA association:	No VA appointment <input checked="" type="checkbox"/> Dually Appointed <input type="checkbox"/> Without Comp <input type="checkbox"/>
If you checked Without Comp, are you performing any VA approved research activities?	Yes <input type="checkbox"/> No <input checked="" type="checkbox"/>
I hereby agree to the Revenue Sharing Agreement as set forth in Part III of the Invention Disclosure Form.	Signature: The signature is handwritten in blue ink and appears to read 'Todd D. Giorgio'. Date: 12/7/2012



CTTC

Center for Technology Transfer
& Commercialization

Invention Disclosure Form

Contributor #3

Must be filled out by each Vanderbilt contributor.

Invention Title: Tissue specific, proximity-activated, folic acid dual targeting polymeric nanoparticles for siRNA drug carrier

**Host-Tumor Interactions Program &
Department of Cancer Biology
12th Annual Joint Retreat
November 30th, 2012**

ABSTRACT

Manipulation of the NF-κB Pathway in Macrophages Using Targeted Nanotherapeutics to Achieve an Anti-Tumor Phenotype

Ryan Ortega, Whitney Barham, Bharat Kumar, Fiona Yull, and Todd Giorgio

The NF-κB pathway is a controller of macrophage phenotype and has been implicated in creating a pro-tumor phenotype in tumor associated macrophages (TAMs); though there is little work elucidating the effective differences between the alternative and classical pathways. TAMs can modify the tumor microenvironment over an extended period to create an inflammatory, pro-tumor niche. We have successfully utilized mannosylated polymer nanoparticles to deliver siRNA sequences targeting mRNA for NF-κB proteins into bone marrow derived macrophages (BMDMs) from NGL mice. Using these *in vitro* studies, we have shown that our nanoparticles are comparable to commercial transfection agents using both gene and protein level readouts for knockdown. We have determined that by delivering siRNA specific to the p52/p100 protein in the alternative pathway, we can knockdown total NF-κB activity by approximately 80% in NGL BMDMs stimulated by TNF-α. By targeting proteins in the classical pathway, we have decreased total NF-κB activity by approximately 50% in the same model, demonstrating the ability to independently inhibit the classical and alternative pathways. Additionally, our previous work has indicated that controlled, local increases in NF-κB activity in macrophages can result in anti-tumor activity. In order to elucidate the mechanism of this activity, we have delivered a liposomal formulation of muramyl tripeptide (Mifamurtide) to NGL BMDMs. We have shown that Mifamurtide delivery increases NF-κB activation and the production of reactive oxygen species, indicating a preliminary mechanistic explanation for therapeutic potential of NF-κB activation. Using our nanoparticles and an siRNA sequence for an inhibitor protein in the NF-κB pathway, we have produced a more than 2-fold increase in total NF-κB activity, showing that we can both increase and decrease NF-κB activity in macrophages using our novel particles.



VANDERBILT
School of Engineering

Manipulation of the NF- κ B Pathway in Macrophages Using Targeted Nanotherapeutics to Achieve an Anti-Tumor Phenotype

Ryan A. Ortega^{1,2}, Whitney Barham², Bharat Kumar¹, Todd D. Giorgio^{1,2}, Fiona Yull²

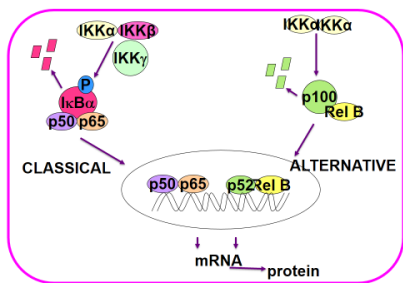
¹Department of Biomedical Engineering, Vanderbilt University, Nashville, TN

²Department of Cancer Biology, Vanderbilt University Medical Center, Nashville TN

**laboratory for
bionanotechnology
AND
nanomedicine**

NF- κ B is a promising target for therapeutic manipulation of tumor associated macrophages (TAMs)

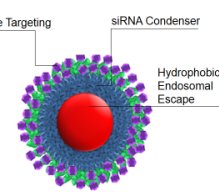
- NF- κ B is implicated in creating a TAM phenotype
- Characterized by constant low levels of inflammation, the recruitment of pro-tumorigenic cells, and the restructuring of local tissue.
- Classical and alternative NF- κ B activation offer highly varied therapeutic targets and effects, specific to each pathway



- Knocking down key NF- κ B proteins with targeted nanotherapeutics could potentially wipe out the TAM phenotype
- Selectively activating a cytotoxic (M1) phenotype could produce a strong anti-tumor inflammatory response that is local and transient

Nanotherapeutic schemes

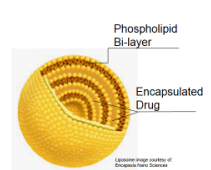
Targeted nanoparticle (Mn-NP) for gene knockdown



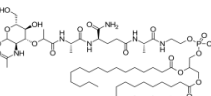
- Mannosylated surface targets the macrophage specific mannose receptor
- Mild surface charge allows for longer transfection times, high biocompatibility, and *in vivo* relevance

- Endosomal pH activates nanoparticle to disrupt endosome and release functional siRNA

Multilamellar liposome for drug delivery



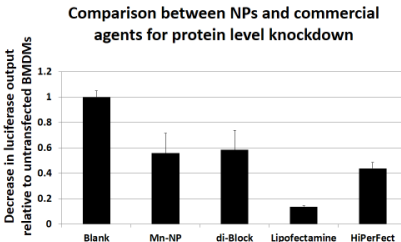
- Liposome ensures preferential uptake by macrophages
- Encapsulated drug, muramyl tripeptide phosphatidylethanolamine (L-MTP-PE), is a synthetic analog of a bacterial protein. Used clinically in the EU to treat osteosarcoma.



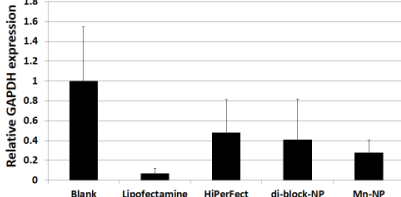
In vitro bone marrow derived macrophage (BMDMs) culturing and transfection

- Bone marrow was harvested from the femurs of NGL reporter mice on an FVB background.
- NGL mice express luciferase and GFP as a reporter of total NF- κ B activity.
- Bone marrow is cultured in media containing a supplemental source of M-CSF for 6 days.
- BMDMs are transfected with siRNA (10 nM) using commercial agent, Lipofectamine (1.6 μ l/ml), or using nanoparticles (4 μ g/ml); or cells are stimulated with an NF- κ B activating agent
- For siRNA transfected cells: After 6 hrs of transfection, cells are stimulated with TNF- α for 6 hrs to elicit strong NF- κ B activation
- For drug stimulated cells: Cells are exposed to L-MTP-PE or other agent for varying time points. Cells are dosed every 24 hours and media is refreshed.

siRNA successfully decreases total NF- κ B activity

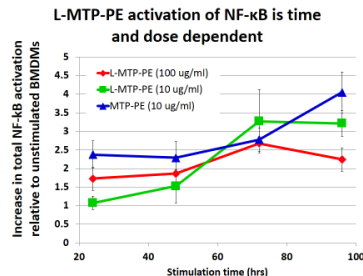


Comparison between NPs and commercial agents for gene level knockdown of GAPDH via qRT-PCR



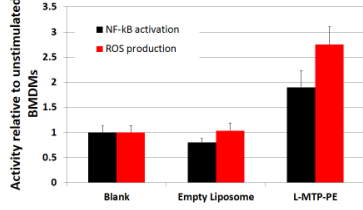
- Nanoparticle siRNA delivery efficiency is comparable to commercial agents with the added bonus of *in vivo* capability and targetability

Controlled *in vitro* activation of NF- κ B requires longer dosing times

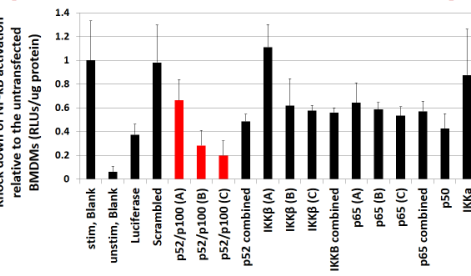


- Liposomal encapsulation of muramyl tripeptide increases its stimulatory effect more than 100 fold

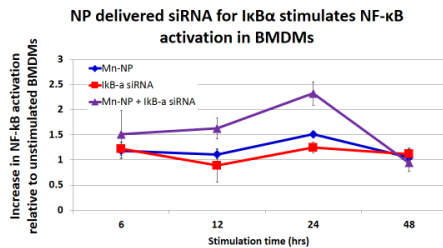
Stimulation of HLL BMDMs with L-MTP-PE show an increase in NF- κ B activation and ROS production



NF- κ B knockdown experiments have produced and effective siRNA library



The classical NF- κ B pathway can be activated by delivering siRNA to the inhibitor protein, IκB α , using Mn-NP



- The transfection times necessary to effectively stimulate NF- κ B by knocking down IκB α with siRNA are impossible to achieve using commercial delivery agents

Conclusions

- NF- κ B specific siRNA are capable of knocking down specific pathway proteins
- Mannosylated nanoparticles exhibit transfection efficiencies comparable to commercial agents
- Using a clinical agent, strategic NF- κ B activation can be correlated to an increase in ROS.
- Targeted activation can be achieved via Mn-NP mediated delivery of siRNA for the IκB α inhibitor protein.

Acknowledgments

This work was made possible in part by a grant from the United States Department of Defense's (USDoD) Congressionally Directed Medical Research Programs (CDMRP) Breast Cancer Research Program (BCRP): Grant BC102690.

Introduction: Folic acid (FA) receptors are overexpressed on numerous cancer cell types and are thus commonly utilized for drug targeting. However, several normal cell types also express low levels of FA receptor, which can lead to off-site effects. In order to increase cancer specificity, we designed a siRNA carrier that specifically targets tissues where there is a co-localization of cell-surface receptors (FA receptors) and environmental factors (high MMP-7 activity) that are both hallmarks of the breast cancer microenvironment. With this dual FA and MMP-7 proximity-activated targeting (PAT) smart polymer nanoparticle (PAT-SPN/FA-SPN), FA is masked by an MMP-7-removable PEG “cloak” that, when removed by MMP-7 activity, exposes FA and triggers uptake by FA receptor-expressing cells (**Fig. 1A**).

Materials and Methods: To generate two versions of the MMP-7-PAT component, a 5 kDa linear or a 20 kDa Y-shaped PEG was conjugated to a reversible addition-fragmentation chain transfer polymerization agent (RAFT-CTA) via an MMP-7 cleavable peptide VPLSLYSGCG linker. An FA-functionalized RAFT-CTA was also synthesized containing a 2 kDa PEG linker. RAFT polymerization of a nanoparticle-forming, pH-responsive diblock copolymer previously described for siRNA delivery [1] was performed with all three of these macro-CTAs (5K-PAT, 20K-PAT, and FA-PEG). Mixed micelle nanoparticles (PAT-SPN/FA-SPN) were made with varied ratios of the FA and PAT functionalized polymers. Dual MMP-7-PAT and FA mediated uptake of fluorescently-labeled siRNA was tested in MDA-MB-231 and MCF-7 breast cancer cells by flow cytometry. Gene knockdown with siRNA delivered by PAT-SPN was evaluated in luciferase-expressing R221A cancer cells.

Results and Discussion: Flow cytometry confirmed that the pre-treatment of complexes with MMP-7 to mimic the breast cancer environment produced to a 2.5 fold increase in uptake of PAT_{5k}-SPN/nucleic acid (0% FA targeting) compared to the uptake of nanoparticles not treated with MMP-7 (not shown). MMP-7-activated PAT_{5k}-SPN knockdown of the model protein luciferase in R221A-Luc cells was greater than that achieved with PAT_{5k}-SPNs not activated by MMP-7 and equal to the commercial reagent Lipofectamine (not shown). As expected, the PAT_{20k}-SPNs were even better than the PAT_{5k}-SPNs at blocking particle nonspecific uptake in the absence of MMP activation, and it was thus used in the mixed compositions with the FA-SPN polymer (PAT_{20k}-SPN/FA-SPNs). In mixed compositions with 25% and 50% FA-SPN, it was found that MMP-7 activation produced a 4 fold increase in uptake relative to PAT_{20k}-SPN/FA-SPNs not activated by MMP-7 ($p<0.005$) (**Fig. 1B**). As expected, higher percentages of the FA-SPN polymer (75-100%) reduced targeting dependency on MMP-7 activity (**Fig. 1B**). Finally, addition of free FA in the media blocked uptake for the FA-SPN-containing particles, confirming that uptake was FA receptor-mediated following MMP activation (**Fig. 1B**).

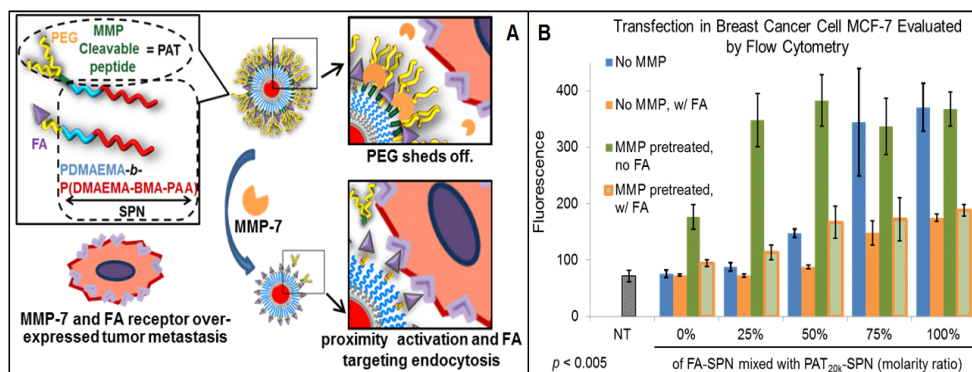


Figure 1 **A.** The PAT-SPN/FA-SPN design incorporates PEG shielding removable in MMP-7-rich tumors to expose FA and trigger uptake. **B.** At ~25-50% FA-containing polymer in the PAT_{20k}-SPN/FA-SPN, dual targeting was finely tuned to be dependent on both MMP-7 activity and FA receptor mediated uptake. (mean+/-SD, n=3).

Conclusions: Novel PAT-SPN/FA-SPN siRNA nanocarriers have been synthesized that are efficiently dual targeted. The optimal PEG length for the PAT element (20 kDa) and FA/PAT ratios (25-50%) have been identified that produce “binary” targeting behavior that is dependent on both MMP-7 and FA receptor-mediated endocytosis. These targeted siRNA nanocarriers hold great promise for improved delivery to breast cancer.

Acknowledgement: Supported DOD CDMRP (W81XWH-10-1-0445/0446)

References: [1] Convertine et al. *J. Contr. Release* 2009.



Dual MMP-7-Proximity-Activated and Folate Targeted Nanoparticles for siRNA Delivery

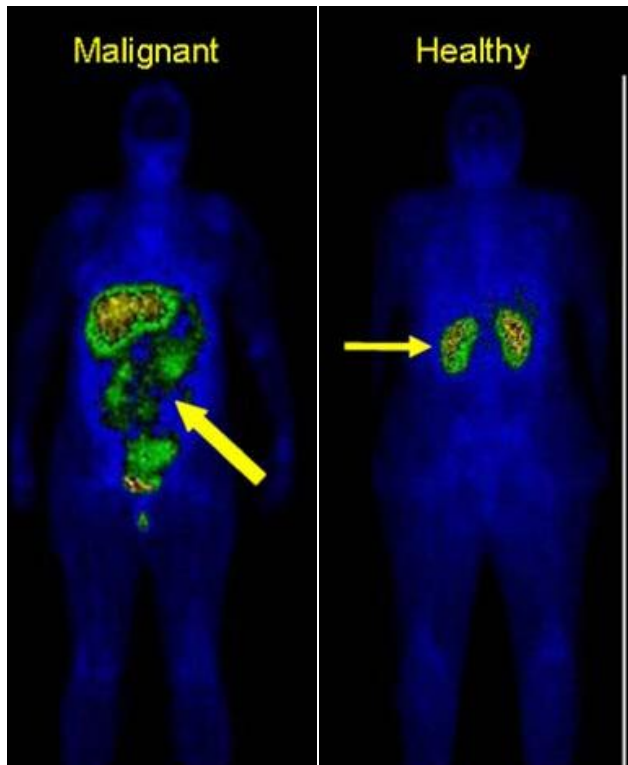
Hongmei Li, Martina Miteva, Ming J. Cheng, Todd D. Giorgio*, Craig L. Duvall*

Biomedical Engineering Department
Vanderbilt University
Nashville, TN

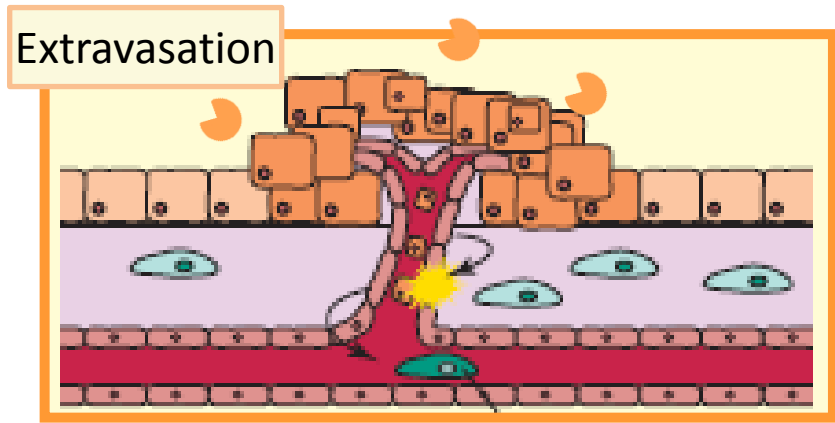


Photos from www.vanderbilt.edu

Folic acid (FA) receptors and matrix metalloproteinases (MMP) are both tumor hallmarks

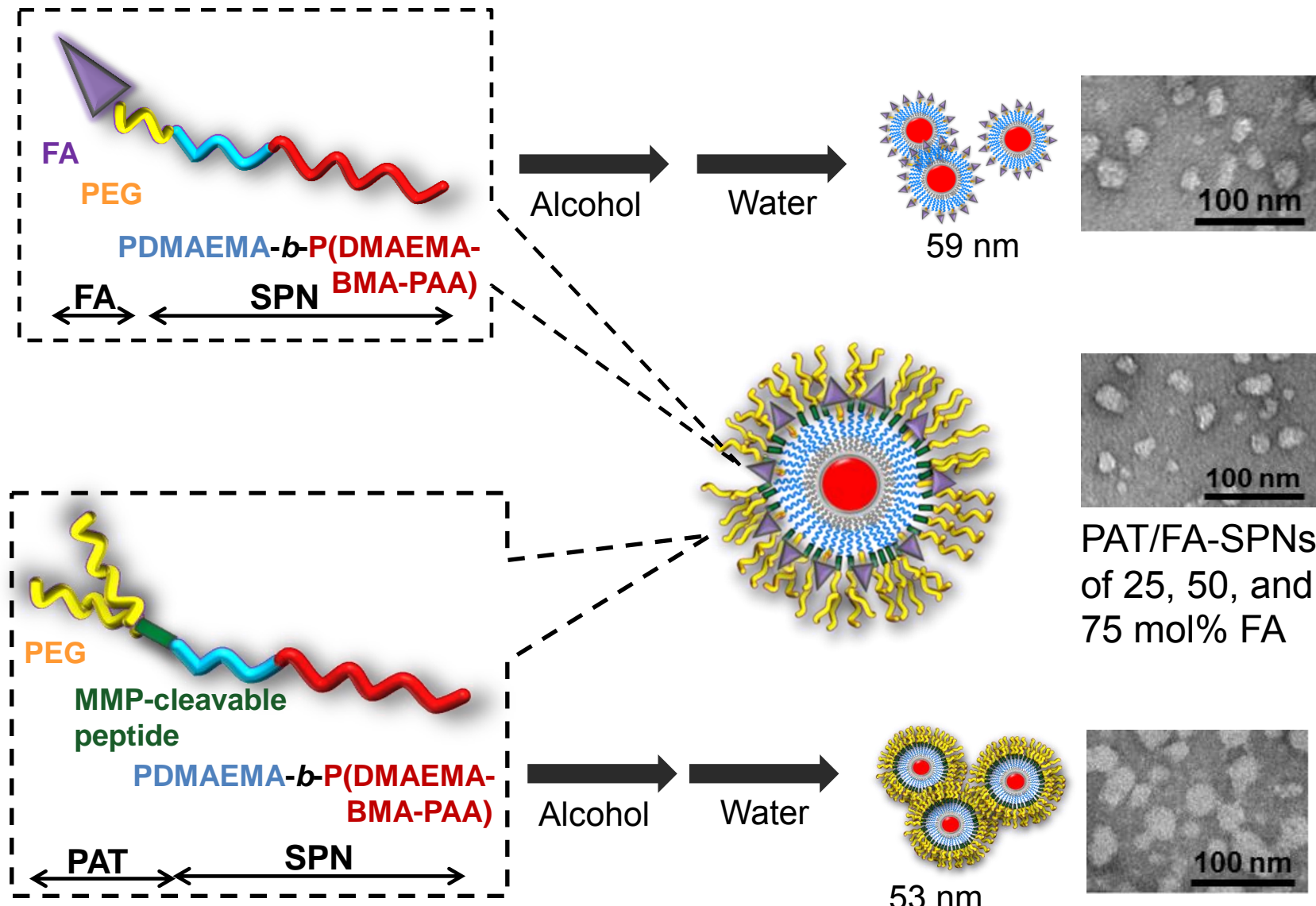


Gamma scintigraphic images of an ovarian cancer patient (left) and healthy volunteer (right) using FR-targeted contrast agents.

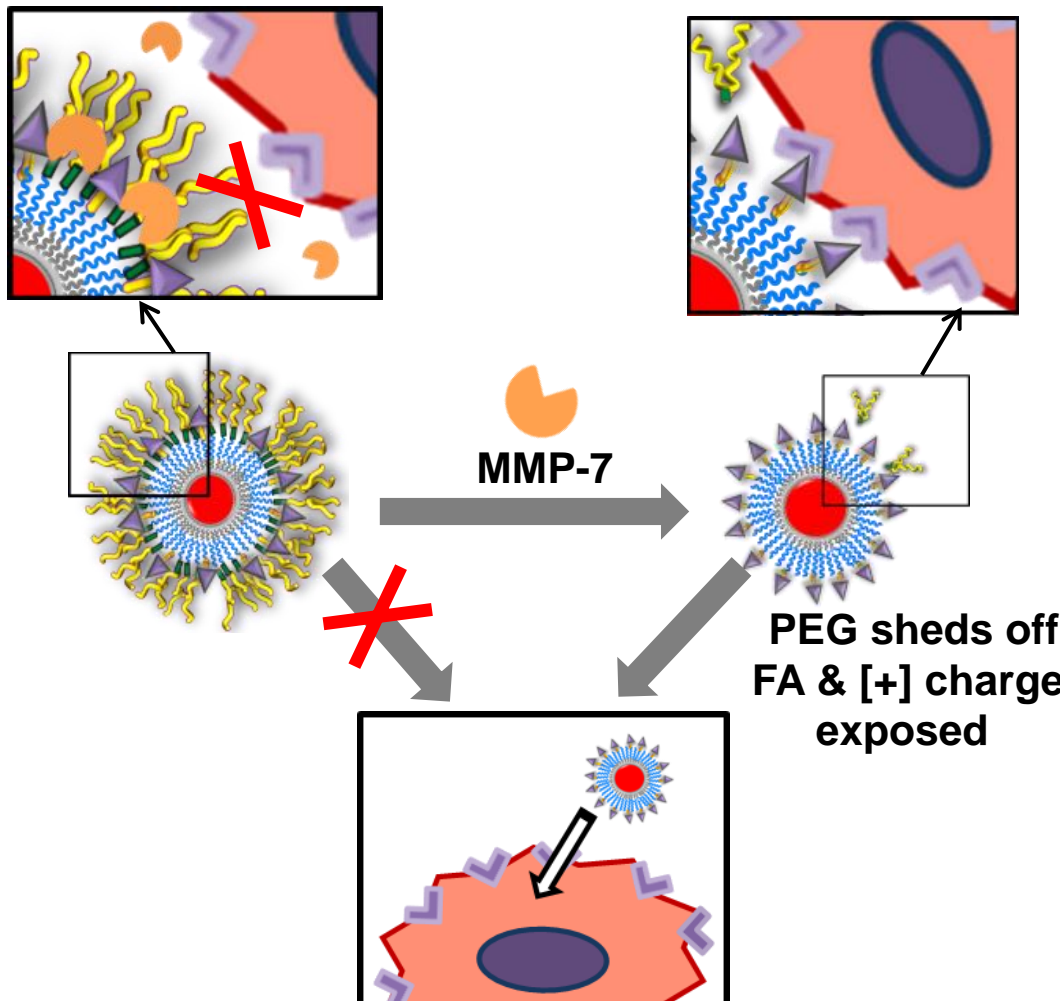


MMP is over-expressed in the proximity of tumor metastases in assisting the tumor cells to proliferate and migrate.

Synthesis of MMP proximity activated targeting (PAT), folic acid (FA) functionalized smart polymeric nanocarriers (SPN)

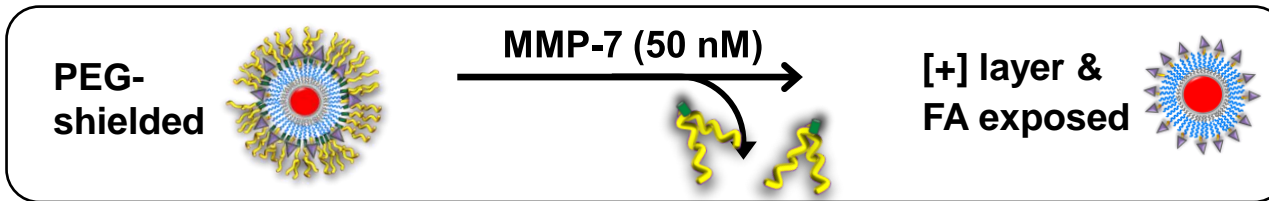


Mechanism of proximity-activated, FA dual targeting by MMP-7 for drug delivery to cancer metastasis

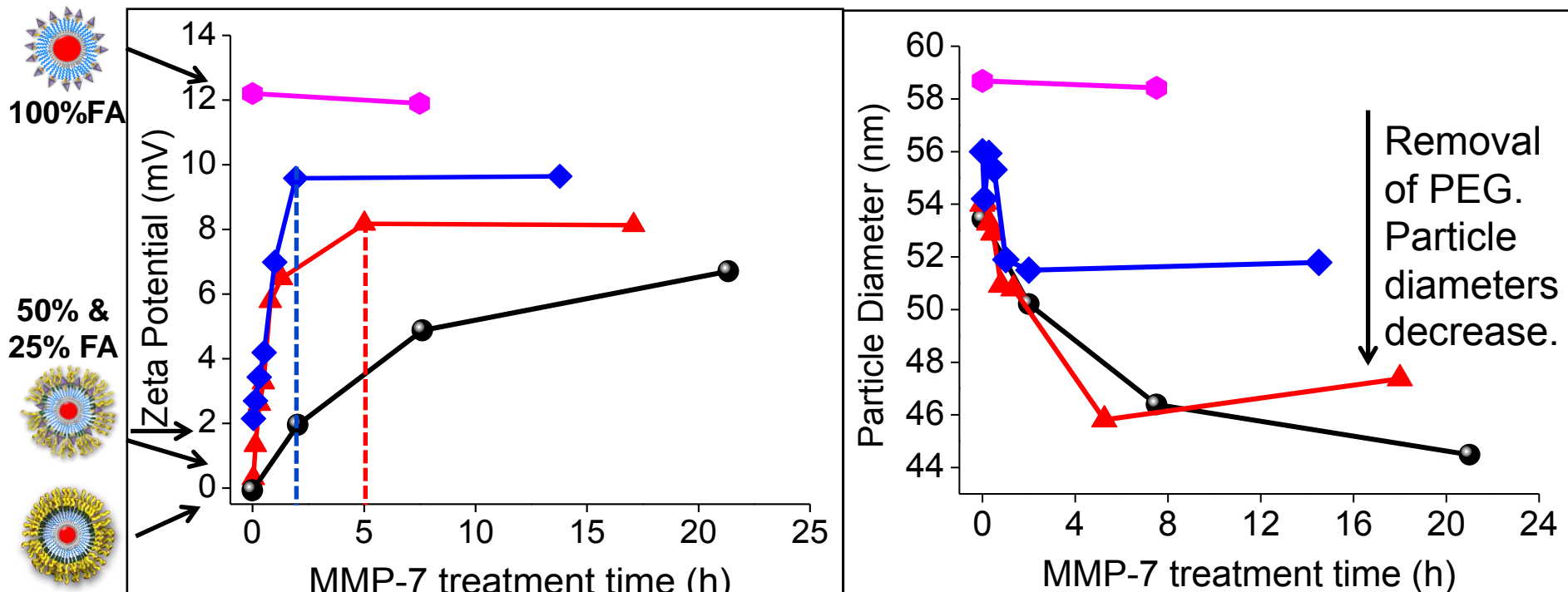


Proximity-activated, FA targeting endocytosis in MMP-7 and FA receptor over-expressed tumor metastasis.

MMP sensitivity--Key to proximity-activated targeting (PAT)



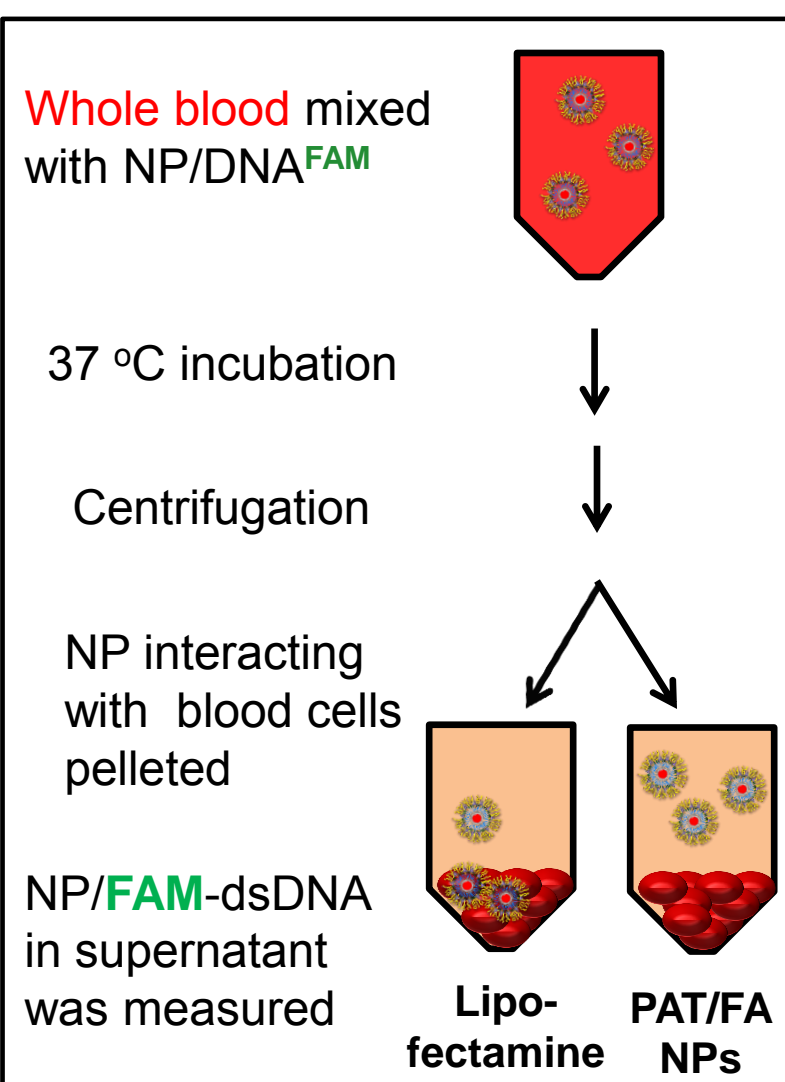
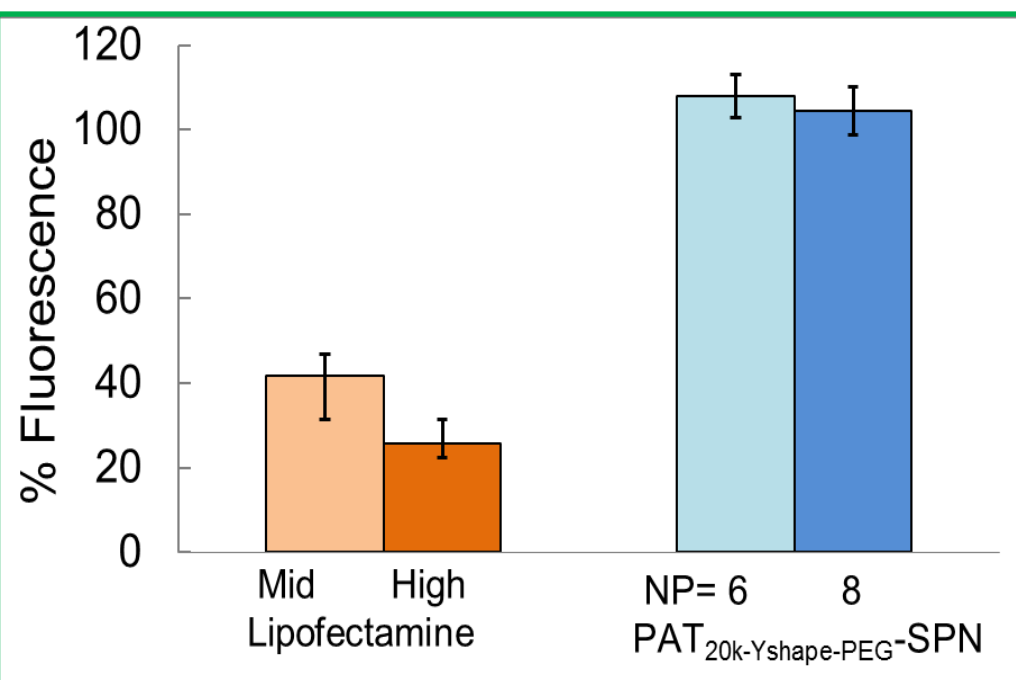
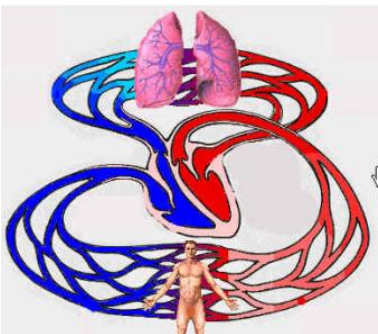
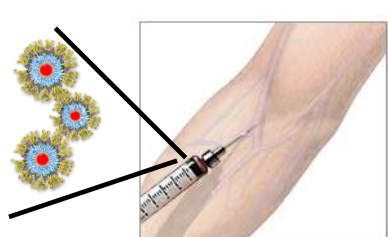
Micelles comprising FA-SPN of  0,  25,  50, and  100 mol% in PAT-SPN



Increased zeta potential (left) and decreased particle diameter (right) of $\text{PAT}_{20\text{kPEG}}/\text{FA-SPN}$ mixed micelles over time after treatment with MMP-7.

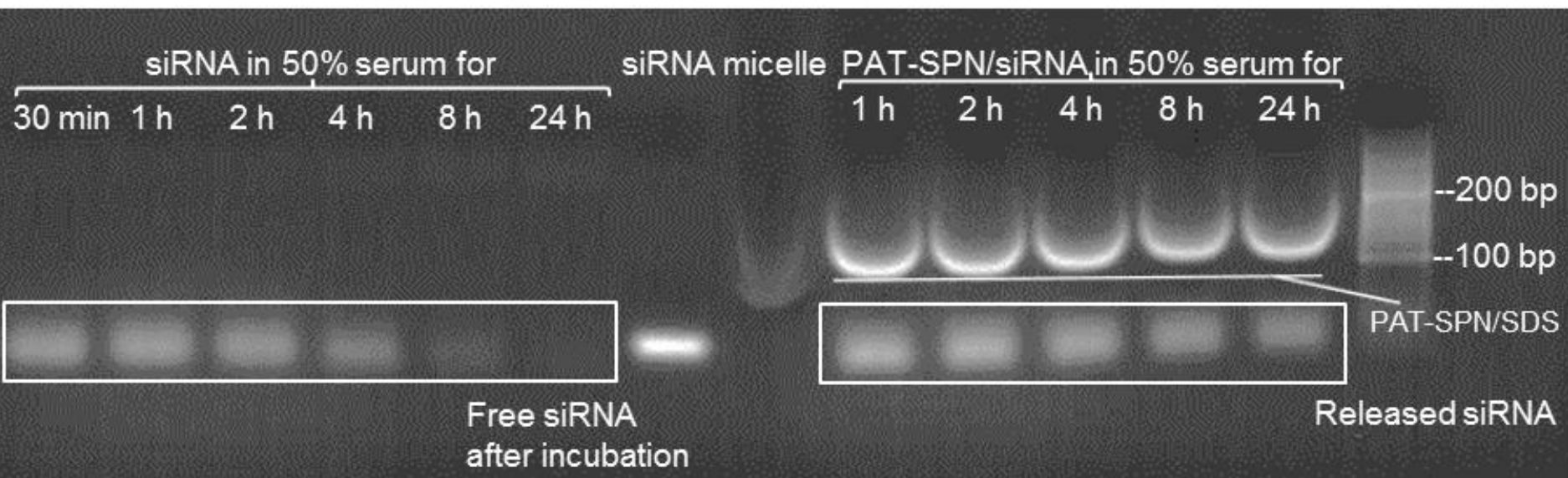


PEG corona greatly reduced the interaction between nanoparticle (NP) and the whole blood



Whole blood compatibility

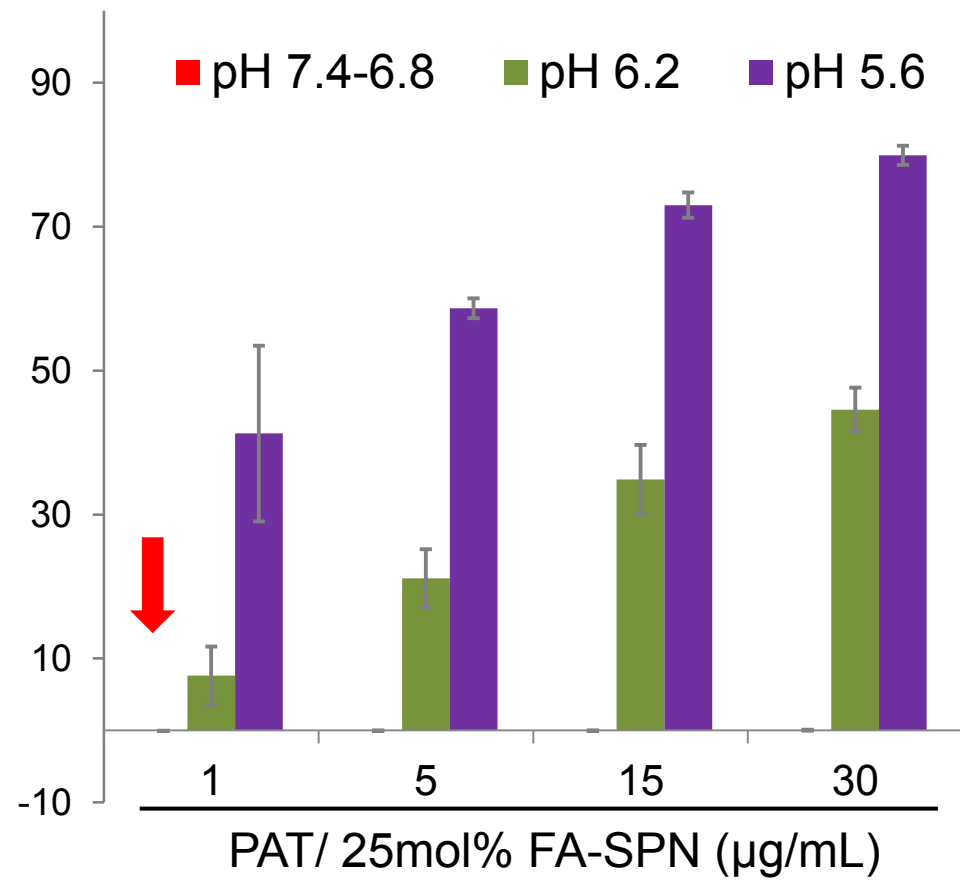
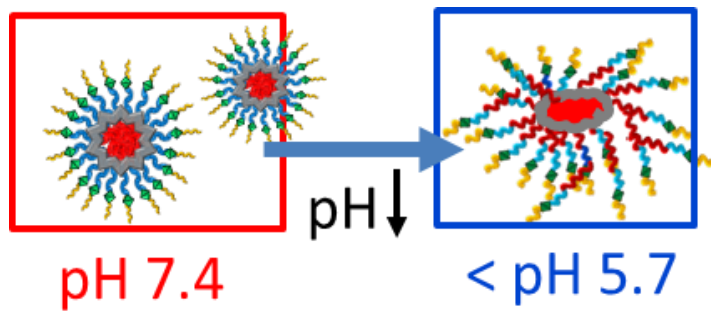
siRNA protection from degradation in serum



Free siRNA (left), relative to siRNA protected by PAT-SPNs from degradation (right), in the presence of 50% serum at 37°C.



pH dependent hemolysis--Feature for endo/lysosome escape

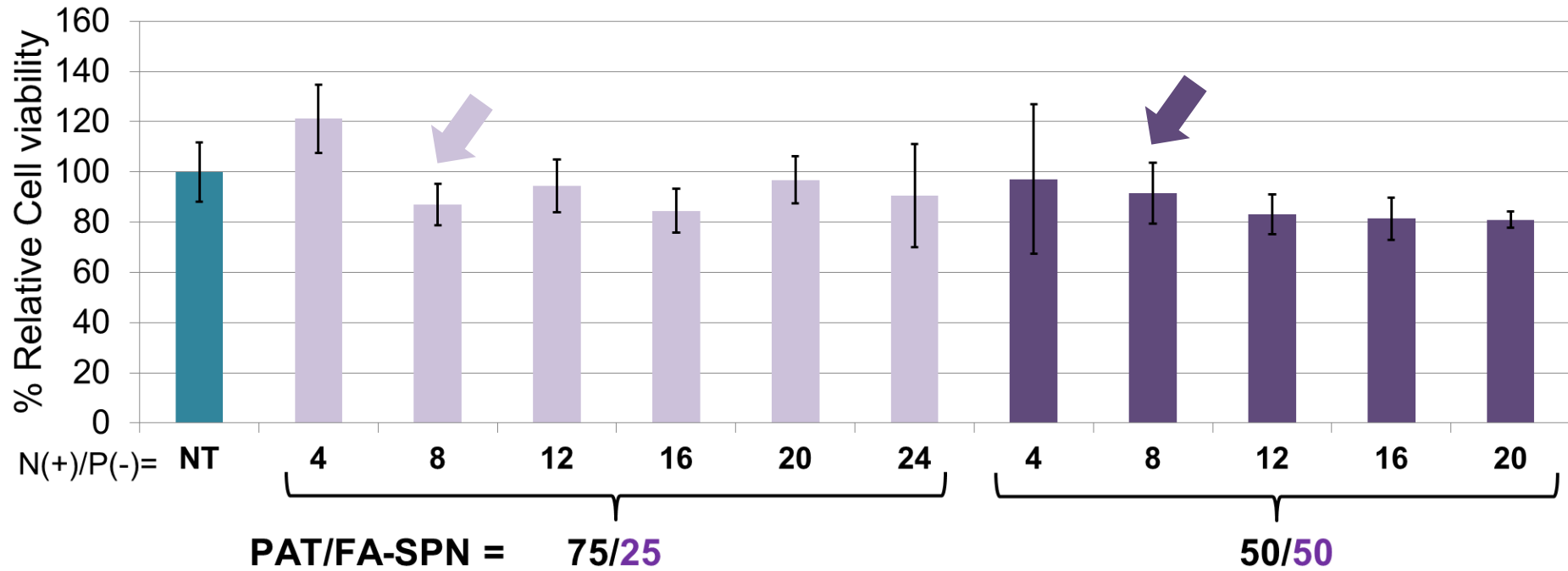


C. L. Duvall et al. *Mol. Pharm.* **2010**, *7*, 468–476.

A. J. Convertine et al., *J. Control. Release* **2009**, *133*, 221–229.



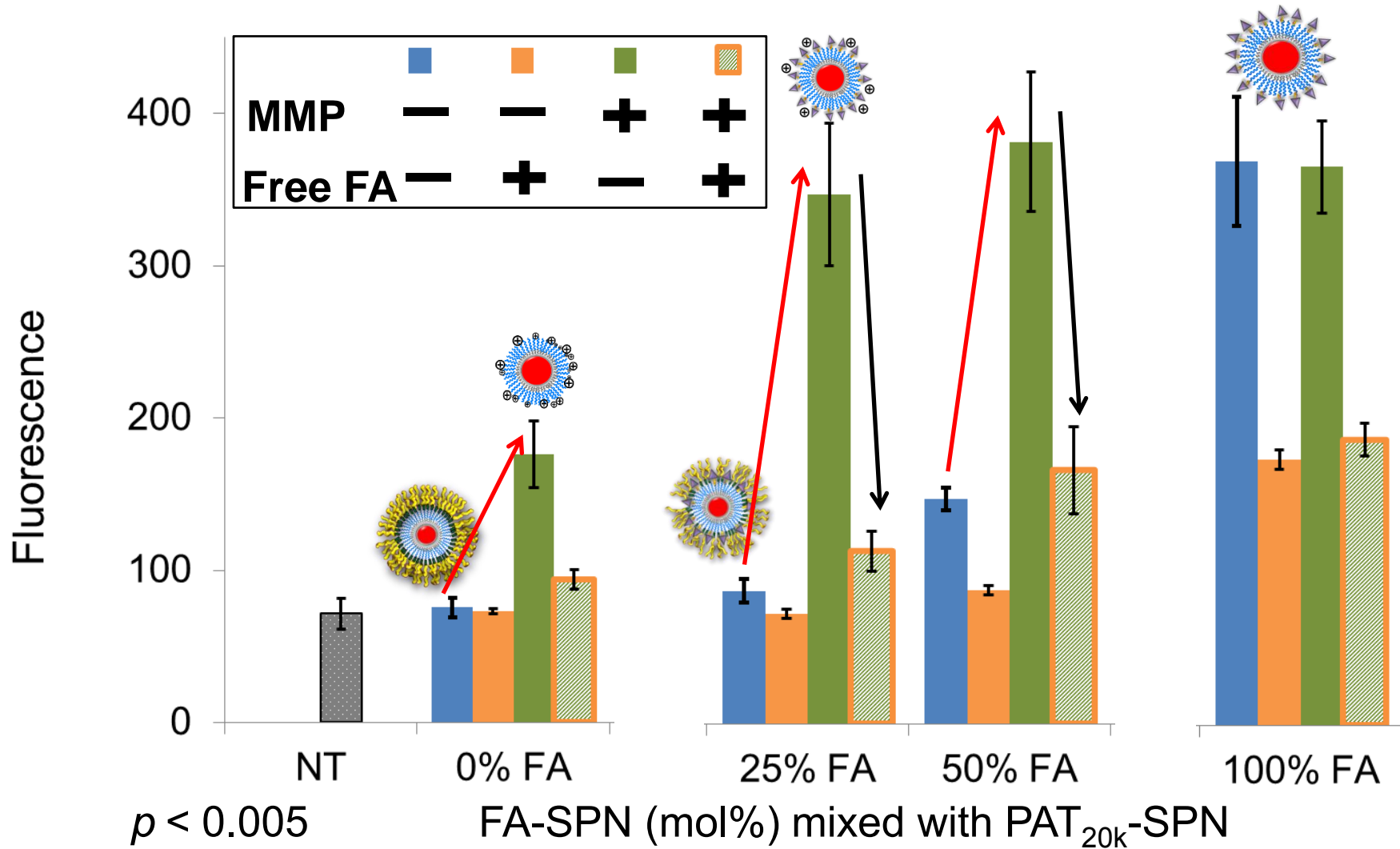
Low cytotoxicity of the nanoparticles



25% and 50% FA in PAT-SPN did not show apparent cytotoxicity across the range of charged polymer/siRNA ratio $N(+)/P(-)$ tested.



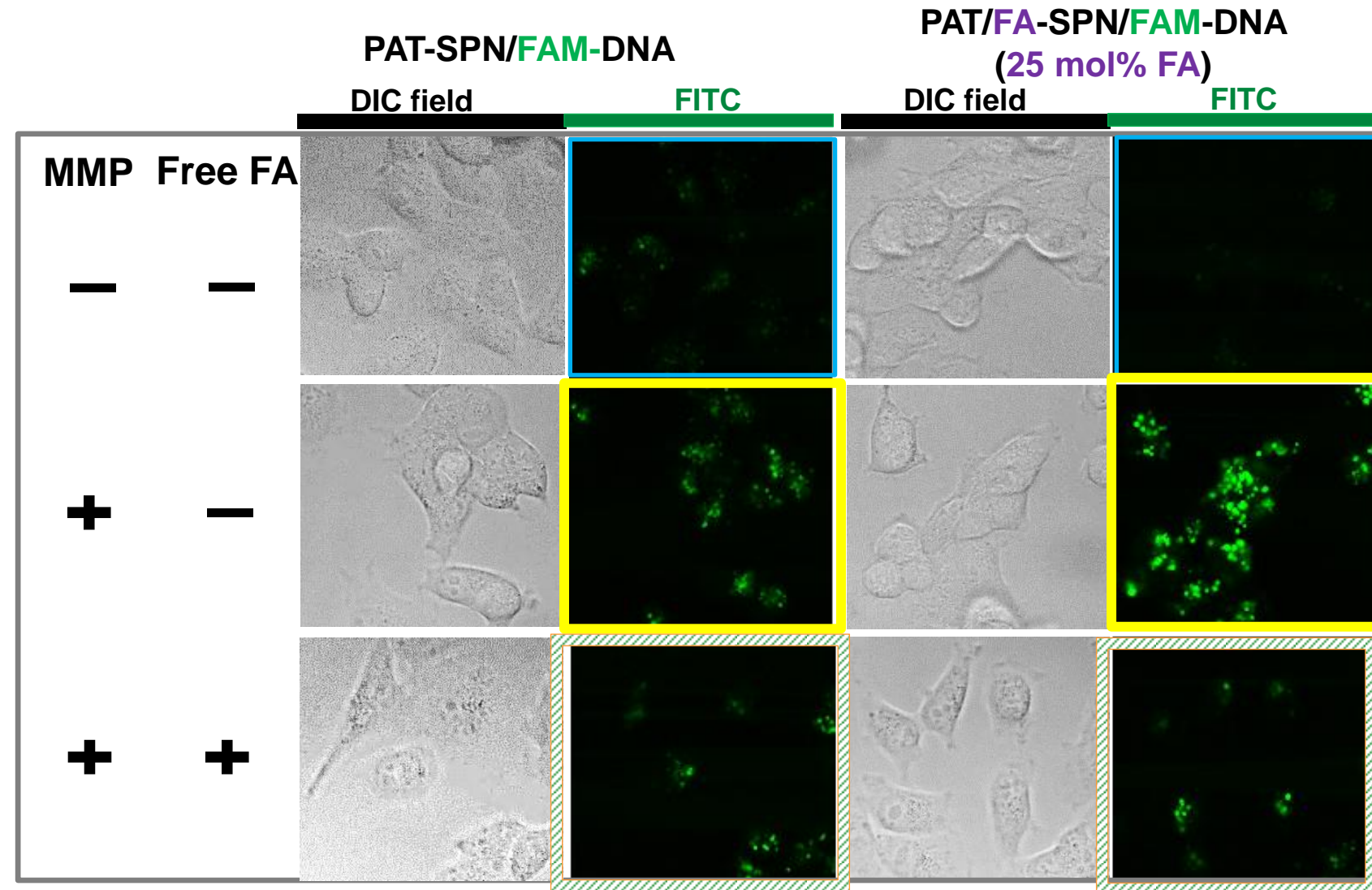
MMP-7 activation triggers dual PAT- and FA-targeting and enhances cell internalization in breast cancer cells



MMP-7 triggered dual targeting

10

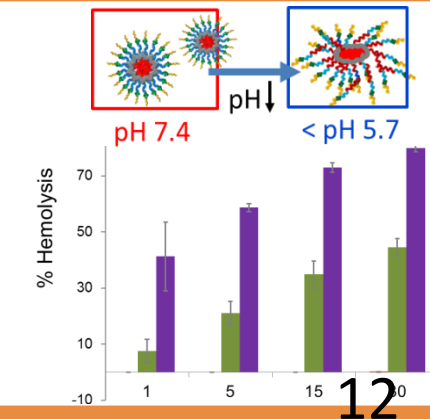
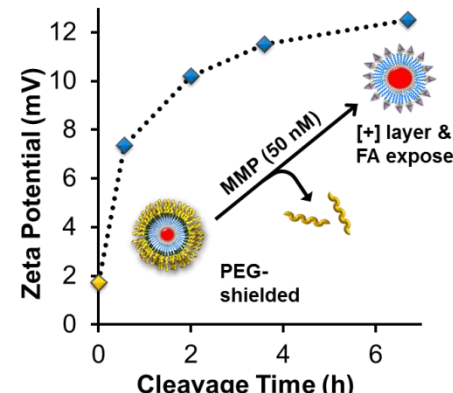
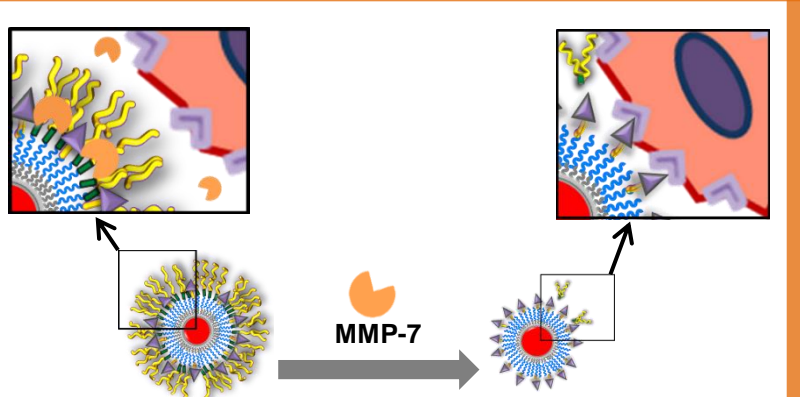
MMP-7 triggered dual PAT- and FA-targeting and enhanced cell internalization in breast cancer cells



Conclusions

Novel MMP proximity activated, folate receptor dual targeting PAT/FA-SPN siRNA nanocarriers are synthesized.

- MMP proximity activated targeting
- Folate mediated cellular uptake
- Agreeable blood compatibility
- Serum stability, protection of siRNA therapeutics
- pH dependent endosome-lysis
- Well cytocompatibility



Acknowledgments



Collaborative Idea
Expansion Awards:
W81XWH-10-1-0446/-
0445



SCHOOL OF ENGINEERING
VANDERBILT UNIVERSITY

Craig Duvall's
research group



Todd Giorgio's
research group



Achieving Cancer Immunotherapy Through RNAi Interference in Tumor-Associated Macrophages via ‘Click’, Mannosylated Polymeric Nanoparticles

S. S. Yu¹, C. M. Lau¹, W. J. Barham², C. E. Nelson¹, F. E. Yull², C. L. Duvall¹, and T. D. Giorgio^{1,2}

¹Vanderbilt University, Nashville, TN, ²Vanderbilt-Ingram Cancer Center, Nashville, TN

Introduction: Tumor-associated macrophages (TAMs) represent a promising therapeutic target in cancer because they have been shown to facilitate tumor growth and invasiveness. However, macrophage-specific drug delivery within tumor sites is a significant challenge, as systemic interference with macrophage behavior may lead to autoimmune manifestations. In this work, we designed and characterized mannosylated polymeric nanoparticles (ManNPs) in order to achieve CD206 (macrophage mannose receptor)-targeted siRNA delivery. CD206 is almost exclusively expressed on macrophages and dendritic cells, and upregulated in tumor-associated macrophages.

Materials and Methods: The ManNPs were tri-block co-polymers synthesized via reversible addition-fragmentation chain transfer (RAFT) polymerization, including the following blocks: (1) an azide-displaying block for the attachment of alkyne-functionalized mannose via ‘click’ chemistry, (2) a cationic block for the condensation of polyanions such as siRNA, and (3) a pH-responsive terpolymer block that facilitates endosomal disruption.¹ ManNPs were complexed with FAM-labeled anti-GAPDH siRNA, and delivery into primary murine bone marrow-derived macrophages (BMDMs) was measured via confocal microscopy and flow cytometry. Knockdown of GAPDH expression was assessed via real-time PCR. The same methods were used to quantify biodistribution and knockdown *in vivo* following 24 h after retro-orbital injection of nanoparticles into tumor-bearing “PyT” mice. The PyT mouse model overexpresses the polyoma middle T oncoprotein in the mammary epithelium, leading to the natural development of mammary tumors at 9–13 weeks after birth.

Results and Discussion: The glycoconjugates improved siRNA delivery into BMDMs by 4.5-fold, relative to a non-mannosylated version of the same carrier.

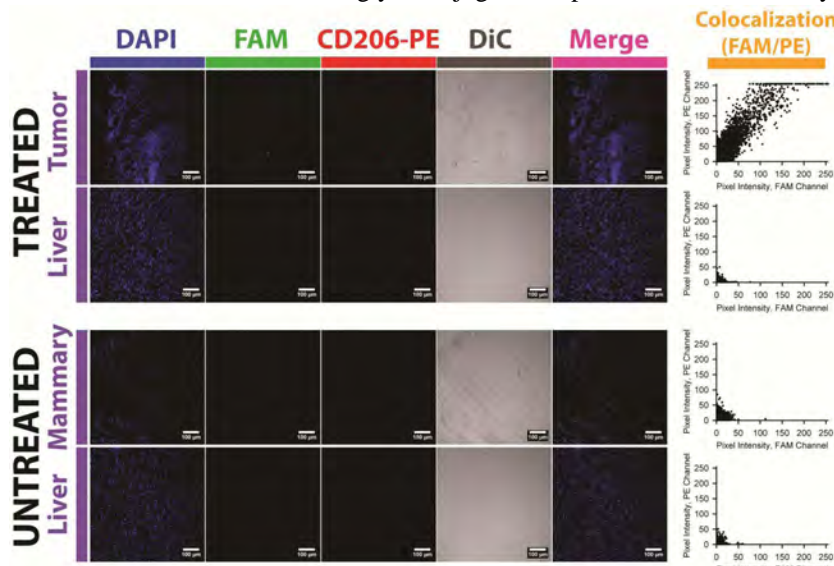


Figure 1. ManNPs deliver FAM-siRNA to CD206+ cells, as shown in frozen sections of mammary tumors of PyT mice treated with nanoparticles for 24h. Moreover, TAMs usually make up <5% of the cells in the tumor, and this is reflected by the limited amount of overall FAM signal in the tumor sections.

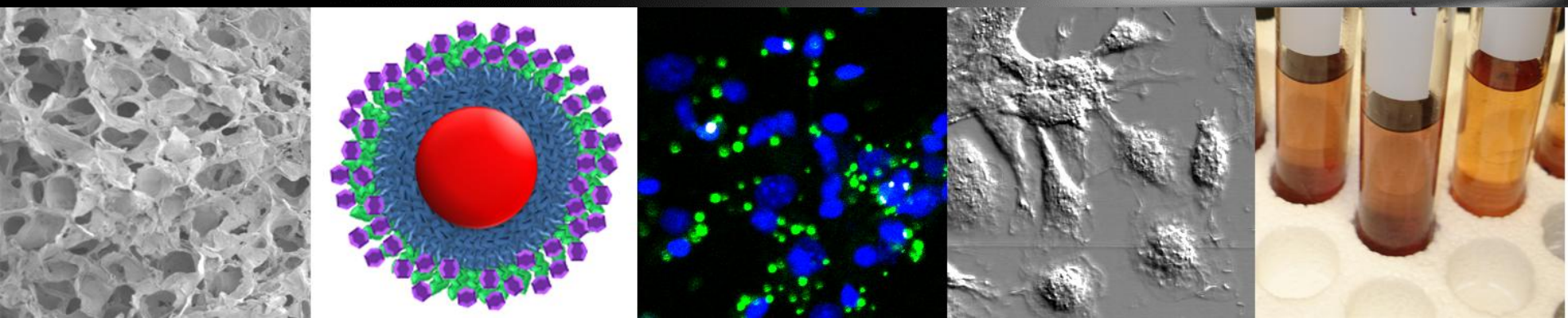
delivered siRNA with tumor-associated F4/80+ cells. This correlated with enhanced knockdown of GAPDH gene expression in CD11b⁺ cells in the tumor.

Conclusions: The ManNPs described here present new opportunities to target TAMs, providing an enabling technology for the modification of the immunosuppressive tumor environment by targeting TAM activity.

Acknowledgements: This work is supported by multiple grants through the Department of Defense CDMRP Breast Cancer Research Program (#W81XWH-10-1-0684, #W81XWH-11-1-0344 & #W81XWH-11-1-0242).

References: ¹AJ Convertine et al. *J Control Release* 2009, 133, 221-9.

Achieving Cancer Immunotherapy Through RNAi in Tumor-Associated Macrophages via 'Click', Mannosylated Polymeric Nanoparticles



**Shann S. Yu, C.M. Lau, W.J. Barham, C.E. Nelson, F.E. Yull,
C.L. Duvall, & T.D. Giorgio**

October 25, 2012

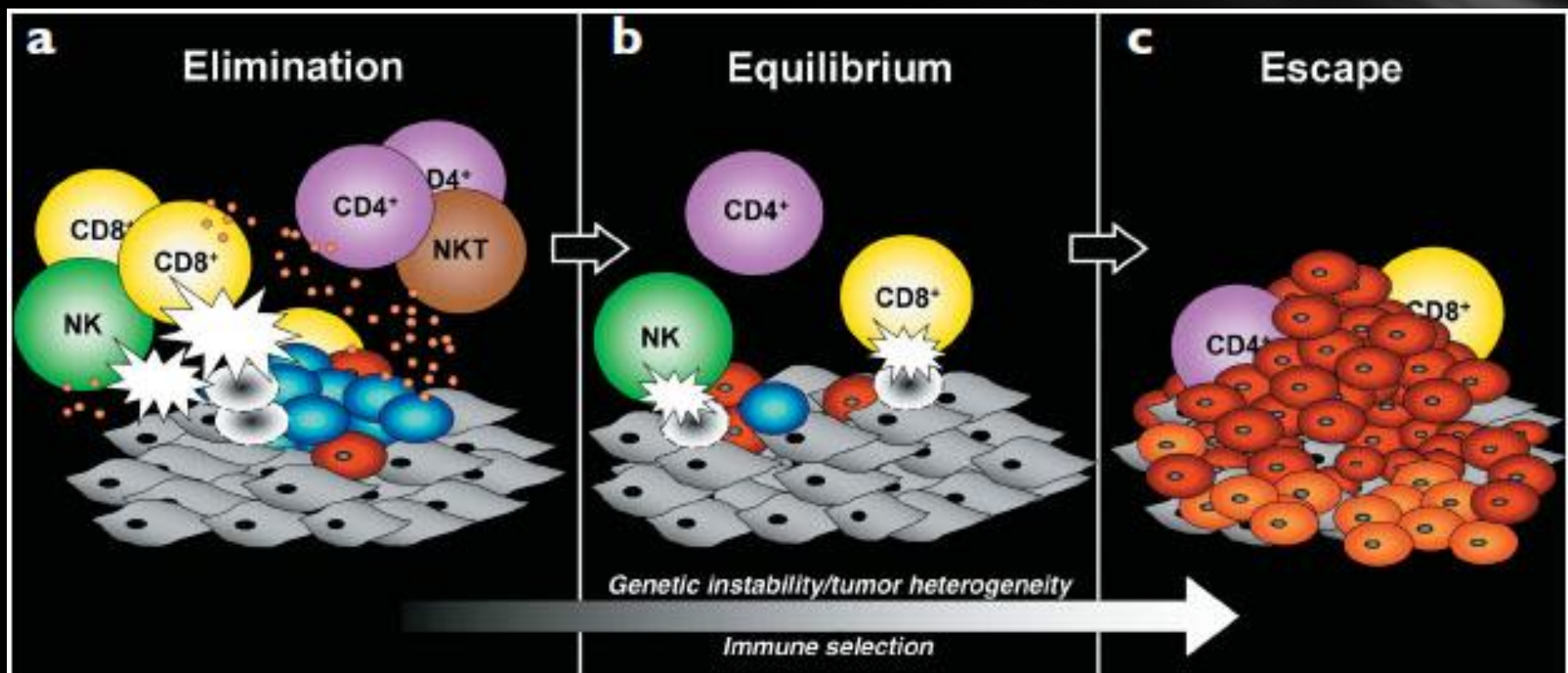
Engineering Immunology and Immunotherapy III

2012 Annual Meeting of the Biomedical Engineering Society



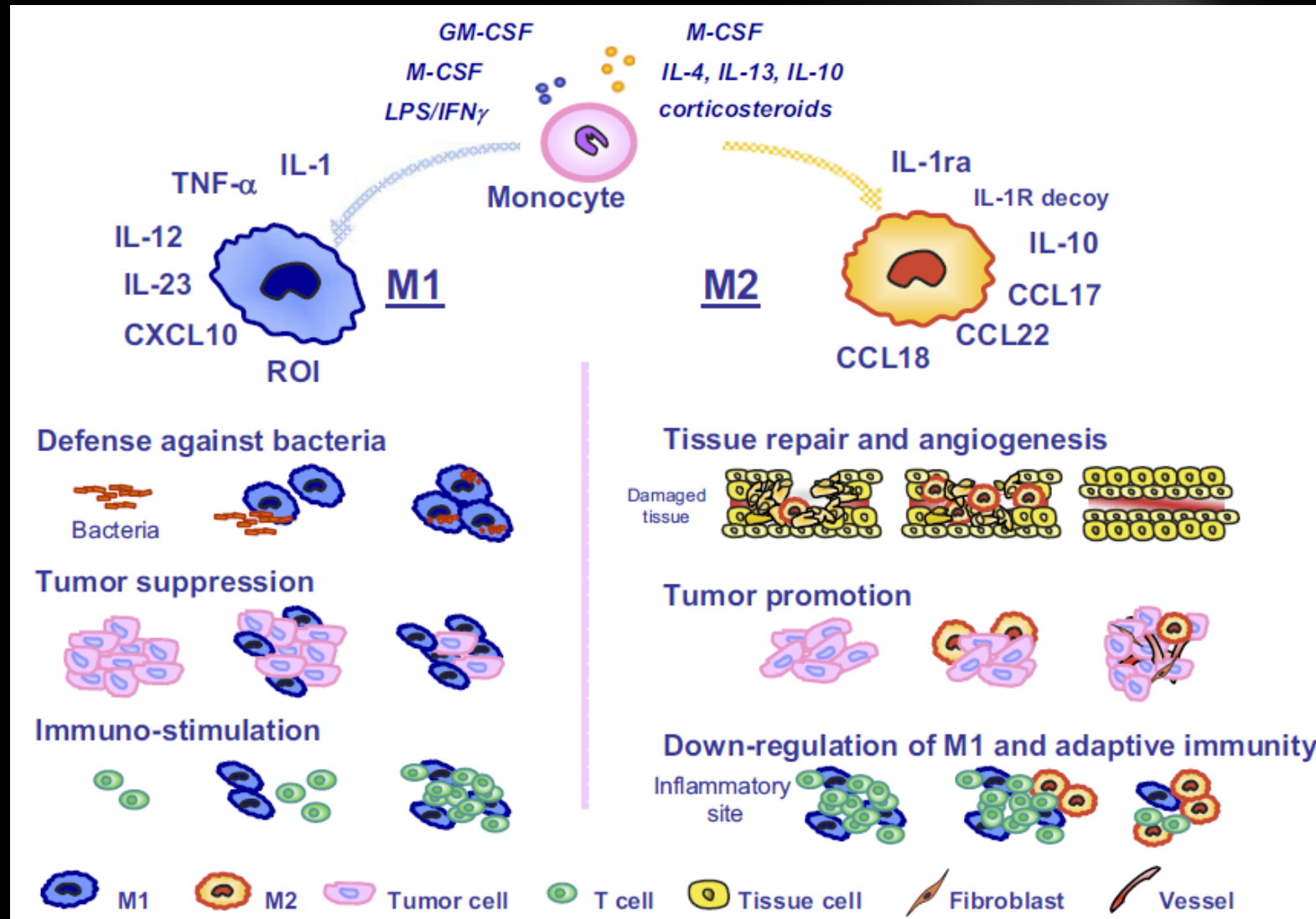
VANDERBILT
School of Engineering

'Immunoediting' as a Tumor Escape Mechanism



GP Dunn et al. (2007) *Nature Immunol.*

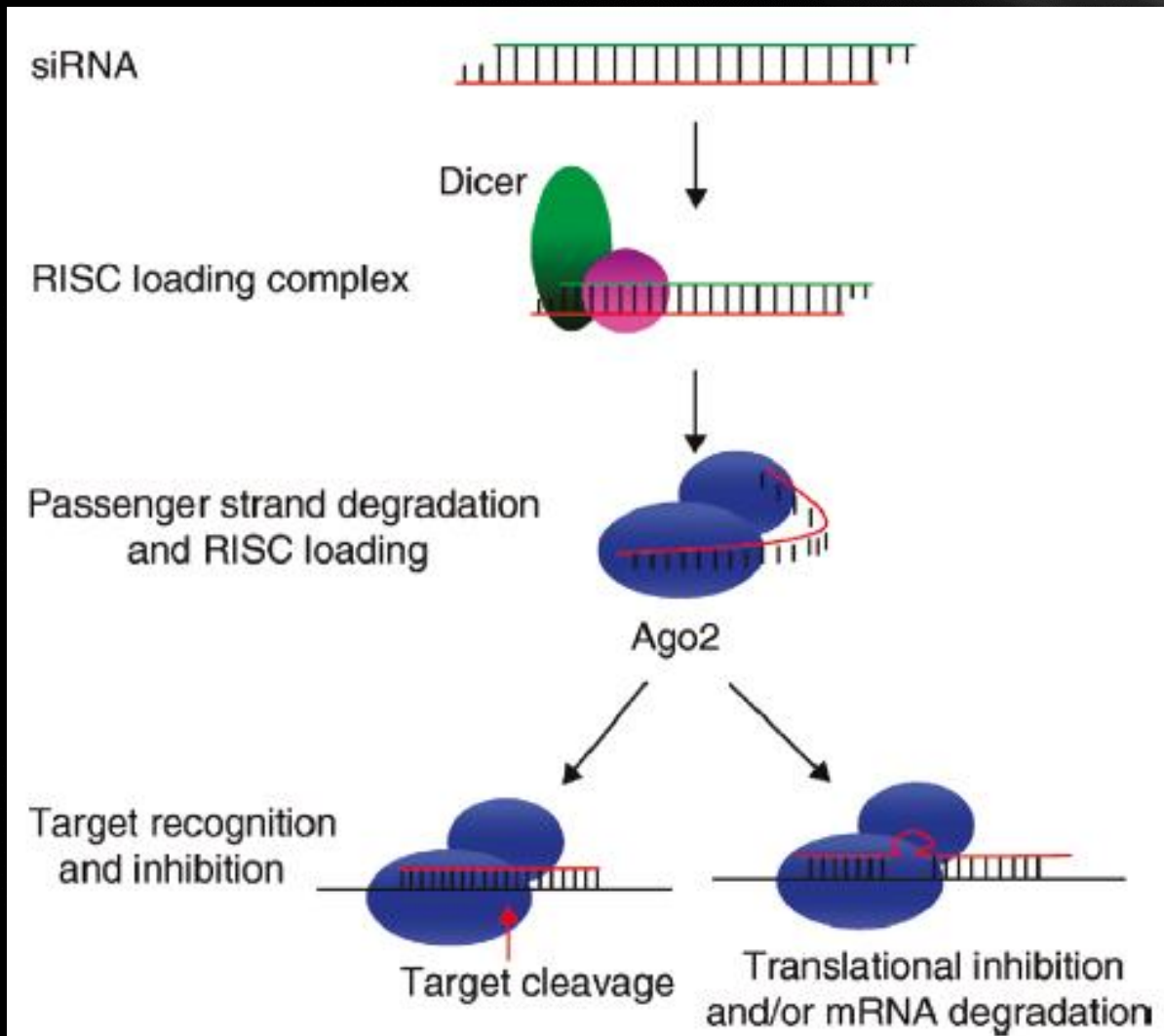
Macrophages are versatile, multifunctional cells that have been 'hijacked' in cancer.



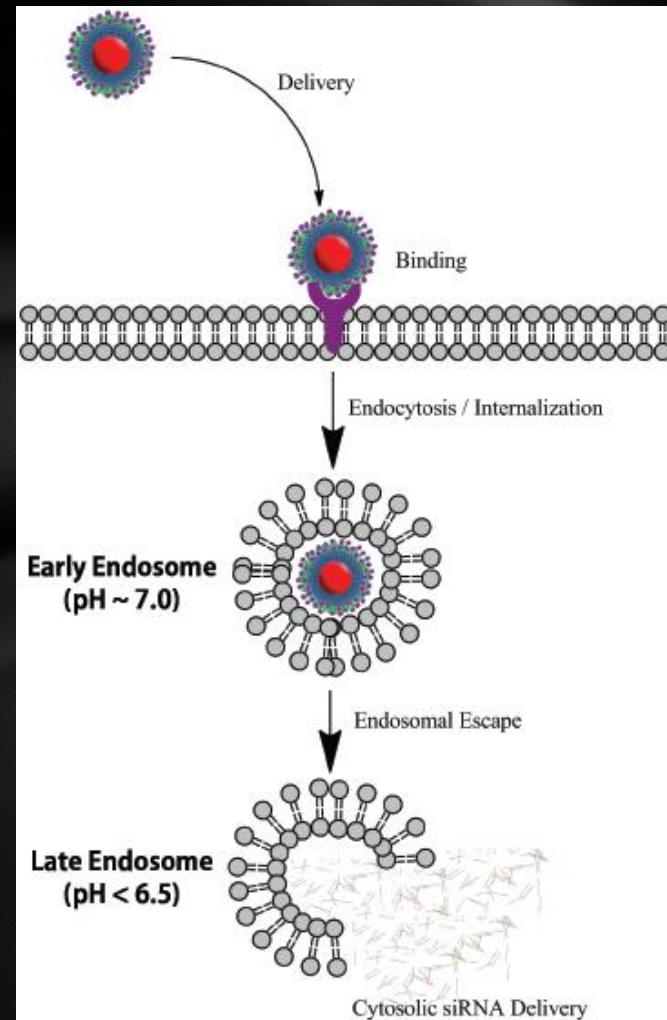
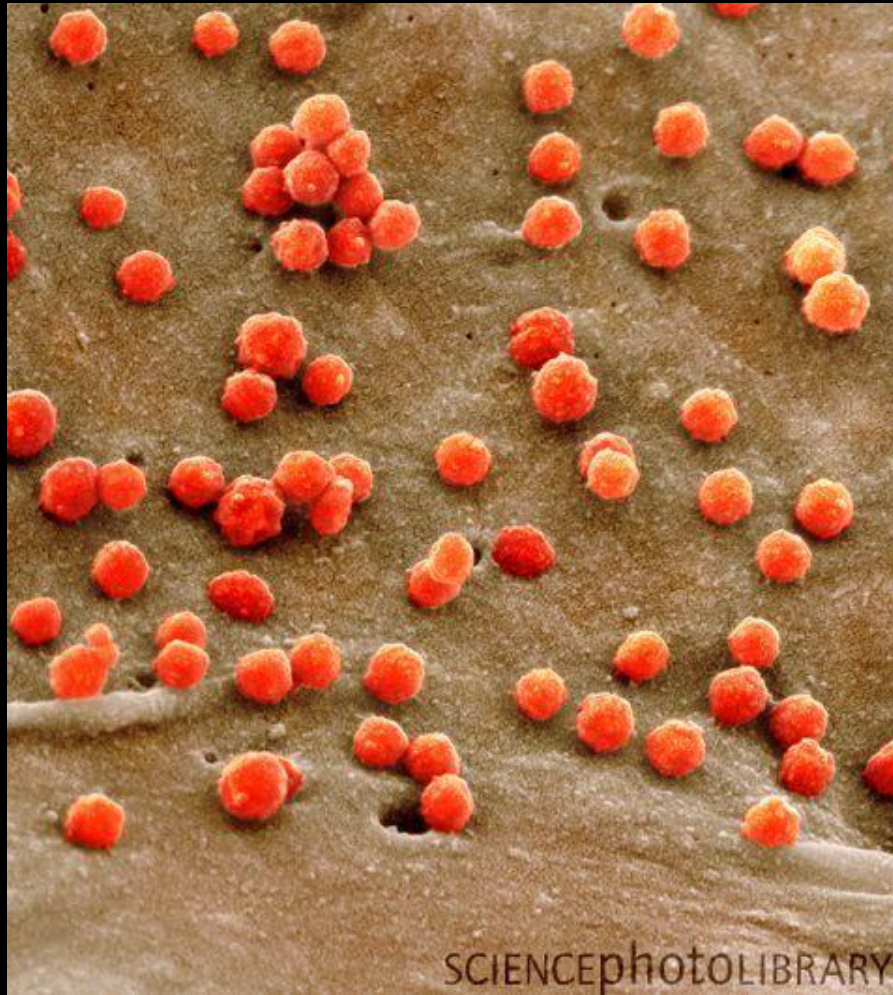
Re-polarization of Tumor-Associated Macrophages Reactivates an Anti-Tumor Immune Response

- C. Guiducci et al. (2005) *Cancer Research*
- A. Saccani et al. (2006) *Cancer Research*
- T. Hagemann et al. (2008) *J Exp Med*
 - GL Beatty et al. (2011) *Science*

Reprogramming TAMs with siRNA: Silencing Pathologic Gene Pathways

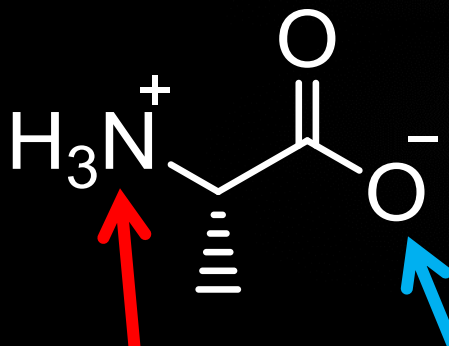


Using Polymers to Mimic Viruses for TAM-Targeted, Intracellular Drug Delivery



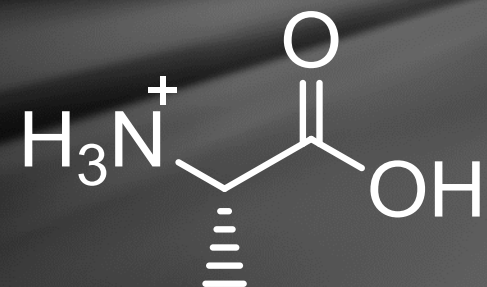
pH-Responsive Polymers are Inspired by Lessons from Nature

pH = 7.4



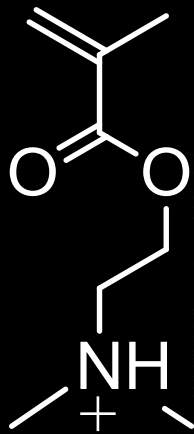
NET CHARGE =
NEUTRAL!!!

pH < 2.3

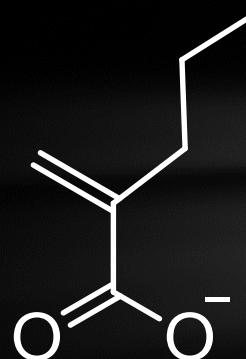


NET CHARGE =
POSITIVE

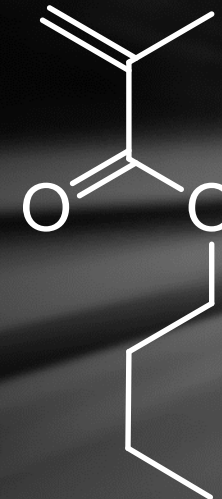
Building pH-Responsive, Endosomolytic Polymers: Rational Monomer Selection



DMAEMA
 $pK_a \sim 7.5$



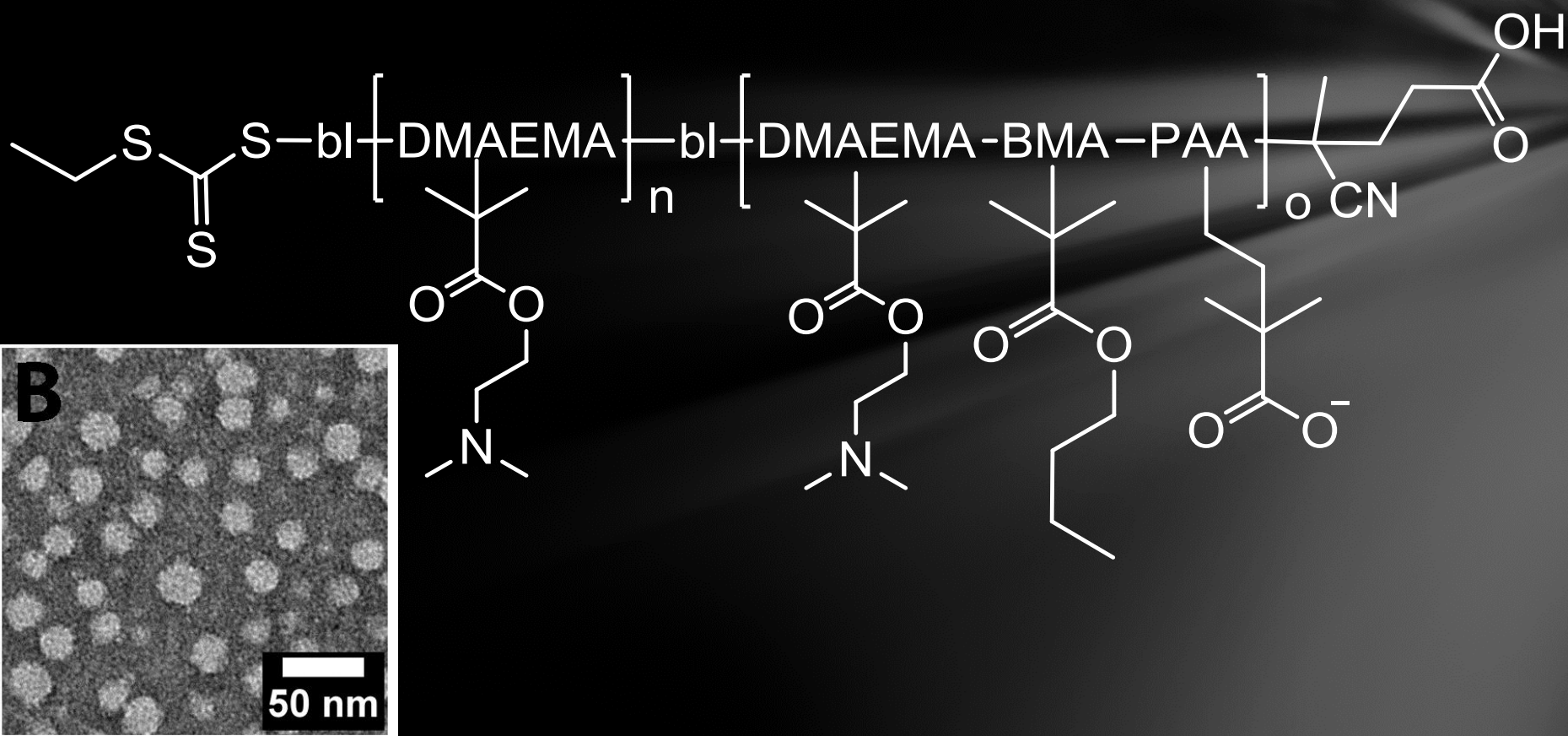
PAA
 $pK_a \sim 6.7$



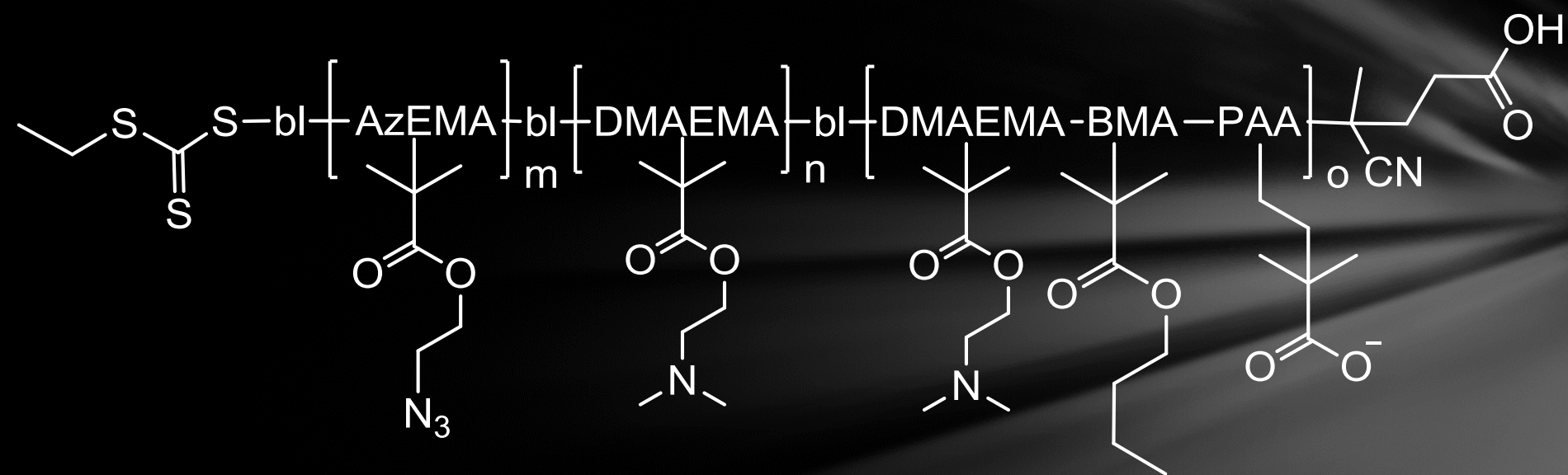
BMA
Hydrophobic
comonomer

S Grainger & MEH El-Sayed. (2010) in **Biologically Responsive Hybrid Biomaterials**, E Jabbari & A Khademhosseini (Eds.): 171-190.
AJ Convertine et al. (2009) **J Controlled Release**.

Attachment of a Polar Polymer to the pH-Responsive Polymer to make Amphiphilic Block Copolymers

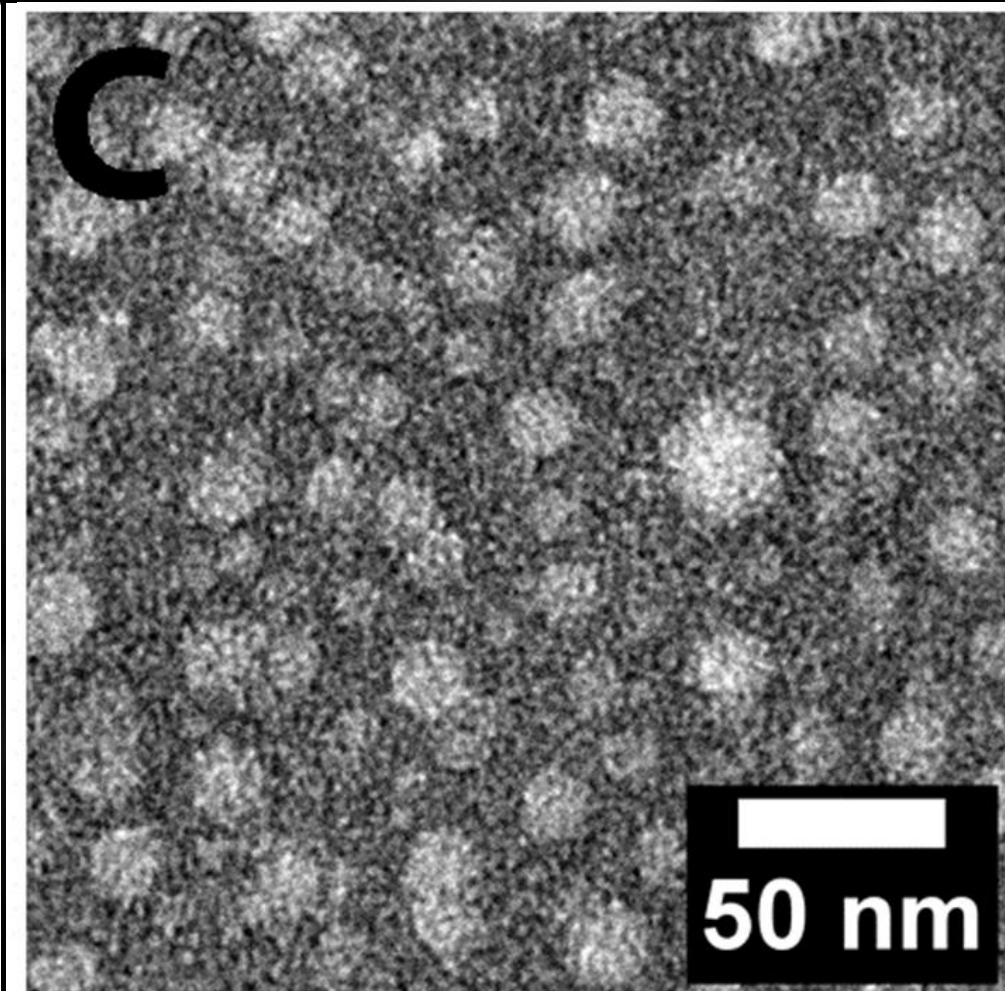
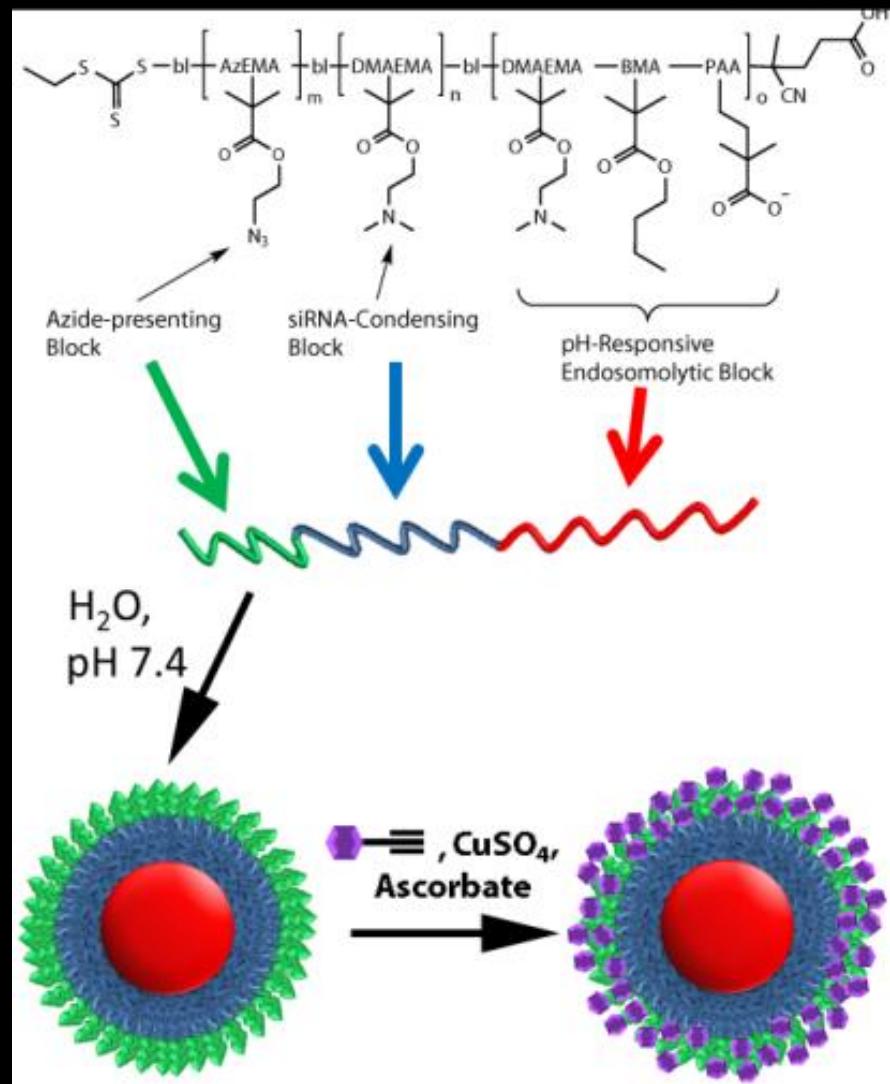


Azide-Containing Block is Added to Enable 'Click' Functionalization

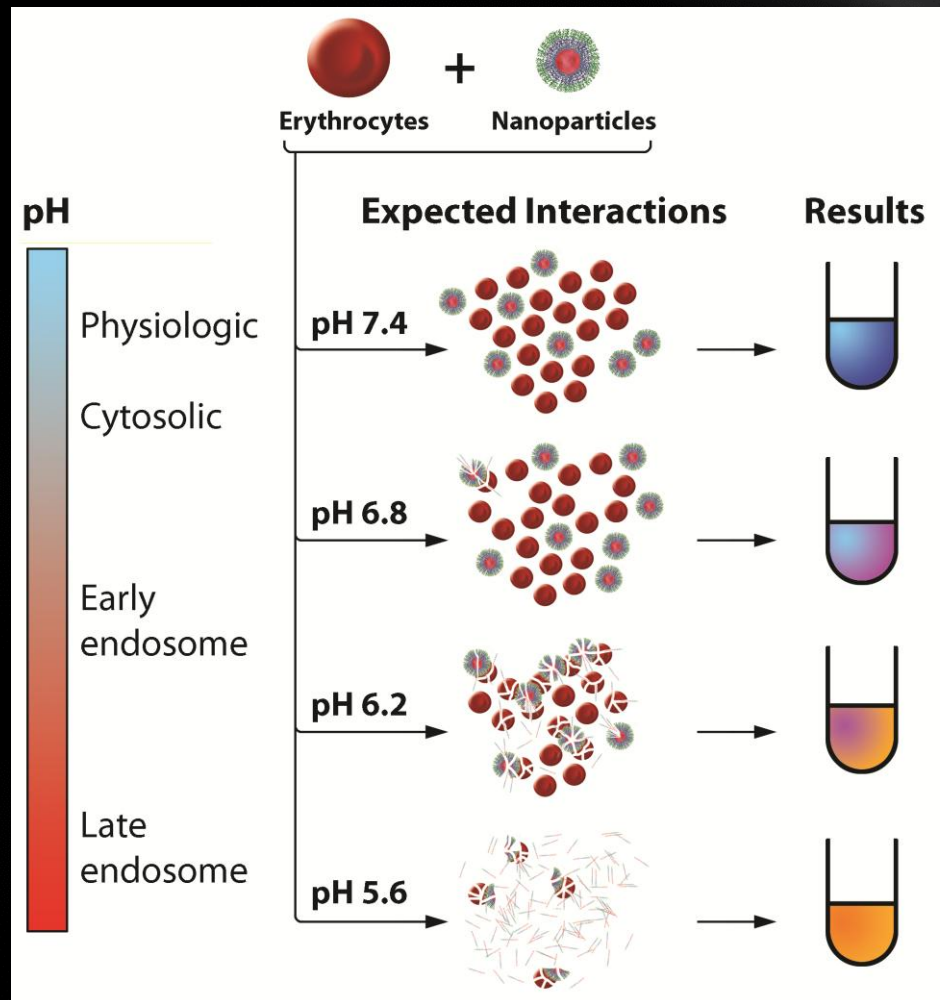


Polymer	dn/dc (mL/g)	Target M _n (Da)	M _n (Da)	M _w (Da)	PDI	D _h (nm)	ζ-Potential (mV)
Terpolymer	0.081	14000	11400	13900	1.22		
Diblock	0.049	21000	16800	20700	1.23	34.2 ± 2.2	+10.8 ± 11.2
Triblock (Before 'click')	---	22000	22300	28900	1.29	28.0 ± 1.5	+19.6 ± 11.7

Schematic of Completed Triblock Polymeric Nanoparticles

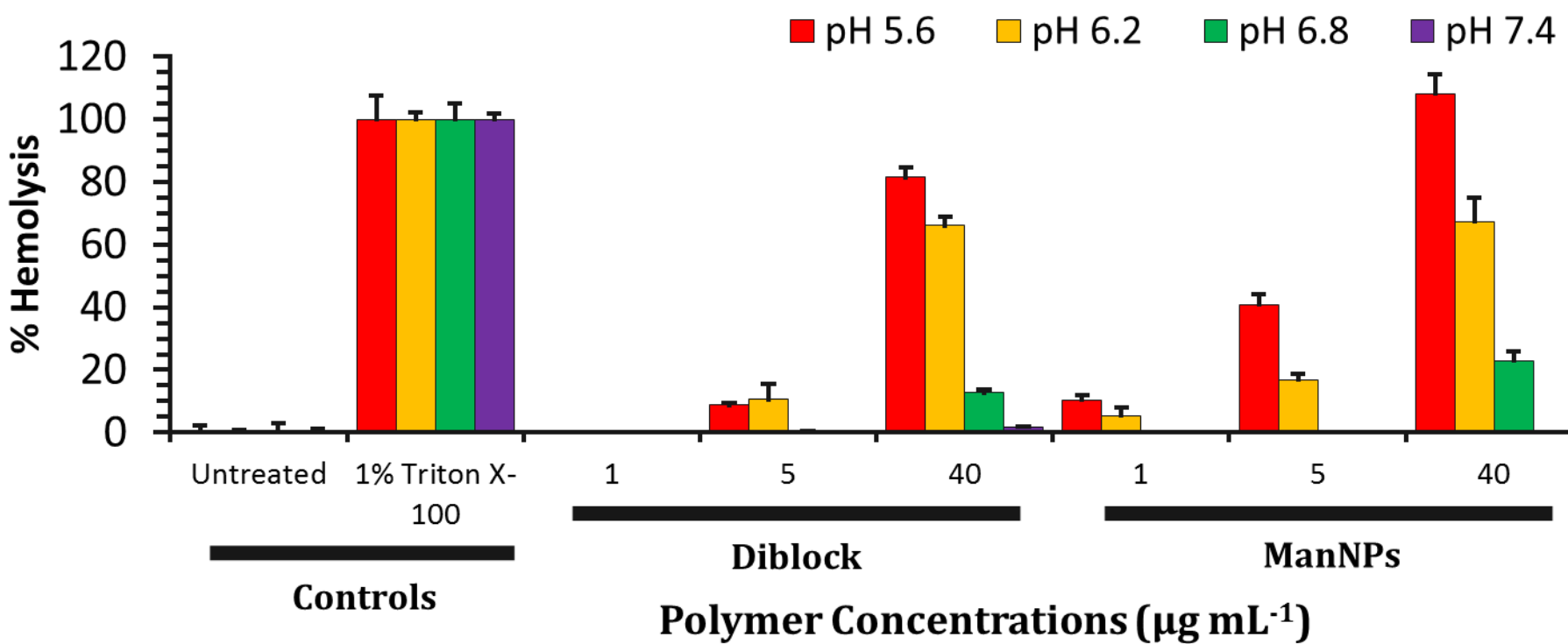


Using the Hemolysis Assay to Model Endosome-Nanoparticle Interactions



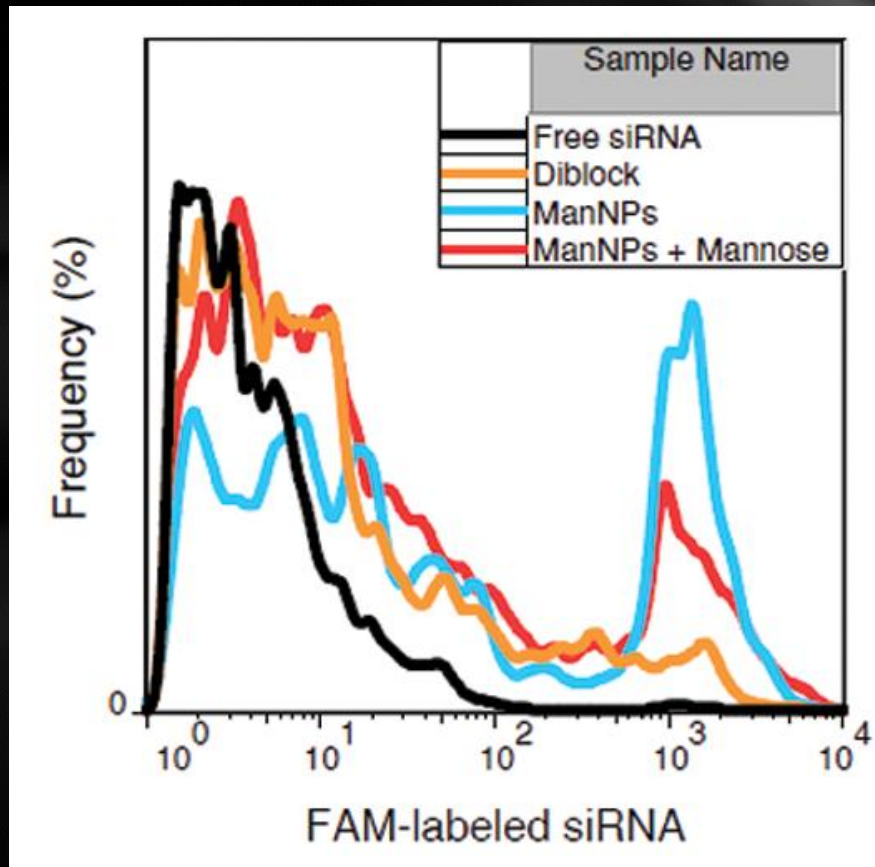
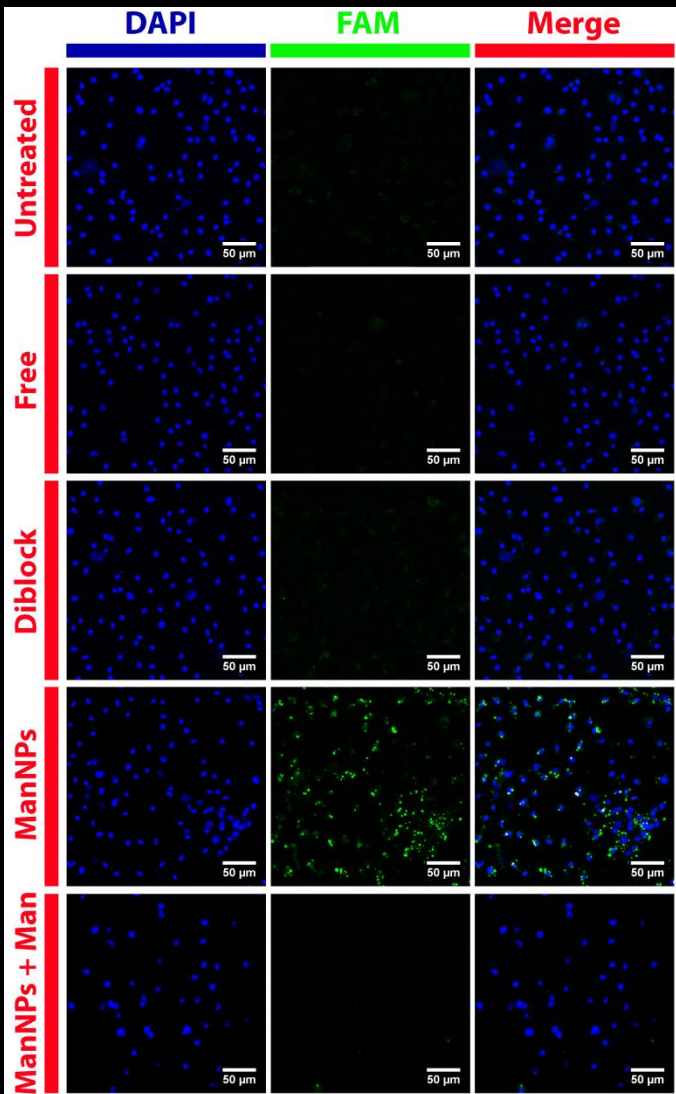
BC Evans, CE Nelson, SS Yu, et al. (2012) *J Visualized Exp.* (in press).

Diblocks and ManNPs Exhibit pH-Responsive Hemolysis



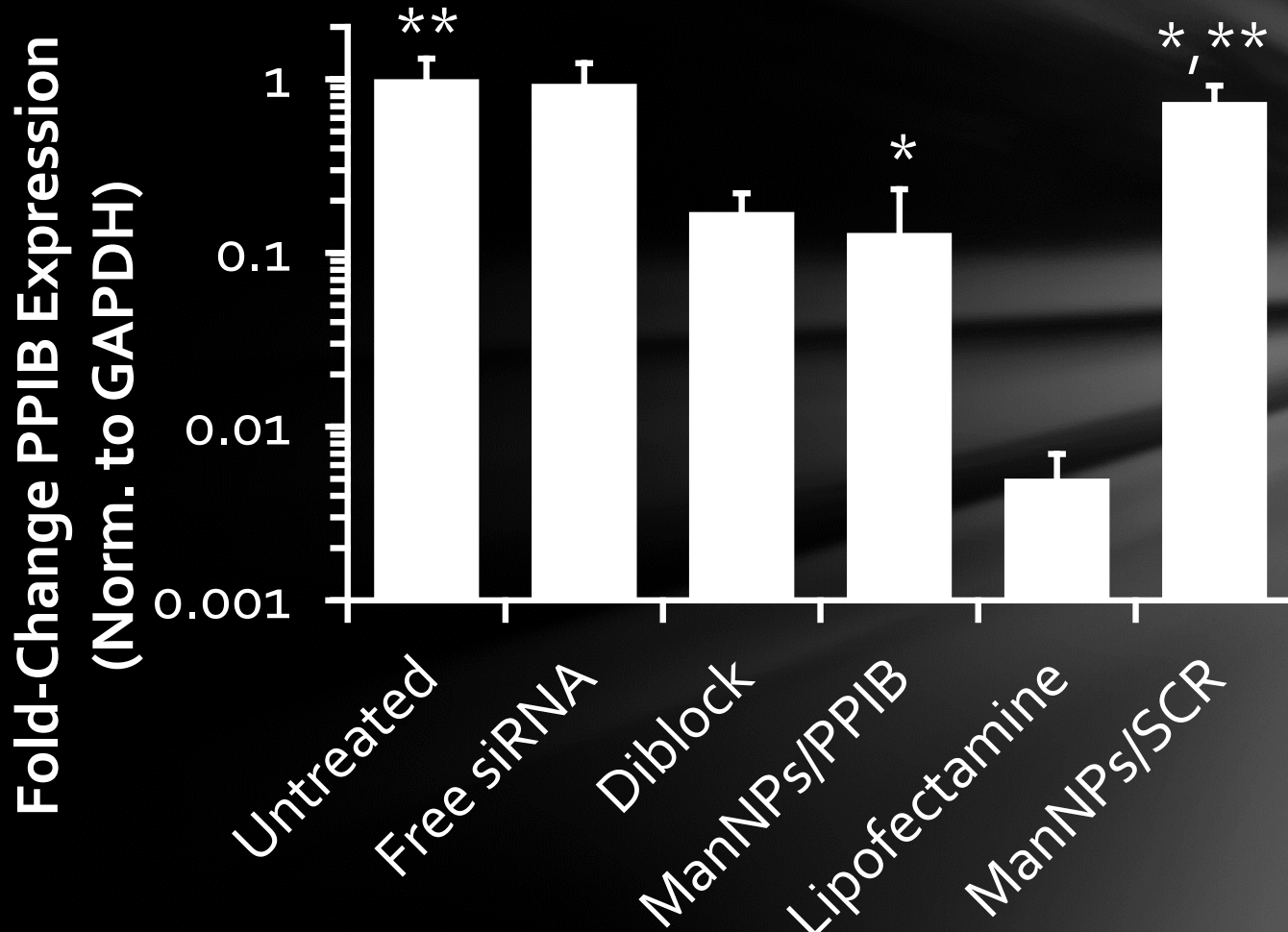
S.S. Yu et al. (2012) *Molecular Pharmaceutics* (Revisions requested).

ManNPs Enhance siRNA Delivery into Primary Macrophages



S.S. Yu et al. (2012) *Molecular Pharmaceutics* (Revisions requested).

siRNA Delivered through ManNPs Retains Ability to Knock Down Target Gene Expression

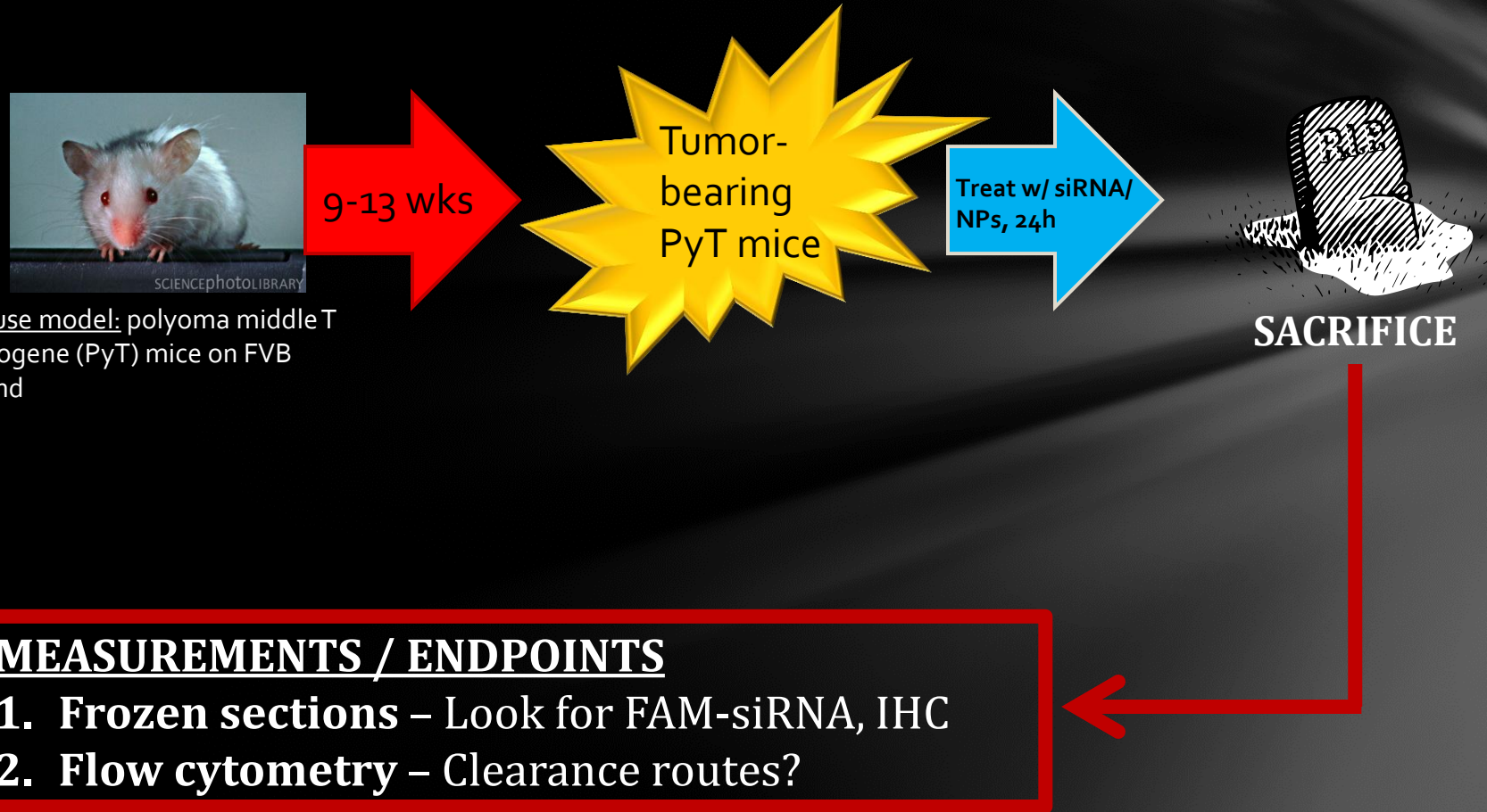


* $p < 0.05$; n = 3

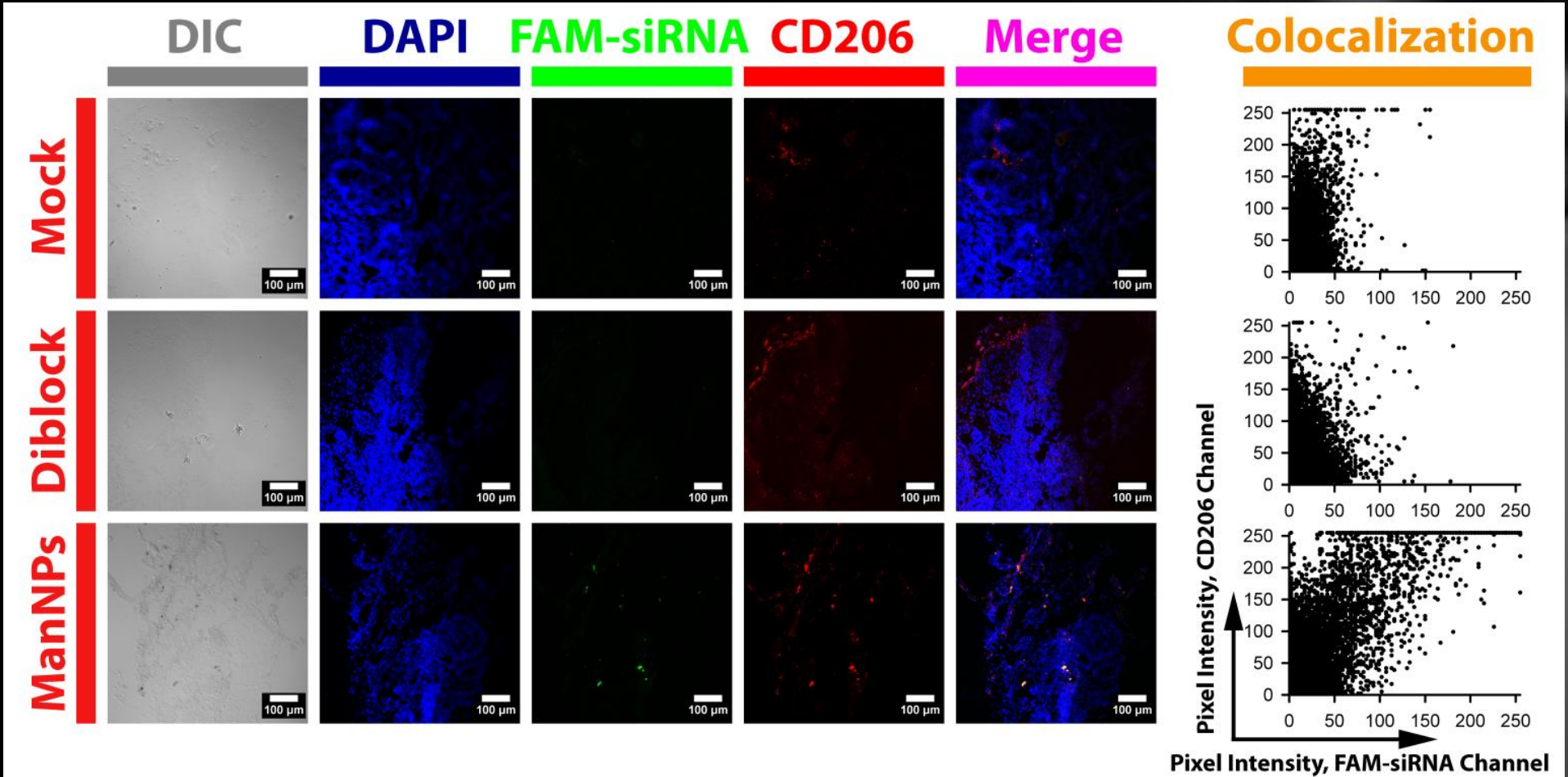
** $p > 0.05$; n = 3

S.S. Yu et al. (2012) *Molecular Pharmaceutics* (Revisions requested).

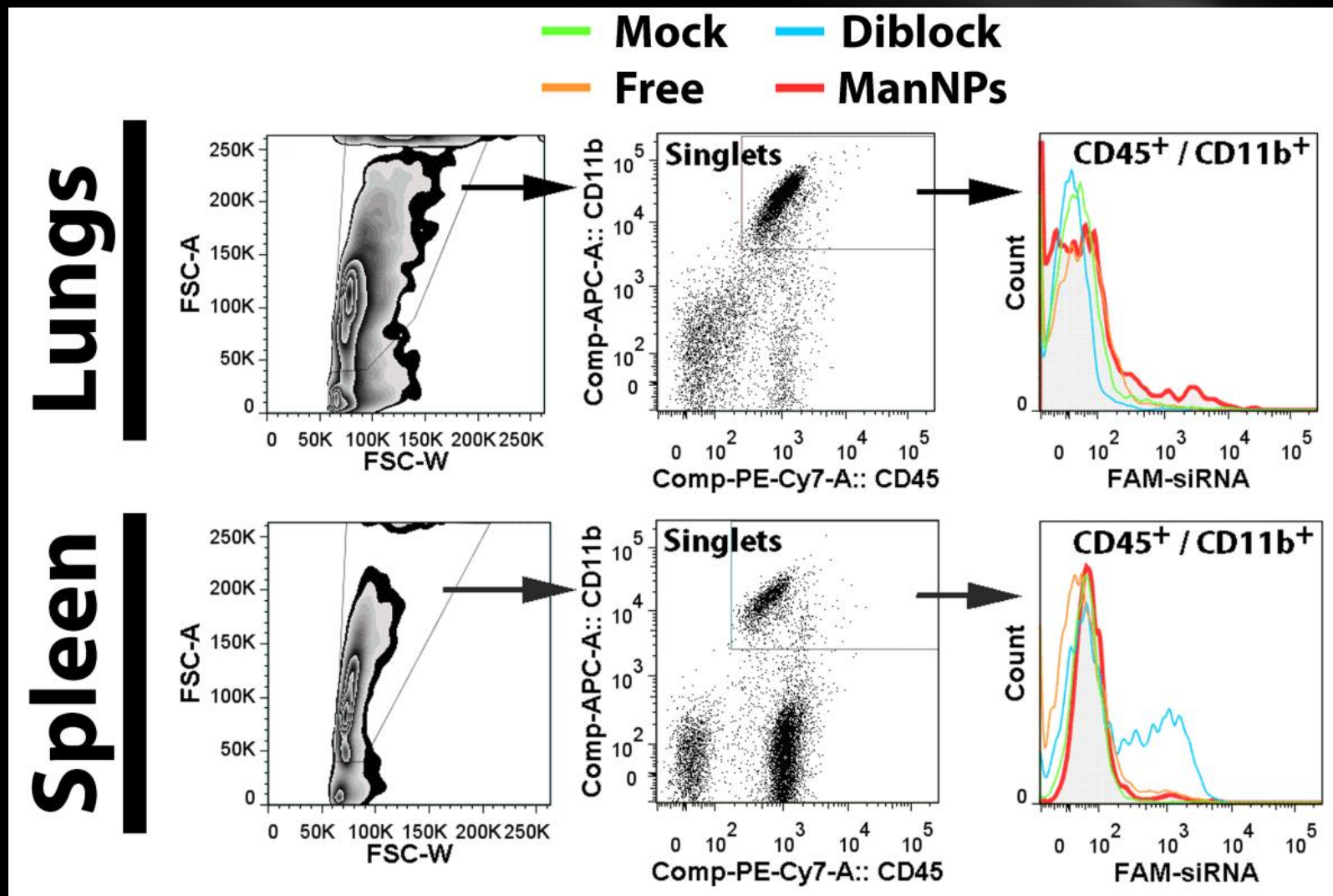
In Vivo Biodistribution of ManNPs in Primary Tumor Model



ManNPs Target CD206⁺ Cells in Primary Tumor Model



Nanoparticles May Also Bind Resident Leukocytes in the Lungs or Spleen



In Vivo Biodistribution of ManNPs in Metastatic Tumor Model



4 wks



Treat w/ siRNA/NPs, 24h



Mouse model: tail vein injection of polyoma cells into FVB mice

MEASUREMENTS / ENDPOINTS

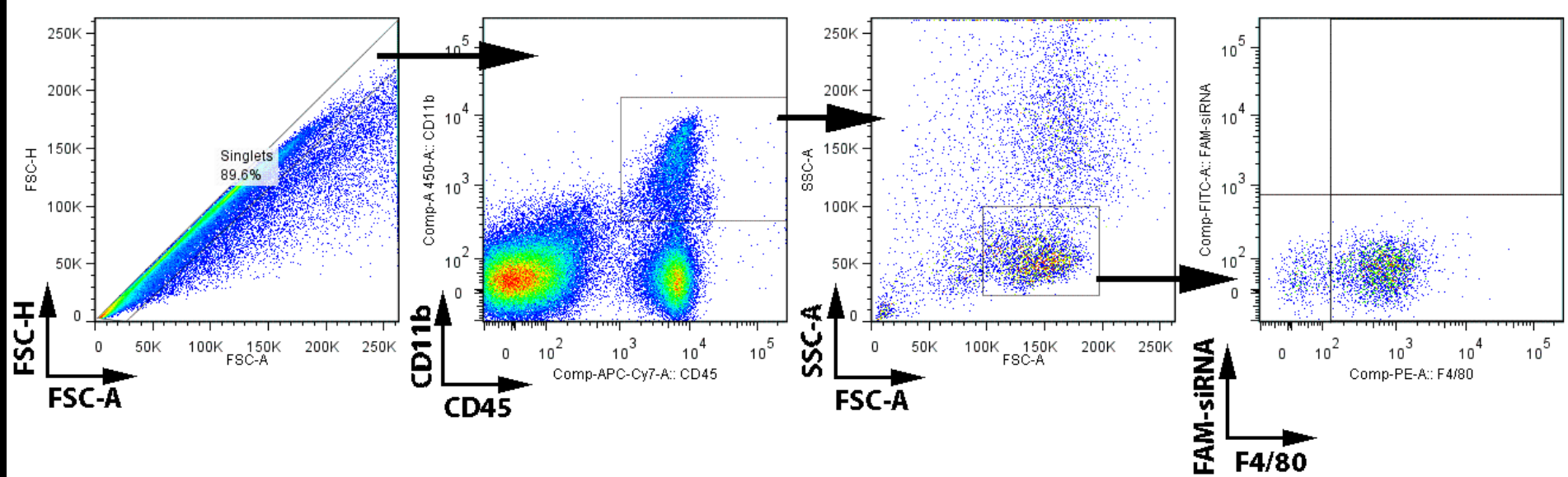
1. Flow cytometry – FAM-siRNA localization?

Formation of Lung Metastases in Tail Vein Injection Model, and Quantification of Macrophages via Flow Cytometry

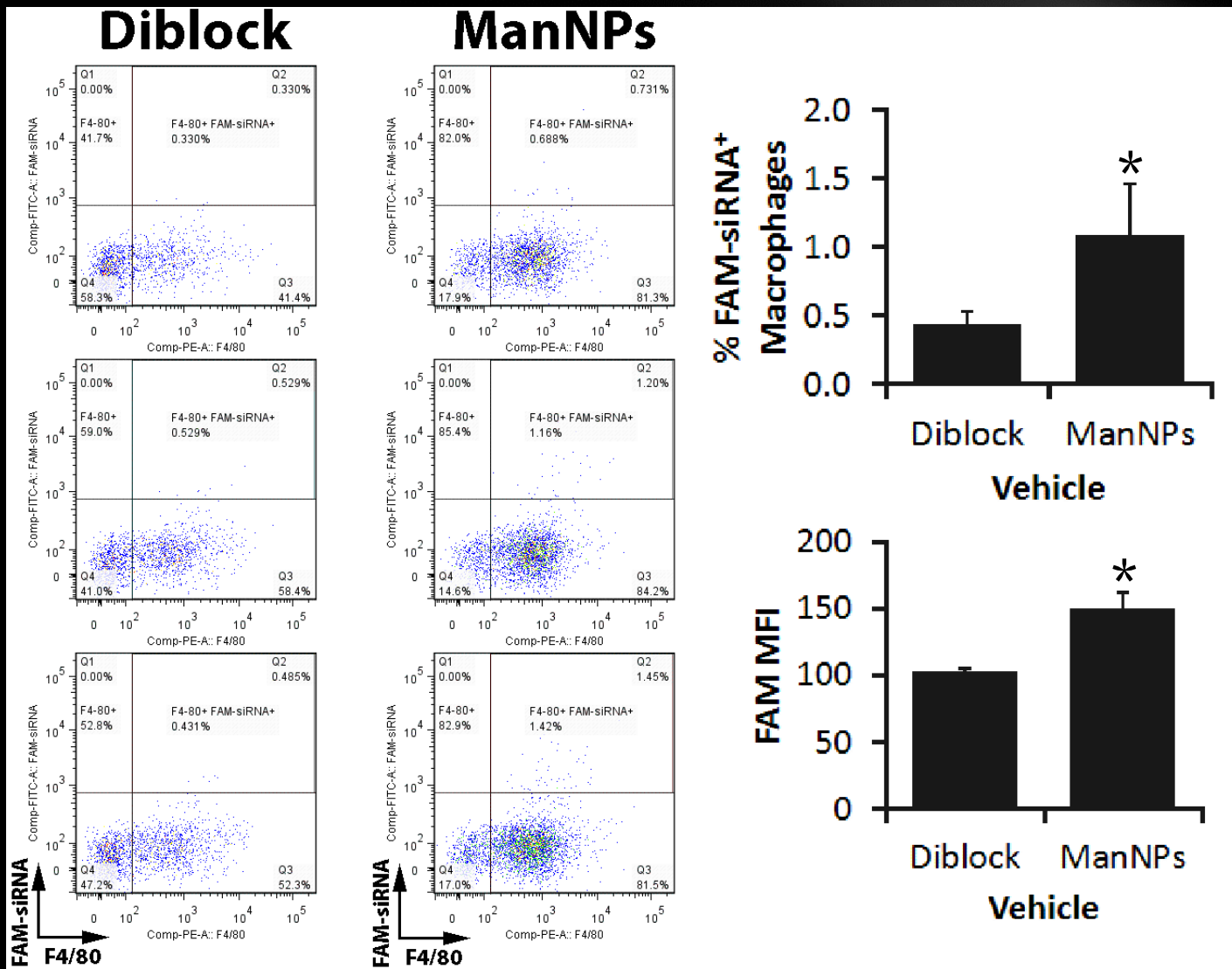


► Lungs inflated w/ Bouin's fixative 2 wks post-injection of polyoma cells.

Flow cytometry gating strategy to identify macrophages in lungs with polyoma metastases.



ManNPs Enhance siRNA Delivery Into Macrophages in Lungs of Mice w/ Overt Lung Metastases

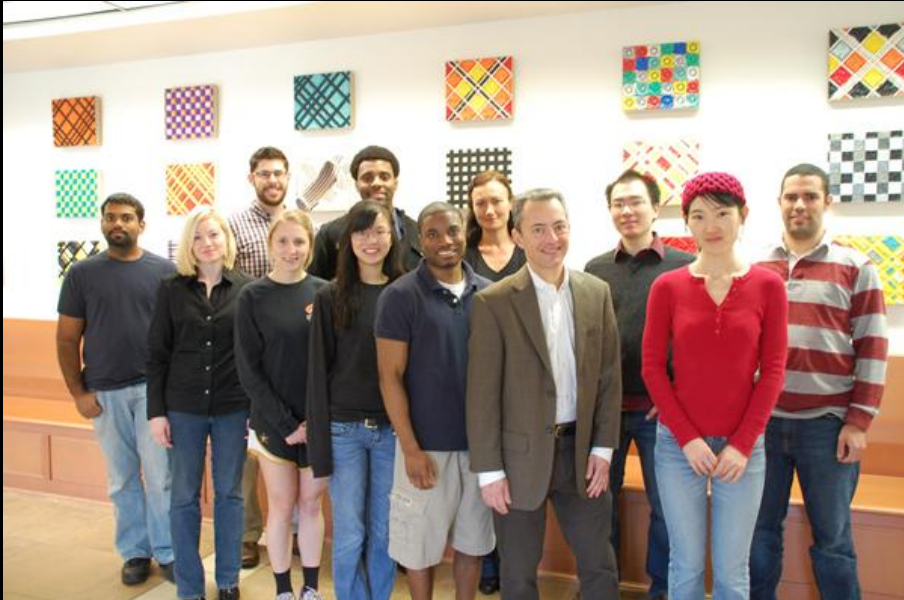


Summary

- Multifunctional triblock copolymers enable systemic targeting of TAMs
 - pH-Responsive behavior enables cytosolic drug delivery
 - Cationic block enables complexation of nucleic acids
 - Azido corona enables attachment of targeting ligands via ‘click’ chemistry
- ManNPs enhance siRNA delivery into primary macrophages *in vitro*
- ManNPs co-localize with CD206⁺ cells in PyMT mice



Acknowledgments



MY PhD COMMITTEE

- Todd Giorgio
- Hak-Joon Sung
- Craig Duvall
- Fiona Yull
- David Harrison

FUNDING SOURCES

- Department of Defense
- Vanderbilt University
- NIH Cancer Center Grant

COLLABORATORS

- Rinat Zaynagetdinov (VUMC)
- Kwangho Kim (VUMC)
- David Bader (VUMC)

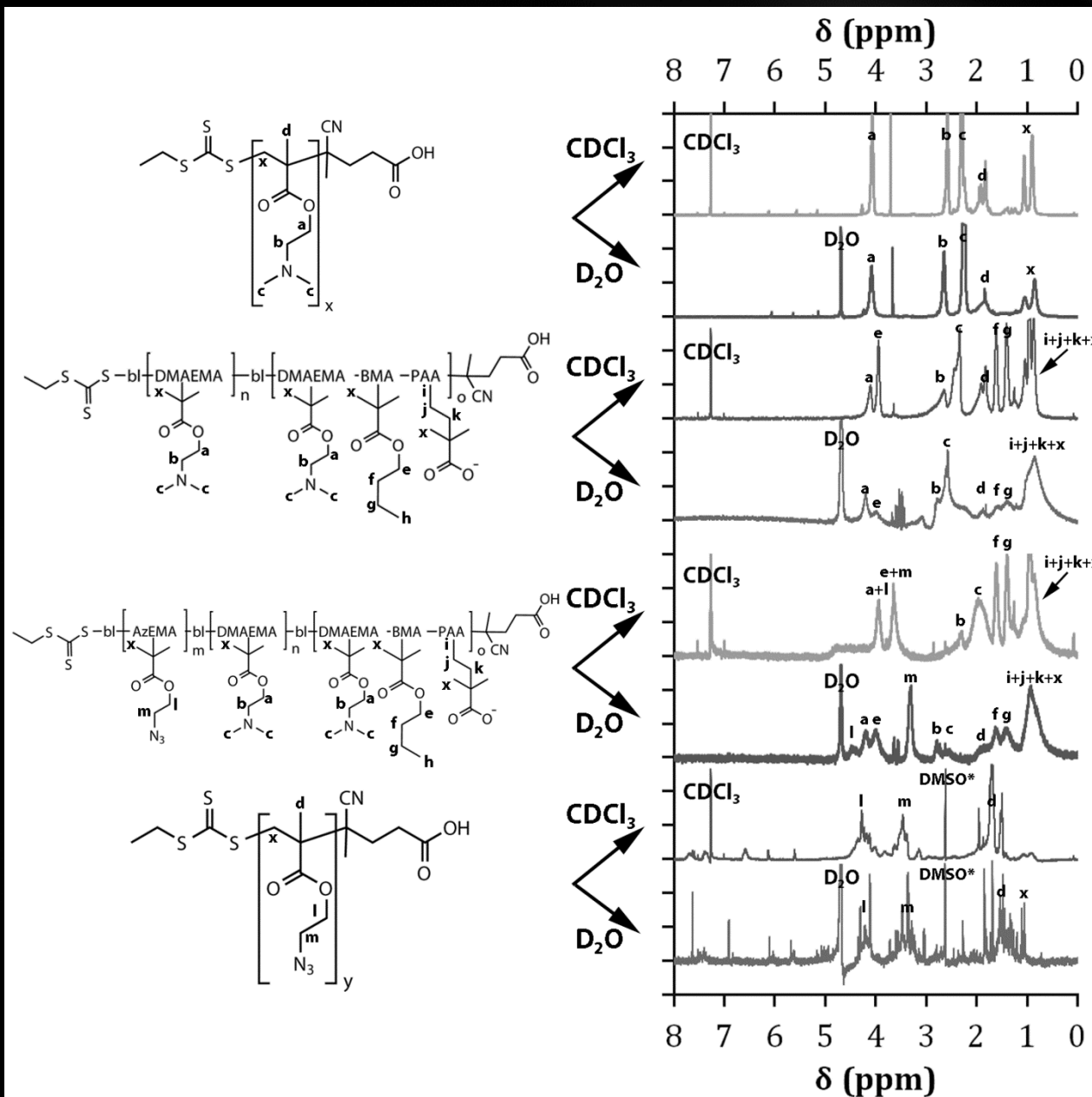
Highlighting Related Work from our Group @ BMES 2012

- P-Fri-A-248 – S.S. Yu et al. See you there if you have any additional questions I am unable to address today!
- P-Th-B-107 – R.A. Ortega, B. Kumar, S.S. Yu, & T.D. Giorgio. More information on what we're therapeutically targeting in TAMs!
- OP-Sat-2-6 – C.L. Duvall, C.E. Nelson, H. Li, S.S. Yu, J.M. Davidson, S.A. Guelcher, & T.D. Giorgio. Overview of our group's local & siRNA delivery technologies!

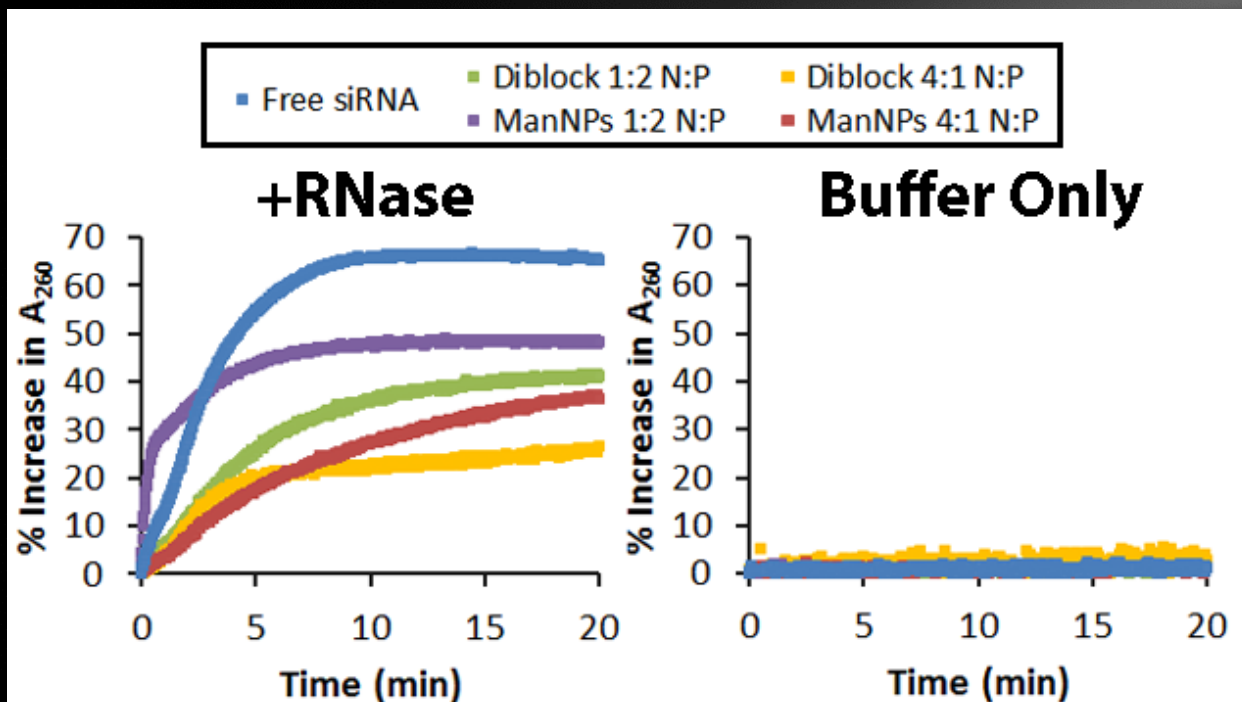
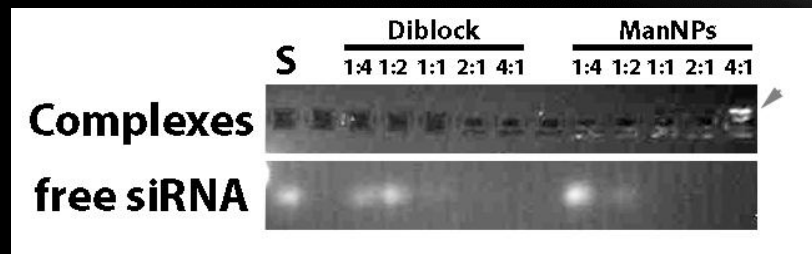
Please pick up a copy of our BMES Presentation Guide from our booth! We have 14 platforms and 34 posters!

Supplementary Slides

NMR Characterization of Polymers

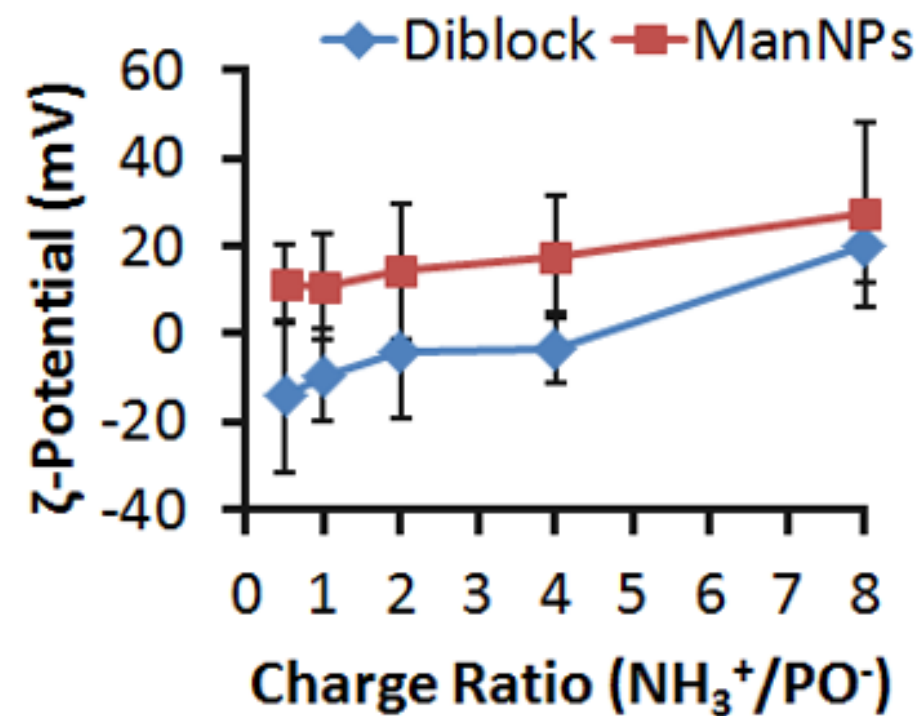
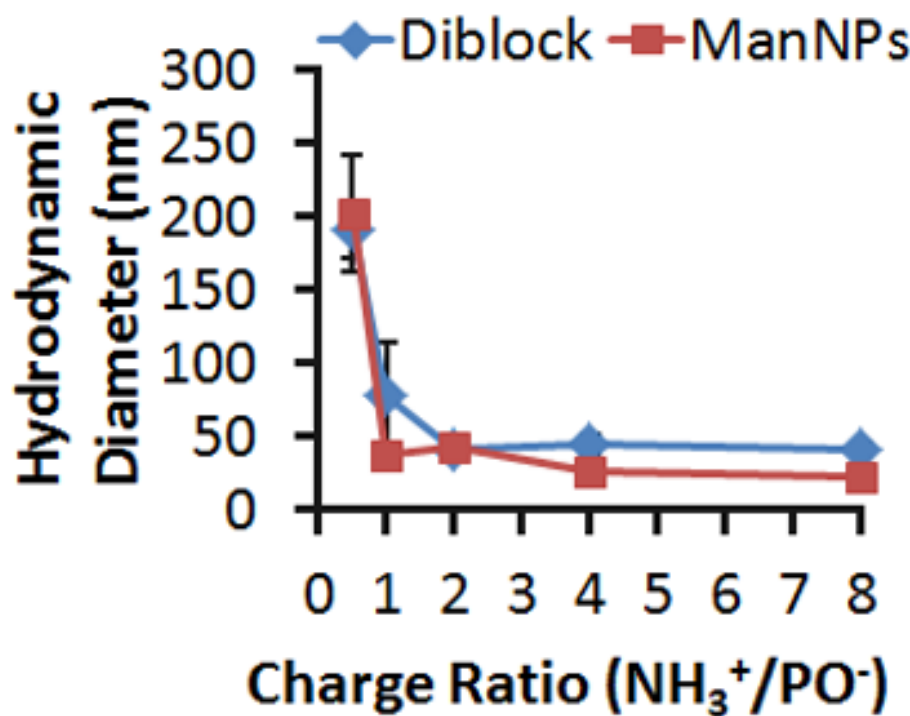


ManNPs Electrostatically Complex siRNA and Protect it from RNases

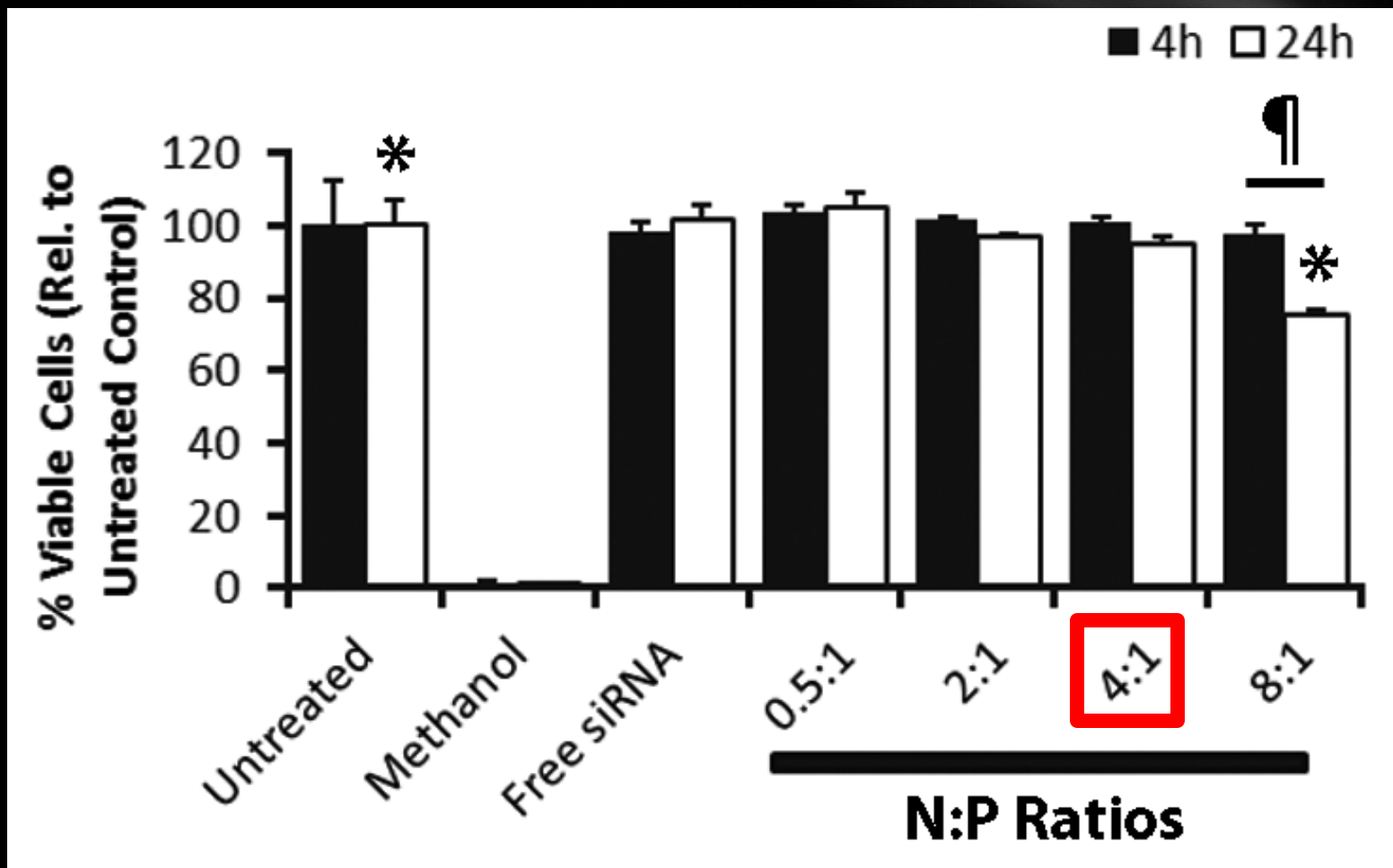


S.S. Yu et al. (2012) *Molecular Pharmaceutics* (Revisions requested).

NP Size and ζ -Potential After Loading w/ siRNA



siRNA-Loaded ManNPs Exhibit Low Cytotoxicity at N:P < 8:1

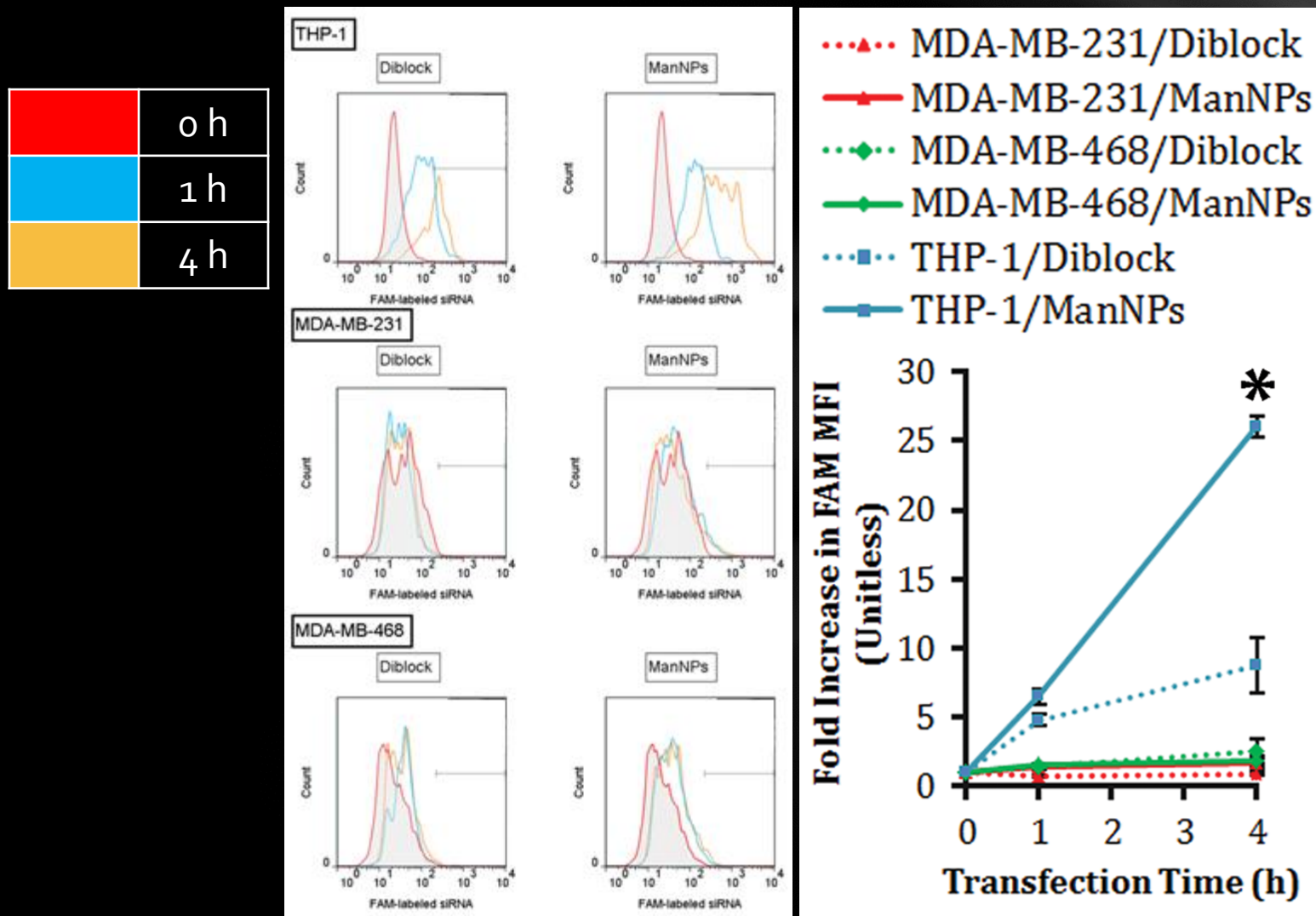


Cell model = THP-1 (immortalized human macrophages); *, ¶ p < 0.01 / n = 3

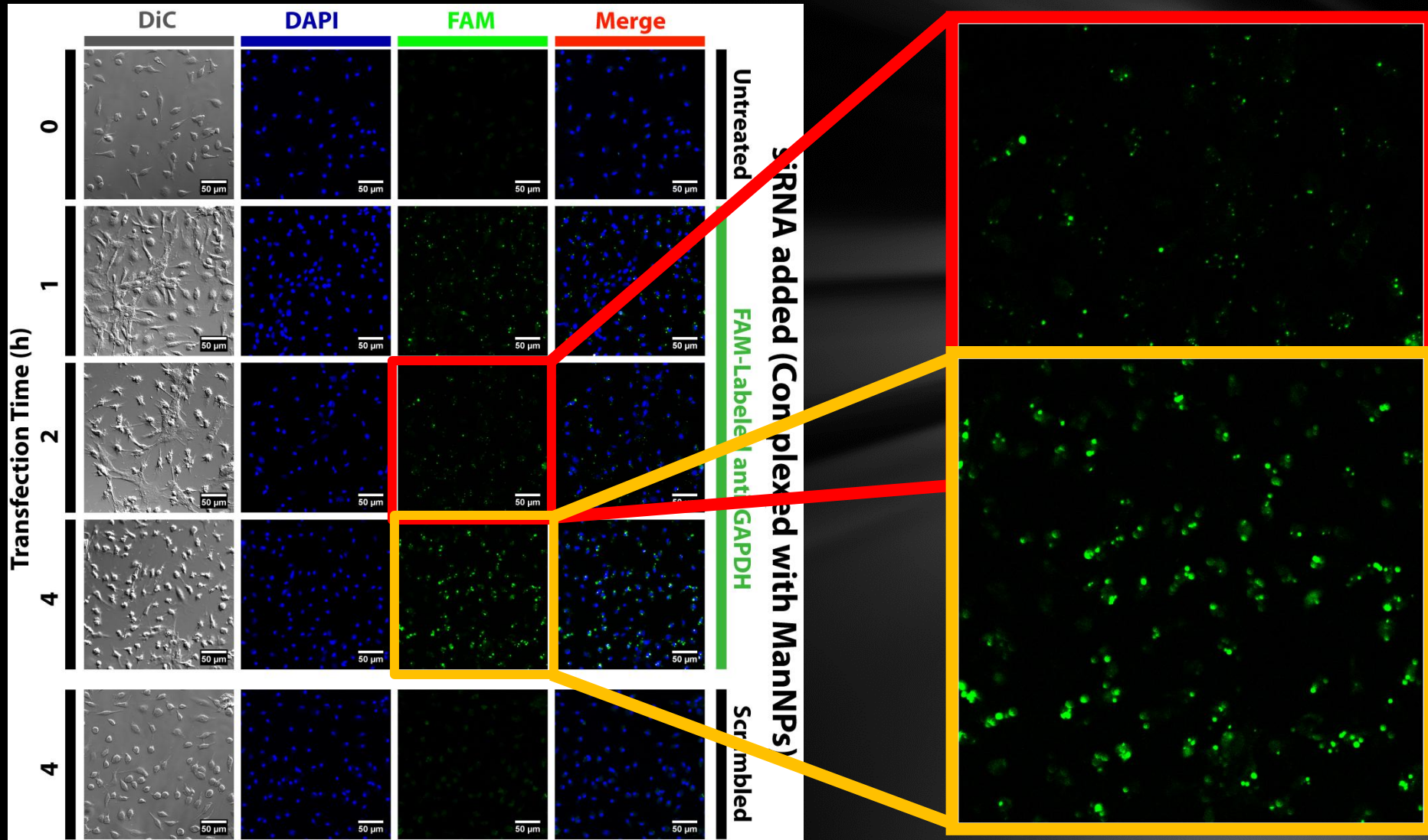
siRNA dose = 50 nM

S.S. Yu et al. (2012) *Molecular Pharmaceutics* (Revisions requested).

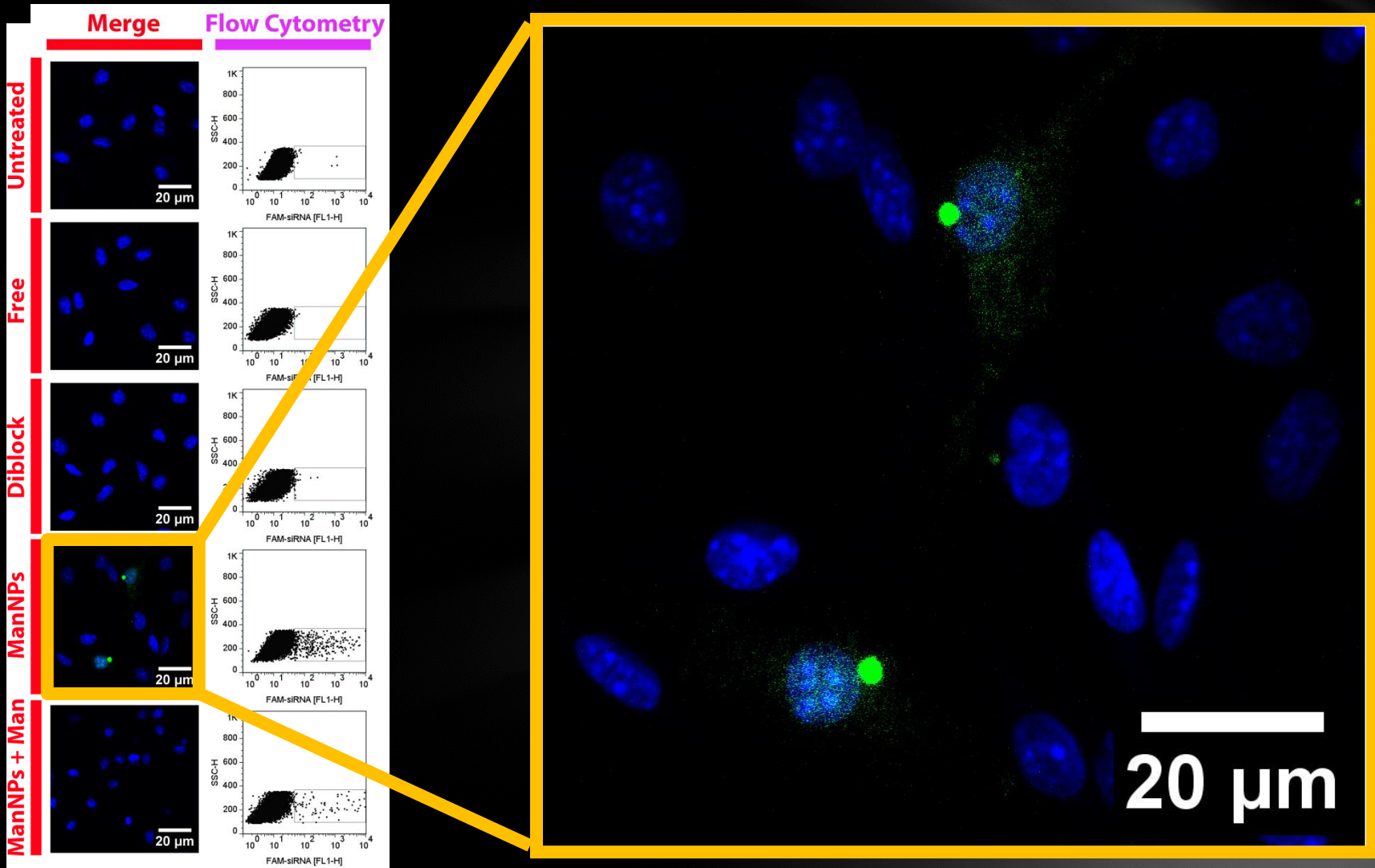
ManNPs Enhance siRNA Delivery into Immortalized Macrophages



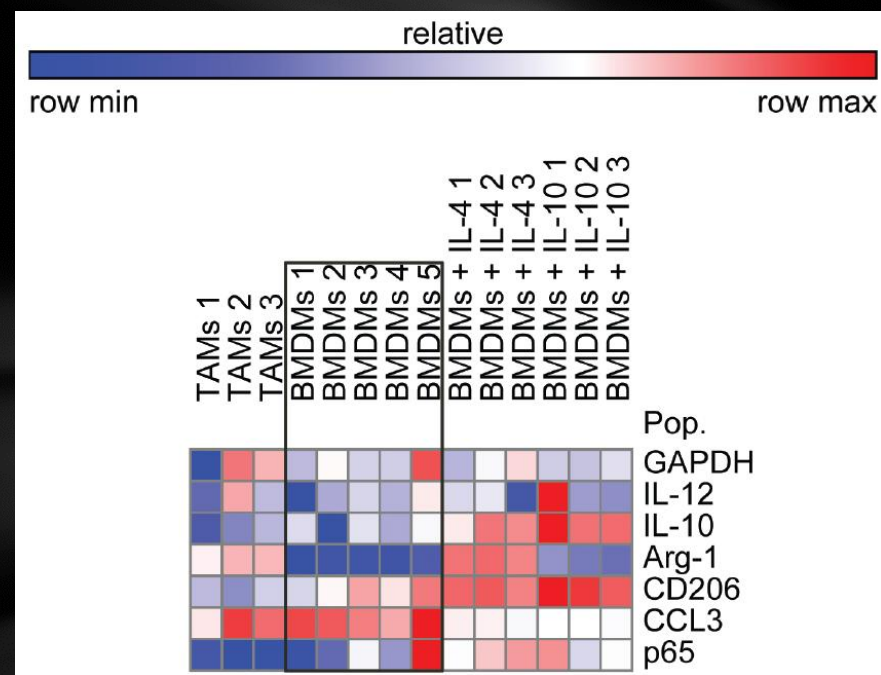
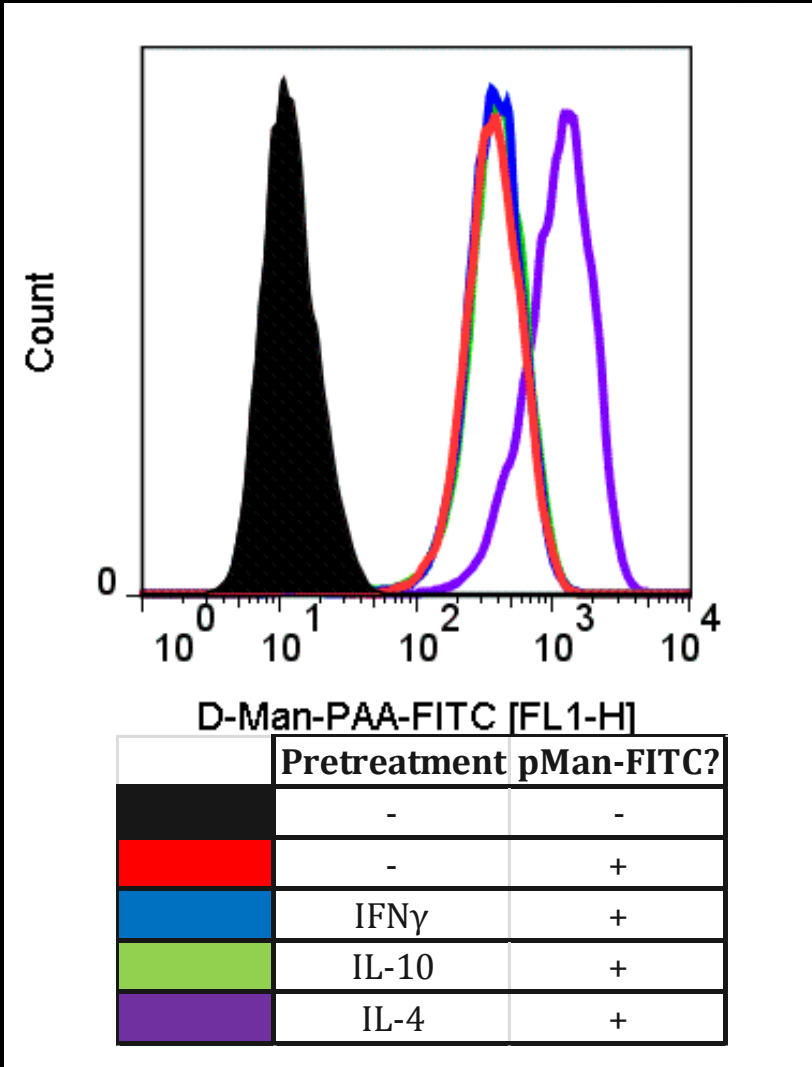
Kinetics of Primary Macrophage Transfection Imaged by Confocal Microscopy



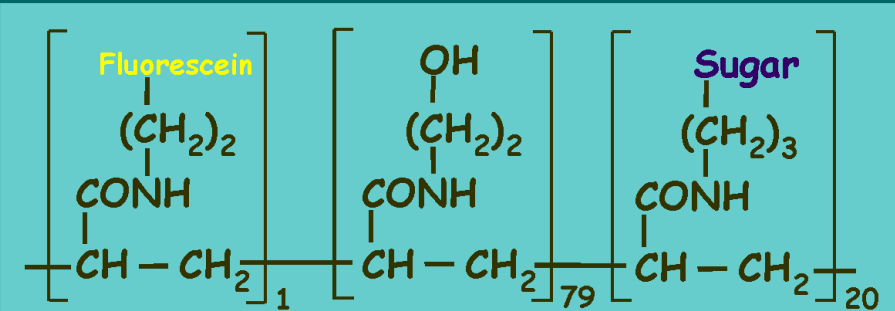
ManNPs Enhance siRNA Delivery Into Primary Macrophages



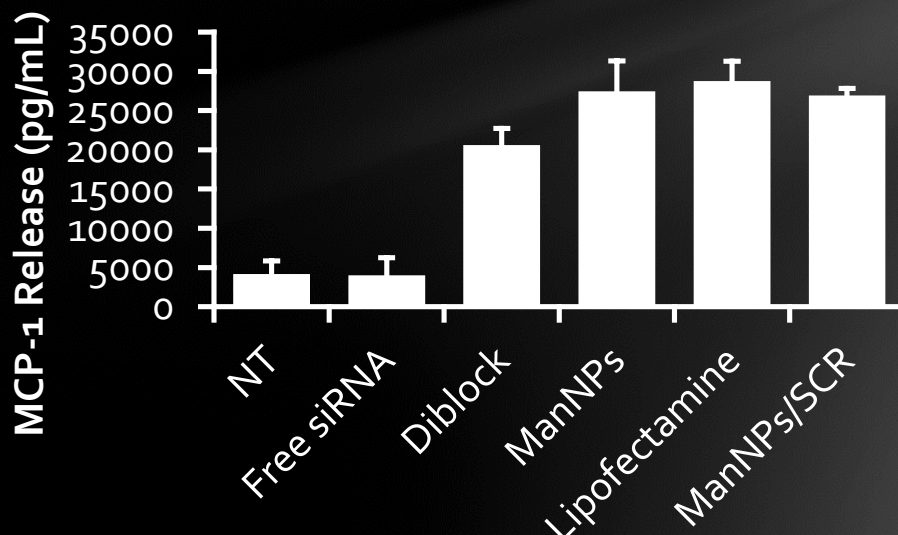
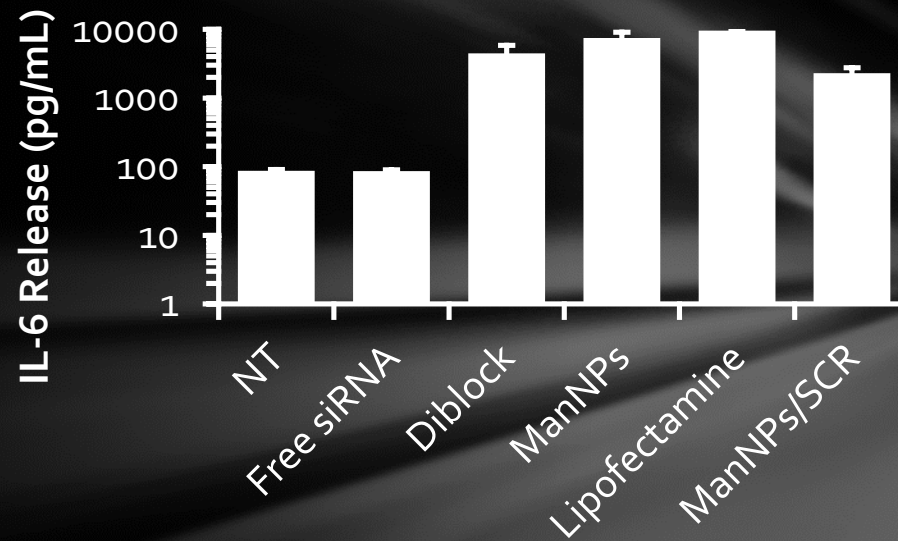
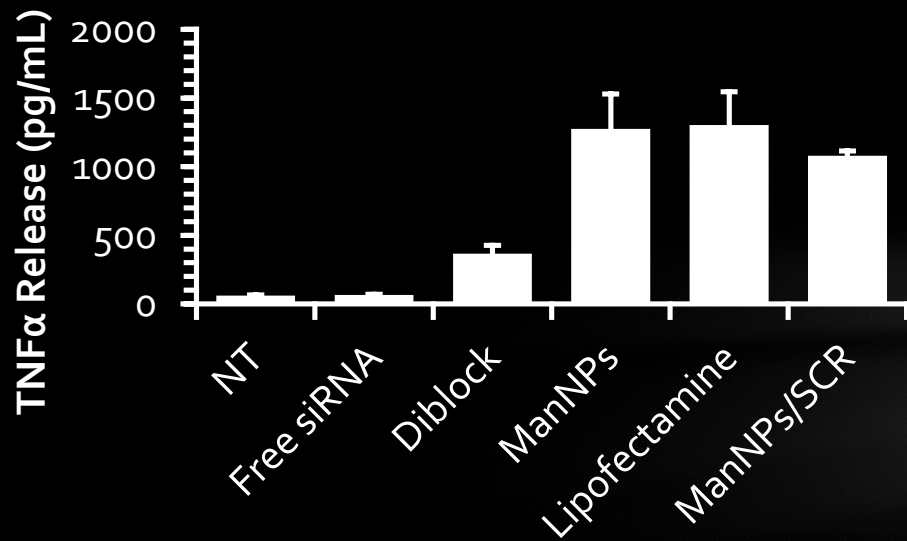
Mannose Receptor Activity vs. Phenotype?



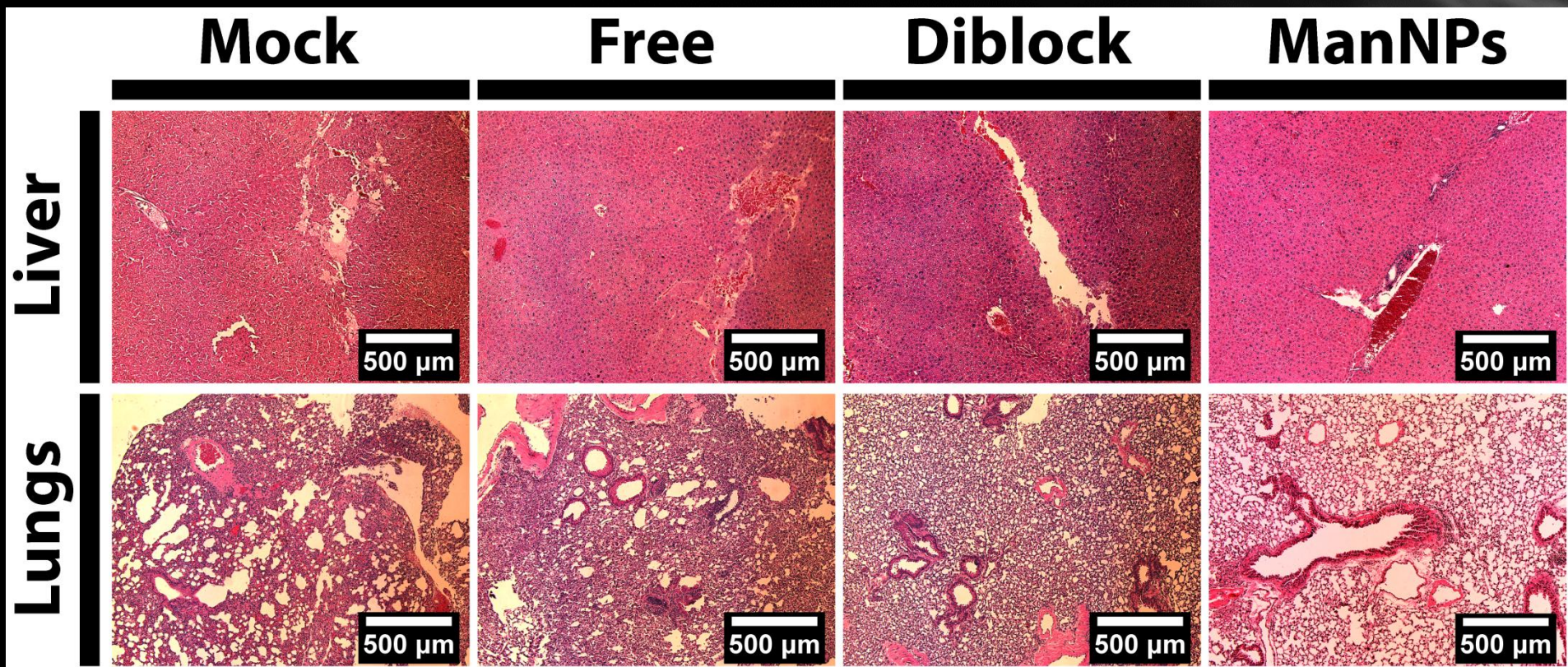
Manufacturer-provided chemical structure of pMan-FITC (Glycotech).



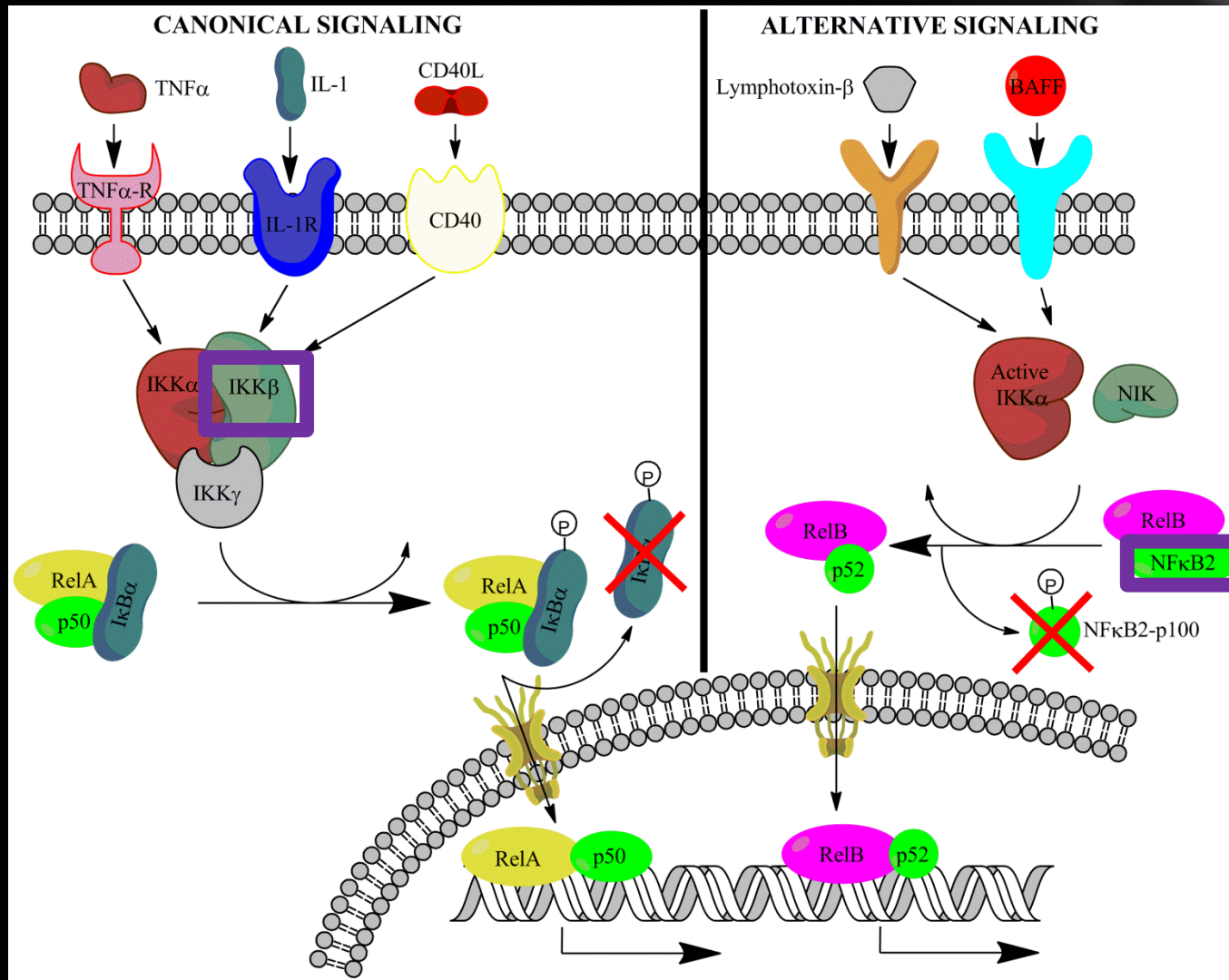
ManNPs Inherently Trigger Pro-Inflammatory Response?



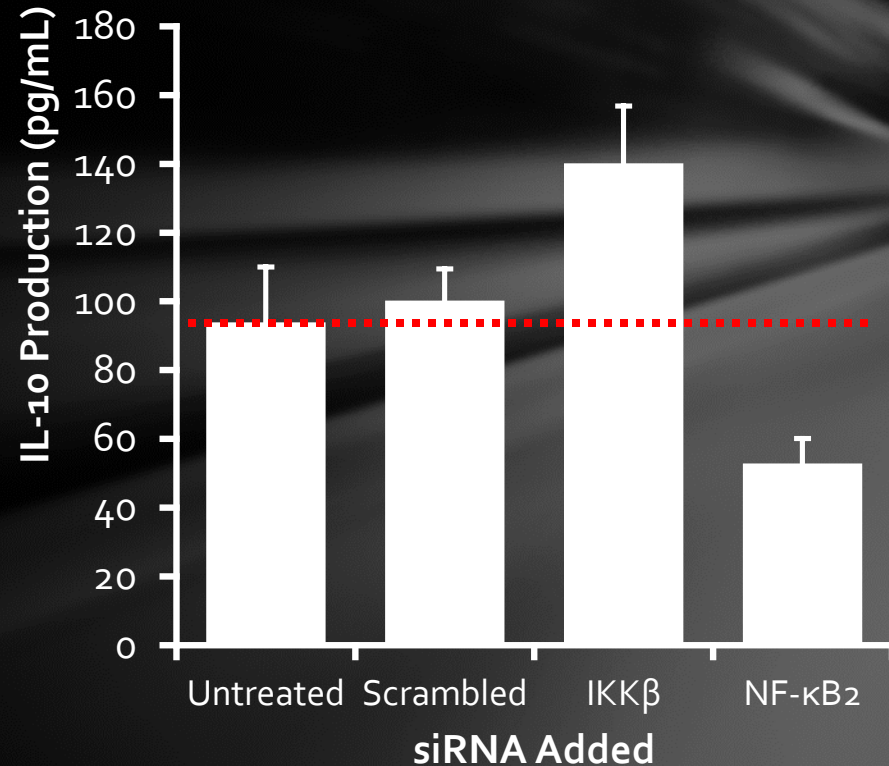
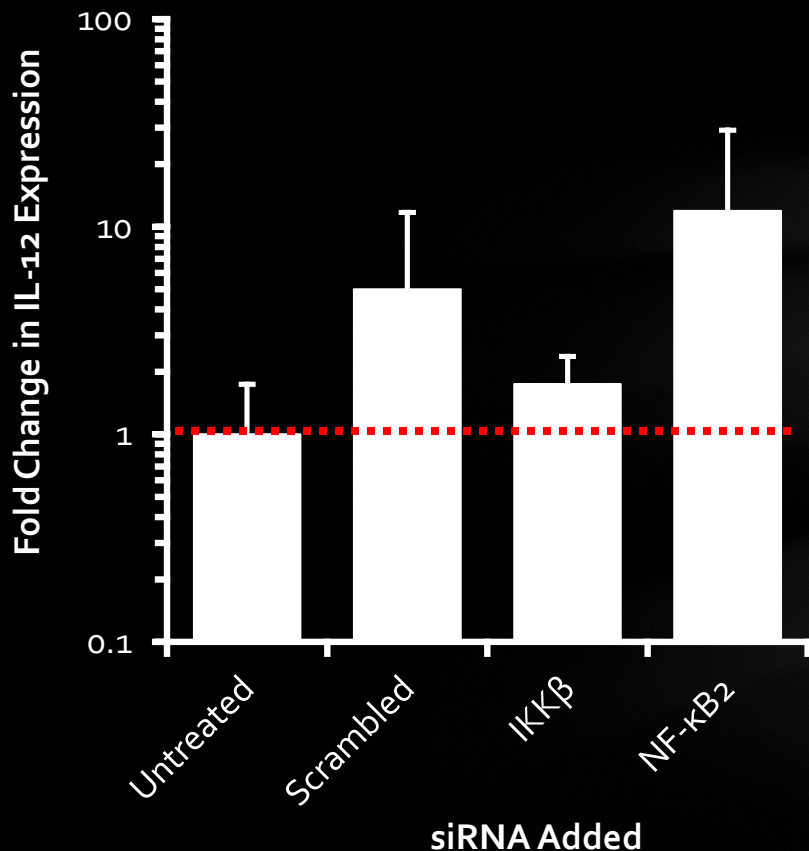
No Significant Changes in Lungs / Liver Morphology within 24 h



Next Steps: What's the Therapeutic Target?



siRNA-Mediated Silencing of NF-κB Family Proteins and BMDM Polarization



Introduction: Macrophages have been proposed as a drug target in breast cancer because they are potent effectors of the immune system, demonstrating the ability to secrete a wide range of pro-inflammatory cytokines and growth factors. The NF- κ B pathways are major controlling factors of macrophage phenotype, consisting of multiple nuclear transcription factor protein dimmers. Aberrant NF- κ B signaling in tumor associated macrophages (TAMs) has been implicated in tumorigenesis. We have developed a polymeric nanoparticle to act as a targeted therapeutic delivery device to treat TAMs by knocking down the production of key proteins in the NF- κ B pathways using small interfering RNA (siRNA). Current delivery of siRNA therapeutics to macrophages generally entails purchasing a commercially available transfection agent and developing an optimized protocol for transfection. The cells of interest for this work, macrophages, are traditionally difficult to transfect effectively. Therefore, the specific objectives of this work is to validate our chosen therapeutic targets, show that the nanoparticle platform developed by our group and our collaborators to deliver siRNA is effective, and show that it is capable of altering macrophage phenotype by knocking down activation of the NF- κ B pathways.

Materials and Methods: Bone marrow cells were isolated from NGL reporter mice on an FVB background. NGL reporter mice have been genetically modified to produce luciferase and green fluorescent protein upon NF- κ B pathway activation. The bone marrow, harvested from the murine femurs, was transformed into bone marrow derived macrophages (BMDMs) using a source of colony stimulating factor-1. BMDMs have been shown to phenotypically mimic TAMs with regards to morphology and cellular products. The cells were transfected with siRNA targeting key proteins in the NF- κ B pathways using a commercial transfection agent (HiPerFect), untargeted nanoparticles, and the targeted nanoparticles. The nanoparticles used consisted of a pH-responsive, endosomolytic core, an siRNA condensing region, and an optional targeting moiety consisting of a mannose chain targeted to the mannose receptor, unique to macrophages. The BMDMs were stimulated with tumor necrotic factor- α (TNF- α) to create model of tumoral presence near the stromal macrophages. After stimulation, the cells were frozen in a luciferase assay lysis buffer and analyzed for NF- κ B pathway activation via luciferase assay. Real time PCR was also performed to analyze levels of cellular RNA as descriptors of macrophage phenotype.

Results and Discussion: Our nanoparticle transfection agent is comparable to commercial agents for transfection efficiency with the added effect of macrophage specific targeting. Initial transfections with commercial agents proved largely ineffective at knocking down NF- κ B activation, showing only a 5-10 % decrease, on average, in pathway activation when a key regulatory protein in the pathways, IKK β , was targeted. PCR revealed that this protein, predicted by literature and our group to be an efficacious target, was in fact a poor target due to an unforeseen lack of upregulation during pathway activation. Other proteins in the pathway, for example the p100/p52 protein (aka: NF- κ B2), are upregulated and are a more efficacious target (Figure 1).

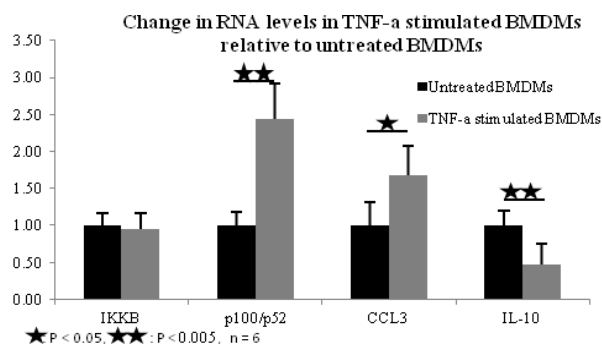


Figure 1: Activation of the NF- κ B pathways using TNF- α showed an increase in p100/p52 but not IKK β . This is corroborated by transfection experiments showing ineffective pathway knockdown with IKK protein targeting and more effective knockdown with NF- κ B protein targeting. Activation was confirmed by the increased presence of inflammatory cytokines such as CCL3 and the decrease in inhibitory cytokine IL-10.

Conclusion: The transcription factors NF- κ B1 and NF- κ B2 are better therapeutic targets for TAM phenotype modulation than initial targets, IKK family proteins, using siRNA. Our targeted nanoparticle transfection agent performed comparably to commercial agents with the added effect of specific targeting.



Targeted Knockdown of NF-κB in Tumor Associated Macrophages

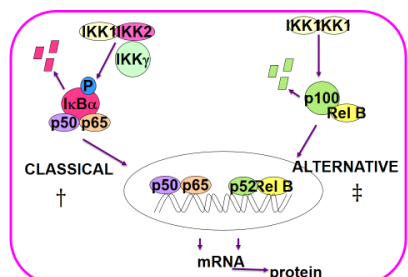
Ryan A. Ortega^{1,2}, Bharat Kumar¹, Shann S. Yu¹, Todd D. Giorgio^{1,2}

¹Department of Biomedical Engineering, Vanderbilt University, Nashville, TN

²Department of Cancer Biology, Vanderbilt University Medical Center, Nashville TN

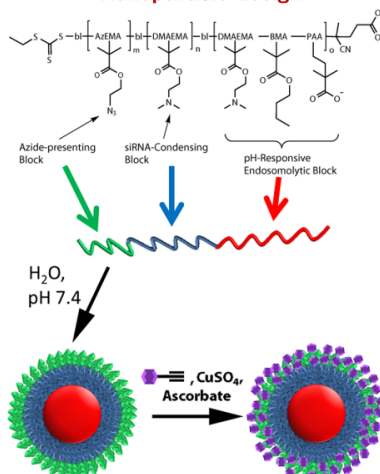
Tumor associated macrophages (TAMs) are a promising therapeutic target for cancer treatment

- Problem: Tumor cells are able to influence TAMs to create a pro-tumor environment around the primary tumor and at potential metastatic sites.
- TAMs can change the local cytokine and growth factor profile, alter the recruitment of other cells, and participate in tissue remodeling.
- The NF-κB pathway is a controller of macrophage behavior and has been implicated in contributing to the TAM phenotype.



- Solution: Develop a biocompatible, targeted nanoparticle to deliver siRNA and/or other therapeutics to macrophages with the intent of modulating NF-κB.

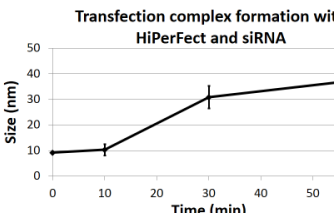
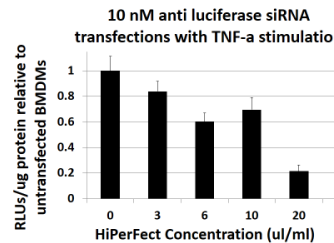
Nanoparticle design



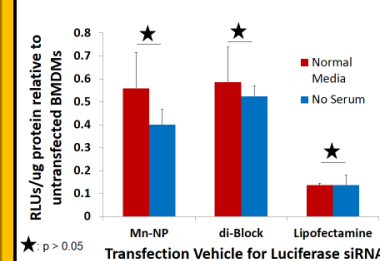
In vitro bone marrow derived macrophage (BMDMs) culturing and transfection

- Bone marrow was harvested from the femurs of NGL reporter mice on an FVB background.
- NGL mice express luciferase as a reporter of total NF-κB activity.
- Bone marrow is cultured in media containing a supplemental source of M-CSF for 6 days.
- After plating, BMDMs are transfected with siRNA (10 nM) using the commercial agents HiPerFect (20 μ l/ml) or Lipofectamine (1.6 μ l/ml), or using nanoparticles (4 μ g/ml).
- After 6 hours of transfection, BMDMs were stimulated with TNF-α to elicit NF-κB activation.
- After 6 hours of stimulation, BMDMs were frozen in a lysis buffer and analyzed for luciferase activity normalized to the total protein per sample.

Optimization of HiPerFect transfection protocol

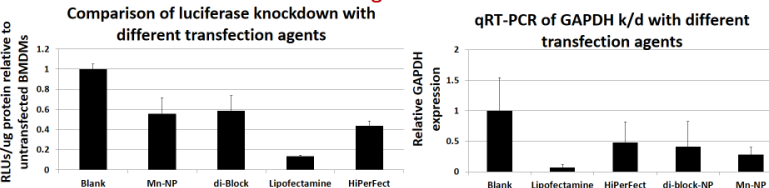


The presence of serum does not significantly effect the transfection ability of nanoparticles or commercial agents



- Transfection complexes are formed in low volume, serum-free solutions for 1 hour, then used for transfection.

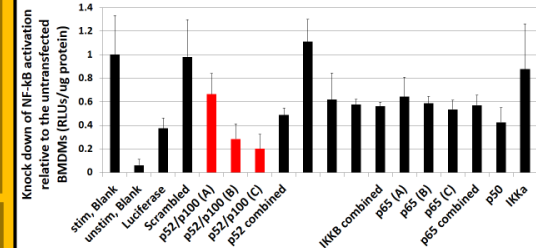
Nanoparticles show transfection activity comparable to commercial transfection agents



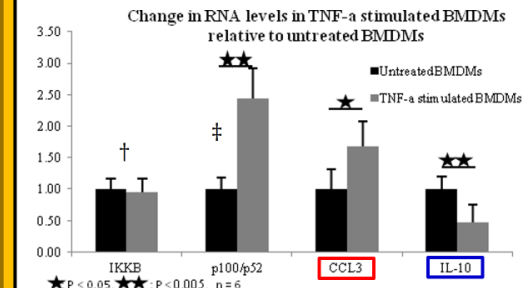
siRNAs are capable of knocking down specific NF-κB pathway proteins

- Initial HiPerFect transfections showed high variability and poor knockdown ability, especially with IKK β siRNA.

- Lipofectamine transfection demonstrated the ability to successfully knockdown pathway proteins:



- Activation of the NF-κB pathways using TNF- α showed an increase in p100/p52 but not IKK β :



Conclusions

- An optimized transfection procedure allows for the formation of transfection complexes in low volume, serum-free solution.
- The presence of serum does not affect actual transfection.
- Mannosylated nanoparticles exhibit transfection activity comparable to commercial agents.
- The transcription factors in the NF-κB pathway are more attractive targets for knockdown than the upstream IKK activating protein subunits.

Acknowledgments

This work was made possible in part by a grant from the United States Department of Defense's (USDoD) Congressionally Directed Medical Research Programs (CDMRP) Breast Cancer Research Program (BCRP); Grant BC10269. Parts of this work were done in collaboration with a group from the Vanderbilt University Medical Center Cancer Biology Department, Fiona Yuli, PI. Mouse colony work was assisted by Whitney Barham.

Whitney Barham MD Anderson Cancer symposium Abstract:

Category: Cancer Inflammation

Title: Education of macrophages through modulation of NF-κB: an opportunity for targeted therapy

Authors: Whitney Barham, Lianyi Chen, Halina Onishko, Oleg Tikhomirov, Taylor Sherrill, Ryan Ortega, Linda Connelly, Timothy S. Blackwell, and Fiona E. Yull

Abstract:

Macrophages are a plastic cell type, capable of adapting to numerous signals within their environment. In the context of a tumor, macrophages can play two very different roles, defined by some as “M1” or “M2”. As part of the innate immune system macrophages were traditionally considered anti-tumor (M1), but it has been well established that macrophages can also help to create a pro-tumor, pro-metastatic tumor niche (M2). NF-κB transcription factors can regulate both pro- (MMP’s, VEGF) and anti-tumor (iNOS) downstream targets within macrophages, suggesting that modulation of NF-κB may play a role in the two different macrophage phenotypes. However, our understanding of NF-κB signaling specifically within macrophages during tumor progression is limited. To this end, we have developed murine transgenic models that enable us to induce expression of an activator or dominant inhibitor of NF-κB in macrophages by adding doxycycline to the drinking water of mice. We have combined these novel transgenics with the polyoma model of mammary cancer for our studies.

We have recently shown that activation of NF-κB in macrophages significantly limits metastasis in a tail vein model of tumor progression. In this model, constitutive IKK2 activity within macrophages leads to an anti-tumor immune response including altered immune cell populations within the lung microenvironment, changes in chemokine and cytokine expression and rapid killing of tumor cells during the seeding phase mediated by reactive oxygen species. Our current work has extended these findings to an orthotopic mammary tumor model. Again, we find that activation of NF-κB in macrophages results in decreased primary tumor growth and decreased tumor seeding into the blood. Ongoing studies will investigate the potential for activation of macrophages to synergize with chemotherapy. Given these findings, we believe that targeted activation of NF-κB signaling in macrophages could be harnessed to overcome the education of macrophages by tumor cells, and could be exploited as a novel targeted therapy.

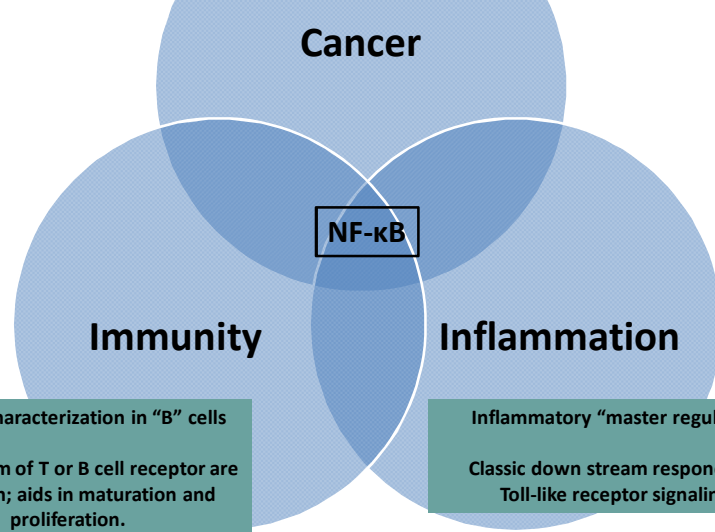
Education of macrophages through modulation of NF-κB: an opportunity for targeted therapy

Whitney Barham, Lianyi Chen, Halina Onishko, Oleg Tikhomirov,
Taylor Sherrill, Ryan Ortega, Rinat Zaynagetdinov, Linda Connelly,
Timothy S. Blackwell, and Fiona E. Yull

Immunology and Inflammation in Cancer
MD Anderson Symposia on Cancer Research 2012

NF-κB up-regulated in solid tumors of the: Breast, cervix, prostate,
kidney, lung, colon, liver, pancreas, esophagus, larynx, thyroid,
parathyroid, bladder, ovary, skin, head, neck, oral cavity, and retina
(as well as many hematological malignancies).

Baud & Karin, *Nature Reviews: Drug Discovery*, 2009.



Review

Cell

PERSPECTIVE SERIES

NF- κ B in defense and disease

Albert S. Hahn, Jr., Scott Lippman

Potential pharmacological control of the NF- κ B pathway

Gautam Sethi¹ and Vinay Tergaonkar^{2,3}

¹Department of Pharmacology, Yong Loo Lin School of Medicine, National University of Singapore, 117587, Singapore
²Institute of Molecular and Cell Biology (IMCB), 61 Biopolis Drive, 138673, Singapore

³Department of Biochemistry, National University of Singapore, 117587, Singapore

Nuclear factor (NF- κ B) mediates cellular responses to environmental stimuli.

It activates transcriptional programs that include proinflammatory genes, tumor promoters to maintain cell growth, and development of a variety of cancers. In addition, NF- κ B mediates development of various diseases, indicates some of which may be chronic. It is clear that several of the approaches described here also work, in part, to regulate the expression of the genetic components of the NF- κ B pathway that get turned on in various diseases.

NF- κ B signaling pathway

DOI: 10.1016/j.cell.2004.01.010

Bullock 29 (2007) 38–35

305 PAGES

NF- κ B as a potential molecular target for cancer therapy

Chae Hyung Lee*, Yong-Tark Jeon*, Su-Hyung Kim*, and Yong-Sang Kang*

*Department of Obstetrics and Gynecology, College of Medicine, Seoul National University, Seoul, Korea

†Cancer Research Institute, College of Medicine, Seoul National University, Seoul, Korea

DOI:

10.1016/j.cell.2004.01.010

305 PAGES

Applenz (2009) 1:434–361

DOI: 10.1016/j.applenz.2008.01.015

CELL DEATH AND DISEASE

NF- κ B signaling in carcinogenesis and as a potential molecular target for cancer therapy

Hsin-Ming Shieh * Vinay Tergaonkar

Published online 11 February 2009
© Springer Science+Business Media, LLC 2009

Abstract: It has been clearly shown that the regulation of NF- κ B signaling cascade is a common underlying factor of many human ailments including cancers. The put two studies of intensive research on NF- κ B signaling pathways have revealed the complex functioning of this pathway but interestingly details of why this pathway works differently in different cellular contexts are still not clear. In this review, we discuss the recent findings that demonstrate how the NF- κ B family undergoes a remarkable transformation during carcinogenesis. In this review, we summarize the literature documenting the involvement of NF- κ B in cancer, and then focus on the mechanisms by which NF- κ B can develop NF- κ B-induced towards promotion of human cancers.

Keywords: NF- κ B; p65; kinase; inhibitors; signaling; Cancer; IBS

General introduction: NF- κ B family proteins and the signaling pathways

Since its discovery over 21 years ago, nuclear factor- κ B (NF- κ B) has emerged as a major regulator of gene transcription factors for its immense importance in vertebrate physiology and for its apparent deregulation in a variety of diseases. The NF- κ B family consists of five members: NF- κ B1/p50, NF- κ B2/p52/RelB, RelA/p65 and NF- κ B3/p105/p52. These proteins form homodimers or heterodimers. Whereas NF- κ B1/p50 is present in all cells, NF- κ B2/p52 is mainly found in hematopoietic tissues.

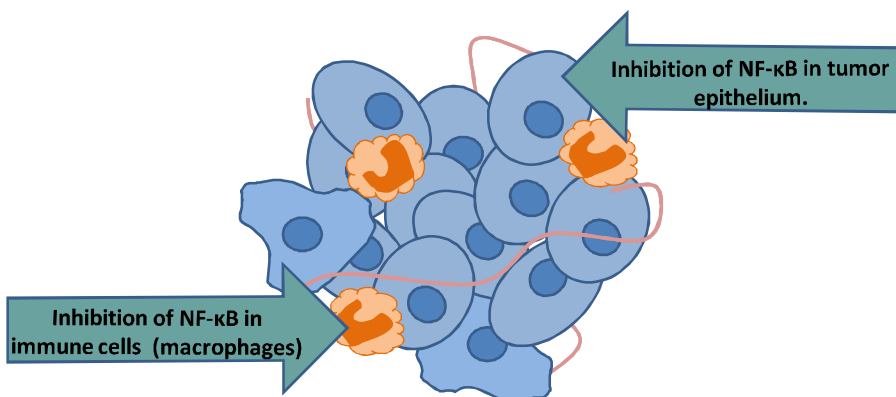
DOI: 10.1016/j.cell.2009.01.010

305 PAGES

DOI: 10.1016/j.applenz.2008.01.010

<div data-bbox="438 2950 50

Systemic inhibitors will inhibit epithelial NF- κ B signaling as well as signaling in the immune cells:

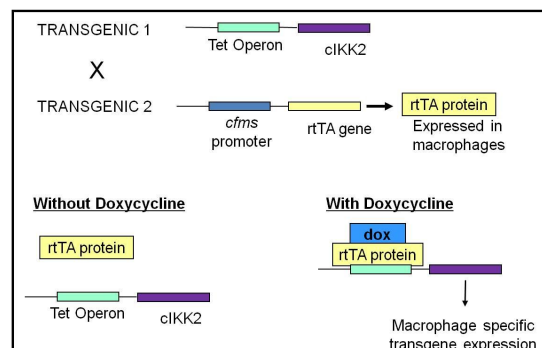
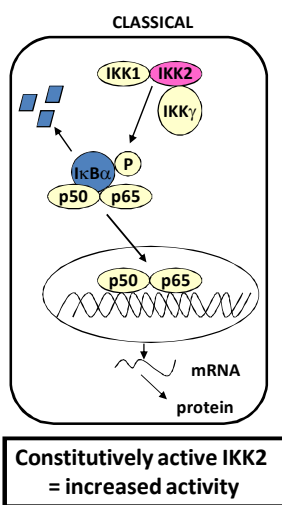


NF-κB signaling in macrophages

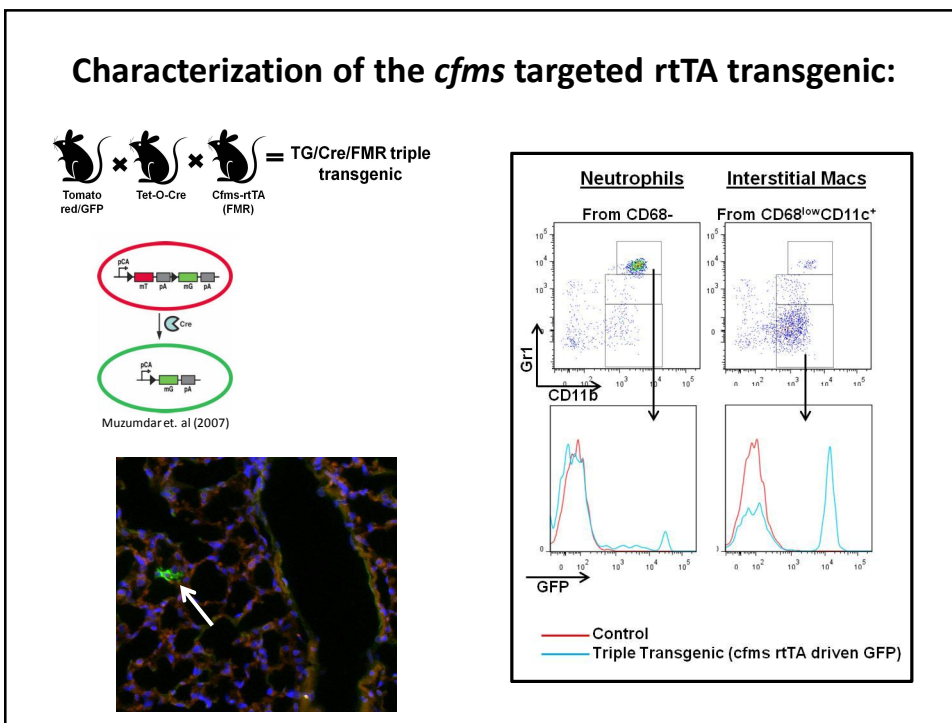
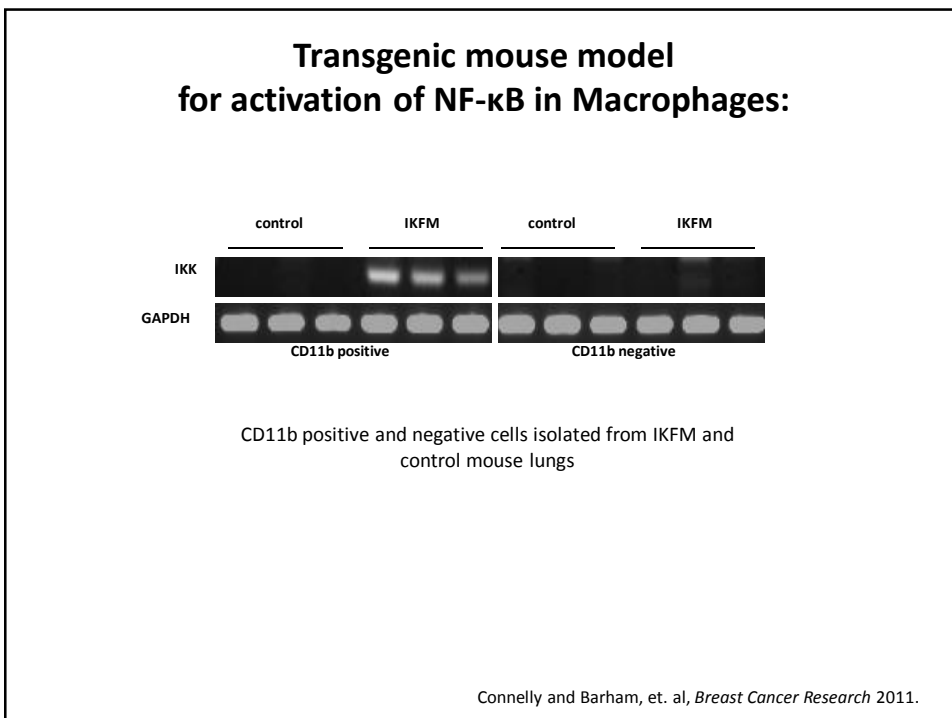
- ~ Many of the proteins generated by macrophages that could be anti-tumor (eg. iNOS) or pro-tumor (eg. MMPs) are regulated by NF-κB signaling.
- ~ Most models have inhibited NF-κB in macrophages and seen tumor inhibition (Hagemann et al. 2008, 2009, and others).
- ~ How about activation of NF-κB in macrophages?

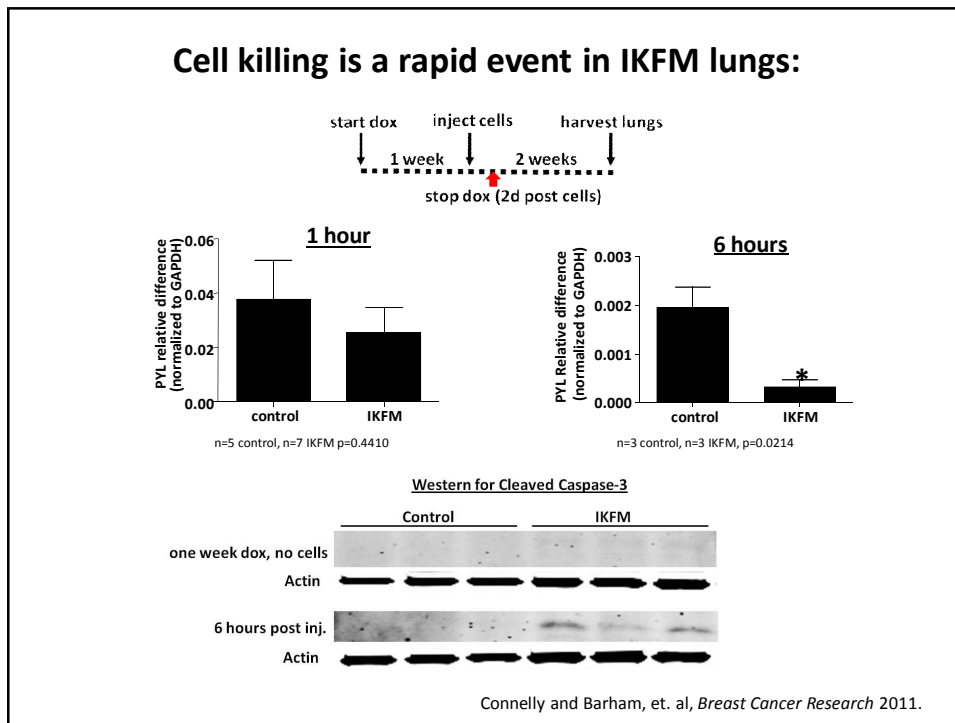
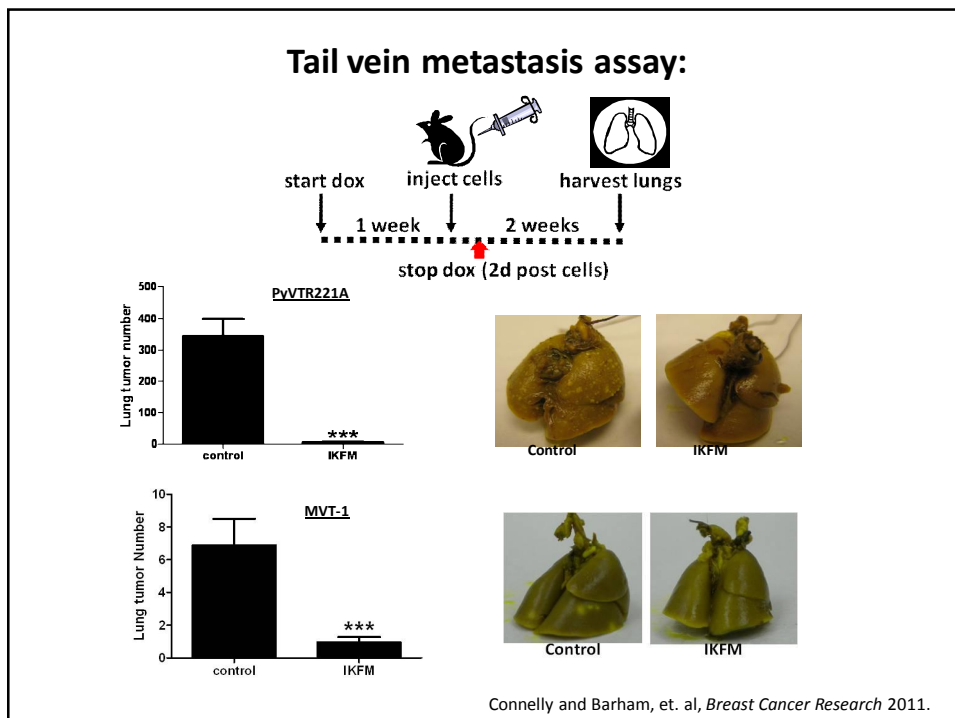
Transgenic mouse model

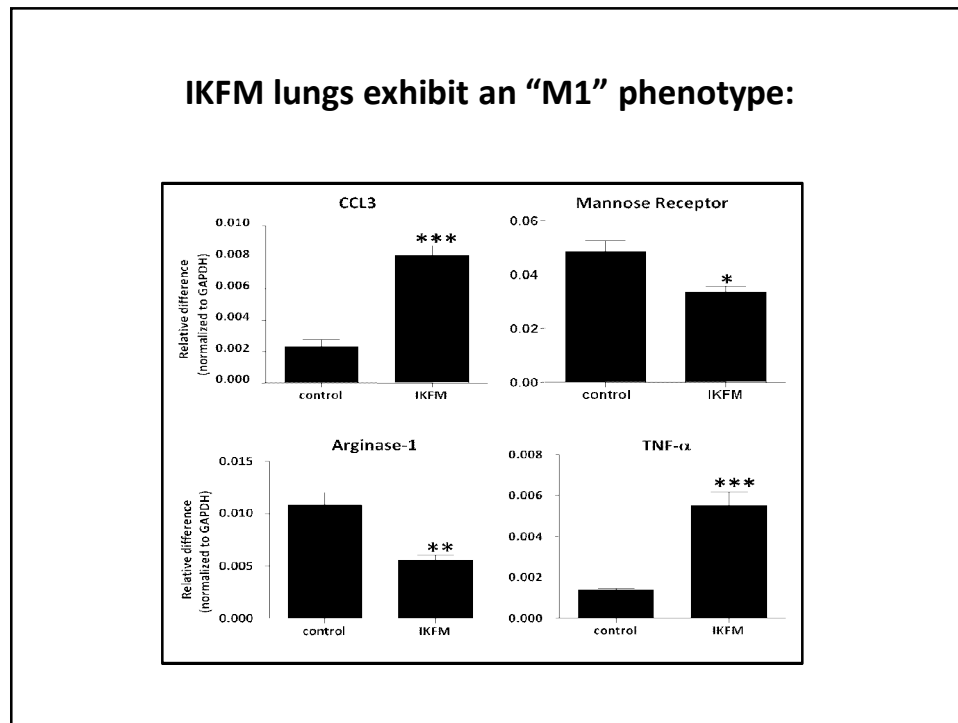
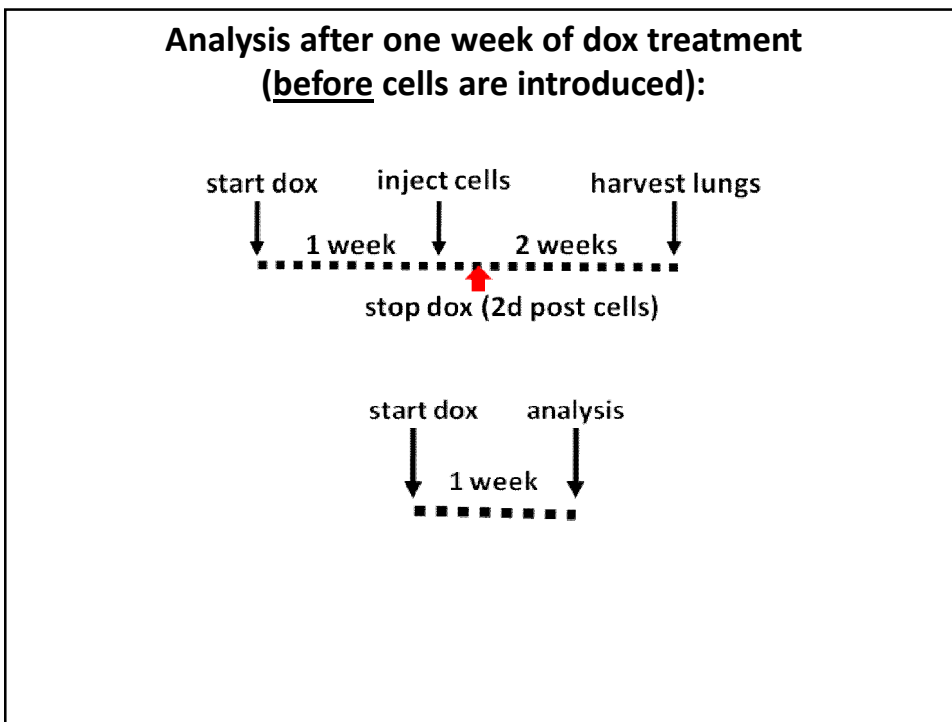
for activation of NF-κB in Macrophages:



IKFM = increased NF-κB signaling in macrophages

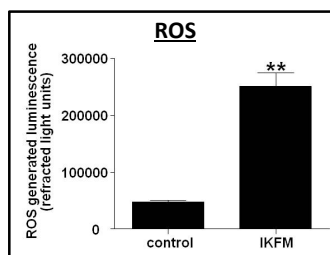




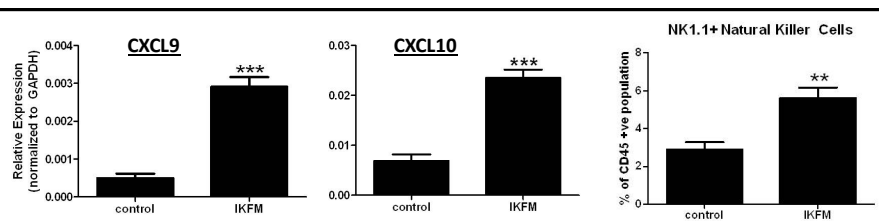


Tumor cell cytotoxicity may be direct or indirect:

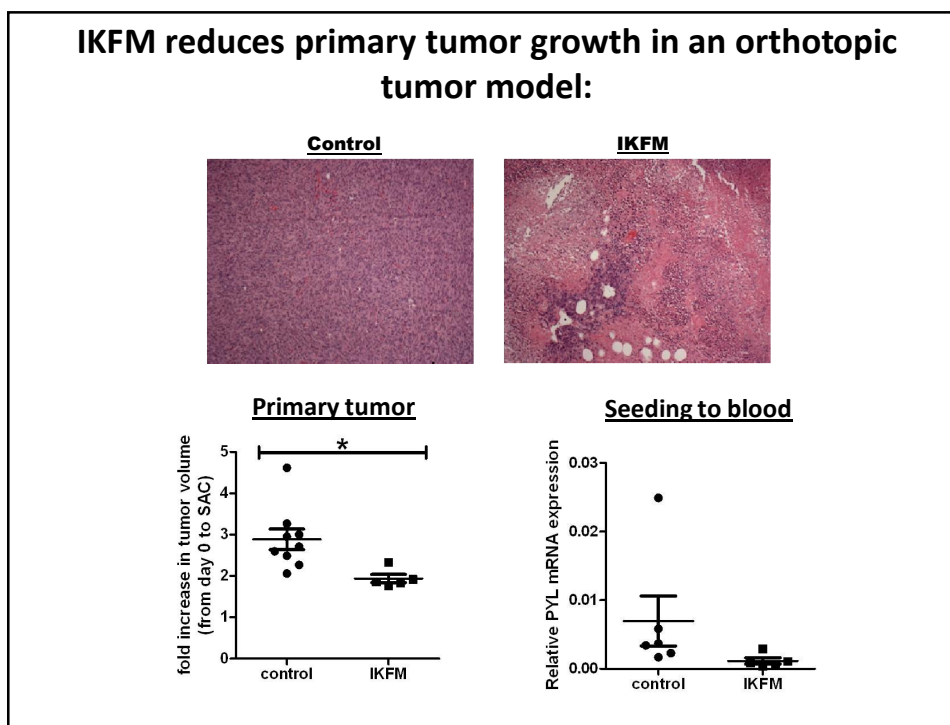
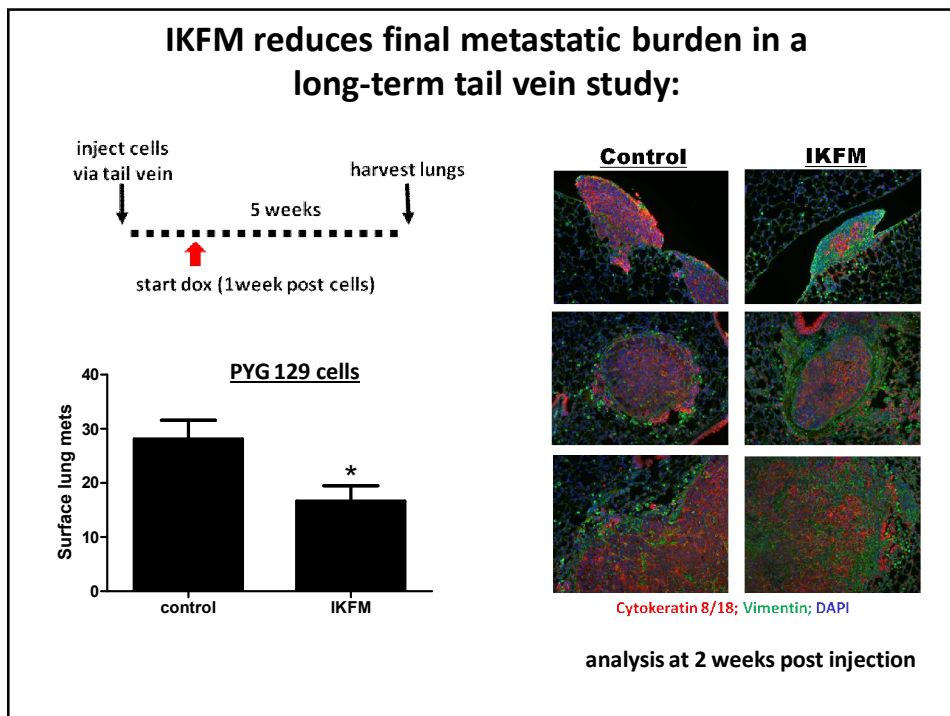
Direct:



Indirect:



What about other models?

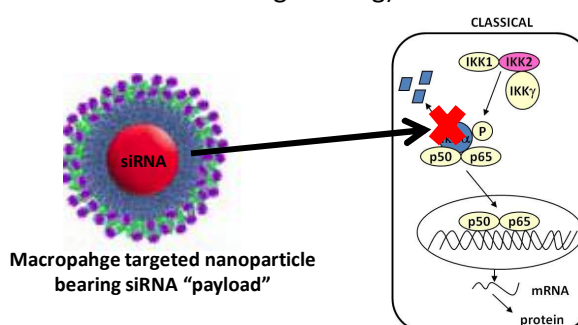


Summary and Conclusions:

- ~ We have created a novel transgenic mouse model that allows macrophage specific induction of cIKK2 during defined time periods.
- ~ This model reveals that activation of NF- κ B in macrophages is anti-tumor in different models of breast cancer tumorigenesis, which include both primary tumor and metastatic growth.
- ~ Can we utilize activation of NF- κ B signaling to manipulate macrophage behavior in clinical cancer therapy?

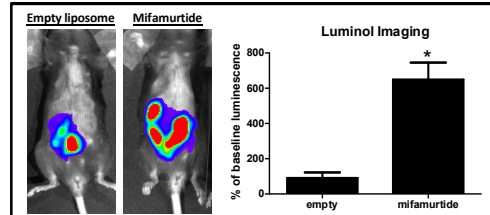
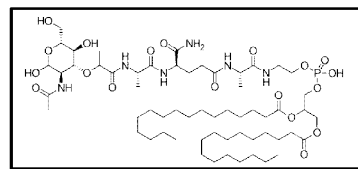
Possible Therapeutic Strategies:

- ~ We have evidence that “inhibition of the inhibitor” ($I\kappa B\alpha$) can also effectively activate NF- κ B and have similar effects as the cIKK2.
- ~ Particles that deliver siRNA to macrophages and silence $I\kappa B\alpha$ are one possible therapeutic strategy (collaboration with Vanderbilt Biomedical Engineering).



Possible Therapeutic Strategies:

Mifamurtide:



“ Liposomized **muramyltripeptide phosphatidylethanolamine (L-MTP-PE)** is a fully synthetic analogue of a lipoprotein from the outer wall of gram negative bacteria.

“ It is not cytotoxic to tumor cells on its own; rather, it activates macrophages and induces cytotoxic behavior of the immune system (simulates infection).

“ Approved in Europe for the treatment of osteosarcoma.

Summary and Conclusions:

Yull lab:

Fiona Yull
Lianyi Chen
Oleg Tikhomirov
Ryan Ortega
Halina Onishko
Linda Connelly (University of Hawaii at Hilo)

Vanderbilt University:

Timothy S. Blackwell
Taylor Sherrill
Wei Hann
DongSheng Cheng
Rinat Zaynagetdinov
Linda Gleaves

Ohio State University:

Mike Ostrowski

Barbara Fingleton

William Lawson

Funding: DOD Breast Cancer Program – IDEA and Concept grants





Cancer Research

Tumor Microenvironment Complexity: Emerging Roles in Cancer Therapy

Melody A. Swartz, Noriho Iida, Edward W. Roberts, et al.

Cancer Res 2012;72:2473-2480. Published OnlineFirst March 13, 2012.

Updated version Access the most recent version of this article at:
doi:[10.1158/0008-5472.CAN-12-0122](https://doi.org/10.1158/0008-5472.CAN-12-0122)

Cited Articles This article cites by 35 articles, 8 of which you can access for free at:
<http://cancerres.aacrjournals.org/content/72/10/2473.full.html#ref-list-1>

Citing articles This article has been cited by 3 HighWire-hosted articles. Access the articles at:
<http://cancerres.aacrjournals.org/content/72/10/2473.full.html#related-urls>

E-mail alerts [Sign up to receive free email-alerts related to this article or journal.](#)

Reprints and Subscriptions To order reprints of this article or to subscribe to the journal, contact the AACR Publications Department at pubs@aacr.org.

Permissions To request permission to re-use all or part of this article, contact the AACR Publications Department at permissions@aacr.org.

Meeting Report

Tumor Microenvironment Complexity: Emerging Roles in Cancer Therapy

Melody A. Swartz¹, Noriho Iida², Edward W. Roberts³, Sabina Sangaletti⁴, Melissa H. Wong⁵, Fiona E. Yull⁶, Lisa M. Coussens⁵, and Yves A. DeClerck⁷

Abstract

The tumor microenvironment (TME) consists of cells, soluble factors, signaling molecules, extracellular matrix, and mechanical cues that can promote neoplastic transformation, support tumor growth and invasion, protect the tumor from host immunity, foster therapeutic resistance, and provide niches for dormant metastases to thrive. An *American Association for Cancer Research (AACR)* special conference held on November 3–6, 2011, addressed five emerging concepts in our understanding of the TME: its dynamic evolution, how it is educated by tumor cells, pathways of communication between stromal and tumor cells, immunomodulatory roles of the lymphatic system, and contribution of the intestinal microbiota. These discussions raised critical questions on how to include the analysis of the TME in personalized cancer diagnosis and treatment. *Cancer Res*; 72(10); 2473–80. ©2012 AACR.

Introduction

The tumor microenvironment (TME) has received growing attention from an increasing number of investigators in the United States and abroad (1) and also by research organizations including the National Cancer Institute (NCI) and the *American Association for Cancer Research (AACR)* over the last decade. As our understanding of the role of the TME in cancer continues to evolve, the complexity of the interactions between neoplastic tumor cells and their microenvironment has become increasingly apparent, and at the same time, the number of agents entering clinical trials that specifically target interactive pathways between neoplastic and stromal cells has increased. On November 3–6, 2011, the AACR, in conjunction with its Tumor Microenvironment Working Group, organized a special conference entitled "Tumor Microenvironment Complexity: Emerging Roles in Cancer Therapy" that brought together in Orlando, FL, more than 280 participants including 42 speakers to discuss recent progress made in the field and to identify future directions of the highest priority. A workshop chaired by Suresh Mohla (NCI, Bethesda, MD) also presented the new TME network (TMEN) program at the NCI funded by U54 and U01 grants that brings together 11 centers and whose

mission is to promote and facilitate interdisciplinary collaborations in understanding the host stroma in tumorigenesis (2).

Many of the presentations focused on the interactions between tumor cells and their surrounding environment. How such interactions are critical for tumor progression was well illustrated by the work of Luis Parada (University of Texas Southwest Medical Center, Dallas, TX), who gave the opening keynote lecture. Using mouse models of neurofibromatosis type 1 (Nf1), he showed that loss of *Nf1* heterozygosity in Schwann cells that give rise to plexiform neurofibroma is insufficient for neurofibroma formation but rather that *Nf1* haploinsufficiency in mast cells is also required for tumor formation. Furthermore, cKIT in mast cells was critical for their recruitment and protumor effects. These elegant studies have led to clinical studies evaluating imatinib (Gleevec) in patients with Nf1 that have thus far indicated a favorable response rate and have bolstered enthusiasm for targeting stromal cells in a diversity of solid tumors.

The present article summarizes the meeting in 5 new emerging concepts (Fig. 1) and 2 critical questions that were the subject of discussion during the conference.

Emerging concept 1: The TME is a dynamic milieu

The TME is in constant evolution as a result of tissue remodeling, metabolic alterations in the tumor, and changes in the recruitment of stromal cells including a diversity of immune cells. Tissue remodeling that occurs in the post-partum breast during mammary gland involution, for example, perpetuates an increased risk of breast cancer (3). Pepper Schedin (University of Colorado, Aurora, CO) described how such remodeling creates a tumor-promoting inflammatory environment similar to the environment of a wound, characterized by an influx of T-helper (T_H)2-type macrophages, abundant fibrillar collagen, and increased COX-2 activity.

Authors' Affiliations: ¹Institute of Bioengineering and Swiss Institute for Experimental Cancer Research, École Polytechnique Fédérale de Lausanne, Lausanne, Switzerland; ²National Cancer Institute, National Institutes of Health, Bethesda, Maryland; ³University of Cambridge, Cambridge, United Kingdom; ⁴Fondazione IRCCS Instituto Nazionale Tumori, Milan, Italy; ⁵Oregon Health and Sciences University, Portland, Oregon; ⁶Vanderbilt University, Nashville, Tennessee; and ⁷University of Southern California, Los Angeles, California

Corresponding Author: Yves A. DeClerck, Children's Hospital Los Angeles, 4650 Sunset Boulevard, MS#54, Los Angeles, CA 90027. Phone: 323-361-2150; Fax: 323-361-4902; E-mail: declerck@usc.edu

doi: 10.1158/0008-5472.CAN-12-0122

©2012 American Association for Cancer Research.

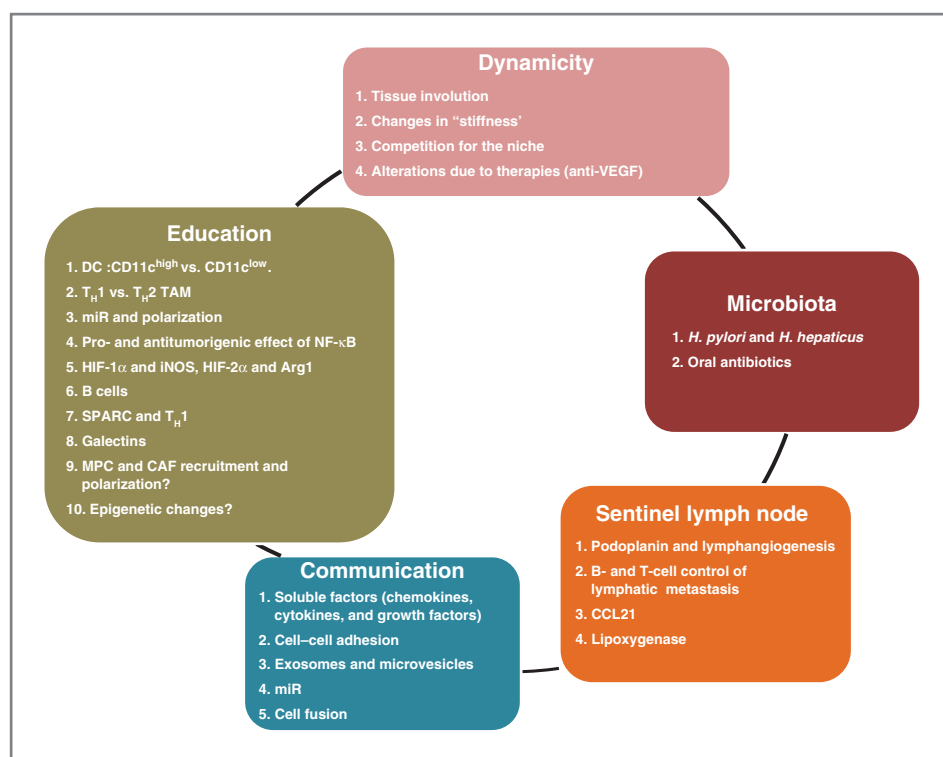


Figure 1. The diagram summarizes the 5 emerging themes that were the subject of presentations and discussions at the special AACR conference entitled "Tumor Microenvironment Complexity: Emerging Roles in Cancer Therapy" that took place in Orlando, FL, on November 3–6, 2011.

Human mammary tumor cells implanted into mouse mammary fat pads formed tumors more readily, with increased metastatic potential, when implanted in involuting (postlactation) mammary glands, rather than during pregnancy, whereas COX-2 inhibition during weaning slowed tumor growth and limited metastasis. These results raise the intriguing possibility that short-term anti-inflammatory treatment during the postpartum period may decrease breast cancer risk, similar to results in colon cancer (4).

Another important feature of the TME is the content and organization of the extracellular matrix (ECM), whose mechanical properties affect neoplastic cell differentiation and invasiveness. Increased stromal stiffness in breast tissue is a known risk factor of breast cancer in humans, and Valerie Weaver (University of California San Francisco, San Francisco, CA) described how inhibition of collagen cross-linking by lysyl oxidase (LOX) in murine models delayed and decreased tumor invasion (5). ECM stiffening promoted activation of ROCK, a Rho kinase effector, which increased collagen deposition by mechanisms associated with increased Wnt signaling, activation of STAT3, and expression of inflammatory cytokines, including CCL2 and granulocyte macrophage colony-stimulating factor (GM-CSF), that recruited bone marrow (BM)-derived cells into the TME. These compelling data indicate that changes in the biomechanical function of the TME impact neoplastic cell proliferation and migration, as well as secretion of immunomodulatory factors. Using second harmonic generation microscopy, Ryan Burke (University of Rochester, New York, NY) from the laboratory of Edward Brown showed that altering the alignment of collagen fibers in solid tumors impacted malignant cell invasion and their metastatic prop-

erties, in part, via regulation of TNF- α and macrophages. Thus, as similarly illustrated in P. Shedin's presentation in the involuting mammary gland not only the amount of stromal collagen but also its organization are drivers of the malignant process.

Dynamic interactions between tumor cells and cells of the osteoblastic niche affect malignant evolution. It has been appreciated for some time that in patients with prostate cancer, increased presence of circulating hematopoietic stem cells (HSC) is an indicator of bone metastasis. Russell Taichman (University of Michigan, Ann Arbor, MI) showed that prostate carcinomas seeded into BM remained dormant and insensitive to drug treatment (6). During bone metastasis, these cells competed with HSCs for occupation of the osteoblastic niche. Conversely, altering the osteoblastic niche in mice by pretreatment with parathormone or by clearing HSCs with a CXCR4 inhibitor promoted prostatic bone metastasis.

Anticancer therapies alter the TME in ways that either promote or inhibit tumorigenicity, depending on a diverse array of heterotypic mechanisms. This concept was elegantly illustrated for the case of anti-VEGF therapy by Gabriele Bergers (University of California San Francisco) who showed that glioblastoma-bearing mice treated with Avastin exhibited a transient beneficial therapeutic response that was followed by tumor revascularization and enhanced invasiveness (7) associated with increased c-Met expression and epithelial-to-mesenchymal transformation (EMT). This is explained by the observation that VEGF receptor (VEGFR)2 and c-Met were antagonistically associated, where c-Met signaling became dominant in the presence of VEGFR2 signaling blockade and vice versa. Thus, combined therapy targeting both signaling

pathways may be required for efficient, durable antitumor responses.

Emerging concept 2: Significance of immune and stromal cell education in the TME

Emerging studies indicate that reciprocal interactions between the diverse assemblages of stromal cells and evolving neoplastic cells fundamentally regulate tumor progression. Adaptive and innate immune cells represent a significant component of the TME. Largely dependent on soluble cytokines and chemokines, immune cells become variably polarized toward $T_{H}1$ - (generally antitumor) or $T_{H}2$ -type (generally protumorigenic) phenotypes. While initially described for $CD4^{+}$ T cells, it is now clear that $T_{H}1$ - and $T_{H}2$ -type factors regulate the phenotype and bioactivity of essentially all immune cells subtypes. Michael Shurin (University of Pittsburgh, Pittsburgh, PA) showed that conventional dendritic cells (DC) exposed to tumor-derived factors polarize into regulatory DCs (regDC) that suppressed the proliferation of preactivated T cells and were phenotypically and functionally different from their precursors and from immature conventional DCs (8). In particular, $CD11c^{low} CD11b^{high}$ DCs exhibited immunosuppressive activity toward implanted 3LL tumors, whereas $CD11c^{high}$ DCs instead promoted their metastasis dependent on RhoGTPase. In the presence of *Clostridium difficile* toxin, DCs failed to polarize and exhibited altered activity and effector functions. Related to DCs, the significance of macrophage $T_{H}2$ polarization was reported by Lisa Coussens (Oregon Health and Science University, Portland, OR). $T_{H}2$ -type tumor-associated macrophages (TAM) are common constituents of many solid tumor types and not only provide proangiogenic and proinvasive factors to growing tumors but also suppress $CD8^{+}$ T-cell-mediated antitumor immunity. Accordingly, blocking recruitment of macrophages into mammary tumors by treating mice with agents that blocked CSF1R signaling not only diminished tumor vascularity and slowed primary tumor development but also reduced formation of pulmonary metastases and improved survival, when given in combination with chemotherapy, by $CD8^{+}$ T-cell-dependent mechanisms (9). These preclinical data highlight the multifunctional role of macrophages in solid tumors and importantly reveal that TAMs blunt cell killing by $CD8^{+}$ T cells as well as by various forms of chemotherapy suggesting a novel combinatorial anticancer approach. A therapeutic CSF1R kinase inhibitor, PLX3397, is currently being tested with eribulin in a phase Ib/II clinical trial in patients with metastatic triple-negative breast cancer.

Macrophage polarization is also modulated by endogenous microRNAs (miR). Michele de Palma (San Raffaele Scientific Institute, Milan, Italy) presented data identifying miR-511-3p, an miRNA encoded by the mannose receptor *Mrc1* gene that was specifically upregulated in $F4/80^{+} MRC1^{+} CD11c^{+}$ TAMs and functioned as a negative regulator of TAM protumorigenic polarization. Also, critical for macrophage phenotype and bioactivity is the expression of the NF- κ B. Using mice in which expression of a constitutive activator of NF- κ B was induced, Fiona Yull (Vanderbilt University, Nashville, TN) reported that NF- κ B activation in macrophages variably affected carcinoma cell metastasis dependent on spatial/temporal features (10).

When activated in the presence of circulating tumor cells, NF- κ B exerted antitumorigenic activities whereas when activated later in tumor progression, for example, in secondary sites of metastasis, protumorigenic activities on macrophages predominated.

Hypoxia can also affect immune cell education in the TME depending on the type of hypoxia-inducible factor (HIF) involved in myeloid cells (11). Jessica Shay (University of Pennsylvania, Philadelphia, PA) of Celeste Simon's laboratory reported that whereas HIF-1 α fostered $T_{H}1$ polarization, HIF-2 α instead favored $T_{H}2$ polarization of immune cells. Experimentally, when HIF-2 α was either inhibited via acriflavine or genetically deleted, $CD68^{+}$ macrophage infiltration into colons of mice challenged with dextran sodium sulphate (DSS) was decreased, and carcinogenesis was reduced. Randall Johnson (University of California San Diego, La Jolla, CA) presented complementary data showing that HIF regulated inducible nitric oxide synthase (iNOS) and arginase 1 (Arg1) expression. In the presence of low IFN- γ , HIF-2 α induced the expression of Arg1, reducing the production of NO and fostering a $T_{H}2$ phenotype. Under conditions of high IFN- γ , HIF-1 α dominated and iNOS was induced converting arginine into NO and promoting a $T_{H}1$ phenotype.

Tumor recruitment of myelocytic cells is also regulated by B cells. Using a mouse model of squamous cell carcinoma induced by K-Ras expression in basal keratinocytes, Andrew Gunderson (Pennsylvania State University, University Park, PA) of Adam Glick's laboratory reported that K-Ras activation led to cutaneous inflammation, including expansion of immunosuppressive myeloid cells. However, when B cells were deleted, myeloid suppressor cells were ablated, indicating the requirement of B cells to stimulate the recruitment and suppressive activity of these myeloid cells. Along these same lines, Tiziana Schioppa (Barts Cancer Institute, London, United Kingdom) from Frances Balkwill's laboratory presented data showing that the clinical efficacy of anti-TNF- α therapy may, in part, be due to its effect on protumorigenic B cells (12). Development of 7,12-dimethylbenz(a)anthracene (DMBA)/12-O-tetradecanoylphorbol-13-acetate (TPA)-induced papillomas was significantly reduced in either TNF- α -deficient or B-cell-deficient mice; transfer of B cells from DMBA-treated mice into TNF- $\alpha^{-/-}$ recipient mice reinstated papilloma development. Notably, B regulatory cell expression of interleukin (IL)-10 was critically dependent on TNF- α expression, suggesting that anti-TNF- α therapy promotes antitumor immunity by suppressing B regulatory expression of IL-10.

ECM proteins also contribute to local immunoregulation. Sabina Sangaletti (Fondazione IRCCS Instituto Nazionale Tumori, Milan, Italy) from the laboratory of Mario Colombo showed that the matricellular secreted protein acidic rich in cysteine (SPARC) with profibrotic actions was expressed in remodeling tissues and in tumors and promoted $T_{H}1$ -type polarization by regulating expression and activation of TGF- β 1 and in turn modulating macrophage production of TNF- α (13). In the absence of SPARC, macrophages did not down-modulate TNF- α in response to TGF- β 1, and thus fostered fibrosis. SPARC could thus be a potential therapeutic target to render the TME unsuitable for cancer cell proliferation.

Galectins, a family of evolutionarily conserved glycan-binding proteins, play an important function in educating immune cells and controlling angiogenesis. Gabriel Rabinovich (Instituto de Biología y Medicina Experimental, Buenos Aires, Argentina) discussed how galectin-1 associated with VEGFR2 in tumor-associated endothelial cell stimulated VEGFR2-mediated signaling and angiogenesis in the absence of VEGF (14). Accordingly, a monoclonal antibody (mAb) against galectin-1 inhibited growth of Kaposi sarcoma and B16 melanomas in mice with increased recruitment of T_H17-type lymphocytes and decreased tumor vascularization.

In addition to polarization, programmed death-1 (PD-1), an inhibitory coreceptor expressed on T and B cells, plays an important role in providing immune-inhibitory signals in the TME. Drew Pardoll (Johns Hopkins University, Baltimore, MD) showed that PD-1 was expressed by activated T and B cells and monocytes and interacted with the ligand B7-H1 expressed by DCs and many tumor cells, providing them with adaptive resistance and an immune escape mechanism. Accordingly, a therapeutic mAb against B7H1 is currently being tested in a phase I clinical trial in patients with advanced solid tumors and preliminary data suggest clinical activity against melanoma and non-small cell lung cancer (15).

Nonimmune mesenchymal cells, such as fibroblasts, myofibroblasts, or adipocytes, play an important role in TMEs where they are "educated" by neoplastic cells. Frank Marini (Wake Forest Comprehensive Cancer Center, Winston-Salem, NC) used mice transplanted with EGFP-labeled BM cells to show that BM-derived mesenchymal progenitor cells (MPC) were recruited into primary tumors where they differentiated into cancer-associated fibroblasts (CAF), expressing fibroblast activation protein (FAP) and fibroblast-specific protein (FSP). The presence of these cells in the tumor affected growth and promoted immune escape. Deletion of CD44 led to a loss of FAP/FSP-producing cells in the tumor, suggesting that CD44 was critical for their recruitment. When in the TME, MPCs and CAFs interact with tumor cells by a variety of mechanisms. One mechanism is activation of the hedgehog (HH) pathway. Yunjung Choi (University of Michigan, Ann Arbor, MI) of Ronald Buckanovich's laboratory showed that HH activation in tumoral stem cells led to induction of bone morphogenic protein (BMP)-2 and -4 (among other factors) that stimulate proliferation of ALDH⁺ ovarian cancer stem cells. MPCs and CAFs are a source of multiple growth factors and chemokines/cytokines including IL-6 and FAP. Yves DeClerck (University of Southern California, Los Angeles, CA) reported that IL-6 expression in MPCs was increased in the presence of tumor (neuroblastoma) cells and that it activated STAT3, which by upregulating expression of survivin, Mcl-1, and Bcl-xL in neoplastic cells, increased their resistance to cytotoxic drugs. Interestingly, TAMs collaborated with MPCs by being a source of the agonistic soluble IL-6 receptor enhancing STAT3 activation. Targeting CAFs may be an attractive therapeutic target; however, it may have a toxic effect as these cells are present in normal tissue. Ed Roberts (University of Cambridge, Cambridge, United Kingdom) from Douglas Fearon's group provided data showing that FAP⁺ cells were present in normal tissues and that their depletion in nontumor-bearing mice

induced a state of cachexia and metabolic waste with a loss in skeletal muscle of follistatin, an inhibitor of procatabolic mediators. Using intravital microscopy and 3-dimensional cell-based models, Eric Sahai (London Research Institute, London, United Kingdom) showed that CAFs contributed to tumor cell migration by locally remodeling the ECM to generate routes used by "following" carcinoma cells (16). ECM remodeling by CAFs depended on Rho-Rock signaling that occurred under the influence of neoplastic cells via IL-6 that induced actomyosin polymerization in CAFs by STAT3 activation (17).

Genetic factors can also contribute to education of the stroma in cancer. Germ line mutations that affect formation of carcinomas such as in the case of familial adenomatous polyposis coli (FAPC) affect mesenchymal cells in the TME. For example, Monica Bertagnolli (Harvard Medical College, Boston, MA) presented data showing that in *Apc*^{Min/+} mice, Wnt signaling was also deregulated in mesenchymal cells and desmoid tumors formed as the result of a COX-2-dependent activation of the mesenchyme associated with an increased production of collagens (18). Furthermore, epigenetic factors may contribute. Benjamin Tycko (Columbia University, New York, NY) showed that in pancreatic intraepithelial neoplasia, there was a decrease in global methylation not only in malignant epithelial cells but also in CAFs. DNA methylation further decreased as lesions progressed from *in situ* to invasive carcinoma. Interestingly, in transgenic mice prone to develop pancreatic cancers, treatment with the hypomethylating agent 5-azacytidine led to a hypomethylation crisis associated with reduction in tumor growth and upregulation of a subset of IFN target genes affecting cell proliferation.

Emerging concept 3: The mechanisms of communication between tumor cells and the microenvironment are diverse: emerging role of exosomes and cell fusion

Two novel mechanisms potentially supporting the communication between tumor cells and stromal cells were the subject of presentations at the meeting. A first mechanism consisted of exosomes (19). Initially considered to be primarily responsible for release of unwanted material by cells, exosomes are now recognized as active entities involved in regulating a variety of extracellular signals. Exosomes have been isolated from the plasma of patients with cancer, and their concentration and protein content correlated with tumor stage and clinical outcome. David Lyden (Cornell University Weill Medical College, New York, NY) presented data suggesting that tumor exosomes, which package not only tumor antigens and immunosuppressive molecules but also miRs, were involved in mobilizing BM-derived cells to premetastatic niches (20). Preconditioning of BM cells with exosomes purified from metastatic melanoma cells, but not from non-malignant cells, transplanted into lethally irradiated recipient mice significantly increased metastasis. Tumor cells within the TME are not the sole source of exosomes, and Ngai-Na Chloe Co (University of Texas MD Anderson Cancer Center, Houston, TX) from Samuel Mok's laboratory presented work showing that CAFs and cancer-associated adipocytes from ovarian tumors released miR21 containing exosomes that in co-culture,

transferred miR21 to tumor cells promoting migration and invasion. Exosomes thus appear to be involved in a 2-way communication between tumor cells and stromal cells. A second newly reported mechanism of communication between tumor and stromal cells is cell fusion. Melissa Wong (Oregon Health and Science University) presented *in vitro* and *in vivo* data showing that functional fusion between TAMs and neoplastic cells occurred and altered the transcriptome by introducing the expression of macrophage-specific genes (21). These macrophage–carcinoma cell fusion hybrid cells may be more prone to migrate and metastasize due to their ability to mimic migratory behaviors of macrophages.

Emerging concept 4: The sentinel lymph node is an active part of the TME

Many tumors metastasize first to the sentinel lymph node after entering lymphatic vessels around the tumor. Although tumor-associated lymphatic vessels were previously considered passive transporters of fluid, molecules, and cells, the last decade has seen numerous reports correlating lymphatic growth factors in the TME with metastatic potential (22). Furthermore, observations that sentinel lymph nodes undergo lymphangiogenesis before metastasis led to the notion that lymph node lymphangiogenesis may be involved in the pre-metastatic niche. Five presentations illustrated how tumor-associated lymphatic vessels, lymph flow, and the sentinel lymph nodes promote immune tolerance and distant metastasis.

Michael Detmar (ETC Zurich Institute of Pharmaceutical Sciences, Zurich, Switzerland) discussed how podoplanin, expressed by lymph node stromal cells in the T-cell zone, can be present in the tumor stroma and how its presence correlated with tumor lymphangiogenesis (23). One mechanism by which podoplanin-induced lymphangiogenesis occurred is via endothelin-1 upregulation. *In vitro*, podoplanin increased tumor cell motility as well as lymphatic endothelial cell (LEC) migration and tubulogenesis. Podoplanin upregulation may be induced by increased lymph flow to the draining lymph nodes, which occurs in lymphangiogenic tumors unless metastasis is extensive enough to be obstructive (24). Interestingly, both increased lymph flow from the tumor as well as lymph node metastasis appear to depend on tumor-draining lymph node lymphangiogenesis, according to new evidence presented by Alanna Ruddell (Fred Hutchison Cancer Research Center, Seattle, WA). She showed that lymphangiogenesis in the tumor-draining lymph nodes was dependent on B cells and that normally metastatic tumors grown in B-cell-deficient mice failed to provoke lymph node lymphangiogenesis, to increase flow or metastasis. Furthermore, in Eμ-c-Myc mice with B-cell expansion in the lymph node, melanoma and lymphoma metastasis to the sentinel lymph node was increased and more rapid, and hematogeneous metastasis also increased (25). However, metastatic colonization of the same tumors after intravenous injection was unchanged in these mice, supporting the hypothesis that B-cell-driven lymph node lymphangiogenesis affects lymphatic spread of lymphoma and melanoma and that hematogeneous spread occurs after lymphatic spread.

Why does sentinel lymph node lymphangiogenesis promote metastasis? Melody Swartz (Swiss Federal Institute of Technology, Lausanne, Switzerland) presented data suggesting that lymphatic involvement by tumors and lymph node lymphangiogenesis promoted tolerance from host immunity (26). B16 melanoma expression of VEGF-C protected tumors against preexisting, vaccine-induced immunity. VEGF-C upregulated CCL21 in the tumor stroma, which attracted naive T cells and promoted their education in the regulatory chemokine environment (27). In addition, LEC in the sentinel lymph node could cross-present tumor antigen MHC class I molecules leading to CD8⁺ T-cell deletion, supporting a new role for LECs in tolerance. On the other hand, CCL21 in tumors and lymphoid stroma drove antitumor as well as protumor effects by attracting naive and regulatory T cells along with antigen-presenting cells. David Peske (University of Virginia, Charlottesville, VA) from the laboratory of Victor Engelhart showed that CCL21 expression in the stroma of ovalbumin-expressing melanomas could attract adoptively transferred naive ovalbumin-specific CD8⁺ T cells after adoptive transfer from T-cell receptor transgenic mice and activated them in the TMEs. In contrast, naturally arising host CD8⁺ T cells proliferated from a rare population of naive CD8⁺ T cells and existed in balance with regulatory T cells. These studies highlight the importance of context and timing for both antitumor immune responses and tumor tolerance to develop.

The session closed with Dotscho Kerjaschki (University of Vienna, Wien, Austria) describing new work on mammary carcinomas, whose lymph node metastasis correlated with lymphangiogenesis in the sentinel lymph nodes and with metastatic tumors but not with the primary tumor. Histopathology of invasive mammary tumors revealed large gaps in lymphatic vessels where tumor cells entered, and this was consistent with *in vitro* data showing tumor spheroids forming gaps in LEC monolayers. Invasive but not benign tumors induced this gap formation, and only in lymphatic but not blood endothelial cells, in a lipoxygenase-dependent manner. In mice with lipoxygenase knockdown, metastasis was prevented, even in VEGF-C-overexpressing tumors. These exciting new data identify lipoxygenase as a potential new drug target to prevent lymphatic spread of mammary carcinomas (28).

Emerging concept 5: The microbial flora can be friend or foe of cancer

The recent possibility of examining the entire microbiome in the gut is shedding new light on the role of commensal/pathogenic bacteria in cancer initiation and progression. One of the burning questions is how the microbiota regulates the inflammatory components of the TME and affects inflammation-associated carcinogenesis (29). The protumorigenic role of gut *Helicobacter hepaticus* in extra-intestinal carcinogenesis was discussed by Susan Erdman (Massachusetts Institute of Technology, Cambridge, MA) who reported that introduction of *H. hepaticus* to Apc^{Min/+}Rag2^{-/-} mice led to development of colitis and intestinal tumors but also to mammary gland tumors heavily infiltrated with macrophages (30). Systemic anti-TNF-α treatment or adoptive transfer of IL-10 producing

CD4⁺ T regulatory cells abolished both intestinal and mammary tumorigenesis. Because Rag2^{-/-} mice lack both T and B cells, inflammation-associated carcinogenesis found in Apc^{Min/+}Rag2^{-/-} mice was mediated by cells of the innate immune system. The presence of mammary tumors in these mice suggest that *H. hepaticus* inhabiting the gut elicits a systemic inflammatory reaction driven by innate immune cells that is also carcinogenic in tissues not directly in contact with the pathogens. Noriho Iida (NCI, Frederick, MD) from Giorgio Trinchieri's group explored the potential ability of intestinal commensal bacteria to augment antitumor immune responses in treatment-induced acute inflammation. They used a model in which mice subcutaneously implanted with melanoma cells and treated with an anti-IL-10R antibody and intratumoral injection of CpG oligonucleotides developed an intratumoral hemorrhagic necrosis due to production of TNF- α by macrophages and exhibited prolonged survival. He showed that depletion of gut commensal bacteria by administration of antibiotics impaired production of TNF- α in the tumor and decreased survival in treated colon carcinoma and melanoma-bearing mice. Thus, proper activation of innate myeloid cells by CpG nucleotides requires an intact intestinal microbiota. These two presentations illustrate the opposite roles that the microbial flora may have on cancer initiation and progression as a function of the type of inflammation present.

Critical question 1: How should we include the TME in the initial evaluation of a tumor and in preclinical cancer models?

Typically, genomic and transcriptomic analyses of tumors are conducted on DNA and RNA extracted from entire tumors and it is generally assumed that genetic and epigenetic alterations and changes in gene expression observed reflect modifications in the tumor cells. This may not necessarily be the case. Morag Park (McGill University, Montreal, Quebec, Canada) reported results from an extensive transcriptomic analysis of breast cancer specimens in which samples were microdissected to separate stroma from malignant epithelium that were individually analyzed (31). She described stromal-specific signatures that allowed classification of breast cancers into 5 TME-based subgroups. Her laboratory also identified 26 stromal-derived genes that predicted outcomes with a power better than the 70 genes used in the mammaprint test (32). Furthermore, data generated from transgenic mice in which oncogenes were targeted in the mammary epithelium suggested that oncogenes produce distinct patterning changes in the mouse mammary stroma similar to those observed in human breast tumors.

Another important question is the development of preclinical cancer mouse models that take the TME into consideration. The important role played by immune cells in the TME indicates that xenotransplanted tumor models in immunodeficient mice are of limited value in the study of TME. Genetically engineered mice have the advantage to recapitulate an oncogenic event within the context of a competent immune system but they represent murine and not human cancer models. Alana Welm (University of Utah, Salt Lake City, UT) discussed a mouse model where fresh human breast cancer

samples were xenografted into immunodeficient mice along with a component of the human stroma to achieve a high rate of engraftment and spontaneous metastasis (33). The pathology of these tumors faithfully reflected the organization of human tumors. Engraftment was also a prognosticator of outcome as women whose tumors engrafted had a poorer survival than women whose tumors did not engraft. Interestingly, although cotransplantation of a stromal component or of human mesenchymal stem cells increased the efficiency of the xenograft, the mouse stroma was quickly recruited to reshape the TME.

Critical question 2: What should be the strategies to target the microenvironment in cancer therapy?

A fundamental question raised by many of the presentations at the meeting is related to the application of our knowledge of the TME to the design of therapeutic strategies. Therapies solely targeted at the TME are unlikely to eradicate cancer, although they could have the potential to convert cancer into a chronic disease. The major focus of ongoing efforts have thus been on strategies that combine targeting tumor cells and the microenvironment and several presentations showed that targeting the microenvironment in combination with therapies aimed at tumor cells is a valuable approach. A first strategy is the use of agents blocking pathways responsible for the recruitment and activation of stromal cells in the TME as first shown for Avastin, that is now part of the armamentarium to combat colon cancer and glioblastoma (34). William Dougall (Amgen, Seattle, WA) presented data illustrating the efficacy of targeting receptor activator of NF- κ B ligand (RANKL) in bone metastasis with denosumab, a fully human mAb against RANKL (35). Three phase III clinical studies with denosumab recently completed in patients with bone metastasis from breast cancer, castration-resistant prostate cancer (CRPC), and other advanced malignancies showed effective inhibition of bone remodeling and the superiority of denosumab over Zometa (zoledronic acid) in decreasing the number of skeletal-related events in these patients. Denosumab was also effective in delaying the development of bone metastasis in men with CRPC, showing that targeting the TME can also have a preventive effect on metastasis. RANKL is also a mediator of the mitogenic activity of progesterone in mouse mammary epithelium and pharmacologic inhibition of RANKL in progesterone-dependent mouse mammary tumors attenuated tumorigenesis. A second strategy is based on the concept that the TME modulates tumor susceptibility to therapy. Combination therapies that include agents targeting pathways affecting tumor cell resistance to drugs with standard chemotherapy or targeted therapy have garnered renewed excitement. William Dalton (H. Lee Moffitt Cancer Center and Research Institute, Tampa, FL) discussed environment-mediated drug resistance (EMDR) as a mechanism where the interaction between tumor cells and the BM environment allows for discrete tumor populations to survive as minimal residual disease and emerge as drug-resistant clones (36). Interfering with these mechanisms may increase cancer response to therapy and prevent resistance. In myeloma, in which such resistance has been extensively studied, the mechanisms

involve activation of specific pathways such as IL-6/STAT3, SDF1/CXCR4, Notch, or TRAIL and miR that provide tumor cells with a survival advantage. Several inhibitors of such pathways are currently in clinical trials. The ECM can also be a factor of therapeutic resistance and thus a target for therapeutic intervention. Sunil Hingorani (Fred Hutchinson Cancer Research Center) showed that the formation of a hyaluronic acid-rich stroma in pancreatic tumors resulted in unperfused blood vessels that provided a drug-free sanctuary for tumor cells. Treatment of the stroma with hyaluronidase in transgenic mice prone to develop pancreatic cancer was followed by a rapid reperfusion of the blood vessels that led to decreased proliferation, increased apoptosis, increased response to therapy, and improved survival.

A third strategy consists of targeting protumorigenic inflammatory pathways, an approach taken by Frances Balkwill's (Barts Cancer Institute) laboratory. She identified TNF, IL-6, and CXCL12 as a TNF network of 3 key cytokine mediators of cancer-related inflammation, having a paracrine action on angiogenesis, infiltration with myeloid cells, and Notch signaling. She reported that siltuximab, an anti-human IL-6 antibody inhibited IL-6 signaling (STAT3 activation) in cancer cells and had therapeutic effects in xenograft models (37). A phase II clinical trial of siltuximab as single agent in platinum-resistant ovarian cancer indicated that it was well-tolerated and had some therapeutic effects.

Conclusion

This conference illustrated well the high level of complexity of the TME and the challenges ahead in our attempt to ultimately identify therapeutic agents that target the TME. This aspect was illustrated by Michael Karin (University of California San Diego), who gave the closing keynote lecture. His work shows how in certain cases, inflammation can suppress antitumor immunity but can also be used to enhance the efficacy of cancer immunotherapy. Central to inflammation is NF- κ B that can have pro- and anti-inflammatory functions (38). Evidence showing its activation in many inflammatory conditions associated with cancer such as inflammatory bowel

disease, rheumatoid arthritis, or psoriasis raised enthusiasm about NF- κ B and IKK β as therapeutic targets in chronic inflammation, autoimmune diseases, and cancer. However, it was a disappointment to later realize that inhibition of NF- κ B increased or even caused inflammation under certain circumstances. In cancer, NF- κ B can have a pro- or antitumorigenic activity depending on the cancer type and also the mechanism of carcinogenesis involved. To understand this complexity will be critical to avoid premature testing in clinical trials of agents whose activity is not entirely understood, which could result in a premature abandonment of these agents as effective anti-cancer agents. We must remember the lessons learned from the clinical testing of inhibitors of matrix metalloproteinases in the late 1990s when the complexity of their role in cancer was not entirely appreciated at the time they were clinically tested (39). This is therefore a challenging but also a very exciting time for investigators studying the TME.

Disclosure of Potential Conflicts of Interest

No potential conflicts of interests were disclosed.

Authors' Contributions

Conception and design: M.A. Swartz, M.H. Wong, Y.A. DeClerck
Writing, review, and/or revision of the manuscript: M.A. Swartz, N. Iida, E. W. Roberts, S. Sangaletti, M.H. Wong, F.E. Yull, L.M. Coussens, Y.A. DeClerck
Administrative, technical, or material support (i.e., reporting or organizing data, constructing databases): Y.A. DeClerck

Y.A. DeClerck chaired the editorial committee that was responsible for summarizing the presentations at the meeting. M.A. Swartz, N. Iida, E.W. Roberts, S. Sangaletti, M.H. Wong, F.E. Yull, and Y.A. DeClerck equally contributed to the summary of the various sessions of the meeting.

Acknowledgments

The authors thank Amy Baran, Amy Flynn, and Kacie Sheppeck for their assistance in the planning and conduct of the meeting. They also thank J. Rosenberg for her assistance in the preparation of the manuscript.

Grant Support

The meeting was supported by Genentech, Teva Pharmaceuticals, Amgen, Bristol Myers Squibb, and Hypoxigen, and a conference grant, R13 CA165812, from the NIH to Y.A. DeClerck and the AACR.

Received January 17, 2012; revised February 23, 2012; accepted March 5, 2012; published OnlineFirst March 13, 2012.

References

1. Hanahan D, Weinberg RA. Hallmarks of cancer: the next generation. *Cell* 2011;144:646–74.
2. Tumor Microenvironment Network [homepage on the Internet]. Bethesda, MD: NCI. Available from: <http://tmen.nci.nih.gov/>.
3. Borges VF, Schedin PJ. Pregnancy-associated breast cancer: an entity needing refinement of the definition. *Cancer*. 2011 Nov 15. [Epub ahead of print].
4. Koehne CH, DuBois RN. COX-2 inhibition and colorectal cancer. *Semin Oncol* 2004;31:12–21.
5. DuFort CC, Paszek MJ, Weaver VM. Balancing forces: architectural control of mechanotransduction. *Nat Rev Mol Cell Biol* 2011;12:308–19.
6. Patel LR, Camacho DF, Shiozawa Y, Pienta KJ, Taichman RS. Mechanisms of cancer cell metastasis to the bone: a multistep process. *Future Oncol* 2011;7:1285–97.
7. Dvorak HF, Weaver VM, Tlsty TD, Bergers G. Tumor microenvironment and progression. *J Surg Oncol* 2011;103:468–74.
8. Shurin GV, Ouellette CE, Shurin MR. Regulatory dendritic cells in the tumor immunoenvironment. *Cancer Immunol Immunother* 2011;61: 223–30.
9. Denardo DG, Brennan DJ, Rexhepaj E, Ruffell B, Shiao SL, Madden SF, et al. Leukocyte complexity predicts breast cancer survival and functionally regulates response to chemotherapy. *Cancer Discov* 2011; 1:54–67.
10. Connelly L, Barham W, Onishko HM, Chen L, Sherrill TP, Zabuwala T, et al. NF- κ B activation within macrophages leads to an anti-tumor phenotype in a mammary tumor lung metastasis model. *Breast Cancer Res* 2011;13:R83.
11. Keith B, Johnson RS, Simon MC. HIF1alpha and HIF2alpha: sibling rivalry in hypoxic tumour growth and progression. *Nat Rev Cancer* 2011;12:9–22.
12. Schioppa T, Moore R, Thompson RG, Rosser EC, Kulbe H, Nedospasov S, et al. B regulatory cells and the tumor-promoting actions of TNF-alpha during squamous carcinogenesis. *Proc Natl Acad Sci U S A* 2011;108:10662–7.
13. Sangaletti S, Tripodo C, Cappetti B, Casalini P, Chiodoni C, Picone S, et al. SPARC oppositely regulates inflammation and fibrosis in bleomycin-induced lung damage. *Am J Pathol* 2011;179: 3000–10.

14. Soldati R, Berger E, Zenclussen AC, Jorch G, Lode HN, Salatino M, et al. Neuroblastoma triggers an immuno-evasive program involving galectin-1-dependent modulation of T cell and dendritic cell compartments. *Int J Cancer* 2011 Oct 23. [Epub ahead of print].
15. Topalian SL, Weiner GJ, Pardoll DM. Cancer immunotherapy comes of age. *J Clin Oncol* 2011;29:4828–36.
16. Calvo F, Sahai E. Cell communication networks in cancer invasion. *Curr Opin Cell Biol* 2011;23:621–9.
17. Sanz-Moreno V, Gaggioli C, Yeo M, Albrengues J, Wallberg F, Viros A, et al. ROCK and JAK1 signaling cooperate to control actomyosin contractility in tumor cells and stroma. *Cancer Cell* 2011;20:229–45.
18. Carothers AM, Rizvi H, Hasson RM, Heit YI, Davids JS, Bertagnolli MM, et al. Mesenchymal stromal cell mutations and wound healing contribute to the etiology of desmoid tumors. *Cancer Res* 2012;72: 346–55.
19. Thery C, Zitvogel L, Amigorena S. Exosomes: composition, biogenesis and function. *Nat Rev Immunol* 2002;2:569–79.
20. Peinado H, Lavotshkin S, Lyden D. The secreted factors responsible for pre-metastatic niche formation: old sayings and new thoughts. *Semin Cancer Biol* 2011;21:139–46.
21. Powell AE, Anderson EC, Davies PS, Silk AD, Pelz C, Impey S, et al. Fusion between intestinal epithelial cells and macrophages in a cancer context results in nuclear reprogramming. *Cancer Res* 2011;71: 1497–505.
22. Alitalo A, Detmar M. Interaction of tumor cells and lymphatic vessels in cancer progression. *Oncogene* 2011 Dec 19. [Epub ahead of print].
23. Kitano H, Kageyama S, Hewitt SM, Hayashi R, Doki Y, Ozaki Y, et al. Podoplanin expression in cancerous stroma induces lymphangiogenesis and predicts lymphatic spread and patient survival. *Arch Pathol Lab Med* 2010;134:1520–7.
24. Proulx ST, Detmar M. Watching lymphatic vessels grow by making them glow. *Cell Res* 2011;22:12–3.
25. Ruddell A, Harrell MI, Furuya M, Kirschbaum SB, Iritani BM. B lymphocytes promote lymphogenous metastasis of lymphoma and melanoma. *Neoplasia* 2011;13:748–57.
26. Lund AW, Swartz MA. Role of lymphatic vessels in tumor immunity: passive conduits or active participants? *J Mammary Gland Biol Neoplasia* 2010;15:341–52.
27. Shields JD, Kourtis IC, Tomei AA, Roberts JM, Swartz MA. Induction of lymphoidlike stroma and immune escape by tumors that express the chemokine CCL21. *Science* 2010;328:749–52.
28. Kerjaschki D, Bago-Horvath Z, Rudas M, Sexl V, Schneckenleithner C, Wolbank S, et al. Lipooxygenase mediates invasion of intrametastatic lymphatic vessels and propagates lymph node metastasis of human mammary carcinoma xenografts in mouse. *J Clin Invest* 2011;121: 2000–12.
29. Parsonnet J, Friedman GD, Vandersteen DP, Chang Y, Vogelman JH, Orentreich N, et al. Helicobacter pylori infection and the risk of gastric carcinoma. *N Engl J Med* 1991;325:1127–31.
30. Fox JG, Ge Z, Whary MT, Erdman SE, Horwitz BH. Helicobacter hepaticus infection in mice: models for understanding lower bowel inflammation and cancer. *Mucosal Immunol* 2011;4:22–30.
31. Bertos NR, Park M. Breast cancer - one term, many entities? *J Clin Invest* 2011;121:3789–96.
32. Glas AM, Floore A, Delahaye LJ, Witteveen AT, Pover RC, Bakx N, et al. Converting a breast cancer microarray signature into a high-throughput diagnostic test. *BMC Genomics* 2006;7:278.
33. DeRose YS, Wang G, Lin YC, Bernard PS, Buys SS, Ebbert MT, et al. Tumor grafts derived from women with breast cancer authentically reflect tumor pathology, growth, metastasis and disease outcomes. *Nat Med* 2011;17:1514–20.
34. Ferrara N. From the discovery of vascular endothelial growth factor to the introduction of avastin in clinical trials - an interview with Napoleone Ferrara by Domenico Ribatti. *Int J Dev Biol* 2011;55:383–8.
35. Dougall WC. Osteoclast-dependent and-independent roles of the RANKL/RANK/OPG pathway in tumorigenesis and metastasis. *Clin Cancer Res* 2012;18:326–35.
36. Meads MB, Gatenby RA, Dalton WS. Environment-mediated drug resistance: a major contributor to minimal residual disease. *Nat Rev Cancer* 2009;9:665–74.
37. Coward J, Kulbe H, Chakravarty P, Leader D, Vassileva V, Leinster DA, et al. Interleukin-6 as a therapeutic target in human ovarian cancer. *Clin Cancer Res* 2011;17:6083–96.
38. Ben Neriah Y, Karin M. Inflammation meets cancer, with NF- κ B as the matchmaker. *Nat Immunol* 2011;12:715–23.
39. Coussens LM, Fingleton B, Matrisian LM. Matrix metalloproteinase inhibitors and cancer: trials and tribulations. *Science* 2002;295: 2387–92.



Size- and charge-dependent non-specific uptake of PEGylated nanoparticles by macrophages

Shann S Yu^{1,2}
Cheryl M Lau¹
Susan N Thomas³
W Gray Jerome⁴
David J Maron⁵
James H Dickerson^{2,6}
Jeffrey A Hubbell³
Todd D Giorgio^{1,2,7,8}

¹Department of Biomedical Engineering, Vanderbilt University, Nashville, ²Vanderbilt Institute of Nanoscale Science and Engineering, Nashville, TN, USA; ³Institute of Bioengineering, École Polytechnique Fédérale de Lausanne, Lausanne, Switzerland, ⁴Department of Pathology, Vanderbilt University Medical Center, Nashville, ⁵Vanderbilt Heart and Vascular Institute, Nashville, ⁶Department of Physics and Astronomy, Vanderbilt University, Nashville, ⁷Department of Cancer Biology, Vanderbilt University Medical Center, Nashville, ⁸Department of Chemical and Biomolecular Engineering, Vanderbilt University, Nashville, TN, USA

Abstract: The assessment of macrophage response to nanoparticles is a central component in the evaluation of new nanoparticle designs for future in vivo application. This work investigates which feature, nanoparticle size or charge, is more predictive of non-specific uptake of nanoparticles by macrophages. This was investigated by synthesizing a library of polymer-coated iron oxide micelles, spanning a range of 30–100 nm in diameter and –23 mV to +9 mV, and measuring internalization into macrophages in vitro. Nanoparticle size and charge both contributed towards non-specific uptake, but within the ranges investigated, size appears to be a more dominant predictor of uptake. Based on these results, a protease-responsive nanoparticle was synthesized, displaying a matrix metalloproteinase-9 (MMP-9)-cleavable polymeric corona. These nanoparticles are able to respond to MMP-9 activity through the shedding of 10–20 nm of hydrodynamic diameter. This MMP-9-triggered decrease in nanoparticle size also led to up to a six-fold decrease in nanoparticle internalization by macrophages and is observable by T_2 -weighted magnetic resonance imaging. These findings guide the design of imaging or therapeutic nanoparticles for in vivo targeting of macrophage activity in pathologic states.

Keywords: macrophage targeting, poly(ethylene glycol) (PEG), poly(propylene sulfide) (PPS), iron oxides, opsonization

Introduction

As one of the most phagocytic cells in the human body, macrophages are among the first cells of the innate immune system to arrive at a site of injury, but also have been observed as permanent residents in certain organs, such as in the liver and bone marrow.^{1–3} They function to clear pathogens and microbes, as well as host cell and matrix debris that are present at sites of tissue injury. Macrophages recognize and interact with this multitude of potential targets through a variety of mechanisms, including phagocytosis and receptor-mediated endocytosis. The latter is mediated primarily through pattern recognition receptors, which include toll-like receptors, the mannose receptor (CD206), and scavenger receptor A (CD204).^{4–6} The polygamous nature of these pattern-recognition receptors is not restricted to natural ligands and targets. For example, CD204 has a wide range of molecular partners, leading to receptor-mediated endocytosis, distinct from the non-specific uptake due to pinocytosis.⁷ For the purposes of this manuscript, we have defined this polygamous behavior as “non-specific” uptake or internalization. This is emphasized by evidence that CD204 has been shown to contribute to the non-specific uptake of nanoparticles surface-functionalized with carboxylic acids, antibodies, as well as synthetic polymers.^{8,9} Therefore, the rational design of nanoparticles for in vivo use requires an application-driven minimization

Correspondence: Todd D Giorgio
Vanderbilt University, VU Station B,
Box 351631, Nashville, TN 37235, USA
Tel +1 615 343 1099
Fax +1 615 343 7919
Email todd.d.giorgio@vanderbilt.edu

or optimization of such non-specific interactions between macrophages and synthetic nanoparticles. However, this area remains largely uninvestigated.

Non-specific interactions between macrophage receptors and nanoparticles may be dictated by a variety of characteristics, including particle size, shape, surface charge, and hydrophobicity, and facilitated by surface chemistry-specific complement activation on the nanoparticle.^{10,11} Doshi and Mitragotri treated macrophages at 4°C with a library of polystyrene microparticles exhibiting a variety of sizes and shapes to mimic bacterial dimensions, and observed optimal attachment for rod-shaped particles with the longest dimension at 2–3 µm.¹¹ However, the smallest particles investigated were in the range of 500 nm; work with such nanoparticles has yet to be extended to the sub-100 nm dimensional range, which is of interest in many in vivo applications. Raynal et al showed that macrophages exhibit size-dependent uptake of nanoparticles functionalized with dextran, but macrophages can interact directly with dextran, as their expression of a dextran receptor (SIGNR1) was later documented.^{12,13}

Therefore, in this work, we sought to investigate non-specific uptake of synthetic nanoparticles by macrophages, extending the work of these earlier groups into sub-100 nm PEGylated nanoparticles. To our knowledge, this is the first investigation of the effects of nanoparticle size, surface chemistry, and charge on non-specific uptake by macrophages. The rationale for using a PEG-functionalized nanoparticle system to accomplish these objectives is that macrophages are unlikely to have specific receptors for poly(ethylene glycol) (PEG). Further, PEG can be easily modified to display various chemical functionalities, enabling the modulation of nanoparticle charge without significantly varying the bulk properties of the PEG coating. This is also a relevant model system for study because PEGylation of nanoparticles is commonly performed in order to render synthetic nanoparticles water-soluble and applicable for in vivo use. This is, in part, because PEG has been shown to discourage protein adsorption and opsonization on nanomaterial surfaces.¹⁴

Therefore, we used block copolymers of poly(ethylene glycol)-bl-poly(propylene sulfide) (PEG-PPS), which are amphiphilic copolymers that are capable of forming micelles and stabilizing hydrophobic drugs and nanoparticles at their liquid, PPS core.^{15,16} The incorporation of ultrasmall superparamagnetic iron oxides (USPIOs) into the micellar core of PEG-PPS block copolymers serves two functional purposes – enabling easy quantification of particle uptake through colorimetric assays, while also being a widely investigated contrast agent for T_2 -weighted magnetic resonance

imaging (MRI). Through the use of a variety of materials processing techniques to form the micelles, including thin film hydration and direct hydration, the same starting PEG-PPS copolymers and iron oxide cores can lead to monodisperse micelles (PEG-PPS-USPIOs) exhibiting hydrodynamic diameters at 30 nm, 40 nm, or 100 nm. Additionally, PEG-PPS-USPIOs can be fashioned with different surface chemistries at the PEG terminus, enabling an examination of charge-dependent non-specific uptake of nanoparticles by the macrophages.

To demonstrate the utility of these studies, we evaluated a protease-activity MRI probe design against these results. To make activity probes, PEG chains containing a protease-cleavable peptide substrate were synthesized and conjugated to PPS, in order to fashion surfactants for the micellization of USPIOs. The resulting nanoparticles are “activatable” by protease activity through a ≥ 10 nm decrease in hydrodynamic diameter. Macrophages are therefore expected to internalize protease-treated nanoparticles differently than untreated nanoparticles. We hypothesize that these differences can be visualized via MRI with the aid of the contrast agent USPIOs encapsulated within the micelles. Taken together, the work presented here shows methods to design ideal nanoparticle dimensions and properties in order to better optimize nanoparticle behavior in vivo.

Materials and methods

All reagents were purchased from Sigma-Aldrich (St Louis, MO) and used as purchased unless otherwise noted below. Matrix metalloproteinase-9 (MMP-9), MMP-9 inhibitor, Fmoc-protected L-amino acids, and resins for solid-phase peptide synthesis were purchased from EMD Biosciences (Gibbstown, NJ). PEG reagents were purchased from Laysan Biosciences (Arab, AL). All dialysis supplies were ordered from Pierce Scientific (Rockford, IL) and used with modifications to the factory-provided protocol as indicated in the appropriate sections below. Copper transmission electron microscopy (TEM) grids with Formvar film and uranyl acetate were purchased from Electron Microscopy Sciences (Hatfield, PA). GIBCO® RPMI-1640 medium, penicillin-streptomycin, and fetal bovine serum (FBS) were purchased from Life Technologies (Carlsbad, CA).

PEG-PPS block copolymers and functionalization

Synthesis of approximately 7 kDa carboxy-PEG-PPS (cPEG-PPS) was carried out as previously described.¹⁶ For fluorescent polymers, FITC-PEG-NH₂ was used

in place of cPEG-NH₂ in the coupling reaction to PPS. The MMP-9-cleavable peptide GGPQRQITAGC (M9C; Gly-Gly-Pro-Arg-Gln-Ile-Thr-Ala-Gly-Cys)¹⁷ was synthesized on a Rink-amide MBHA resin support, via standard Fmoc-based solid phase peptide synthesis on an automated system (Protein Technologies PS3, Tucson, AZ).¹⁸ The peptide (1.5 eq, 45 mmol) was then reacted overnight with 1 eq of 5 kDa methoxy-PEG-maleimide (mPEG-MAL; 30 mmol; 150 mg), in an aqueous buffer containing 0.1 M Na₃PO₄ and 0.15 M NaCl at pH 7.2. Unbound peptide was removed by dialysis across a 2 kDa molecular weight cutoff membrane overnight at room temperature. The completed mPEG-[M9C] conjugate was lyophilized, then coupled to cPEG-PPS via standard carbodiimide chemistry to yield mPEG-[M9C]-PEG-PPS block copolymers.

For Fourier transform infrared (FT-IR) spectroscopy, polymer samples were prepared by mixing with IR-grade KBr and pelleting on a KBr press (Specac, Slough, UK). FT-IR was performed on a Bruker Tensor 27 system (Billerica, MA).

Proton nuclear magnetic resonance (¹H NMR) spectra were obtained at 400 MHz using a 9.4 Tesla Oxford magnet operated by a Bruker AV-400 console. The main NMR probe for the instrument is a 5 mm Z-gradient broadband inverse (BBI) probe with automatic tuning and matching capability (ATM).

Gel permeation chromatography (GPC) was performed on three resolving columns running in series (1 × TSKGel Alpha4000, 2 × TSKGel Alpha3000; Tosoh Bioscience, King of Prussia, PA) with dimethylformamide (DMF) + 0.1 M LiBr mobile phase. Columns were incubated at 60°C, and chromatograms were obtained with a Shimadzu SPD-10A UV detector and RID-10A refractive index detector (Shimadzu Scientific Instruments, Columbia, MD), and a Wyatt miniDAWN Treos multi-angle light scattering detector (MALS; Wyatt Technology, Santa Barbara, CA). Data collection and analysis was achieved through the Wyatt ASTRA software (v 5.3.4).

Encapsulation of USPIOs in PEG-PPS copolymers

Synthesis of hydrophobic, monodisperse USPIO core particles and their encapsulation in PEG-PPS copolymers was carried out as previously described.¹⁶ In brief, USPIO cores of predictable diameters were first synthesized through thermal decomposition, by controlling the molar ratios of iron precursor to oleic acid introduced in the reaction feed (Supplementary Figure S1). A 1:2 mass ratio of dried

hydrophobic USPIO cores to PEG-PPS polymers were then dissolved in toluene, vortexed to mix, sonicated for 5 seconds to break apart clumps, and then dried by rotary evaporation for 20 minutes. The dried polymer/USPIO mixture was then rehydrated in 3 mL of nanopure water and vortexed vigorously to suspend all particulates. Large clumps and byproducts were removed by magnetic pelletting, and the colloidal phase was collected and further centrifuged at 2500 g for 5 minutes to precipitate excess polymers. The supernatant is gently aspirated by pipette into fresh scintillation vials and stored at 4°C.

To fabricate fluorescent micelles, a 1:40:20.5 mass ratio of FITC-PEG-PPS:PEG-PPS:iron oxide cores was mixed and micellized as described above. Therefore, the overall mass ratio of polymers to iron oxides is preserved at 1:2 for all micellization procedures. To make “proximity-activated” USPIOs (PA-USPIOs) – which are able to respond to local MMP-9 activity, OA-USPIOs were encapsulated in MMP-9-cleavable mPEG-[M9C]-PEG-PPS polymers using the same protocol.

Pluronic®-PPS nanoparticles and loading with USPIOs

Pluronic-stabilized PPS nanoparticles (NPs) were synthesized by inverse emulsion polymerization as described previously.^{10,19} Pluronic F-127 (a block copolymer of polyethylene glycol and polypropylene glycol terminated by α and ω hydroxyl groups) was used alone or in combination with carboxyl-terminated Pluronic derivatized as previously described.²⁰ The hydrophobic core was stabilized by disulfide crosslinking of the linear PPS chains.¹⁹ However, since crosslinking cannot reach completion, remaining free sulphydryl groups on the NP surface were irreversibly capped by reaction with the alkylating reagent iodoacetamide. NP solutions were sterile-filtered, and then loaded with 3 nm USPIO cores through a direct hydration process. Then 100 μ L of the hydrophobic OA-USPIOs (20 mg/mL in tetrahydrofuran [THF]) was added to 1 mL of the Pluronic-PPS NPs (15 mg/mL in water) with swirling, and was followed by removal of THF by rotary evaporation, and removal of non-encapsulated OA-USPIOs by filtration through 0.45 μ m Teflon filters (Whatman Inc, Piscataway, NJ).

Nanoparticle characterization

Size and ζ -potential of NPs were investigated by dynamic light scattering (DLS) in a Malvern Zetasizer Nano-ZS with the reusable dip-cell kit (Malvern Instruments Ltd, Worcestershire, UK). For measurements of ζ -potential in

serum media, nanoparticles were mixed with THP-1 growth medium and allowed to incubate at 37°C for 24 hours prior to DLS measurements. No further purification of the nanoparticles was performed. This is because the purification process ends up diluting the particles (along with the adsorbed proteins), and may lead to further protein exchange interactions with media used downstream of isolation procedures, as per the Vroman effect.¹⁴ Therefore, in order to best mimic in vivo conditions, the nanoparticles were measured in the presence of serum. Measurements of hydrodynamic diameter demonstrated the presence of a peak at <5 nm that corresponded to proteins, while nanoparticles could still be easily discerned within the 20–100 nm diameter range.

Transmission electron microscopy (TEM) was conducted on a Philips CM20 system (Amsterdam, the Netherlands) operating at 200 kV. Carbon film-backed copper grids were inverted onto droplets containing nanoparticle suspensions of interest and blotted dry. Images were collected using a CCD camera with AMT Image Capture Engine software (v 600.335h built on 29 Apr 2010; Advanced Microscopy Techniques, Danvers, MA), and sizing of the particles was automated using a particle analyzer on ImageJ software (v 1.43u). Images were thresholded, and then the built-in (Analyze Particles) function was used to measure the major and minor axes of the fit ellipses around each particle. After artificially discarding clumps of particles encompassed within single fit ellipses (usually identified by major and minor axes that were >10% different from one another), or ellipses drawn around globs in the carbon grid (usually identified by any dimension <1 nm), the diameter of individual particles was taken to be the average of the major and minor axis.

For aqueous samples, nanoparticles on TEM grids were also counterstained with 3% uranyl acetate in water for 2 minutes, gently blotted dry, and dried in a vacuum desiccator for 2 hours prior to imaging.

Cell culture and nanoparticle co-incubation experiments

Non-adherent THP-1 human leukemic monocytes (American Type Culture Collection, Manassas, VA) were grown in RPMI-1640 medium supplemented with 10% FBS, 1% penicillin-streptomycin, 1 × MEM vitamins (Mediatech, Manassas, VA), 120 μM β-mercaptoethanol, and 10 mM HEPES® (Sigma-Aldrich) at 37°C in a 5% CO₂ incubator. For all cell experiments, monocytes were seeded into standard tissue culture-treated plates at a density of 300,000 cells/cm², and differentiated for 3 days in growth medium (above) supplemented with 200 nM of phorbol myristate acetate (PMA).

The differentiation process leads to induction of cell adherence onto tissue culture polystyrene surfaces.

For nanoparticle co-incubation experiments, cells were washed once with phosphate buffered saline (PBS) to remove unbound cells, prior to addition of growth medium. The medium was supplemented with nanoparticles and fucoidan. Nanoparticle dosing was based on total iron concentration as measured through the colorimetric phenanthroline assay as previously described.²¹ Final iron concentrations in the wells were calculated to be between 30 μM and 200 μM. For fucoidan competition experiments, media was supplemented with fucoidan to a final concentration of 0–500 μM.

At selected time points, cells were washed three times with PBS to remove unbound nanoparticles, and then lysed in 3 N HCl and 0.25% Triton X-100 for at least 2 hours. The strongly acidic environment also promotes solubilization of the endocytosed USPIOS via oxidation of the amphiphilic PEG-PPS shell on the nanoparticles into fully hydrophilic polymers,¹⁹ as well as leaching and mineralization of the iron in the USPIO core. The cell lysate was analyzed for protein content using a commercial Lowry protein assay kit (Bio-Rad Laboratories, Hercules, CA), while iron content was measured using the colorimetric phenanthroline assay as previously described.²¹ While the acidic conditions for the Lowry protein assay deviate significantly from the protocol described by the supplier (alkaline conditions), this does not significantly affect the sensitivity or results of the assay (Supplementary Figure S2).

Calculation of nanoparticle internalization was dependent upon nanoparticle type, as shown in Table 1. The rationale behind the two different measurement types is inherent to the loading efficiencies possible. Because PEG-PPS-USPIO samples are purified, all cell-nanoparticle interactions in experiments involving them involve an iron “tag”. However, since Pluronic-PPS-USPIOS are a subpopulation of the nanoparticles used in this system, not all cell-nanoparticle interactions here involve the iron tag. Due to differing USPIO loading efficiencies across the different Pluronic-PPS surface chemistries available to us, an additional normalization method was required in order that resulting figures fully represented charge-dependent uptake of nanoparticles. The normalization of internalization data to the initially administered dose of iron was therefore used to report internalization of Pluronic-PPS-USPIOS (Table 1).

For cell viability experiments, cells were incubated for 24 hours with PEG-PPS-USPIOS, at a final iron dose of 30 μM, 60 μM, or 120 μM. After rinsing cells three times with PBS to remove unbound nanoparticles, they were

Table I Quantification of nanoparticle uptake into THP-1 cells

Nanoparticle type	Required measurements	Units	Equation	Rationale
PEG-PPS-USPIOS	[Fe] and [Protein] in cell lysates	µg Fe/mg protein	$\frac{[Fe]}{[Protein]}$	Result is a quantity normalized to cell number, but reflects dose-dependence and cell number-dependence of quantified internalization
Pluronic-PPS-USPIOS	[Fe] and [Protein] in cell lysates, and $[Fe]_0$ (concentration of iron administered at time 0)	%/mg protein	$\left(\frac{[Fe]}{[Fe]_0} \right) \times 100$	Different surface chemistries led to differing loading efficiencies of Pluronic-PPS nanoparticles with USPIOS. Quantification method enables experiments to be run at constant nanoparticle concentrations, without worry of effects of different loading efficiencies on measured iron internalization

Notes: PEG-PPS-USPIO internalization data was also represented as %ID/mg once in this manuscript (Figure 3E) in order to facilitate comparison of results.

Abbreviations: PEG, poly(ethylene glycol); PPS, poly(propylene sulfide); USPIO, ultrasmall superparamagnetic iron oxides.

stained with a commercial calcein-AM/ethidium homodimer live/dead assay kit (Invitrogen, Carlsbad, CA), and quantified according to the manufacturer's instructions.

Protease-activatable nanoparticles

"Proximity-activated" USPIOS (PA-USPIOS) – which are able to respond to local MMP-9 activity, were formed as described for other PEG-PPS-USPIOS above. For protease experiments, 50 µL PA-USPIOS (iron dose = 600 µM) were incubated with 10 µL MMP-9 (final concentration = 2 µg/mL) in an aqueous buffer containing 0.1 M HEPES, 0.15 M NaCl, and 5 mM CaCl₂ (pH 7.2) for 24 hours at 37°C. For control experiments, PA-USPIOS were incubated with buffer only. Following cleavage, nanoparticles were added directly to cell cultures. The final concentration of iron and MMP-9 in the cell cultures were 120 µM and 400 ng/mL, respectively. In some control experiments, MMP-9 inhibitor was also added to the cell cultures, to a final concentration of 300 ng/mL.

Magnetic resonance imaging (MRI)

MRI was performed on a Varian 4.7 T horizontal bore imaging system. *T*₂ signal decay was measured using a Carr-Purcell-Meiboom-Gill (CPMG) spin-echo pulse sequence with N = 8 echoes with 6.5 ms echo spacing. The signal from each voxel at the eight imaging time points was fit to a mono-exponential signal decay model to determine *T*₂ for each voxel:

$$S = S_0 e^{-\frac{t}{T_2}} \quad (1)$$

A region of interest (ROI) was manually drawn using MATLAB (MathWorks, Inc, Natick, MA) for the first imaging time point and translated to the images from later echoes. The mean *T*₂ and standard deviation for each well

was then calculated from all voxels within this ROI. Other imaging parameters included TR = 2 seconds, field of view = 22 mm × 22 mm, data matrix = 128 × 128, slice thickness = 1 mm, number of acquisitions = 24 (total scan time approximately 1 hour 45 minutes).

To prepare cells for MRI, the supernatant containing unbound nanoparticles in medium was aspirated and replaced with PBS, prior to scraping of the cells into the buffer (Corning Life Sciences, Lowell, MA). Cells were centrifuged into a pellet at 300 g for 5 minutes, and rinsed with PBS twice more. Cells were then fixed with 10% buffered formalin, gently mixed, and allowed to incubate for 30 minutes at room temperature before they were pelleted and imaged.

Results and discussion

The primary objective of this study was to investigate size- and charge-dependent non-specific uptake of nanoparticles by macrophages. With the targeted size range being in the sub-100 nm hydrodynamic diameter range, the objectives required the synthesis of a library of highly monodisperse, water-soluble nanoparticles in order to reduce size overlap between different nanoparticle formulations and elucidate trends between size and uptake. Therefore, USPIO cores were synthesized by thermal decomposition in organic solvents, which led to oleic acid-stabilized USPIOS (OA-USPIOS) of 3.0 ± 0.4 nm (Figure 1A, n approximately 200) and 12.0 ± 1.0 nm (Figure 1B, n > 400). Control over USPIO core diameters was accomplished by adjusting the molar ratios of oleic acid surfactant to iron pentacarbonyl precursor in the reaction feed, and to date, we have synthesized OA-USPIOS of up to 24 nm in diameter using this method (Supplementary Figure S1). These results extend previous work by Woo et al,²² who showed the ability to synthesize particles from 5 nm to 19 nm in diameter using this same exact method. Additionally, we were also able to scale up this original synthesis and now are able to produce the uniform OA-USPIOS in 1 g amounts.

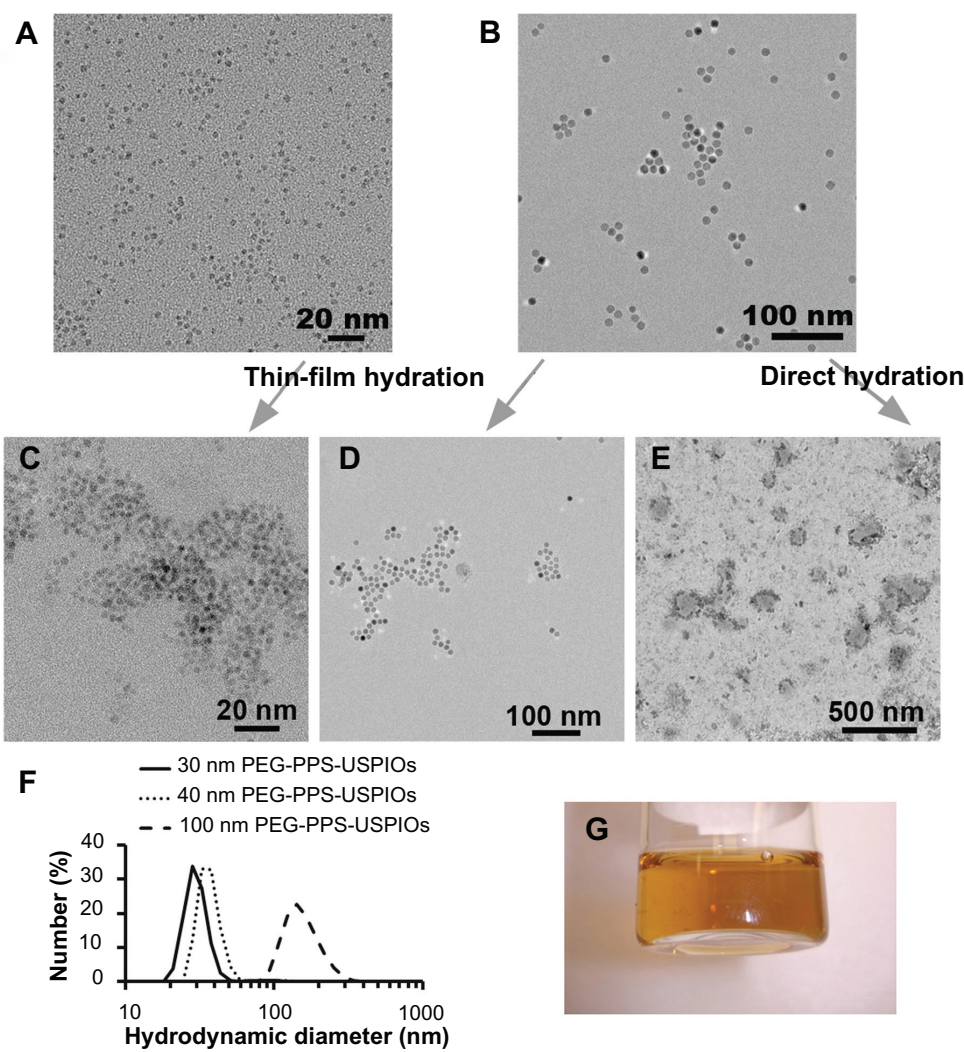


Figure 1 Characterization of USPIOs and PEG-PPS-USPIO micelles. HRTEM images of (A) 3 nm and (B) 12 nm hydrophobic, oleic acid-stabilized USPIO cores ($\gamma\text{-Fe}_3\text{O}_4$), which were synthesized via thermal decomposition. To render particles water-soluble, they were coated with PEG-PPS block copolymers via thin-film hydration to yield, respectively, (C) 30 nm and (D) 40 nm PEG-PPS-USPIO micelles. (E) 100 nm PEG-PPS-USPIO micelles can also be synthesized via direct hydration using the same feed materials used to create micelles in (D); this TEM image has been counterstained with 3% uranyl acetate. (F) Size-number distributions of these PEG-PPS-USPIO micelles were obtained by dynamic light scattering. (G) As shown in this representative photograph, 40 nm PEG-PPS-USPIOs remain stable in water and do not flocculate even after storage at room temperature over 4 months.

Note: Scale bars: (A and C) 20 nm; (B and D) 100 nm; (E) 500 nm.

Abbreviations: HRTEM, high resolution transmission electron microscope; PEG, poly(ethylene glycol); PPS, poly(propylene sulfide); TEM, transmission electron spectroscopy; USPIO, ultrasmall superparamagnetic iron oxides.

To render the OA-USPIOs water-soluble, either a thin-film hydration or a direct hydration method was employed, effectively encapsulating OA-USPIOs within micelles composed of amphiphilic PEG-PPS block copolymers (1.65 kDa PPS block, 4.2 kDa PEG block; Figure 1C–E). Prior to cell experiments, the micelles were sterile-filtered; size-number distributions of the completed USPIO-loaded micelles are shown in Figure 1F. However, due to the larger size of the 100 nm micelles, these materials tended to be caught in the Teflon filters and were thus used as synthesized. The 30 nm and 40 nm micelles were particularly stable in water and flocculated minimally even after storage for several months

at room temperature (Figure 1G). These two formulations were also extremely difficult to pellet by centrifugation or through the influence of an externally-applied 1 T neodymium magnet. The completed micelles exhibited ζ -potentials that were weakly anionic (Table 2), owing partly to the terminal mono-methyl ether group on the PEG block that is displayed on the nanoparticle surface.

Nanoparticles were next administered to THP-1 human leukemic macrophages in order to establish a quantitative basis for the remainder of the experiments, while also examining the kinetics of particle uptake. THP-1 cells were chosen for this study because uptake and processing of lipid nanoparticles by

Table 2 Size and ζ -potential of as-synthesized PEG-PPS-USPIO micelles

Sample name	USPIO core diameter (nm)	Micelle diameter range (nm) ^a	ζ -potential (mV)
30 nm PEG-PPS-USPIOS	3	30.0 ± 2.6	-2.8 ± 5.9
40 nm PEG-PPS-USPIOS	12	36.6 ± 11.9	-1.7 ± 4.6
100 nm PEG-PPS-USPIOS	12		-7.8 ± 5.1

Notes: ^aDetermined after filtration through a 0.45 μ m PTFE filter. 100 nm PEG-PPS-USPIOS were not as stable to filtration and were not subjected to this additional treatment step prior to use in cell experiments.

Abbreviations: PEG, poly(ethylene glycol); PPS, poly(propylene sulfide); USPIO, ultrasmall superparamagnetic iron oxides.

THP-1 and primary human monocyte-derived macrophages is not significantly different between the two cell types.^{23,24} We expected, therefore, that macrophage interactions with synthetic nanoparticles can be similarly modeled through this readily available, *in vitro* system.

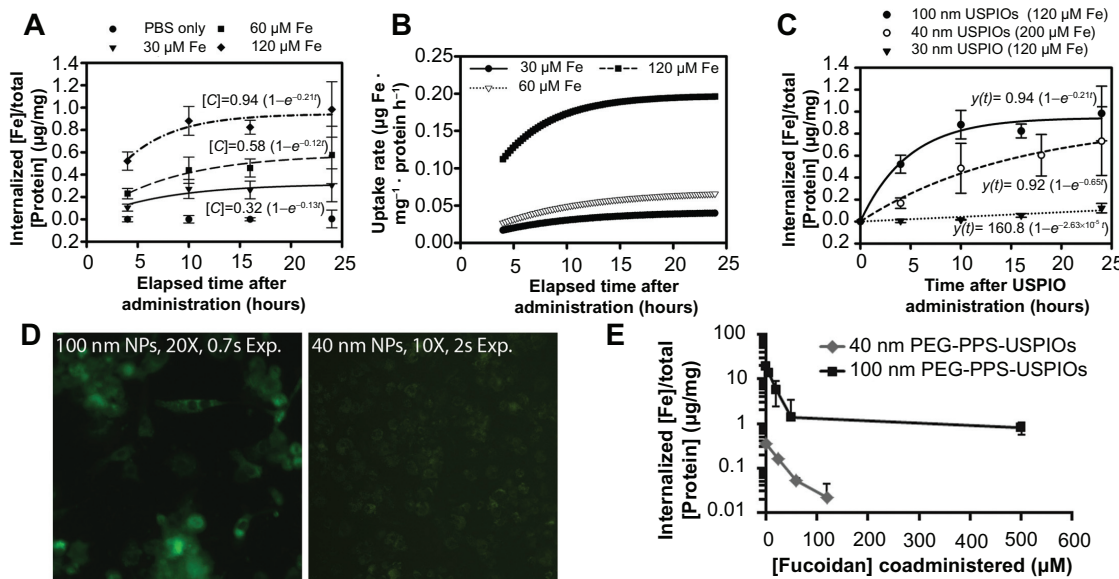


Figure 2 Dose- and size-dependent internalization of PEG-PPS-USPIOS by THP-1 macrophages. THP-1 cells were treated for up to 24 hours with standard growth serum medium supplemented with varying doses of PEG-PPS-USPIOS in PBS. As a negative control, PBS was used in place of the PEG-PPS-USPIO colloidal suspension. Iron internalization and initial doses were quantified using a colorimetric phenanthroline assay, and internalized iron content was normalized to cell number indirectly via a protein assay. (A) Internalization of nanoparticles over the time period of interest is described by first-order rate kinetics, indicating that initial dose of nanoparticles is the primary determinant of internalization rate and total internalization amount. Relative to the initial doses of USPIOS, macrophages receiving 30 μ M, 60 μ M, and 120 μ M of iron endocytosed 8.4% ± 3.7%, 7.7% ± 3.2%, and 6.2% ± 0.9% of the maximum possible USPIOS, respectively. Error bars indicate standard deviations from six independent experiments. (B) Derivatives of the best-fit kinetic equations plotted in (A) demonstrate further the dependence of uptake rate on initial dose of PEG-PPS-USPIOS. (C) Of the three sizes investigated, 100 nm nanoparticles were most effectively internalized by the macrophages. Smaller nanoparticles were internalized less effectively, and 30 nm nanoparticles experienced almost negligible uptake levels over the 24 hour experimental period. Normalization of the 24 hour uptake amounts to the initially administered doses shows that macrophages internalized 6.2% ± 0.9%, 1.4% ± 2.3%, and 1.1% ± 0.3% of the 100 nm, 40 nm, and 30 nm PEG-PPS-USPIOS, respectively. Error bars represent standard deviation from three to six independent experiments. (D) Fluorescent imaging of the delivery of 40 nm and 100 nm fluorescent PEG-PPS-USPIO micelles. The uptake of 100 nm nanoparticles was easily visualized at 20X magnification with a 0.7 second exposure time, but even with a lower magnification and roughly a three-fold higher exposure time, the microscope was insufficiently sensitive to visualize the internalization of the 40 nm nanoparticles. (E) 40 nm PA-USPIOS (at 200 μ M Fe) or 100 nm PEG-PPS-USPIOS (at 120 μ M Fe) were co-administered to THP-1 macrophages with varying amounts of fucoidan for 24 hours, and allowed to incubate overnight prior to cell lysis and measurement of internalized iron. Increasing concentrations of fucoidan correlated with decreased uptake of the nanoparticles, suggesting that the mechanism of PEG-PPS-USPIO uptake is via receptor-mediated endocytosis, and facilitated by the scavenger receptor CD204. Error bars represent standard deviation of three independent experiments.

Abbreviations: PA-USPIOS, proximity-activated ultrasmall superparamagnetic iron oxides; PBS, phosphate buffered saline; PEG, poly(ethylene glycol); PPS, poly(propylene sulfide); THP, human acute monocytic leukemia cell line.

As an example, varying doses of the 100 nm PEG-PPS-USPIOS were administered to THP-1 macrophages. Because first-order rate equations are often used as governing equations in efforts to model receptor-mediated endocytosis of nanoparticles by macrophages,²⁵ the resulting 24-hour uptake profiles (Figure 2A) were fit to first-order rate kinetic equations (Figure 2A and B). The successful curve-fit suggested that USPIO concentration is the primary determinant of uptake rate. The best-fit equations take the form:

$$[C] = [C]_{\max}(1 - e^{-kt}) \quad (2)$$

where $[C]_{\max}$ represents the maximum possible concentration of iron in the cells and $[C]$ is a measure of the accumulated iron content in the cells. As the fit equations show (Figure 2A), the calculated $[C]_{\max}$ values are proportional to the initially administered doses of PEG-PPS-USPIOS (standard errors < 13%), while the calculated rate constants k do not vary significantly across the doses (standard

errors 25%–40%). Relative to the initial doses of USPIOs, macrophages receiving 30 μM , 60 μM , and 120 μM of iron endocytosed $8.4\% \pm 3.7\%$, $7.7\% \pm 3.2\%$, and $6.2\% \pm 0.9\%$ of the maximum possible USPIOs, respectively. In order to ensure that the measurements excluded USPIO binding events not resulting in uptake, some experiments were also conducted at 4°C to block endocytosis, resulting in insignificant iron levels quantified in the lysates (Supplementary Figure S3). In addition, a live/dead cytotoxicity assay was also conducted in order to confirm that treatment of macrophages with the PEG-PPS-USPIOs resulted in minimal cell death (Supplementary Figure S4).

Similar nanoparticle uptake kinetics were also observed for particles of smaller hydrodynamic diameters (Figure 2C). The results also show that by mass, smaller nanoparticles are internalized less effectively than their larger counterparts. The 40 nm nanoparticles shown in this graph were based on a higher iron dose for easier visualization; however, the same nanoparticles, administered at the same 120 μM Fe dose as the other two samples, were internalized at $0.36 \pm 0.55 \mu\text{g}/\text{mg}$ protein (curve not shown). Normalization of the 24-hour uptake data to the initially administered doses shows that THP-1 macrophages were able to internalize $1.1\% \pm 0.3\%$, $1.4\% \pm 2.3\%$, and $6.2\% \pm 0.9\%$ of the 30 nm, 40 nm, and 100 nm PEG-PPS-USPIOs, respectively. When nanoparticle internalization is normalized to cell number, a 70% decrease in PEG-PPS-USPIO diameter corresponded with almost a ten-fold decrease in iron uptake per cell. This was supported by fluorescence microscopy experiments, where macrophages were treated with FITC-tagged nanoparticles (Figure 2D), demonstrating the accumulation of 100 nm micelles within the macrophages. Despite longer exposure times at a lower magnification, the microscope was insufficiently sensitive to visualize the internalization of the 40 nm micelles by the macrophages. Taken together, these data suggest a positive correlation between nanoparticle size and their non-specific recognition and internalization by macrophages.

Given the lack of any specific targeting moieties on the micelle surface, this evidence suggested that within the nanoparticle size range investigated, macrophages were able to optimally recognize and internalize PEGylated nanoparticles of >100 nm diameter. Further, smaller nanoparticles seemed to experience significantly less non-specific uptake by the macrophages. One of the mechanisms of uptake is likely through receptor-mediated endocytosis via CD204 – as PEG-PPS-USPIO internalization can be effectively blocked by co-administration of nanoparticles with fucoidan, which is a well-known CD204 ligand (Figure 2E).⁴

We next investigated the effects of nanoparticle charge on non-specific uptake. Because the sub-40 nm nanoparticles provided a satisfactorily minimal baseline uptake over 24 hours, we opted to focus on nanoparticles of this size for this section of the study. End-carboxylated, -aminated, and -thiolated Pluronic were used as surfactants in inverse emulsion polymerization as described previously.¹⁰ The resulting Pluronic-PPS nanoparticles were loaded with USPIOs via direct hydration (Figure 3A–C), and delivered to THP-1 macrophages under the same conditions described for the other cell experiments above. Since Pluronic polymers are PEG-containing block co-polymers, the properties of Pluronic-PPS are not very different from those of PEG-PPS used in the other studies shown here, and, in effect, still produce PEG-PPS-coated USPIOs. Pluronic-PPS enables facile synthesis schemes necessary to produce the various end-functionalized polymers used in this work that would otherwise be more difficult to generate from PEG-PPS coatings.¹⁹

In order to account for differences in USPIO loading efficiencies across the library of Pluronic-PPS nanoparticle formulations, uptake was not only reported as $[\text{Fe}]/[\text{Protein}]$ as above, but further normalized to initial doses of iron and reported as percent injected dose/protein (%ID/mg protein; Figure 3D, Table 1). We hypothesized that this system would enable us to parse out the roles of surface charge from size on nanoparticle internalization, leading us to identify the sensitivity of size and charge on nanoparticle non-specific uptake by macrophages.

The Pluronic-PPS-USPIOS initially exhibited surface charges from -23 mV up to $+9$ mV, but following incubation in 10% serum media for 4 hours, all nanoparticle formulations experienced significant changes in ζ potential (Figure 3D). Therefore, while the ζ potential of the nanoparticles was tunable to some extent by varying the surface chemistry of the nanoparticles, electrostatic interactions with serum proteins and components, as well as protein adsorption and opsonization processes contributed to significant changes in nanoparticle properties. The addition of serum into the incubation medium for these studies is intended to reflect an interaction environment that includes important components of the *in vivo* environment. Since there is no opportunity for nanoparticle purification following intravenous injection, we elected to allow nanoparticle interaction with serum proteins during ζ potential measurements, and later on, incubation with THP-1 cells. One outcome of this approach, and equally true *in vivo*, is the modulation of initial nanoparticle ζ potential by serum protein adsorption. These processes have been studied in detail for the Pluronic-PPS nanoparticle system, as

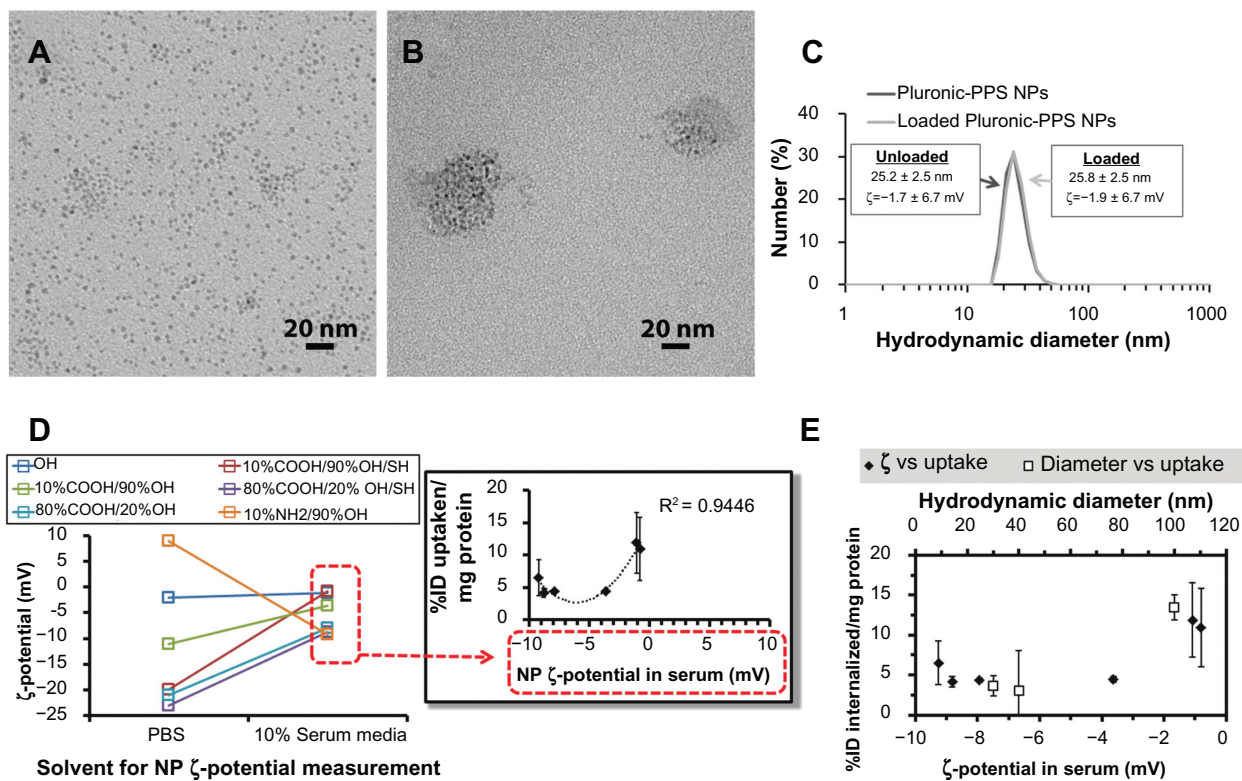


Figure 3 Effects of nanoparticle surface charge and chemistry on macrophage uptake. Representative TEM images of (A) hydrophobic, unloaded 3 nm OA-USPIOs and (B) water-soluble Pluronic-PPS nanoparticles after loading with the OA-USPIOs. (C) The loading process does not significantly affect the hydrodynamic diameters or the ζ potentials inherent to the Pluronic-PPS nanoparticles. (D) ζ -potential of all nanoparticle formulations (color-coded by surface chemistry) was originally measured in PBS following synthesis, and again following incubation in 10% serum media. While modulation of surface chemistry allows for a wide range of ζ -potentials, this range is compressed due to interactions between nanoparticles and media components. Uptake of nanoparticles correlated with their surface charge as measured in media (inset; red dotted boxes indicate source of data for x-axis), according to a parabolic distribution. To account for differences in USPIO loading efficiency across the different Pluronic-PPS nanoparticle formulations, nanoparticle uptake was normalized to the initial dose administered as well as cell content indirectly, via a protein assay. Error bars indicate standard deviation for three independent experiments. (E) Cell internalization data is plotted versus nanoparticle ζ -potentials measured in 10% serum media (solid squares). In order to determine which nanoparticle feature may be more determinant of non-specific interactions with macrophages, the effects of nanoparticle diameter have also been plotted for comparison (open squares).

Abbreviations: OA-USPIOs, oleic acid-stabilized ultrasmall superparamagnetic iron oxides; PBS, phosphate buffered saline; PPS, poly(propylene sulfide); TEM, transmission electron microscopy.

reported by Thomas et al.¹⁰ In particular, varying the surface chemistry of this nanoparticle system influenced the ability of the nanoparticles to become functionalized with the C3 complement proteins.¹⁰ More generally, this phenomena is well known in the synthetic gene delivery field, in which cationic nanoscale carriers of pDNA or siRNA rapidly interact with albumin and other serum proteins *in vivo*, and is consistent with the findings reported here.²⁶ This is significant because many consider that a minimum ζ potential of ± 30 mV is necessary in order to form stable nanoparticle suspensions.²⁷ Because electrostatic interactions and adsorption processes between serum proteins and the nanoparticle surface are inevitable following *in vivo* administration, higher ζ potential magnitudes may actually promote these processes, and in turn, opsonization processes ultimately leading to nanoparticle clearance from the bloodstream.

The observed decrease in the magnitude of the nanoparticle ζ potentials did not correspond with increased

agglomeration, as no flocculation or sedimentation was observed in any of the samples following treatment with serum. This observation was true of all nanoparticle formulations regardless of surface chemistry, possibly owing to the colloidal stability of Pluronic-PPS nanoparticles as shown previously.¹⁹

The two formulations that were most efficiently internalized were the nanoparticles displaying the terminal OH ($12\% \pm 5\%$ ID/mg protein) and the 10%COOH/90% OH/SH ($11\% \pm 5\%$ mg). Uptake correlated with nanoparticle charge as measured in serum, yielding a parabolic trend with maximum uptake observed for cationic and strongly anionic nanoparticles (Figure 3D, $R^2 = 0.94$, inset). However, because interactions with serum compressed the range of nanoparticle ζ potentials, we were unable to experimentally explore uptake of the nanoparticles beyond the -10 mV to 0 mV range. Despite the narrow window of ζ potentials covered by the data, the trends suggest that

non-specific uptake of nanoparticles may be promoted by nanoparticle cationicity or high anionicity. This is consistent with previous observations.¹³

Uptake of nanoparticles in serum was minimized in the range of ζ potentials from -9.0 mV to -3.5 mV. A three-fold increase in uptake was measured for identically sized nanoparticles having ζ potentials in serum from -3.5 mV to -0.8 mV, representing a 77% decrease in anionicity. In comparison, a four-fold change in uptake was observed for a 60% decrease in PEG-PPS-USPIO diameter (100 nm to 40 nm). Over these ranges and conditions, macrophage uptake of these nanoparticles is 42% more sensitive to size than to ζ potential (Figure 3E).

To expand on this conclusion, we synthesized PEG-PPS-USPIOS containing an MMP-9-degradable peptide (M9C) within the PEG chain (Figure 4A and B). This design results in particles that respond to active MMP-9 in the environment by releasing a layer of PEG, effectively leading to a decrease in nanoparticle diameter. Probes for MMP-9 activity are of wide interest because of the upregulation of MMP-9 in the progression of atherosclerosis.^{28–30} Based on the studies described earlier, we hypothesized that this experimental contrast agent would experience less uptake by macrophages following treatment with MMP-9, relative to the as-synthesized, intact form.

These MMP-9-responsive contrast agents were synthesized by encapsulating 10 nm and 3 nm OA-USPIOS using approximately 10 kDa mPEG-[M9C]-PEG-PPS (subsequently referred to as “PA” for protease-activatable), to produce 60 nm and 30 nm PA-USPIOS (Figure 4C and D). Both PA-USPIO formulations responded to MMP-9 treatment with a 10–20 nm decrease in nanoparticle hydrodynamic diameters as measured by DLS, while ζ -potentials were not significantly affected (30 nm PA-USPIOS: -3.9 ± 6.4 mV pre-cleavage, -2.8 ± 5.9 mV post-cleavage; 60 nm PA-USPIOS: 0.0 ± 7.1 mV pre-cleavage, -4.7 ± 5.5 mV post-cleavage). For cell experiments, PA-USPIOS were incubated with MMP-9 for 24 hours prior to their administration to THP-1 cells at equivalent iron doses. In both cases, MMP-9-treated PA-USPIOS were internalized significantly less effectively than their non-cleaved counterparts (Figure 4E). Most notably, the 30 nm PA-USPIOS experienced a six-fold decrease in nanoparticle uptake following MMP-9 cleavage (0.12 ± 0.04 $\mu\text{g Fe}/\text{mg protein}$ pre-cleavage vs 0.02 ± 0.02 $\mu\text{g}/\text{mg}$ post-cleavage). Also of note is the slightly higher uptake of the MMP-9-treated 60 nm PA-USPIOS (final diameter = 40.0 ± 6.2 nm) relative to the untreated 30 nm PA-USPIOS (30.0 ± 2.6 nm).

Because these changes in nanoparticle internalization may be due to MMP-9-mediated modifications on the cell membranes, a series of control experiments were also performed, using non-cleavable, 40 nm PEG-PPS-USPIOS (Supplementary Figure S5). In these experiments, co-administration of non-cleavable nanoparticles with MMP-9 did not lead to significant differences in nanoparticle internalization. Further, co-administration with a MMP-9 inhibitor also did not affect internalization. Taken together, the results suggest that the variations in PA-USPIO internalization by the THP-1 cells were attributable to the size of the nanoparticles, as the nanoparticle ζ potentials did not vary significantly before versus after treatment with MMP-9. Further, cellular capacity for nanoparticle internalization was unaffected by exposure to protease.

To determine if these MMP-9-dependent differences in nanoparticle internalization result in statistically significant changes in sample T_2 relaxation, and therefore, clinically relevant detection of MMP-9 activity in cell samples, 60 nm PA-USPIO-treated cells were pelleted and imaged on a 4.7 T magnetic resonance imaging scanner (Figure 4F). Through the use of a CPMG spin-echo pulse sequence, MMP-9-treated PA-USPIOS appeared to exhibit higher mean gray intensities versus cells incubated with untreated PA-USPIOS.

While the PA-USPIOS exhibited $T_2 = 4.82 \pm 0.02$ ms, the PA-USPIOS on the macrophages exhibited $T_2 = 23.2 \pm 3.5$ ms. These rather strong changes in T_2 are somewhat surprising assuming that approximately 1% of the administered dose was taken up by the macrophages as measured in the earlier sections of this work. This implies that for each imaging slice, the concentration of iron responsible for T_2 signal modulation within that slice is about 100-fold less in the nanoparticle-treated cell samples versus the positive control. To quantify this phenomenon, the calculated values above (from first-principle measurements) can be plugged into the R_2 relaxivity equation:

$$R_2 = \frac{1}{T_2 \times [Fe]} \quad (3)$$

in order to produce a measure of how effective the USPIOS are in modulating the local negative contrast. Given that measured T_2 in the cell samples is only approximately five times higher than the measurements in the positive control, the iron concentration in the cell samples would need to be about a fifth of the concentration in the positive control in order to maintain the same R_2 value. As we have seen, this

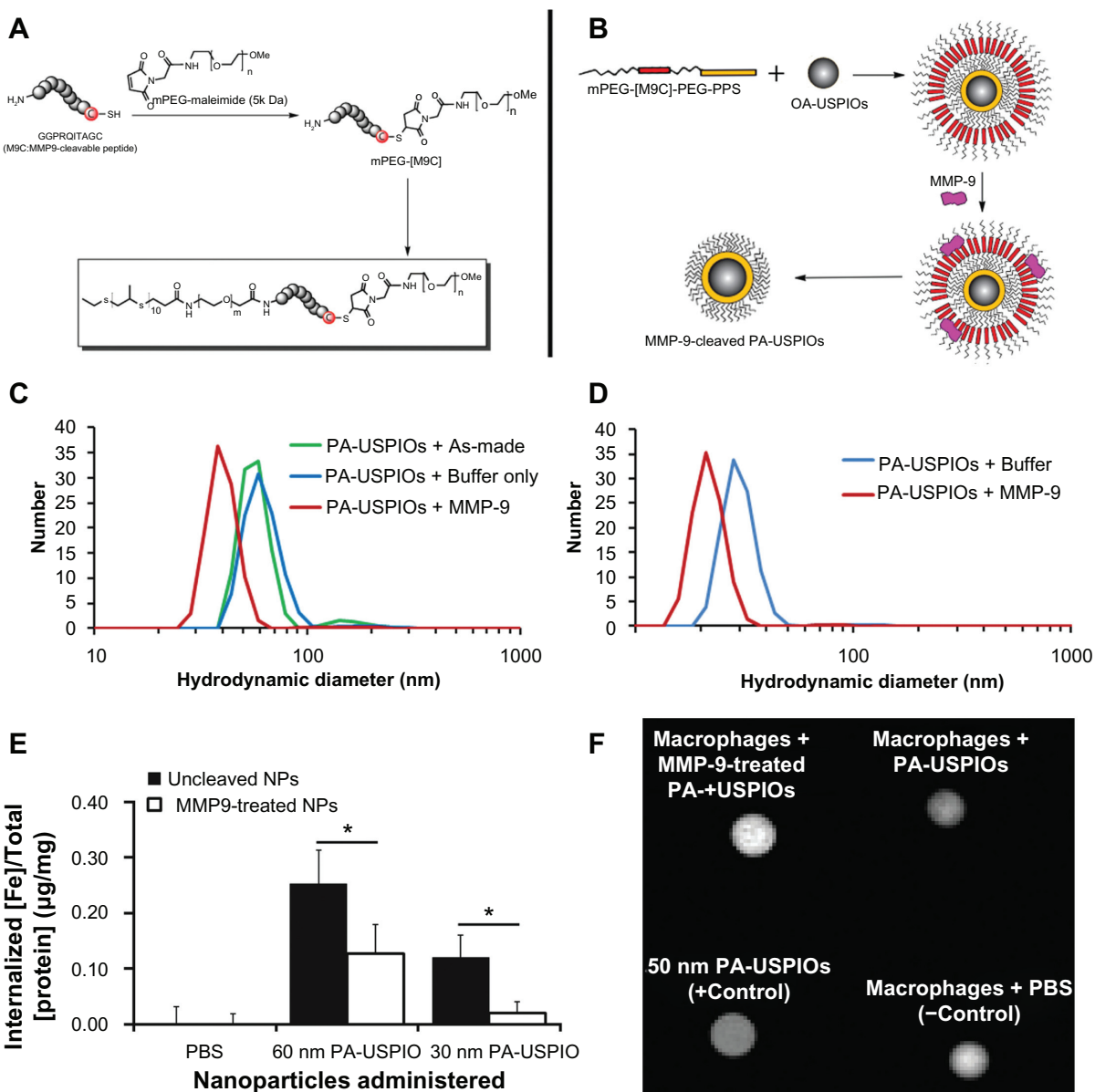


Figure 4 Behavior of MMP-9-responsive PA-USPIOs. **(A)** Synthesis of MMP-9-cleavable PEG-PPS chains (mPEG-[M9C]-PEG-PPS; PA) and **(B)** encapsulation of USPIOs to form PA-USPIOs. MMP-9 is able to recognize and cleave the (M9C) peptide sequence, resulting in release of a layer of PEG from the nanoparticle surface, accompanied by a decrease in nanoparticle hydrodynamic diameter. **(C)** DLS characterization of hydrodynamic diameters of as-synthesized 60 nm PA-USPIOs (**C**; green) and 30 nm PA-USPIOs (**D**; blue) demonstrates a loss in hydrodynamic diameter following treatment with MMP-9. **(E)** Buffer-treated or MMP-9-pretreated nanoparticles were delivered to THP-1 macrophages for 24 hours in standard growth medium. As a control, PBS was used in place of the nanoparticles. For both PA-USPIO formulations tested, the decrease in nanoparticle size following MMP-9 treatment results in less effective nanoparticle internalization by the macrophages. Error bars represent standard deviations from three to six independent experiments. **(F)** T_2 -weighted MRI of THP-1 cells treated with MMP-9-cleaved PA-USPIOs appeared brighter than cells incubated with untreated PA-USPIOs, indicating that less cleaved nanoparticles were internalized by the macrophages versus the untreated PA-USPIOs.

Note: * $P < 0.05$ by Student's t-test.

Abbreviations: DLS, dynamic light scattering; MMP-9, matrix metalloproteinase-9; PA-USPIOs, proximity-activated ultrasmall superparamagnetic iron oxides; MRI, magnetic resonance imagery; PBS, phosphate buffered saline; PEG, poly(ethylene glycol); PPS, poly(propylene sulfide).

is hardly the case, and based on our data, we can conclude that the R_2 values in the cell sample would have to be on the order of 20-fold larger than the R_2 of the free-floating PA-USPIOs. These results indicate that following internalization by the macrophages, the PA-USPIOs are being manipulated in such a way that increases their ability to exert T_2 contrast.

This phenomenon can be explained by previous observations that aggregated or clustered superparamagnetic nanoparticles result in higher R_2 versus fully dispersed, singlet nanoparticles.^{16,31} Others have demonstrated via TEM that following endocytosis of iron oxide nanoparticles, macrophages can process the particles into lysosomes, where dense clusters of particles can usually be observed.³²

Taken together, these other observations help explain how even a small amount of nanoparticle uptake results in a marked change in T_2 contrast in the system.

Conclusion

PEGylated nanoparticles are internalized by macrophages in a size-dependent fashion for diameters between 30 nm and 100 nm. Charge-uptake relationships were investigated by varying the surface properties of nanoparticles. While the data supports the possibility that cationic and strongly anionic nanoparticles may be internalized most effectively, within the ranges investigated, nanoparticle size, not charge, is a stronger determinant of non-specific uptake by macrophages. Based on this information, an MMP-9-sensitive nanoparticle was developed that decreases in size following treatment with MMP-9. Macrophages respond to MMP-9-treated nanoparticles in a predictable fashion, and cleaved nanoparticles were consistently phagocytosed less efficiently than their untreated counterparts, demonstrating the effects of dynamic nanoparticle size modulation on macrophage uptake. These MMP-9-induced differences in uptake are also detectable via MRI. Despite the low levels of overall uptake over the 24 hour incubation periods ($\leq 1\%$ initially administered dose), a significant increase in macrophage R_2 was observed. Presumably, and consistent with quantitative analysis, the clustering of nanoparticles into endosomes following endocytosis results in an increase in nanoparticle R_2 , providing amplification of negative MR image contrast. The results presented here inform the design of nanoparticles to target or evade macrophages in future *in vivo* applications.

Acknowledgments

This work was supported by a Vanderbilt University Intramural Discovery Grant (4-48-999-9132), the Department of Defense Congressionally Directed Medical Research Programs (W81XWH-08-1-0502), and a Whitaker International Scholarship to SNT. CML acknowledges support through a fellowship from the Vanderbilt University Undergraduate Summer Research Program (VUSR). Dynamic light scattering and TEM were conducted through the use of the core facilities of the Vanderbilt Institute of Nanoscale Sciences and Engineering (VINSE), using facilities renovated under NSF ARI-R2 DMR-0963361. We thank Dr Daniel Colvin of the Vanderbilt University Institute of Imaging Science (VUIIS) for his assistance with MRI imaging and analysis. We also acknowledge the laboratories of Professors Hak-Joon Sung and Craig L Duvall (Vanderbilt Biomedical Engineering), whose equipment were instrumental to the execution of this work.

Disclosure

The authors have no conflicts of interest to disclose.

References

- Martin P. Wound healing – aiming for perfect skin regeneration. *Science*. 1997;276(5309):75–81.
- Bouwens L, Baekeland M, De Zanger R, Wisse E. Quantitation, tissue distribution and proliferation kinetics of Kupffer cells in normal rat liver. *Hepatology*. 1986;6(4):718–722.
- Felix R, Cecchini MG, Hofstetter W, Elford PR, Stutzer A, Fleisch H. Impairment of macrophage colony-stimulating factor production and lack of resident bone marrow macrophages in the osteopetrotic op/op Mouse. *J Bone Miner Res*. 1990;5(7):781–789.
- Brown MS, Goldstein JL. Lipoprotein metabolism in the macrophage: implications for cholesterol deposition in atherosclerosis. *Annu Rev Biochem*. 1983;52:223–261.
- Linehan SA, Martinez-Pomares L, Gordon S. Mannose receptor and scavenger receptor: two macrophage pattern recognition receptors with diverse functions in tissue homeostasis and host defense. *Adv Exp Med Biol*. 2000;479:1–14.
- Kindt TJ, Goldsby RA, Osborne BA, Kuby J. *Kuby Immunology*. 6th ed. New York: W.H. Freeman; 2007.
- Plüddemann A, Neyen C, Gordon S. Macrophage scavenger receptors and host-derived ligands. *Methods*. 2007;43(3):207–217.
- Chnari E, Nikitczuk JS, Wang J, Uhrich KE, Moghe PV. Engineered polymeric nanoparticles for receptor-targeted blockage of oxidized low density lipoprotein uptake and atherogenesis in macrophages. *Biomacromolecules*. 2006;7(6):1796–1805.
- Lipinski MJ, Amirbekian V, Frias JC, et al. MRI to detect atherosclerosis with gadolinium-containing immunomicelles targeting the macrophage scavenger receptor. *Magn Reson Med*. 2006;56(3):601–610.
- Thomas SN, van der Vlies AJ, O’Neil CP, et al. Engineering complement activation on polypropylene sulfide vaccine nanoparticles. *Biomaterials*. 2011;32(8):2194–2203.
- Doshi N, Mitragotri S. Macrophages recognize size and shape of their targets. *PLoS One*. 2010;5(4):e10051.
- Taylor PR, Brown GD, Herre J, Williams DL, Willment JA, Gordon S. The role of SIGNR1 and the beta-glucan receptor (dectin-1) in the nonopsonic recognition of yeast by specific macrophages. *J Immunol*. 2004;172(2):1157–1162.
- Raynal I, Prigent P, Peyramaure S, Najid A, Rebuzzi C, Corot C. Macrophage endocytosis of superparamagnetic iron oxide nanoparticles: mechanisms and comparison of ferumoxides and ferumoxtran-10. *Invest Radiol*. 2004;39(1):56–63.
- Ratner BD. *Biomaterials Science: an Introduction to Materials in Medicine*. San Diego, CA: Academic Press; 1996.
- Velluto D, Demurtas D, Hubbell JA. PEG-b-PPS diblock copolymer aggregates for hydrophobic drug solubilization and release: cyclosporin A as an example. *Mol Pharm*. 2008;5(4):632–642.
- Yu SS, Scherer RL, Ortega RA, et al. Enzymatic- and temperature-sensitive controlled release of ultrasmall superparamagnetic iron oxides (USPIOs). *J Nanobiotechnology*. 2011;9:7.
- Deguchi JO, Aikawa M, Tung CH, et al. Inflammation in atherosclerosis: visualizing matrix metalloproteinase action in macrophages *in vivo*. *Circulation*. 2006;114(1):55–62.
- Chan WC, White PD, editors. *Fmoc Solid Phase Peptide Synthesis: a Practical Approach*. Oxford, UK: Oxford University Press; 2000.
- Rehor A, Hubbell JA, Tirelli N. Oxidation-sensitive polymeric nanoparticles. *Langmuir*. 2005;21(1):411–417.
- van der Vlies AJ, O’Neil CP, Hasegawa U, Hammond N, Hubbell JA. Synthesis of pyridyl disulfide-functionalized nanoparticles for conjugating thiol-containing small molecules, peptides, and proteins. *Bioconjug Chem*. 2010;21(4):653–662.
- Christian GD. *Analytical Chemistry*. 5th ed. New York: Wiley & Sons; 1994.

22. Woo K, Hong J, Choi S, et al. Easy synthesis and magnetic properties of iron oxide nanoparticles. *Chem Mater.* 2004;16(14):2814–2818.
23. Griffin EE, Ullery JC, Cox BE, Jerome WG. Aggregated LDL and lipid dispersions induce lysosomal cholesterol ester accumulation in macrophage foam cells. *J Lipid Res.* 2005;46(10):2052–2060.
24. Jerome WG, Cox BE, Griffin EE, Ullery JC. Lysosomal cholesterol accumulation inhibits subsequent hydrolysis of lipoprotein cholesterol ester. *Microsc Microanal.* 2008;14(2):138–149.
25. Ece Gamsiz D, Shah LK, Devalapally H, Amiji MM, Carrier RL. A model predicting delivery of saquinavir in nanoparticles to human monocyte/macrophage (Mo/Mac) cells. *Biotechnol Bioeng.* 2008;101(5):1072–1082.
26. Phillips NC, Heydari C. Modulation of cationic liposomal DNA zeta potential and liposome-protein interaction by amphiphilic poly (ethylene glycol)*. *Pharm Pharmacol Commun.* 1996;2(2):73–76.
27. Han F, Li S, Yin R, Liu H, Xu L. Effect of surfactants on the formation and characterization of a new type of colloidal drug delivery system: nanostructured lipid carriers. *Colloids Surf A: Physicochem Eng Asp.* 2008;315(1–3):210–216.
28. Gough PJ, Gomez IG, Wille PT, Raines EW. Macrophage expression of active MMP-9 induces acute plaque disruption in apoE-deficient mice. *J Clin Invest.* 2006;116(1):59–69.
29. Schellenberger E, Rudloff F, Warmuth C, Taupitz M, Hamm B, Schnorr J. Protease-specific nanosensors for magnetic resonance imaging. *Bioconjug Chem.* 2008;19(12):2440–2445.
30. Sluijter JP, Pulskens WP, Schoneveld AH, et al. Matrix metalloproteinase 2 is associated with stable and matrix metalloproteinases 8 and 9 with vulnerable carotid atherosclerotic lesions: a study in human endarterectomy specimen pointing to a role for different extracellular matrix metalloproteinase inducer glycosylation forms. *Stroke.* 2006;37(1):235–239.
31. Perez JM, O'Loughlin T, Simeone FJ, Weissleder R, Josephson L. DNA-based magnetic nanoparticle assembly acts as a magnetic relaxation nanoswitch allowing screening of DNA-cleaving agents. *J Am Chem Soc.* 2002;124(12):2856–2857.
32. Müller K, Skepper JN, Posfai M, et al. Effect of ultrasmall superparamagnetic iron oxide nanoparticles (Ferumoxtran-10) on human monocyte-macrophages in vitro. *Biomaterials.* 2007;28(9):1629–1642.

Supplementary figures

Online supplementary materials include the following Figures: (S1) control over iron oxide nanoparticle size, (S2) Lowry protein assay standard curves, (S3) nanoparticle

binding experiments, (S4) nanoparticle cytotoxicity assay, and (S5) control internalization experiments involving MMP-9, MMP-9 inhibitor, and protease-insensitive nanoparticles.

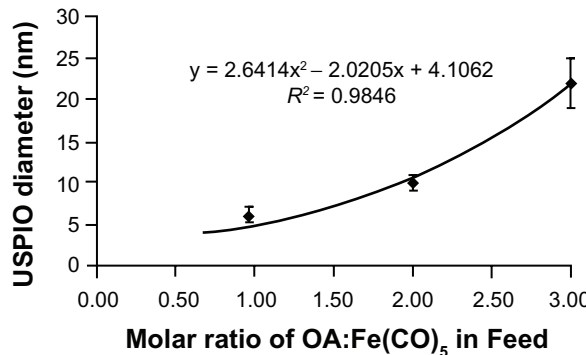


Figure S1 Feed ratio of oleic acid surfactant to iron pentacarbonyl precursors and resulting USPIO diameters. A 6 mmol quantity of Fe(CO)₅ was introduced into reactors containing 40 mL octyl ether and varying amounts of oleic acid at 100°C. USPIO cores were allowed to grow and then oxidize as described in materials and methods, and then imaged by HRTEM. Core diameters were measured via ImageJ software.

Abbreviations: HRTEM, high resolution transmission electron microscope; USPIO, ultrasmall superparamagnetic iron oxides.

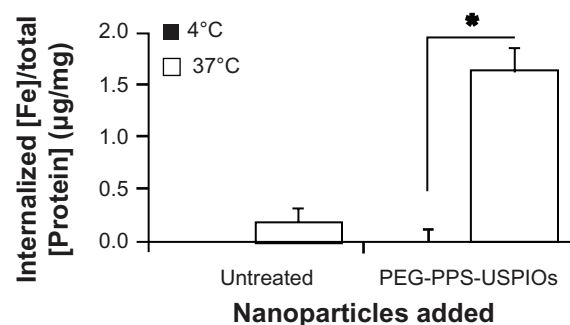


Figure S3 Twenty-four hour uptake of nanoparticles by THP-I macrophages. Cells were treated with 40 nm PEG-PPS-USPIOS for 24 hours, and then measured for iron content via the phenanthroline assay. Iron content was normalized to cell number indirectly via a protein assay. To confirm that the phenanthroline assay measures internalized nanoparticles and not just nanoparticles that have bound to macrophage receptors, some cells were incubated with nanoparticles at 4°C. Results showed about ten-fold lower iron content in these samples relative to samples treated at 37°C, indicating that the protocol successfully lyses cells and enables measurements of internalized iron.

Note: Error bars indicate standard deviation of three independent experiments (*P < 0.01).

Abbreviations: PEG, poly(ethylene glycol); PPS, poly(propylene sulfide); USPIO, ultrasmall superparamagnetic iron oxides; THP, human acute monocytic leukemia cell line.

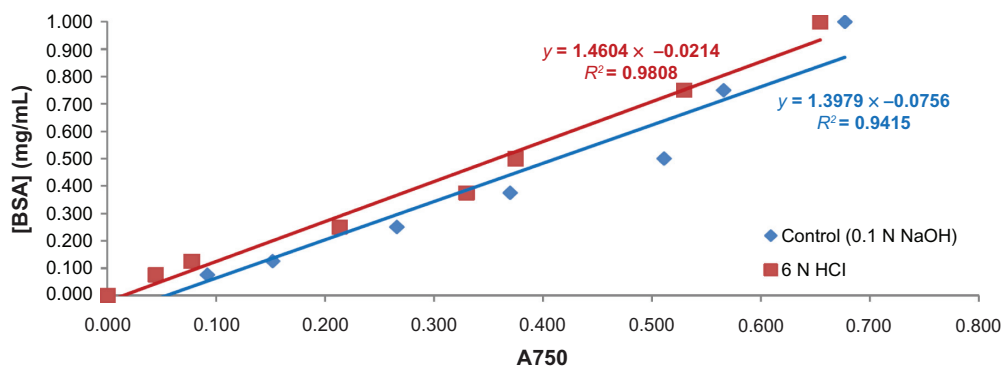


Figure S2 Lowry protein assay standard curves. BSA was dissolved in PBS and treated with either 0.1 N NaOH or 6 N HCl prior to performance of the Lowry protein assay. While the assay is typically run under alkaline conditions (blue), strong acidic conditions do not significantly affect the sensitivity or reliability of this assay.

Abbreviations: BSA, bovine serum albumin; PBS, phosphate buffered saline.

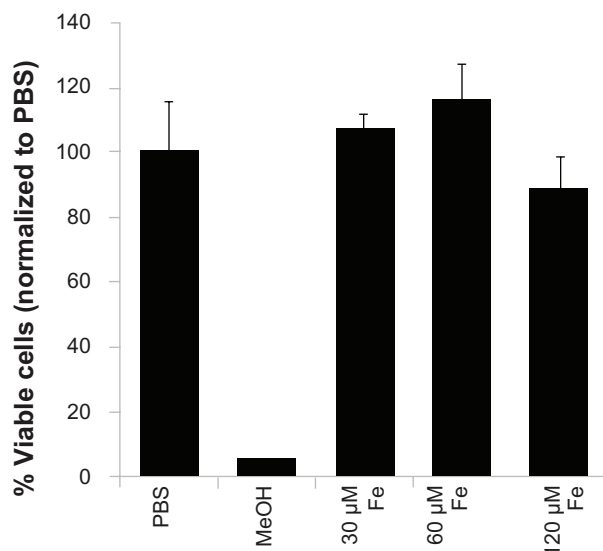


Figure S4 Cell viability measurements on nanoparticle-treated THP-1 cells, normalized to untreated cells (media + PBS). Cells were treated with increasing doses of 100 nm PEG-PPS-USPIOs for 24 hours, prior to removal of unbound nanoparticles and assessment of cell viability via quantification of calcein-AM/ethidium homodimer staining. Dosage on the x-axis represents actual iron concentration within the samples. No statistically significant differences in viability were observed between any of the treatment groups ($n = 3$).

Abbreviations: PBS, phosphate buffered saline; PEG, poly(ethylene glycol); PPS, poly(propylene sulfide); USPIO, ultrasmall superparamagnetic iron oxides; THP, human acute monocytic leukemia cell line.

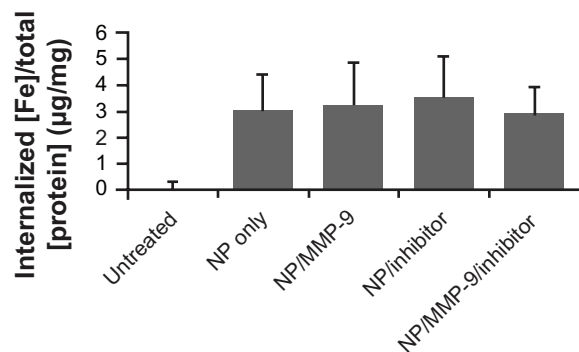


Figure S5 Co-administration of 40 nm PEG-PPS-USPIOs (do not contain MMP-9-cleavable peptide) with MMP-9 does not significantly affect internalization of nanoparticles. THP-1 cells were treated with media only (untreated), nanoparticles only, or nanoparticles co-administered with 200 ng/mL MMP-9 and/or 300 ng/mL MMP-9 inhibitor. Because these nanoparticles do not contain MMP-9-cleavable elements, their diameter is unaffected by treatment (data not shown). MMP-9 treatment does not change the properties of the THP-1 cell membrane in a way that affects their interactions with nanoparticles. Error bars indicate standard deviation for three independent experiments.

Abbreviations: MMP-9, matrix metalloproteinase-9; PEG, poly(ethylene glycol); PPS, poly(propylene sulfide); USPIO, ultrasmall superparamagnetic iron oxides; THP, human acute monocytic leukemia cell line.

Manipulation of the Tumor Associate Macrophage Phenotype into an Anti-Tumor Phenotype by Modulating the NF-κB Pathway

Ryan A. Ortega

Department of Biomedical Engineering

Vanderbilt University, Nashville, TN

Dissertation Committee

Advisor: Prof. Todd Giorgio, Dept. of Biomedical Engineering, Vanderbilt University

Prof. Fiona Yull, Dept. of Cancer Biology, Vanderbilt University

Prof. Craig Duvall, Dept. of Biomedical Engineering, Vanderbilt University

Prof. Frederick Haselton, Dept. of Biomedical Engineering, Vanderbilt University

Prof. Barbara Fingleton, Dept. of Cancer Biology, Vanderbilt University

I. Abstract

Tumor associated macrophages (TAMs) have been implicated in creating a pro-tumor environment in multiple types of cancer resulting in increased malignancy, rapid tumor progression, and a poorer prognosis. Preliminary studies depleting macrophages or ablating macrophage recruiting and maturation factors have demonstrated the efficacy of targeting TAMs with therapeutic intent. Instead of simply destroying TAMs or shutting them down, a better therapeutic approach would be to stimulate them to recapitulate their normal immune response and activate tumor cell immunity. The NF- κ B pathways are major controllers of macrophage phenotype. By manipulating these pathways using RNAi therapeutics it should be possible to replace the TAM phenotype with an activated, anti-tumor phenotype.

The first section of this work is to show that it is possible to manipulate the NF- κ B pathway in murine macrophages *in vitro*. Using commercial agents and novel mannosylated nanoparticles, I have shown efficacious knockdown of total NF- κ B activity *in vitro* using siRNA against specific NF- κ B proteins. The next goal of this work is to produce and characterize an NF- κ B modulated, anti-tumor ‘Terminator’ phenotype for macrophages. Macrophages from mice with activated classical or alternative NF- κ B pathways will be isolated and their RNA analyzed with microarray. Differences between these two macrophage types and TAMs will be elucidated and used to describe the Terminator phenotype, which will then be created *in vitro* using siRNA. An anti-tumor macrophage phenotype will then be created *in vivo* in a mouse model of human breast cancer. Mannosylated nanoparticles will be used to target TAMs in the tumor and in the metastatic niche and deliver siRNA for specific NF- κ B proteins, manipulating the TAMs to adopt the previously described Terminator phenotype. This work will develop a novel immunological engineering approach to cancer treatment by selectively targeting and manipulating the tumor stroma.

Table of Contents

I.	Abstract	1
II.	Hypothesis and Specific Aims	3
III.	Abbreviations	4
IV.	Introduction	5
V.	Background and Significance	
	Tumor associated macrophages as a therapeutic target in breast cancer	6
	Defining the TAM phenotype	7
	NF- κ B deregulation in macrophages creates a pro-tumor environment	9
	Manipulating NF- κ B by transfecting macrophages with siRNA	11
VI.	Preliminary Data and Proposed Work	
a.	Aim #1: <i>In vitro</i> validation of commercial transfection agents and Mn-NP	14
b.	Aim #2: Definition and creation of an NF- κ B mediated, anti-tumor ‘Terminator’ macrophage phenotype	21
c.	Aim #3: Investigate the therapeutic potential of Terminator macrophages and nucleotide delivery to TAMs	24
VII.	Proposed Timeline	29
VIII.	Acknowledgements	30
IX.	References	31
X.	Appendix I: Previous Publications and Conference Abstracts	34
XI.	Appendix 2: Writing Removed for Revised Version	35

II. Hypothesis and Specific Aims

Hypothesis: Tumor associated macrophages create a potent pro-tumor effect in many solid tumors by promoting tumor cell proliferation, angiogenesis, and metastasis and by suppressing normal immune response. By strategically manipulating the NF- κ B pathways in these macrophages it is possible to reduce the pro-tumor effects typically seen in tissue remodeling macrophages and create a set of anti-tumor, immunogenic traits to stimulate tumor cell immunity.

Aim #1: In order to show efficacious manipulation of the NF- κ B pathways *in vitro*, commercial agents and novel mannosylated nanoparticles (Mn-NP) will be used to deliver siRNA to macrophages to knockdown NF- κ B proteins. A library of effective sequences will be made and effective transfection protocols for the commercial agents and nanoparticles will be developed.

Aim #2: An NF- κ B mediated, anti-tumor, “Terminator” phenotype for macrophages will be defined using microarray analysis of macrophages from mice with upregulated classical and alternative activation, as well as tumor associated macrophages from mammary targeted polyoma middle T oncogene mice. The differences between these cell populations will inform the selection of NF- κ B controllable, anti-tumor traits and suggest possible therapeutic targets within the NF- κ B pathway. The Terminator phenotype will be produced *in vitro* using the siRNA and transfection agents from Aim #1 and tested using quantitative real time PCR.

Aim #3: A biodistribution study will be performed with siRNA-loaded Mn-NP and the *in vivo* targeting ability of the mannose ligand will be assessed in mammary tumor bearing mice. The siRNA therapeutic regimen designed in Aim #2 will be used to inform the delivery of active siRNAs to tumor associated macrophages in murine mammary tumors. The macrophages will be removed and their phenotype analyzed following treatment.

III. Abbreviations

TAM	Tumor associated macrophage
SPM	Splenic macrophage
BMDM	Bone marrow derived macrophage
siRNA	Small interfering RNA
NF-κB	Nuclear factor kappa-light-chain-enhancer of activated B cells
P105/p50 (NF-κB1)	Class 1 NF-κB protein of the classical NF-κB pathway
P100/p52 (NF-κB2)	Class 1 NF-κB protein of the alternative NF-κB pathway
RelA (p65)	Class 2 NF-κB protein of the classical NF-κB pathway
RelB	Class 2 NF-κB protein of the alternative NF-κB pathway
IκB-α	Inhibitor of the NF-κB transcription factor; inhibitor of classical NF-κB pathway
IKKα (IKK1, CHUK)	IκB kinase alpha; activator of classical and alternative NF-κB pathway
IKKβ (IKK2)	IκB kinase beta; activator of classical NF-κB pathway
NEMO (IKKγ)	NF-κB essential modulator; activator of classical NF-κB pathway
NIK	NF-κB inducing kinase; activator of classical NF-κB pathway
TRAF3	TNF receptor-associated factor 3; Inhibitor of NIK
CSF-1 (M-CSF)	Colony stimulating factor 1 (macrophage colony stimulating factor)
IFN	Interferon; immune activating cytokine
TNF	Tumor necrosis factor
IL-1	Interleukin 1; pro-inflammatory cytokine
IL-10	Interleukin 10; anti-inflammatory cytokine
IL-12	Interleukin 12; an activator of immune cells
MMP	Matrix metalloproteinase
ROS	Reactive oxygen species
MIIF	Macrophage migration inhibitory factor
CSF-1R	CSF-1 receptor; a macrophage surface marker
CD11B (ITGAM, CR3)	Integrin alpha M (compliment receptor 3); a myeloid cell surface marker
F4/80	A murine macrophage surface marker
Gr1	A negative macrophage surface marker; lost during macrophage maturation
RAFT	Reversible addition-fragmentation chain transfer
BME	Butyl methacrylate
PAA	Propylacrylic acid
DMAEMA	2-(Dimethylamino)ethyl methacrylate
AzEMA	2-Azidoethyl methacrylate
Mn-NP	Mannosylated endosomal escape nanoparticle
OH-NP	OH terminated endosomal escape nanoparticle
PyVT	Polyoma middle T oncogene
NGL	Transgenic mouse expressing luciferase and GFP as an NF-κB activation readout
IKFM	Transgenic mouse w/ upregulated classical NF-κB activation in macrophages
ALFM	Transgenic mouse w/ upregulated alternative NF-κB activation in macrophages
wt	Wild type
qRT-PCR	Quantitative reverse transcription polymerase chain reaction
AST	Aspartate aminotransferase
ALT	Alanine aminotransferase
BUN	Blood urea nitrogen

IV. Introduction

Tumor associated macrophages (TAMs) play an important role in establishing a pro-tumorigenic local microenvironment in many tumor types. These macrophages stimulate angiogenesis, promote tumor growth and metastasis, and suppress the normal immune response.^{4,5} TAMs display a phenotype that is a blend of the two classical macrophage phenotypic categories. Like the classically immunogenic (M1) macrophage, TAMs produce low levels of inflammatory cytokines which creates pro-tumorigenic smoldering inflammation.⁶ Like the classical description of a tissue remodeling (M2) macrophage, TAMs break down the surrounding extracellular matrix, secrete growth factors, and inhibit the adaptive immune response.³

It has been demonstrated that tumor associated macrophages are a viable therapeutic target in cancer treatment and ablating these cells can have a powerful anti-tumor effect.⁷ A more elegant solution would be to target these pro-tumor macrophages with a therapeutic agent that can alter their behavior to a strongly immunogenic phenotype capable of stimulating tumor immunity. In order to facilitate this immunological engineering, a target for phenotypic modulation must be elucidated. The NF-κB pathways control macrophage phenotype and the inflammatory response.⁸ Tumor cell induced NF-κB deregulation has also been implicated in creating many of the pro-tumor traits of TAMs.⁹ By selectively manipulating NF-κB in TAMs, it should be possible to eradicate the TAM phenotype and recapitulate the normal immune response.

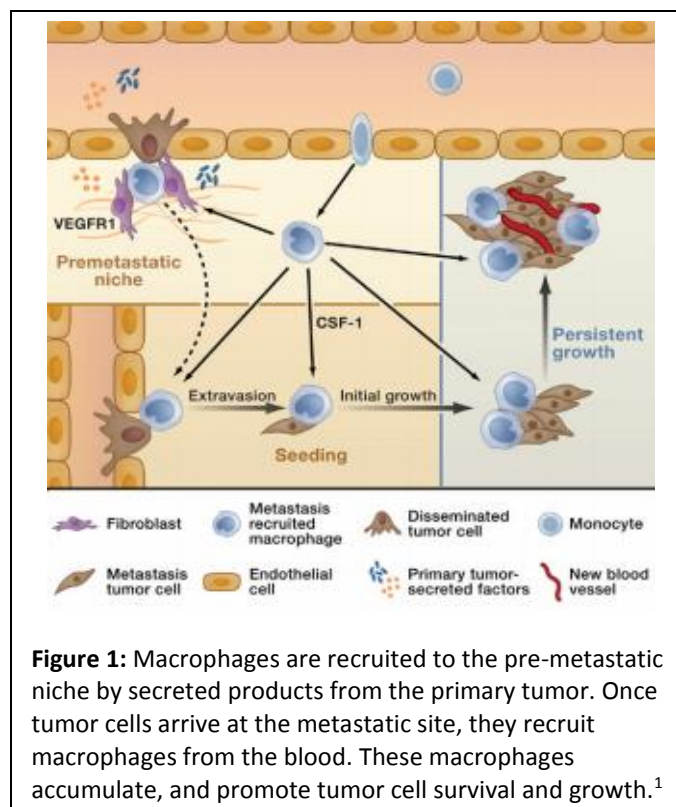
siRNA is a potent therapeutic agent capable of selectively knocking down the translation of specific mRNA into protein.¹⁰ Clinical trials of siRNA therapeutics utilize targeted nanoparticles as a delivery device to reach specific cell populations.¹¹ A mannose functionalized nanoparticle with an siRNA condensing region would be capable of targeting the macrophage mannose receptor (upregulated in TAMs) and deliver NF-κB specific siRNAs in order to change the TAM phenotype.^{12,13}

V. Background and Significance

Tumor associated macrophages (TAMs) as a therapeutic target for cancer treatment

The tumor supportive stroma has been identified as an attractive target for therapeutic intervention in breast cancer. While most tumors exhibit a large degree of cellular heterogeneity, the tumor stroma is potentially more homogenous with respect to local stromal cell phenotype. In particular, macrophages have been implicated in supporting tumor associated angiogenesis, promotion of local tumor growth and invasion, tumor cell migration, intravasation, and suppression of an anti-tumor immune response.^{4, 5, 7} Macrophages play an important trophic role in tissue development and one suggested mechanism for the TAM phenotype is that these trophic roles are recapitulated in the tumor microenvironment.¹⁴ An increase in TAMs at the site of tumor progression has proven to be predictive of poor prognosis and survival in mouse models of human breast cancer.^{15, 16}

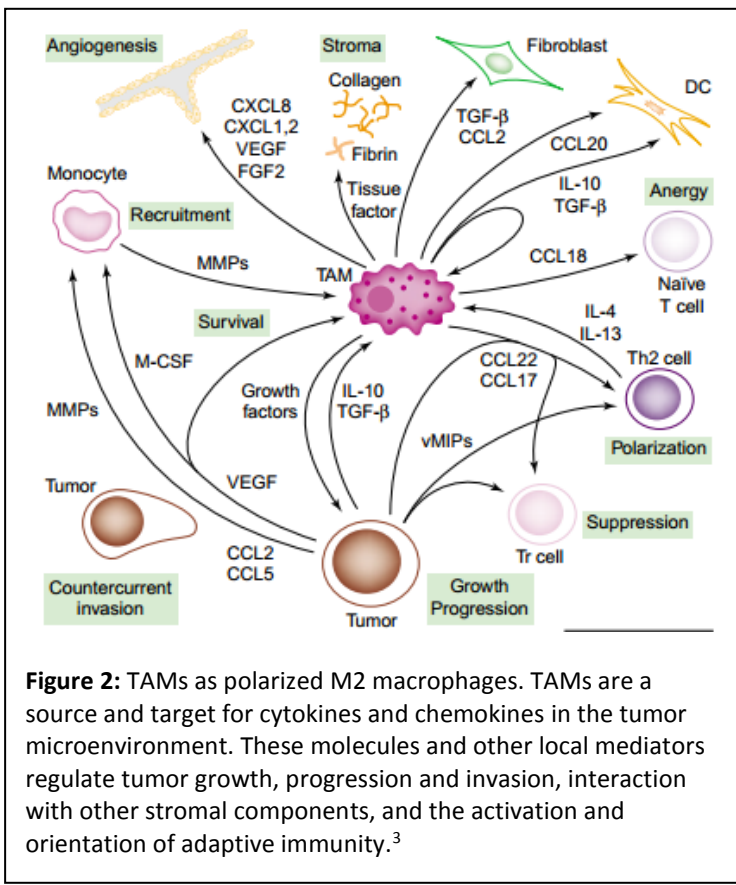
Over expression of one of the major factors controlling macrophage maturation, CSF-1 (M-CSF), has been associated with poor prognosis in breast, ovarian, prostate, hepatocellular, and colorectal cancer.^{7, 17, 18} One of the more insidious characteristics of TAMs driven in part by CSF-1 is their ability to prepare a metastatic niche for circulating tumor cells (Figure 1).⁷ Ablation of CSF-1 in the polyoma middle T oncogene (PyVT) mouse model of human breast cancer



greatly reduces macrophage density in the tumor, resulting in a decreased rate of tumor progression and an inhibition of metastases.¹⁹ In addition to data from studies of CSF-1 in cancer, CCL-2, a major macrophage chemotaxis factor has been shown to be upregulated in a wide range of cancers, and is associated with poor prognosis in breast cancer.¹⁷ Depletion of macrophages reduces tumor growth in melanoma, ovarian cancer, Lewis lung carcinoma, and prostate tumor graft models.⁷ All of this evidence supports the role of TAMs as a viable therapeutic target for treating breast cancer. Furthermore, unlike tumor cells, the genomes of macrophages are stable, indicating that they may not become resistant to therapy as readily as tumor cells.

Defining the TAM phenotype

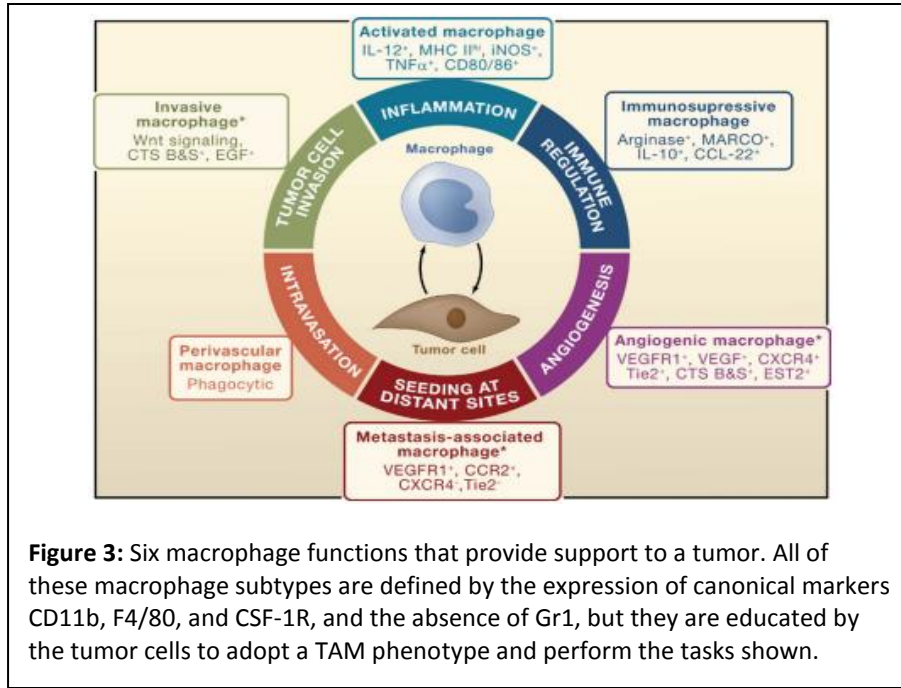
TAMs are phenotypically distinct from the classic M1/M2 description of macrophage phenotype, but blend together several characteristics of both. In the classic description of macrophages, M1 or ‘classically activated’ macrophages are thought of as the pro-inflammatory, immune response-controlling macrophages. M1 activation is associated with an increase in inflammatory cytokines IFN- γ , TNF- α , IL12, chemoattractants for CD8+ T-cells, and reactive oxygen species. This phenotype describes a cell that acts as a first responder to the site of injury or microorganism invasion and controls local inflammation and the total immune response.³ M2 or ‘alternatively activated’ macrophages exhibit an increase in scavenger and mannose receptors, an increased production of anti-inflammatory cytokines IL-10 and IL-1 receptor antagonist, and an increased production of T-regulatory cell chemoattractant, CCL-22.³ The M2 phenotype describes a cell that tunes and inhibits inflammation and the adaptive immune response as well as promotes tissue repair, angiogenesis and tissue remodeling facilitated by increased production of MMP-1 and MMP-9.²⁰ Many, if not all of these key properties of M2 macrophages are present in TAMs. Alberto Mantovani and collaborators have published a model of TAMs as an M2 macrophage; a summary of their findings are depicted in Figure 2.



Initially, it appears as if the M2 phenotype is a perfect model for the TAM phenotype. However, the M2 phenotype cannot account for one of the defining characteristics of TAMs: smoldering inflammation. Smoldering inflammation is a pro-tumorigenic state characterized by low levels of local inflammation combined with a paradoxical blunting of innate and adaptive immunity.^{6,21} While in a state of smoldering inflammation, a pre-cancerous niche is constantly exposed

to reactive oxygen species (ROS), which reacts with DNA in the surrounding cells resulting in permanent genomic alterations, but not enough to result in cell death. In addition to low levels of ROS and other inflammatory cytokine production, TAMs produce migration inhibitory factor (MIF), a cytokine that overcomes p53 function by suppressing its transcriptional activity.²² These phenotypic traits are usually associated with M1 macrophages.

The TAM phenotype does not map cleanly onto the classical M1/M2 description of macrophages. Instead it displays a blended phenotype in which traits from both M1 and M2 macrophages are selected to create a strongly pro-tumor microenvironment. TAMs produce growth factors to promote tumor cell growth, tissue remodeling, and angiogenesis. They suppress the immune response to tumor cells while simultaneously creating low levels of local inflammation. When taken together, these traits show that TAMs play a critical role in tumor progression, summarized in Figure 3.



NF- κ B deregulation in macrophages creates a pro-tumor environment

NF- κ B is a transcriptional pathway that has been studied for over 25 years and is known to regulate hundreds of genes. This pathway is active in many cell types and plays a major role in controlling the inflammatory response in macrophages in particular.⁸ Investigations of NF- κ B as have pro-tumorigenic function revealed a critical positive role for NF- κ B in linking inflammation with tumor development.²¹ In myeloid cells such as macrophages, the inflammatory state is controlled by NF- κ B activation which is essential for the inflammatory macrophage phenotype.²³ NF- κ B activation is needed to create many of the traits of TAMs including the critical smoldering inflammation state.¹⁷ The total effect that NF- κ B activation in macrophages has on the tumor microenvironment is complicated. The NF- κ B pathway is actually comprised of the two parallel pathways seen in Figure 4.² The classical pathway is well understood and has been studied in great detail; however, the alternative NF- κ B pathway remains critically understudied, and the effects that alternative NF- κ B activation has in specific cell populations is not well understood.²⁴

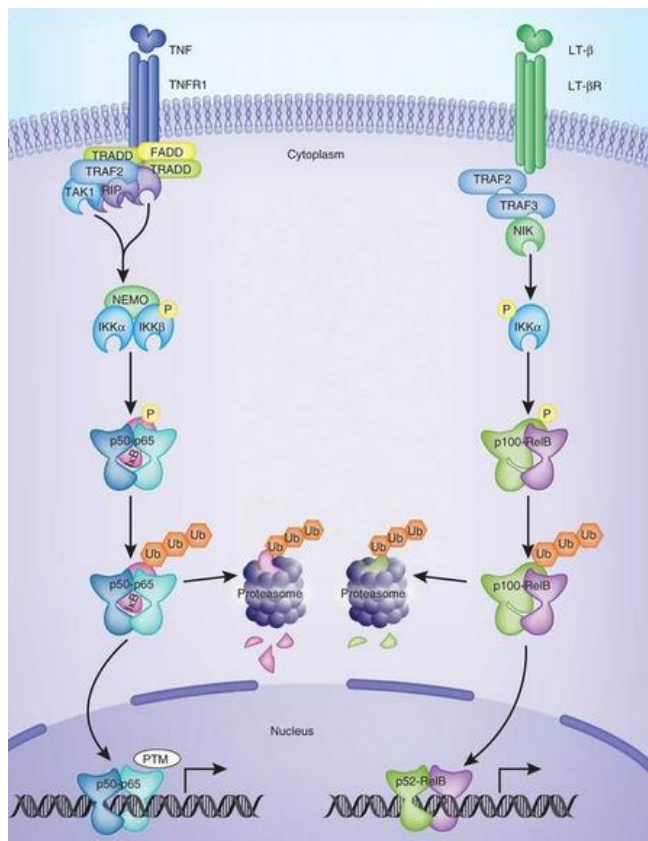


Figure 4: Classical (left) and alternative (right) pathways of NF-κB activation. The classical pathway is induced by most physiological NF-κB stimuli and is represented here by TNFR1 signaling. In the classical pathway, IκB-α is phosphorylated in an IKKβ and NEMO-dependent manner, which results in the nuclear translocation of mostly p65-containing heterodimers. In contrast, the alternative pathway, induced by certain TNF family cytokines, such as RANKL and LT-β, involves IKKα-mediated phosphorylation of p100 associated with RelB, which leads to partial processing of p100 to p52 and the generation of transcriptionally active p52-RelB complexes. IKKα activation is NIK dependent.²

It is well established that the classical NF-κB pathway controls the classical immune response of activated macrophages as well as many other non-immunogenic macrophage behaviors. The classical pathway is activated by binding of ligands to toll-like receptors at the cell surface, and by inflammatory cytokines such as lipopolysaccharide and tumor necrosis factor family members.² In response to these stimulatory signals, the classical NF-κB pathway causes macrophages to produce more inflammatory cytokines and recruit cells of the innate and adaptive immune system to the site of activation. The classical pathway also exhibits a low level of constitutive activation in mature macrophages. In contrast, alternative pathway function is

far more selective and specific than classical NF-κB activation. Alternative activation of NF-κB in activated macrophages is poorly understood relative to the classical pathway but it is broadly known to play an important role in organogenesis and tissue architecture organization.^{24, 25} The alternative pathway is not constitutively active in normal macrophages and is held in abeyance by sequestration

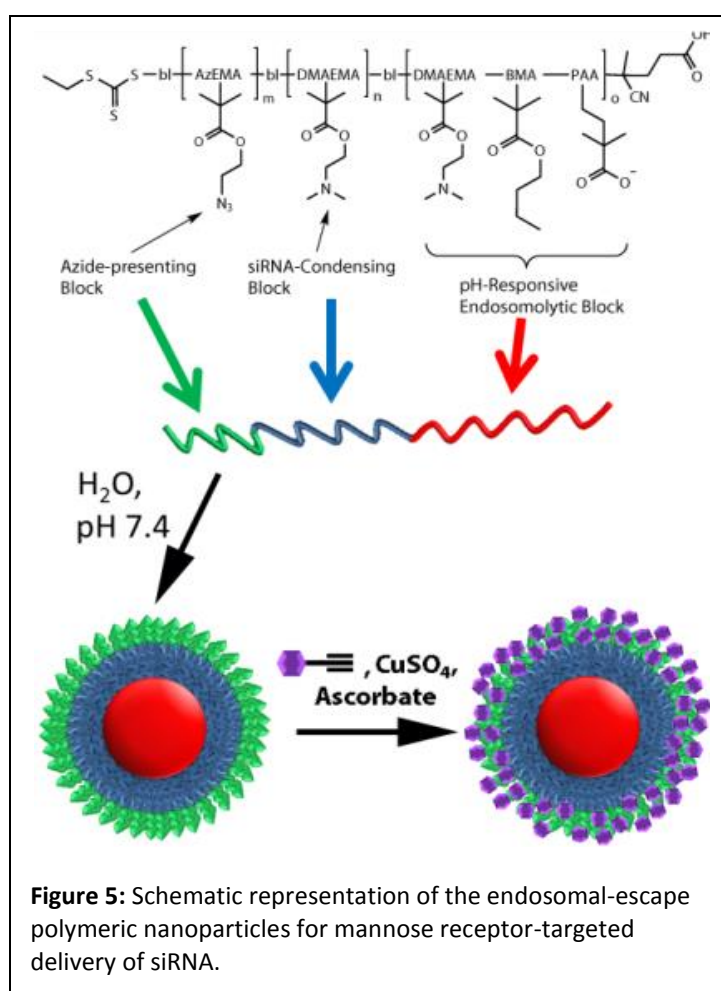
and constant degradation of its activating kinase, NIK, by TRAF3.²⁶ Signal induced activation of protein kinases is usually mediated through post-translational modifications; however, NIK is unique in that its function is controlled by a steady level of expression. The expression level of NIK is normally kept low and bound by TRAF3, but is drastically elevated in response to a specific alternative NF-κB activating signal.²⁷ In the tumor microenvironment signals exist which stimulate macrophages to undergo broad NF-κB activation. Though the NF-κB pathways are functioning normally, the activation of the pathways is deregulated by the tumor cells; the tissue remodeling effects of alternative NF-κB activation would be tumorigenic in this context.^{9, 28}

The NF-κB pathways together produce complex pro- or anti-inflammatory and pro- or anti-tumorigenic effects. The interplay between the two pathways is made more confounding in that there is some unknown level of cross talk between the two, resulting in activation or depression of one or both pathways in different circumstances. This inherent complexity makes NF-κB a useful tool for tumor cells to utilize via local deregulation using tumor secreted cytokines, but it also makes NF-κB a very desirable target to manipulate in order to activate the innate cytotoxic, immunogenic properties of mature macrophages. One approach for manipulation of NF-κB in macrophages to create an anti-tumor environment is to selectively activate the strong immunogenic response associated with normal classical pathway activation while simultaneously turning off the tissue remodeling, trophic effects associated with the alternative pathway. This method of turning off one pathway while activating the other would rob the tumor of its trophic macrophages, reduce the complexity of NF-κB cross talk in TAMs, and create actively anti-tumor macrophages (Terminator macrophages).

Manipulating NF-κB by transfecting macrophages with siRNA

NF-κB is a promising therapeutic target for manipulation of macrophage phenotype to induce anti-tumor behavior. However, a broad, untargeted manipulation of NF-κB would likely result in

negative side effects and would not produce the precise activity required to induce an anti-tumor phenotype in macrophages. In order to deliver a therapeutic agent to this specific cell population, a targeted delivery method would be ideal.²⁹ In a current collaboration between the Giorgio, Yull, and Duvall laboratories, a novel mannosylated nanoparticle has been developed that is capable of targeting the mannose receptor found on the surface of macrophages and upregulated in TAMs.^{12, 13, 30} The core of the particle is created by RAFT polymerization of BME, PAA, and DMAEMA to create a hydrophobic, terpolymer with tunable endosomal escape properties.^{31, 32} Next, a polycationic DMAEMA block is added



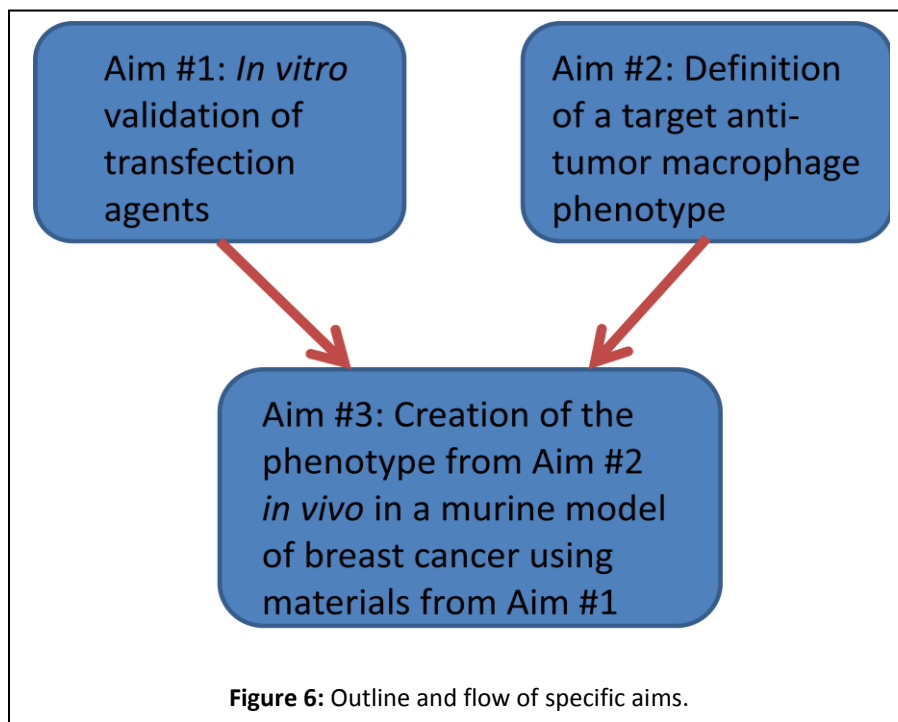
by RAFT polymerization to add the capability to condense polyanionic therapeutics onto the particle. Finally, an AzEMA block is polymerized onto the diblock polymer to form a triblock polymer terminated in an AzEMA block to support further functionalization. In order to create a mannose functionalized polymer, click chemistry is performed with alkyne –functionalized mannose to attach a mannose moiety to the end of the polymer.^{13, 33} The completed polymer assembles into positively charged micelles when

reconstituted in an aqueous solution, forming mannosylated nanoparticles (Mn-NP; Figure 5).

siRNAs are short therapeutically active RNA strands capable of knocking down the translational activities of specific mRNAs without significant off-target side effects.³⁴ siRNA knocks down levels of

target proteins by binding to complementary mRNA strands, resulting in the degradation of the target mRNA strand.¹⁰ Far from being just a laboratory tool, siRNA has been shown to have clinical translational potential, and targeted delivery of therapeutic siRNA has been accomplished in humans.^{11,35} As a therapeutic with tunable activity and high specificity, this polyanion is well suited for incorporation into Mn-NP to be used to target and treat TAMs *in vivo*. There are many commercial transfection agents, such as Lipofectamine, capable of efficacious delivery of siRNA to cells *in vitro*; however, the Mn-NPs have a more neutral surface charge, indicating potential *in vivo* biocompatibility.¹³ This vehicle is uniquely suited for use in experiments targeting TAMs in *in vivo* models of cancer and delivering NF-κB modulating siRNA sequences. Mn-NP can be used to target TAMs *in vivo* and deliver siRNA sequences against alternative NF-κB proteins, knocking down trophic and immunosuppressive TAM activity, while simultaneously delivering an siRNA sequence against the inhibitor of the classical pathway, IκB-α. By knocking down an inhibitor protein, this second siRNA will activate the classical pathway and induce a local immune response at the site of the primary tumor or metastasis.

VI. Preliminary Data and Proposed Work



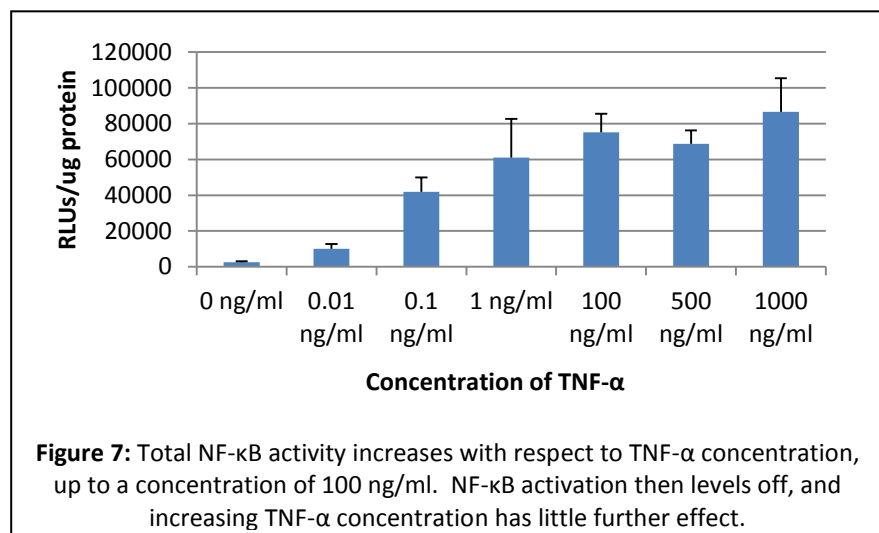
Specific Aim #1: *In vitro* validation of commercial transfection agents and Mn-NP transfection agent

The first specific aim sought to develop *in vitro* siRNA transfection protocols for Mn-NP and commercial agents that can be used in Aims #2 and #3. An efficacious transfection protocol was developed with commercial transfection agents for primary murine macrophages *in vitro* by modulating the concentrations of siRNA and transfection agent, as well as transfection time. This protocol will be used to investigate the molecular biology of NF- κ B manipulation in macrophages for Aim #2. Transfection protocols for macrophages have been reported for cell lines such as RAW 264.7, but primary macrophages are notoriously difficult to transfect effectively. Development of effective transfection protocols is an important first step in the overall goal of this work and is integral for Aims #2 and #3.

1a. Development of commercial agent siRNA transfection protocol: Initially, commercial agents HiPerFect and Lipofectamine RNAiMAX were considered for use as the standard commercially available agent. Lipofectamine is an aqueous formulation of cationic lipids designed to carry polyanionic molecules, such as nucleic acids, across cell membranes. The RNAiMAX formulation is optimized to protect fragile siRNA and deliver it into the cells' cytoplasm in a functional state. HiPerFect is an aqueous formulation of neutral and cationic lipids designed for *in vitro* transfection purposes. *In vitro* transfection studies for Aim #1 were performed in murine bone marrow derived macrophages (BMDMs) from FVB mice which express luciferase as a readout of total NF- κ B activity.^{15, 36, 37}

BMDM preparation from NGL mice: Bone marrow was harvested from the femurs of NGL mice and plated as a single cell suspension in media with a 10% supplement of L-929 murine fibroblast culture media as a source of colony stimulating factor-1 (CSF-1, M-CSF). After 6 days of culture, the transformed cells are mature, adherent macrophages and were scraped from their plates and re-plated in 12 well plates (300,000 cells per well, approximately 80-90% confluency).^{15, 38} The NGL transgenic mice allow total NF- κ B activity to be measured in a simple luciferase activity assay and reported as a dimensionless number of relative light units, normalized to the amount of protein in the sample.³⁹

Commercial agent transfection: HiPerFect, was initially selected as the commercial transfection agent based on manufacturers' claims and previous studies indicating that its formulation was optimal for transfecting macrophages due to the lower cationic charge of the lipids used to form the transfection complexes. To form transfection complexes, a control siRNA against luciferase was incubated with HiPerFect for 1 hour before the transfection solution was added to the cells' media. siRNA concentration and HiPerFect volume were varied. BMDMs were then transfected for 6 hours with the HiPerFect_siRNA complexes. After transfection, the cells were washed and stimulated with TNF- α for 6 hours to activate the NF- κ B pathways as evidenced by an increase in luciferase production. Several concentrations of TNF-



α were initially considered to activate the BMDMs; this experiment is shown in Figure 7. 10 ng/ml was chosen as the stimulating concentration in future experiments. After 6 hours of stimulation, the cells

were washed in PBS, lysed, and frozen in a luciferase assay lysis buffer. The cell supernatant was then measured for luciferase activity and normalized to sample protein concentration. The results of the HiPerFect optimization studies are shown in Figure 8.

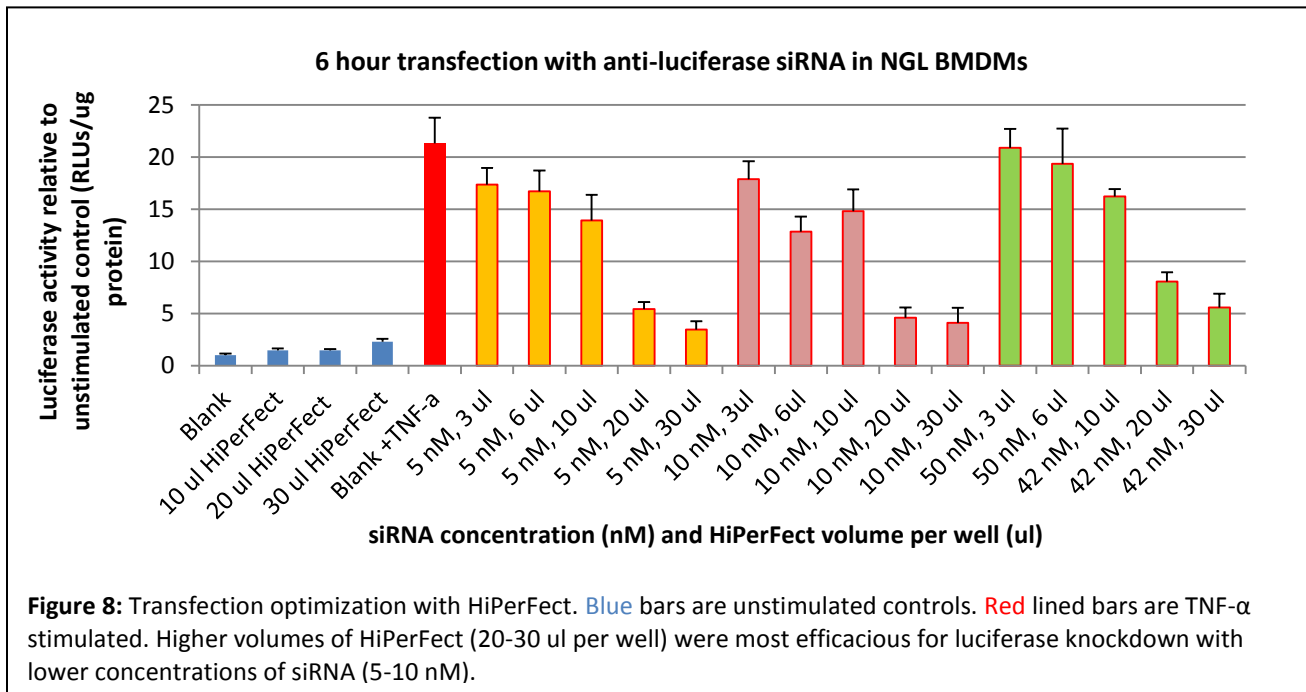


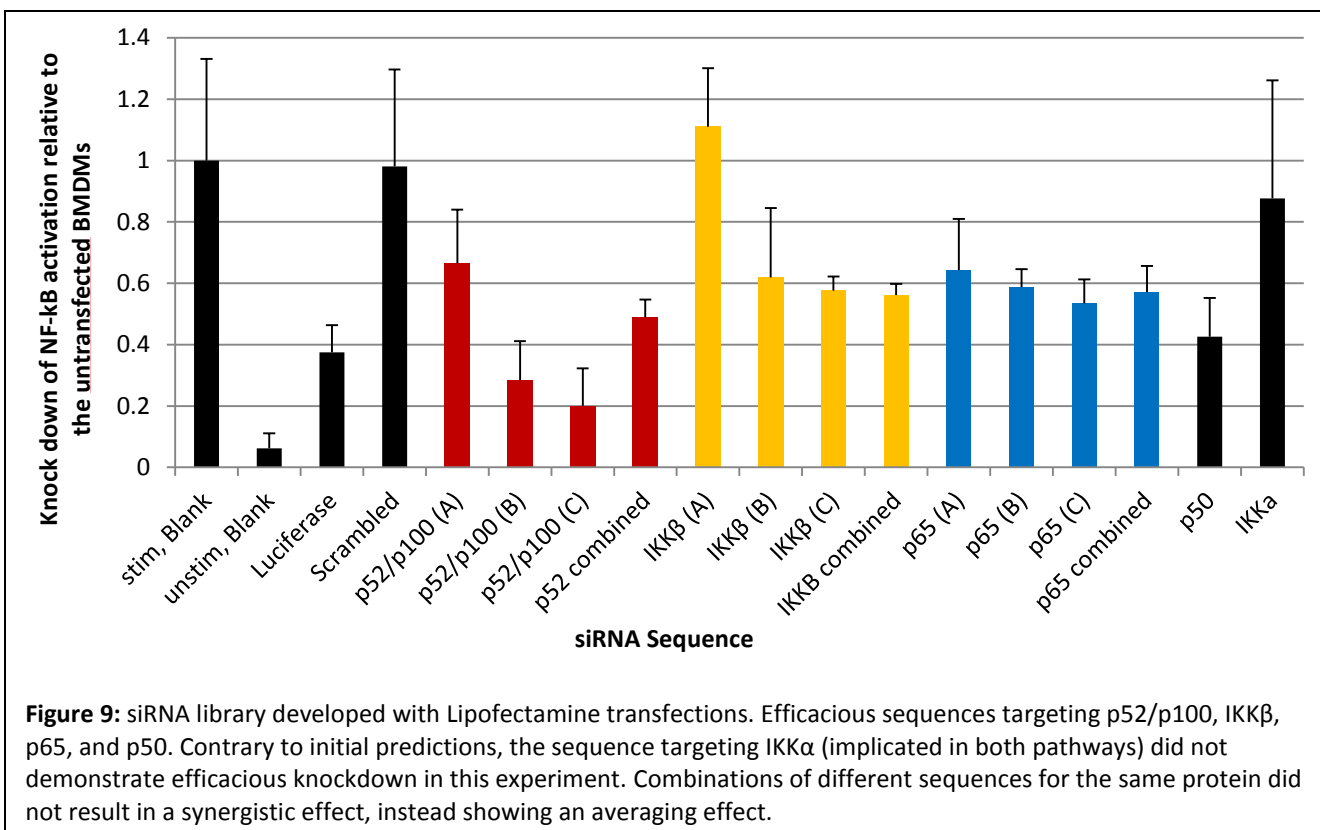
Figure 8: Transfection optimization with HiPerFect. Blue bars are unstimulated controls. Red lined bars are TNF- α stimulated. Higher volumes of HiPerFect (20-30 ul per well) were most efficacious for luciferase knockdown with lower concentrations of siRNA (5-10 nM).

Knockdown of luciferase using an anti-luciferase positive control siRNA was shown to be more dependent on HiPerFect concentration, rather than siRNA concentration. Based on these results, I

chose to use HiPerFect at a concentration of 20 ul per well, with 10 nM siRNA in each well for further experiments.

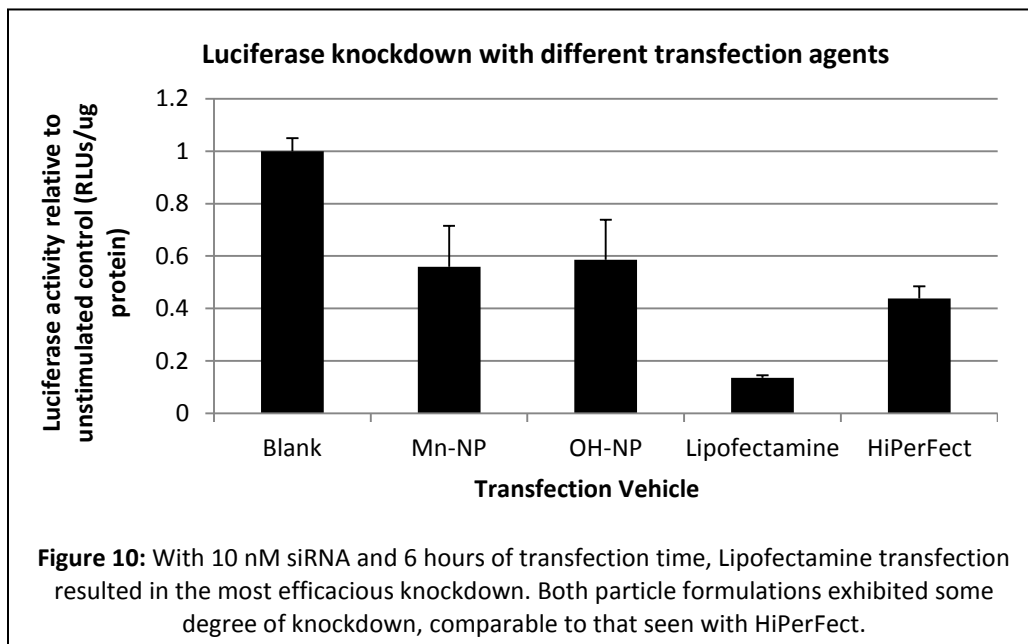
Practical application of the HiPerFect transfection agent would prove difficult. Experiments with HiPerFect in Aims 1b and 1c demonstrated poor repeatability (data not shown) when NF- κ B relevant siRNA were used and the amount of HiPerFect needed to perform the optimized protocol was cost prohibitive due to the large number of experiments being performed. For these reasons, Lipofectamine RNAiMAX (referred to hereafter in Aim #1 as ‘Lipofectamine’) was investigated as a replacement for HiPerFect. It was decided to continue using the optimized concentration of siRNA (10 nM) and to utilize the suggested Lipofectamine dose of 2 ul to form transfection complexes with 10 nM in 1 ml of media for BMDMs in 12 well plates. Later experiments in Aims 1b and 1c showed that Lipofectamine is more effective at transfecting the BMDMs.

1b. Creation of an effective siRNA library: Once an effective transfection protocol with Lipofectamine was developed, several NF- κ B specific sequences of siRNAs were investigated for efficacy in knocking down total NF- κ B activity in the stimulated NGL BMDM model. 3 different sequences of siRNAs were selected (indicated by A, B, and C) for the following initial targets: IKK β , p65 (RelA), and p52/p100. Preliminary studies were done with single sequences of the following targets: p50 and IKK α . Transfections were done in 12 well plates with NGL BMDMs cultured with 300,000 cells per well. 10 nM siRNA was delivered with 2 ul of Lipofectamine per well with a total volume of 1 ml of media per well. Total NF- κ B knockdown was measured via luciferase assay and the knockdown from each sequence is reported in Figure 9.



1c. Development of a macrophage transfection protocol with Mn-NP: Mannose terminated endosomal escape polymers with an siRNA condensing region were prepared in the Duvall and Giorgio labs by Shann Yu, lyophilized, and stored at -20 °C. OH-terminated polymers OH-NP were also prepared as a control for mannose targeting. The polymers were reconstituted in PBS at a concentration of 4 mg/ml and sonicated for 10 minutes (see background section on Mn-NP for particle diagram).¹³ 100 ul aliquots were frozen and used as needed. An initial experiment was performed to compare different transfection vehicles using a control siRNA for luciferase with stimulated NGL BMDMs. Transfections with the commercial agents were performed as previously described. Previous work with the nanoparticles has shown that the optimum N:P ratio for protection of the associated siRNA is an N:P charge ratio of 4, corresponding to a polymer mass of 160 ug per nmol of siRNA.¹³ siRNA was mixed with either a commercial agent or one of the two polymer formulations and allowed to form transfection complexes for 1 hour. After an hour, the complexes were added and allowed to incubate for 6 hours. The cells were

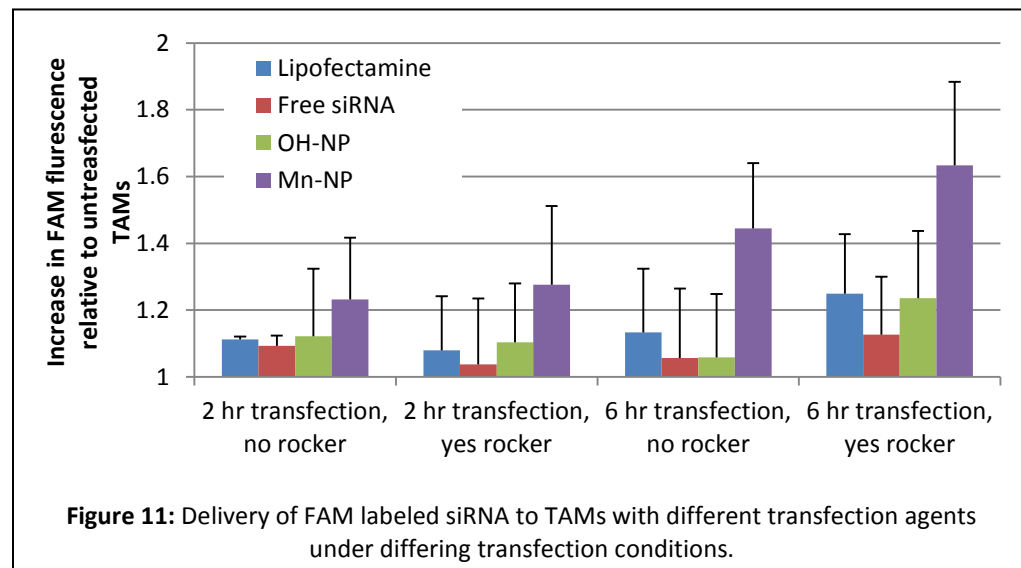
then stimulated for 6 hours with TNF- α and prepared for the luciferase activity assay as described above. Figure 10 shows that while Lipofectamine provided the most efficacious knockdown, the two nanoparticle formulations showed some knockdown in this initial experiment.



Delivery of FAM labeled siRNA to tumor associated macrophages (TAMs) under multiple conditions:

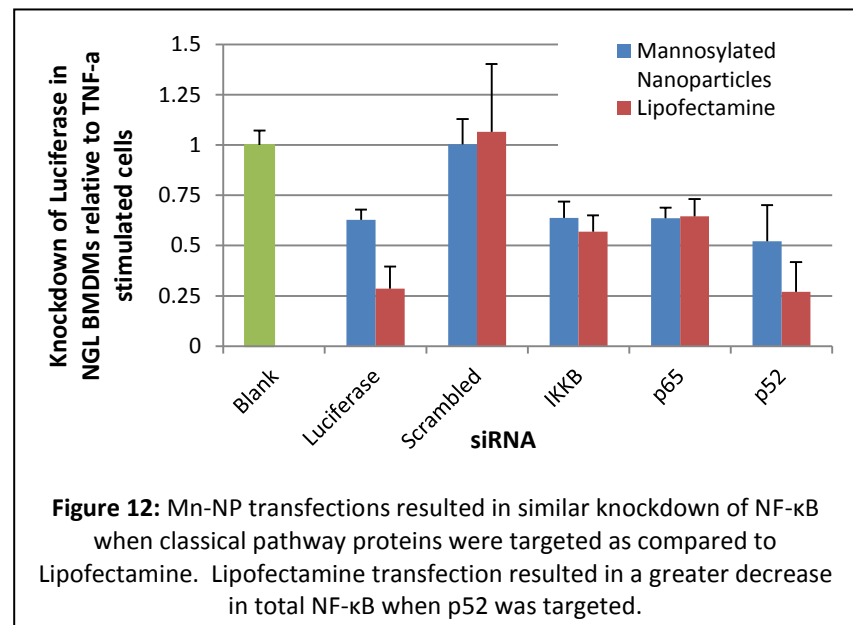
TAMs were isolated from the mammary tumors of mice bearing the polyoma middle T oncogene (PyVT) targeted to the mammary epithelium by a 60 minute rapid adhesion protocol and plated in 12 well plates.⁴⁰ The PyVT model is an accepted mouse model of human breast cancer progression and these cells are the *in vivo* targets of this work.⁴¹ FAM labeled scrambled siRNA was delivered to the cells in free form, with Lipofectamine, and with Mn-NP and OH-NP. 2 and 6 hour transfection times were used and TAMs were transfected both with and without fluid motion in the wells. Fluid motion was created with a cell rocker installed in the incubator, rocking at a rate of approximately 10 rocks per minute. FAM fluorescence was measured using a Tecan Infinite M1000 Pro plate reader. The Mn-NP resulted in the most FAM fluorescence under all conditions (Figure 11). This effect was more pronounced with the longer transfection time and with fluid motion in the well. Previous work by the Giorgio lab has shown

that convective fluid flow increases delivery of nucleotide containing transfection particles, and it is expected that this effect is more pronounced in particles targeting an endosomal receptor such as the mannose receptor.⁴²



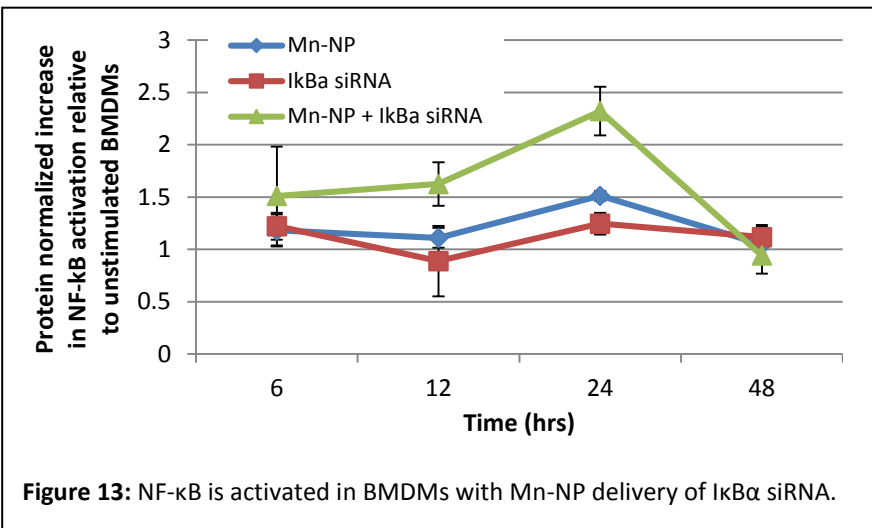
Transfection of BMDMs with NF- κ B specific siRNAs using Mn-NPs:

The next transfection experiments utilized the most efficacious NF- κ B siRNAs determined previously. Transfection times were increased to 18 hours based on the expected high biocompatibility of the nanoparticle transfection agents in order to



increase transfection efficiency and performed with fluid motion introduced as previously described.

Under these conditions, the use of Mn-NPs resulted in significant total NF- κ B knockdown; in many cases comparable to that measured with the use of Lipofectamine (Figure 12). One interesting result of



experiments using Mn-NP to deliver siRNA against NF-κB proteins to BMDMs is the observation that NF-κB can be activated by using siRNA to knockdown the IκBa inhibitor protein

in these cells (Figure 13). When free siRNAs or empty Mn-NPs are incubated with BMDMs there is no effect. However, when the two are combined, there is an increase in total NF-κB activation as measured in NGL BMDMs dosed with the complexes for 24 hours.

Outcomes and deliverables: Aim #1 has resulted in transfection protocols for Lipofectamine and Mn-NP using a relatively small concentration of siRNA (10 nM). The efficacy of the Mn-NP transfection agents has been demonstrated to be similar to Lipofectamine in *in vitro* transfection studies, and experiments with fluid motion and longer transfection times suggest that these results will translate well to *in vivo* usage of Mn-NP in Aim #3. Data from the knockdown of NF-κB proteins would be useful for developing a model of NF-κB activation and deactivation. Several conference abstracts have been prepared from this work, and a publication is planned for submission in May, aimed at a nanotechnology journal.

Specific Aim #2: Definition of an NF-κB mediated, anti-tumor, "Terminator" phenotype for macrophages

The NF-κB pathway has been implicated in creating the pro-tumor TAM phenotype in many cancers.^{4, 19, 43} However, classical NF-κB activation is strongly associated with the classically activated macrophage phenotype, which produces several cytokines leading to acute inflammation capable of

killing microorganisms and tumor cells such as IFN- γ , TNF- α , IL-12, pro-inflammatory CXCL cytokines, and others.^{3, 44, 45} The inherent complexity of NF- κ B control of macrophage phenotype has been a barrier to therapeutic techniques targeting NF- κ B in macrophages as a point of intervention. Part of this complexity stems from a lack of knowledge about downstream effects of alternative NF- κ B activation in macrophages. Aim #2 seeks to investigate NF- κ B activation in macrophages in a pathway specific fashion and develop a phenotypic profile for a macrophage that has induced anti-tumor activity due to NF- κ B manipulation (Terminator macrophage).

2. Manipulation of the NF- κ B pathway in primary macrophages to create the Terminator phenotype:

Once the Terminator phenotype has been defined, it will be reproduced *in vitro* in a macrophage population by manipulation of NF- κ B using siRNA. The optimized transfection protocol from Aim #1a will be used with siRNA from Aim #1b to selectively knock down NF- κ B proteins in the classical and alternative pathway. Background research and preliminary experiments suggest that an efficacious anti-tumor phenotype can be produced by knocking down the alternative pathway and activating the classical pathway. Experiments in Aim #1 have shown that it is possible to efficaciously deliver siRNA against p100/p52 to murine NGL BMDMs and decrease total NF- κ B activity. Similar experiments have shown that it is possible to increase NF- κ B activation by delivering siRNA against the I κ B α inhibitor protein in the classical pathway.

Transfection of murine macrophages to create a Terminator phenotype: BMDMs, splenic macrophages (SPMs), and TAMs from PyVT mammary tumors will be plated at a density of 3×10^6 cells per well in 6-well plates. SPMs and TAMs will be isolated from dissociated whole tissue cell suspensions with a 60 minute rapid adhesion protocol.^{40, 46} 10 nM siRNA will be delivered to the cells for 18 hours using Lipofectamine® RNAiMAX transfection agent using the optimized protocol from Aim #1. Fluid motion will be created in the wells using a cell rocker, rocking at approximately 10 rocks per minute. Sequences

used will be sequences against I κ B α to activate the classical pathway and sequences against p100/p52 to knock down the alternative pathway. These sequences will be delivered separately and together, and untransfected cells and cells exposed to only Lipofectamine will be used as negative controls. After transfection, one group of cells will be immediately prepared for qRT-PCR analysis and another group will be stimulated with TNF- α for 6 hours, then prepared for qRT-PCR analysis. RNA will be isolated from the cells as described in Aim #2a and cDNA libraries for the cells will be made for real-time analysis. qRT-PCR will focus on analyzing key genes identified for the Terminator phenotype in 2a. In a parallel experiment, TAMs will be modified using the same transfection scheme described above. The cells will then be co-incubated with tumor cells using a macrophage cytotoxicity assay currently under development in the Yull lab.

Alternate plan: SPMs were chosen for use in Aim #2 as a primary population of mature, immunocompetent macrophages with which to experiment. Other sources of macrophages meeting these criteria are resident macrophages from the lung or the mammary glands, though these sources are not as abundant as the spleen. Mammary TAMs were chosen for use as a primary source of macrophages which have been repurposed by tumor cells to exhibit a pro-tumor phenotype because this is the cell type that ideally will be targeted for manipulation *in vivo*. Another source of tumor educated macrophages that could be used is murine ovarian ascites fluid. The Yull lab is currently cultivating expertise in creating and isolating this type of macrophage. In addition to targeting p100/p52 for knockdown of the alternative NF- κ B pathway, targeting of the NIK enzyme should also produce efficacious results; especially considering that NIK is unique in that it is normally expressed at a low level and its function is primarily controlled by a steady level of expression. NIK activation of the alternative NF- κ B pathway is very sensitive to changes in levels of NIK enzyme.²⁷

Outcomes and deliverables: The Terminator phenotype described in 2 will be used for *in vivo* Aim #3.

The NF-κB pathway is a major pathway in all cell types and has a profound controlling influence on macrophage phenotype.⁹ The use of siRNA to create a designed macrophage phenotype by manipulating NF-κB is a novel approach for engineering cancer immunity. The alternative NF-κB pathway is an important contributor to total NF-κB activity, but is critically under-studied with respect to how it functions in specific cell types.⁴⁷ A description of the effects that alternative NF-κB manipulation has on macrophage phenotype would be novel and impactful. The results of Aim #2 will be presented in an article submitted to a high impact immunology journal; estimated submission date: Summer 2013.

Specific Aim #3: Investigate the therapeutic potential of Terminator macrophages and nucleotide delivery to TAMs

The completion of Aim 1 provides an *in vitro* validated nanoparticle for the transfection of tumor associated macrophages with nucleic acid therapeutics. Aim 2 elucidates a target phenotype for anti-tumor macrophages and describes a method of creating this phenotype by manipulating the NF-κB pathway. Aim 3 seeks to combine the two previous aims to investigate their therapeutic potential in the PyVT mouse model of human breast cancer. The goal of Aim 3 is to begin to test the hypothesis that Mn-NP delivered siRNA can change TAM phenotype and produce a tumor cytotoxic or cytostatic effect (directly or indirectly) with positive therapeutic potential. The *in vitro* work published previously regarding Mn-NP and the completion of Aims #1 and #2 will be used as preliminary evidence for the *in vivo* efficacy of using Mn-NP to create a Terminator macrophage phenotype within tumor stroma. In order to simplify initial *in vivo* investigations, I will seek to answer the following questions:

1. Do modified Terminator macrophages have therapeutic potential in a simple tumor system?
2. Is it possible to target macrophages *in vivo* using Mn-NP, especially at the site of metastases?

3a. Investigating the therapeutic potential of terminator macrophages: Aim #2 will result in the description of the Terminator macrophage phenotype. Aim #3a will investigate the therapeutic potential of these macrophages in a simplified tumor model. A simple method of modifying macrophages would be to do so *in vitro*. Once the macrophages have been modified, a simple method of tumor delivery would be to directly inject the cells into a tumor. This approach is reminiscent of adoptive cell transfer therapy, which has been used as a clinical model to develop new cancer therapies and as a pre-clinical model to test the effects of manipulating certain cell types.^{48, 49} I propose to use the latter paradigm to test the therapeutic potential of macrophages that have been modified *ex vivo* by directly injecting the cells into orthotopic mammary tumors in mice. Some of the most significant technical issues associated with testing a cell phenotype for therapeutic potential (modification of cells, cell numbers) are simplified by using this model system.

Determination of appropriate macrophage numbers and macrophage retention time in tumors:

Orthotopic PyVT cell line tumors will be made in the left or right, fourth mammary fat pad of 15 adult FVB mice. Once the tumors reach a palpable size, macrophages labeled with Qtracker® 800 (Invitrogen) near infrared quantum dot cell tracking agent will be injected into the tumors at variable cell densities (3 different densities, n=4 mice per density), with PBS injections used as a control (n=3).^{50, 51} The animals will be imaged at 1, 6, 24, 48, 72, 96 hrs post injection using an IVIS imaging system to measure near infrared fluorescence as a measure of injected macrophage load retained in the tumor.

Injection of modified macrophages into orthotopic tumors: Orthotopic PyVT cell line tumors will be made in the left and right mammary fat pads of 20 adult FVB mice. The right tumors will receive experimental treatment and the left tumors will serve as internal controls. Once the tumors reach a palpable size, macrophages will be injected into the tumors in the following scheme: 5 mice will receive a PBS injection as a negative control, 5 mice will receive an injection of unmodified macrophages, 5 mice

will receive and injection of LPS+IFN- γ treated macrophages as a positive control for M1 phenotype, and 5 mice will receive an injection of macrophages modified with siRNA. The previous study will inform macrophage dosing density, dosing regimen (single or multiple doses), and the timeline of the experiment. During the experiment, tumor size will be measured 3 times per week. At the end of the experiment, the tumors will be measured, weighed, and dissociated to a single cell suspension. M1 markers will be measured with qRT-PCR in whole tumor tissue and in the macrophage population, enriched via a 60 minute rapid adhesion assay.^{40, 46} Additionally, tissue levels of ki67 and caspase3 will be analyzed as markers of cell proliferation and cell death, respectively. Cytospins will be performed on aliquots of single cell tissue suspensions and stained with a Giemsa stain to analyze the immune cell composition of the tumors, providing insight into possible indirect immunologic effects caused by modified macrophages.

3b. Determine the efficacy of Mn-NP for delivery of nucleotides to TAMs in lung metastases: Once the *in vitro* efficacy of Mn-NP for siRNA delivery to macrophages has been demonstrated, the next step will be to test *in vivo* delivery and efficacy of mannose as a targeting ligand. To that end, a tail vein lung metastasis model will be set up in 20 FVB mice via injection of PyVT cell line cells. Approximately 2 weeks after injection of the PyVT cells, mice will receive intratracheal delivery (i.t.) of Mn-NP with cy3 labeled DNA as a nucleotide payload (1 mg/kg) as well as controls: 5 mice will receive i.t. delivery of PBS, 5 mice will receive i.t. delivery of free DNA-cy3, 5 mice will receive i.t. delivery of OH-NP_DNA-cy3 as a control for mannose targeting, and 5 mice will receive i.t. delivery of Mn-NP_DNA-cy3. After the particles or controls are allowed to incubate in the mouse lungs (exact time will be informed by *in vitro* experiments from Aim #1 and #2), the mice will be sacrificed and the lungs removed. Half of the lungs will be dissociated to a single cell suspension for quantitative fluorescence analysis and half of the lungs will be fixed for whole tissue section imaging.

Quantitative fluorescence measurement in single cells: A portion of the lungs will be dissociated into a single-cell suspension and the macrophage population will be enriched via a 60 minute rapid adhesion assay on 12-well plates.^{40, 46} The non-macrophage cell population will be removed after 60 minutes and plated in new 12-well plates. The cy3 fluorescence for each sample (macrophage and non-macrophage populations) will be quantitatively measured on a Tecan Infinite M1000 plate reader. Approximately 20 measurements per well will be taken, with a scan sequence designed to measure areas at the periphery and center of the wells. Fluorescence measurements will be controlled for differences in cell number with a Bradford assay for protein concentration.

Whole tissue immunohistochemistry (IHC): A portion of the lungs will be fixed and sectioned for use in an immunohistochemical analysis of Mn-NP uptake. In order to investigate the efficacy of mannose targeting of macrophages in the context of tumor metastases, the tissue will be stained with an antibody for the mannose receptor (CD206) and imaged to correlate cy3 positive cells with CD206 positive cells.

Alternate plan: An alternate route of nanoparticle delivery is retro-orbital injection, although this route will result in reduced delivery to the lungs. A non-IV delivery method considered for alternate delivery is intraperitoneal injection. After fluorescence measurements are taken of the dissociated cells, the same cells could be fixed with paraformaldehyde and stained overnight for immunofluorescence by a direct staining method using a fluorescently labeled CD206 antibody at a 1:100 dilution.⁷ The cells would be counterstained with a 1:1000 dilution DAPI nuclear stain. The stained cells would be imaged with a fluorescent microscope (Nikon Eclipse Ti) and the imaged cells analyzed for co-localization of cy3 fluorescence and CD206 antibody fluorescence.

Outcomes and deliverables: Aim #3 will investigate the therapeutic potential of Terminator macrophages and the *in vivo* nucleotide delivery ability of Mn-NP in simplified model systems. These

experiments will provide *in vivo* evidence to support the therapeutic potential of NF-κB manipulation in TAMs and the ability of Mn-NP to deliver therapeutic nucleotides to TAMs. This data will be useful for future grant applications and would be appropriate for publication in a high impact scientific journal with broad readership; estimated submission date: late fall/early winter 2013.

VII. Proposed Timeline

		2011	2012				2013			
			Winter	Spring	Summer	Fall	Winter	Spring	Summer	Fall
AIM 1	Transfection agent protocol									
	siRNA Library									
	Mn-NP validation									
AIM 2	Microarray of macrophages									
	Terminator Macrophages									
AIM 3	Biodistribution of Mn-NP									
	<i>In vivo</i> manipulation of TAMs									
Other Milestones	DOD annual Report									
	Mn-NP manuscript									
	Terminator macrophage manuscript									
	<i>In vivo</i> manuscript									
	Dissertation Defense									

VIII. Acknowledgements

I would like to thank everyone who has helped me to get this far in my research and my career; those who have offered their support, both professional and personal. First, I would like to express a deep sense of gratitude to my PI and mentor, Todd Giorgio. When I was left without an advisor after my first year in graduate school, he took me into his lab and has helped me to grow and thrive as an engineer and scientist for the past 4 years. For that and for much more, I will be eternally grateful. I would also like to give special thanks to Fiona Yull for welcoming an engineer into her microbiology/cancer immunology lab. She bore with me as I learned the language and techniques of immunology and mouse models. The experience of working in laboratories with two very different backgrounds has been, and continues to be an engaging challenge and extremely rewarding. I am a better investigator, engineer, and scientist because of the collaboration between the Giorgio and Yull labs. The positive aspects of my work are a reflection of the skills of my mentors. Any faults are my own. Thank you also to the other members of my PhD committee for taking the time out of your schedules to mentor me through this arduous process. Each member of my committee brings something different and important to the table.

The labmates I have worked with during my tenure at Vanderbilt so far have uplifted and sustained me. In the Giorgio lab, my friend and former roommate Shann Yu deserves special thanks. We worked closely together for several years and I couldn't have asked for a better friend and research partner. I'd also like to thank the post docs, graduate students, and undergrads (past and present) I have worked with so far: Amanda Lowery, Hongmei Li, Virgina Pensabene, Kellye Kirkbride, Ian McFadden, Charleson Bell, Bharat Kumar, Jordan Fernandez, Becca Hudson, Chelsey Smith, Kavya Sharman, and any others I may have accidentally forgot. I'd also like to thank the members of the Yull lab I have worked with for the past year and a half: Whitney Barham, Hala Onishko, Oleg Tikhomirov, and Lianyi Chen. I also, want to thank the members of the Duvall, Sung, and Haselton labs for their input, encouragement, and friendship. The open and collaborative environment in our biomaterials/nanomaterials group makes me look forward to coming in to the lab every day.

My family has always been there to support me and let me know how proud they are of me and my decision to pursue a PhD in BME. If I have ever second guessed myself, they have been there to tell me unequivocally that they support me and believe in me. For that and everything else, I'd like to thank my father and mother, Albert and Lorenda Ortega, my brother Logan, and my sister Clara. Finally, I'd like to thank my girlfriend of 6 years, Alex Barker, for her continuing and unwavering support and understanding. She looks after me when I'm too busy to do so myself, and is understanding of the times when I have to spend my evenings and weekends in lab. I couldn't do this without her support.

IX. References

1. Qian, B.Z. *et al.* A Distinct Macrophage Population Mediates Metastatic Breast Cancer Cell Extravasation, Establishment and Growth. *Plos One* **4** (2009).
2. Oeckinghaus, A., Hayden, M.S. & Ghosh, S. Crosstalk in NF-kappaB signaling pathways. *Nat Immunol* **12**, 695-708.
3. Mantovani, A., Sozzani, S., Locati, M., Allavena, P. & Sica, A. Macrophage polarization: tumor-associated macrophages as a paradigm for polarized M2 mononuclear phagocytes. *Trends in Immunology* **23**, 549-555 (2002).
4. Pollard, J.W. Tumour-educated macrophages promote tumour progression and metastasis. *Nature Reviews Cancer* **4**, 71-78 (2004).
5. Condeelis, J. & Pollard, J.W. Macrophages: Obligate partners for tumor cell migration, invasion, and metastasis. *Cell* **124**, 263-266 (2006).
6. Coussens, L.M. & Werb, Z. Inflammation and cancer. *Nature* **420**, 860-867 (2002).
7. Qian, B.Z. & Pollard, J.W. Macrophage Diversity Enhances Tumor Progression and Metastasis. *Cell* **141**, 39-51 (2010).
8. Ben-Neriah, Y. & Karin, M. Inflammation meets cancer, with NF-kappa B as the matchmaker. *Nature Immunology* **12**, 715-723 (2011).
9. DiDonato, J.A., Mercurio, F. & Karin, M. NF-kappa B and the link between inflammation and cancer. *Immunological Reviews* **246**, 379-400 (2012).
10. Fire, A. *et al.* Potent and specific genetic interference by double-stranded RNA in *Caenorhabditis elegans*. *Nature* **391**, 806-811 (1998).
11. Davis, M.E. *et al.* Evidence of RNAi in humans from systemically administered siRNA via targeted nanoparticles. *Nature* **464**, 1067-1070.
12. Allavena, P. *et al.* Engagement of the Mannose Receptor by Tumoral Mucins Activates an Immune Suppressive Phenotype in Human Tumor-Associated Macrophages. *Clinical & Developmental Immunology* (2010).
13. Yu, S.S. *et al.* Macrophage-Specific RNA Interference Targeting via "Click", Mannosylated Polymeric Micelles. *Molecular Pharmaceutics* **10**, 975-987 (2013).
14. Pollard, J.W. Trophic macrophages in development and disease. *Nature Reviews Immunology* **9**, 259-270 (2009).
15. Ojalvo, L.S., King, W., Cox, D. & Pollard, J.W. High-Density Gene Expression Analysis of Tumor-Associated Macrophages from Mouse Mammary Tumors. *American Journal of Pathology* **174**, 1048-1064 (2009).
16. Zabuwala, T. *et al.* An Ets2-Driven Transcriptional Program in Tumor-Associated Macrophages Promotes Tumor Metastasis. *Cancer Research* **70**, 1323-1333 (2010).
17. Mantovani, A. & Sica, A. Macrophages, innate immunity and cancer: balance, tolerance, and diversity. *Current Opinion in Immunology* **22**, 231-237 (2010).
18. Sharma, M. *et al.* CSF-1 and Fibromatosis Expression in Stroma of Ductal Carcinoma In Situ. *Modern Pathology* **22**, 67a-67a (2009).
19. Lin, E.Y., Nguyen, A.V., Russell, R.G. & Pollard, J.W. Colony-stimulating factor 1 promotes progression of mammary tumors to malignancy. *Journal of Experimental Medicine* **193**, 727-739 (2001).
20. Gordon, S. Alternative activation of macrophages. *Nature Reviews Immunology* **3**, 23-35 (2003).
21. Greten, F.R. *et al.* IKK beta links inflammation and tumorigenesis in a mouse model of colitis-associated cancer. *Cell* **118**, 285-296 (2004).

22. Hudson, J.D. *et al.* A proinflammatory cytokine inhibits p53 tumor suppressor activity. *Journal of Experimental Medicine* **190**, 1375-1382 (1999).
23. Karin, M. & Greten, F.R. NF kappa B: Linking inflammation and immunity to cancer development and progression. *Nature Reviews Immunology* **5**, 749-759 (2005).
24. Sun, S.C. The noncanonical NF-kappa B pathway. *Immunological Reviews* **246**, 125-140 (2012).
25. Weih, F. & Caamano, J. Regulation of secondary lymphoid organ development by the nuclear factor-kappa B signal transduction pathway. *Immunological Reviews* **195**, 91-105 (2003).
26. Xiao, G.T., Fong, A. & Sun, S.C. Induction of p100 processing by NF-kappa B-inducing kinase involves docking I kappa B kinase alpha (IKK alpha) to p100 and IKK alpha-mediated phosphorylation. *J. Biol. Chem.* **279**, 30099-30105 (2004).
27. Liao, G.X., Zhang, M.Y., Harhaj, E.W. & Sun, S.C. Regulation of the NF-kappa B-inducing kinase by tumor necrosis factor receptor-associated factor 3-induced degradation. *J. Biol. Chem.* **279**, 26243-26250 (2004).
28. Beinke, S. & Ley, S.C. Functions of NF-kappa B1 and NF-kappa B2 in immune cell biology. *Biochem. J* **382**, 393-409 (2004).
29. Chellat, F., Merhi, Y., Moreau, A. & Yahia, L. Therapeutic potential of nanoparticulate systems for macrophage targeting. *Biomaterials* **26**, 7260-7275 (2005).
30. Luo, Y.P. *et al.* Targeting tumor-associated macrophages as a novel strategy against breast cancer. *Journal of Clinical Investigation* **116**, 2132-2141 (2006).
31. Convertine, A.J., Benoit, D.S.W., Duvall, C.L., Hoffman, A.S. & Stayton, P.S. Development of a novel endosomolytic diblock copolymer for siRNA delivery. *J. Controlled Release* **133**, 221-229 (2009).
32. Boyer, C. *et al.* Bioapplications of RAFT Polymerization. *Chem. Rev.* **109**, 5402-5436 (2009).
33. Kolb, H.C. & Sharpless, K.B. The growing impact of click chemistry on drug discovery. *Drug Discovery Today* **8**, 1128-1137 (2003).
34. Elbashir, S.M. *et al.* Duplexes of 21-nucleotide RNAs mediate RNA interference in cultured mammalian cells. *Nature* **411**, 494-498 (2001).
35. Davis, M.E. The first targeted delivery of siRNA in humans via a self-assembling, cyclodextrin polymer-based nanoparticle: from concept to clinic. *Mol Pharm* **6**, 659-668 (2009).
36. Han, W. *et al.* Myeloid cells control termination of lung inflammation through the NF-kappa B pathway. *American Journal of Physiology-Lung Cellular and Molecular Physiology* **296**, L320-L327 (2009).
37. Everhart, M.B. *et al.* Duration and intensity of NF-kappa B activity determine the severity of endotoxin-induced acute lung injury. *Journal of Immunology* **176**, 4995-5005 (2006).
38. Connelly, L., Jacobs, A.T., Palacios-Callender, M., Moncada, S. & Hobbs, A.J. Macrophage endothelial nitric-oxide synthase autoregulates cellular activation and pro-inflammatory protein expression. *J. Biol. Chem.* **278**, 26480-26487 (2003).
39. Everhart, M.B. *et al.* Duration and intensity of NF-kappaB activity determine the severity of endotoxin-induced acute lung injury. *J Immunol* **176**, 4995-5005 (2006).
40. Schonhegrad, M.A. & Holt, P.G. Improved Method for the Isolation of Purified Mouse Peritoneal-Macrophages. *Journal of Immunological Methods* **43**, 169-173 (1981).
41. Lin, E.Y. *et al.* Progression to malignancy in the polyoma middle T oncogene mouse breast cancer model provides a reliable model for human diseases. *American Journal of Pathology* **163**, 2113-2126 (2003).
42. Harris, S.S. & Giorgio, T.D. Convective flow increases lipoplex delivery rate to in vitro cellular monolayers. *Gene Therapy* **12**, 512-520 (2005).
43. Mantovani, A., Bottazzi, B., Colotta, F., Sozzani, S. & Ruco, L. The Origin and Function of Tumor-Associated Macrophages. *Immunology Today* **13**, 265-270 (1992).

44. Mantovani, A. The chemokine system: redundancy for robust outputs. *Immunology Today* **20**, 254-257 (1999).
45. Sica, A. et al. Macrophage polarization in tumour progression. *Semin Cancer Biol* **18**, 349-355 (2008).
46. Dethloff, L.A. & Lehnert, B.E. Pulmonary Interstitial Macrophages - Isolation and Flow Cytometric Comparisons with Alveolar Macrophages and Blood Monocytes. *Journal of Leukocyte Biology* **43**, 80-90 (1988).
47. Sun, S.C. Non-canonical NF-kappa B signaling pathway. *Cell Research* **21**, 71-85 (2011).
48. Dudley, M.E. & Rosenberg, S.A. Adoptive-cell-transfer therapy for the treatment of patients with cancer. *Nature Reviews Cancer* **3**, 666-U662 (2003).
49. Andreesen, R. et al. Adoptive Transfer of Tumor Cytotoxic Macrophages Generated Invitro from Circulating Blood Monocytes - a New Approach to Cancer-Immunotherapy. *Cancer Research* **50**, 7450-7456 (1990).
50. Lin, S. et al. Quantum dot imaging for embryonic stem cells. *Bmc Biotechnology* **7** (2007).
51. Muccioli, M., Pate, M., Omosebi, O. & Benencia, F. Generation and labeling of murine bone marrow-derived dendritic cells with Qdot nanocrystals for tracking studies. *J Vis Exp.*
52. Sasmono, R.T. et al. A macrophage colony-stimulating factor receptor-green fluorescent protein transgene is expressed throughout the mononuclear phagocyte system of the mouse. *Blood* **101**, 1155-1163 (2003).
53. Connelly, L. et al. Activation of nuclear factor kappa B in mammary epithelium promotes milk loss during mammary development and infection. *J Cell Physiol* **222**, 73-81.
54. Connelly, L. et al. NF-kappaB activation within macrophages leads to an anti-tumor phenotype in a mammary tumor lung metastasis model. *Breast Cancer Res* **13**, R83.
55. Connelly, L. et al. Inhibition of NF-kappa B activity in mammary epithelium increases tumor latency and decreases tumor burden. *Oncogene* **30**, 1402-1412 (2011).
56. Yamashita, K. et al. Silica and titanium dioxide nanoparticles cause pregnancy complications in mice. *Nature Nanotechnology* **6**, 321-328 (2011).
57. De Ritis, F., Coltorti, M. & Giusti, G. An enzymic test for the diagnosis of viral hepatitis: The transaminase serum activities (Reprinted from Clinica Chimica Acta, vol 2, pg 70-74, 1957). *Clin. Chim. Acta* **369**, 148-152 (2006).
58. Joyce, J.A. & Pollard, J.W. Microenvironmental regulation of metastasis. *Nature Reviews Cancer* **9**, 239-252 (2009).

Manipulation of the Tumor Associated Macrophage Phenotype into an Anti-Tumor Phenotype by Modulating the NF-κB Pathway

Qualifying Exam Presentation for Ryan Ortega
5/8/13

Dissertation Committee:

Todd Giorgio
Fiona Yull
Craig Duvall
Frederick Haselton
Barbara Fingleton

**Cancer is one of the most prevalent
health problems in the first world**

Leading New Cancer Cases and Deaths – 2013 Estimates

Estimated New Cases*		Estimated Deaths	
Male	Female	Male	Female
Prostate 238,590 (28%)	Breast 232,340 (29%)	Lung & bronchus 87,260 (28%)	Lung & bronchus 72,220 (26%)
Lung & bronchus 118,080 (14%)	Lung & bronchus 110,110 (14%)	Prostate 29,720 (10%)	Breast 39,620 (14%)
Colon & rectum 73,680 (9%)	Colon & rectum 69,140 (9%)	Colon & rectum 26,300 (9%)	Colon & rectum 24,530 (9%)
Urinary bladder 54,610 (6%)	Uterine corpus 49,560 (6%)	Pancreas 19,480 (6%)	Pancreas 18,980 (7%)
Melanoma of the skin 45,060 (5%)	Thyroid 45,310 (6%)	Liver & intrahepatic bile duct 14,890 (5%)	Ovary 14,030 (5%)
Kidney & renal pelvis 40,430 (5%)	Non-Hodgkin lymphoma 32,140 (4%)	Leukemia 13,660 (4%)	Leukemia 10,060 (4%)
Non-Hodgkin lymphoma 37,600 (4%)	Melanoma of the skin 31,630 (4%)	Esophagus 12,220 (4%)	Non-Hodgkin lymphoma 8,430 (3%)
Oral cavity & pharynx 29,620 (3%)	Kidney & renal pelvis 24,720 (3%)	Urinary bladder 10,820 (4%)	Uterine corpus 8,190 (3%)
Leukemia 27,880 (3%)	Pancreas 22,480 (3%)	Non-Hodgkin lymphoma 10,590 (3%)	Liver & intrahepatic bile duct 6,780 (2%)
Pancreas 22,740 (3%)	Ovary 22,240 (3%)	Kidney & renal pelvis 8,780 (3%)	Brain & other nervous system 6,150 (2%)
All sites 854,790 (100%)	All sites 805,500 (100%)	All sites 306,920 (100%)	All sites 273,430 (100%)

*Excludes basal and squamous cell skin cancers and in situ carcinoma except urinary bladder.

©2013, American Cancer Society, Inc., Surveillance Research

Cancer cells are an obvious therapeutic target, but the tumor stroma is becoming recognized as a viable target

CANCER CELLS

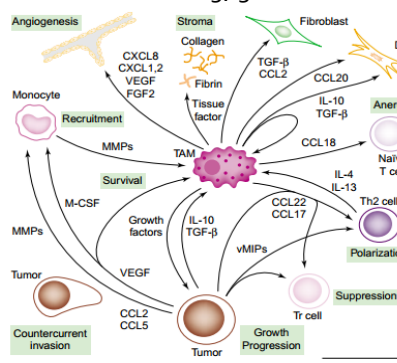
- Large population of heterogenous cells
- Loss of normal function; genetic instability
- Can become resistant to therapy

STROMAL CELLS

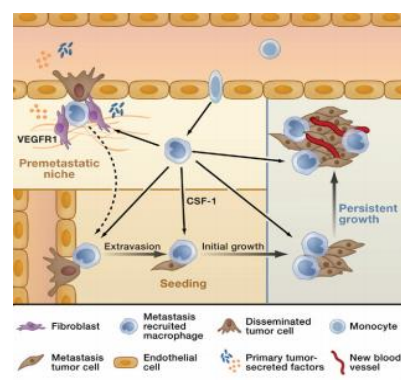
- Relatively more homogenous cell population
- Deregulation of normal functions; stable genome
- May not become resistant to therapy
 - Stable genetics
 - Regular renewal

Tumor associated macrophages (TAMs) regulate the pro-tumor stromal response

- TAMs create local, pro-tumor effects
 - Smoldering inflammation, angiogenesis, immunosuppression, tissue remodeling, growth factors
- TAMs participate in the metastatic process
 - Invasion, intravasation, preparation of the metastatic niche

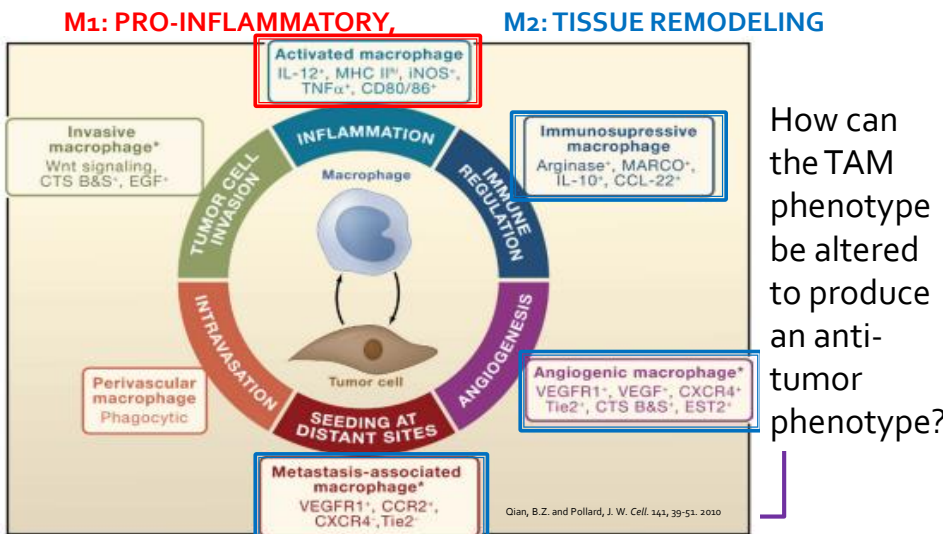


Qian, B.Z. et al. Plos One. 4 (2009)



Mantovani, A. et al. Trends in Immunology. 23: 549-555. (2002)

The TAM phenotype is a complex blend of classical M ϕ phenotypes

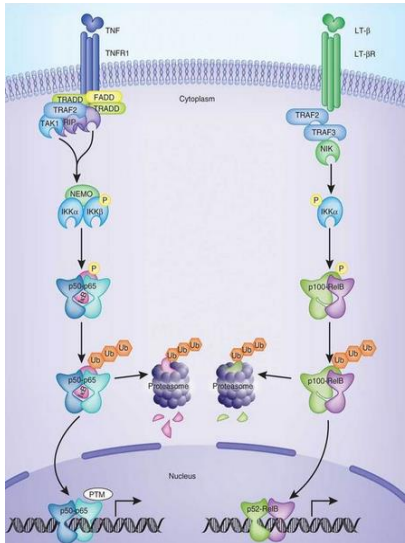


How can the TAM phenotype be altered to produce an anti-tumor phenotype?

The TAM phenotype is induced via tumor-macrophage (M ϕ) signaling

- Immature macrophages invade the tumor and become trapped in the necrotic core
- One of the most important secreted factors tumors use to hijack macrophages is CSF-1
 - CSF-1 is a M ϕ maturation factor
 - Ablation of CSF-1 in mouse models of human cancer reduces TAM population and slows tumor progression and metastasis
- What if we could override the tumor-macrophage signaling and create an anti-tumor phenotype?

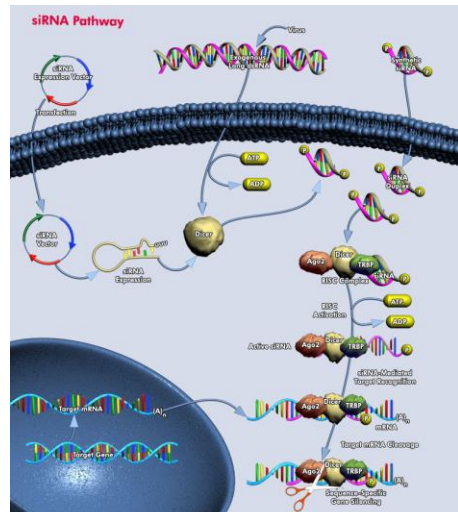
The NF-κB pathway is a major controller of Mφ phenotype



- The NF-κB pathway is actually 2 pathways
- The classical pathway regulates inflammation
 - Constitutively active, broadly activated
- The alternative pathway is understudied; thought to play a role in tissue remodeling
 - Has a specific group of activators

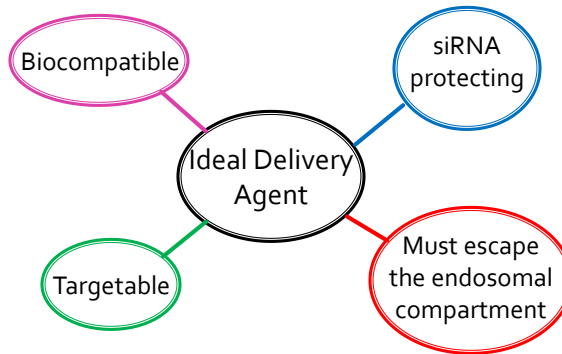
The NF-κB pathway can be manipulated *in vivo* using siRNA

- siRNA bind to complementary strands of mRNA and inhibit translation
 - 2006 Nobel Prize in Medicine or Physiology
- siRNA is being tested in Phase I clinical trials by Calando Pharmaceuticals

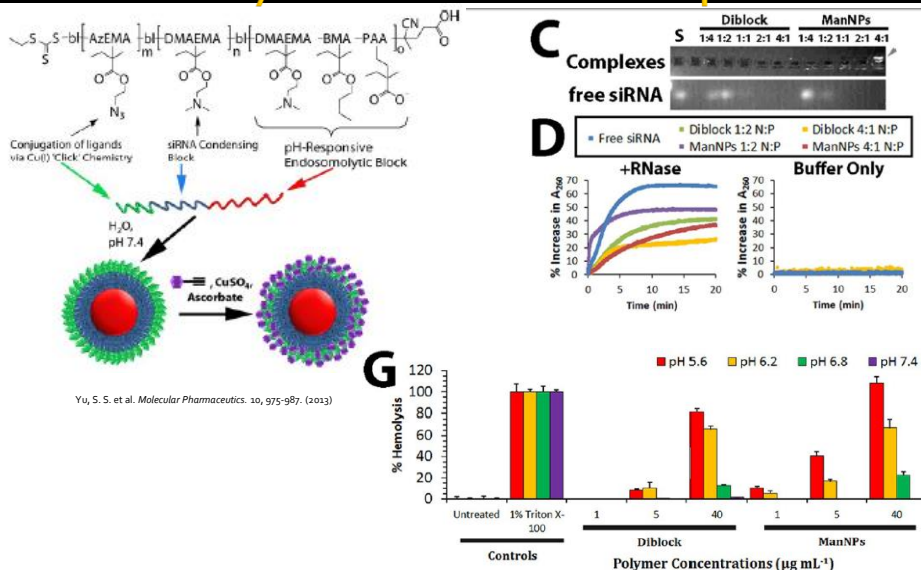


What does the ideal siRNA-to-TAM delivery device look like?

Design Criteria



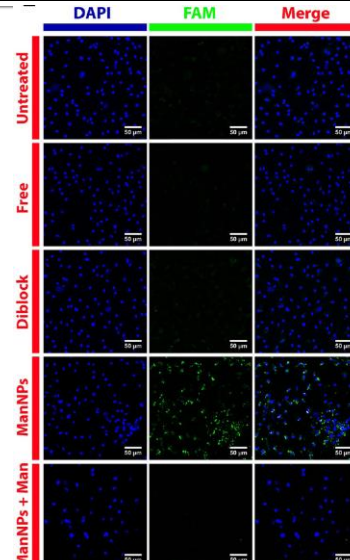
siRNA condensing, endosomal escape nanoparticles (NP) protect siRNA and become membrane-lytic at late-endosomal pH



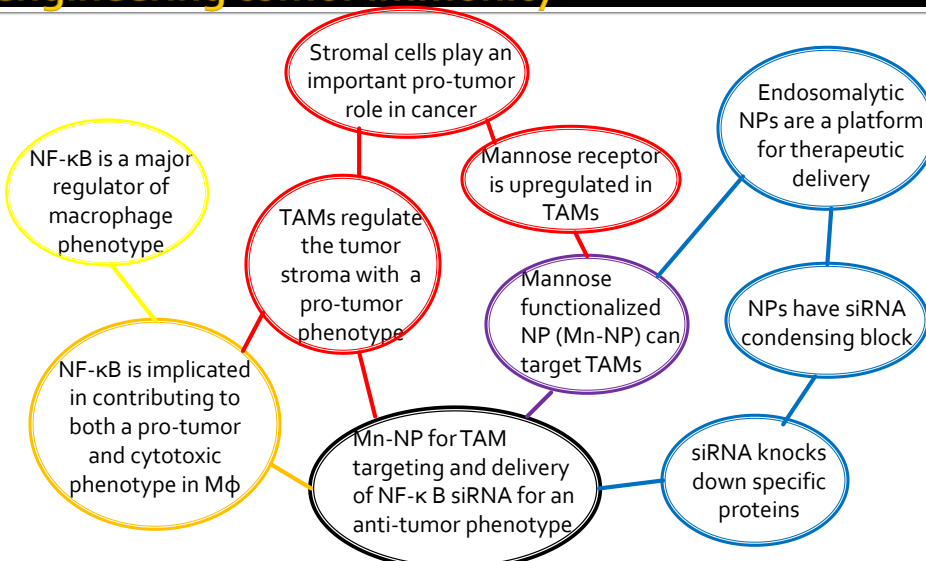
Mannose targeted NP (Mn-NP) for creating an anti-tumor phenotype in TAMs

- Mannose receptor (CD206) is present on the surface of M ϕ
- CD206 is upregulated on the surface of TAMs
- Mn-NP delivers siRNA to M ϕ in a mannose dependent manner

Yu, S. S. et al. *Molecular Pharmaceutics*. 10, 975-987. (2013)



A multi-disciplinary approach can plan, create, and utilize novel nanotherapeutics for engineering tumor immunity



Hypothesis and Specific Aims

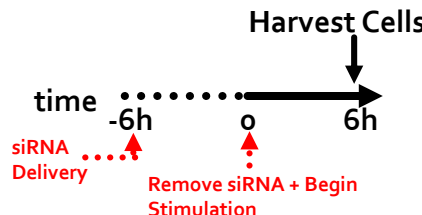
Hypothesis: By strategically manipulating the NF- κ B pathways in tumor associated macrophages it is possible to reduce the pro-tumor effects typically seen in tissue remodeling macrophages and create a set of anti-tumor, immunogenic traits to stimulate tumor cell immunity.

- Aim 1: *In vitro* validation of commercial and nanoparticle siRNA delivery agents
- Aim 2: Definition of an NF- κ B mediated, anti-tumor, "Terminator" phenotype for macrophages
- Aim 3: Targeted delivery of siRNA to TAMs *in vivo*.

Aim 1: *In vitro* siRNA transfection

1a: Development of a commercial transfection agent protocol

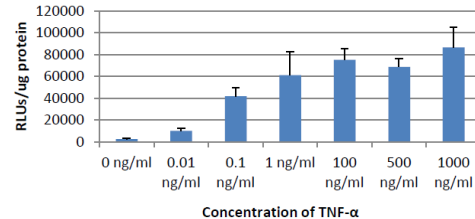
- Initial transfections performed in bone marrow derived macrophages (BMDMs) from NGL mice.
- Cells are transfected with siRNA_transfection agent complexes and then stimulated with TNF- α



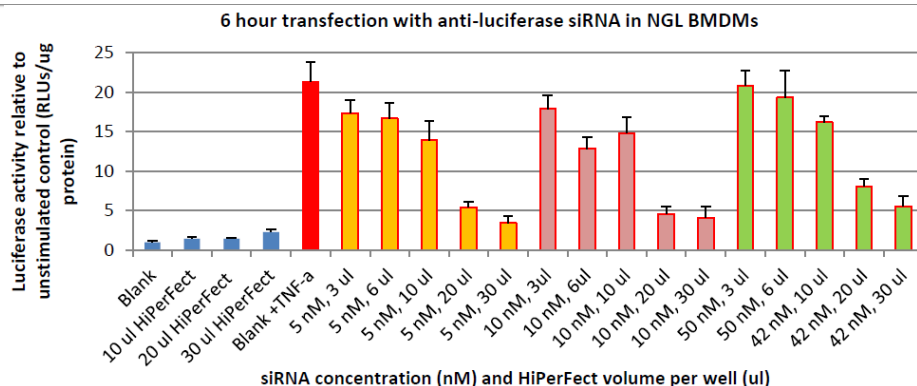
- HiPerFect was initially chosen as the commercial agent

TNF- α stimulation reaches an asymptotic response after 1 ng/ml in BMDM cell culture

- BMDMs were stimulated for 6 hours with TNF- α
- Cells were lysed and the cell supernatant was analyzed for luciferase activity relative to protein concentration
- A 10 ng/ml TNF- α concentration has been used by the Yull lab; this concentration was verified for BMDM stimulation in transfection experiments.



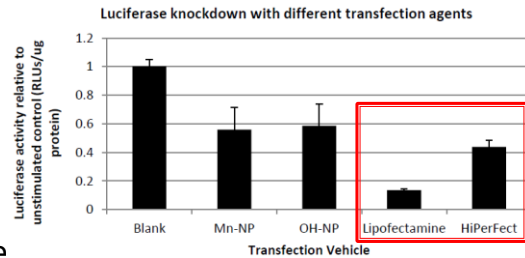
A HiPerFect concentration of 20 μ l/ml and 10 nM siRNA were chosen for transfection



- Though initial experiments were promising, HiPerFect transfections had poor repeatability and were cost prohibitive.

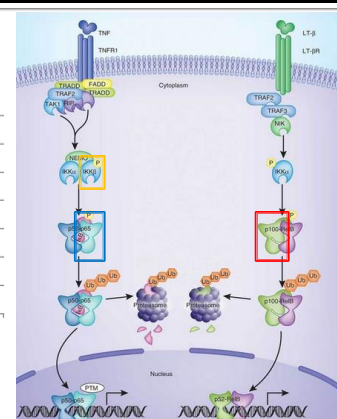
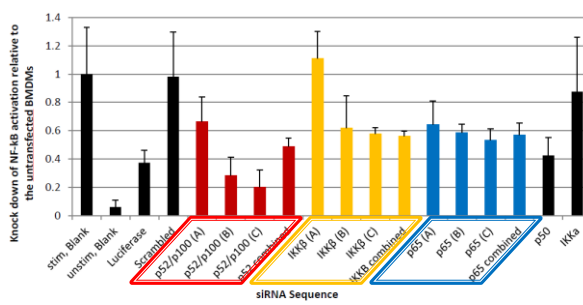
Lipofectamine RNAiMAX was selected as a potential substitute for HiPerFect

- Transfection agent comparison study
 - 10 nM siRNA (consistent with previous experiment)
 - 2 μ l/ml Lipofectamine 20 μ l/ml HiPerFect
 - 6 hrs transfection
 - 6 hrs stimulation
- Lipofectamine proved more efficacious, cost effective, and repeatable than HiPerFect



Lipofectamine was used to investigate NF- κ B specific siRNA sequences

1b: Creation of an effective siRNA library

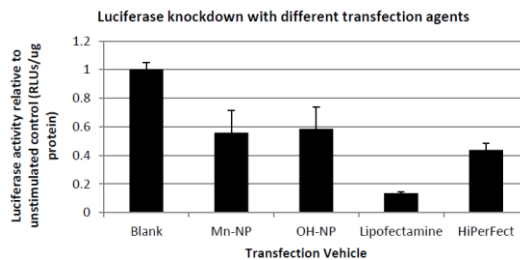


- 6 hrs transfection with 10 nM siRNA, 2 μ l/ml Lipofectamine (suggested dose from manufacturer)

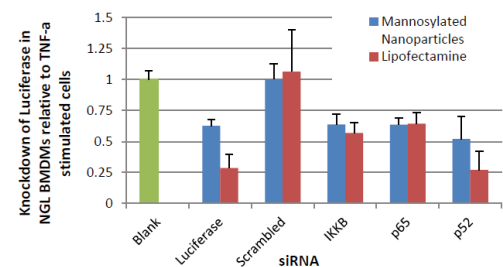
Nanoparticles are efficacious at delivering siRNA to knock down the luciferase reporter in NGL BMDMs

1c: Development of an Mn-NP transfection protocol

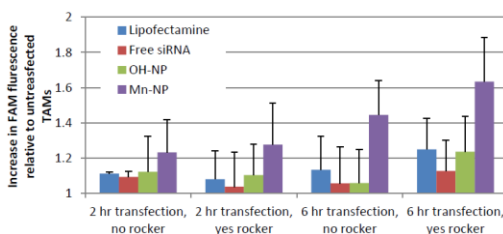
- 10 nM siRNA was used
- NPs complexed with siRNA for an optimal N:P ratio of 4
 - 160 ug polymer per nmol of siRNA
- 6 hrs transfection
- Protocol used was optimized for commercial agents



Longer transfection times and convective fluid motion were introduced in the transfection protocol to improve NP transfection



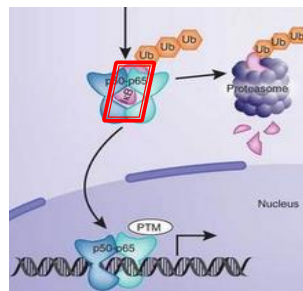
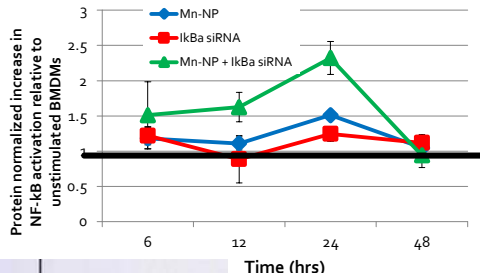
- NF- κ B specific knockdown was repeated with Mn-NP
 - 18 hrs transfection
 - Performed on rocker, approximately 10 rocks/min



- FAM labeled scrambled siRNA was delivered to TAMs with different agents
 - Transfection time was varied
 - TAMs were transfected with and without fluid motion

Mn-NP are capable of activating NF-κB in BMDMs by delivering siRNA to I κ B α

- NGL BMDMs were transfected with I κ B α siRNA by Mn-NP for different times
- No stimulation occurred other than what could be created by knocking down the classical NF-κB inhibitor



Aim 1 Outcomes

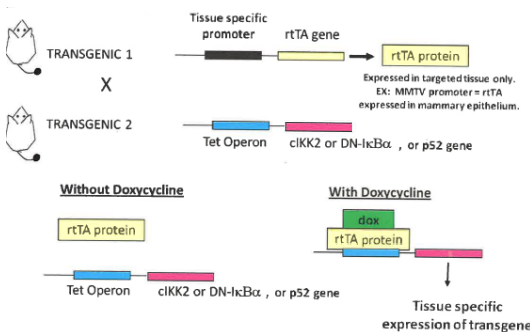
- Effective *in vitro* transfection protocols have been developed for Lipofectamine and Mn-NP
- A Library of effective NF-κB siRNA has been compiled
- Activation of NF-κB by k/d of inhibitor demonstrated
- Several conference abstracts have been presented
 - Publication planned for May submission

Aim 2: Defining the Terminator macrophage phenotype

- TAMs have a blended, pro-tumor phenotype
- NF- κ B is a controller of M ϕ phenotype
 - Inflammation, survival, immune manipulation, tissue modification
- Hypothesis: There exists some manipulation of NF- κ B in macrophages (TAMs specifically) that will remove the TAM phenotype, and induce a phenotype capable of creating a strong, local, transient immune response to tumor cells

Microarray analysis of macrophages will show different phenotypes for classical vs alternative NF- κ B activation

2a: Microarray analysis of IKFM, ALFM, TAM and wt macrophages

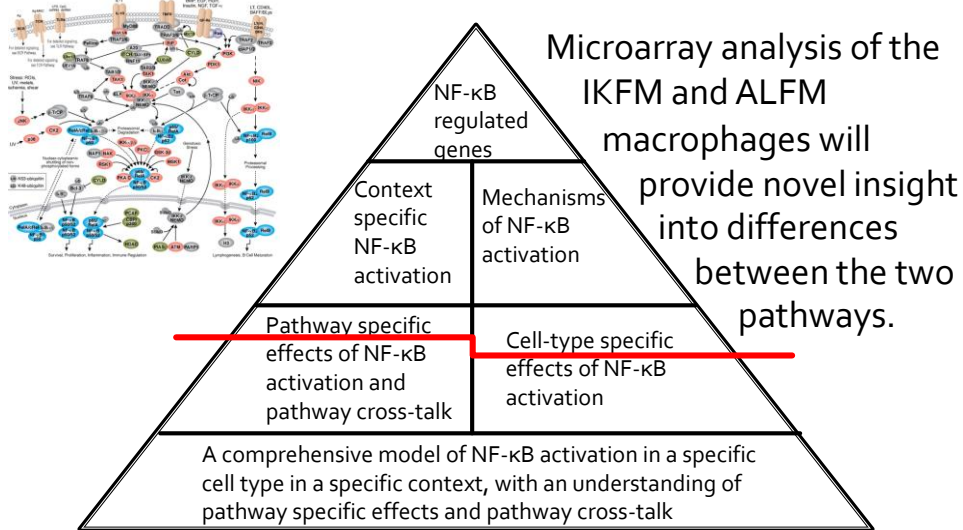


- Analysis of the mRNA from these macrophages will provide insight into how NF- κ B contributes to TAM and how it might be used to create the Terminator macrophage

■ Mice from the Yull lab upregulate classical or alternative NF- κ B

■ After activation, M ϕ s can be separated via CD11B+ magnetic bead pulldown

NF-κB: Understand the complexity; embrace the complexity



State of the microarray

- IKFM samples have been prepared and analyzed previously
- wt and TAM samples have been submitted and are awaiting hybridization
- ALFM samples have mRNA prepared and are awaiting test results for contamination

NF-κB will be manipulated using siRNA in primary macrophages to create the Terminator phenotype

2b: Creation of the Terminator phenotype *in vitro*

- wt BMDMs, splenic macrophages (SPMs), and PyVT TAMs will be cultured in 6 well plates
- The cells will be transfected with siRNA overnight to manipulate NF-κB
 - Background research suggests that k/d of the alternative pathway and activation of the classical pathway will be the most efficacious combination
- qRT-PCR will be used to analyze the cells' phenotypes; gene targets informed by microarray

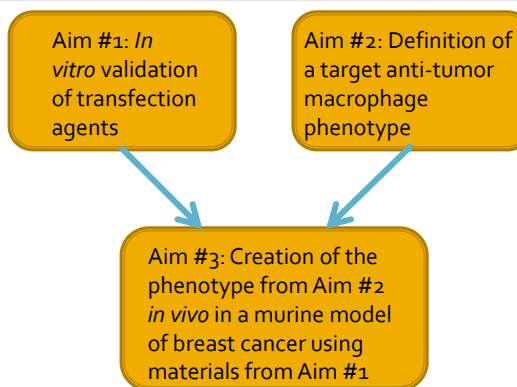
Aim 2b: Alternate plans

- SPMs are one source of primary, immunocompetent Mφs, but other sources are possible: lung, mammary
- Other sources of TAMs: ovarian ascites fluid
- Alternate knockdown target in alternative NF-κB pathway: NIK
 - Activating kinase of the alt pathway
 - Constantly produced but regulated via rapid degradation

Aim 2 Outcomes

- The Terminator phenotype described in 2a will be the target from *in vivo* aim 3
- Microarray analysis will reveal actionable information about the alternative pathway in Mφs
 - Robust information about alternative pathway will be highly publishable
- A manuscript from Aim 2 is tentatively planned for the end of summer 2013

Aim 3: Targeted delivery of siRNA to TAMs *in vivo*



Aim 3 will investigate the biodistribution of the Mn-NP and examine their therapeutic potential in an *in vivo* mouse model of human breast cancer (PyVT)

Biodistribution in PyVT mice will be examined using fluorescent dsDNA

3a: Biodistribution study of the Mn-NP

- FAM-dsDNA will be delivered to wt and MMTV-PyVT mice with Mn-NP via 2 retro-orbital (RO) injections
 - 5 mg/kg (approx 15 nmol dsDNA/kg), N:P = 4
 - 3 control groups: saline injection, free FAM-dsDNA, OH-NP_dsdNA
 - 1 experimental group: Mn-NP_dsdNA
- Samples will be taken from: liver, kidney, lung, blood, mammary/tumor
 - Blood serum tested at Pathology Core for AST:ALT for liver function and BUN for kidney toxicity
 - Tissue macrophages will be separated via rapid adhesion, plated, and analyzed for FAM fluorescence in a plate reader
 - Plated cells will be stained with fluorescent CD11B antibody, fixed, and imaged

Aim 3a: alternate plan

- If FAM dyes will not work on the plate reader, PE based dyes on dsDNA can be used; IR dyes would allow whole animal imaging
- Alternate routes of NP delivery: Tail vein, intratumoral
- Frozen tissue sections can be taken to do qualitative fluorescent imaging of FAM-dsDNA

Terminator M ϕ s will be created *in vivo* in PyVT mammary tumors

3b: Targeted manipulation of TAM phenotype with Mn-NP_siRNA

- siRNAs used to create the Terminator phenotype in Aim 2 will be delivered using the Mn-NP vetted in 1c and 3a
 - Research suggests that siRNAs will be used to k/d the alternative pathway and activate the classical pathway
- Female MMTV-PyVT mice will be grown to 7 weeks and treated with Mn-NP_siRNA via RO injection

Terminator M ϕ s will be created *in vivo* in PyVT mammary tumors

3b: Targeted manipulation of TAM phenotype with Mn-NP_siRNA

- 4 control mice groups, n=5, 2 mg/kg dose
 - Saline injection, unloaded Mn-NP, Mn-NP_siRNA₁, Mn-NP_siRNA₂
- 1 experimental group, n=5, 2 mg/kg dose
 - Mn-NP_siRNA₁ + Mn-NP_siRNA₂
- Mice will be injected before formation of palpable tumor and injected 3 times per week for 4 weeks or until the humane endpoint is reached

Analysis of therapeutic effect of Mn-NP delivered siRNA

- Tumors will be measured with calipers before each injection
- After sacrifice, all tumor tissue will be removed and weighed
- Lungs will be inflated with Bouin's fixative and the number of lung metastases will be counted
- Tumors will be dissociated and the Mφ population enriched by rapid adhesion to tissue culture plates
 - qRT-PCR will be performed on TAM mRNA to determine phenotypic changes brought about by siRNA delivery
 - Liver and kidney toxicity will be measured by AST:ALT and BUN

Aim 3b: alternate plan

- Completion of Aims 2 and 3a may inform changes in the dosing plan
- Alternate tumor models:
 - primary tumor model - orthotopic injection of L129 cells (murine polyoma) into the mammary fat pad
 - lung metastasis model - tail vein injection of tumor cells
- PyVT mice could be crossed with NGL to use luciferase/GFP as a readout of NF-κB in TAMs

Aim 3 Outcomes

- Aim 3 will provide a biodistribution profile of the Mn-NP_nucleotide complex and show *in vivo* manipulation of tumor stromal cell phenotype using siRNA
- Successful completion of Aim 3 would result in high impact, clinically translatable data. This data will be put into a manuscript aimed at a high impact factor journal with broad readership.

Proposed Timeline

		2011		2012				2013			
		Winter	Spring	Summer	Fall	Winter	Spring	Summer	Fall	Winter	
AIM 1	Transfection agent protocol										
	siRNA Library										
	Mn-NP validation										
AIM 2	Microarray of macrophages										
	Terminator Macrophages										
AIM 3	Biodistribution of Mn-NP										
	<i>In vivo</i> manipulation of TAMs										
Other Milestones	DOD annual Report										
	Mn-NP manuscript										
	Terminator macrophage manuscript										
	<i>In vivo</i> manuscript										
	Dissertation Defense										

Peer reviewed original research and review articles

- T. Soike, A.K. Streff, C. Guan, R. Ortega, M. Tantawy, C. Pino, V.P. Shastri. Engineering a Material Surface for Drug Delivery and Imaging using Layer-by-Layer Assembly of Functionalized Nanoparticles. *Adv. Mater.* 22, 1392-1397. 2010.
- S.S. Yu, R.L. Scherer, R.A. Ortega, C.S. Bell, C.P. Soman, C.P. O'Neil, J.A. Hubbell, and T.D. Giorgio. Enzymatic- and temperature-sensitive controlled release of ultrasmall superparamagnetic iron oxides (USPIOs). *Journal of Nanobiotechnology*. 9:7. 2011.
- S.S. Yu, R.A. Ortega, B.W. Reagan, J.A. McPherson, H.J. Sung, T.D. Giorgio. Emerging applications of nanotechnology for the diagnosis and management of vulnerable atherosclerotic plaques. *WIREs Nanomedicine and Nanobiotechnology*. 3:6. 2011.
- R.A. Ortega, T.E. Yankeelov, T.D. Giorgio. Magnetic nanoparticles in magnetic resonance imaging: a translational push toward theranostics. Ed. R. Bawa, G. F. Audette, I. Rubinstein. *Clinical Nanomedicine – From Bench to Bedside*. Pan Stanford Series in Nanomedicine, Pan Stanford Publishing, Singapore, 2012.
- R.A. Ortega and T.D. Giorgio. A Mathematical Model of Superparamagnetic Iron Oxide Nanoparticle Magnetic Behavior to Guide the Design of Novel Nanomaterials. *Journal of Nanoparticle Research*. 14: 1282. 2012.

Acknowledgements

PhD Committee

Todd Giorgio
 Fiona Yull
 Craig Duvall
 Frederick Haselton
 Barbara Fingleton



VANDERBILT
 School of Engineering



Giorgio Lab

Shann Yu
 Hongmei Li
 Kellye Kirkbride
 Virginia Pensabene
 Ian McFadden
 Charleson Bell
 Bharat Kumar
 Chelsey Smith
 Kavya Sharman

Yull Lab

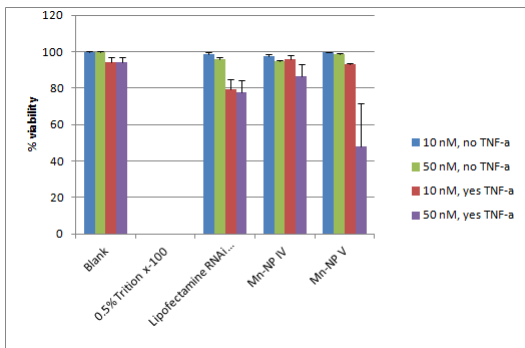
Whitney Barham
 Oleg Tikhomirov
 Hala Onishko
 Lianyi Chen

Members of the
 Duvall, Haselton,
 and Sung Labs

Funding

DoD BCRP

Particle formulation IV is well tolerated



- Trypan Blue viability assay done with Mn-NP formulations and lipofectamine

NPs go to tumor tissue; some end up in spleen and lungs

